

**Design, synthesis and optimization of receptor ligands:
tools for studying purine-activated and related orphan G
protein-coupled receptors**

Dissertation

zur

Erlangung des Doktorgrades (Dr. rer. nat.)

der

Mathematisch-Naturwissenschaftlichen Fakultät

der

Rheinischen Friedrich-Wilhelms-Universität Bonn

vorgelegt von

Tim Harms

Aus Wilhelmshaven, Deutschland

Bonn 2021

Angefertigt mit Genehmigung der Mathematisch-Naturwissenschaftlichen Fakultät
der Rheinischen Friedrich-Wilhelms-Universität Bonn

Promotionskommission:

Erstgutachterin: Prof. Dr. Christa E. Müller

Zweitgutachter: Prof. Dr. Finn Hansen

Fachnahes Mitglied: Prof. Dr. Günther Weindl

Fachfremdes Mitglied: Prof. Dr. Rainer Manthey

Tag der Promotion: 07.01.2022

Erscheinungsjahr: 2022

Die vorliegende Arbeit wurde in der Zeit von Oktober 2017 bis September 2021 am Pharmazeutischen Institut der Rheinischen Friedrich-Wilhelms-Universität Bonn unter der Leitung von Frau Prof. Dr. Christa E. Müller angefertigt.

Mein besonderer Dank gilt Frau Prof. Dr. Christa E. Müller für die interessanten Promotionsthemen, ihre Anleitung und den lehrreichen Gesprächen.

Ebenso möchte ich Herrn Prof. Dr. Finn Hansen, Herrn Prof. Dr. Günther Weindl und Herrn Prof. Dr. Rainer Manthey für ihre Mitgliedschaft in meiner Prüfungskommission danken.

Table of contents

1. Introduction	1
1.1 G protein-coupled receptors.....	1
1.1.1. GPCR structures	1
1.1.2. Classification of GPCRs	2
1.2 Purinergic receptors.....	3
1.3 Adenosine receptors.....	3
1.3.1. Adenosine	4
1.3.2. The A _{2A} adenosine receptor.....	6
1.3.3. The A _{2B} adenosine receptor.....	17
1.4. Orphan GPCRs.....	24
1.4.1. MRGPRX3.....	24
1.5. General methods to study GPCR ligand binding	27
1.5.1. Approaches to study GPCR ligand binding using fluorescent-labeled ligands.....	27
1.6. Fluorescent ligands.....	35
1.6.1. Cyanine dyes.....	38
1.6.2. NIR fluorophores	40
2. Aims of the study	42
2.1. Exploration of <i>N</i> -acyl-8-(4-piperazine-1-sulfonyl) phenylxanthines as potent and selective adenosine A _{2B} receptor antagonists	42
2.2. Functionalized potent and selective 8-(4-acylpiperazinyl-1-sulfonyl)phenylxanthines providing a platform for fluorescence-labeling of adenosine A _{2B} receptor antagonists.....	43
2.3. Synthesis of 3-amino- <i>N</i> -benzyl-1-phenyl-1 <i>H</i> -pyrazole-4-carboxamides as A _{2A} AR antagonists	44
2.4. Synthesis of 2,4,6,8-tetrasubstituted pyrimido[5,4- <i>d</i>]pyrimidines as MRGPRX3 agonists	45
3. References.....	46
4. Results and discussion	71

4.1. Part I: Exploration of <i>N</i> -acyl-8-(4-piperazine-1-sulfonyl) phenylxanthines as potent and selective adenosine A _{2B} receptor antagonists	71
4.1.1. Keywords:.....	71
4.1.2. Abstract	71
4.1.3. Introduction.....	72
4.1.4. Results and discussion	73
4.1.5. Conclusions.....	80
4.1.6. Experimental section	80
4.1.7. References	91
4.1.8. Supporting information.....	94
4.2. Part II: Functionalized potent and selective 8-(4-acylpiperazinyl-1-sulfonyl)phenylxanthines providing a platform for fluorescence-labeling of adenosine A _{2B} receptor antagonists	119
4.2.1. Keywords.....	119
4.2.2. Abstract	119
4.2.3. Introduction.....	120
4.2.4. Results and discussion	122
4.2.5. Conclusions.....	135
4.2.6. Material and methods	136
4.2.7. References	154
4.2.8. Supporting Information	160
4.3. Part III: Synthesis of 3-amino- <i>N</i> -benzyl-1-phenyl-1 <i>H</i> -pyrazole-4-carboxamides as A _{2A} AR antagonists	172
4.3.1. SAR analysis of 5-aminotriazoles as A _{2A} AR antagonists based on computational studies.....	172
4.3.2. Compound design	174
4.3.3. Synthesis of 3-amino- <i>N</i> -benzyl-1-phenyl-1 <i>H</i> -pyrazole-4-carboxamides.....	177
4.3.4. Synthesis.....	181
4.3.5. Reactivity of 3-aminopyrazole derivatives	209
4.3.6. Resynthesis of 1-(5-(6-fluoro-5-methyl-3 <i>H</i> -imidazo[4,5- <i>b</i>]pyridine-2-yl)-1 <i>H</i> -indazol-1-yl)propan-2-ol (PZB00712006)	209

4.3.7. Biological evaluation.....	211
4.3.8. Summary and outlook.....	225
4.3.9. Experimental Part.....	229
4.3.10. References.....	260
4.4. Part IV: Synthesis of 2,4,6,8-tetrasubstituted pyrimido[5,4- <i>d</i>]pyrimidines as MRGPRX3 agonists.....	265
4.4.1. Dipyridamole and derivatives.....	265
4.4.2. Compound design.....	267
4.4.3. Synthesis.....	272
4.4.4. Pharmacological evaluation.....	307
4.4.5. Conclusions and outlook.....	321
4.4.6. Experimental part.....	324
4.4.7. References.....	353
5. Summary and outlook.....	356
5.1. Adenosine receptors.....	356
5.1.1. Exploration of <i>N</i> -acyl-8-(4-piperazine-1-sulfonyl)phenylxanthines as potent and selective adenosine A _{2B} receptor antagonists.....	357
5.1.2. Functionalized potent and selective 8-(4-acylpiperazinyl-1-sulfonyl)phenylxanthines providing a platform for fluorescence-labeling of adenosine A _{2B} receptor antagonists.....	358
5.1.3. Synthesis of 3 amino- <i>N</i> -benzyl-1-phenyl-1 <i>H</i> -pyrazole-4-carboxamides as A _{2A} AR antagonists.....	359
5.2. Synthesis of 2,4,6,8-tetrasubstituted pyrimido[5,4- <i>d</i>]pyrimidines as MRGPRX3 agonists.....	360
5.3. References.....	361

1. Introduction

1.1 G protein-coupled receptors

Receptors are proteins that translate signals from the extracellular to the intracellular space. Aside from some special stimuli like light, thermal energy or protons, receptors are typically activated by endogenous ligands including hormones, peptides, ions, amino acids and other transmitters. They can additionally be addressed by synthetic compounds making them a target for drugs.¹⁻³ G protein-coupled receptors (GPCRs) are the most important class of drug targets. About 34% of all drugs on the market act on around 100 GPCRs.⁴⁻⁷ The name “GPCR” is based on the heterotrimeric guanine nucleotide-binding proteins (G proteins) that are bound and activated by the receptors.⁴ With more than 800 members, GPCRs represent the largest gene superfamily in the human genome.⁸ Their signal transduction is based on stimulating or inhibiting secondary messenger release including cAMP (cyclic adenosine monophosphate), IP₃ (inositol-1,4,5-triphosphate) and DAG (diacylglycerol), transmitted by a guanine-nucleotide-binding protein (G_s, G_i and G_q or G_{12/13}).^{3,4}

1.1.1. GPCR structures

GPCRs are composed of seven hydrophobic transmembrane α -helices and are consequently also called seven-transmembrane (7TM) receptors. Those helices are connected via three extracellular loops (ECL1-3) and three intracellular loops (ICL1-3), the N-terminus is located extracellularly and the C-terminus is found inside the cell. One important intramolecular interaction of class A GPCRs are disulfide bridges that are formed by highly conserved cysteine residues located at TM3 / ECL1 and ECL2. These bridges induce and stabilize the overall three-dimensional conformation of the receptors.⁹

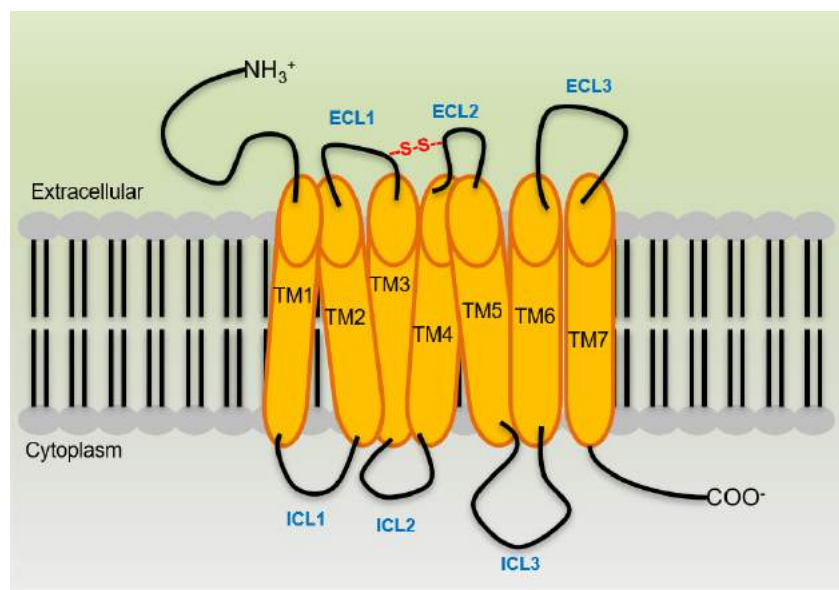


Figure 1. Schematic structure of a G protein-coupled receptor (GPCR).

GPCRs share the greatest sequence identity in the TM regions but strongly vary in the sequence and length of the extracellular N-terminus.^{8;10;11} The different N-termini make GPCRs remarkably versatile signaling molecules. Monoamine and peptide receptors exhibit short sequences between 10 and 50 amino acids while much larger domains (350-600 amino acids) are found for glycoprotein hormone receptors, and the glutamate family of receptors.¹¹

GPCRs can be addressed by various modulators binding to different binding sites. Small molecules bind mostly to the TM region while peptides and other large structures rather bind to the easier accessible N-terminus. Allosteric ligands can bind to a separate site or various sites on the same receptor, altering the signal transduction of orthosteric ligands.^{12;13}

1.1.2. Classification of GPCRs

In 1994, Attwood, Findlay¹⁴ and Kolakowski¹⁵ introduced a classification system for GPCRs that was based on structural and physiological features defining different classes (A - F) in order to classify all GPCRs in vertebrates and invertebrates.¹⁶ The largest and best studied group refers to the Rhodopsin-like receptors and is called class **A**.^{4;17} Receptors of this class are commonly addressed by biogenic amines, peptides or lipid-like ligands. The adenosine receptor family is a well-known example of this class. Class **B** describes secretin-like receptors that bind larger proteins like secretin, calcitonin or glucagon, while class **C** defines metabotropic glutamate receptors that bind glutamate. The other receptor classes, class **D**, the fungal pheromone receptors, class **E**, cAMP receptors, and class **F**, the frizzled / smoothed receptors, cannot be found in the human genome. All these classes can be distinguished according to physiological functions and the nature of their ligands.¹⁷

Another system of classification is the GRAFS system that was established by Fredriksson et al. in 2003 (cf. table 1). It is based on a phylogenetic comparison and may be a more convenient approach for pharmaceutical research since only human GPCRs are classified.¹⁸

Table 1. Overview of the GPCR-classes according to the GRAFS-system.¹⁸

Receptor Family	Examples
<u>G</u> lutamate receptors	Metabotropic and GABA receptors
<u>R</u> hodopsin receptors	Purine receptors, opioid receptors, chemokine receptors, olfactory receptors, neuropeptide receptors
<u>A</u> dhesion receptors	Lectomidin receptor
<u>F</u> rizzled/Taste 2 receptors	FZD 1-10 (glycoprotein Wnt binding frizzled receptors), TAS2 receptor (taste receptor)
<u>S</u> ecretin receptors	Secretin receptor, glucagon receptor, calcitonin receptor, corticotropin-releasing hormone receptor

1.2 Purinergic receptors

Purinergic receptors belong to the largest family of GPCRs, the rhodopsin-like receptors. The family was firstly defined in 1976 and was later subdivided into P1 and P2 receptors.^{19;20} Receptors of the P1 family are activated by adenosine while P2 receptors are activated by various nucleotides such as adenosine triphosphate (ATP), adenosine diphosphate (ADP), uridine triphosphate (UTP), uridine diphosphate (UDP) and others (see Figure 2).^{20;21} Four subtypes of adenosine receptors (A_1 -, A_{2A} -, A_{2B} - and A_3 ARs) are distinguished according to their structural features and their ability to increase (A_{2A} - and A_{2B} ARs) or decrease (A_1 - and A_3 ARs) cAMP levels in cells by regulating the activity of the adenylate cyclase (AC).^{22;23} The nucleotide receptors (P2) are subdivided into P2X and P2Y receptors, P2Y are GPCRs, while P2X receptors are ligand-gated ion channels (LGICs).²⁴ There are seven subtypes of the ionotropic P2X receptors (P2X1-7), all being activated by ATP. The eight metabotropic P2Y receptors (P2Y_{1,2,4,6,11-14}), on the other hand, are responsive to ATP, ADP, UTP, UDP or UDP-glucose, depending on the subtype. The subscripted numbers refer to the chronological order of cloning the respective receptor whereby the missing numbers are receptors that are not responsive for nucleotides or that are not found in mammals.^{25;26} In 2002, Bender et al. identified another purinergic receptor in rat that is sensitive to adenine (P0).²⁷ Those adenine receptors have not been found in humans yet, however they were cloned and characterized from rat (rAdeR1 or MrgA), mouse (mAdeR1 or MrgA10, mAdeR2 or MrgA9) and hamster (cAdeR1).^{27;28} Adenine receptors belong to the family of mas-related gene (MRG) receptors.^{27;29}

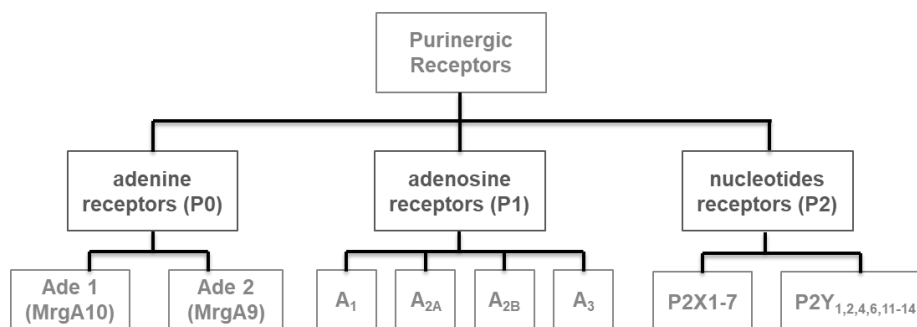


Figure 2. Classification of the purinergic receptors.

1.3 Adenosine receptors

Adenosine-activated receptors (ARs) are an important subfamily among class A rhodopsin-like GPCRs, firstly cloned in the 1990s. These membrane-bound receptors have been studied in great detail. As mentioned before, four different subtypes are classified due to genetic and pharmacologic features, namely the A_1 , A_{2A} , A_{2B} and A_3 receptor.^{5;30} ARs can be found all over the human body, be it in the central nervous system (brain, spinal cord) or in many organs such as heart, colon, liver or lung.³⁰ The receptor family is of high interest as drug targets since

ARs involved are in a variety of physiological but also pathological functions including pain, inflammatory diseases, ischemia, epilepsy, neurodegenerative diseases, and noteworthy in cancer.^{31;32}

1.3.1. Adenosine

The purinergic nucleoside adenosine is composed of the nucleobase adenine and the sugar β -D-ribose, and is an important core structure for all kinds of biomolecules. Its derivative ATP embodies the ubiquitous energy source for biochemical reactions and a ligand for P2 receptors. Furthermore, adenosine is a building block of RNA and S-adenosylmethionine which acts as a biochemical methylation reagent.^{33;34} Adenosine is the natural ligand for the four ARs, however at a basal extracellular concentration of 30 - 200 nM, the A_{2B}AR is not activated since it has the lowest affinity for adenosine (EC₅₀ >10 μ M).^{35;36} Nevertheless, the concentration can increase 100-fold under pathophysiological conditions such as inflammation, ischemia, hypoxia and tissue injury and then activate the A_{2B}AR as well.^{21;36}

Instead of being released into the extracellular compartment by vesicles (like classic neurotransmitters), adenosine is mainly transported from the intracellular compartment by equilibrative nucleoside transporters like ENT1, or it is formed by enzymatic breakdown of extracellular adenine nucleotides such as ATP (cf. Figure 3).³⁷⁻³⁹ As the name “equilibrative nucleoside transporter” suggests, the direction of adenosine-transport is depending on the gradient of concentration. Adenosine cannot pass the cell-membrane by passive diffusion. Intracellular adenosine originates from the hydrolysis of S-adenosylhomocysteine (SAH) to adenosine and homocysteine (Hcy) via the enzyme SAH-hydrolase or via hydrolysis of adenosine monophosphate (AMP) by 5'-nucleotidases.⁴⁰ Another source of extracellular adenosine can be extracellular nucleotides that emerge from traversing through channel proteins, by exocytosis or by cell lysis.³⁹ Nucleotides can be hydrolyzed by certain membrane-bound enzymes, the ectonucleodases. The human ectonucleotidase NTPDase2 (nucleoside triphosphate diphosphohydrolase 2) can convert ATP to ADP, while CD39 (also known as NTPDase1) converts ATP and ADP to AMP. Finally, adenosine is formed by the hydrolysis of AMP by the enzyme CD73 (ecto-5'-nucleotidase).³⁹ Normally, the concentration of adenosine is much higher inside the cells, however, the extracellular concentration rises dramatically under pathological conditions (e.g. hypoxia or tissue injury) when nucleotide breakdown is expedited by the aforementioned enzymes.⁴¹ Adenosine has a lifetime of about 1 s in the extracellular compartment, then it is either (re)phosphorylated by adenosine kinase (ADK) to produce AMP, or converted to inosine by adenosine deaminase (ADA).³³

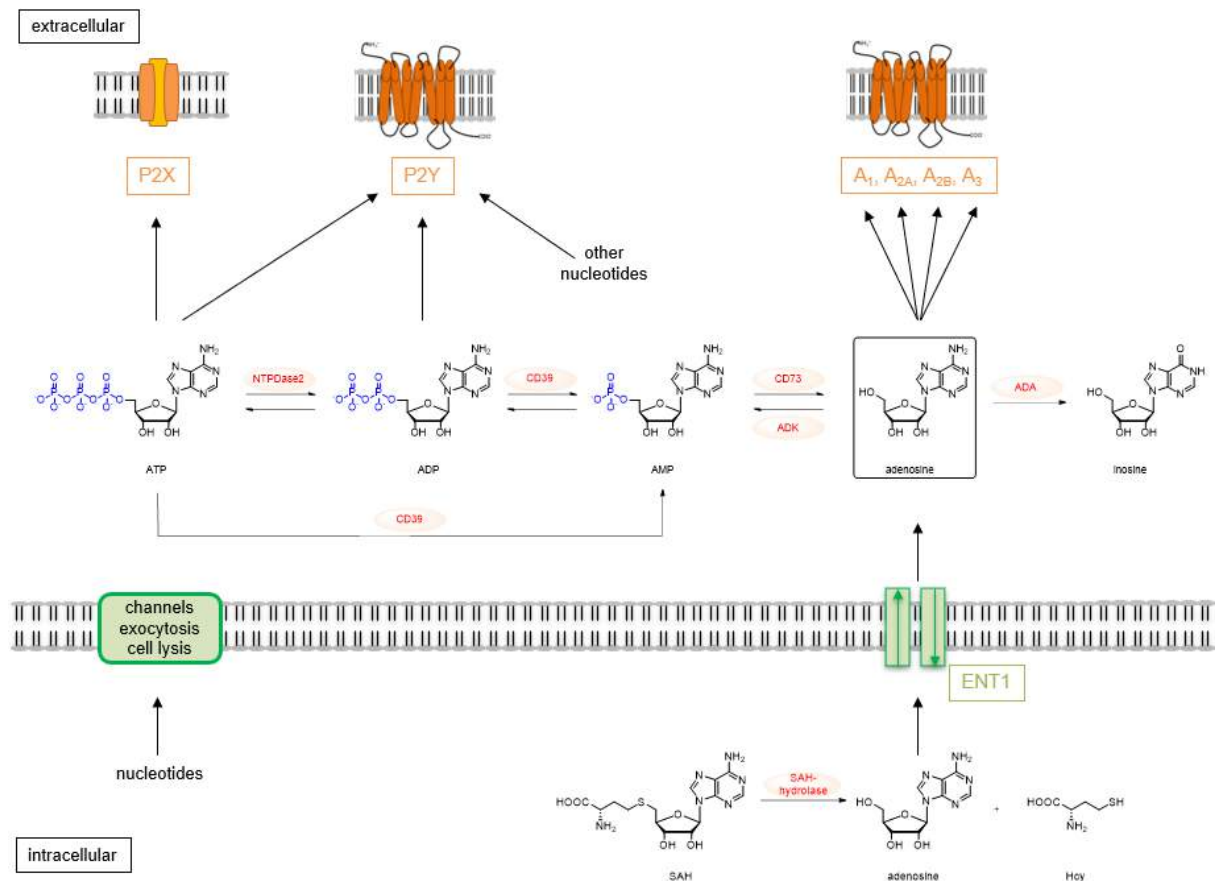


Figure 3. Schematic representation of adenine nucleotides and adenosine interconversion in the intra- and extracellular space and their associated signaling pathways.³⁹

Adenosine is an important neurotransmitter and neuromodulator regulating many tissue functions under physiological and pathophysiological conditions.^{42;43} Among other impacts, adenosine promotes vasodilatation and angiogenesis and decreases inflammation, and it counteracts prolonged ischemia and consequently plays a cardioprotective role.⁴⁴ Adenosine is clinically approved for the treatment of paroxysmal supraventricular tachycardia under the tradename Adenocard®.⁴⁵ Despite its protective role under physiological condition, high adenosine concentrations can be very harmful under certain pathological conditions, e.g. in asthma, diabetes, neurodegenerative diseases, ischemia or cancer.⁴⁶ For example, adenosine plays a role in promoting cancer development by evoking immunosuppressive effects and directly affecting growth, metastasis and angiogenesis of tumor cells.^{46;47} In particular, the A_{2A}- and A_{2B}ARs exhibit similar immunosuppressive and pro-angiogenic functions, yet have distinct biological roles in cancer.⁴⁸ Blocking the A_{2A}- and A_{2B}ARs and/or ectonucleotidases like CD39 and CD73 could reduce the pathological production and impact of adenosine and hence lead to an activation of the immune system to defeat cancer.⁴⁹

1.3.2. The A_{2A} adenosine receptor

The human A_{2A}AR is encoded on the gene ADORA2A on chromosome number 22 (22q11.2), and it consists of 412 amino acids (cf. Figure 4).⁵⁰ The A_{2A} receptor has ~46% sequence identity with the A_{2B}AR, ~37% sequence identity with the A₁AR and approx. 31% with the A₃AR.⁵¹ The A_{2A}AR possesses common features that are observed in the GPCR family. However, in contrast to many other GPCRs, an eighth transmembrane helix is present which, unlike the other helices, is parallel to the cytoplasmic surface of the receptor.⁵² Structure-based drug design methods such as modeling became more and more successful since several X-ray crystallography studies made 3D crystal structures of the A_{2A}AR available and greatly helped to rationally design and discover novel A_{2A}AR ligands including agonists, antagonists and allosteric modulators (cf. Figure 4).⁵²⁻⁵⁵ The A_{2A}AR was the non-rhodopsin, first non-adrenergic GPCR of which an X-ray crystallographic structure was reported.^{5;25}

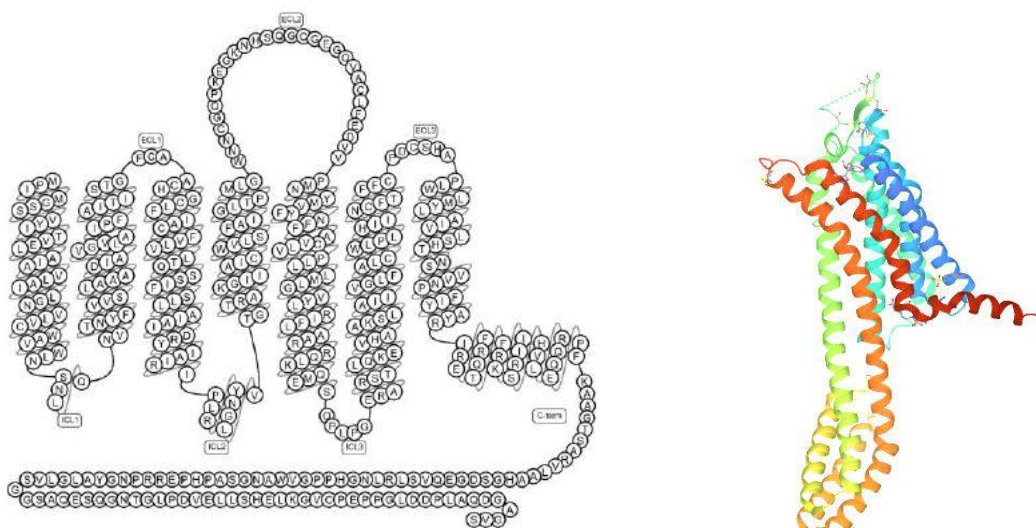


Figure 4. Snakelike plot of the human A_{2A} adenosine receptor (left) and crystal structure of adenosine A_{2A} receptor bound to a triazole-carboximidamide antagonist (right) (PDB id: 5UIG). The C-terminus is truncated in the X-ray structure.^{53;56;57}

1.3.2.1. (Patho)physiological functions and modulation of the A_{2A} adenosine receptor

In the human body, the A_{2A}AR is mainly expressed in the spleen, on blood platelets, the thymus, leukocytes and certain regions of the brain (striatopallidal GABAergic neurons and tuberculum olfactorium and dorsal striatum neurons) and it can be found in lesser amounts in heart, lung, kidney, liver and blood vessels.^{30;58;59}

The A_{2A}AR plays important roles in inflammation processes, since it is expressed on macrophages, T-lymphocytes and neutrophils, which are involved in inflammatory activity. The activation of the A_{2A}AR leads to inhibitory effects on these inflammatory cells, making

A_{2A} agonists potential anti-inflammatory drugs.⁶⁰ Activating A_{2A}ARs on immune cells significantly reduces inflammation processes such as the secretion of elastase as well as many pro-inflammatory cytokines. Additionally, A_{2A}AR activation stimulates the production of the anti-inflammatory peptide interleukin 10 (IL-10), further reducing inflammation.⁶¹

A_{2A}AR agonists might have a potential use in the treatment of various inflammatory conditions such as asthma. This respiratory disease is characterized by chronic inflammation and reversible obstruction of the airways, and ~8% of adults are affected.⁶² The inflammation process in the airways involves many immune cells expressing the A_{2A}AR, making these cells a potential target for asthma therapy.⁶³ As shown by Tiago et al. in 2017, the A_{2A}AR is upregulated in alveolar macrophages when subjected to pro-inflammatory stimuli, and activation of A_{2A}AR attenuated the impact of pro-inflammatory stimuli.⁶⁴ On the other hand, the application of A_{2A} antagonists can worsen asthmatic conditions in animal models, proving the concept.⁶⁵

Inflammation is furthermore involved in wound healing. After remission of the inflammatory process, angiogenesis and remodeling of the affected tissue takes place.⁶⁶ This process can be impaired, for example, due to the pathological consequences of diabetes mellitus.⁶⁷ Since the A_{2A}AR has shown to be involved in wound healing, agonists have been investigated towards potential applications.⁶⁸ The application of the A_{2A}AR agonist polydeoxyribonucleotide (PDRN), for example, showed improved wound healing in patients suffering from chronic diabetic foot ulcers in a clinical study.⁶⁹ The activation of A_{2A}ARs is furthermore involved in fibrosis as activation leads to the production of cAMP and subsequently the activation of the PKA (protein kinase A), which, in turn, can activate fibroblasts and stimulate the production of collagen.⁷⁰

Since the A_{2A}AR is widely expressed in the brain, it is an attractive target for neurodegenerative diseases, e.g. Parkinson's disease (PD), Alzheimer's disease (AD), or depression.⁵² Parkinson's disease is a highly prevalent neurodegenerative disorder being characterized by progressive loss of dopaminergic neurons present in the substantia nigra in the brain. As a result, the dopamine-level in the striatum is significantly diminished. Bradykinesia, postural instability and tremors are the main symptoms of PD.^{52;71-73} The current therapy uses the prodrug L-DOPA (*L*-3,4-dihydroxyphenylalanine) as a dopamine replacement. L-DOPA can penetrate the blood-brain barrier by active transport through amino acid transporter and is converted to dopamine in the brain to substitute the lacking dopamine. Although it reduces the common symptoms of PD, the therapy is accompanied by side-effects like hypotension, dyskinesia, nausea and vomiting.⁷⁴ Antagonizing the A_{2A}AR has shown relief for the symptoms of PD presumably due to several reasons. A physical inhibitory interaction between the A_{2A}AR and the dopamine receptors present in the striatum has been observed, and A_{2A}AR antagonists

might therefore compensate for the reduced levels of dopamine.^{75;76} It should be noted, that the A_{2A}AR, like many other GPCRs, is known to dimerize or oligomerize. Homo- and hetero dimerization as well as oligomerization have been reported.^{77;78} In the striatum, a well-explored A_{2A}AR / D₂ dopamine receptor heterodimer can be addressed by antagonists to treat PD.^{5;79} This needs to be considered during drug discovery because the formation of dimers or oligomers might alter the conformation of the entire protein and thus change the potency of ligands.⁸⁰ Furthermore, an association between high levels of A_{2A}AR and the development of dyskinesia has been observed.⁸¹ Accordingly, A_{2A}AR antagonists may also diminish the unpleasant side effects of an L-DOPA-therapy.⁸² A_{2A}AR antagonists might additionally exert their anti-Parkinsonian activity via the inhibition of MAO-B (monoamine oxidase B) enzymes that play a major role in the metabolism of dopamine. By reducing metabolic degradation, the dopamine level will rise.⁸³ The xanthine-based A_{2A}AR antagonist istradefylline (see Figure 6, **10**), for example, was observed to reversibly inhibit MAO-B with a K_i value of 28 μM.⁸⁴ This is, however, very high, and probably not therapeutically relevant.

Alzheimer's disease is a highly prevalent neurodegenerative disorder that results in progressive impairment of cognitive functions, especially cognition and memory. The development of AD is influenced by genetic and environmental factors. Two hallmark characteristics of AD are known: abnormally phosphorylated tau-proteins that result in the formation of intraneuronal fibrillar aggregates, and the accumulation of β-amyloid peptides form amyloid plaques outside of brain neurons thereby impeding neuronal function.^{85;86} It has been observed that the consumption of caffeine (see Figure 6, **9**) is inversely correlated with the development of Alzheimer's disease as well as other cognitive impairments in the elderly. These findings were correlated with A_{2A}AR-blocking activity of caffeine.⁸⁷ The pathological role of the A_{2A}AR in AD was confirmed by a study using a gene-based association analysis⁸⁸ and the investigation of A_{2A}-knockout mice that indicated that deletion of A_{2A}AR is protective in a mouse model of tauopathy.⁸⁹ The suitability of A_{2A} antagonists as potential AD treatment has been widely explored. The first successful *in vivo* study was performed by Dall'Igna et al. in 2007 and revealed that A_{2A} antagonists (including caffeine) have a protective effect against cognitive impairment induced by β-amyloid.⁹⁰ In another study, genetically modified mice were treated with the A_{2A} antagonist MSX-3 (see Figure 6, **11a**) (daily 0.3 g/l in water) over 6 months. As a result, the treatment prevented memory impairment in the APP / PS1dE9 mouse model of AD and partially inhibited amyloidogenesis in the brain.⁹¹

Major depressive disorder (MDD) is a highly prevalent psychotic disorder that is associated with loss of interest, depressed mood, appetite abnormalities and sleep disorders.⁹² One of the assumed causes of MDD is a disbalance of neurotransmitters in the presynaptic cleft.⁹³ This situation can be addressed by many drugs nowadays, however, these drugs still suffer from

adverse effects, withdrawal symptoms and lack of efficacy.⁹⁴ It was shown that intake of caffeine has (yet unclear) negative effects on anxiety and depression.⁹⁵ Increased levels of adenosine, on the other hand, were associated with the development of depression in animal models.^{96;97} Animal models that investigated depressive behavior of rats overexpressing the A_{2A}AR⁹⁸ or A_{2A}AR-knockout mice⁹⁹ indicated that A_{2A}-stimulation is related to an increase of depression and thus, that antagonism at A_{2A}AR could be a therapeutic approach to treat MDD.⁵²

The term cancer refers to mutated cells whose division occurs in a rapidly abnormal and uncontrolled manner. This happens in contrast to normal physiological conditions since cell division is a highly controlled process that is regulated by many internal and external factors.⁵² Common approaches to fight cancer include surgery, radiation therapy chemotherapy and recently immunotherapy.^{100;101} Several lines of evidence indicate that adenosine plays a crucial role in tumor development. It has been reliably established that the tumor microenvironment has relatively high levels of adenosine as a result of hypoxia and tissue damage. Adenosine has contrary effects on cell proliferation depending on the involvement of different adenosine receptor subtypes in various cancer types.^{52;102} It was furthermore observed that adenosine inhibits immune cell responses. The activation of the A_{2A}ARs on natural killer T cells, for example, leads to a reduced response of these cells, showing the suppressing role of the A_{2A}AR in the immune system.¹⁰³ Waickman et al. found out that mice lacking the A_{2A}AR showed significantly delayed growth of lymphoma cells in comparison to wild type-mice, showing the tumor-supportive role of the A_{2A}AR in tumor-growth.¹⁰⁴ These findings suggest the possibility of utilizing A_{2A}AR-antagonism in cancer immunotherapy. Furthermore, cancer cells can alter the expression levels of the immune checkpoints leading to inhibitory effects on the T cells. The A_{2A}AR has been demonstrated to participate in the protection of cancer cells from T cells.¹⁰⁵ Consequently, blocking A_{2A}ARs would help the immune system to fight cancer.

1.3.2.2. Selective ligands for the A_{2A} adenosine receptor

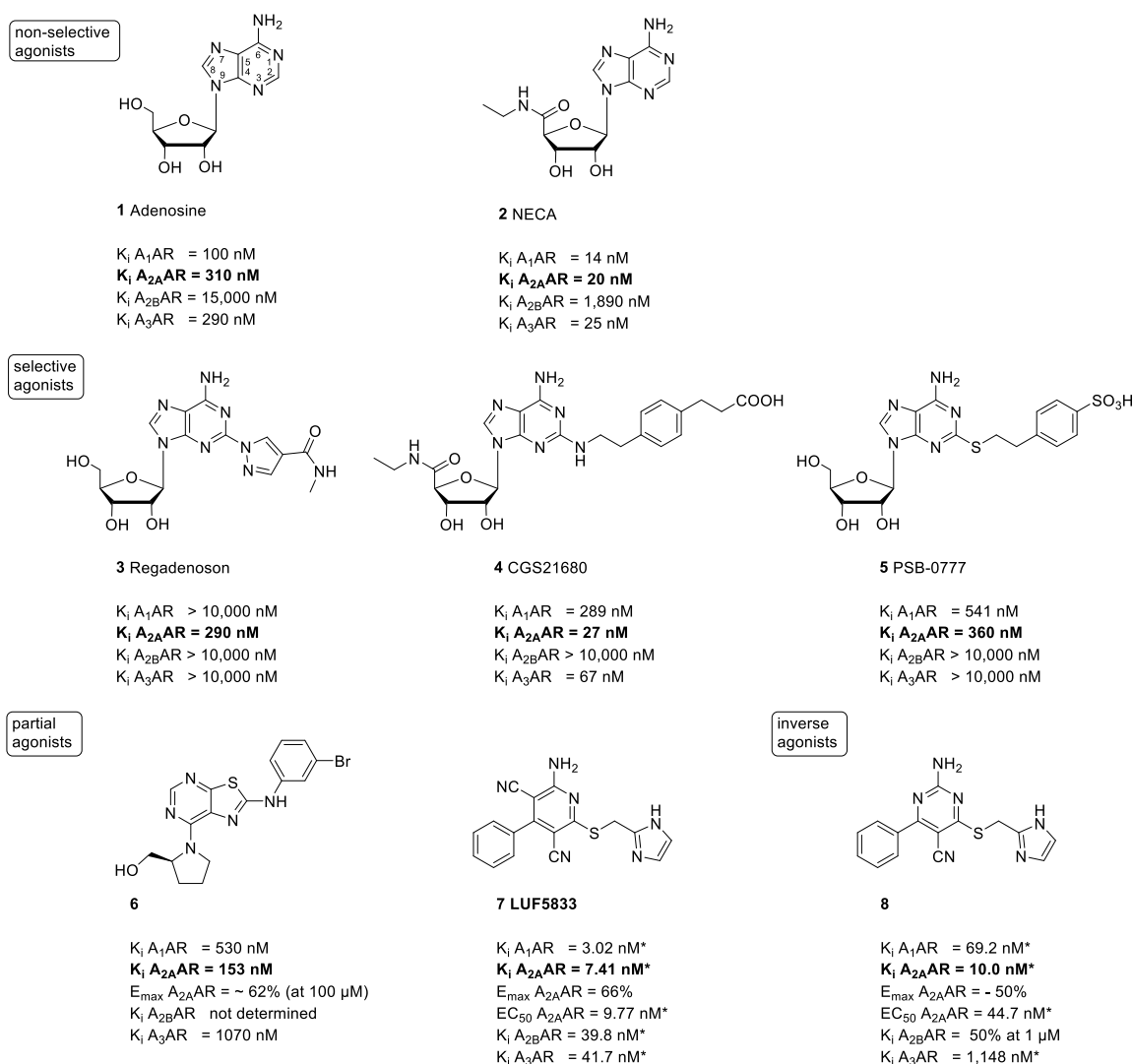
A large number of chemical compounds has been synthesized and evaluated with regard to activity at the ARs in general and the A_{2A}AR in particular. Three major scaffolds have been found to bind to A_{2A}ARs:

- modified nucleosides on the basis of adenosine and adenine-derivatives
- modified purines, particularly xanthine-derivatives
- various heterocyclic scaffolds such as bicyclic and tricyclic heterocycles, some of them being mimics of adenine and xanthines

Generally, the first class (modified nucleosides) are mostly agonists while the other two classes (modified purines and heterocycles) turned out to be mostly antagonists for the $A_{2A}AR$.^{59;106} The following chapters will introduce some chosen selective ligands of the $A_{2A}AR$.

1.3.2.2.1. A_{2A} adenosine receptor agonists

Most $A_{2A}AR$ agonists are derivatives of adenosine. The receptor exhibits a hydrophilic pocket that binds to the sugar moiety of adenosine derivatives which is typically not occupied by antagonists.¹⁰⁷ The natural agonist for all AR subtypes adenosine (**1**) has a very short half-life (~1 s) in the body so that more stable adenosine derivatives are normally used as pharmacological probes or drugs.^{5;108} 5'-(*N*-Ethylcarboxamido)adenosine (NECA, **2**), for example, is an adenosine-derived, non-selective agonist active on all AR subtypes and it is widely used tool compound and for the measurement of $A_{2B}AR$ binding affinities as a radioligand ($[^3H]NECA$).¹⁰⁹



* calculated from pK_i or pEC_{50} values

Figure 5. Chemical structures and affinities at human AR subtypes of $A_{2A}AR$ agonists.^{5;108-115}

The introduction of bulky modifications at the C2-position of adenosine or NECA can improve the selectivity for the A_{2A} AR over the other AR subtypes. The marketed drug regadenoson (LexiscanTM, **3**) is an example for a successful therapeutic application of a selective A_{2A} AR agonists.¹¹⁰ Because of its vasodilatory effects, it was introduced as a diagnostic for stress testing.¹¹¹ With a K_i value of 290 nM it shows good affinity for A_{2A} and is highly selective towards the other AR subtypes. CGS21680 (**4**) is a highly potent A_{2A} agonist ($K_i = 27$ nM) and was recently co-crystallized with the A_{2A} AR in its active conformation, giving very important information regarding the binding of agonists to the receptor through analysis of the CGS21680 binding pose.¹¹² El-Tayeb et al. synthesized PSB-0777 (**5**) and used it in a study exploiting the synergistic effect due to combining the A_{2A} AR agonist with an A_{2B} AR antagonist for treating inflammatory bowel disease.¹¹³ In order to ensure exclusive local activity in the gastrointestinal tract, the very polar sulfonate group was introduced to the molecule to prevent absorption. The compound showed a good K_i value of 360 nM at the human A_{2A} AR and significantly improved impaired acetylcholine-induced contractions in inflamed rat ileum / jejunum preparations. In 2016, Bharati et al. discovered compound **6** as a novel chemotype of non-nucleoside partial agonists for the A_{2A} AR.¹¹⁴ Molecular modeling studies were performed to design the thiazolo[5,4-*d*]pyrimidine scaffold. The group predicted that the (*S*)-2-hydroxymethylene-pyrrolidine residue could mimic the sugar moiety of adenosine in the receptor. In experimental assays a K_i value of 153 nM and ~ 62% efficacy for the human A_{2A} AR was determined along with moderate selectivity towards A_1 AR and A_3 AR. Recently, Amelia et al. reported the nonriboside partial agonist LUF5833 (**7**). It binds to the A_{2A} AR with a K_i value of 7.41 nM but binds to the other AR subtypes with comparable affinity. **7** reached up to 66% of E_{max} with an EC_{50} of 9.77 nM. Guided by a crystal structure of **7** in complex with the A_{2A} AR, the group synthesized new derivatives including compound **8** that turned out to be an inverse agonist. **8** exhibited an E_{max} value of -50% with good binding to the A_{2A} AR ($K_i = 10$ nM).¹¹⁵

1.3.2.2.2. Competitive selective A_{2A} adenosine receptor antagonists

While the agonists mostly comprise of modifications of adenosine, the antagonists show much broader structural diversity. On the basis of caffeine, many xanthine-based compounds have been explored as antagonists. On the other hand, numerous antagonists containing a variety of mono-, bi- or tricyclic structures have been described.

1.3.2.2.2.1. Selective xanthine-based A_{2A} adenosine receptor antagonists

One of the first identified compounds and the structural prototype of xanthine-based A_{2A} AR antagonists is the natural alkaloid caffeine (**9**, Figure 6). Its potency is in about the same range for all four AR subtypes. The xanthine scaffold has been intensely studied as a basis for AR antagonists. Structure-activity relationship (SAR) studies and selectivities towards various AR subtypes have been explored with regard to substitutions at the 1-, 3-, 7- and 8-position.^{49;116}

A_{2A} -selective antagonists have been developed through substitution of the 8-position with styryl residues. Istradefylline (**10**) was one of the first reported selective A_{2A} AR antagonists and the first approved drug of that kind. It is clinically used for the treatment of Parkinson's disease in Japan and the USA.^{82;117;118} The compound is potent (K_i human A_{2A} AR = 12 nM) and selective towards the other ARs, especially A_{2B} and A_3 . Similar to most other xanthine derivatives, Istradefylline suffers from poor water solubility. Additionally, it has to be protected from light since the styryl-double bond is prone to dimerization in the solid state or *E/Z*-isomerization in dilute solution.¹¹⁹ The compound MSX-2 (**11**) suffers from the same drawbacks, however, the OH group in the structure offers the possibility of water-soluble prodrug approaches: the phosphate prodrug MSX-3 (**11a**) and the *L*-valine ester prodrug MSX-4 (**11b**) could be established and have been used for *in vivo* studies.^{117;120-122} The potency and selectivity of MSX-2 are superior compared to istradefylline.

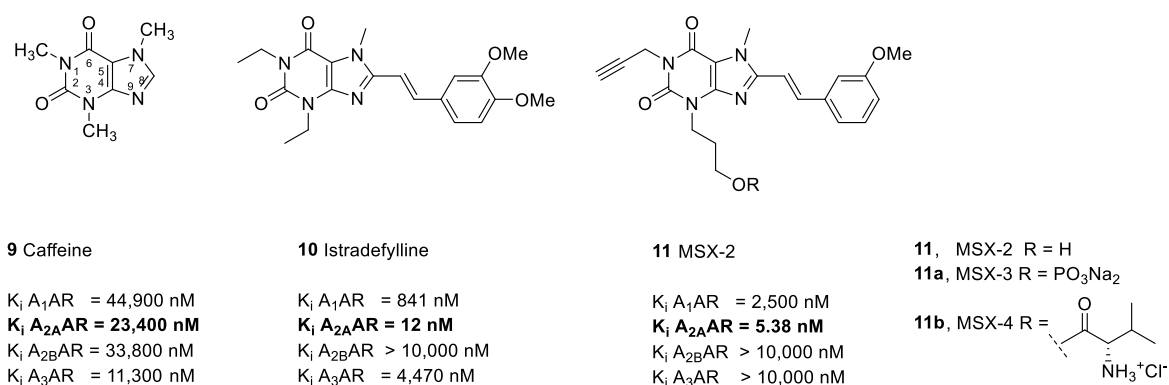


Figure 6. Chemical structures and affinities at human AR subtypes of important xanthine-based A_{2A} AR antagonists.^{49;82;116;120;121}

1.3.2.2.2. Selective non-xanthine selective A_{2A} adenosine receptor antagonists

Numerous antagonists containing a mono-, bi- or tricyclic structure have been described. The aromatic part of these molecules often mimics the adenine moiety of adenosine in the receptor, while the sugar part is missing.

The triazolopyrimidine derivative ZM241385 (**12**, Figure 7) is a highly potent A_{2A} AR antagonist (K_i = 1.6 nM) but also moderately binds to A_{2B} AR. Its tritiated and iodinated derivatives have been used as radioligands for the A_{2A} AR and also for labeling the A_{2B} AR in highly overexpressing cell lines.¹²³ The first X-ray crystallographic structure of the A_{2A} AR was obtained in complex with ZM241385.¹²⁴ The triazolopyrimidine vipadenant (**13**) was prepared by Gillespie et al. and showed (beneath high potency at the A_{2A} AR and good selectivity towards the A_3 AR) activity in commonly used models of Parkinson's disease after peroral application.¹²⁵ Although it demonstrated excellent preclinical pharmacokinetics and successfully completed phase I clinical studies, vipadenant was terminated due to concerns over the outcome of

preclinical toxicology testing.¹²⁶ Later on, it was repurposed for cancer therapy.¹²⁷ The pyrazolotriazolopyrimidine SCH442416 (**14**) demonstrates high potency at the A_{2A} AR ($K_i = 4.1$ nM) and selectivity towards all other ARs.¹²⁸ Its ^{11}C -radiolabeled form is widely used for mapping the distribution of A_{2A} ARs in the brain.¹²⁹ A structurally related compound is preladenant (**15**), it shows slightly higher A_{2A} -affinity and was clinically studied for PD. Unfortunately, it showed no benefits although the compound was well tolerated.¹³⁰

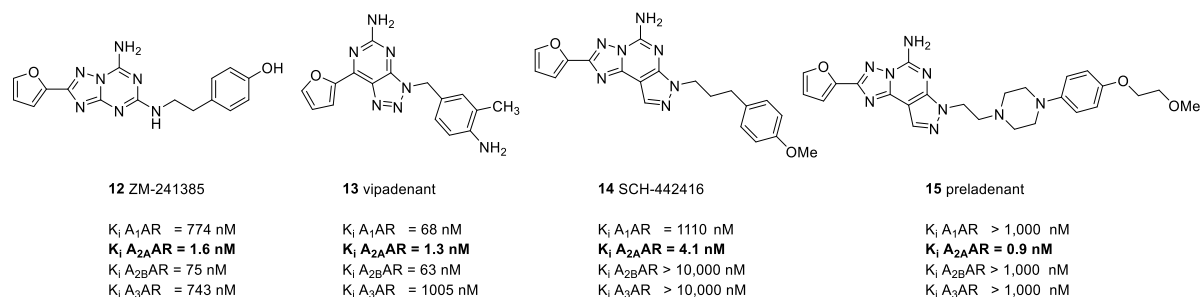
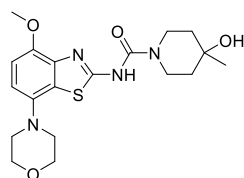


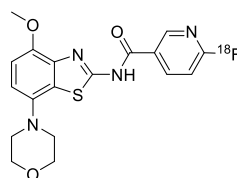
Figure 7. Chemical structures and affinities at human AR subtypes of non-xanthine A_{2A} AR antagonists.^{125;128;131;132}

The company Roche reported the benzothiazole tozadenant (SYN115, **16**) as potent (K_i A_{2A} AR = 5 nM) and selective A_{2A} AR antagonist.¹³³ **16** significantly reduced motor deficits in a 2-[(2-aminoethylamino)carbonylethylphenylethylamino]-5'-ethylcarboxamidoadenosine (APEC) induced hypolocomotion rat model and revealed good pharmacokinetic parameters in rat and dog.¹³⁴ The efficacy and safety dose ranges of tozadenant were accessed in several clinical trials in PD patients. A shortening of positive off-time was observed after a twice daily dose of 120 mg of **16**. However, a placebo-controlled phase III study (NCT02453386) needed to be interrupted due to serious adverse effects.¹³⁵ Recently, Lai et al. reported novel fluorinated analogs of **16**. The compound TOZ1 was selected for radiofluorination aiming at the development of a positron emission tomography (PET) radiotracer for non-invasive imaging.¹³⁵ The cold ligand showed low nanomolar affinity at the A_{2A} AR ($K_i = 1.00$ nM) and was selective towards the A_1 AR. [^{18}F]TOZ1 (**17**) proved A_{2A} AR-selective binding to striatum of mouse and pig brain determined in autoradiography studies. Dynamic PET studies in mice displayed penetration of the blood brain barrier (BBB), however, the specific binding was insufficient and would need to be improved in the future.



16 Tozadenant (SYN 115)

K_i A₁AR = 1,350 nM
 K_i A_{2A}AR = 5.0 nM
 K_i A_{2B}AR = 700 nM
 K_i A₃AR = 1,570 nM

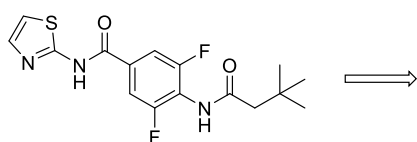


17 [¹⁸F]TOZ1

K_i A₁AR = 618 nM
 K_i A_{2A}AR = 1.00 nM

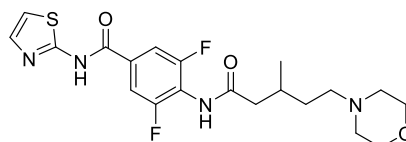
Figure 8. Chemical structures and affinities at human AR subtypes of benzothiazole-based A_{2A}AR antagonists.^{133;135;136}

The group of Mikkelsen et al. optimized the A_{2A}AR antagonist Lu AA411063 (**18**) with regard to enhanced water solubility and A₁AR-selectivity.¹³⁷ The study highlighted compound **19** which still binds in a nanomolar range and showed better A₁ selectivity and solubility than the parent compound. During *in vitro* pharmacokinetic evaluation tests, the compound showed no significant cytochrome P450 (CYP) inhibition.



18 Lu AA41063

A_{2A} K_i = 5.9 nM
A₁ K_i = 410 nM
aq. solubility @ pH 7.4 = 1 µg/ml

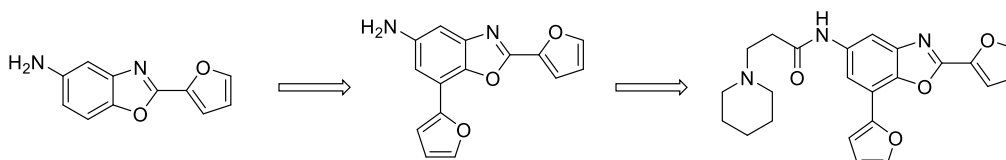


19

A_{2A} K_i = 110 nM
A₁ IC₅₀ >2000 nM
aq. solubility @ pH 7.4 = 116 µg/ml

Figure 9. Chemical structures, human A_{2A} and human A₁ receptor binding affinities and water solubility of A_{2A}AR antagonists based on 3,5-difluoro-N-thiazol-2-yl-benzamides.¹³⁷

On the basis of a 2-arylbenzoxazole scaffold, Duroux et al. improved the properties of an initial screening hit at the A_{2A}AR (**20**) with support of molecular docking studies.¹³⁸ Several compounds with affinities in the low nanomolar range were described whereby compound **21** showed particularly good affinity, and compound **22** exhibited notably good DMPK properties.



20

A_{2A} K_i = 10,000 nM

21

A_{2A} K_i = 40 nM

22

A_{2A} K_i = 81 nM

Figure 10. Chemical structures and affinities at human A_{2A}AR of antagonists based on a 2-arylbenzoxazole scaffold.¹³⁸

Further examples for non-xanthine scaffolds as A_{2A} AR antagonists include the very potent and selective 7-imino-2-thioxo-3,7-dihydro-2*H*-thiazolo[4,5-*d*]pyrimidine derivative **23** ($K_i A_{2A}$ = 0.0038 nM),¹³⁹ the adenine derivative ST-1535 (**24**, $K_i A_{2A}$ = 6.6 nM)¹⁴⁰ or the 1,2,4-triazine derivative **25** ($K_i A_{2A}$ = 7.76 nM),¹⁴¹ all depicted in Figure 11.

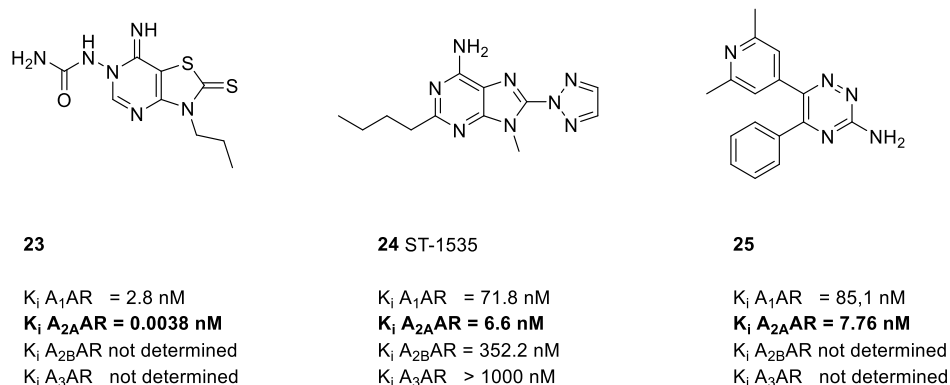


Figure 11. Chemical structures and affinities at human AR subtypes of different non-xanthine A_{2A} AR antagonists.¹³⁹⁻¹⁴¹

Recently, the 5-aminotriazole Cmp-1 (**26**) has been crystallized with the A_{2A} AR. Antagonist **26** showed a good affinity to A_{2A} with a K_i value of 11.2 nM.⁵³ The study proposed a potential allosteric pocket in the receptor. Compounds **27** and **28** were found by molecular docking studies searching for dual antagonists at the A_{2A} AR and the MAO-B, this combination would be particularly meaningful with regard to PD therapy.⁵⁴ Among others, the two compounds were prepared and pharmacologically tested. Both showed high affinity to the A_{2A} AR. However, only compound **27** showed high inhibition of MAO-B.

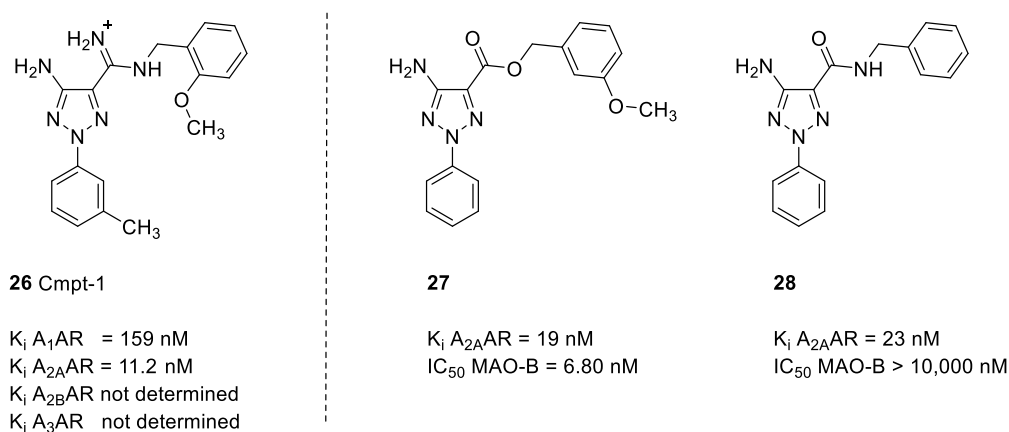


Figure 12. Chemical structures and affinities at human AR subtypes of A_{2A} AR antagonists based on 5-aminotriazoles.^{53,54}

1.3.2.2.3. Allosteric modulators of the A_{2A} adenosine receptor

The binding of allosteric modulators to a GPCR induces a conformational change of the protein that affects binding and accordingly kinetics and signal transduction of orthosteric ligands. Allosteric ligands are divided into negative allosteric modulators (NAMs) and positive allosteric modulators (PAMs). Allosteric binding sites are found on other domains of the proteins than the orthosteric binding site.¹⁴² Several class A GPCRs feature a conserved allosteric site called “sodium ion pocket”. This has been proven for the A_{2A}AR via X-ray crystallography studies.^{53;143;144}

In 2016, Massink et al. reported the synthesis and evaluation of 5'-substituted amiloride derivatives as NAMs at the A_{2A}AR.¹⁴³ As a result, the 4-ethoxyphenethyl-substituted amiloride derivative **29** showed the highest potency, it diminished the binding of [³H]ZM-241385 (cf. Figure 13). A shift in potencies between the wild-type receptor and a variant that was mutated in the sodium ion pocket (W246A) confirmed binding of **29** at the allosteric binding site. Recently, an affinity mass spectrometry-based fragment screening was performed by Lu et al. yielding the NAM Fg754 (**30**).¹⁴⁵ The compound displaced the agonist [³H]CGS21680 (**4**) and it displayed moderate potency in inhibiting G_s-coupled cAMP signaling. The group reported that **30** might function in a mixed mode since molecular dynamics simulations indicated penetration of **30** into the allosteric sodium ion pocket as well as an overlap of **30** with the bottom of the orthosteric site. The allosteric modulation, however, seemed to be the major mode of action. Due to this special binding mode, **30** was suggested as a novel template for the development of bitopic A_{2A}AR ligands. Chen et al. performed a fragment-based drug discovery approach (FBDD) and screened a fragment library using thermostabilized GPCRs and target immobilized NMR screening (TINS). Among other hits, they discovered the NAM **31** and the PAM **32**.¹⁴⁶ Treating the A_{2A}AR with **31** resulted in an increase of the k_{off} of [³H]ZM-241385 while the k_{off} of [³H]NECA was increased. Additionally, the group showed concentration-dependence of the allosteric modulation, suggesting that **31** is a NAM. **32**, on the other hand, potentiated the action of [³H]ZM-241385 and [³H]NECA. Moreover, the group reported a dose-dependent increase of the E_{max} of the agonist CGS21680 (Figure 5, **4**), suggesting that **32** is a PAM. Compound **33** was discovered to be a potent PAM at the A_{2A}AR, it significantly decreased the dissociation rate of [³H]ZM-241385.¹⁴⁷ Furthermore, it significantly amplified vasodilatory capacity for agonist CGS21680 in a rodent aortic ring assay.

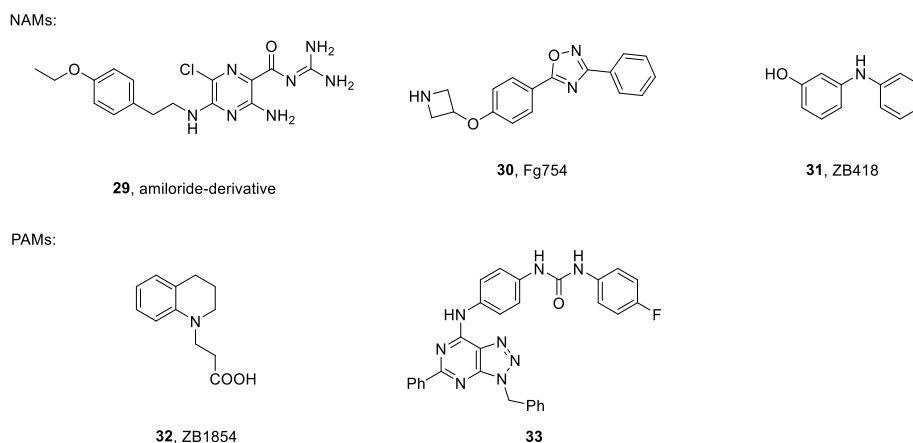


Figure 13. Allosteric modulators of the human $A_{2A}AR$ **29-33** and their potencies and kinetic influence of $A_{2A}AR$ modulators.^{143;145-147}

1.3.3. The A_{2B} adenosine receptor

The human $A_{2B}AR$ is encoded on the gene *ADORA2B* on chromosome number 17 (17p12-p11.2) and consists of 332 amino acids (cf. Figure 14).⁵⁷ It shows a sequence identity of ~42% to the A_1AR , ~46% to the $A_{2B}AR$ and ~35% to the A_3AR .⁵¹ Since no X-ray crystallography structure is available for the $A_{2B}AR$, only homology models (based on the most closely related $A_{2A}AR$) can be utilized to envision the structure of the receptor.¹⁴⁸⁻¹⁵⁰ The binding sites of A_{2A} - and $A_{2B}AR$ s are similar, differing in only one amino acid (namely leucine L249 in the $A_{2A}AR$ for valine V250 in the $A_{2B}AR$). It is unclear whether this results in the big difference in affinities of adenosine for the two receptors.¹⁵¹ Another explanation might be the difference in the extracellular domains, e.g. of EL2 which is much longer in the $A_{2B}AR$. The EL2 has been proposed to play a role as a gate-keeper for ligand binding, subtype-selectivity and receptor activation.¹⁵² Moreover, the $A_{2B}AR$ has only one required disulfide bridge in its extracellular domains while the $A_{2A}AR$ has four disulfide bridges, making it much more rigid in its conformation in comparison to the $A_{2B}AR$.^{153;154}

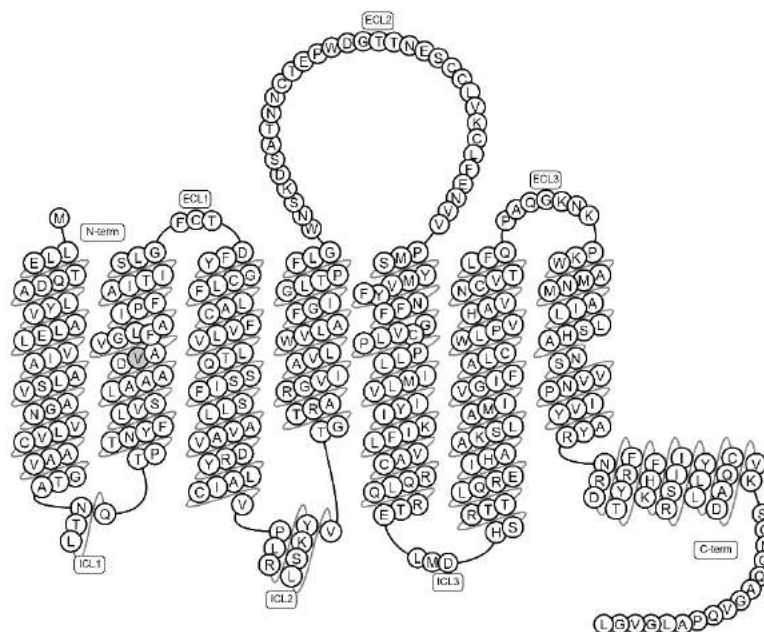


Figure 14. Snakelike plot of the human A_{2B} adenosine receptor.⁵⁷

1.3.3.1 (Patho)physiological functions and modulation of the A_{2A} adenosine receptor

The $A_{2B}AR$ is widely distributed in the periphery of the human body; abundant expression of the receptor is observed in smooth muscles, monocytes, mast cells, bronchial epithelium and the digestive tract including colon and ileum. In the CNS, on the other hand, the $A_{2B}AR$ can be found on neurons and in glia but to a much lesser extent. Moreover, the $A_{2B}AR$ is expressed in the urinary bladder, vasculature and alveolar cells.¹⁵⁵⁻¹⁵⁷ The $A_{2B}AR$ shows the lowest affinity for adenosine of all four subtypes and thus remains silent under normal physiological conditions. Only under pathological conditions such as hypoxia, inflammatory and cancer, where extracellular adenosine levels increase up to micromolar concentrations, the receptor is considerably stimulated.^{5;30} Its expression is upregulated under certain pathological conditions as well (e.g. by hypoxia-inducible factor 1- α (HIF-1 α), under inflammatory conditions and in cancer), suggesting a possible maladaptive role of the $A_{2B}AR$ in many processes.¹⁵⁸⁻¹⁶⁰

The $A_{2B}AR$ is expressed on cells that modulate inflammation, and it can both inhibit and increase inflammation.¹⁶¹ The proinflammatory effects are mediated via secretion of IL-6 from macrophages, and of several interleukins and VEGF from mast cells, as well as the production of IL-19 and TNF- α from bronchial epithelial cells.¹⁶²⁻¹⁶⁴ Stimulation of $A_{2B}ARs$ can also have anti-inflammatory effects, this includes the inhibition of adhesion of neutrophils to endothelial cells, the suppression of TNF- α and IL-1 β production and macrophage proliferation as well as the stimulation of IL-10 secretion from macrophages.^{165;166} Moreover, the receptor can delay the deactivation of myofibroblasts and thus regulate myocardial repair and remodeling.¹⁶⁷

The blockage of A_{2B}ARs using the antagonists CVT-6883 and MRS-1754 (see Figure 16, **39** and **40**) alleviated clinical symptoms of experimental autoimmune encephalitis in mice and could thus protect the CNS from immune damage.^{164;168}

In the lung, pathophysiological effects such as inflammation, airway reactivity and remodeling in asthma are mediated by G_q and G_s proteins that bind to the A_{2B}AR.¹⁶⁹ Inflammatory mediators (leading to bronchoconstriction) are released by mast cells when the A_{2B}AR is activated and this could be prevented by the application of antagonists.¹⁷⁰ For example, the A_{2B}AR antagonist CVT-6883 (**39**) decreased asthmatic effects including inflammation and airway reactivity in a mouse model.¹⁷¹ Chronic obstructive pulmonary disease (COPD) is a nonspecific term that describes several debilitating disorders resulting in a relentless, progressive, and essentially irreversible remission of lung function. The application of the selective A_{2B}AR (partial) agonist BAY 60-6583 (see Figure 15, **34**) in combination with dexamethasone could provide a potential therapy for COPD by inducing genes with anti-inflammatory effects.^{164;172} Additionally, studies confirmed that A_{2B}-stimulation plays an important role in the pathogenesis of COPD and pulmonary fibrosis by inducing the differentiation of pulmonary fibroblasts into myofibroblasts and the secretion of IL-6.^{173;174}

Although the A_{2B}AR seems to have no direct impact on ventricular myocytes, it was proven to be involved with A₁AR-mediated cardioprotection.^{175;176} Myocardial ischemia-reperfusion injury refers to the tissue damage that occurs when the blood supply returns to tissues after an ischemic event in the heart.¹⁷⁷ During this pathological conditions, the level of adenosine is increased enough to stimulate the low-affinity A_{2B}ARs, therefore it can mediate a cardioprotective role upon stimulation.¹⁷⁸ The cardioprotective effects involve transcription factor hypoxia-inducible factor (HIF1 α) and specificity protein 1 (SP1).¹⁷⁹ In this situation, the A_{2B}AR can promote tissue adaption to the occurring hypoxia, neutralizing hypoxia-induced inflammation. Moreover, A_{2B}ARs can reduce infarction by decreasing platelet aggregation, by mediating vasodilatory effects and by adjusting carbohydrate metabolism.¹⁵⁷

The A_{2B}AR and adenosine play an important, pro-tumorigenic role in cancer. On the one hand, the adenosine level is increased in tumor tissues which promotes cancer growth by suppressing the immune system.¹⁸⁰ On the other hand, high levels of A_{2B}ARs can be found on many tumor cells, and stimulation of A_{2B}AR is involved in tumor cell proliferation, angiogenesis and metastasis.^{181;182} Metastasis might be supported by A_{2B}AR-mediated expression of Fos-related antigen-1 (Fra-1, a metastasis transcription factor),¹⁸³ while angiogenesis is induced through the production of angiogenic cytokines by mast cells and the vascular endothelial growth factor (VEGF).¹⁸⁴ In human prostate cancer cell lines, the A_{2B}AR was found to be the most highly expressed AR. Its activation decreased chemotherapy and TNF α -induced cell death protecting the cancer cells.¹⁶⁸ These findings lead to the attempt to fight cancer by

blocking the A_{2B} AR. A prominent example for this approach is the antagonist PSB-1115 (see Figure 16, **38**). Its application decreased tumor metastasis of CD73⁺ melanoma cells and mammary carcinoma cells,¹⁸⁵ it delayed tumor growth and increased NK cells and tumor-infiltrating CD8⁺ T cells¹⁸⁶ and it demonstrated synergistic effects with other chemotherapeutics such as doxorubicin or dacarbazine.¹⁸⁶ Several A_{2B} AR antagonists are in clinical trials for cancer-treatment.^{182;187}

1.3.3.2. A_{2B} adenosine receptor ligands

1.3.3.2.1. A_{2B} adenosine receptor agonists

Animal studies for several diseases, including lung injury, ischemia and vascular leakage, suggested a therapeutic advantage for A_{2B} AR stimulation, however, a selective and potent full agonist has not yet been identified.¹⁸⁸ Only BAY 60-6583 (**34**, Figure 15) and few derivatives based on the 2-aminopyridine-3,5-dicarbonitrile scaffold showed noteworthy agonism for A_{2B} ARs combined with selectivity.¹⁸⁹ Even so, studies involving compound **34** should be interpreted carefully since **34** acts as a partial agonist or even as a functional antagonist at A_{2B} ARs, based on the receptor expression level and local adenosine concentrations.¹⁵¹ Moreover, **34** showed antagonism at other AR subtypes, namely the A_1 AR, the A_{2A} AR and the A_3 AR.¹⁹⁰

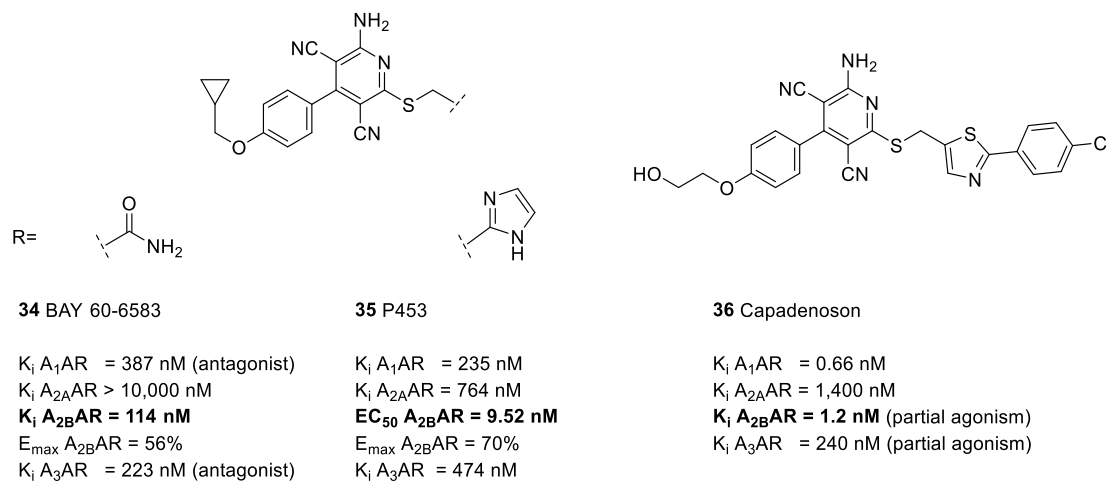


Figure 15. Chemical structures and affinities at human AR subtypes of partial A_{2B} AR agonists.

189;191;192

Despite these limitations, **34** was employed in several *in vivo* studies to activate the A_{2B} AR. The compound significantly reduced myocardial infarct size by promoting the differentiation of anti-inflammatory macrophages over the PI3K/PKB pathway (phosphoinositide 3-kinases / protein kinase B). These protective effects could be blocked by either ATL-801 (A_{2B} AR antagonist) or wortmannin (PI3K-inhibitor).^{193;194} In a study by Jafari et al., **34** induced a cell cycle arrest and apoptosis in breast cancer stem cells.¹⁹⁵ In 2019, Catarzi et al. synthesized

several derivatives of **34** leading to unselective pan AR-ligands and to A_1/A_{2B} -selective partial agonists. Compound P453 (**35**) (cf. Figure 15)¹⁹¹ turned out to be the most potent and selective agonist in this series, exhibiting an EC_{50} value of 9.52 nM and showing 70% efficacy in a cAMP assay. Activation of A_{2B} ARs by **35** led to significantly reduced paired pulse facilitation in CA1 hippocampal preparations of rat brain (cornu ammonis).¹⁹⁶ The clinically trialed A_1 AR agonist capadenoson (**36**) was recently found to be a partial A_{2B} AR agonist as well.¹⁹² The compound had been evaluated in phase IIa clinical trials on patients with stable angina and atrial fibrillation but was eventually withdrawn.^{197;198}

1.3.3.2.2. Selective A_{2B} adenosine receptor antagonists

1.3.3.2.2.1. Xanthine-based selective A_{2B} adenosine receptor antagonists

A large number of selective A_{2B} AR antagonists have been described, many of which are based on the xanthine scaffold. Similar to the A_{2A} AR, caffeine (**9**) was the first noteworthy antagonist described for A_{2B} ARs.¹¹⁶ XAC (**37**) is an example for a non-selective AR-antagonist; it has high affinities in a comparable range on all ARs (cf. Figure 16).¹⁵¹ The compound could be crystallized with the A_{2A} AR, yielding an X-ray structure of the inactive receptor conformation.¹⁹⁹ Highly potent and selective A_{2B} AR antagonists can be obtained by carefully choosing the residues at the xanthine scaffold. Alkylation of N1 and N3, and particularly the structural nature of the residue in position 8 are important for subtype-selectivity. In 2002, the Müller group reported the potent and A_{2B} -selective antagonist PSB-1115 (**38**).²⁰⁰ In contrast to many other xanthines, **38** showed good water-solubility due to the sulfonic acid group. Accordingly, it could be employed for *in vivo* studies as done by Michael et al.. The group showed that the blockade of the A_{2B} AR with **38** can impede the inflammation-induced disturbance of the acetylcholine-induced contraction in TNBS (2,4,6-trinitrobenzenesulfonic acid) pre-treated small intestinal preparations of rats.²⁰¹ CVT-6883 (**39**) is a potent and selective antagonist ($K_i A_{2B}AR = 22$ nM),²⁰² it was used in *in vivo* mouse models of pulmonary inflammation and injury. The compound diminished pulmonary inflammation and injury in the lungs of adenosine deaminase-deficient mice and in a model of bleomycin-induced lung injury.²⁰³ MRS-1745 (**40**) was described as another potent and selective antagonist for $A_{2B}AR$.²⁰⁴ It was used to inhibit angiogenesis in microvascular endothelial cell lines and it inhibited the growth of colon carcinoma cells.^{205;206} However, the molecule suffers from poor oral bioavailability and is metabolically unstable.²⁰⁷

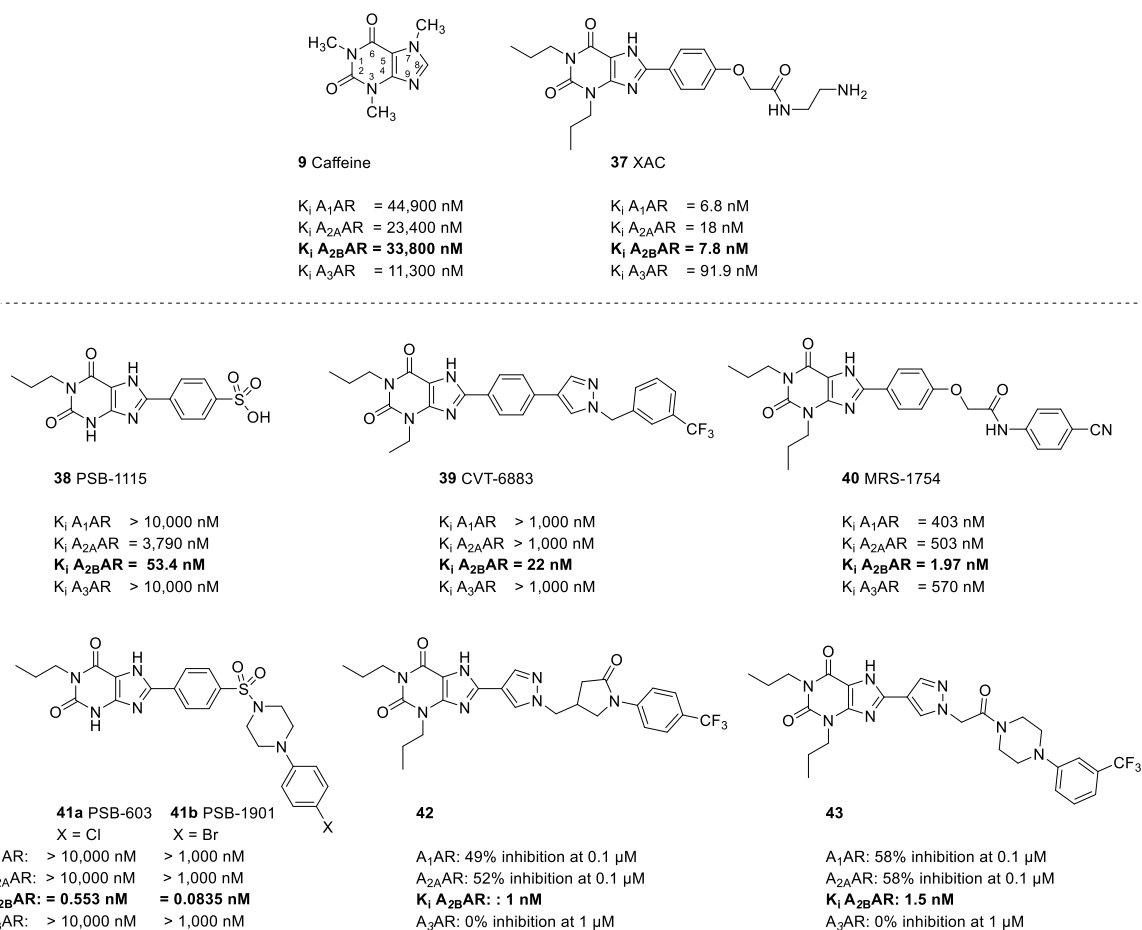


Figure 16. Chemical structures and affinities at the human AR subtypes of xanthine-based A_{2B}AR antagonists.^{116;150;197;199;202;204;208;209}

PSB-603 (**41a**) is an extremely potent and selective A_{2B}AR antagonist for human, rat and mouse (K_i human A_{2B}AR = 0.553 nM, K_i rat A_{2B}AR = 0.355 nM, K_i mouse A_{2B}AR = 0.265 nM >18,000-fold selectivity). Moreover, it is metabolically stable in all three species.^{49;190;209} Its tritiated derivative [³H]PSB-603 is frequently used as a radioligand in binding studies to identify new antagonists for the A_{2B}AR.²⁰⁹ Mølck et al. found that PSB-603 can change the cellular metabolism in colorectal cancer cells and it enhanced their responsiveness to chemotherapy.²¹⁰ Moreover, **41a** could diminish the proliferation of prostate cancer cells and it mediated a concentration-dependent decrease in baseline cAMP levels, suggesting that **41a** acts as an inverse agonist.¹⁶⁰ One of the most potent and selective A_{2B}AR antagonists is the lately published compound **41b**. With a K_i value of 0.0835 nM, and >10,000-fold selectivity versus all other AR subtypes it might be a promising tool for preclinical studies. Computational studies suggested, that the compound might form a rare halogen bond with the receptor.¹⁵⁰ Similar to **41a**, the compound suffers from poor water-solubility.⁴⁹ Two newly published antagonists, **42** and **43** exhibited high binding affinity (K_i = 1 and 1.5 nM, respectively) and selectivity for the A_{2B}AR. Those compounds were particularly interesting since they displayed good pharmacokinetic properties in mice with 27% and 65% oral bioavailability, respectively.²⁰⁸

1.3.3.2.2. Selective non-xanthine A_{2B} adenosine receptor antagonists

Beside the widely explored xanthine scaffold, many other A_{2B}AR antagonists, based on heterocyclic structures, have been reported. Recently, a “nitrogen-walk” approach has been applied to explore bioisosteric replacements for the furan and thiophene rings in a series of potent A_{2B}AR antagonists based on 4-substituted-2-methyl-1,4-dihydrobenzo-[4,5]imidazo[1,2-*a*]pyrimidine-3-carboxylic acid alkyl esters. Several new ligands that combine good affinity ($K_i < 30$ nM) and selectivity were identified, e.g. **44**. It exhibits a K_i value of 3.66 nM at the A_{2B}AR (cf. Figure 17).²¹¹ In 2018, Bayer carried out a high-throughput screening using their corporate substance library of around 2.8 million compounds and found that thienouracils are promising A_{2B}AR antagonists. A hit-to-lead optimization yielded BAY-545 (**45**, K_i A_{2B}AR = 66 nM) which was used for subsequent *in vivo* studies. It inhibited the release of pro-inflammatory interleukin 6 (IL-6) from human fibroblasts *in vitro* and showed efficacy in *in vivo* mouse models of lung fibrosis.²¹² The pyrazine derivative LAS101057 (**46**) was reported as a potent, selective and orally efficacious antagonist for the A_{2B}AR (K_i A_{2B}AR = 24 nM).²¹³ It showed good potency in both cell-based and mechanistic functional assays and exhibited good *in vivo* activity in the ovalbumin-sensitized mouse model of asthma.

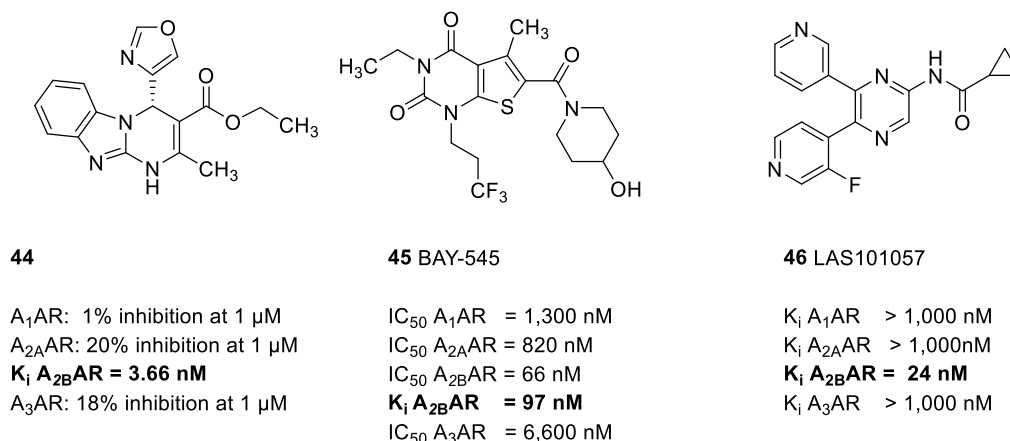


Figure 17. Chemical structures and affinities at human AR subtypes of non-xanthine A_{2B}AR antagonists.²¹¹⁻²¹³

Comparable to many xanthines, the majority of heterocyclic A_{2B}AR antagonists suffer from low water solubility. Although high affinity and selectivity can be achieved by many drug molecules, physicochemical properties often need to be improved.

1.4. Orphan GPCRs

A receptor is considered an “orphan receptor” when the native activating ligand is yet unknown. Nonetheless, they can be categorized into receptor families based on sequence homology with identified receptors whose signaling molecules are already known.²¹⁴ The identification of the respective natural ligand and the elucidation of the physiological roles of the receptor are a great challenge. These facts are important for the overall understanding of biological processes and also for drug research. This process is called “deorphanization”. After the establishment of an appropriate screening assay, compound libraries can be screened to find active ligands. The utilization of bioinformatics to predict candidate ligands and then test them is another possible technique.²¹⁵⁻²¹⁹ Interestingly, the P2Y₁₂ receptor was targeted by the antiplatelet drug clopidogrel before it was deorphanized. Only later it was found to be activated by ADP and directly became a candidate for further drug development.²²⁰⁻²²² Today, about 100 orphan GPCRs exist.^{217;219}

1.4.1. MRGPRX3

MRGPRX3 belongs to the family of MAS-related G protein-coupled receptors (MRGPRs) which is one of the largest families of GPCRs.^{29;223} Modulation of these receptors may lead to analgesic and antipruritogenic therapies, hence, this receptor family became an appealing pharmacological target.^{29;223} Reportedly, the MRGPR family represents the largest non-rodent GPCR family with 40 members, which belong to the rhodopsin-like class A, specifically to the δ branch, along with glycochormone, nucleotide, lipid-activated and olfactory receptors.²²³ The MRGPR family is subdivided into nine subfamilies (**A-H** and **X**) based on sequence homology (cf. Figure 18).²⁹

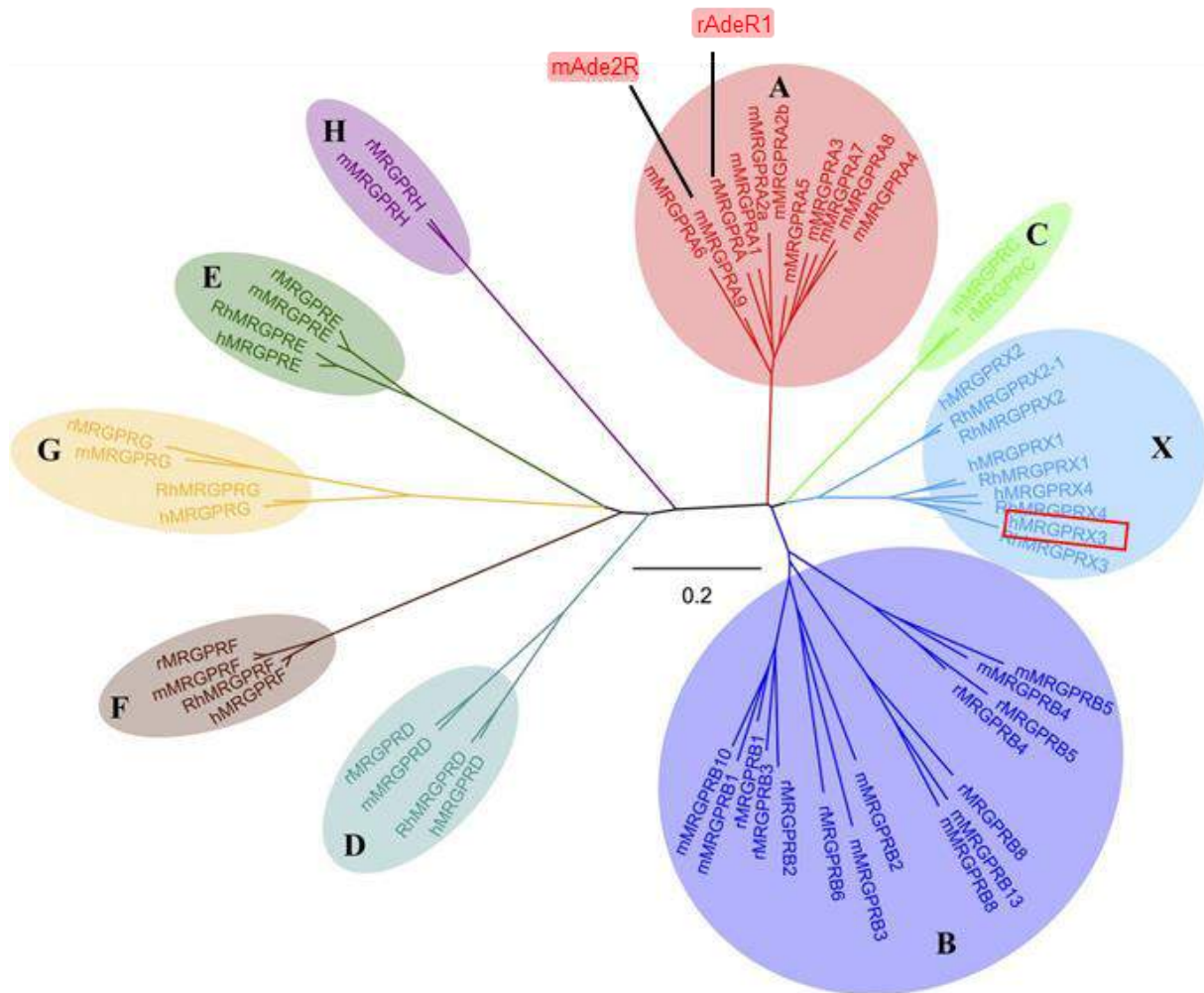


Figure 18. Phylogeny of Mas-related G protein-coupled receptors.²⁹

While subfamilies **A**, **B**, **C** and **H** are rodent-specific, **D**, **E**, **F** and **G** are conserved subfamilies in mammalian species. Only subfamily **X** is primate-specific and thus particularly interesting.^{29;224}

The MRGPRX subfamily consists of four distinct genes being located on the chromosome 11p15.1 in humans.²⁹ Four receptors, namely MRGPRX1, MRGPRX2, MRGPRX3, and MRGPRX4 belong to the MRGPRX subfamily, of which MRGPRX3 is the least studied receptor.²⁹ No ligand, endogenous or artificial, has been identified yet. MRGPRX3 was discovered in the early 2000s with the breakthrough discovery of MRGPR family. It consists of 322 amino acids, being illustrated in Figure 19.^{225;226}

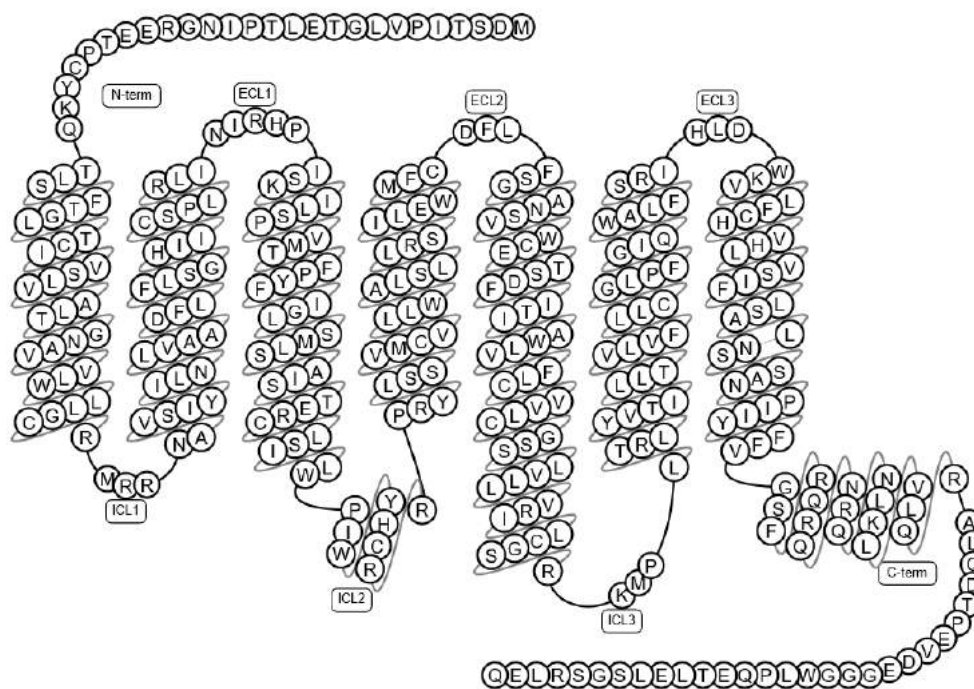


Figure 19. Snake plot of MRGPRX3.⁵⁷

In humans, MRGPRX3 is highly expressed in the dorsal root ganglia (DRG) both on the RNA and the protein level. Accordingly, it may play role in the regulation of pain and itch perceptions.^{225;226} Thus, addressing this receptor via drugs might be a potential therapy for neuropathic pain. Furthermore, high levels of RNA transcripts were detected in the cerebellum, salivary glands, lungs, breast and testis. The high expression of MRGPRX3 in the lungs was reported to be reduced after oxidative stress caused by the exposure to electronic cigarettes, which suggests, that the downregulation of MRGPRX3 as a potential pathophysiological effects in pulmonary diseases.²²⁷ The MRGPRX3 was reported to be highly expressed in human corneal endothelial cells.²²⁸ Previously, overexpression of MRGPRX3 in mice led to several symptoms affecting the skin and the eyes related to hyper proliferation of cells.²²⁹ However, the relevance of these observations to humans is still unknown.

1.5. General methods to study GPCR ligand binding

The measurement of receptor ligand binding is crucial in pharmacology. Therefore, radioligand binding assays are often used. They provide sensitive and quantitative information about GPCR expression and the affinity of ligands, making them important tools to study the structure-activity relationships of potential drug molecules.^{123;209;230-232} Radioactively labeled ligands can be used for kinetic studies, for saturation studies and for competition experiments to determine binding affinities of unlabeled compounds (K_i values) or equilibrium dissociation constants (K_D values).²³³ One of many examples for the application radioligand binding assays was published by Jiang et al. who found several xanthine-based $A_{2B}AR$ antagonists with picomolar affinity, showing the high sensitivity of these assays.¹⁵⁰ However, radioligand binding studies are by far not the only approaches to investigate receptor-ligand binding parameters:

Examples for a label-free ligand-receptor binding assays would be surface plasmon resonance (SPR) assays,²³⁴ plasmon-waveguide resonance studies,²³⁵ microscale thermophoresis (MST),²³⁶ backscattering interferometry (BSI)²³⁷ or the usage of bilayer interferometry biosensors (BIB).²³⁸ Beneath structure-based ligand binding assays that use nuclear magnetic resonance (NMR)²³⁹ or X-ray crystallography,²⁴⁰ methods are used that employ thermodynamics like the isothermal titration calorimetry (ITC).²⁴¹ Methods using fluorescent-labeled ligands have recently gained attention and became a valuable addition to the pool of techniques available in pharmacology.^{149;242}

1.5.1. Approaches to study GPCR ligand binding using fluorescent-labeled ligands

1.5.1.1. Fluorescence

A molecule can absorb energy in form of light characterized by a specific wavelength. The energy of the resulting excited state can either be released in form of heat (internal conversion) or emitted as light (fluorescence or phosphorescence, respectively). The emission of light can be detected and quantified by fluorescence spectroscopy. The wavelength of emitted fluorescent light is always longer than the corresponding excitation wavelength due to a loss of thermal energy (vibrational relaxation). This difference of energy or wavelength, resp., the so-called Stoke's shift, provides the background for modern highly sensitive methods like resonance energy transfer (RET) assays.²⁴³⁻²⁴⁵ These assays use the principle of RET: The non-radiant energy emitted by a donor is absorbed by an acceptor and newly emitted with a higher wavelength. Most biological macromolecules such as proteins and nucleic bases are non-fluorescent. Linking them to fluorescent dyes or attaching them to a fluorescent protein by biotechnological methods allows their visualization and detection by appropriate methods.²⁴²

A fluorescent molecule must possess particular properties:

- the presence of a large delocalized π -electrons system (often including aromatic structures)
- a certain rigidity of the structure²⁴⁶
- the presence of auxochromes/antiauxochromes²⁴⁷

Figure 20 shows examples of common fluorophores used for ligand or biomolecule labeling. All selected molecules provide a functional group that can be reacted either with a biomolecule or an appropriate functionalized ligand. Reactive free amino or thiol groups which are present e.g. in proteins are frequently used in order to form fluorescent conjugates.^{244;248;249}

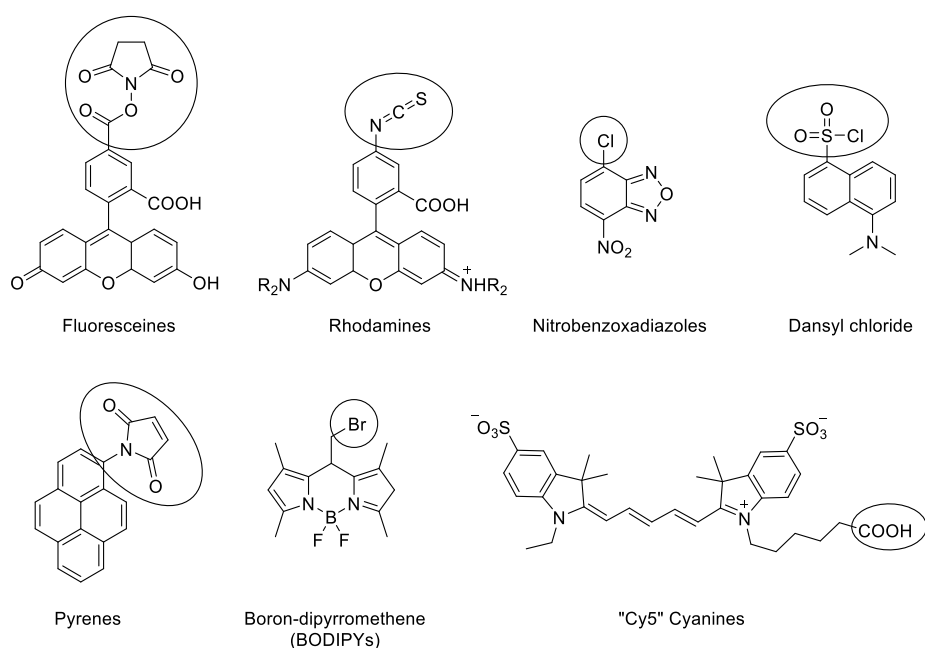


Figure 20. Common fluorescent dyes containing functional groups (circled in blue) for chemical attachment.²⁴⁴

Methods using fluorescent ligands can offer several advantages compared to e.g. radioligand binding studies. The synthesis of radioligands requires special know-how, radioactive reagents, and is in general rather expensive. In contrast, the preparation of fluorescent dyes is not accompanied by similar legal and environmental issues. An additional advantage of methods using fluorescent ligands is the possibility of a direct measurement due to the distance-dependence ($< 100 \text{ \AA}$) e.g. in a BRET (bioluminescence resonance energy transfer) system. Using fluorescent ligands enables to monitor ligand-receptor interactions at 37°C and in real time using live cells, cell lysates or purified proteins. Nevertheless, it has to be noted that the attachment of a big fluorophore moiety will alter the overall structure of a ligand and might thus affect the target affinity.^{242;250-252}

An optimal fluorescent probe should possess the following characteristics:^{253;254}

- high affinity and selectivity for the target
- a high quantum yield ($\Phi > 0.3$) when bound to the target
- an excitation- and emission-wavelength that neither interacts with the cell tissue's autofluorescence nor affects the properties of the investigated cell
- small size
- sufficient photostability and minor photobleaching effects
- a readily alterable structure to be versatile for the adaptation of spectral properties and target affinity
- a high stability against hydrolysis
- a high extinction coefficient (ϵ) in the region of detection
- a suitable excited-state lifetime

A large number of techniques which use fluorescent ligands of biomolecules can be used to gain pharmacological information. The following section highlights the most important methods using fluorescent ligands.

1.5.1.2. Fluorescence polarization

Fluorescence polarization is based on the possibility to distinguish whether a fluorescent molecule is bound to a target or not. A fluorescent ligand is excited by normal and also by polarized light. When polarized light is used, the fast rotation of the free fluorescent ligand leads to the emission of light with a higher degree of depolarization. Bound to a macromolecule, the fluorescent ligand is fixed and the rotation is hindered. It will stay aligned during the process of emission, and more of the light remains polarized.^{128;242;244}

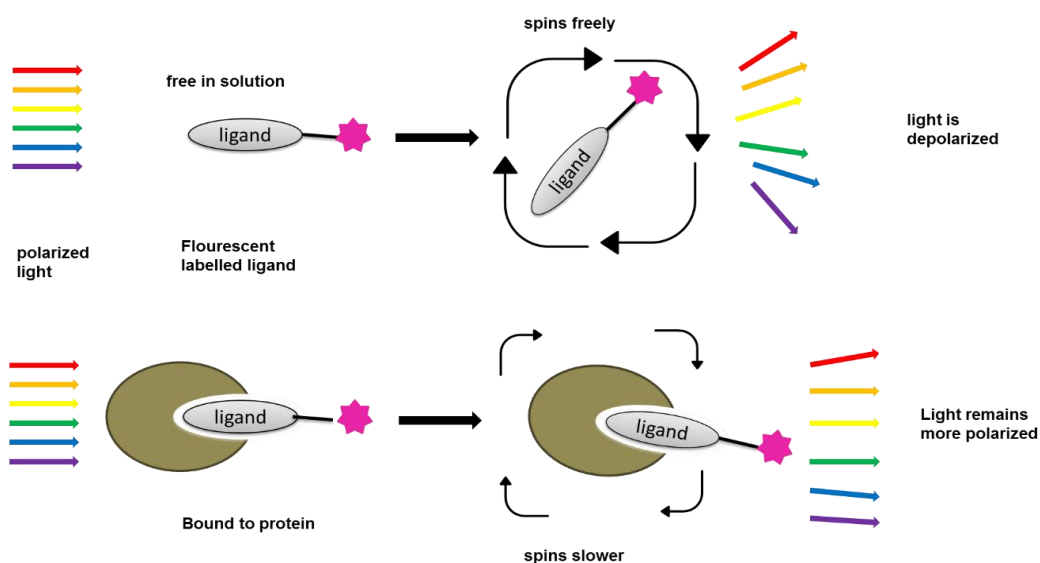


Figure 21. Principal of fluorescence polarization.^{128;242;244}

In 2010, Kecskes et al. used a fluorescence-labeled $A_{2A}AR$ antagonist (MRS5346, $K_i A_{2A}AR = 111$ nM) conjugated to the fluorescent dye Alexa Fluor-488 (cf. Figure 26, compound **47**) in order to develop an $A_{2A}AR$ binding assay on the basis of fluorescence polarization. This assay has now become a tool for kinetic analyses and testing of A_{2A} -affinity.¹²⁸

1.5.1.3. Confocal microscopy

Confocal microscopy allows the direct imaging of the fluorescent ligand's location. In contrast to conventional light microscopy, not the entire specimen is illuminated but only a small part of it. This illumination is scanned all over the specimen step by step. The light intensities of reflected or fluorescence-emitted light are measured successively at all locations of the area to be imaged. As a result, only light from a small volume around the focus point passes to the detector delivering high-contrast sectional images. This method allows reconstruction of three-dimensional structures from sets of images obtained at different depths of specimen.²⁵⁵

In 2003, Baker et al. published one of the first examples to quantify the binding of a fluorescent ligand to a receptor by confocal microscopy. The experiment was performed on live cells expressing the β_2 -adrenoceptor. As a fluorescent probe, the partial agonist CGP 12177 covalently bound to a borondipyrrromethene (BODIPY) dye, namely BODIPY-TMR-CGP, was used (Figure 26, compound **48**, $EC_{50} ADRB2 = 28.1$ nM). They obtained confocal images with increasing concentrations of the fluorescent ligand indicating a significant binding to the cell membrane. A saturation binding curve was generated using pixel intensity from the pictures yielding a K_D value similar to the value obtained by radioligand binding studies (cf. Figure 22).²⁵⁶

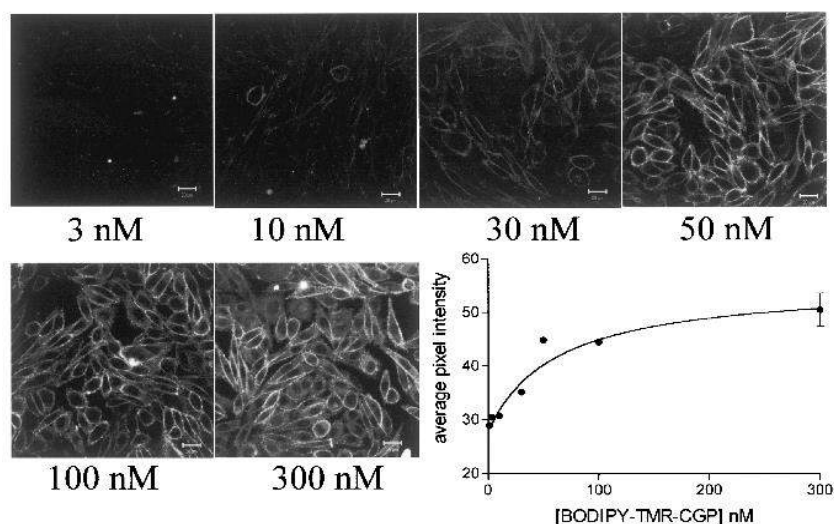


Figure 22. Saturation curve of fluorescence-labeled BODIPY-TMR-CGP: quantification of the fluorescence by average pixel intensity.²⁵⁶

1.5.1.4. Flow cytometry

Flow cytometry measures the mean fluorescence of a single cell focused in a sheath fluid that intersects an argon laser. A forward angle light scatter detector, a light scatter detector (1, Figure 23) and multiple fluorescence emission detectors (see 2 - 4 in Figure 23) collect the resulting signals. This versatile detection process allows both qualitative and quantitative evaluation.²⁵⁷ This technique can be used for ligand binding studies on single live cells. When an appropriate fluorescent ligand is available, ligand binding data can be collected in microsecond timescale and without removing unbound ligands from the media, making this probe very efficient.²⁴²

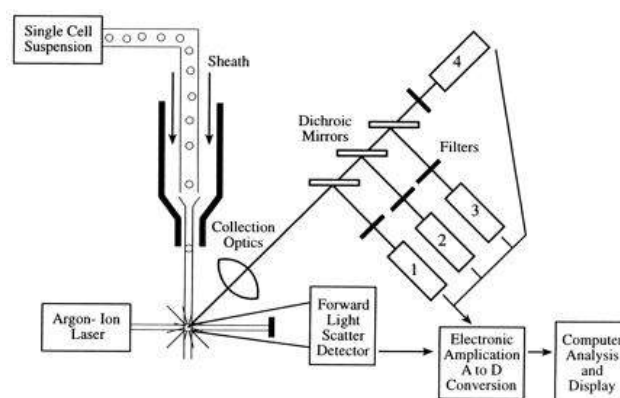


Figure 23. Principle of flow cytometry.²⁵⁷

In 2013, Kozma et al. used flow cytometry to compare various fluorescent agonists at the A_3 adenosine receptor and suggested, that the cyanine 5-tagged, adenosine-based agonist MRS5218 ($K_i A_3AR = 17.2$ nM, 94 % efficacy) is the most useful compound to characterize the A_3AR (Figure 26, **49**).^{258;259}

In 2018, Köse et al published the first potent and selective fluorescent-labeled $A_{2B}AR$ antagonist PSB-12105 ($K_i A_{2B}AR = 1.83$ nM) and successfully used it to establish a homogeneous receptor-ligand binding assay using flow cytometry (Figure 26, **50**).¹⁴⁹ The compound combined a selective xanthine ligand with a BODIPY dye.

1.5.1.5. FRET assays

For FRET (Förster resonance energy transfer) experiments a fluorescent-labeled biomolecule (e.g. a GPCR) and a fluorescent-labeled ligand are required. The fluorophore attached to the N-terminus of the receptor is initially excited by its particular wavelength (1, Figure 24). Subsequently, non-radiant energy (dipole-dipole interactions) is transferred from the donor fluorophore to an acceptor fluorophore (2). Excitation of the acceptor results in emission of fluorescence with a higher wavelength (3).²⁴³ The secondary fluorescence (emitted by the acceptor) is detected and can be quantified as a measure of the bound acceptor. FRET can

be used for binding assays if a sufficient overlap of the donor emission spectrum and the acceptor excitation spectrum is given (Figure 24, right). The fluorophores need to be located in close proximity ($< 100 \text{ \AA}$), and correct donor-acceptor orientation of dipole moments is required.²⁶⁰ This method can readily be adapted to investigate the interaction of labeled proteins²⁶¹ or to perform binding assays using a fluorescent ligand with suitable spectral properties and a fluorophore-tagged protein. Both interactions are close enough to be investigated with FRET.²⁴²

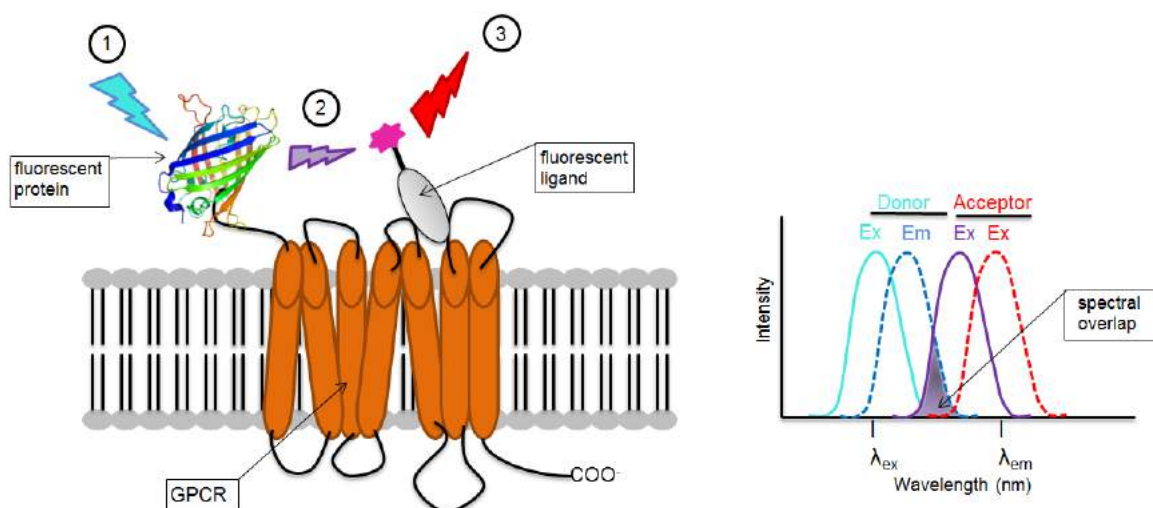


Figure 24. Functional principle of Förster resonance energy transfer (FRET).²⁴³

A FRET competition binding assay using a combination of a BODIPY-linked pirenzepine probe Bo-PZ as acceptor (Figure 26, compound **51**) and an eGFP-tagged muscarinic ACh M1 receptor as a donor (eGFP = enhanced green fluorescent protein) was described to determine binding affinities of unlabeled muscarinic receptor antagonists by Ilien et al. in 2003.²⁶² The ligand showed a K_i value of 22 nM.

1.5.1.6. BRET assays - NanoLuc

The same non-radiative energy emission required for a FRET experiment can also be provided by a luciferase enzyme oxidizing its photon-emitting substrate (1, Figure 25) instead of a synthetic fluorophore.²⁵¹ The so called “bioluminescence resonance energy transfer” (BRET) is not only artificial but was also found naturally in organisms like bacteria, insects, fungi, and an abundance of marine organisms.^{263;264} The emission wavelength (2) is depending on the luciferase and its substrate. Comparable to FRET probes, a fluorescence acceptor is excited and emits at a higher wavelength (3) which can be detected and evaluated (cf. Figure 25). The luciferase of the sea pansy (*Renilla reniformis*, “Rluc”) and its corresponding substrate coelenterazine, have extensively been used to investigate GPCR protein-protein interactions.

This assay has been optimized by point mutations of the luciferase (Rluc2 and Rluc8, respectively) and by using altered substrates.^{260;265-267}

More recently, the NanoLuc technology has gained much interest. It utilizes a small 19 kDa luciferase subunit from the deep-sea shrimp *Oplophorus gracilirostris* and the corresponding substrate furimazine, both designed and optimized by Hall et al. (cf. Figure 25).²⁶³

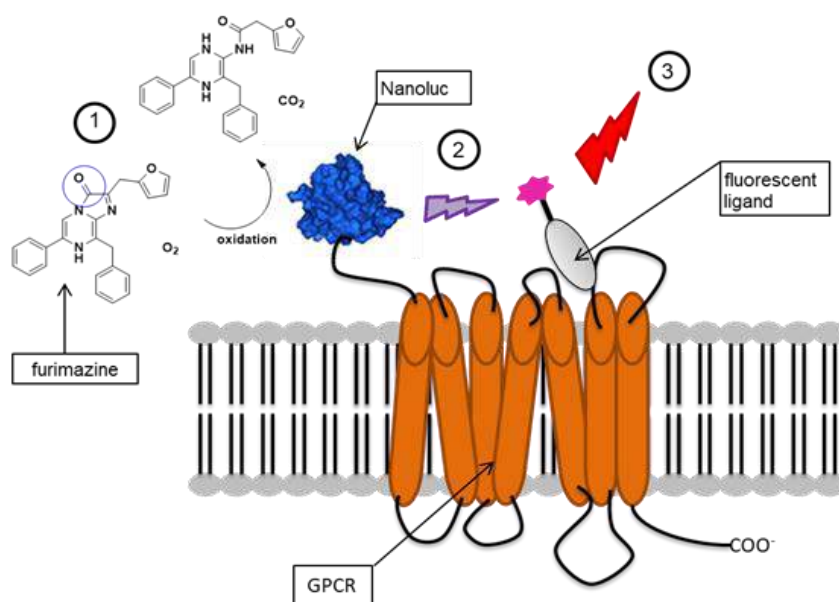


Figure 25. Principle of bioluminescence resonance energy transfer (BRET).^{251;260;265-267}

This donor-acceptor pair is outstanding due to its intense luminescence (approximately 150-fold more luminescent as the aforementioned Rluc), its physical stability and its high quantum yield.²⁶³ Although having an emission peak at 460 nm, the very high luminescence intensity enables NanoLuc to have sufficient emission at longer wavelengths and the transfer of resonance energy to red fluorophores. Red fluorophores are considered to be most desirable for biological assays since emission in this range of the spectrum can be well distinguished from possible cellular autofluorescence.^{242;251}

In 2015, Stoddard et al. successfully demonstrated live cell BRET ligand binding using a range of different fluorescent ligands in saturation, competition and kinetic binding assays at β 2-adrenoceptors, adenosine A₁ and A₃ receptors, and angiotensin AT₁ receptors.²⁵²

With the A_{2A}AR antagonist preladenant as a basis and a Cy5 cyanine (Alexa Flour 647) as a fluorophore, the compound AF647 (**54**) was prepared by Comeo et al. (see Figure 27). Which allowed a clear visualization of the specific receptor localization through confocal imaging.²⁶⁸ Furthermore, the measurement of ligand binding affinities of unlabeled human A_{2A}AR antagonists using a NanoBRET assay was performed. The values obtained through fluorescent binding assays were comparable to the reported literature values.

1.5.2. Förster distance

Alongside binding, saturation and competition assays, resonance energy transfer (RET) approaches can be used to determine the distance between fluorescence donor and acceptor, offering insights into binding modes of protein-protein interaction or ligand-protein binding, respectively.²⁶⁰ The calculation of this distance is based on the Förster rate equation (eq. 1) which describes the non-radiative energy transfer (k) of dipolar interactions.^{269;270}

$$k = \frac{1}{\tau_D} * \left(\frac{R_0}{r}\right)^6 \quad (1)$$

τ_D is the donor lifetime in the absence of acceptor, r is the donor-acceptor distance. The Förster distance (R_0), describing the intermolecular separation characterized by 50% of the maximum possible energy transfer, is a critical parameter for resonance energy transfer. It can link the measured changes of the RET ratio to a physical dimension scale and thus allows estimation of the range of distances determinable by any donor-acceptor pair.²⁶⁰ As a result, a RET based ligand binding assay can not only determine if and how strong, but also *where* in the protein a ligand is binding. It is particularly notable, that the transferred energy is inversely proportional to the sixth power of the distance between the RET pair, making a close proximity of donor and acceptor crucial for binding detection.²⁵¹ This distance-dependence is beneficial since ligand binding can directly be measured without the need of washing-steps to discriminate unbound ligands.²⁴² With the help of FRET probes, the active center of several receptors could be determined, giving important insight about the structure and the function of the corresponding receptors.^{271;272}

1.6. Fluorescent ligands

Recently, numerous approaches based on fluorescent ligands have been used to determine receptor binding using various methods. As these probes proved to be fruitful, many new fluorescent ligands were designed, evaluated and established to provide more suitable ligands.²⁷³

Figure 26 illustrates five selected ligands that were used in the aforementioned studies.^{128;149;256;258;262}

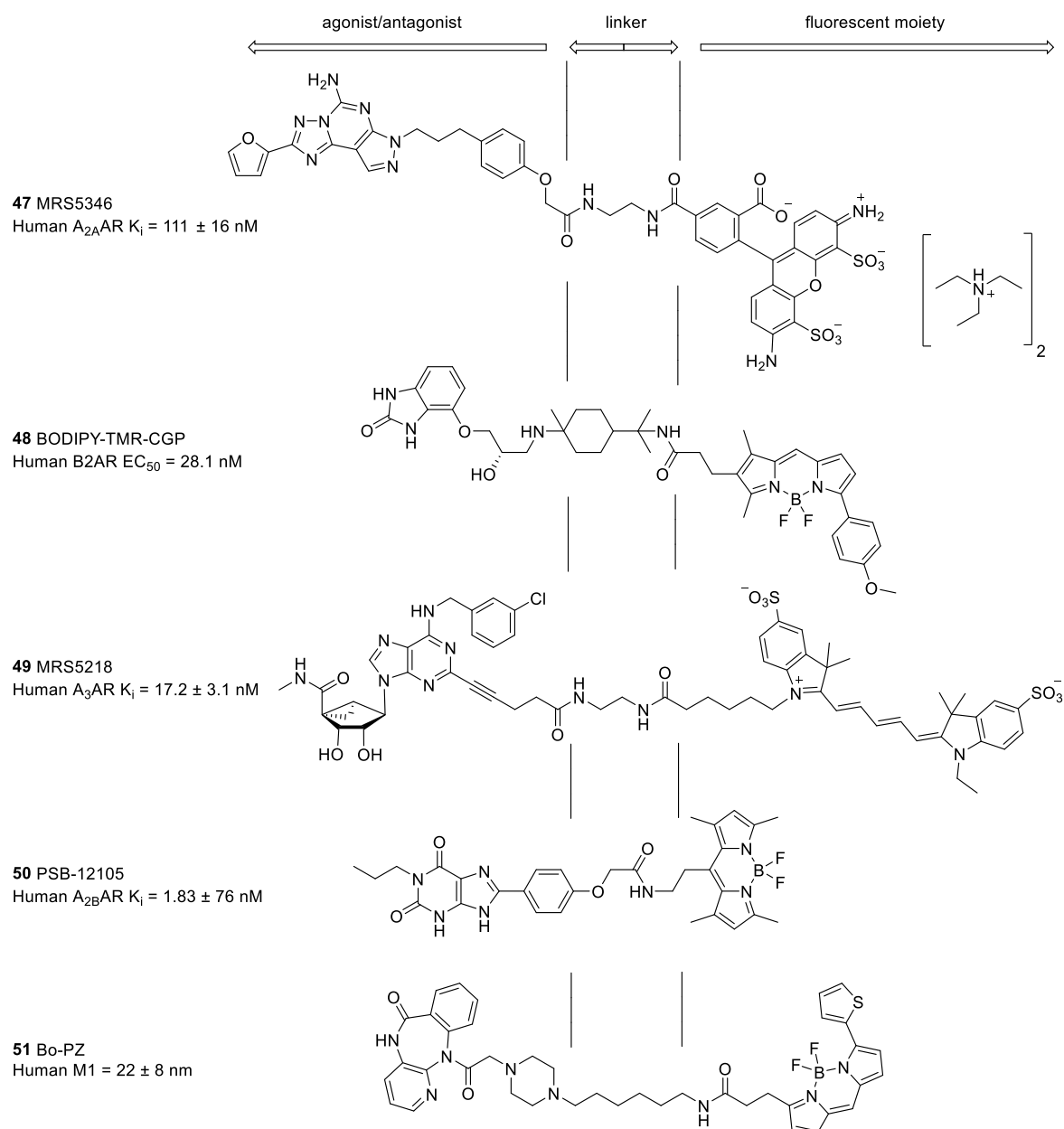


Figure 26. Typical structures of fluorescent receptor ligands.^{128;149;256;258;259;262}

It can be seen, that all abovementioned ligands consist of three regions: An agonist/antagonist moiety and a fluorescent dye conjugated by a linker.²⁷³ For the design of a new fluorescent ligand, the following considerations need to be made: A highly potent and selective agonist or antagonist moiety is required. Properties including structure, size, lipophilicity and solubility of the parent compound will likely be changed by attaching a large residue, and may influence affinity and selectivity to the target unfavorably.²⁴² In order to maintain potency and selectivity, the position of the linker must be chosen carefully. Preliminary SAR studies elucidate the best position for a modification of a parent ligand.²⁷⁴ An appropriate fluorescent dye has to be chosen according to the required spectral properties for the particular assay. In the special case of RET probes the rate of overlap between the donor emission and the acceptor excitation spectrum is crucial. In addition, the quantum yield of the fluorescent donor as well as the extinction coefficient need to be sufficiently high.²⁵¹ Furthermore, the lipophilicity of the fluorescent moiety has to be considered with regard to membrane crossing and binding.²⁷⁴

In general, the fluorescent dye is not closely conjugated to the ligand moiety but separated by a linker. It is intended to have an appropriate distance between the ligand binding domain in order to avoid a decrease in affinity.²⁵⁰ The linker between the fluorescent moiety and the protein can be used not only to fine-tune the distance but to modify physicochemical properties like solubility or lipophilicity as well. Polyethyleneglycols (PEGs), for example, can improve water solubility compared to a lipophilic alkyl chain.^{275;276}

Many fluorescent probes and fluorescence-labeled ligands for the ARs have been reported and reviewed.²⁷⁷⁻²⁷⁹ Figure 27 illustrates selected examples:

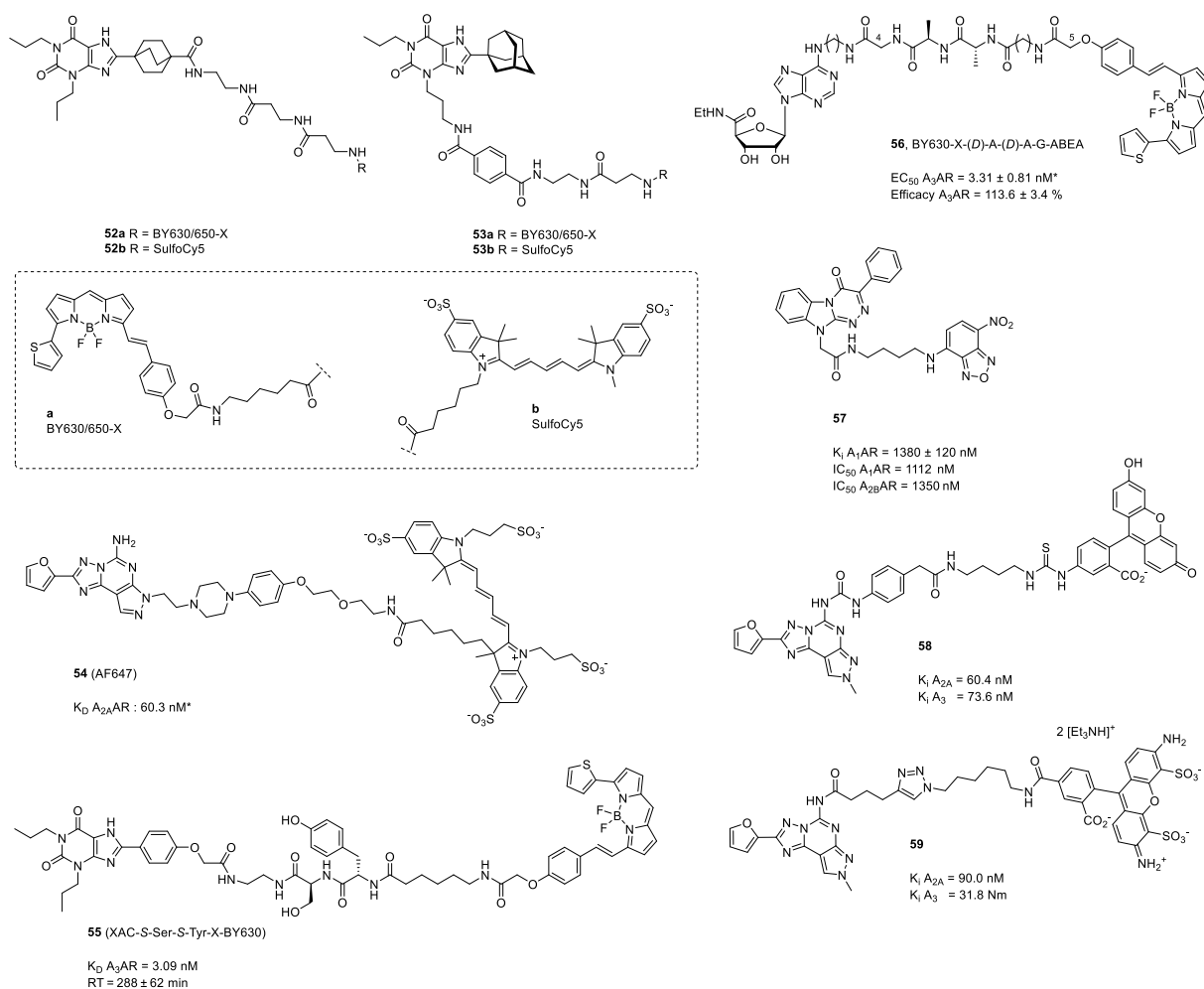


Figure 27. Selected fluorescent-labeled AR ligands.^{268;280-284} *calculated from pK_D value

Recently, Cameo et al. reported several xanthine-based fluorescent ligands for the study of the A_1AR in live cells, Figure 27 illustrates the best compounds (**52a** / **52b** and **53a** / **53b**).²⁸⁰ The group demonstrated that both, the 3- and the 8-position of the prototypic xanthine scaffold can be functionalized with linkers and fluorescent dyes. The ligands allowed NanoBRET studies for the quantification of kinetic and equilibrium ligand binding parameters as well as the visualization of specific A_1AR distribution patterns in living cells using different microscopy techniques. Especially the derivatives **52b** and **53a** showed good selectivity towards the other AR subtypes. The $A_{2A}AR$ antagonist preladenant was the basis for the fluorescent labeled antagonist AF647 (**54**).²⁶⁸ The ligand was used for the measurement of ligand binding affinities of unlabeled $A_{2A}AR$ antagonists via NanoBRET assays and for the visualization of receptor localization through confocal imaging. Recently, a live cell NanoBRET ligand binding assay using fluorescent-labeled A_3AR antagonists to measure kinetic parameters of labeled and unlabeled compounds at the A_3AR at physiological temperatures was developed.²⁸¹ In a series of fluorescence-labeled xanthine derivatives, the antagonist XAC-S-Ser-S-Tyr-X-BY630 (**55**) had the longest residence time at the A_3AR (RT = 288 min). The group of Stoddard reported the fluorescent A_3AR agonist BY630-X-(D)-A-(D)-A-G-ABEA (**56**).²⁸³ It showed high potency

(K_i A_3AR = 3.31 nM) and full efficacy and could be employed for receptor internalization studies of untagged receptors. In 2018, the 7-nitrobenzofurazan-coupled triazinobenzimidazole derivative **57** was reported by Barresi et al. as a useful tool to investigate the expression pattern of both A_1AR s and $A_{2B}AR$ s.²⁸⁴ The compound acted as an antagonist at the A_1AR and the $A_{2B}AR$, binding with similar micromolar affinities to both receptors. Fluorescence confocal microscopy studies of **57** showed specific labeling of ARs on cell membranes on bone marrow-derived mesenchymal stem cells. Based on a pyrazolo[4,3-*e*]-1,2,4-triazolo[1,5-*c*]pyrimidine scaffold, Federico et al. described several conjugatable A_3AR antagonists and highlighted two subtype-selective fluorescence-labeled ligands for the A_3AR .²⁸² The fluorescein-bearing derivative **58** and the Alexa-fluor-488-bearing derivative **59** showed high potency at the A_3AR (K_i = 73.6 nM and K_i = 31.8 nM, respectively) but were not selective towards the $A_{2A}AR$, making them dual-acting probes.

1.6.1. Cyanine dyes

Many different fluorescent dyes with various spectral properties and applications have recently been described. Beneath the extensively used class of BODIPYs, cyanine dyes proved to be versatile and useful in a wide range of chemical and biological applications.²⁴⁸ Cyanines are synthetic, positively charged polymethine dyes containing nitrogen atoms. Polymethines are composed of all-trans configured polyenes being framed by at least two heteroatoms (cf. Figure 28):²⁸⁵

- Anions: vinylogous carbonic acid ($X = X' = O$) → oxonoles,
- Cations: vinylogous amidine ($X = X' = N$) → cyanines
- Neutral molecules: vinylogous amide ($X = O, X' = N$) → merocyanines.

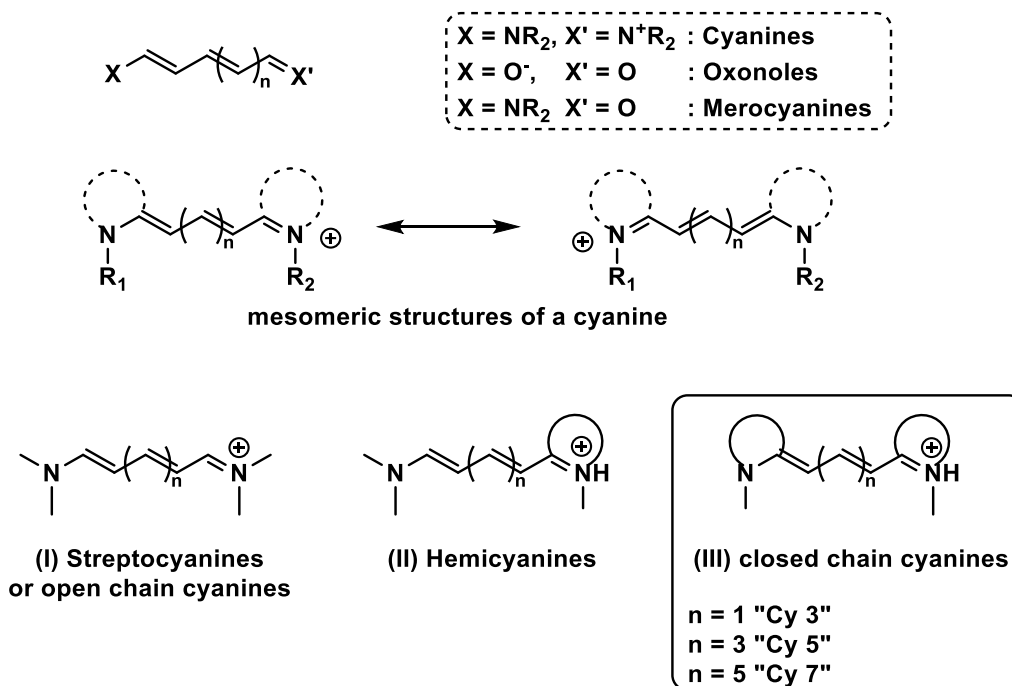


Figure 28. Different classes of polymethine dyes and cyanines.²⁸⁶

Cyanines are divided into three subclasses which include open chained streptocyanines (I), hemicyanines (II) and “closed chain” cyanines (III) where both N-atoms are members of heterocyclic rings.²⁸⁶

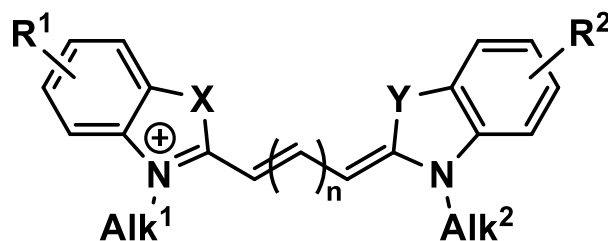


Figure 29. Prototype of “closed chain” cyanine dyes.

The number of double bonds (n) in a cyanine dye has crucial impact on the spectroscopic properties. An additional double bond in the polyene chain results in a shift of λ_{abs} to longer wavelength of about 100 nm.^{248;287;288} Apart from the polyene chain, the absorption and the emission wavelength as well as the absorption coefficient of the “closed chain” cyanines can be fine-tuned by chemical variation at different positions:

- a) Variation of substituents R^1 and R^2
- b) Introduction of different heteroatoms (X, Y can be e.g. O, S or CR_2)
- c) A change of the N -alkyl residues Alk^1 and Alk^2 (both substituents can independently be introduced and combined)

Water-soluble fluorescent dyes can be obtained by the introduction of sulfonic acid groups (at R¹ and/or R² or at the end of the alkyl chain) without a significant impact on the spectroscopic properties. Carefully designed, the abovementioned “closed chain” cyanine dyes offer a large number of possible modifications in order to provide a broad range of spectral properties.^{287;288} Cyanine dyes are appreciated because they offer good water solubility, high stability, sharp fluorescence band, high sensitivity, and versatility.^{248;289} The alkyl moieties of these dyes can exhibit reactive groups on either one or both heterocyclic rings so that they can be chemically conjugated to other functional molecules.²⁹⁰

1.6.2. NIR fluorophores

Fluorescence imaging is one of the most powerful techniques to monitor biological targets and processes.²⁹¹⁻²⁹³ Many different fluorescent dyes are available to visualize and evaluate biological and pharmacological probes. RET probes for BRET and FRET assays using fluorescent dyes with absorption and emission in the visible spectral range of the donor fluorophore (normally a fluorescent protein or a luciferase) overlap well with an acceptor fluorophore being excited in the UV/VIS light range.^{266;294;295} When it comes to *in vivo* probes, however, UV/Vis-fluorescent compounds are difficult to be used for sensing and imaging targets as the absorption and auto-fluorescence of biomolecules (e.g. hemoglobin and water) are high in this region (cf. Figure 30).^{291;293;296}

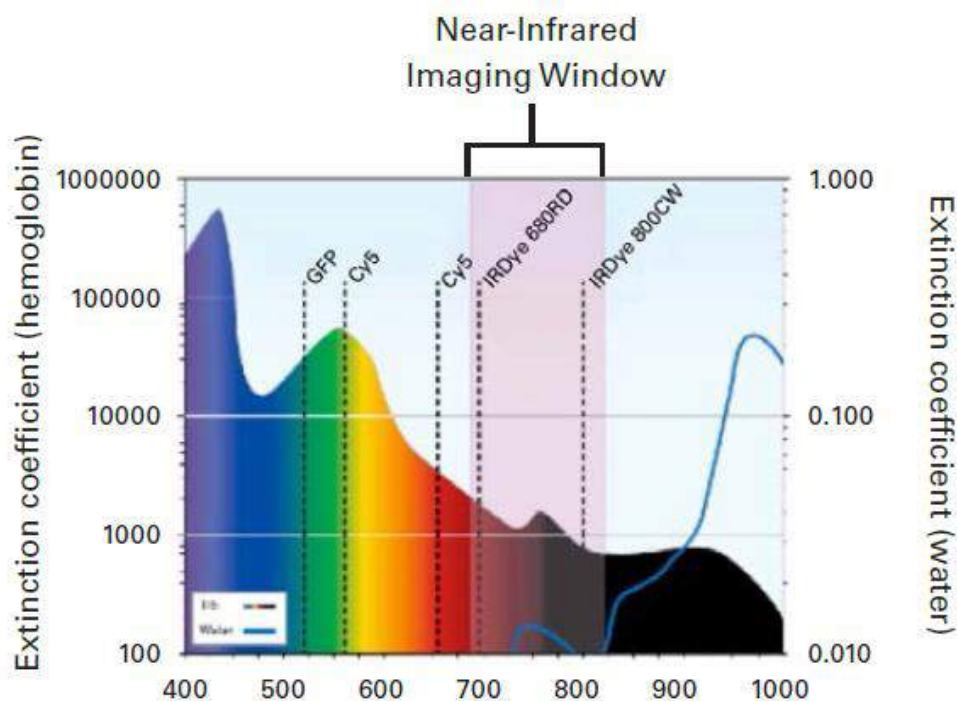


Figure 30. Extinction coefficients of hemoglobin (color) and water (blue).²⁹³

By contrast, fluorescent probes with absorption and emission in the near infrared (NIR) region (650-900 nm) are favorable for *in vivo* bioimaging because of minimum photo-damage to biological samples, deep tissue penetration of the fluorophore and minimum interference from background auto-fluorescence by biomolecules in the living systems. The low light scattering, deep penetration of the NIR light and the possibility to use low-cost excitation light sources make the NIR spectral range even more advantageous.^{291;292;296}

A special class of cyanine dyes, namely the heptamethine-cyanines, relate to this class. These cyanines exhibit seven methine units ($n = 3$, see Figure 29) and absorb and emit light in a range of 600 nm and 900 nm, depending on the modification of the cyanine scaffold.^{248;297} The basic scaffold (also called “Cy7”) combines two modified indole moieties with seven unsubstituted methine units, the maxima of absorption and emission circle around 750 nm (cf. Figure 31, left compound).

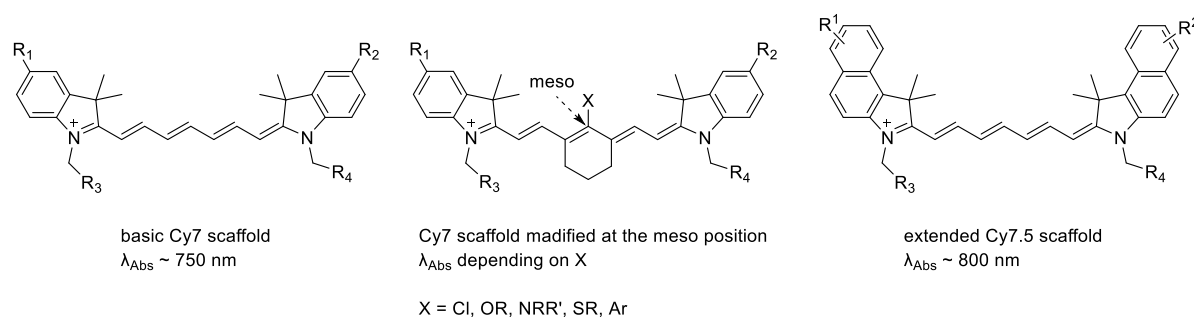


Figure 31. Different types of heptamethine-cyanines.

Moreover, heptamethine-cyanines often bear a cyclohexene ring structure to stabilize the double bonds and to improve the quantum yields. The *meso*-position can be modified as well by introducing heteroatoms or aryl residues at this position (cf. Figure 31, central compound). This can strongly alter the spectral properties of the fluorophore in dependence of the nature of the *meso*-substituent. Finally, cyanine dyes can exhibit an extended chromophore and fluorophore by introducing two additional phenyl rings at the indole moiety. These 4,5-benzo-3*H*-indole moieties shift the spectral properties into the NIR range by around 50 nm to around 800 nm.

2. Aims of the study

2.1. Exploration of *N*-acyl-8-(4-piperazine-1-sulfonyl)phenylxanthines as potent and selective adenosine A_{2B} receptor antagonists

Many selective and potent A_{2B}AR antagonists based on the xanthine scaffold were reported by our group. 1-Propyl-8-(4-phenylpiperazine-1-sulfonyl)phenylxanthines such as **PSB-603** and 1-propyl-8-(4-benzylpiperazine-1-sulfonyl)phenylxanthines such as **PSB-0788** proved to be particularly potent scaffolds (cf. Figure 32).^{150;209}

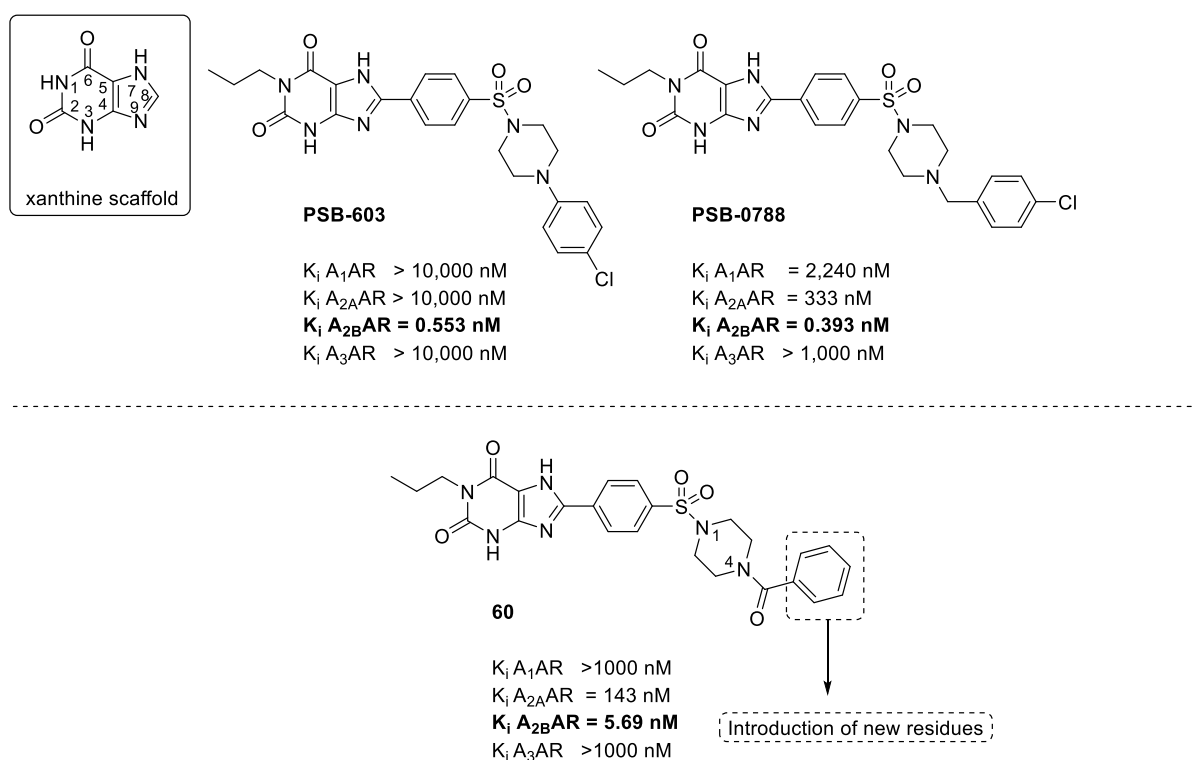


Figure 32. Xanthine derivatives as modulators of the A_{2B}AR.^{150;209}

So far, only on xanthine derivative bearing a benzoyl residue at the piperazine-position 4 (**60**) is described in literature.^{150;209} On the basis of this potent and selective A_{2B}AR antagonist, the scaffold of 8-(4-acylpiperazine-1-sulfonyl)phenyl-1-propylxanthines was to be explored by introducing a variety of carboxylic acids to the 4-position of the scaffold's piperazine moiety.

2.2. Functionalized potent and selective 8-(4-acylpiperazinyl-1-sulfonyl)phenylxanthines providing a platform for fluorescence-labeling of adenosine A_{2B} receptor antagonists

Recently, our group reported the first potent and selective fluorescent A_{2B}AR ligands, **PSB-12105** being the best of them (cf. figure 33).¹⁴⁹ The aim of this study was the design and synthesis of potent and selective fluorescent-labeled A_{2B}AR antagonists as the second generation of fluorescent probes. Therefore, our approach was to prepare 8-substituted xanthine derivatives based on parent compound **60**, bearing different reactive groups at the benzoyl moiety as a platform for functionalization with fluorescent dyes.

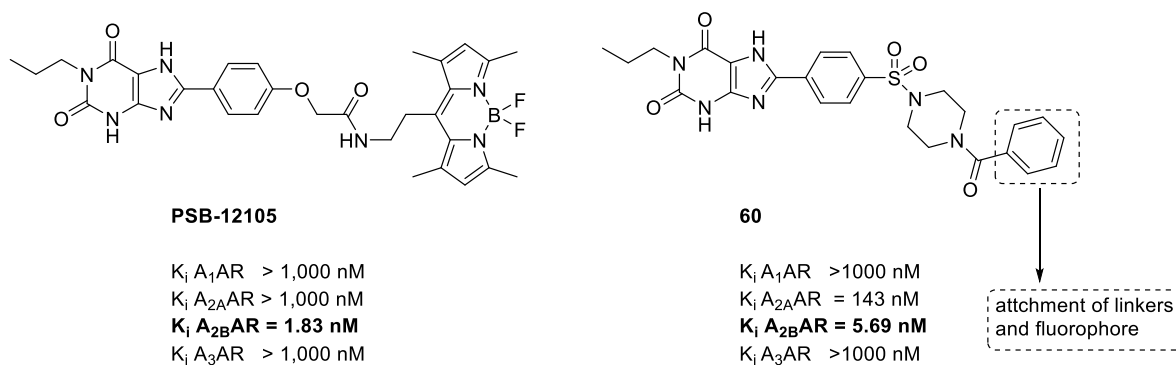


Figure 33. First generation fluorescent probe **PSB-12105** and parent compound **60**.^{149;150;209}

2.3. Synthesis of 3-amino-*N*-benzyl-1-phenyl-1*H*-pyrazole-4-carboxamides as A_{2A}AR antagonists

Several 5-aminotriazoles have been described as antagonists for the A_{2A}AR.^{53;54} Until this point, a 3-aminopyrazole scaffold, as illustrated in Figure 34, has never been described as A_{2A}AR antagonist, thus a new class of antagonists is introduced in the present study.

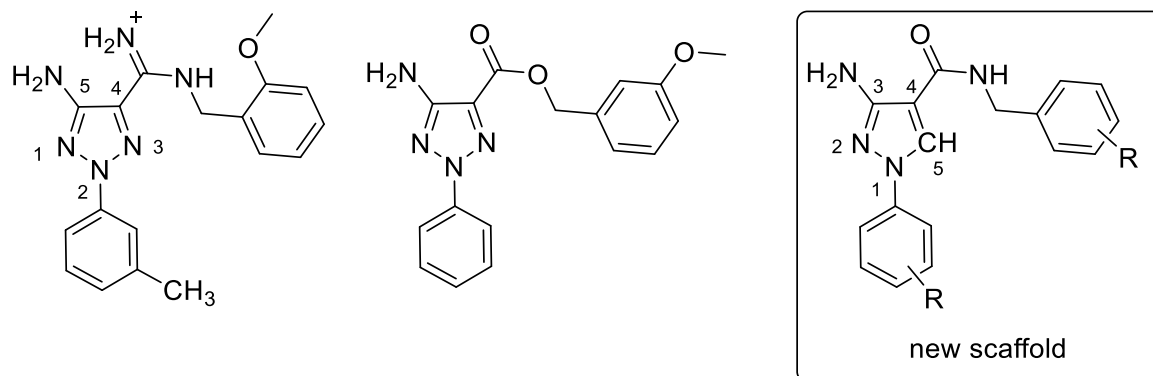


Figure 34. Different scaffolds of A_{2A}AR antagonists.^{53;54}

By switching the scaffold from an amidine or ester structure at position 4 to a bioisosteric carboxamide, metabolic stability and chemical accessibility should be improved. The phenyl ring at position 1 of the pyrazole and the benzylamine moiety are the main structures of the scaffold that are planned to be varied.

2.4. Synthesis of 2,4,6,8-tetrasubstituted pyrimido[5,4-*d*]pyrimidines as MRGPRX3 agonists

The overall goal of this study was the deorphanization of the MRGPRX3 receptor that belongs to the family of MAS-related G protein-coupled receptors. Employing a β -arrestin recruitment assay, the receptor was screened for agonists using an approved drug library. Our research team found one hit: Dipyridamole showed weak potency with an EC_{50} value of 71.5 μ M (cf. Figure 35). With Dipyridamole as a screening hit for MRGPRX3, 2,4,6,8-tetrasubstituted pyrimido[5,4-*d*]pyrimidines will therefore be investigated to establish the first structure-activity relationship for MRGPRX3 agonists and to improve its potency. Moreover, a screening campaign to identify antagonists was planned. Inhibition of MRGPRX3 might lead to novel treatments for pain.

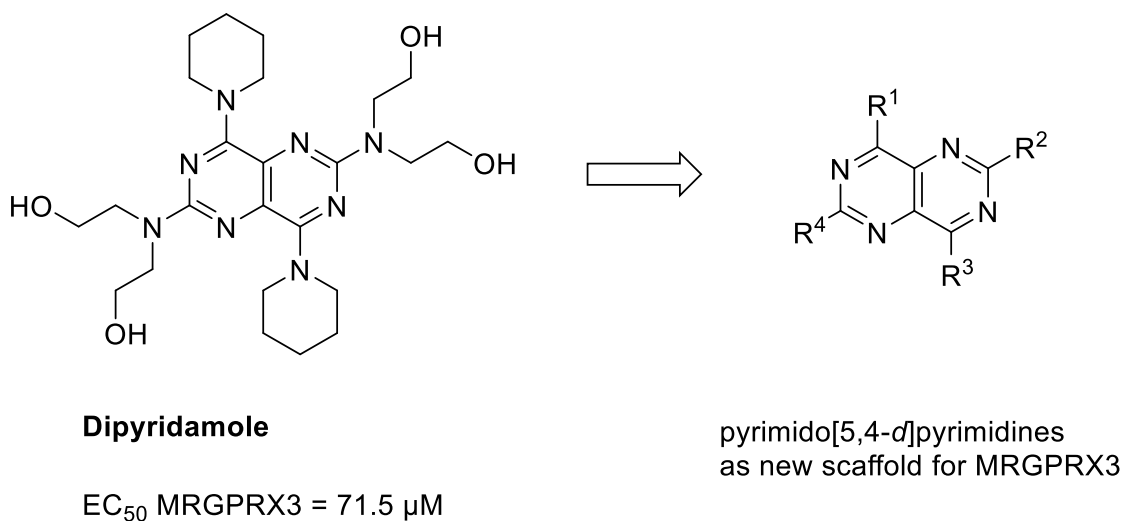


Figure 35. Structure of screening hit dipyridamole and its potency at MRGPRX3; new scaffold.

3. References

- (1) *Römpp Chemie Lexikon*; Thieme Verlag: Stuttgart, 1995.
- (2) George, S. R.; O'Dowd, B. F.; Lee, S. P. G protein-coupled receptor oligomerization and its potential for drug discovery. *Nat. Rev. Drug Discov.* **2002**, *1*, 808-820.
- (3) Mutschler, E. *Mutschler Arzneimittelwirkungen*; 9th Edition; Wiss. Verl.-Ges: Stuttgart, 2013.
- (4) Jacoby, E.; Bouhelal, R.; Gerspacher, M.; Seuwen, K. The 7 TM G-protein-coupled receptor target family. *ChemMedChem.* **2006**, *1*, 761-782.
- (5) Müller, C. E.; Jacobson, K. A. Recent developments in adenosine receptor ligands and their potential as novel drugs. *Biochim. Biophys. Acta.* **2011**, *1808*, 1290-1308.
- (6) Müller, C. E.; Schiedel, A. C.; Baqi, Y. Allosteric modulators of rhodopsin-like G protein-coupled receptors: opportunities in drug development. *Pharmacol. Ther.* **2012**, *135*, 292-315.
- (7) Overington, J. P.; Al-Lazikani, B.; Hopkins, A. L. How many drug targets are there? *Nat. Rev. Drug Discov.* **2006**, *5*, 993-996.
- (8) Katritch, V.; Cherezov, V.; Stevens, R. C. Structure-function of the G protein-coupled receptor superfamily. *Annu. Rev. Pharmacol.* **2013**, *53*, 531-556.
- (9) Ballesteros, J. A.; Weinstein, H. Integrated methods for the construction of three-dimensional models and computational probing of structure-function relations in G protein-coupled receptors. *Methods Neurosci.*, 1995, 366-428.
- (10) Baldwin, J. M. The probable arrangement of the helices in G protein-coupled receptors. *EMBO J.* **1993**, *12*, 1693-1703.
- (11) Kobilka, B. K. G protein coupled receptor structure and activation. *Biochim. Biophys. Acta.* **2007**, *1768*, 794-807.
- (12) Pin, J.-P.; Galvez, T.; Prézeau, L. Evolution, structure, and activation mechanism of family 3/C G-protein-coupled receptors. *Pharmacol. Ther.* **2003**, *98*, 325-354.
- (13) Baker, J. G.; Hill, S. J. Multiple GPCR conformations and signalling pathways: implications for antagonist affinity estimates. *Trends Pharmacol. Sci.* **2007**, *28*, 374-381.
- (14) Attwood, T. K.; Findlay, J. B. Fingerprinting G-protein-coupled receptors. *Protein Eng.* **1994**, *7*, 195-203.
- (15) Kolakowski, L. F. GCRDb: A G protein-coupled receptor database. *Recept. Channels.* **1994**, *2*, 1-7.

- (16) Schiöth, H. B.; Fredriksson, R. The GRAFS classification system of G-protein coupled receptors in comparative perspective. *Gen. Comp. Endocrinol.* **2005**, *142*, 94-101.
- (17) Davies, M. N.; Secker, A.; Freitas, A. A.; Mendao, M.; Timmis, J.; Flower, D. R. On the hierarchical classification of G protein-coupled receptors. *Bioinformatics.* **2007**, *23*, 3113-3118.
- (18) Fredriksson, R.; Lagerström, M. C.; Lundin, L.-G.; Schiöth, H. B. The G protein-coupled receptors in the human genome form five main families. Phylogenetic analysis, paralogon groups, and fingerprints. *Mol. Pharm.* **2003**, *63*, 1256-1272.
- (19) Burnstock, G. Purinergic receptors. **1962**, *62*, 491-503.
- (20) Burnstock, G. A basis for distinguishing two types of purinergic receptor, in cell membrane receptors for drug and hormones; a multidisciplinary approach. (Strub, R. W.; Bolis, L.; eds.) Raven Press: New York 1978, 107-118.
- (21) Yan, L.; Burbiel, J. C.; Maass, A.; Müller, C. E. Adenosine receptor agonists: from basic medicinal chemistry to clinical development. *Expert Opin. Emerg. Drugs.* **2003**, *8*, 537-576.
- (22) Müller, C. E.; Stein, B. Adenosine receptor antagonists: Structures and potential therapeutic applications. *Curr. Pharm. Des.* **1996**, 501-530.
- (23) Zhou, Q. Y.; Li, C.; Olah, M. E.; Johnson, R. A.; Stiles, G. L.; Civelli, O. Molecular cloning and characterization of an adenosine receptor: the A₃ adenosine receptor. *Proc. Natl. Acad. Sci. U. S. A.* **1992**, *89*, 7432-7436.
- (24) Burnstock, G.; Kennedy, C. Is there a basis for distinguishing two types of P₂-purinoceptor? *Gen. Pharmacol.* **1985**, *16*, 433-440.
- (25) Abbracchio, M. P.; Burnstock, G.; Boeynaems, J.-M.; Barnard, E. A.; Boyer, J. L.; et al. International Union of Pharmacology LVIII: update on the P₂Y G protein-coupled nucleotide receptors: from molecular mechanisms and pathophysiology to therapy. *Pharmacol. Rev.* **2006**, *58*, 281-341.
- (26) Burnstock, G. Physiology and pathophysiology of purinergic neurotransmission. *Pharmacol. Rev.* **2007**, *87*, 659-797.
- (27) Bender, E.; Buist, A.; Jurzak, M.; Langlois, X.; Baggerman, G.; Verhasselt, P.; Ercken, M.; Guo, H.-Q.; Wintmolders, C.; van den Wyngaert, I.; van Oers, I.; Schoofs, L.; Luyten, W. Characterization of an orphan G protein-coupled receptor localized in the dorsal root ganglia reveals adenine as a signaling molecule. *Proc. Natl. Acad. Sci. U. S. A.* **2002**, *99*, 8573-8578.
- (28) Brunschweiler, A.; Müller, C. E. P₂ receptors activated by uracil nucleotides - an update. *Curr. Med. Chem.* **2006**, *13*, 289-312.

- (29) Solinski, H. J.; Gudermann, T.; Breit, A. Pharmacology and signaling of MAS-related G protein-coupled receptors. *Pharmacol. Rev.* **2014**, *66*, 570-597.
- (30) Fredholm, B. B.; IJzerman, A. P.; Jacobson, K. A.; Klotz, K. N.; Linden, J. International union of pharmacology. XXV. Nomenclature and classification of adenosine receptors. *Pharmacol. Rev.* **2001**, *53*, 527-552.
- (31) Chen, J.-F.; Eltzschig, H. K.; Fredholm, B. B. Adenosine receptors as drug targets - what are the challenges? *Nat. Rev. Drug Discov.* **2013**, *12*, 265-286.
- (32) Fredholm, B. B.; IJzerman, A. P.; Jacobson, K. A.; Linden, J.; Müller, C. E. International union of basic and clinical pharmacology. LXXXI. Nomenclature and classification of adenosine receptors - an update. *Pharmacol. Rev.* **2011**, *63*, 1-34.
- (33) Müller, C. E.; Scior, T. Adenosine receptors and their modulators. *Pharm. Acta Helv.* **1993**, *68*, 77-111.
- (34) Fredholm, B. B.; Arslan, G.; Halldner, L.; Kull, B.; Schulte, G.; Wasserman, W. Structure and function of adenosine receptors and their genes. *Naunyn. Schmiedebergs. Arch. Pharmacol.* **2000**, *362*, 364-374.
- (35) Ballarín, M.; Fredholm, B. B.; Ambrosio, S.; Mahy, N. Extracellular levels of adenosine and its metabolites in the striatum of awake rats: inhibition of uptake and metabolism. *Acta Physiol. Scand.* **1991**, *142*, 97-103.
- (36) Beukers, M. W.; Dulk, H. den; van Tilburg, E. W.; Brouwer, J.; IJzerman, A. P. Why are A_{2B} receptors low-affinity adenosine receptors? Mutation of Asn273 to Tyr increases affinity of human A_{2B} receptor for 2-(1-hexynyl)adenosine. *Mol. Pharm.* **2000**, *58*, 1349-1356.
- (37) Dal Ben, D.; Lambertucci, C.; Vittori, S.; Volpini, R.; Cristalli, G. GPCRs as therapeutic targets: a view on adenosine receptors structure and functions, and molecular modeling support. *J. Iran. Chem. Soc.* **2005**, *2*, 176-188.
- (38) Antonioli, L.; Blandizzi, C.; Csóka, B.; Pacher, P.; Haskó, G. Adenosine signalling in diabetes mellitus - pathophysiology and therapeutic considerations. *Nat. Rev. Endocrinol.* **2015**, *11*, 228-241.
- (39) Jacobson, K. A. Introduction to adenosine receptors as therapeutic targets. *Handb. Exp. Pharmacol.* **2009**, 1-24.
- (40) Kloor, D.; Osswald, H. S-Adenosylhomocysteine hydrolase as a target for intracellular adenosine action. *Trends Pharmacol. Sci.* **2004**, *25*, 294-297.

- (41) Sperlágh, B.; Vizi, E. S. The role of extracellular adenosine in chemical neurotransmission in the hippocampus and Basal Ganglia: pharmacological and clinical aspects. *Curr. Top. Med. Chem.* **2011**, *11*, 1034-1046.
- (42) Ciccarelli, R.; Ballerini, P.; Sabatino, G.; Rathbone, M. P.; D'Onofrio, M.; Caciagli, F.; Di Iorio, P. Involvement of astrocytes in purine-mediated reparative processes in the brain. *Int. J. Dev. Neurosci.* **2001**, *19*, 395-414.
- (43) Borea, P. A.; Gessi, S.; Merighi, S.; Varani, K. Adenosine as a multi-signalling guardian angel in human diseases: when, where and how does it exert its protective effects? *Trends Pharmacol. Sci.* **2016**, *37*, 419-434.
- (44) Forman, M. B.; Stone, G. W.; Jackson, E. K. Role of adenosine as adjunctive therapy in acute myocardial infarction. *Cardiovasc. Drug Rev.* **2006**, *24*, 116-147.
- (45) Borea, P. A.; Varani, K.; Gessi, S.; Merighi, S.; Vincenzi, F., Eds. *The adenosine receptors*; Springer International Publishing: Cham, 2018.
- (46) Borea, P. A.; Gessi, S.; Merighi, S.; Vincenzi, F.; Varani, K. Pathological overproduction: the bad side of adenosine. *Br. J. Pharmacol.* **2017**, *174*, 1945-1960.
- (47) Ohta, A. A metabolic immune checkpoint: Adenosine in tumor microenvironment. *Front. Immunol.* **2016**, *7*, 109.
- (48) Allard, D.; Turcotte, M.; Stagg, J. Targeting A₂ adenosine receptors in cancer. *Immunol. Cell Biol.* **2017**, *95*, 333-339.
- (49) Müller, C. E.; Baqi, Y.; Namasivayam, V. Agonists and antagonists for purinergic receptors. In *Pelegrín (Hg.) 2020 -Purinergic Signaling*; pp. 45-64.
- (50) Le, F.; Townsend-Nicholson, A.; Baker, E.; Sutherland, G. R.; Schofield, P. R. Characterization and chromosomal localization of the human A_{2A} adenosine receptor gene: ADORA2A. *Biochem. Biophys. Res. Commun.* **1996**, *223*, 461-467.
- (51) Piirainen, H.; Ashok, Y.; Nanekar, R. T.; Jaakola, V.-P. Structural features of adenosine receptors: from crystal to function. *Biochim. Biophys. Acta.* **2011**, *1808*, 1233-1244.
- (52) Al-Attraqchi, O. H. A.; Attimarad, M.; Venugopala, K. N.; Nair, A.; Al-Attraqchi, N. H. A. Adenosine A_{2A} receptor as a potential drug target - current status and future perspectives. *Curr. Pharm. Design.* **2019**, *25*, 2716-2740.
- (53) Sun, B.; Bachhawat, P.; Chu, M. L.-H.; Wood, M.; Ceska, T.; Sands, Z. A.; Mercier, J.; Lebon, F.; Kobilka, T. S.; Kobilka, B. K. Crystal structure of the adenosine A_{2A} receptor bound to an antagonist reveals a potential allosteric pocket. *P. Natl. Acad. Sci. U.S.A.* **2017**, *114*, 2066-2071.

- (54) Jaiteh, M.; Zeifman, A.; Saarinen, M.; Svenningsson, P.; Brea, J.; Loza, M. I.; Carlsson, J. Docking screens for dual inhibitors of disparate drug targets for Parkinson's Disease. *J. Med. Chem.* **2018**, *61*, 5269-5278.
- (55) Landin, E. J. B.; Lovera, S.; Fabritiis, G. de; Kelm, S.; Mercier, J.; McMillan, D.; Sessions, R. B.; Taylor, R. J.; Sands, Z. A.; Joedicke, L.; Crump, M. P. The aminotriazole antagonist Cmpd-1 stabilizes a distinct inactive state of the adenosine 2A receptor. *Angew. Chem. Int. Edit.* **2019**, *58*, 9399-9403.
- (56) Sun, B.; Bachhawat, P.; Ling-Hon Chu, M.; Ceska, T.; Sands, Z.; Lebon, F.; Kobilka, T. S.; Kobilka, B. *Crystal structure of adenosine A_{2A} receptor bound to a novel triazole-carboximidamide antagonist*, 2017.
- (57) Kooistra, A. J.; Mordalski, S.; Pándy-Szekeres, G.; Esguerra, M.; Mamyrbekov, A.; Munk, C.; Keserű, G. M.; Gloriam, D. E. GPCRdb in 2021: integrating GPCR sequence, structure and function. *Nucleic Acids Res.* **2021**, *49*, D335-D343.
- (58) Fredholm, B. B.; Cunha, R. A.; Svenningsson, P. Pharmacology of adenosine A_{2A} receptors and therapeutic applications. *Curr. Top. Med. Chem.* **2003**, *3*, 413-426.
- (59) Diniz, C.; Borges, F.; Santana, L.; Uriarte, E.; Oliveira, J. M. A.; Gonçalves, J.; Fresco, P. Ligands and therapeutic perspectives of adenosine A_{2A} receptors. *Curr. Pharm. Des.* **2008**, *14*, 1698-1722.
- (60) Deng, Q.; Lim, Y.-H.; Anand, R.; Yu, Y.; Kim, J.; Zhou, W.; Zheng, J.; Tempest, P.; Levorse, D.; Zhang, X.; Greene, S.; Mullins, D.; Culberson, C.; Sherborne, B.; Parker, E. M.; Stamford, A.; Ali, A. Use of molecular modeling aided design to dial out hERG liability in adenosine A_{2A} receptor antagonists. *Bioorg. Med. Chem. Lett.* **2015**, *25*, 2958-2962.
- (61) Csóka, B.; Németh, Z. H.; Virág, L.; Gergely, P.; Leibovich, S. J.; Pacher, P.; Sun, C.-X.; Blackburn, M. R.; Vizi, E. S.; Deitch, E. A.; Haskó, G. A_{2A} adenosine receptors and C/EBPβ are crucially required for IL-10 production by macrophages exposed to Escherichia coli. *Blood.* **2007**, *110*, 2685-2695.
- (62) Lambrecht, B. N.; Hammad, H. The immunology of asthma. *Nature Immunol.* **2015**, *16*, 45-56.
- (63) Lappas, C. M.; Sullivan, G. W.; Linden, J. Adenosine A_{2A} agonists in development for the treatment of inflammation. *Expert Opin. Inv. Drugs.* **2005**, *14*, 797-806.
- (64) Alfaro, T. M.; Rodrigues, D. I.; Tomé, Â. R.; Cunha, R. A.; Robalo Cordeiro, C. Adenosine A_{2A} receptors are up-regulated and control the activation of human alveolar macrophages. *Pulm. Pharmacol. Ther.* **2017**, *45*, 90-94.

- (65) Pejman, L.; Omrani, H.; Mirzamohammadi, Z.; Shahbazfar, A. A.; Khalili, M.; Keyhanmanesh, R. The effect of adenosine A_{2A} and A_{2B} antagonists on tracheal responsiveness, serum levels of cytokines and lung inflammation in guinea pig model of asthma. *Adv. Pharm. Bull.* **2014**, *4*, 131-138.
- (66) Andrews, J. P.; Marttala, J.; Macarak, E.; Rosenbloom, J.; Uitto, J. Keloids: The paradigm of skin fibrosis - Pathomechanisms and treatment. *Matrix Biol.* **2016**, *51*, 37-46.
- (67) Yan, J.; Tie, G.; Wang, S.; Tutto, A.; DeMarco, N.; Khair, L.; Fazzio, T. G.; Messina, L. M. Diabetes impairs wound healing by Dnmt1-dependent dysregulation of hematopoietic stem cells differentiation towards macrophages. *Nat. Commun.* **2018**, *9*, 33.
- (68) Ialenti, A.; Caiazzo, E.; Morello, S.; Carnuccio, R.; Cicala, C. Adenosine A_{2A} receptor agonist, 2-*p*-(2-carboxyethyl)phenethylamino-5'-*N*-ethylcarboxamidoadenosine hydrochloride hydrate, inhibits inflammation and increases fibroblast growth factor-2 tissue expression in carrageenan-induced rat paw edema. *J. Pharmacol. Exp. Ther.* **2018**, *364*, 221-228.
- (69) Squadrito, F.; Bitto, A.; Altavilla, D.; Arcoraci, V.; Caridi, G. de; Feo, M. E. de; Corrao, S.; Pallio, G.; Sterrantino, C.; Minutoli, L.; Saitta, A.; Vaccaro, M.; Cucinotta, D. The effect of PDRN, an adenosine receptor A_{2A} agonist, on the healing of chronic diabetic foot ulcers: results of a clinical trial. *J. Clin. Endocrinol. Metab.* **2014**, *99*, E746-53.
- (70) Shaikh, G.; Cronstein, B. Signaling pathways involving adenosine A_{2A} and A_{2B} receptors in wound healing and fibrosis. *Purinerg. Signal.* **2016**, *12*, 191-197.
- (71) Cieślak, M.; Komoszyński, M.; Wojtczak, A. Adenosine A_{2A} receptors in Parkinson's disease treatment. *Purinerg. Signal.* **2008**, *4*, 305-312.
- (72) Pringsheim, T.; Jette, N.; Frolkis, A.; Steeves, T. D. L. The prevalence of Parkinson's disease: a systematic review and meta-analysis. *Mov. Disord.* **2014**, *29*, 1583-1590.
- (73) Morelli, M.; Carta, A. R.; Jenner, P. Adenosine A_{2A} receptors and Parkinson's disease. *Handb. Exp. Pharmacol.* **2009**, 589-615.
- (74) Connolly, B. S.; Lang, A. E. Pharmacological treatment of Parkinson disease: a review. *JAMA.* **2014**, *311*, 1670-1683.
- (75) Bara-Jimenez, W.; Sherzai, A.; Dimitrova, T.; Favit, A.; Bibbiani, F.; Gillespie, M.; Morris, M. J.; Mouradian, M. M.; Chase, T. N. Adenosine A_{2A} receptor antagonist treatment of Parkinson's disease. *Neurology.* **2003**, *61*, 293-296.
- (76) Chen, J.-F.; Fredduzzi, S.; Bastia, E.; Yu, L.; Moratalla, R.; Ongini, E.; Schwarzschild, M. A. Adenosine A_{2A} receptors in neuroadaptation to repeated dopaminergic stimulation: implications for the treatment of dyskinesias in Parkinson's disease. *Neurology.* **2003**, *61*, S74-81.

- (77) Franco, R.; Casado, V.; Cortes, A.; Perez-Capote, K.; Mallol, J.; Canela, E.; Ferre, S.; Lluís, C. Novel pharmacological targets based on receptor heteromers. *Brain Res. Rev.* **2008**, *58*, 475-482.
- (78) Canals, M.; Marcellino, D.; Fanelli, F.; Ciruela, F.; Benedetti, P. de; Goldberg, S. R.; Neve, K.; Fuxe, K.; Agnati, L. F.; Woods, A. S.; Ferre, S.; Lluís, C.; Bouvier, M.; Franco, R. Adenosine A_{2A}-dopamine D₂ receptor-receptor heteromerization: qualitative and quantitative assessment by fluorescence and bioluminescence energy transfer. *J. Biol. Chem.* **2003**, *278*, 46741-46749.
- (79) Ferre, S.; Baler, R.; Bouvier, M.; Caron, M. G.; Devi, L. A.; Durroux, T.; Fuxe, K.; George, S. R.; Javitch, J. A.; Lohse, M. J.; Mackie, K.; Milligan, G.; Pflieger, K. D. G.; Pin, J.-P.; Volkow, N. D.; Waldhoer, M.; Woods, A. S.; Franco, R. Building a new conceptual framework for receptor heteromers. *Nat. Chem. Biol.* **2009**, *5*, 131-134.
- (80) Cacciari, B.; Spalluto, G.; Federico, S. A_{2A} Adenosine receptor antagonists as therapeutic candidates: are they still an interesting challenge? *Mini-Rev. Med. Chem.* **2018**, *18*, 1168-1174.
- (81) Calon, F.; Dridi, M.; Hornykiewicz, O.; Bédard, P. J.; Rajput, A. H.; Di Paolo, T. Increased adenosine A_{2A} receptors in the brain of Parkinson's disease patients with dyskinesias. *Brain.* **2004**, *127*, 1075-1084.
- (82) Takahashi, M.; Fujita, M.; Asai, N.; Saki, M.; Mori, A. Safety and effectiveness of istradefylline in patients with Parkinson's disease: interim analysis of a post-marketing surveillance study in Japan. *Expert. Opin. Pharmacol.* **2018**, *19*, 1635-1642.
- (83) Armentero, M. T.; Pinna, A.; Ferré, S.; Lanciego, J. L.; Müller, C. E.; Franco, R. Past, present and future of A_{2A} adenosine receptor antagonists in the therapy of Parkinson's disease. *Pharmacol. Ther.* **2011**, *132*, 280-299.
- (84) Petzer, J. P.; Steyn, S.; Castagnoli, K. P.; Chen, J.-F.; Schwarzschild, M. A.; van der Schyf, C. J.; Castagnoli, N. Inhibition of monoamine oxidase B by selective adenosine A_{2A} receptor antagonists. *Bioorgan. Med. Chem.* **2003**, *11*, 1299-1310.
- (85) Duyckaerts, C.; Braak, H.; Brion, J.-P.; Buée, L.; Del Tredici, K.; Goedert, M.; Halliday, G.; Neumann, M.; Spillantini, M. G.; Tolnay, M.; Uchihara, T. PART is part of Alzheimer disease. *Acta Neuropathol.* **2015**, *129*, 749-756.
- (86) Pietrowski, M. J.; Gabr, A. A.; Kozlov, S.; Blum, D.; Halle, A.; Carvalho, K. Glial purinergic signaling in neurodegeneration. *Front. Neurol.* **2021**, *12*, 743.
- (87) Maia, L.; Mendonça, A. de. Does caffeine intake protect from Alzheimer's disease? *Eur. J. Neurol.* **2002**, *9*, 377-382.

- (88) Horgusluoglu-Moloch, E.; Nho, K.; Risacher, S. L.; Kim, S.; Foroud, T.; Shaw, L. M.; Trojanowski, J. Q.; Aisen, P. S.; Petersen, R. C.; Jack, C. R.; Lovestone, S.; Simmons, A.; Weiner, M. W.; Saykin, A. J. Targeted neurogenesis pathway-based gene analysis identifies ADORA2A associated with hippocampal volume in mild cognitive impairment and Alzheimer's disease. *Neurobiol. Aging*. **2017**, *60*, 92-103.
- (89) Laurent, C.; Burnouf, S.; Ferry, B.; Batalha, V. L.; Coelho, J. E.; Baqi, Y.; Malik, E.; Mariciniak, E.; Parrot, S.; van der Jeugd, A.; Faivre, E.; Flaten, V.; Ledent, C.; D'Hooge, R.; Sergeant, N.; Hamdane, M.; Humez, S.; Müller, C. E.; Lopes, L. V.; Buée, L.; Blum, D. A2A adenosine receptor deletion is protective in a mouse model of tauopathy. *Mol. Psychiatr.* **2016**, *21*, 97-107.
- (90) Dall'Igna, O. P.; Fett, P.; Gomes, M. W.; Souza, D. O.; Cunha, R. A.; Lara, D. R. Caffeine and adenosine A_{2A} receptor antagonists prevent β -amyloid (25-35)-induced cognitive deficits in mice. *Exp. Neurol.* **2007**, *203*, 241-245.
- (91) Faivre, E.; Coelho, J. E.; Zornbach, K.; Malik, E.; Baqi, Y.; Schneider, M.; Cellai, L.; Carvalho, K.; Sebda, S.; Figeac, M.; Eddarkaoui, S.; Caillierez, R.; Chern, Y.; Heneka, M.; Sergeant, N.; Müller, C. E.; Halle, A.; Buée, L.; Lopes, L. V.; Blum, D. Beneficial effect of a selective adenosine A_{2A} receptor antagonist in the APP^{swe}/PS1^{dE9} mouse model of Alzheimer's disease. *Front. Mol. Neurosci.* **2018**, *11*, 235.
- (92) Otte, C.; Gold, S. M.; Penninx, B. W.; Pariante, C. M.; Etkin, A.; Fava, M.; Mohr, D. C.; Schatzberg, A. F. Major depressive disorder. *Nat. Rev. Dis. Primers.* **2016**, *2*, 16065.
- (93) Nutt, D. J. Relationship of neurotransmitters to the symptoms of major depressive disorder. *J. Clin. Psychiatr.* **2008**, *69 Suppl E1*, 4-7.
- (94) Kok, R. M.; Reynolds, Charles F., III. Management of depression in older adults: A review. *JAMA.* **2017**, *317*, 2114-2122.
- (95) Yamada, K.; Kobayashi, M.; Kanda, T. Involvement of adenosine A_{2A} receptors in depression and anxiety. *Int. Rev. Neurobiol.* **2014**, *119*, 373-393.
- (96) Hunter, A. M.; Balleine, B. W.; Minor, T. R. Helplessness and escape performance: glutamate-adenosine interactions in the frontal cortex. *Behav. Neurosci.* **2003**, *117*, 123-135.
- (97) Lindquist, B. E.; Shuttleworth, C. W. Evidence that adenosine contributes to Leao's spreading depression in vivo. *J. Cereb. Blood. Flow. Metab.* **2017**, *37*, 1656-1669.
- (98) Coelho, J. E.; Alves, P.; Canas, P. M.; Valadas, J. S.; Shmidt, T.; Batalha, V. L.; Ferreira, D. G.; Ribeiro, J. A.; Bader, M.; Cunha, R. A.; do Couto, F. S.; Lopes, L. V. Overexpression of adenosine A_{2A} receptors in rats: Effects on depression, locomotion, and anxiety. *Front. Psychiatry.* **2014**, *5*, 67.

- (99) López-Cruz, L.; Carbó-Gas, M.; Pardo, M.; Bayarri, P.; Valverde, O.; Ledent, C.; Salamone, J. D.; Correa, M. Adenosine A_{2A} receptor deletion affects social behaviors and anxiety in mice: Involvement of anterior cingulate cortex and amygdala. *Behav. Brain Res.* **2017**, *321*, 8-17.
- (100) Lumniczky, K.; Candéias, S. M.; Gaipl, U. S.; Frey, B. Editorial: Radiation and the immune system: Current knowledge and future perspectives. *Front. Immunol.* **2018**, *8*, 1933.
- (101) Yu, Y.; Cui, J. Present and future of cancer immunotherapy: A tumor microenvironmental perspective. *Oncol. Lett.* **2018**, *16*, 4105-4113.
- (102) Gessi, S.; Bencivenni, S.; Battistello, E.; Vincenzi, F.; Colotta, V.; Catarzi, D.; Varano, F.; Merighi, S.; Borea, P. A.; Varani, K. Inhibition of A_{2A} adenosine receptor signaling in cancer cells proliferation by the novel antagonist TP455. *Front. Pharmacol.* **2017**, *8*, 888.
- (103) Ohta, A.; Sitkovsky, M. Role of G-protein-coupled adenosine receptors in downregulation of inflammation and protection from tissue damage. *Nature.* **2001**, *414*, 916-920.
- (104) Waickman, A. T.; Alme, A.; Senaldi, L.; Zarek, P. E.; Horton, M.; Powell, J. D. Enhancement of tumor immunotherapy by deletion of the A_{2A} adenosine receptor. *Cancer Immunol. Immun.* **2012**, *61*, 917-926.
- (105) Pardoll, D. M. The blockade of immune checkpoints in cancer immunotherapy. *Nat. Rev. Cancer.* **2012**, *12*, 252-264.
- (106) Shaik, K.; Deb, P. K.; Mailavaram, R. P.; Chandrasekaran, B.; Kachler, S.; Klotz, K.-N.; Jaber, A. M. Y. 7-Amino-2-aryl/hetero-aryl-5-oxo-5,8-dihydro1,2,4-triazolo1,5-apyridine-6-carbonitriles: Synthesis and adenosine receptor binding studies. *Chem. Biol. Drug Des.* **2019**, *94*, 1568-1573.
- (107) El-Tayeb, A.; Gollos, S. Synthesis and structure-activity relationships of 2-hydrazinyladenosine derivatives as A_{2A} adenosine receptor ligands. *Bioorg. Med. Chem.* **2013**, *21*, 436-447.
- (108) Knight, B. P.; Zivin, A.; Souza, J.; Goyal, R.; Man, K. C.; Strickberger, A.; Morady, F. Use of adenosine in patients hospitalized in a university medical center. *Am. J. Med.* **1998**, *105*, 275-280.
- (109) Hinz, S.; Alnouri, W. M.; Pleiss, U.; Müller, C. E. Tritium-labeled agonists as tools for studying adenosine A_{2B} receptors. *Purinerg. Signal.* **2018**, *14*, 223-233.
- (110) Hage, F. G.; Ghimire, G.; Lester, D.; McKay, J.; Bleich, S.; El-Hajj, S.; Iskandrian, A. E. The prognostic value of regadenoson myocardial perfusion imaging. *J. Nucl. Cardiol.* **2015**, *22*, 1214-1221.

- (111) Al Jaroudi, W.; Iskandrian, A. E. Regadenoson: a new myocardial stress agent. *J. Am. Coll. Cardiol.* **2009**, *54*, 1123-1130.
- (112) Lebon, G.; Edwards, P. C.; Leslie, A. G. W.; Tate, C. G. Molecular determinants of CGS21680 binding to the human adenosine A_{2A} receptor. *Mol. Pharmacol.* **2015**, *87*, 907-915.
- (113) El-Tayeb, A.; Michael, S.; Abdelrahman, A.; Behrenswerth, A.; Gollos, S.; Nieber, K.; Müller, C. E. Development of polar adenosine A_{2A} receptor agonists for inflammatory bowel disease: Synergism with A_{2B} antagonists. *ACS Med. Chem Lett.* **2011**, *2*, 890-895.
- (114) Bharate, S. B.; Singh, B.; Kachler, S.; Oliveira, A.; Kumar, V.; Bharate, S. S.; Vishwakarma, R. A.; Klotz, K.-N.; Gutiérrez de Terán, H. Discovery of 7-(prolinol-*N*-yl)-2-phenylamino-thiazolo5,4-dpyrimidines as novel non-nucleoside partial agonists for the A_{2A} adenosine receptor: Prediction from molecular modeling. *J. Med. Chem.* **2016**, *59*, 5922-5928.
- (115) Amelia, T.; van Veldhoven, J. P. D.; Falsini, M.; Liu, R.; Heitman, L. H.; van Westen, G. J. P.; Segala, E.; Verdon, G.; Cheng, R. K. Y.; Cooke, R. M.; van der Es, D.; IJzerman, A. P. Crystal structure and subsequent ligand design of a nonriboside partial agonist bound to the adenosine A_{2A} receptor. *J. Med. Chem.* **2021**, *64*, 3827-3842.
- (116) Müller, C. E.; Jacobson, K. A. Xanthines as adenosine receptor antagonists. *Handb. Exp. Pharmacol.* **2011**, 151-199.
- (117) Abo-Salem, O. M.; Hayallah, A. M.; Bilkei-Gorzo, A.; Filipek, B.; Zimmer, A.; Müller, C. E. Antinociceptive effects of novel A_{2B} adenosine receptor antagonists. *J. Pharmacol. Exp. Ther.* **2004**, *308*, 358-366.
- (118) Chen, J.-F.; Cunha, R. A. The belated US FDA approval of the adenosine A_{2A} receptor antagonist istradefylline for treatment of Parkinson's disease. *Purinerg. Signal.* **2020**, *16*, 167-174.
- (119) Hockemeyer, J.; Burbiel, J. C.; Müller, C. E. Multigram-scale syntheses, stability, and photoreactions of A_{2A} adenosine receptor antagonists with 8-styrylxanthine structure: potential drugs for Parkinson's disease. *J. Org. Chem.* **2004**, *69*, 3308-3318.
- (120) Sauer, R.; Maurinsh, J.; Reith, U.; Fülle, F.; Klotz, K. N.; Müller, C. E. Water-soluble phosphate prodrugs of 1-propargyl-8-styrylxanthine derivatives, A_{2A}-selective adenosine receptor antagonists. *J. Med. Chem.* **2000**, *43*, 440-448.
- (121) Vollmann, K.; Qurishi, R.; Hockemeyer, J.; Müller, C. E. Synthesis and properties of a new water-soluble prodrug of the adenosine A_{2A} receptor antagonist MSX-2. *Molecules.* **2008**, *13*, 348-359.
- (122) Worden, L. T.; Shahriari, M.; Farrar, A. M.; Sink, K. S.; Hockemeyer, J.; Müller, C. E.; Salamone, J. D. The adenosine A_{2A} antagonist MSX-3 reverses the effort-related effects of

dopamine blockade: differential interaction with D1 and D2 family antagonists. *Psychopharmacology (Berl)*. **2009**, *203*, 489-499.

(123) Alexander, S. P.; Millns, P. J. [³H]ZM241385 - an antagonist radioligand for adenosine A_{2A} receptors in rat brain. *Eur. J. Pharmacol.* **2001**, *411*, 205-210.

(124) Jaakola, V.-P.; Griffith, M. T.; Hanson, M. A.; Cherezov, V.; Chien, E. Y. T.; Lane, J. R.; IJzerman, A. P.; Stevens, R. C. The 2.6 angstrom crystal structure of a human A_{2A} adenosine receptor bound to an antagonist. *Science*. **2008**, *322*, 1211-1217.

(125) Gillespie, R. J.; Bamford, S. J.; Botting, R.; Comer, M.; Denny, S.; Gaur, S.; Griffin, M.; Jordan, A. M.; Knight, A. R.; Lerpiniere, J.; Leonardi, S.; Lightowler, S.; McAteer, S.; Merrett, A.; Misra, A.; Padfield, A.; Reece, M.; Saadi, M.; Selwood, D. L.; Stratton, G. C.; Surry, D.; Todd, R.; Tong, X.; Ruston, V.; Upton, R.; Weiss, S. M. Antagonists of the human A_{2A} adenosine receptor. 4. Design, synthesis, and preclinical evaluation of 7-aryltriazolo-4,5-dpyrimidines. *J. Med. Chem.* **2009**, *52*, 33-47.

(126) Pinna, A. Adenosine A_{2A} receptor antagonists in Parkinson's disease: progress in clinical trials from the newly approved istradefylline to drugs in early development and those already discontinued. *CNS Drugs*. **2014**, *28*, 455-474.

(127) Huck, B. R.; Kötzner, L.; Urbahns, K. Small molecules drive big improvements in immuno-oncology therapies. *Angew. Chem. Int. Edit.* **2018**, *57*, 4412-4428.

(128) Kecskés, M.; Kumar, T. S.; Yoo, L.; Gao, Z.-G.; Jacobson, K. A. Novel Alexa Fluor-488 labeled antagonist of the A_{2A} adenosine receptor: Application to a fluorescence polarization-based receptor binding assay. *Biochem. Pharmacol.* **2010**, *80*, 506-511.

(129) Moresco, R. M.; Todde, S.; Belloli, S.; Simonelli, P.; Panzacchi, A.; Rigamonti, M.; Galli-Kienle, M.; Fazio, F. In vivo imaging of adenosine A_{2A} receptors in rat and primate brain using 11CSCH442416. *Eur. J. Nucl. Med. Mol. Imaging*. **2005**, *32*, 405-413.

(130) Stocchi, F.; Rascol, O.; Hauser, R. A.; Huyck, S.; Tzontcheva, A.; Capece, R.; Ho, T. W.; Sklar, P.; Lines, C.; Michelson, D.; Hewitt, D. J. Randomized trial of pramipexole, given as monotherapy, in patients with early Parkinson Disease. *Neurology*. **2017**, *88*, 2198-2206.

(131) Jacobson, K. A.; Gao, Z.-G. Adenosine receptors as therapeutic targets. *Nat. Rev. Drug Discov.* **2006**, *5*, 247-264.

(132) Müller, C. E.; Ferré, S. Blocking striatal adenosine A_{2A} receptors: a new strategy for basal ganglia disorders. *Recent Pat. CNS Drug Discov.* **2007**, *2*, 1-21.

(133) Flohr, A.; Moreai, L.-J.; Poli, S.; Riemer, C.; Steward, Lucinda. 4-Hydroxy-4-methylpiperidine-1-carboxylic acid (4-methoxy-7-morpholin-4-yl-benzothiazol-2-yl)-amide. US20050261289 A1, 2005.

- (134) Woiwode, T.; Moran, M. 4-Hydroxy-4-methyl-piperidine-1-carboxylic acid (4-Methoxy-7-morpholin-4-yl-benzothiazol-2-yl)-amide for the treatment of post-traumatic stress disorder. PCT Int. Appl. WO2009015236 A1, 2009.
- (135) Lai, T. H.; Toussaint, M.; Teodoro, R.; Dukić-Stefanović, S.; Kranz, M.; Deuther-Conrad, W.; Moldovan, R.-P.; Brust, P. Synthesis and biological evaluation of a novel ¹⁸F-labeled radiotracer for PET imaging of the adenosine A_{2A} receptor. *Int. J. Mol. Sci.* **2021**, *22*.
- (136) Lera Ruiz, M. de; Lim, Y.-H.; Zheng, J. Adenosine A_{2A} receptor as a drug discovery target. *J. Med. Chem.* **2014**, *57*, 3623-3650.
- (137) Mikkelsen, G. K.; Langgård, M.; Schrøder, T. J.; Kreilgaard, M.; Jørgensen, E. B.; Brandt, G.; Griffon, Y.; Boffey, R.; Bang-Andersen, B. Synthesis and SAR studies of analogues of 4-(3,3-dimethyl-butyrylamino)-3,5-difluoro-*N*-thiazol-2-yl-benzamide (Lu AA41063) as adenosine A_{2A} receptor ligands with improved aqueous solubility. *Bioorg. Med. Chem. Lett.* **2015**, *25*, 1212-1216.
- (138) Duroux, R.; Agouridas, L.; Renault, N.; El Bakali, J.; Furman, C.; Melnyk, P.; Yous, S. Antagonists of the adenosine A_{2A} receptor based on a 2-arylbenzoxazole scaffold: Investigation of the C5- and C7-positions to enhance affinity. *Eur. J. Med. Chem.* **2018**, *144*, 151-163.
- (139) Luthra, P. M.; Mishra, C. B.; Jha, P. K.; Barodia, S. K. Synthesis of novel 7-imino-2-thioxo-3,7-dihydro-2*H*-thiazolo 4,5-*d* pyrimidine derivatives as adenosine A_{2A} receptor antagonists. *Bioorg. Med. Chem. Lett.* **2010**, *20*, 1214-1218.
- (140) Minetti, P.; Tinti, M. O.; Carminati, P.; Castorina, M.; Di Cesare, M. A.; Di Serio, S.; Gallo, G.; Ghirardi, O.; Giorgi, F.; Giorgi, L.; Piersanti, G.; Bartocchini, F.; Tarzia, G. 2-*n*-Butyl-9-methyl-8-1,2,3-triazol-2-yl-9*H*-purin-6-ylamine and analogues as A_{2A} adenosine receptor antagonists. Design, synthesis, and pharmacological characterization. *J. Med. Chem.* **2005**, *48*, 6887-6896.
- (141) Congreve, M.; Andrews, S. P.; Doré, A. S.; Hollenstein, K.; Hurrell, E.; Langmead, C. J.; Mason, J. S.; Ng, I. W.; Tehan, B.; Zhukov, A.; Weir, M.; Marshall, F. H. Discovery of 1,2,4-triazine derivatives as adenosine A(2A) antagonists using structure-based drug design. *J. Med. Chem.* **2012**, *55*, 1898-1903.
- (142) Foster, D. J.; Conn, P. J. Allosteric modulation of GPCRs: New insights and potential utility for treatment of schizophrenia and other CNS disorders. *Neuron.* **2017**, *94*, 431-446.
- (143) Massink, A.; Louvel, J.; Adlere, I.; van Veen, C.; Huisman, B. J. H.; Dijksteel, G. S.; Guo, D.; Lenselink, E. B.; Buckley, B. J.; Matthews, H.; Ranson, M.; Kelso, M.; IJzerman, A. P. 5'-

Substituted amiloride derivatives as allosteric modulators binding in the sodium ion pocket of the adenosine A_{2A} receptor. *J. Med. Chem.* **2016**, *59*, 4769-4777.

(144) Yuan, G.; Gedeon, N. G.; Jankins, T. C.; Jones, G. B. Novel approaches for targeting the adenosine A_{2A} receptor. *Expert. Opin. Drug Dis.* **2015**, *10*, 63-80.

(145) Lu, Y.; Liu, H.; Yang, D.; Zhong, L.; Xin, Y.; Zhao, S.; Wang, M.-W.; Zhou, Q.; Shui, W. Affinity mass spectrometry-based fragment screening identified a new negative allosteric modulator of the adenosine A_{2A} receptor targeting the sodium ion pocket. *ACS Chem. Biol.* **2021**.

(146) Chen, D.; Errey, J. C.; Heitman, L. H.; Marshall, F. H.; IJzerman, A. P.; Siegal, G. Fragment screening of GPCRs using biophysical methods: identification of ligands of the adenosine A(2A) receptor with novel biological activity. *ACS Chem. Biol.* **2012**, *7*, 2064-2073.

(147) Giorgi, I.; Biagi, G.; Bianucci, A. M.; Borghini, A.; Livi, O.; Leonardi, M.; Pietra, D.; Calderone, V.; Martelli, A. N6-1,3-diphenylurea derivatives of 2-phenyl-9-benzyladenines and 8-azaadenines: synthesis and biological evaluation as allosteric modulators of A_{2A} adenosine receptors. *Eur. J. Med. Chem.* **2008**, *43*, 1639-1647.

(148) Sherbiny, F. F.; Schiedel, A. C.; Maass, A.; Müller, C. E. Homology modelling of the human adenosine A_{2B} receptor based on X-ray structures of bovine rhodopsin, the beta2-adrenergic receptor and the human adenosine A_{2A} receptor. *J. Comput. Aided Mol. Des.* **2009**, *23*, 807-828.

(149) Köse, M.; Gollos, S.; Karcz, T.; Fiene, A.; Heisig, F.; Behrenswerth, A.; Kieć-Kononowicz, K.; Namasivayam, V.; Müller, C. E. Fluorescent-labeled selective adenosine A_{2B} receptor antagonist enables competition binding assay by flow cytometry. *J. Med. Chem.* **2018**, *61*, 4301-4316.

(150) Jiang, J.; Seel, C. J.; Temirak, A.; Namasivayam, V.; Arridu, A.; Schabikowski, J.; Baqi, Y.; Hinz, S.; Hockemeyer, J.; Müller, C. E. A_{2B} adenosine receptor antagonists with picomolar potency. *J. Med. Chem.* **2019**, *62*, 4032-4055.

(151) Müller, C. E.; Baqi, Y.; Hinz, S.; Namasivayam, V. Medicinal chemistry of A_{2B} adenosine receptors. In *The adenosine receptors*. Borea, P. A.; Varani, K.; Gessi, S.; Merighi, S.; Vincenzi, F., Eds.; Springer International Publishing: Cham; pp. 137-168.

(152) Seibt, B. F.; Schiedel, A. C.; Thimm, D.; Hinz, S.; Sherbiny, F. F.; Müller, C. E. The second extracellular loop of GPCRs determines subtype-selectivity and controls efficacy as evidenced by loop exchange study at A₂ adenosine receptors. *Biochem. Pharmacol.* **2013**, *85*, 1317-1329.

- (153) Filippo, E. de; Namasivayam, V.; Zappe, L.; El-Tayeb, A.; Schiedel, A. C.; Müller, C. E. Role of extracellular cysteine residues in the adenosine A_{2A} receptor. *Purinerg. Signal.* **2016**, *12*, 313-329.
- (154) Schiedel, A. C.; Hinz, S.; Thimm, D.; Sherbiny, F.; Borrmann, T.; Maass, A.; Müller, C. E. The four cysteine residues in the second extracellular loop of the human adenosine A_{2B} receptor: role in ligand binding and receptor function. *Biochem. Pharmacol.* **2011**, *82*, 389-399.
- (155) Feoktistov, I.; Biaggioni, I.; Polosa, R.; Holgate, S. T. Adenosine A_{2B} receptors: a novel therapeutic target in asthma? *Trends Pharmacol. Sci.* **1998**, *19*, 148-153.
- (156) Yaar, R.; Jones, M. R.; Chen, J.-F.; Ravid, K. Animal models for the study of adenosine receptor function. *J. Cell. Physiol.* **2005**, *202*, 9-20.
- (157) Aherne, C. M.; Kewley, E. M.; Eltzschig, H. K. The resurgence of A_{2B} adenosine receptor signaling. *Biochim. Biophys. Acta.* **2011**, *1808*, 1329-1339.
- (158) Ham, J.; Rees, D. A. The adenosine A_{2B} receptor: its role in inflammation. *Endocr. Metab. Immune Disords. Drug Targets.* **2008**, *8*, 244-254.
- (159) Kong, T.; Westerman, K. A.; Faigle, M.; Eltzschig, H. K.; Colgan, S. P. HIF-dependent induction of adenosine A_{2B} receptor in hypoxia. *FASEB J.* **2006**, *20*, 2242-2250.
- (160) Vecchio, E. A.; Tan, C. Y. R.; Gregory, K. J.; Christopoulos, A.; White, P. J.; May, L. T. Ligand-independent adenosine A_{2B} receptor constitutive activity as a promoter of prostate cancer cell proliferation. *J. Pharmacol. Exp. Ther.* **2016**, *357*, 36-44.
- (161) Antonioli, L.; Csóka, B.; Fornai, M.; Colucci, R.; Kókai, E.; Blandizzi, C.; Haskó, G. Adenosine and inflammation: what's new on the horizon? *Drug Discov. Today.* **2014**, *19*, 1051-1068.
- (162) Ryzhov, S.; Zaynagetdinov, R.; Goldstein, A. E.; Novitskiy, S. V.; Blackburn, M. R.; Biaggioni, I.; Feoktistov, I. Effect of A_{2B} adenosine receptor gene ablation on adenosine-dependent regulation of proinflammatory cytokines. *J. Pharmacol. Exp. Ther.* **2008**, *324*, 694-700.
- (163) Zhong, H.; Wu, Y.; Belardinelli, L.; Zeng, D. A_{2B} adenosine receptors induce IL-19 from bronchial epithelial cells, resulting in TNF-alpha increase. *Am. J. Resp. Cell Mol.* **2006**, *35*, 587-592.
- (164) Effendi, W. I.; Nagano, T.; Kobayashi, K.; Nishimura, Y. Focusing on adenosine receptors as a potential targeted therapy in human diseases. *Cells.* **2020**, *9*.
- (165) Blackburn, M. R.; Vance, C. O.; Morschl, E.; Wilson, C. N. Adenosine receptors and inflammation. In *Wilson, Mustafa (Hg.) 2009 - Adenosine receptors in health*; pp. 215-269.

- (166) Linden, J. New insights into the regulation of inflammation by adenosine. *J. Clin. Invest.* **2006**, *116*, 1835-1837.
- (167) Ryzhov, S.; Sung, B. H.; Zhang, Q.; Weaver, A.; Gumina, R. J.; Biaggioni, I.; Feoktistov, I. Role of adenosine A_{2B} receptor signaling in contribution of cardiac mesenchymal stem-like cells to myocardial scar formation. *Purinerg. Signal.* **2014**, *10*, 477-486.
- (168) Wei, W.; Du, C.; Lv, J.; Zhao, G.; Li, Z.; Wu, Z.; Haskó, G.; Xie, X. Blocking A_{2B} adenosine receptor alleviates pathogenesis of experimental autoimmune encephalomyelitis via inhibition of IL-6 production and Th17 differentiation. *J. Immunol.* **2013**, *190*, 138-146.
- (169) Wilson, C. N.; Mustafa, S. J., Eds. *Adenosine Receptors in Health and Disease*; Springer Berlin Heidelberg: Berlin, Heidelberg, 2009.
- (170) van den Berge, M.; Hylkema, M. N.; Versluis, M.; Postma, D. S. Role of adenosine receptors in the treatment of asthma and chronic obstructive pulmonary disease: recent developments. *Drugs R D.* **2007**, *8*, 13-23.
- (171) Mustafa, S. J.; Nadeem, A.; Fan, M.; Zhong, H.; Belardinelli, L.; Zeng, D. Effect of a specific and selective A_{2B} adenosine receptor antagonist on adenosine agonist AMP and allergen-induced airway responsiveness and cellular influx in a mouse model of asthma. *J. Pharm. Exp. Ther.* **2007**, *320*, 1246-1251.
- (172) Greer, S.; Page, C. W.; Joshi, T.; Yan, D.; Newton, R.; Giembycz, M. A. Concurrent agonism of adenosine A_{2B} and glucocorticoid receptors in human airway epithelial cells cooperatively induces genes with anti-inflammatory potential: a novel approach to treat chronic obstructive pulmonary disease. *J. Pharmacol. Exp. Ther.* **2013**, *346*, 473-485.
- (173) Bruce N. Cronstein. Adenosine receptors and fibrosis: a translational review. *F1000 Biol. Rep.* **2011**, *3*.
- (174) Zhong, H.; Belardinelli, L.; Maa, T.; Zeng, D. Synergy between A_{2B} adenosine receptors and hypoxia in activating human lung fibroblasts. *Am. J. Resp. Cell Mol. Biol.* **2005**, *32*, 2-8.
- (175) Peart, J. N.; Headrick, J. P. Adenosinergic cardioprotection: multiple receptors, multiple pathways. *Pharmacol. Ther.* **2007**, *114*, 208-221.
- (176) Zhan, E.; McIntosh, V. J.; Lasley, R. D. Adenosine A_{2A} and A_{2B} receptors are both required for adenosine A₁ receptor-mediated cardioprotection. *Am. J. Physiol. Heart Circ. Physiol.* **2011**, *301*, H1183-9.
- (177) Carden, D. L.; Granger, D. N. Pathophysiology of ischaemia-reperfusion injury. *J. Pathol.* **2000**, *190*, 255-266.

- (178) Lasley, R. D. Adenosine receptor-mediated cardioprotection - current limitations and future directions. *Front. Pharmacol.* **2018**, *9*, 310.
- (179) Eltzhig, H. K.; Bonney, S. K.; Eckle, T. Attenuating myocardial ischemia by targeting A_{2B} adenosine receptors. *Trends Mol. Med.* **2013**, *19*, 345-354.
- (180) Antonioli, L.; Blandizzi, C.; Pacher, P.; Haskó, G. Immunity, inflammation and cancer: a leading role for adenosine. *Nat. Rev. Cancer.* **2013**, *13*, 842-857.
- (181) Sun, Y.; Huang, P. Adenosine A_{2B} Receptor: From cell biology to human diseases. *Front. Chem.* **2016**, *4*, 37.
- (182) Gao, Z.-G.; Jacobson, K. A. A_{2B} adenosine receptor and cancer. *Int. J. Mol. Sci.* **2019**, *20*.
- (183) Belguise, K.; Kersual, N.; Galtier, F.; Chalbos, D. FRA-1 expression level regulates proliferation and invasiveness of breast cancer cells. *Oncogene.* **2005**, *24*, 1434-1444.
- (184) Feoktistov, I.; Goldstein, A. E.; Ryzhov, S.; Zeng, D.; Belardinelli, L.; Voynoyasenetskaya, T.; Biaggioni, I. Differential expression of adenosine receptors in human endothelial cells: role of A_{2B} receptors in angiogenic factor regulation. *Circ. Res.* **2002**, *90*, 531-538.
- (185) Mittal, D.; Sinha, D.; Barkauskas, D.; Young, A.; Kalimutho, M.; Stannard, K.; Caramia, F.; Haibe-Kains, B.; Stagg, J.; Khanna, K. K.; Loi, S.; Smyth, M. J. Adenosine 2B receptor expression on cancer cells promotes metastasis. *Cancer Res.* **2016**, *76*, 4372-4382.
- (186) Iannone, R.; Miele, L.; Maiolino, P.; Pinto, A.; Morello, S. Blockade of A_{2B} adenosine receptor reduces tumor growth and immune suppression mediated by myeloid-derived suppressor cells in a mouse model of melanoma. *Neoplasia.* **2013**, *15*, 1400-1409.
- (187) Kalla, R. V.; Zablocki, J. Progress in the discovery of selective, high affinity A_{2B} adenosine receptor antagonists as clinical candidates. *Purinerg. Signal.* **2009**, *5*, 21-29.
- (188) Eltzhig, H. K. Adenosine: an old drug newly discovered. *Anesthesiology.* **2009**, *111*, 904-915.
- (189) Hinz, S.; Lacher, S. K.; Seibt, B. F.; Müller, C. E. BAY60-6583 acts as a partial agonist at adenosine A_{2B} receptors. *J. Pharm. Exp. Ther.* **2014**, *349*, 427-436.
- (190) Alnouri, M. W.; Jepards, S.; Casari, A.; Schiedel, A. C.; Hinz, S.; Müller, C. E. Selectivity is species-dependent: Characterization of standard agonists and antagonists at human, rat, and mouse adenosine receptors. *Purinerg. Signal.* **2015**, *11*, 389-407.

- (191) Catarzi, D.; Varano, F.; Varani, K.; Vincenzi, F.; Pasquini, S.; Dal Ben, D.; Volpini, R.; Colotta, V. Amino-3,5-dicyanopyridines targeting the adenosine receptors ranging from pan ligands to combined A₁/A_{2B} partial agonists. *Pharmaceuticals*. **2019**, *12*.
- (192) Baltos, J.-A.; Vecchio, E. A.; Harris, M. A.; Qin, C. X.; Ritchie, R. H.; Christopoulos, A.; White, P. J.; May, L. T. Capadenoson, a clinically trialed partial adenosine A₁ receptor agonist, can stimulate adenosine A_{2B} receptor biased agonism. *Biochem. Pharmacol.* **2017**, *135*, 79-89.
- (193) Tian, Y.; Piras, B. A.; Kron, I. L.; French, B. A.; Yang, Z. Adenosine 2B receptor activation reduces myocardial reperfusion injury by promoting anti-inflammatory macrophages differentiation via PI3K/Akt pathway. *Oxid. Med. Cell Longv.* **2015**, *2015*, 585297.
- (194) Powis, G.; Bonjouklian, R.; Berggren, M. M.; Gallegos, A.; Abraham, R.; Ashendel, C.; Zalkow, L.; Matter, W. F.; Dodge, J.; Grindey, G. Wortmannin, a potent and selective inhibitor of phosphatidylinositol-3-kinase. *Cancer Res.* **1994**, *54*, 2419-2423.
- (195) Jafari, S. M.; Joshaghani, H. R.; Panjehpour, M.; Aghaei, M. A_{2B} adenosine receptor agonist induces cell cycle arrest and apoptosis in breast cancer stem cells via ERK1/2 phosphorylation. *Cell. Oncol. (Dordr)*. **2018**, *41*, 61-72.
- (196) Fusco, I.; Cherchi, F.; Catarzi, D.; Colotta, V.; Varano, F.; Pedata, F.; Pugliese, A. M.; Coppi, E. Functional characterization of a novel adenosine A_{2B} receptor agonist on short-term plasticity and synaptic inhibition during oxygen and glucose deprivation in the rat CA1 hippocampus. *Brain Res. Bull.* **2019**, *151*, 174-180.
- (197) Elzein, E.; Zablocki, J. A₁ adenosine receptor agonists and their potential therapeutic applications. *Expert Opin. Inv. Drugs.* **2008**, *17*, 1901-1910.
- (198) Bhatt, K. N.; Butler, J. Myocardial energetics and heart failure: a review of recent therapeutic trials. *Curr. Heart Fail. Rep.* **2018**, *15*, 191-197.
- (199) Doré, A. S.; Robertson, N.; Errey, J. C.; Ng, I.; Hollenstein, K.; Tehan, B.; Hurrell, E.; Bennett, K.; Congreve, M.; Magnani, F.; Tate, C. G.; Weir, M.; Marshall, F. H. Structure of the adenosine A_{2A} receptor in complex with ZM241385 and the xanthines XAC and caffeine. *Structure*. **2011**, *19*, 1283-1293.
- (200) Hayallah, A. M.; Sandoval-Ramírez, J.; Reith, U.; Schobert, U.; Preiss, B.; Schumacher, B.; Daly, J. W.; Müller, C. E. 1,8-disubstituted xanthine derivatives: synthesis of potent A_{2B}-selective adenosine receptor antagonists. *J. Med. Chem.* **2002**, *45*, 1500-1510.
- (201) Michael, S.; Warstat, C.; Michel, F.; Yan, L.; Müller, C. E.; Nieber, K. Adenosine A_{2A} agonist and A_{2B} antagonist mediate an inhibition of inflammation-induced contractile disturbance of a rat gastrointestinal preparation. *Purinerg. Signal.* **2010**, *6*, 117-124.

- (202) Elzein, E.; Kalla, R. V.; Li, X.; Perry, T.; Gimbel, A.; Zeng, D.; Lustig, D.; Leung, K.; Zablocki, J. Discovery of a novel A_{2B} adenosine receptor antagonist as a clinical candidate for chronic inflammatory airway diseases. *J. Med. Chem.* **2008**, *51*, 2267-2278.
- (203) Sun, C.-X.; Zhong, H.; Mohsenin, A.; Morschl, E.; Chunn, J. L.; Molina, J. G.; Belardinelli, L.; Zeng, D.; Blackburn, M. R. Role of A_{2B} adenosine receptor signaling in adenosine-dependent pulmonary inflammation and injury. *J. Clin. Invest.* **2006**, *116*, 2173-2182.
- (204) Kim, Y. C.; Ji, X.; Melman, N.; Linden, J.; Jacobson, K. A. Anilide derivatives of an 8-phenylxanthine carboxylic congener are highly potent and selective antagonists at human A_{2B} adenosine receptors. *J. Med. Chem.* **2000**, *43*, 1165-1172.
- (205) Du, X.; Ou, X.; Song, T.; Zhang, W.; Cong, F.; Zhang, S.; Xiong, Y. Adenosine A_{2B} receptor stimulates angiogenesis by inducing VEGF and eNOS in human microvascular endothelial cells. *Exp. Biol. Med.* **2015**, *240*, 1472-1479.
- (206) Ma, D.-F.; Kondo, T.; Nakazawa, T.; Niu, D.-F.; Mochizuki, K.; Kawasaki, T.; Yamane, T.; Kato, R. Hypoxia-inducible adenosine A_{2B} receptor modulates proliferation of colon carcinoma cells. *Hum. Pathol.* **2010**, *41*, 1550-1557.
- (207) Zablocki, J.; Kalla, R.; Perry, T.; Palle, V.; Varkhedkar, V.; Xiao, D.; Piscopio, A.; Maa, T.; Gimbel, A.; Hao, J.; Chu, N.; Leung, K.; Zeng, D. The discovery of a selective, high affinity A_{2B} adenosine receptor antagonist for the potential treatment of asthma. *Bioorg. Med. Chem. Lett.* **2005**, *15*, 609-612.
- (208) Basu, S.; Barawkar, D. A.; Ramdas, V.; Waman, Y.; Patel, M.; Panmand, A.; Kumar, S.; Thorat, S.; Bonagiri, R.; Jadhav, D.; Mukhopadhyay, P.; Prasad, V.; Reddy, B. S.; Goswami, A.; Chaturvedi, S.; Menon, S.; Quraishi, A.; Ghosh, I.; Dusange, S.; Paliwal, S.; Kulkarni, A.; Karande, V.; Thakre, R.; Bedse, G.; Rouduri, S.; Gundu, J.; Palle, V. P.; Chugh, A.; Mookhtiar, K. A. A_{2B} adenosine receptor antagonists: Design, synthesis and biological evaluation of novel xanthine derivatives. *Eur. J. Med. Chem.* **2017**, *127*, 986-996.
- (209) Borrmann, T.; Hinz, S.; Bertarelli, D. C. G.; Li, W.; Florin, N. C.; Scheiff, A. B.; Müller, C. E. 1-alkyl-8-(piperazine-1-sulfonyl)phenylxanthines: development and characterization of adenosine A_{2B} receptor antagonists and a new radioligand with subnanomolar affinity and subtype specificity. *J. Med. Chem.* **2009**, *52*, 3994-4006.
- (210) Mølck, C.; Ryall, J.; Failla, L. M.; Coates, J. L.; Pascussi, J.-M.; Heath, J. K.; Stewart, G.; Hollande, F. The A_{2B} adenosine receptor antagonist PSB-603 promotes oxidative phosphorylation and ROS production in colorectal cancer cells via adenosine receptor-independent mechanism. *Cancer Lett.* **2016**, *383*, 135-143.

- (211) Mallo-Abreu, A.; Prieto-Díaz, R.; Jespers, W.; Azuaje, J.; Majellaro, M.; Velando, C.; García-Mera, X.; Caamaño, O.; Brea, J.; Loza, M. I.; Gutiérrez-de-Terán, H.; Sotelo, E. Nitrogen-walk approach to explore bioisosteric replacements in a series of potent A_{2B} adenosine receptor antagonists. *J. Med. Chem.* **2020**, *63*, 7721-7739.
- (212) Härter, M.; Kalthof, B.; Delbeck, M.; Lustig, K.; Gerisch, M.; Schulz, S.; Kast, R.; Meibom, D.; Lindner, N. Novel non-xanthine antagonist of the A_{2B} adenosine receptor: From HTS hit to lead structure. *Eur. J. Med. Chem.* **2019**, *163*, 763-778.
- (213) Eastwood, P.; Esteve, C.; González, J.; Fonquerna, S.; Aiguadé, J.; Carranco, I.; Doménech, T.; Aparici, M.; Miralpeix, M.; Albertí, J.; Córdoba, M.; Fernández, R.; Pont, M.; Godessart, N.; Prats, N.; Loza, M. I.; Cadavid, M. I.; Nueda, A.; Vidal, B. Discovery of LAS101057: A potent, selective, and orally efficacious A_{2B} adenosine receptor antagonist. *ACS Med. Chem. Lett.* **2011**, *2*, 213-218.
- (214) Davenport, A. P.; Harmar, A. J. Evolving pharmacology of orphan GPCRs: IUPHAR Commentary. *Br. J. Pharmacol.* **2013**, *170*, 693-695.
- (215) Wise, A.; Jupe, S. C.; Rees, S. The identification of ligands at orphan G-protein coupled receptors. *Annu. Rev. Pharmacol.* **2004**, *44*, 43-66.
- (216) Jiang, Z.; Zhou, Y. Using silico methods predicting ligands for orphan GPCRs. *Curr. Protein Pept. Sci.* **2006**, *7*, 459-464.
- (217) Laschet, C.; Dupuis, N.; Hanson, J. The G protein-coupled receptors deorphanization landscape. *Biochem. Pharmacol.* **2018**, *153*, 62-74.
- (218) Ngo, T.; Kufareva, I.; Coleman, J. L.; Graham, R. M.; Abagyan, R.; Smith, N. J. Identifying ligands at orphan GPCRs: current status using structure-based approaches. *Br. J. Pharmacol.* **2016**, *173*, 2934-2951.
- (219) Yasi, E. A.; Kruyer, N. S.; Peralta-Yahya, P. Advances in G protein-coupled receptor high-throughput screening. *Curr. Opin. Biotech.* **2020**, *64*, 210-217.
- (220) Savi, P.; Labouret, C.; Delesque, N.; Guette, F.; Lupker, J.; Herbert, J. M. P2Y₁₂, a new platelet ADP receptor, target of clopidogrel. *Biochem. Biophys. Res. Commun.* **2001**, *283*, 379-383.
- (221) Hollopeter, G.; Jantzen, H. M.; Vincent, D.; Li, G.; England, L.; Ramakrishnan, V.; Yang, R. B.; Nurden, P.; Nurden, A.; Julius, D.; Conley, P. B. Identification of the platelet ADP receptor targeted by antithrombotic drugs. *Nature.* **2001**, *409*, 202-207.
- (222) Nothacker, H.-P. Orphan Receptors. In *Encyclopedia of molecular pharmacology*. Offermanns, S., Ed.; Springer: Berlin, Heidelberg, New York, NY; pp. 914-917.

- (223) Bader, M.; Alenina, N.; Andrade-Navarro, M. A.; Santos, R. A. MAS and its related G protein-coupled receptors, Mrgprs. *Pharmacol. Rev.* **2014**, *66*, 1080-1105.
- (224) Zylka, M. J.; Dong, X.; Southwell, A. L.; Anderson, D. J. Atypical expansion in mice of the sensory neuron-specific Mrg G protein-coupled receptor family. *Proc. Natl. Acad. Sci.* **2003**, *100*, 10043-10048.
- (225) Dong, X.; Han, S.; Zylka, M. J.; Simon, M. I.; Anderson, D. J. A diverse family of GPCRs expressed in specific subsets of nociceptive sensory neurons. *Cell.* **2001**, *106*, 619-632.
- (226) Lembo, P. M. C.; Grazzini, E.; Groblewski, T.; O'Donnell, D.; Roy, M.-O.; Zhang, J.; Hoffert, C.; Cao, J.; Schmidt, R.; Pelletier, M.; Labarre, M.; Gosselin, M.; Fortin, Y.; Banville, D.; Shen, S. H.; Ström, P.; Payza, K.; Dray, A.; Walker, P.; Ahmad, S. Proenkephalin A gene products activate a new family of sensory neuron - specific GPCRs. *Nat. Neurosci.* **2002**, *5*, 201-209.
- (227) Solleti, S. K.; Bhattacharya, S.; Ahmad, A.; Wang, Q.; Mereness, J.; Rangasamy, T.; Mariani, T. J. MicroRNA expression profiling defines the impact of electronic cigarettes on human airway epithelial cells. *Sci. Rep.* **2017**, *7*, 1081.
- (228) Yoshihara, M.; Ohmiya, H.; Hara, S.; Kawasaki, S.; Hayashizaki, Y.; Itoh, M.; Kawaji, H.; Tsujikawa, M.; Nishida, K. Discovery of molecular markers to discriminate corneal endothelial cells in the human body. *PLoS ONE.* **2015**, *10*.
- (229) Kaisho, Y.; Watanabe, T.; Nakata, M.; Yano, T.; Yasuhara, Y.; Shimakawa, K.; Mori, I.; Sakura, Y.; Terao, Y.; Matsui, H.; Taketomi, S. Transgenic rats overexpressing the human MrgX3 gene show cataracts and an abnormal skin phenotype. *Biochem. Biophys. Res. Commun.* **2005**, *330*, 653-657.
- (230) Klotz, K. N.; Lohse, M. J.; Schwabe, U.; Cristalli, G.; Vittori, S.; Grifantini, M. 2-Chloro-N6-[³H]cyclopentyladenosine (3HCCPA)--a high affinity agonist radioligand for A₁ adenosine receptors. *N-S Arch. Pharmacol.* **1989**, *340*, 679-683.
- (231) Müller, C. E.; Diekmann, M.; Thorand, M.; Ozola, V. [³H]8-Ethyl-4-methyl-2-phenyl-(8R)-4,5,7,8-tetrahydro-1H-imidazo[2,1-*f*]-purin-5-one ([³H]PSB-11), a novel high-affinity antagonist radioligand for human A₃ adenosine receptors. *Bioorg. Med. Chem. Lett.* **2002**, *12*, 501-503.
- (232) Müller, C. E.; Maurinsh, J.; Sauer, R. Binding of ³HMSX-2 (3-(3-hydroxypropyl)-7-methyl-8-(*m*-methoxystyryl)-1-propargylxanthine) to rat striatal membranes - a new, selective antagonist radioligand for A_{2A} adenosine receptors. *Eur. J. Pharm. Sci.* **2000**, *10*, 259-265.
- (233) Flanagan, C. A. GPCR-radioligand binding assays. *Method. Cell Biol.* **2016**, *132*, 191-215.

- (234) Vachali, P. P.; Li, B.; Bartschi, A.; Bernstein, P. S. Surface plasmon resonance (SPR)-based biosensor technology for the quantitative characterization of protein-carotenoid interactions. *Arch. Biochem. Biophys.* **2015**, *572*, 66-72.
- (235) Salamon, Z.; Fitch, J.; Cai, M.; Tumati, S.; Navratilova, E.; Tollin, G. Plasmon-waveguide resonance studies of ligand binding to integral proteins in membrane fragments derived from bacterial and mammalian cells. *Anal. Biochem.* **2009**, *387*, 95-101.
- (236) Asmari, M.; Ratih, R.; Alhazmi, H. A.; El Deeb, S. Thermophoresis for characterizing biomolecular interaction. *Methods.* **2018**, *146*, 107-119.
- (237) Saetear, P.; Perrin, A. J.; Bartholdson, S. J.; Wanaguru, M.; Kussrow, A.; Bornhop, D. J.; Wright, G. J. Quantification of Plasmodium-host protein interactions on intact, unmodified erythrocytes by back-scattering interferometry. *Malar. J.* **2015**, *14*, 88.
- (238) Verzijl, D.; Riedl, T.; Parren, P. W. H. I.; Gerritsen, A. F. A novel label-free cell-based assay technology using bilayer interferometry. *Biosens. Bioelectron.* **2017**, *87*, 388-395.
- (239) Bartoschek, S.; Klabunde, T.; Defossa, E.; Dietrich, V.; Stengelin, S.; Griesinger, C.; Carlomagno, T.; Focken, I.; Wendt, K. U. Drug design for G-protein-coupled receptors by a ligand-based NMR method. *Angew. Chem. Int. Edit.* **2010**, *49*, 1426-1429.
- (240) Carlsson, J.; Yoo, L.; Gao, Z.-G.; Irwin, J. J.; Shoichet, B. K.; Jacobson, K. A. Structure-based discovery of A_{2A} adenosine receptor ligands. *J. Med. Chem.* **2010**, *53*, 3748-3755.
- (241) Rajarathnam, K.; Rösgen, J. Isothermal titration calorimetry of membrane proteins - progress and challenges. *Biochim. Biophys. Acta.* **2014**, *1838*, 69-77.
- (242) Stoddart, L. A.; White, C. W.; Nguyen, K.; Hill, S. J.; Pflieger, K. D. G. Fluorescence- and bioluminescence-based approaches to study GPCR ligand binding. *Br. J. Pharmacol.* **2016**, *173*, 3028-3037.
- (243) Albani, J. R. *Structure and dynamics of macromolecules*; Elsevier: Amsterdam, Oxford, 2004.
- (244) Baidur, N.; Triggler, D. J. Concepts and progress in the development and utilization of receptor-specific fluorescent ligands. *Med. Res. Rev.* **1994**, *14*, 591-664.
- (245) Rücker, G.; Neugebauer, M.; Willems, G. G. *Instrumentelle pharmazeutische Analytik*; Wiss. Verl.-Ges: Stuttgart, 2013.
- (246) Colón, W. [39] Analysis of protein structure by solution optical spectroscopy. In *Amyloid, prions, and other protein aggregates*. Wetzel, R., Ed.; Academic Press: San Diego; pp. 605-632.
- (247) White, C. E.; Argauer, R. J. *Fluorescence analysis*; Dekker: New York, 1970.

- (248) Park, J. W.; Kim, Y.; Lee, K.-J.; Kim, D. J. Novel cyanine dyes with vinylsulfone group for labeling biomolecules. *Bioconjugate Chem.* **2012**, *23*, 350-362.
- (249) Hall, L. M.; Gerowska, M.; Brown, T. A highly fluorescent DNA toolkit. Synthesis and properties of oligonucleotides containing new Cy3, Cy5 and Cy3B monomers. *Nucleic Acids Res.* **2012**, *40*, e108.
- (250) Dale, C. L.; Hill, S. J.; Kellam, B. New potent, short-linker BODIPY-630/650™ labelled fluorescent adenosine receptor agonists. *Med. Chem. Commun.* **2012**, *3*, 333-338.
- (251) Pflieger, K. D. G.; Eidne, K. A. Illuminating insights into protein-protein interactions using bioluminescence resonance energy transfer (BRET). *Nat. Methods.* **2006**, *3*, 165-174.
- (252) Stoddart, L. A.; Johnstone, E. K. M.; Wheal, A. J.; Goulding, J.; Robers, M. B.; Machleidt, T.; Wood, K. V.; Hill, S. J.; Pflieger, K. D. G. Application of BRET to monitor ligand binding to GPCRs. *Nat. Methods.* **2015**, *12*, 661-663.
- (253) Waggoner, A. S.; Melamed, M. R.; Lindmo, T.; Mendelsohn M. L. "Fluorescent probes for cytometry," in flow cytometry and sorting, Eds., 2nd ed., Wiley-Liss, New York, 1990, 209-225.
- (254) Johannes, H.-H. Cyanine: Direkte Funktionalisierung, Oligomerisierung, linear und nichtlinear optische Eigenschaften. **2000**.
- (255) Pawley, J. B., Ed. *Handbook of biological confocal microscopy*; Springer: New York, NY, 2006.
- (256) Baker, J. G.; Hall, I. P.; Hill, S. J. Pharmacology and direct visualization of BODIPY-TMR-CGP: a long-acting fluorescent beta2-adrenoceptor agonist. *Br. J. Pharmacol.* **2003**, *139*, 232-242.
- (257) Brown, M.; Wittwer, C. Flow Cytometry. Principles and clinical applications in hematology. *Clin. Chem.* **2000**, *46*, 1221-1229.
- (258) Kozma, E.; Gizewski, E. T.; Tosh, D. K.; Squarzialupi, L.; Auchampach, J. A.; Jacobson, K. A. Characterization by flow cytometry of fluorescent, selective agonist probes of the A₃ adenosine receptor. *Biochem. Pharmacol.* **2013**, *85*, 1171-1181.
- (259) Tosh, D. K.; Chinn, M.; Ivanov, A. A.; Klutz, A. M.; Gao, Z.-G.; Jacobson, K. A. Functionalized congeners of A₃ adenosine receptor-selective nucleosides containing a bicyclo[3.1.0]hexane ring system. *J. Med. Chem.* **2009**, *52*, 7580-7592.
- (260) Dacres, H.; Michie, M.; Wang, J.; Pflieger, K. D. G.; Trowell, S. C. Effect of enhanced Renilla luciferase and fluorescent protein variants on the Förster distance of Bioluminescence resonance energy transfer (BRET). *Biochem. Bioph. Res. Commun.* **2012**, *425*, 625-629.

- (261) Kenworthy, A. K. Imaging protein-protein interactions using fluorescence resonance energy transfer microscopy. *Methods*. **2001**, *24*, 289-296.
- (262) Ilien, B.; Franchet, C.; Bernard, P.; Morisset, S.; Odile Weill, C.; Bourguignon, J.-J.; Hibert, M.; Galzi, J.-L. Fluorescence resonance energy transfer to probe human M1 muscarinic receptor structure and drug binding properties. *J. Neurochem*. **2003**, *85*, 768-778.
- (263) Hall, M. P.; Unch, J.; Binkowski, B. F.; Valley, M. P.; Butler, B. L.; Wood, M. G.; Otto, P.; Zimmerman, K.; Vidugiris, G.; Machleidt, T.; Robers, M. B.; Benink, H. A.; Eggers, C. T.; Slater, M. R.; Meisenheimer, P. L.; Klaubert, D. H.; Fan, F.; Encell, L. P.; Wood, K. V. Engineered luciferase reporter from a deep sea shrimp utilizing a novel imidazopyrazinone substrate. *ACS Chem. Biol*. **2012**, *7*, 1848-1857.
- (264) Widder, E. A. Bioluminescence in the ocean: origins of biological, chemical, and ecological diversity. *Science*. **2010**, *328*, 704-708.
- (265) Kocan, M.; See, H. B.; Seeber, R. M.; Eidne, K. A.; Pflieger, K. D. G. Demonstration of improvements to the bioluminescence resonance energy transfer (BRET) technology for the monitoring of G protein-coupled receptors in live cells. *J. Biomol. Screen*. **2008**, *13*, 888-898.
- (266) Machleidt, T.; Woodroffe, C. C.; Schwinn, M. K.; Méndez, J.; Robers, M. B.; Zimmerman, K.; Otto, P.; Daniels, D. L.; Kirkland, T. A.; Wood, K. V. NanoBRET - A novel BRET platform for the analysis of protein-protein interactions. *ACS Chem. Biol*. **2015**, *10*, 1797-1804.
- (267) Pflieger, K. D. G.; Seeber, R. M.; Eidne, K. A. Bioluminescence resonance energy transfer (BRET) for the real-time detection of protein-protein interactions. *Nat. Protoc*. **2006**, *1*, 337-345.
- (268) Comeo, E.; Kindon, N. D.; Soave, M.; Stoddart, L. A.; Kilpatrick, L. E.; Scammells, P. J.; Hill, S. J.; Kellam, B. Subtype-selective fluorescent ligands as pharmacological research tools for the human adenosine A_{2A} receptor. *J. Med. Chem*. **2020**, *63*, 2656-2672.
- (269) Förster; T. 10th Spiers memorial lecture - Transfer mechanisms of electronic excitation. *Discuss. Faraday Soc*. **1959**, 7-17.
- (270) Wu, P.; Brand, L. Resonance energy transfer: methods and applications. *Anal. Biochem*. **1994**, *218*, 1-13.
- (271) Carraway, K. L.; Koland, J. G.; Cerione, R. A. Location of the epidermal growth factor binding site on the EGF receptor. A resonance energy transfer study. *Biochemistry*. **1990**, *29*, 8741-8747.
- (272) Fay, S. P.; Domalewski, M. D.; Sklar, L. A. Evidence for protonation in the human neutrophil formyl peptide receptor binding pocket. *Biochemistry*. **1993**, *32*, 1627-1631.

- (273) Jacobson, K. A. Functionalized congener approach to the design of ligands for G protein-coupled receptors (GPCRs). *Bioconjugate Chem.* **2009**, *20*, 1816-1835.
- (274) Vernall, A. J.; Hill, S. J.; Kellam, B. The evolving small-molecule fluorescent-conjugate toolbox for Class A GPCRs. *Br. J. Pharmacol.* **2014**, *171*, 1073-1084.
- (275) Banerjee, S. S.; Aher, N.; Patil, R.; Khandare, J. Poly(ethyleneglycol)-prodrug conjugates: Concept, design, and applications. *J. Drug Deliv.* **2012**, *2012*, 103973.
- (276) Veronese, F. M.; Pasut, G. PEGylation, successful approach to drug delivery. *Drug Discov. Today.* **2005**, *10*, 1451-1458.
- (277) Kozma, E.; Kumar, T. S.; Federico, S.; Phan, K.; Balasubramanian, R.; Gao, Z.-G.; Paoletta, S.; Moro, S.; Spalluto, G.; Jacobson, K. A. Novel fluorescent antagonist as a molecular probe in A₃ adenosine receptor binding assays using flow cytometry. *Biochem. Pharmacol.* **2012**, *83*, 1552-1561.
- (278) Kozma, E.; Jayasekara, P. S.; Squarcialupi, L.; Paoletta, S.; Moro, S.; Federico, S.; Spalluto, G.; Jacobson, K. A. Fluorescent ligands for adenosine receptors. *Bioorg. Med. Chem. Lett.* **2013**, *23*, 26-36.
- (279) Federico, S.; Lassiani, L.; Spalluto, G. Chemical probes for the adenosine receptors. *Pharmaceuticals.* **2019**, *12*, 168.
- (280) Comeo, E.; Trinh, P.; Nguyen, A. T.; Nowell, C. J.; Kindon, N. D.; Soave, M.; Stoddart, L. A.; White, J. M.; Hill, S. J.; Kellam, B.; Halls, M. L.; May, L. T.; Scammells, P. J. Development and application of subtype-selective fluorescent antagonists for the study of the human adenosine A₁ receptor in living cells. *J. Med. Chem.* **2021**.
- (281) Bouzo-Lorenzo, M.; Stoddart, L. A.; Xia, L.; IJzerman, A. P.; Heitman, L. H.; Briddon, S. J.; Hill, S. J. A live cell NanoBRET binding assay allows the study of ligand-binding kinetics to the adenosine A₃ receptor. *Purinerg. Signal.* **2019**, *15*, 139-153.
- (282) Federico, S.; Margiotta, E.; Moro, S.; Kozma, E.; Gao, Z.-G.; Jacobson, K. A.; Spalluto, G. Conjugable A₃ adenosine receptor antagonists for the development of functionalized ligands and their use in fluorescent probes. *Eur. J. Med. Chem.* **2020**, *186*, 111886.
- (283) Stoddart, L. A.; Vernall, A. J.; Briddon, S. J.; Kellam, B.; Hill, S. J. Direct visualization of internalization of the adenosine A₃ receptor and localization with arrestin3 using a fluorescent agonist. *Neuropharmacology.* **2015**, *98*, 68-77.
- (284) Barresi, E.; Giacomelli, C.; Daniele, S.; Tonazzini, I.; Robello, M.; Salerno, S.; Piano, I.; Cosimelli, B.; Greco, G.; Da Settimo, F.; Martini, C.; Trincavelli, M. L.; Taliani, S. Novel fluorescent triazinobenzimidazole derivatives as probes for labeling human A₁ and A_{2B} adenosine receptor subtypes. *Bioorg. Med. Chem.* **2018**, *26*, 5885-5895.

- (285) Dost, T. L.; Gressel, M. T.; Henary, M. Synthesis and optical properties of pentamethine cyanine dyes with carboxylic acid moieties. *Anal. Chem. Insights*. **2017**, *12*, 1177390117711938.
- (286) Kim, E.; Park, S. B. Discovery of new synthetic dyes: Targeted synthesis or combinatorial approach? In *Advanced fluorescence reporters in chemistry and biology I : fundamentals and molecular design*.
- (287) Ernst, L. A.; Gupta, R. K.; Mujumdar, R. B.; Waggoner, A. S. Cyanine dye labeling reagents for sulfhydryl groups. *Cytometry*. **1989**, *10*, 3-10.
- (288) Mason, S. J.; Hake, J. L.; Nairne, J.; Cummins, W. J.; Balasubramanian, S. Solid-phase methods for the synthesis of cyanine dyes. *J. Org. Chem.* **2005**, *70*, 2939-2949.
- (289) Mujumdar, R. B.; Ernst, L. A.; Mujumdar, S. R.; Waggoner, A. S. Cyanine dye labeling reagents containing isothiocyanate groups. *Cytometry*. **1989**, *10*, 11-19.
- (290) Wolf, N.; Kersting, L.; Herok, C.; Mihm, C.; Seibel, J. High-yielding water-soluble asymmetric cyanine dyes for labeling applications. *J. Org. Chem.* **2020**, *85*, 9751-9760.
- (291) Yuan, L.; Lin, W.; Zheng, K.; He, L.; Huang, W. Far-red to near infrared analyte-responsive fluorescent probes based on organic fluorophore platforms for fluorescence imaging. *Chem. Soc. Rev.* **2013**, *42*, 622-661.
- (292) He, S.; Song, J.; Qu, J.; Cheng, Z. Crucial breakthrough of second near-infrared biological window fluorophores: design and synthesis toward multimodal imaging and theranostics. *Chem. Soc. Rev.* **2018**, *47*, 4258-4278.
- (293) Osterman, H. L.; Schutz-Geschwender, A. *Near-infrared fluorescence imaging: Seeing beyond the visible with IRDye infrared dyes*: NE, USA, 2012.
- (294) Ciruela, F.; Fernández-Dueñas, V.; Jacobson, K. A. Lighting up G protein-coupled purinergic receptors with engineered fluorescent ligands. *Neuropharmacology*. **2015**, *98*, 58-67.
- (295) Ciruela, F.; Jacobson, K. A.; Fernández-Dueñas, V. Portraying G protein-coupled receptors with fluorescent ligands. *ACS Chem. Biol.* **2014**, *9*, 1918-1928.
- (296) Yuan, L.; Lin, W.; Yang, Y.; Chen, H. A unique class of near-infrared functional fluorescent dyes with carboxylic-acid-modulated fluorescence ON/OFF switching: rational design, synthesis, optical properties, theoretical calculations, and applications for fluorescence imaging in living animals. *J. Am. Chem. Soc.* **2012**, *134*, 1200-1211.
- (297) Sheng, Z.; Hu, D.; Xue, M.; He, M.; Gong, P.; Cai, L. Indocyanine Green Nanoparticles for Theranostic Applications. *Nano-Micro Lett.* **2013**, *5*, 145-150.

4. Results and discussion

4.1. Part I: Exploration of *N*-acyl-8-(4-piperazine-1-sulfonyl)phenylxanthines as potent and selective adenosine A_{2B} receptor antagonists

Exploration of *N*-acyl-8-(4-piperazine-1-sulfonyl)phenylxanthines as potent and selective adenosine A_{2B} receptor antagonists

Tim Harms,¹ Jörg Hockemeyer,¹ Christin Vielmuth,¹ Sonja Hinz,^{1,2} and Christa E. Müller^{1,*}

¹PharmaCenter Bonn, Pharmaceutical Institute, Pharmaceutical Sciences Bonn (PSB), Pharmaceutical & Medicinal Chemistry, University of Bonn, An der Immenburg 4, 53121, Bonn, Germany.

²Institute of Pharmacology and Toxicology, Center for Biomedical Education and Research (ZBAF), School of Medicine, Faculty of Health, University of Witten/Herdecke, D-58453 Witten, Germany.

Email: tim.harms@uni-bonn.de ; christa.mueller@uni-bonn.de

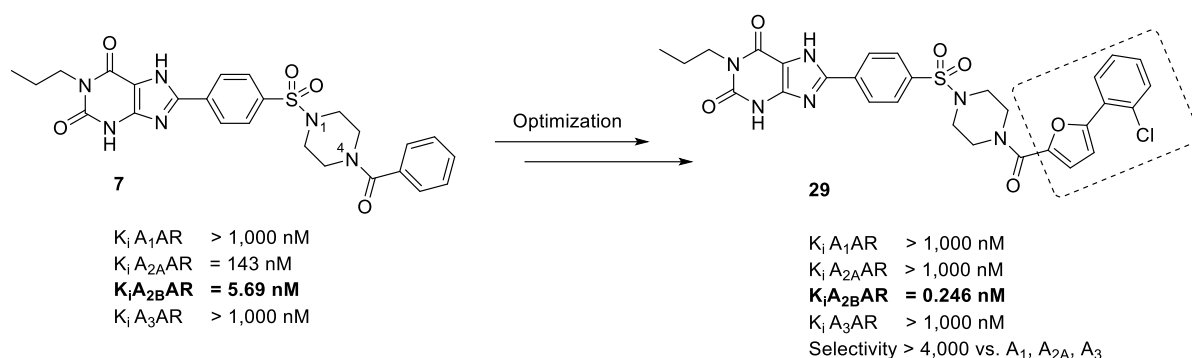
4.1.1. Keywords:

Antagonists, adenosine A_{2B} receptor, xanthines, reaction products, acylation

4.1.2. Abstract

The A_{2B} adenosine receptor (A_{2B}AR) has been investigated as a novel target for the treatment of cancer, inflammatory diseases and further indications since its blockade results in antiproliferative, antimetastatic, antiangiogenic, and immunostimulatory effects. In this study, we explored the structure-activity relationships of 8-(4-piperazine-1-sulfonyl)phenylxanthine derivatives by introducing a variety of residues at the position 4 of the piperazine structure by straightforward acylation. Based on prototype **7**, 8-(4-((4-(5-(2-chlorophenyl)furan-2-carbonyl)piperazine-1-yl)sulfonyl)phenyl)-1-propyl-3,7-dihydro-1*H*-purine-2,6-dione (**29**) could be identified as the most potent and selective A_{2B}-antagonist among the series with a subnanomolar K_i value of 0.246 nM and >4,000-fold selectivity versus all other AR subtypes.

4.1.2.1. Graphical abstract



4.1.3. Introduction

Adenosine A_{2B} receptors (A_{2B}ARs) belong to the superfamily of G protein-coupled receptors (GPCRs). Four different AR subtypes exist, designated A₁-, A_{2A}-, A_{2B}- and A₃ARs.^{1;2} The receptor is ubiquitously expressed but mostly silent under normal physiological conditions since it has the lowest affinity for adenosine among the four AR subtypes. However, it is considerably stimulated under pathological conditions including hypoxia, inflammation or cancer, when extracellular adenosine levels increase up to 100-fold and A_{2B}AR expression levels are upregulated.^{1;3-5} A_{2B}AR antagonists are currently in the focus of interest as therapeutics for cancer, inflammatory diseases, autoimmune diseases, diabetes, Alzheimer's disease and further indications.^{3;5-10} The plant alkaloid caffeine (Figure 1, **1**), a widely consumed central stimulatory drug present in tea and coffee, is therapeutically used e.g. in analgesic drugs in combination with paracetamol (acetamidophen) and/or non-steroidal anti-inflammatory drugs. The analgesic activity of caffeine is due to its A_{2B}AR blockade.^{11;12} Caffeine inhibits all four AR subtypes with micromolar affinity and is thus only moderately potent and non-selective.¹³ Alkylation at N1 and/or N3 and particularly substitution of position 8 of the xanthine core structure have yielded subtype-selective AR antagonists. PSB-1115 (**2**) is a water-soluble antagonist with increased potency and subtype selectivity that has been widely used for *in vivo* studies.^{11;14-17} Further optimization led to sulfonamide-derivatives of **2** showing strongly increased potency and selectivity.^{18;19} PSB-603 (**3a**) has become a tool compound for studying A_{2B}ARs antagonist in human and in rodents due to its superior potency and selectivity across species.^{13;20} Its tritiated derivative [³H]PSB-603 is frequently employed in radioligand binding studies.^{3;13;18;20} Recently, PSB-1901 (**3b**) was reported, with a K_i value of 0.0835 nM, and >10,000-fold selectivity versus all other AR subtypes, it is one of the most potent A_{2B}AR antagonist known thus far.¹⁸ Xanthine-based antagonists bearing a pyrazole core structure, e.g. **4**, displayed high binding affinity (K_i = 1 nM) and 100-fold selectivity for the A_{2B}AR, showing high oral bioavailability in C57BL/6J mice at 10 mg/kg.²¹ Besides xanthines, various non-xanthine scaffolds have been developed as A_{2B}AR antagonists.²²⁻²⁴

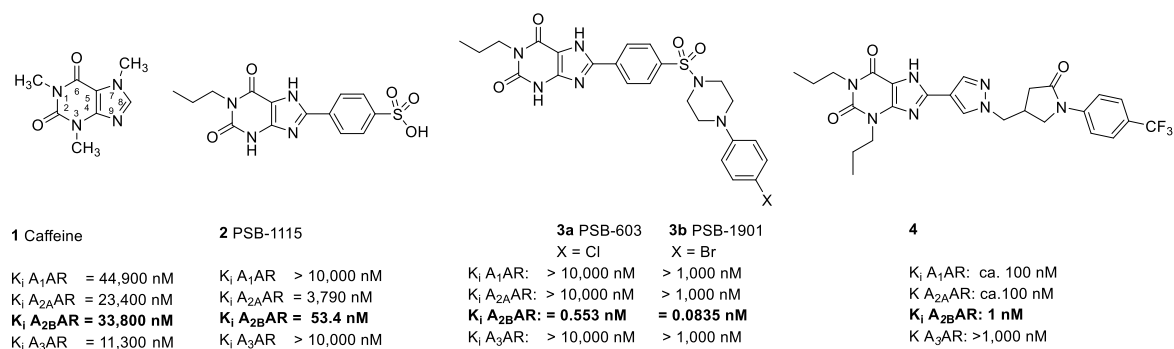


Figure 1. Selected xanthine-based A_{2B}AR antagonists and their affinities for human AR subtypes.^{13,14,18,20,21}

While phenyl- and benzyl-substituted 8-(4-piperazine-1-sulfonyl)phenyl-1-propylxanthines are well established scaffolds for xanthine-based A_{2B}AR antagonists (for prototypes see **5** and **6**, Figure 2), compound **7** is the only benzoyl-substituted 8-(4-piperazine-1-sulfonyl)phenyl-1-propylxanthine derivative that has been described thus far.^{18,19} It is a potent A_{2B}AR antagonist ($K_i = 5.69$ nM) with selectivity versus the other AR subtypes. Due to its promising pharmacological properties and straightforward synthetic accessibility, **7** was selected as a lead structure for the synthesis and exploration of novel 8-(4-acylpiperazine-1-sulfonyl)phenyl-1-propylxanthines as A_{2B}AR antagonists. In the present study, we modified the acyl residue of **7** and studied structure-activity relationships (SARs).

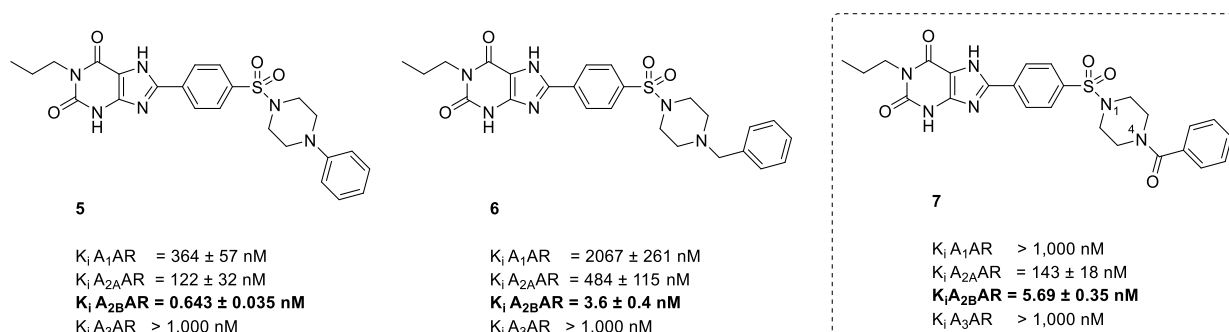


Figure 2. Affinities of xanthine-8-yl-benzenesulfonamide derivatives **5**, **6** and **7** at the human adenosine receptor subtypes.^{18,19}

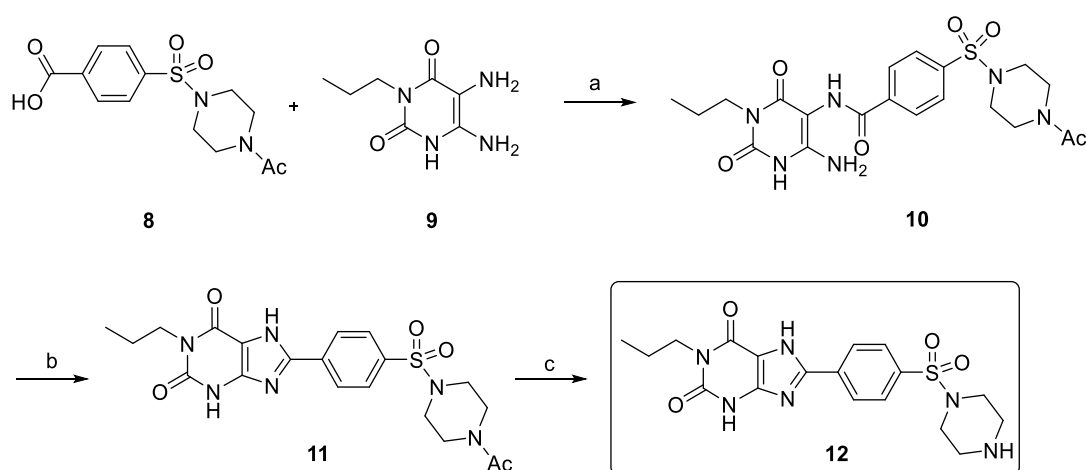
4.1.4. Results and discussion

4.1.4.1. Synthesis of 8-(4-acylpiperazine-1-sulfonyl)phenyl-1-propylxanthines

8-(Piperazine-1-sulfonyl)phenyl-1-propylxanthine (**12**), unsubstituted at the N₄-position of the piperazine ring, was prepared as a suitable starting compound. Substitution at N₁ (propyl), N₃ (H) and N₇ (H) was kept constant, since this substitution pattern was previously found to be optimal for high A_{2B}AR affinity and selectivity.^{18,19} This new scaffold allows the straightforward introduction of substituents via acylation of the piperazine-4-NH group. This procedure is

milder, more economic and results in better yields than e.g. the aminolysis of *p*-nitrophenoxysulfonylphenylxanthines that has been previously used to prepare 8-(4-piperazine-1-sulfonyl)phenylxanthine derivatives.^{13;18-20}

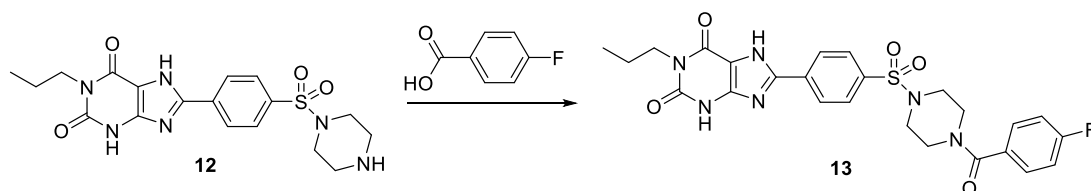
Amide formation of 4-((4-acetylpiperazine-1-yl)sulfonyl)benzoic acid (**8**)²⁵ and 5,6-diamino-3-propyluracil (**9**)²⁶ afforded intermediate **10**. Treatment of **10** with phosphorus pentoxide in *N,N*-dimethylformamide (DMF) at 100 °C afforded **11** as previously described.¹⁸ Saponification of **11** employing aqueous NaOH solution led to the formation of the desired precursor **12** (see Scheme 1).



Scheme 1. Synthesis of 8-(piperazinylsulfonyl)phenyl-1-propylxanthine (**12**).

Reaction conditions: (a) 1-ethyl-3-(3-dimethylaminopropyl)carbodiimide hydrochloride (EDC • HCl), methanol (MeOH), rt, 2 h. (b) P₂O₅, DMF, reflux, 15 min. (c) H₂O / ethanol (EtOH), NaOH, 60 °C, 5 h.^{18;25;26}

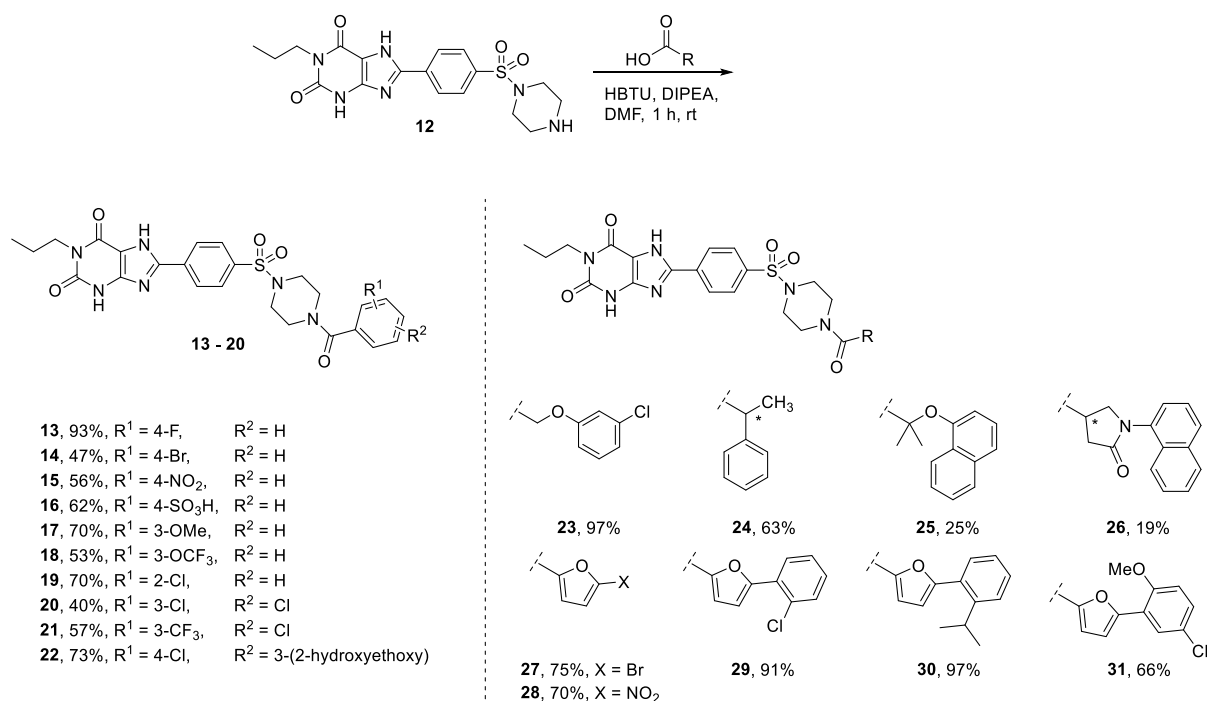
The piperazine-NH function of **12** was subsequently acetylated using a variety of carboxylic acid derivatives. Reaction of **12** with 4-fluorobenzoic acid (affording **13**) was initially performed as a test system to optimize the conditions for amide formation of the corresponding 8-(4-acetylpiperazine-1-sulfonyl)phenyl-1-propylxanthine derivatives (see Scheme 2).



Scheme 2. Synthesis of derivative 8-(4-((4-(4-fluorobenzoyl)piperazin-1-yl)sulfonyl)phenyl)-1-propyl-3,7-dihydro-1*H*-purine-2,6-dione (**13**)

Precursor **12** and 4-fluorobenzoic acid were reacted in a 1 : 1.3 ratio under different conditions at rt. The reactions were monitored by thin-layer chromatography (TLC). The main challenge

for the coupling reaction was the poor solubility of precursor **12**. An initial approach employing 4-fluorobenzoyl chloride in the presence of N,N-diisopropylethylamine (DIPEA) in DMF resulted in too many side products. Using EDC • HCl as a condensation reagent in tetrahydrofuran (THF) or a mixture of MeOH and dimethyl sulfoxide (DMSO) (1 : 1) led to incomplete conversion of the starting material. Satisfactory results were only obtained when DMF was used as a solvent. The best results were obtained when 2-(1*H*-benzotriazol-1-yl)-1,1,3,3-tetramethyluronium hexafluorophosphate (HBTU) was used as a coupling reagent in the presence of DIPEA as a base in DMF. After one hour of stirring at rt, TLC analysis showed completion of the reaction. Product **13** was obtained by precipitation with water from the reaction mixture in an excellent yield of 93% and high purity of 97%. These conditions could subsequently be successfully applied to a variety of carboxylic acid derivatives affording 19 new 8-(4-acylpiperazine-1-sulfonyl)phenyl-1-propylxanthines (**13-31**, see scheme 3). The employed carboxylic acid derivatives were selected according to the following criteria: (i) similarity to selected 8-(4-benzylpiperazine-1-sulfonyl)phenyl-1-propyl xanthines¹⁸ (**13,14** and **17**), (ii) new substitution patterns on the benzoyl moiety (**15, 18, 19-22**), including diversity e.g. regarding sterical properties (**23 - 26**). Benzoylsulfonate **16** was designed to enhance water solubility. Additionally, different furanyl-substituted derivatives were selected to replace the phenyl ring (**27-31**). The carboxylic acids were commercially available or prepared according to the literature.^{27:28}



Scheme 3. Synthesis of 8-(4-acylpiperazine-1-sulfonyl)phenyl-1-propylxanthines **13-31** and yields.

The final products could be obtained in yields ranging from 19-97%. Depending on the physicochemical properties of the employed carboxylic acids, the purification of the products had to be adapted. In all cases the crude products were precipitated by the addition of water. Further purification (if needed) was achieved by reprecipitation from DMF. Some yields were decreased by the necessity of reprecipitation. Product **25** (25% yield) and **26** (19% yield) were particularly hard to purify while the furan derivatives were easily obtained in pure form by a single precipitation. Only the most polar compound of the present series, sulfonate **16**, was purified by column chromatography.

4.1.4.2. Biological evaluation

4.1.4.2.1. Radioligand binding studies

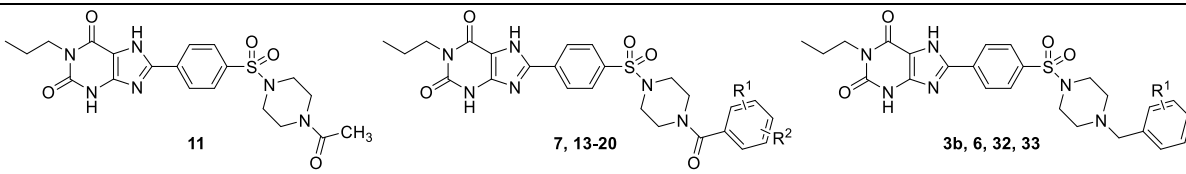
The synthesized 8-(4-acylpiperazine-1-sulfonyl)phenyl-1-propylxanthines **13-31** were investigated in radioligand binding studies at all four human AR subtypes stably expressed in human embryonic kidney (HEK-293) or Chinese hamster ovary (CHO) cells versus the following receptor subtype-selective radioligands: [³H]2-Chloro-*N*6-cyclo-pentyladenosine ([³H]CCPA)²⁹ for the A₁AR, [³H](*E*)-3-(3-hydroxypropyl)-8-(2-(*m*-methoxyphenyl)vinyl)-7-methyl-1-prop-2-ynyl-3,7-dihydropurine-2,6-dione ([³H]MSX-2)³⁰ for the A_{2A}AR, [³H]8-(4-(4-(4-chlorophenyl)piperazine-1-sulfonyl)phenyl)-1-propyl-3,7-dihydropurine-2,6-dione ([³H]PSB-603)¹³ for the A_{2B}AR and [³H]2-phenyl-8-ethyl-4-methyl-(8*R*)-4,5,7,8-tetrahydro-1*H*-imidazo[2.1-*f*]purin-5-one ([³H]PSB-11)³¹ for the A₃AR. The radioligand receptor binding assays were performed as previously described.^{18;20;32;33}

4.1.4.2.2. Structure-activity relationships analysis of 8-(4-acylpiperazine-1-sulfonyl)phenyl-1-propylxanthines

Most of the investigated 8-(4-acylpiperazine-1-sulfonyl)phenyl-1-propylxanthines (except for the sulfonate derivative **16**, K_i A_{2B} 460 nM) displayed high affinities at the A_{2B}AR with K_i values in the low nanomolar (**13**, **15**, **17**, **19**, **22**, **23-27**) or subnanomolar range (**14**, **18**, **20**, **21**, **29-31**). The moderate potency of **16** indicates that the A_{2B}AR does not well tolerate polar or charged moieties on the benzoyl residue. Introduction of small lipophilic groups led in most cases to improved affinities and selectivities in comparison to the unsubstituted parent compound **7**¹⁸ (K_i A_{2B} 5.69 nM) with regard to A_{2B}-affinity and A_{2B}/A_{2A}-selectivity. Compounds **14**, **18**, **20** and **21**, bearing halogen(-containing) substituents at the *meta*-and/or *para*-position of the benzoyl moiety, showed subnanomolar potency for the A_{2B}AR. The trifluoromethoxy group of **18** resulted in an 8-fold higher potency and 9-fold higher selectivity than the very similar methoxy group of **17**. *Ortho*-substitution of the benzoyl residue (see **19**, K_i A_{2B} 8.34 nM) was tolerated by the A_{2B}AR but did not seem to be beneficial in comparison to *meta* or *para*-substitution. Derivatives **18**, **20** and **21** showed very high selectivity (>800-fold). Compounds

23-26 showed similar K_i values between 1.46 nM and 6.95 nM despite being substituted with very diverse residues. Compound **22** exhibited a well tolerated 2-hydroxyethoxy chain in *meta*-position of the benzoyl residue ($K_i A_{2B}$ 4.72 nM), suggesting that the attachment of linkers for further modifications might be tolerated by the $A_{2B}AR$. The three 5-phenyl-2-furancarboxyl derivatives **29**, **30** and **31** showed particularly high potencies ($K_i A_{2B}$ 0.246 nM, 0.424 nM and 0.831 nM, respectively) and selectivity (>1000-fold) within this series. Compounds **27** and **28**, bearing comparably small substituents at the piperazine moiety, exhibited lower potency and only poor selectivity towards the $A_{2A}AR$. Acetyl derivative **11** showed high affinity for the $A_{2B}AR$ with moderate selectivity for the other AR subtypes. Hence, small substituents at the 4-position of the piperazine ring are tolerated but not beneficial, big lipophilic residues like disubstituted benzoyl- or 5-phenyl-2-furancarboxyl-moieties are strongly preferred. All tested compounds were inactive at the A_3AR ($K_i >1000$ nM), and except for **14**, **20** and **23**, most compounds also displayed K_i values >1000 nM at the A_1AR . Derivatives **15**, **19**, **22-24** and **26-28** showed only moderate selectivity towards the $A_{2A}AR$ and can almost be considered as dual-acting $A_{2A}/A_{2B}AR$ antagonists, making them interesting drug molecules for the treatment of cancer or Parkinson's Disease.⁷

Table 1. Binding affinities of xanthine derivatives **11**, **13-22**, **3b**, **6**, **32** and **33** at the human AR subtypes.

							
$K_i \pm SEM$ (nM)							
(or % inhibition of radioligand binding at 1 μ M)							
Compd	R ¹	R ²	A_1AR^a	$A_{2A}AR^b$	$A_{2B}AR^c$	A_3AR^d	Selectivity index ^e
11	-	-	>1000 (16%)	531 \pm 98	21.6 \pm 3.1	>1000 (16%)	25
Substitutions on the benzoyl ring							
7 ¹⁸	H	H	>1000 (15%)	143 \pm 18	5.69 \pm 0.35	>1000 (26%)	25
13	4-F	H	>1000 (35%)	304 \pm 106	2.20 \pm 0.23	>1000 (44%)	138
14	4-Br	H	612 \pm 88	91.9 \pm 13.2	0.820 \pm 0.191	>1000 (39%)	112

15	4-NO ₂	H	>1000 (36%)	73.9 ± 24.5	3.87 ± 0.66	>1000 (33%)	19
16	4-SO ₃ H	H	>1000 (6%)	>1000 (19%)	460 ± 157	>1000 (4%)	>0.46
17	3-OMe	H	>1000 (29%)	341 ± 85	3.68 ± 0.78	>1000 (9%)	93
18	3-OCF ₃	H	>1000 (32%)	395 ± 68	0.456 ± 0.04	>1000 (12%)	866
19	2-Cl	H	>1000 (38%)	304 ± 52	8.34 ± 3.29	>1000 (26%)	36
20	3-Cl	4-Cl	595 ± 176	374 ± 103	0.419 ± 0.012	>1000 (31%)	893
21	3-CF ₃	4-Cl	>1000 (44%)	408 ± 96	0.498 ± 0.039	>1000 (20%)	819
22	3-(2-hydroxy-ethoxy)	4-Cl	>1000 (30%)	300 ± 119	4.72 ± 0.50	>1000 (28%)	64
Benzyl-substitution analogues for comparison							
6¹⁹	H	H	2067 ± 261	484 ± 115	3.6 ± 0.4	>1000 (29%)	134
33^{13;18}	4-F	H	9090 ± 1260	255 ± 3.0	0.595 ± 0.101	758 ± 229	428
3b¹⁸	4-Br	H	>1000 (13%)	>1000 (33%)	0.0835 ± 0.0327	>1000 (29%)	>11,980
32¹⁸	3-OMe	H	205 ± 13	131 ± 15	1.28 ± 0.21	>1000 (27%)	102

^avs. [³H]CCPA (n = 3); ^bvs. [³H]MSX-2 (n = 3); ^cvs. [³H]PSB-603 (n = 3); ^dvs. [³H]PSB-11 (n = 3)

^eSelectivity index was calculated by dividing the second lowest K_i value by the A_{2B}AR K_i value.

Table 2. Binding affinities of xanthine derivatives **23-31** at the human AR subtypes.

K _i ± SEM (nM)					
(or % inhibition of radioligand binding at 1 μM)					
Compd	A ₁ AR ^a	A _{2A} AR ^b	A _{2B} AR ^c	A ₃ AR ^d	Selectivity index ^e
23	607 ± 44	32.7 ± 15.6	1.46 ± 0.09	>1000 (24%)	22
24	>1000 (29%)	232 ± 52	4.55 ± 0.65	>1000 (38%)	51
25	>1000 (26%)	574 ± 104	2.66 ± 0.73	>1000 (36%)	216
26	>1000 (42%)	195 ± 38	6.95 ± 1.1	>1000 (28%)	28
27	>1000 (37%)	217 ± 30	4.61 ± 1.79	>1000 (25%)	47
28	>1000 (18%)	335 ± 90	18.4 ± 8.7	>1000 (19%)	18
29	>1000 (15%)	>1000 (41%)	0.246 ± 0.014	>1000 (44%)	>4,065
30	>1000 (12%)	>1000 (22%)	0.424 ± 0.136	>1000 (15%)	>2,358
31	>1000 (19%)	>1000 (26%)	0.831 ± 0.221	>1000 (20%)	>1,203

^avs. [³H]CCPA (n = 3); ^bvs. [³H]MSX-2 (n = 3); ^cvs. [³H]PSB-603 (n = 3); ^dvs. [³H]PSB-11 (n = 3)

^eSelectivity index was calculated by dividing the second lowest K_i value by the A_{2B}AR K_i value.

Compounds **13**, **14** and **17** were designed for comparison with the previously reported corresponding 8-(4-**benzyl**piperazine-1-sulfonyl)phenyl-1-propylxanthines (see Table 1). Mostly, K_i values of related analogues (**7**¹⁸ vs. **5**¹⁹, **13** vs. **33**^{13;18}, **14** vs. **3b**¹⁸ and **18** vs. **32**¹⁸, respectively) were in a comparable range with regard to A_{2B}AR affinity and selectivity (see Table 1). Only **3b** was an outlier being significantly more potent and selective than **14**. All in all, substituted benzoyl residues and a variety of other acyl moieties attached to the 4-piperazine position of 8-(piperazine-1-sulfonyl)phenyl-1-propylxanthines are well tolerated by the A_{2B}AR. Mostly, benzoyl derivatives do not show lower potency or selectivity as compared to related benzyl-substituted 8-(piperazine-1-sulfonyl)phenyl-1-propylxanthines.¹⁸

4.1.5. Conclusions

In this study, we established SARs for *N*-acylated 8-(4-piperazine-1-sulfonyl)phenyl-1-propylxanthines as antagonists for the A_{2B}AR. Based on straightforward acylation of intermediate **12** bearing a piperazine moiety with an unsubstituted nitrogen atom, 19 novel compounds were synthesized and explored with regard to their affinities at all four human AR subtypes. Many of the derivatives displayed subnanomolar affinities at the A_{2B}AR and high selectivity. A comparison of selected acyl derivatives with established 8-(4-**benzyl**piperazine-1-sulfonyl)phenyl-1-propylxanthines revealed similar binding profiles. Derivatives bearing substituted 2-phenylfuran moieties (**29-31**) turned out to be particularly potent with subnanomolar affinities at the A_{2B}AR and over 1000-fold selectivity. Those derivatives can be considered as new lead structures for further explorations of the scaffold. The scaffold is particularly advantageous with regard to the preparation: precursor **12** can be synthesized with high yields, the subsequent acylation is straightforward and many benzoic acid derivatives are available, readily yielding a variety of derivatives in short time. This leads to a fast and easy exploration of SARs that can be presumably extrapolated to corresponding benzyl derivatives. The feasible introduction of new substituents via acylation of **12** could be a basis for the functionalization of the scaffold with fluorescent dyes or other reporter groups. Moreover, some derivatives (**15**, **19**, **23**, **26-28**) showed dual affinity for A_{2A}-/A_{2B}ARs.

4.1.6. Experimental section

4.1.6.1. General method

Reagents that were commercially available (e.g. from ABCR, Acros, Aldrich, Merck, and Sigma) were directly used without further purification. The used solvents were not purified or dried before usage. Thin-layer chromatography (TLC) (utilizing 0.2 mm silica gel-coated aluminum sheets with nanosilica gel 60 and fluorescence indicator UV₂₅₄; Merck) was used to control the reaction progress. Silica gel 60 (Merck) with a mesh size of 0.040-0.063 mm was utilized for column chromatography. Melting points were determined using open capillary tubes in a Wepa Apotec capillary melting-point apparatus (Wepa). Purity measurements were performed using HPLC-UV on a liquid chromatography-mass spectrometry (LC-MS) instrument (Applied Biosystems API 2000 LC-MS/MS, HPLCAgilent 1100) applying the following conditions: A mixture of methanol / H₂O / NH₃ (aq) (1:1:0.1) was used to dissolve the compounds at a concentration of 0.5 mg/ml. Each sample was injected (10 µl) into a Phenomenex Luna C18 HPLC column (column size of 50 mm × 2.00 mm; particle size of 3 µm). A gradient of water / methanol (containing 2 mM ammonium acetate) at a flow rate of 250 µl/min (from 90:10 to 0:100 over 20 min) was employed. Absorption from 200 to 950 nm was measured via a diode array UV/Vis detector. Mass spectra were determined with an API 2000 mass spectrometer (electron spray ion source, Applied Biosystems, Darmstadt,

Germany) coupled with an Agilent 1100 HPLC system. High resolution mass spectra were recorded on a micrOTOF-Q mass spectrometer (Bruker) with ESI-source coupled with a HPLC Dionex Ultimate 3000 (Thermo Scientific) using flow injection mode. Sample solution was injected to a flow of 0.3 ml/min acetonitrile containing 0.1 % acetic acid or 0.1 % formic acid. Positive or negative full scan MS was observed from 50 - 1000 m/z. Sodium acetate or sodium formate was used as calibrant. ^1H and ^{13}C NMR data were collected on a Bruker Avance 500 MHz NMR spectrometer at 500 MHz (^1H) and 126 MHz (^{13}C), or on a 600 MHz NMR spectrometer at 600 MHz (^1H) and 151 MHz (^{13}C) using DMSO- d_6 or CDCl_3 as solvents. Chemical shifts were reported in parts per million (ppm) in relation to the deuterated solvent, i.e., chloroform, δ ^1H : 7.26 ppm; ^{13}C : 77.36 ppm; DMSO, ^1H : 2.49 ppm; ^{13}C : 39.7 ppm. Coupling constants (J) were given in hertz, the spin multiplicities are given as s (singlet), d (doublet), t (triplet), m (multiplet), or in variations.

4.1.6.2. Synthesis

Synthesis of 4-((-acetylpiperazin-1-yl)sulfonyl)-*N*-(6-amino-2,4-dioxo-3-propyl-1,2,3,4-tetrahydropyrimidin-5-yl)benzamide (**10**)^{25;26}

A suspension of 4-((4-acetylpiperazin-1-yl)sulfonyl)benzoic acid (**8**) (3.9 g, 12.5 mmol), 5,6-diamino-3-propyluracil (**9**) (2.3 g, 12.5 mol) and EDC·HCl (3.1 g, 16.3 mol) in MeOH (75 ml) was stirred for 2 h at rt. The product was filtered off under reduced pressure, washed with MeOH (30 ml) and dried at 70°C affording 4.13 g (69%) of a colorless solid. ^1H NMR (500 MHz, DMSO- d_6) δ : 10.49 (s, 1H, NH), 9.12 (s, 1H, NH), 8.17 (d, 2H, $J = 8.3$ Hz, $\text{CH}_{\text{arom.}}$), 7.83 (d, 2H, $J = 8.3$ Hz, $\text{CH}_{\text{arom.}}$), 6.16 (s, 2H, NH_2), 3.66 (t, 2H, $J = 7.4$ Hz, NCH_2), 3.50 (s, 4H, NCH_2 (piperazine)), 2.91 (m NCH_2 (piperazine)), 1.92 (s, 3H, COCH_3), 1.50 (q, 2H, $J = 7.4$ Hz, CH_2CH_3), 0.83 (t, 3H, $J = 7.4$ Hz, CH_2CH_3) ppm. ^{13}C NMR (126 MHz, DMSO- d_6) δ : 168.5 ($\text{N}_{\text{(piperazine)}}\text{C}=\text{OCH}_3$), 165.3 ($\text{NHC}=\text{O}$), 160.7 (C_6 uracil), 150.6 (C_4 uracil), 150.1 (C_2 uracil), 139.0 ($\text{C}_{\text{arom.}}$), 137.1 ($\text{C}_{\text{arom.}}$), 130.4 ($\text{C}_{\text{arom.}}$), 129.1 ($\text{C}_{\text{arom.}}$), 127.9 ($\text{C}_{\text{arom.}}$), 127.4 ($\text{C}_{\text{arom.}}$), 86.7 (C_5 uracil), 46.2 (NCH_2), 45.9 (NCH_2 (piperazine)) 45.0 (NCH_2 (piperazine)), 41.1 (NCH_2 (piperazine)), 21.2 (COCH_3), 21.09 (CH_2CH_3), 11.3 (CH_2CH_3) ppm. MS (ESI) (m/z): 461.1 [$\text{M} + \text{H}$] $^+$. Mp.: 194 °C.

Synthesis of 8-(4-((4-acetylpiperazin-1-yl)sulfonyl)phenyl)-1-propyl-3,7-dihydro-1*H*-purine-2,6-dione (**11**)¹⁸

A solution of **10** (500 mg, 1.05 mmol) in DMF (2 ml) was treated with P_2O_5 (800 mg, 2.8 mmol) and stirred at 100°C for 15 min. Subsequently, water (20 ml) was added and the precipitated product was filtered off under reduced pressure, washed with water (20 ml) dried at 70 °C affording 446 mg (92 %) of a colorless solid. ^1H NMR (500 MHz, DMSO- d_6) δ : 10.49 (s br, 1H, NH), 9.12 (s br, 1H, NH), 8.17 (d, 2H, $J = 8.3$ Hz, $\text{CH}_{\text{arom.}}$), 7.83 (d, 2H, $J = 8.3$ Hz, $\text{CH}_{\text{arom.}}$), 6.16 (s, 2H, NH_2), 3.66 (t, 2H, $J = 7.4$ Hz, NCH_2), 3.50 (s, 4H, NCH_2 (piperazine)), 2.91 (d,

4H, $J = 28.9$ Hz, NCH_2 (piperazine)), 1.92 (s, 3H, COCH_3), 1.50 (q, 2H, $J = 7.4$ Hz, CH_2CH_3), 0.83 (t, 3H, $J = 7.4$ Hz, CH_2CH_3) ppm. ^{13}C NMR (126 MHz, $\text{DMSO}-d_6$) δ : 168.5 (N (piperazine) COCH_3), 165.3 (NHCO), 160.7 (C_6 uracil), 150.6 (C_4 uracil), 150.1 (C_2 uracil), 139.0 ($\text{C}_{\text{arom.}}$), 137.1 ($\text{C}_{\text{arom.}}$), 130.4 ($\text{C}_{\text{arom.}}$), 129.1 ($\text{C}_{\text{arom.}}$), 127.9 ($\text{C}_{\text{arom.}}$), 127.4 ($\text{C}_{\text{arom.}}$), 86.7 (C_5 uracil), 46.2 (NCH_2), 45.9 (NCH_2 (piperazine)) 45.0 (NCH_2 (piperazine)), 41.1 (NCH_2 (piperazine)), 21.2 (COCH_3), 21.09 (CH_2CH_3), 11.3 (CH_2CH_3) ppm. HPLC-UV (254 nm) ESI-MS, purity: 97.2%. MS (ESI) (m/z): 461.2 $[\text{M} + \text{H}]^+$. HRMS (ESI-TOF) m/z: $[\text{M} + \text{H}]^+$ calcd. for $\text{C}_{20}\text{H}_{24}\text{N}_6\text{O}_5\text{S}$ 461.1602 found 461.1580. Mp.: 223-224 °C.

Synthesis of 8-(4-(piperazine-1-ylsulfonyl)phenyl)-1-propyl-3,7-dihydro-1H-purine-2,6-dione (12)

A solution of **11** (440 mg, 0.96 mmol) in EtOH (15 ml) was treated with 2 M aqueous NaOH solution (15 ml) and heated to 60 °C for 5 h. Subsequently, the solution was neutralized with diluted aqueous HCl solution to pH 7. The precipitated product was filtered off under reduced pressure, washed with water (20 ml) and dried at 70 °C affording 371 mg (93 %) of a colorless solid. ^1H NMR (500 MHz, $\text{DMSO}-d_6$) δ : 8.31 (d, 2H, $J = 8.5$ Hz, $\text{CH}_{\text{arom.}}$), 7.81 (d, 2H, $J = 8.5$ Hz, $\text{CH}_{\text{arom.}}$), 3.85-3.78 (m, 2H, NCH_2), 2.84 (s, 4H, NCH_2 (piperazine)), 2.77-2.72 (m, 4H, NCH_2 (piperazine)), 1.57 (h, 2H, $J = 7.4$ Hz, CH_2CH_3), 0.87 (t, 3H, $J = 7.4$ Hz, CH_2CH_3) ppm. no NH-proton detectable. ^{13}C NMR (125 MHz, $\text{DMSO}-d_6$) δ : 163.1 (C_4 xanth.), 155.4 (C_8 xanth.), 151.2 (C_2 xanth.), 148.7 (C_6 xanth.), 147.9 ($\text{C}_{\text{arom.}}$), 135.3 ($\text{C}_{\text{arom.}}$), 134.0 ($\text{C}_{\text{arom.}}$), 128.4 (C_5 xanth.), 109.8 ($\text{C}_{\text{arom.}}$), 46.6 (NCH_2 (piperazine)), 44.6 (NCH_2 (piperazine)), 41.6 (NCH_2), 21.0 (CH_2CH_3), 11.3 (CH_2CH_3) ppm. MS (ESI) (m/z): 419.3 $[\text{M} + \text{H}]^+$.

General procedure for 8-(4-(4-acylpiperazine-1-sulfonyl)phenyl)-1-propylxanthines 13-31

A stirred solution of **12** (30 mg, 0.072 mmol), the appropriate carboxylic acid (0.094 mmol, 1.3 eq.), and DIPEA (31 μl , 0.18 mmol, 2.5 eq.) in DMF (1 ml), was treated with HBTU (36 mg, 0.094 mmol, 1.3 eq.). The solution was stirred at rt for 1 h and subsequently water (10 ml) was added to precipitate the product. The product was filtered off under reduced pressure, washed with water (50 ml) and dried at 70 °C. If necessary, reprecipitation was performed by dissolving the crude product in a minimum of DMF (ca. 1 ml) followed by treatment with water (10 ml). The solid thus obtained was isolated as described above.

8-(4-((4-(4-Fluorobenzoyl)piperazine-1-yl)sulfonyl)phenyl)-1-propyl-3,7-dihydro-1H-purine-2,6-dione (13)

Colorless solid, 36 mg, 93%. ^1H NMR (600 MHz, $\text{DMSO}-d_6$) δ : 14.01 (s, 1H, NH), 11.95 (s, 1H, NH), 8.33 (d, $J = 8.1$ Hz, 2H, $\text{CH}_{\text{arom.}}$), 7.85 (d, $J = 8.2$ Hz, 2H, $\text{CH}_{\text{arom.}}$), 7.40 (d, $J = 7.3$ Hz, 2H, $\text{CH}_{\text{arom.}}$), 7.21 (t, $J = 8.8$ Hz, 2H, $\text{CH}_{\text{arom.}}$), 3.82 (t, $J = 7.6$ Hz, 2H, NCH_2), 3.70-3.60 (br s, 4H, NCH_2), 3.02 (br s, 4H, NCH_2 Piperazine), 1.57 (q, $J = 7.9, 6.7$ Hz, 2H, CH_2CH_3), 0.87 (t, $J = 7.2$ Hz,

3H, CH₂CH₃) ppm. ¹³C NMR (151 MHz, DMSO-*d*₆) δ: 168.4 (C=O), 162.79 (d, ¹J_{CF} = 246.9 Hz, CF), 155.1 (C₄ xanth.), 151.1 (C₂ xanth.), 148.1 (C₈ xanth.), 147.7 (C₆ xanth.), 135.9 (C_{arom.}), 133.3 (C_{arom.}), 131.8 (C_{arom.}), 129.9 (d, ³J_{CF} = 8.6 Hz, C_{arom.}), 128.4 (C₅ xanth.), 127.2 (C_{arom.}), 115.50 (d, ²J_{CF} = 22 Hz, C_{arom.}), 108.8 (C_{arom.}), 46.6 (br, NCH₂ (piperazine)), 45.9 (NCH₂ (piperazine)), 41.7 (NCH₂), 21.0 (CH₂CH₃), 11.4 (CH₂CH₃) ppm. HPLC-UV (254 nm) ESI-MS, purity: 97.5%. MS (ESI) (m/z): 541.2 [M + H]⁺. HRMS (ESI-TOF) m/z: [M + H]⁺ calcd. for C₂₅H₂₅FN₆O₅S, 541.1664 found 541.1642. Mp.: 308-309 °C.

8-(4-((4-(4-Bromobenzoyl)piperazine-1-yl)sulfonyl)phenyl)-1-propyl-3,7-dihydro-1H-purine-2,6-dione (14)

Off-white solid, 20 mg, 47%. ¹H NMR (500 MHz, DMSO-*d*₆) δ: 13.99 (s, 1H, NH), 11.93 (s, 1H, NH), 8.33 (d, *J* = 8.2 Hz, 2H, CH_{arom.}), 7.84 (d, *J* = 8.2 Hz, 2H, CH_{arom.}), 7.58 (d, *J* = 8.1 Hz, 2H, CH_{arom.}), 7.30 (d, *J* = 8.1 Hz, 2H, CH_{arom.}), 3.82 (t, *J* = 7.6 Hz, 2H, NCH₂), 3.63 (br s, 4H, NCH₂ (piperazine)), 3.02 (s, 4H, NCH₂ (piperazine)), 1.58 (h, *J* = 7.8 Hz, 2H, CH₂CH₃), 0.88 (t, *J* = 7.4 Hz, 3H, CH₂CH₃) ppm. ¹³C NMR (126 MHz, DMSO-*d*₆) δ: 168.3 (C=O), 155.1 (C₄ xanth.), 151.1 (C₂ xanth.), 148.1 (C₈ xanth.), 147.7 (C₆ xanth.), 136.0 (C_{arom.}), 134.6 (C_{arom.}), 133.4 (C_{arom.}), 131.5 (C_{arom.}), 129.4 (C_{arom.}), 128.4 (C₅ xanth.), 127.2 (C_{arom.}), 123.2 (C_{arom.}), 108.8 (C_{arom.}), 46.5 (br m, NCH₂ (piperazine)), 45.8 (NCH₂ (piperazine)), 41.6 (NCH₂), around 41.0 (br m, NCH₂(piperazine)), 21.0 (CH₂CH₃), 11.3 (CH₂CH₃) ppm. HPLC-UV (254 nm) ESI-MS, purity: 95.5%. MS (ESI) (m/z): 601.2 [M + H]⁺. HRMS (ESI-TOF) m/z: [M + H]⁺ calcd. for C₂₅H₂₅BrN₆O₅S, 601.0863 found 601.0828. Mp.: 318-319.5°C.

8-(4-((4-(4-Nitrobenzoyl)piperazine-1-yl)sulfonyl)phenyl)-1-propyl-3,7-dihydro-1H-purine-2,6-dione (15)

Off-white solid, 23 mg, 56%. ¹H NMR (600 MHz, DMSO-*d*₆) δ: 13.96 (s, 1H, NH), 11.93 (s, 1H, NH), 8.33 (s, 2H, CH_{arom.}), 8.22 (s, 2H, CH_{arom.}), 7.84 (s, 2H, CH_{arom.}), 7.62 (s, 2H, CH_{arom.}), 3.81 (s, 2H, NCH₂), 3.72 (s, 2H, NCH₂ (piperazine)), 3.09 (s, 2H, NCH₂ (piperazine)), 2.98 (s, 4H, NCH₂ (piperazine)), 1.57 (s, 2H, CH₂CH₃), 0.89-0.85 (m, 3H, CH₂CH₃) ppm. ¹³C NMR (151 MHz, DMSO-*d*₆) δ: 167.7 (C=O), 155.1 (C₄ xanth.), 151.1 (C₂ xanth.), 148.6 (C_{arom.}), 148.3 (C₈ xanth.), 148.1 (C₆ xanth.), 142.1 (C_{arom.}), 136.2 (C_{arom.}), 133.9 (C_{arom.}), 128.9 (C_{arom.}), 128.7 (C₅ xanth.), 127.5 (C_{arom.}), 124.1 (C_{arom.}), 109.5 (C_{arom.}), 46.7 (NCH₂ (piperazine)), 46.0 (NCH₂ (piperazine)), 42.0 (NCH₂ (piperazine)), 41.3 (NCH₂), 21.0 (CH₂CH₃), 11.3 (CH₂CH₃) ppm. HPLC-UV (254 nm) ESI-MS, purity: 95.4%. MS (ESI) (m/z): 568.2 [M + H]⁺. HRMS (ESI-TOF) m/z: [M + H]⁺ calcd. for C₂₅H₂₅N₇O₇S, 568.1609 found 568.1603. Mp.: 320-321 °C.

4-(4-((4-(2,6-Dioxo-1-propyl-2,3,6,7-tetrahydro-1H-purine-8-yl)phenyl)sulfonyl)piperazine-1-carbonyl)benzenesulfonic acid (16)

Compound **16** was synthesized according to the general procedure starting with 4-sulfobenzoic acid potassium salt and compound **12**. Deviating from the general, procedure the product was precipitated by diluted hydrochloric acid (10 ml). The crude product **16** was purified by column chromatography on silica gel 60 using a mixture of dichloromethane and methanol (3:1, containing 2% of acetic acid) as an eluent. Yield: 27 mg of a colorless solid (62 %). ¹H NMR (500 MHz, DMSO-*d*₆) δ: 14.05 (s, 1H, NH), 11.95 (s, 1H, NH), 8.20 (d, *J* = 8.1 Hz, 2H, CH_{arom.}), 7.63 (d, *J* = 7.8 Hz, 2H, CH_{arom.}), 7.59 (d, *J* = 7.7 Hz, 2H, CH_{arom.}), 7.28 (d, *J* = 7.6 Hz, 2H), 3.78 (t, *J* = 7.4 Hz, 2H, NCH₂), 2.97 (s, 5H, NCH₂ (piperazine)), 1.53 (q, *J* = 7.5 Hz, 2H, CH₂CH₃), 0.85 (t, *J* = 7.5 Hz, 3H, CH₂CH₃) ppm. ¹³C NMR (126 MHz, DMSO-*d*₆) δ: 169.1 (C=O), 158.0 (C₄ xanth.), 151.8 (C₂ xanth.), 149.6 (C₈ xanth.), 148.9 (C₆ xanth.), 135.3 (C_{arom.}), 131.8 (C_{arom.}), 128.2 (C₅ xanth.), 127.7 (C_{arom.}), 126.7 (C_{arom.}), 125.7 (C_{arom.}), 125.65 (C_{arom.}), 125.5 (C_{arom.}), 45.9 (NCH₂ (piperazine)), 41.1 (NCH₂), 21.4 (CH₂CH₃), 11.4 (CH₂CH₃) ppm. HPLC-UV (254 nm) ESI-MS, purity: 96.3%. MS (ESI) (m/z): 603.3 [M + H]⁺. HRMS (ESI-TOF) m/z: [M + H]⁺ calcd. for C₂₅H₂₆N₆O₈S₂ 603.1326, found 603.1290. Mp.: 332 °C.

8-(4-((4-(3-Methoxybenzoyl)piperazine-1-yl)sulfonyl)phenyl)-1-propyl-3,7-dihydro-1H-purine-2,6-dione (17)

Off-white solid, 28 mg, 70 %. ¹H NMR (600 MHz, DMSO-*d*₆) δ: 14.97 (br s, 1H, NH), 11.93 (br s, 1H, NH), 8.32 (d, *J* = 8.1 Hz, 2H, CH_{arom.}), 7.84 (d, *J* = 8.2 Hz, 2H, CH_{arom.}), 7.29 (t, *J* = 8.0 Hz, 1H, CH_{arom.}), 6.97 (dd, *J* = 8.1, 2.6 Hz, 1H, CH_{arom.}), 6.89-6.82 (m, 2H, CH_{arom.}), 3.81 (t, *J* = 7.5 Hz, 2H, NCH₂), 3.72 (s, 3H, OCH₃), 3.68 (br s, 4H, NCH₂ (piperazine)), 3.01 (br s, 4H, NCH₂ (piperazine)), 1.57 (q, *J* = 7.5 Hz, 2H, CH₂CH₃), 0.87 (t, *J* = 7.4 Hz, 3H, CH₂CH₃) ppm. ¹³C NMR (151 MHz, DMSO-*d*₆) δ: 169 (C=O), 159.2 (C_{arom.}), 155.1 (C₄ xanth.), 151.1 (C₂ xanth.), 148.1 (C₈ xanth.), 147.7 (C₆ xanth.), 136.8 (C_{arom.}), 135.8 (C_{arom.}), 133.7 (C_{arom.}), 129.8 (C_{arom.}), 128.4, 127.1 (C_{arom.}), 119.1 (C_{arom.}), 115.4 (C_{arom.}), 112.6 (C_{arom.}), 109.3 (C_{arom.}), 55.4 (OCH₃), 45.8 (NCH₂ (piperazine)), 41.6 (NCH₂ (piperazine)), 21.1 (CH₂CH₃), 11.4 (CH₂CH₃) ppm. HPLC-UV (254 nm) ESI-MS, purity: 98.3%. MS (ESI) (m/z): 553.1 [M + H]⁺. HRMS (ESI-TOF) m/z: [M + H]⁺ calcd. for C₂₆H₂₈N₆O₆S 553.1864, found 553.1840. Mp.: 303-306 °C.

1-Propyl-8-(4-((4-(3-(trifluoromethoxy)benzoyl)piperazine-1-yl)sulfonyl)phenyl)-3,7-dihydro-1H-purine-2,6-dione (18)

Colorless solid, 23 mg, 53%. ¹H NMR (600 MHz, DMSO-*d*₆) δ: 14.02 (s, 1H, NH), 11.95 (s, 1H, NH), 8.33 (d, *J* = 8.1 Hz, 2H, CH_{arom.}), 7.85 (d, *J* = 8.0 Hz, 2H, CH_{arom.}), 7.53 (t, *J* = 7.9 Hz, 1H, CH_{arom.}), 7.42 (d, *J* = 8.2 Hz, 1H, CH_{arom.}), 7.40-7.34 (m, 2H, CH_{arom.}), 3.82 (t, *J* = 7.4 Hz, 2H, NCH₂), 3.69 (s, 2H, NCH₂ (piperazine)), 3.38 (s, 2H, NCH₂ (piperazine)), 3.07 (s, 2H, NCH₂ (piperazine)),

3.04-2.98 (m, 2H, NCH₂(piperazine)), 1.57 (m, $J = 7.3$ Hz, 2H, CH₂CH₃), 0.87 (t, $J = 7.4$ Hz, 3H, CH₂CH₃) ppm. ¹³C NMR (151 MHz, DMSO-*d*₆) δ: 167.5 (C=O) 155.1 (C₄ xanth.), 151.1 (C₂ xanth.), 148.1 (C₈ xanth.), 148.2 (C_{arom.}), 147.7 (C₆ xanth.), 137.7 (C_{arom.}), 136.1 (C_{arom.}), 133.3 (C_{arom.}), 130.8 (C_{arom.}), 128.4 (C₅ xanth.), 127.2 (C_{arom.}), 126.3 (C_{arom.}), 122.3 (C_{arom.}), 120.15 (q, ¹J_{CF} = 257 Hz), 119.9 (C_{arom.}), 46.5 (NCH₂(piperazine)), 45.7 (NCH₂(piperazine)), 41.7 (NCH₂), 41.2 (NCH₂(piperazine)), 21.1 (CH₂CH₃), 11.4 (CH₂CH₃) ppm. HPLC-UV (254 nm) ESI-MS, purity: 98.0%. MS (ESI) (m/z): 607.2 [M + H]⁺. HRMS (ESI-TOF) m/z: [M + H]⁺ calcd. for C₂₆H₂₅F₃N₆O₆S 607.1581, found 607.1556. Mp.: 311-313.5 °C.

8-(4-((4-(2-Chlorobenzoyl)piperazine-1-yl)sulfonyl)phenyl)-1-propyl-3,7-dihydro-1H-purine-2,6-dione (19)

Colorless solid, 28 mg, 70%. ¹H NMR (500 MHz, DMSO-*d*₆) δ: 14.00 (br s, 1H, NH), 11.94 (s, 1H, NH), 8.33 (d, $J = 8.1$ Hz, 2H, CH_{arom.}), 7.85 (d, $J = 8.2$ Hz, 2H, CH_{arom.}), 7.49-7.29 (m, 4H, CH_{arom.}), 3.81 (br m, 2H, NCH₂), 3.67, 3.21, 3.07 and 2.94 (broad signals, complex spin system, 8H, NCH₂(piperazine)), 1.58 (q, $J = 7.2$ Hz, 2H, CH₂CH₃), 0.87 (t, $J = 7.5$ Hz, 3H, CH₂CH₃) ppm. ¹³C NMR (126 MHz, DMSO-*d*₆) δ: 165.8 (C=O), 155.1 (C₄ xanth.), 151.1 (C₂ xanth.), 148.1 (C₈ xanth.), 147.7 (C₆ xanth.), 135.9 (C_{arom.}), 135.2 (C_{arom.}), 133.3 (C_{arom.}), 130.9 (C_{arom.}), 129.6 (C_{arom.}), 129.2 (C_{arom.}), 128.4 (C₅ xanth.), 128.2 (C_{arom.}), 127.8 (C_{arom.}), 127.2 (C_{arom.}), 108.9 (C_{arom.}), 46.0 (NCH₂(piperazine)), 45.8 (NCH₂(piperazine)), 45.7 (NCH₂(piperazine)), 41.7 (NCH₂), 40.6 (NCH₂(piperazine)), 21.0 (CH₂CH₃), 11.3 (CH₂CH₃) ppm. HPLC-UV (254 nm) ESI-MS, purity: 96.9%. MS (ESI) (m/z): 557.1 [M + H]⁺. HRMS (ESI-TOF) m/z: [M + H]⁺ calcd. for C₂₅H₂₅ClN₆O₅S 557.1368, found 557.1349. Mp.: 321-322 °C.

8-(4-((4-(3,4-Dichlorobenzoyl)piperazine-1-yl)sulfonyl)phenyl)-1-propyl-3,7-dihydro-1H-purine-2,6-dione (20)

Off-white solid, 17 mg, 40%. ¹H NMR (600 MHz, DMSO-*d*₆) δ: 14.02 (s, 1H, NH), 11.96 (s, 1H, NH), 8.33 (d, $J = 8.2$ Hz, 2H, CH_{arom.}), 7.85 (d, $J = 8.4$ Hz, 2H, CH_{arom.}), 7.65 (d, $J = 8.7$ Hz, 2H, CH_{arom.}), 7.38-7.29 (m, 1H, CH_{arom.}), 3.82 (t, $J = 7.4$ Hz, 2H, NCH₂), 3.76-3.52 (m, 4H, NCH₂(piperazine)), 3.02 (dt, $J = 29.6/14.1$ Hz, 4H, NCH₂(piperazine)), 1.57 (h, $J = 7.4$ Hz, 2H, CH₂CH₃), 0.87 (t, $J = 7.4$ Hz, 3H, CH₂CH₃) ppm. ¹³C NMR (151 MHz, DMSO-*d*₆) δ: 167.2 (C=O), 165.9 (C_{arom.}), 155.4 (C₄ xanth.), 151.4 (C₂ xanth.), 148.4 (C₈ xanth.), 148.0 (C₆ xanth.), 136.4 (C_{arom.}), 133.6 (C_{arom.}), 132.8 (C_{arom.}), 131.8 (C_{arom.}), 131.5 (C_{arom.}), 131.2 (C_{arom.}), 129.8 (C_{arom.}), 129.6 (C_{arom.}), 128.7 (C₅ xanth.), 127.8 (C_{arom.}), 127.5 (C_{arom.}), 109.1 (C_{arom.}), 46.9 (NCH₂(piperazine)), 46.0 (NCH₂(piperazine)), 44.0 (NCH₂(piperazine)), 41.7 (NCH₂), 21.3 (CH₂CH₃), 11.7 (CH₂CH₃) ppm. HPLC-UV (254 nm) ESI-MS, purity: 93.8%. MS (ESI) (m/z): 591.1 [M + H]⁺. HRMS (ESI-TOF) m/z: [M + H]⁺ calcd. for C₂₅H₂₄Cl₂N₆O₅S 591.0963, found 591.0958. Mp.: 317 °C.

8-(4-((4-(4-Chloro-3-(trifluoromethyl)benzoyl)piperazine-1-yl)sulfonyl)phenyl)-1-propyl-3,7-dihydro-1H-purine-2,6-dione (21)

Colorless solid, 25 mg, 57%. ¹H NMR (500 MHz, DMSO-*d*₆) δ: 14.02 (s, 1H, NH), 11.96 (s, 1H, NH), 8.33 (d, *J* = 8.2 Hz, 2H, CH_{arom.}), 7.88-7.78 (m, 3H, CH_{arom.}), 7.75 (d, *J* = 8.2 Hz, 1H, CH_{arom.}), 7.67 (dd, *J* = 8.4, 1.9 Hz, 1H, CH_{arom.}), 3.82 (t, *J* = 7.5 Hz, 2H, NCH₂), 3.69 (s, 4H, NCH₂ Piperazine), 3.04 (s, 4H, NCH₂ Piperazine), 1.58 (q, *J* = 7.5 Hz, 2H, CH₂CH₃), 0.88 (t, *J* = 7.4 Hz, 3H, CH₂CH₃) ppm. ¹³C NMR (126 MHz, DMSO-*d*₆) δ: 166.8 (C=O), 155.1 (C₄ xanth.), 151.1 (C₂ xanth.), 148.1 (C₈ xanth.), 147.7 (C₆ xanth.), 135.9 (C_{arom.}), 135.1 (C_{arom.}), 133.4 (C_{arom.}), 132.8 (C_{arom.}), 132.0 (C_{arom.}), 131.8 (C_{arom.}), 128.3 (C₅ xanth.), 127.1 (C_{arom.}), 126.9 (C_{arom.}), 122.64 (q, ¹J_{CF} = 273 Hz), 108.7 (C_{arom.}), around 46.6 (br m, NCH₂ (piperazine)), 45.6 (NCH₂ (piperazine)), 41.6 (NCH₂), 41.1 (br m, NCH₂ (piperazine)), 21.0 (CH₂CH₃), 11.3 (CH₂CH₃) ppm. HPLC-UV (254 nm) ESI-MS, purity: 95.2%. MS (ESI) (m/z): 625.3 [M + H]⁺. HRMS (ESI-TOF) m/z: [M + H]⁺ calcd. for C₂₆H₂₄ClF₃N₆O₅S 625.1242, found 625.1229. Mp.: 324-325 °C.

8-(4-((4-(4-Chloro-3-(2-hydroxyethoxy)benzoyl)piperazine-1-yl)sulfonyl)phenyl)-1-propyl-3,7-dihydro-1H-purine-2,6-dione (22)

Colorless solid, 15 mg, 73%. ¹H NMR (500 MHz, DMSO-*d*₆) δ: 14.00 (s, 1H, NH), 11.93 (s, 1H, NH), 8.33 (d, *J* = 8.3 Hz, 2H, CH_{arom.}), 7.85 (d, *J* = 8.3 Hz, 2H, CH_{arom.}), 7.42 (d, *J* = 7.9 Hz, 1H, CH_{arom.}), 7.11 (s, 1H, CH_{arom.}), 6.94-6.86 (m, 1H, CH_{arom.}), 4.83 (s, 1H, OH), 4.04 (br m, 2H, OCH₂), 3.82 (m, 2H, NCH₂), 3.70 (d, *J* = 5.3 Hz, 2H, OCH₂), 3.41 (s, 4H, NCH₂ (piperazine)), 3.03 (br s, 4H, NCH₂ (piperazine)), 1.58 (h, *J* = 7.5 Hz, 2H, CH₂CH₃), 0.88 (t, *J* = 7.3 Hz, 3H, CH₂CH₃) ppm. ¹³C NMR (126 MHz, DMSO-*d*₆) δ: 168.2 (C=O), 155.1 (C₄ xanth.), 154.1 (C_{arom.}), 151.1 (C₂ xanth.), 148.1 (C₈ xanth.), 147.7 (C₆ xanth.), 136.2 (C_{arom.}), 135.5 (C_{arom.}), 133.3 (C_{arom.}), 130.0 (C_{arom.}), 128.3 (C₅ xanth.), 127.2 (C_{arom.}), 122.8 (C_{arom.}), 112.9 (C_{arom.}), 70.9 (NCH₂), 59.5 (NCH₂), around 46.6 (br m, NCH₂ (piperazine)), 45.8 (NCH₂ (piperazine)), 41.7 (NCH₂), 41.0 (br m, NCH₂ (piperazine)), 21.0 (CH₂CH₃), 11.3 (CH₂CH₃) ppm. HPLC-UV (254 nm) ESI-MS, purity: 94.0%. MS (ESI) (m/z): 617.3 [M + H]⁺. HRMS (ESI-TOF) m/z: [M + H]⁺ calcd. for C₂₇H₂₉ClN₆O₇S 617.1580, found 617.1556. Mp.: 315-316 °C.

8-(4-((4-(2-(3-Chlorophenoxy)acetyl)piperazine-1-yl)sulfonyl)phenyl)-1-propyl-3,7-dihydro-1H-purine-2,6-dione (23)

Colorless solid, 41 mg, 97%. ¹H NMR (500 MHz, DMSO-*d*₆) δ: 14.00 (s, 1H, NH), 11.93 (s, 1H, NH), 8.33 (d, *J* = 8.2 Hz, 2H, CH_{arom.}), 7.85 (d, *J* = 8.2 Hz, 2H, CH_{arom.}), 7.20 (d, *J* = 8.7 Hz, 1H, CH_{arom.}), 6.91 (d, *J* = 6.7 Hz, 2H, CH_{arom.}), 6.84-6.78 (m, 1H, CH_{arom.}), 4.81 (s, 2H, CH₂O), 3.81 (d, *J* = 8.1 Hz, 2H, NCH₂), 3.54 (s, 4H, NCH₂ (piperazine)), 3.00 (s, 2H, NCH₂ (piperazine)), 2.98-2.92 (m, 2H, NCH₂ (piperazine)), 1.58 (q, *J* = 7.4 Hz, 2H, CH₂CH₃), 0.91-0.84 (t, *J* = 7.4 Hz, 3H, CH₂CH₃) ppm. ¹³C NMR (126 MHz, DMSO-*d*₆) δ: 165.7 (C=O), 159.0 (C_{arom.}), 155.1 (C₄ xanth.), 151.1

(C₂ xanth.), 148.1 (C₈ xanth.), 135.7 (C_{arom.}), 133.5 (C_{arom.}), 130.7(C_{arom.}), 128.4(C₅ xanth.), 127.1(C_{arom.}), 120.9 (C_{arom.}), 114.64 (C_{arom.}), 114.0(C_{arom.}), 65.9 (COCH₂O), 45.9(NCH₂ (piperazine)), 43.6 (NCH₂ (piperazine)), 41.6 (NCH₂), 40.6 (NCH₂ (piperazine)), 21.0 (CH₂CH₃), 11.3 (CH₂CH₃) ppm. HPLC-UV (254 nm) ESI-MS, purity: 97.3%. MS (ESI) (m/z): 587.3 [M + H]⁺. HRMS (ESI-TOF) m/z: [M + H]⁺ calcd. for C₂₆H₂₇ClN₆O₆S 587.1474 found 587.1451. Mp.: 308 °C.

8-(4-((4-(2-Phenylpropanoyl)piperazine-1-yl)sulfonyl)phenyl)-1-propyl-3,7-dihydro-1H-purine-2,6-dione (24)

Colorless solid, 25 mg, 63%. ¹H NMR (500 MHz, DMSO-*d*₆) δ: 14.04 (s, 1H, NH), 11.95 (s, 1H, NH), 8.30 (d, *J* = 8.2 Hz, 2H, CH_{arom.}), 7.71 (d, *J* = 8.2 Hz, 2H, CH_{arom.}), 7.11 (tt, *J* = 9.8, 4.8 Hz, 5H, CH_{arom.}), 3.83 (t, *J* = 7.5 Hz, 2H, NCH₂), 3.66 (s, 1H, NCH₂ (piperazine)), 3.62-3.35 (m, 4H, NCH₂ (piperazine)), 2.99 (d, *J* = 11.9 Hz, 1H, NCH₂ (piperazine)), 2.81 (s, 1H, NCH₂ (piperazine)), 2.64 (d, *J* = 11.3 Hz, 1H, NCH₂ (piperazine)), 2.13 (q, 1H, CHCH₃) 1.58 (h, *J* = 7.3 Hz, 2H, CH₂CH₃), 1.19 (d, *J* = 6.7 Hz, 3H, CHCH₃), 0.88 (t, *J* = 7.4 Hz, 3H, CH₂CH₃). ¹³C NMR (126 MHz, DMSO-*d*₆) δ: 171.5 (C=O), 155.1 (C₄ xanth.), 151.1 (C₂ xanth.), 148.1 (C₈ xanth.), 147.7 (C₆ xanth.), 141.9 (C_{arom.}), 135.3 (C_{arom.}), 133.2 (C_{arom.}), 128.7 (C₅xanth.), 128.2 (C_{arom.}), 127.2 (C_{arom.}), 127.1 (C_{arom.}), 126.6 (C_{arom.}), 108.7 (C_{arom.}), 45.7 (NCH₂ (piperazine)), 45.5 (NCH₂ (piperazine)), 44.3 (NCH₂ (piperazine)), 41.6 (NCH₂), 40.9 (CHCH₃), 21.0 (CH₂CH₃), 20.4 (CHCH₃), 11.3 (CH₂CH₃) ppm. HPLC-UV (254 nm) ESI-MS, purity: 95.3%. MS (ESI) (m/z): 551.3 [M + H]⁺. HRMS (ESI-TOF) m/z: [M + H]⁺ calcd. for C₂₇H₃₀N₆O₅S 551.2071 found 551.2049. Mp.: 307 °C.

8-(4-((4-(2-Methyl-2-(naphthalene-1-yloxy)propanoyl)piperazine-1-yl)sulfonyl)phenyl)-1-propyl-3,7-dihydro-1H-purine-2,6-dione (25)

Off-white solid, 11 mg, 25%. ¹H NMR (500 MHz, DMSO-*d*₆) δ: 14.11 (s, 1H, NH), 12.01 (s, 1H, NH), 8.24 (d, *J* = 8.0 Hz, 2H, CH_{arom.}), 8.10 (d, *J* = 8.3 Hz, 1H, CH_{arom.}), 7.77 (d, 2H, *J* = 8.0 Hz, CH_{arom.}), 7.52 (dt, *J* = 22.4, 7.2 Hz, 2H, CH_{arom.}), 7.41 (d, *J* = 8.1 Hz, 1H, CH_{arom.}), 6.99 (d, *J* = 8.2 Hz, 1H, CH_{arom.}), 6.90 (t, *J* = 8.0 Hz, 1H, CH_{arom.}), 6.47 (d, *J* = 7.7 Hz, 1H, CH_{arom.}), 3.84 (m, 4HNCH₂ / NCH₂ (piperazine)), 3.71-3.51 (m, 4H, NCH₂ (piperazine)), 2.72 (s, 2H, NCH₂ (piperazine)), 1.79-1.35 (m, 8H, CH₂CH₃/CH₃), 0.90 (t, *J* = 7.4 Hz, 3H, CH₂CH₃) ppm. ¹³C NMR (126 MHz, DMSO-*d*₆) δ: 170.1 (C=O), 155.1 (C₄ xanth.), 151.1 (C₂ xanth.), 150.0, 148.2 (C₈ xanth.), 147.9 (C₆ xanth.), 134.6 (C_{arom.}), 134.1 (C_{arom.}), 133.3 (C_{arom.}), 127.8 (C_{arom.}), 128.4 (C₅ xanth.), 127.7 (C_{arom.}), 127.0 (C_{arom.}), 126.6 (C_{arom.}), 125.8 (C_{arom.}), 125.7 (C_{arom.}), 125.0 (C_{arom.}), 121.5 (C_{arom.}), 120.7 (C_{arom.}), 108.1 (C_{arom.}), 80.9 COC(CH₃)₂O, 45.9 (NCH₂ (piperazine)), 45.0 (NCH₂ (piperazine)), 44.8 (NCH₂ (piperazine)), 41.9 (NCH₂ (piperazine)), 41.7 (NCH₂), 25.8 C(CH₃)₂, 21.0 (CH₂CH₃), 11.4 (CH₂CH₃) ppm. HPLC-UV (254 nm) ESI-MS, purity: 94.3%. MS (ESI) (m/z): 631.3 [M + H]⁺. HRMS (ESI-TOF) m/z: [M + H]⁺ calcd. for C₃₂H₃₄N₆O₆S 631.2333 found 631.2305. Mp.: 340-342 °C.

8-(4-((4-(1-(Naphthalene-1-yl)-5-oxopyrrolidine-3-carbonyl)piperazine-1-yl)sulfonyl)phenyl)-1-propyl-3,7-dihydro-1H-purine-2,6-dione (26)

Off-white solid, 9 mg, 19%. ¹H NMR (500 MHz, DMSO-*d*₆) δ: 13.99 (s, 1H, NH), 11.93 (s, 1H, NH), 8.31 (d, *J* = 8.2 Hz, 2H, CH_{arom.}), 8.00-7.78 (m, 5H, CH_{arom.}), 7.50 (qd, *J* = 9.5, 7.6, 4.9 Hz, 3H, CH_{arom.}), 7.40 (d, *J* = 7.3 Hz, 1H, CH_{arom.}), 3.92 (t, *J* = 8.8 Hz, 1H, COCH₂), 3.83 (ddd, *J* = 19.3, 9.6, 5.6 Hz, 4H, NCH₂), 3.66 - 3.58 (m, 4H, NCH₂ (piperazine)), 3.02 (ddd, *J* = 34.6, 13.3, 7.4 Hz, 4H, NCH₂ (piperazine)), 2.78 (dd, *J* = 16.9, 9.5 Hz, 2H, COCH₂ (lactam)), 2.66 (dd, *J* = 16.8, 5.8 Hz, 2H, COCH₂ (lactam)), 1.57 (h, *J* = 7.3 Hz, 2H, CH₂CH₃), 0.87 (t, *J* = 7.4 Hz, 3H, CH₂CH₃) ppm. ¹³C NMR (126 MHz, DMSO-*d*₆) δ: 172.6 (CO (lactam)), 171.0 (C=O), 155.07 (C₄ xanth.), 151.1 (C₂ xanth.), 148.1 (C₈ xanth.), 147.7 (C₆ xanth.), 136.0 (C_{arom.}), 135.6 (C_{arom.}), 134.1 (C_{arom.}), 133.3 (C_{arom.}), 129.6 (C_{arom.}), 128.3 (C₅ xanth.), 128.0 (C_{arom.}), 127.2 (C_{arom.}), 126.6 (C_{arom.}), 126.4 (C_{arom.}), 125.9 (C_{arom.}), 124.9 (C_{arom.}), 123.3 (C_{arom.}), 108.7 (C_{arom.}), 53.1 (lactam), 46.0 (NCH₂ (piperazine)), 45.8 (NCH₂ (piperazine)), 44.3 (lactam), 41.7 (NCH₂), 41.0 (lactam), 34.5 (lactam), 33.7 (lactam), 21.0 (CH₂CH₃), 11.3 (CH₂CH₃) ppm. HPLC-UV (254 nm) ESI-MS, purity: 96.7%. MS (ESI) (m/z): 656.2 [M + H]⁺. HRMS (ESI-TOF) m/z: [M + H]⁺ calcd. for C₃₃H₃₃N₇O₆S 656.2286 found 656.2259. Mp.: 329-330 °C.

8-(4-((4-(5-Bromofuran-2-carbonyl)piperazine-1-yl)sulfonyl)phenyl)-1-propyl-3,7-dihydro-1H-purine-2,6-dione (27)

Off-white solid, 32 mg, 75%. ¹H NMR (500 MHz, DMSO-*d*₆) δ: 13.95 (s, 1H, NH), 11.93 (s, 1H, NH), 8.32 (d, *J* = 8.2 Hz, 2H, CH_{arom.}), 7.85 (d, *J* = 8.2 Hz, 2H, CH_{arom.}), 6.98 (d, *J* = 3.4 Hz, 1H, CH_{furanyl}), 6.70 (d, *J* = 3.3 Hz, 1H, CH_{furanyl}), 3.82 (d, *J* = 7.6 Hz, 2H, NCH₂), 3.72 (s, 4H, NCH₂ (piperazine)), 3.11 - 2.96 (m, 4H, NCH₂ (piperazine)), 1.57 (h, *J* = 8.5, 7.8 Hz, 2H, CH₂CH₃), 0.87 (t, *J* = 7.2 Hz, 3H, CH₂CH₃). ¹³C NMR (126 MHz, DMSO-*d*₆) δ: 162.4 (C=O), 157.5 (C_{arom.}), 155.1 (C₄ xanth.), 151.1 (C₂ xanth.), 148.3 (C_{arom.}), 148.1 (C₈ xanth.), 147.7 (C₆ xanth.), 135.9 (C_{arom.}), 133.3 (C_{arom.}), 128.4 (C₅ xanth.), 127.2 (C_{arom.}), 124.5 (C_{arom.}), 118.4 (C_{arom.}), 113.6 (C_{arom.}), 108.8 (C_{arom.}), 45.9 (NCH₂ (piperazine)), 41.6 (NCH₂), 21.0, (CH₂CH₃), 11.3 (CH₂CH₃). HPLC-UV (254 nm) ESI-MS, purity: 95.8%. MS (ESI) (m/z): 593.1 [M + H]⁺. HRMS (ESI-TOF) m/z: [M + H]⁺ calcd. for C₂₃H₂₃BrN₆O₆S 591.0656 found 591.0625. Mp.: 295-296 °C.

8-(4-((4-(5-Nitrofuran-2-carbonyl)piperazine-1-yl)sulfonyl)phenyl)-1-propyl-3,7-dihydro-1H-purine-2,6-dione (28)

Off-white solid, 28 mg, 70%. ¹H NMR (500 MHz, DMSO-*d*₆) δ: 14.01 (s, 1H, NH), 11.93 (s, 1H, NH), 8.33 (d, *J* = 8.3 Hz, 2H, CH_{arom.}), 7.86 (d, *J* = 8.5 Hz, 2H, CH_{arom.}), 7.70 (d, *J* = 3.8 Hz, 1H, CH_{furanyl}), 7.21 (d, *J* = 4.0 Hz, 1H, CH_{furanyl}), 3.81 (m, 2H, NCH₂), 3.75 (m, 4H, NCH₂ (piperazine)), 3.18-3.00 (m, 4H, NCH₂ (piperazine)), 1.56 (q, *J* = 7.4 Hz, 2H, CH₂CH₃), 0.97-0.81 (m, 3H, CH₂CH₃). ¹³C NMR (126 MHz, DMSO-*d*₆) δ: 157.0 (C=O), 155.1 (C₄ xanth.), 151.1 (C₂ xanth.), 148.1

(C₈ xanth.), 147.7 (C₆ xanth.), 147.3 (C_{arom.}), 135.9 (C_{arom.}), 133.2 (C_{arom.}), 128.4 (C₅ xanth.), 127.2 (C_{arom.}), 117.4 (C_{arom.}), 112.9 (C_{arom.}), 108.7 (C_{arom.}), 45.8 (NCH₂ (piperazine)), 41.64 (NCH₂), 21.0 (CH₂CH₃), 11.3 (CH₂CH₃). HPLC-UV (254 nm) ESI-MS, purity: 95%. MS (ESI) (m/z): 558.1 [M + H]⁺. HRMS (ESI-TOF) m/z: [M + H]⁺ calcd. for C₂₃H₂₃N₇O₈S 558.1402 found 558.1375. Mp.: 298-299 °C.

8-(4-((4-(5-(2-Chlorophenyl)furan-2-carbonyl)piperazine-1-yl)sulfonyl)phenyl)-1-propyl-3,7-dihydro-1H-purine-2,6-dione (29)

Off-white solid, 41 mg, 91%. ¹H NMR (500 MHz, DMSO-*d*₆) δ: 13.96 (s, 1H, NH), 11.92 (s, 1H, NH), 8.32 (d, *J* = 8.1 Hz, 2H, CH_{arom.}), 7.82 (d, *J* = 7.8 Hz, 1H, CH_{furanyl}), 7.56 (d, *J* = 7.8 Hz, 1H, CH_{furanyl}), 7.48-7.37 (m, 3H, CH_{arom.}), 7.18-7.09 (m, 2H, CH_{arom.}), 3.84-3.78 (m, 6H, NCH₂ (piperazine)), 2.49 (s, 4H, NCH₂ (piperazine)), 1.61-1.52 (m, 2H, CH₂CH₃), 0.87 (t, *J* = 7.3 Hz, 3H, CH₂CH₃) ppm. ¹³C NMR (126 MHz, DMSO-*d*₆) δ: 158.1 (C=O), 155.1 (C₄ xanth.), 151.1 (C₂ xanth.), 150.8 (C_{arom.}), 148.1 (C₈ xanth.), 147.6 (C₆ xanth.), 146.3 (C_{arom.}), 135.9 (C_{arom.}), 133.4 (C_{arom.}), 130.9 (C_{arom.}), 130.1 (C_{arom.}), 129.8 (C_{arom.}), 128.8 (C_{arom.}), 128.3 (C₅ xanth.), 127.8 (C_{arom.}), 127.6 (C_{arom.}), 127.1 (C_{arom.}), 118.0 (C_{arom.}), 112.1 (C_{arom.}), 108.8 (C_{arom.}), 46.0 (NCH₂ (piperazine)), 41.6 (NCH₂), 21.0 (CH₂CH₃), 11.3 (CH₂CH₃) ppm. HPLC-UV (254 nm) ESI-MS, purity: 92.7%. MS (ESI) (m/z): 623.1 [M + H]⁺. HRMS (ESI-TOF) m/z: [M + H]⁺ calcd. for C₂₉H₂₇ClN₆O₆S 623.1474 found 623.1461. Mp.: 335-337 °C.

8-(4-((4-(5-(2-Isopropylphenyl)furan-2-carbonyl)piperazin-1-yl)sulfonyl)phenyl)-1-propyl-3,7-dihydro-1H-purine-2,6-dione (30)

Off-white solid, 44 mg, 97%. ¹H NMR (500 MHz, DMSO-*d*₆) δ: 13.99 (s, 1H, NH), 11.93 (s, 1H, NH), 8.35-8.29 (m, 2H, CH_{arom.}), 7.89-7.81 (m, 2H, CH_{arom.}), 7.50-7.35 (m, 3H, CH_{arom.}), 7.27 (dtd, *J* = 10.8, 7.5 and 1.7 Hz, 1H, CH_{arom.}), 7.09 (d, *J* = 3.5 Hz, 1H, CH_{furanyl}), 6.69 (d, *J* = 3.6, 1H, CH_{furanyl}), 3.85-3.77 (m, 6H, NCH₂ (piperazine)), 3.25 (m, 1H, CH(CH₃)₂), 3.06 (t, *J* = 5.2 Hz, 4H, NCH₂ (piperazine)), 1.63-1.51 (m, 2H, CH₂CH₃), 1.15 (d, *J* = 6.8 Hz, 6H, CH(CH₃)₂), 0.87 (t, *J* = 7.4 Hz, 3H, CH₂CH₃) ppm. ¹³C NMR (126 MHz, DMSO-*d*₆) δ: 158.4 (C=O), 155.1 (C₄ xanth.), 154.8 (C_{arom.}), 151.1 (C₂ xanth.), 148.1 (C₈ xanth.), 147.7 (C₆ xanth.), 146.5 (C_{arom.}), 146.3 (C_{arom.}), 135.8 (C_{arom.}), 133.3 (C_{arom.}), 129.6 (C_{arom.}), 129.2 (C_{arom.}), 128.4 (C₅ xanth.), 128.1 (C_{arom.}), 127.1 (C_{arom.}), 126.2 (C_{arom.}), 126.1 (C_{arom.}), 118.1 (C_{arom.}), 117.2 (C_{arom.}), 110.4 (C_{arom.}), 108.7 (C_{arom.}), 46.1 (NCH₂ (piperazine)), 41.6 (NCH₂), 29.3 (CH(CH₃)₂), 23.9 (CH(CH₃)₂), 21.0 (CH₂CH₃), 11.3 (CH₂CH₃) ppm. HPLC-UV (254 nm) ESI-MS, purity: 98.1%. MS (ESI) (m/z): 631.4 [M + H]⁺. HRMS (ESI-TOF) m/z: [M + H]⁺ calcd. for C₃₂H₃₄N₆O₆S 631.2333 found 631.2320. Mp.: 329-330 °C.

8-(4-((4-(5-(5-Chloro-2-methoxyphenyl)furan-2-carbonyl)piperazine-1-yl)sulfonyl)phenyl)-1-propyl-3,7-dihydro-1*H*-purine-2,6-dione (31)

Off-white solid, 31 mg, 66%. ¹H NMR (500 MHz, DMSO-*d*₆) δ: 14.01 (s, 1H, NH), 11.93 (s, 1H, NH), 8.32 (d, *J* = 8.4 Hz, 2H, CH_{furan}yl), 7.84 (d, *J* = 8.4 Hz, 2H, CH_{furan}yl), 7.45 (d, *J* = 9.7 Hz, 1H, CH_{arom.}), 7.26 (s, 1H, CH_{arom.}), 7.19 (s, 1H, CH_{arom.}), 7.10 (s, 1H, CH_{arom.}), 6.97 (d, *J* = 8.7 Hz, 1H, CH_{arom.}), 3.81 (d, *J* = 10.1 Hz, 10H, NCH₂ (piperazine)), 3.18 (s, 1H), 3.09 (s, 4H, NCH₂ (piperazine)), 1.61-1.53 (m, 2H, CH₂CH₃), 1.20 (s, 3H, OCH₃), 0.90-0.83 (m, 3H, CH₂CH₃) ppm. ¹³C NMR (126 MHz, DMSO-*d*₆) δ: 158.31 (C=O), 155.1 (C₄ xanth.), 151.1 (C₂ xanth.), 150.6 (C_{arom.}), 150.3 (C_{arom.}), 148.1 (C₈ xanth.), 147.7 (C₆ xanth.), 146.3 (C_{arom.}), 135.9 (C_{arom.}), 133.3 (C_{arom.}), 131.9 (C_{arom.}), 128.3 (C₅ xanth.), 127.1 (C_{arom.}), 121.2 (C_{arom.}), 118.0 (C_{arom.}), 117.5 (C_{arom.}), 116.3 (C_{arom.}), 113.1 (C_{arom.}), 112.3 (C_{arom.}), 55.7 (OCH₃), 46.0 (NCH₂ (piperazine)), 41.6 (NCH₂), 21.0 (CH₂CH₃), 11.3 (CH₂CH₃) ppm. HPLC-UV (254 nm) ESI-MS, purity: 96.8%. MS (ESI) (*m/z*): 653.1 [M + H]⁺. HRMS (ESI-TOF) *m/z*: [M + H]⁺ calcd. for C₃₀H₂₉ClN₆O₇S 653.1580 found 653.1550. Mp.: 331-333 °C.

Synthesis of 5-(2-isopropylphenyl)-furan-2-carboxylic acid

A mixture of 2-isopropylphenylboronic acid (1 g, 6.1 mmol), methyl-5-bromo-2-furanate (1.13 g, 5.6 mmol), Na₂CO₃ (1.15 g, 10.9 mmol) and Pd(PPh₃)₄ (0.31 g, 0.27 mmol) in ethylenglycoldimethylether (42 ml) and water (10 ml) was stirred at 80 °C for 18 h. Subsequently, the mixture was extracted with water (50 ml) and diethyl ether (50 ml, 3 x). The combined organic layers were dried over MgSO₄ and concentrated under reduced pressure. The crude product was purified by column chromatography (petrol ether / ethyl acetate - 9 : 1) and was obtained as 1.37 g (92%) of a colorless oil. MS (ESI) (*m/z*): 245.3 [M + H]⁺.

The methyl ester (1.37 g, 5.61 mmol) and NaOH (2.31 g, 57.8 mmol) were stirred in a mixture of water (40 ml), methanol (20 ml) and THF (40 ml) at rt for 30 min. Subsequently, the mixture was treated with 1 N HCl (60 ml) and the precipitated product was collected by filtration. The product was obtained as 1.12 g (87%) of a colorless solid. ¹H NMR (500 MHz, DMSO-*d*₆) δ = 13.03 (s, 1H, COOH), 7.51-7.46 (m, 1H), 7.44-7.40 (m, 1H), 7.31 (d, *J* = 3.6 Hz, 1H, CH_{furan}yl), 7.32-7.25 (m, 1H), 6.76 (d, *J* = 3.5 Hz, 1H, CH_{furan}yl), 3.29 (hept, *J* = 6.7 Hz, 2H, CH), 1.20 (d, *J* = 6.9 Hz, 6H, (CH₃)₂) ppm. ¹³C NMR (126 MHz, DMSO-*d*₆) δ 159.4, 156.7, 146.7, 144.4, 129.8, 129.2, 128.2, 126.2, 126.1, 119.3, 110.9, 29.5, 23.9 ppm. MS (ESI) (*m/z*): 231.3 [M + H]⁺.

4.1.7. References

- (1) Fredholm, B. B.; IJzerman, A. P.; Jacobson, K. A.; Linden, J.; Müller, C. E. International union of basic and clinical pharmacology. LXXXI. Nomenclature and classification of adenosine receptors - an update. *Pharmacol. Rev.* **2011**, *63*, 1-34.
- (2) Fredholm, B. B.; IJzerman, A. P.; Jacobson, K. A.; Klotz, K. N.; Linden, J. International union of pharmacology. XXV. Nomenclature and classification of adenosine receptors. *Pharmacol. Rev.* **2001**, *53*, 527-552.
- (3) Müller, C. E.; Baqi, Y.; Namasivayam, V. Agonists and antagonists for purinergic receptors. In *Pelegrín (Hg.) 2020 - Purinergic Signaling*; pp. 45-64.
- (4) Hinz, S.; Navarro, G.; Borroto-Escuela, D.; Seibt, B. F.; Ammon, Y.-C.; Filippo, E. de; Danish, A.; Lacher, S. K.; Červinková, B.; Rafehi, M.; Fuxe, K.; Schiedel, A. C.; Franco, R.; Müller, C. E. Adenosine A_{2A} receptor ligand recognition and signaling is blocked by A_{2B} receptors. *Oncotarget.* **2018**, *9*, 13593-13611.
- (5) Allard, D.; Turcotte, M.; Stagg, J. Targeting A₂ adenosine receptors in cancer. *Immunol. Cell Biol.* **2017**, *95*, 333-339.
- (6) Jacobson, K. A.; Gao, Z.-G. Adenosine receptors as therapeutic targets. *Nat. Rev. Drug Discov.* **2006**, *5*, 247-264.
- (7) Müller, C. E.; Baqi, Y.; Hinz, S.; Namasivayam, V. Medicinal chemistry of A_{2B} adenosine receptors. In *The adenosine receptors*. Borea, P. A.; Varani, K.; Gessi, S.; Merighi, S.; Vincenzi, F., Eds.; Springer International Publishing: Cham; pp. 137-168.
- (8) El-Tayeb, A.; Michael, S.; Abdelrahman, A.; Behrenswerth, A.; Gollos, S.; Nieber, K.; Müller, C. E. Development of polar adenosine A_{2A} receptor agonists for inflammatory bowel disease: Synergism with A_{2B} antagonists. *ACS Med. Chem Lett.* **2011**, *2*, 890-895.
- (9) Chen, M.; Liang, D.; Zuo, A.; Shao, H.; Kaplan, H. J.; Sun, D. An A_{2B} adenosine receptor agonist promotes Th17 autoimmune responses in experimental Autoimmune Uveitis (EAU) via dendritic cell activation. *PLoS ONE.* **2015**, *10*, e0132348.
- (10) Rüsing, D.; Müller, C. E.; Verspohl, E. J. The impact of adenosine and A(2B) receptors on glucose homeostasis. *J. Pharm. Pharmacol.* **2006**, *58*, 1639-1645.
- (11) Abo-Salem, O. M.; Hayallah, A. M.; Bilkei-Gorzo, A.; Filipek, B.; Zimmer, A.; Müller, C. E. Antinociceptive effects of novel A_{2B} adenosine receptor antagonists. *J. Pharmacol. Exp. Ther.* **2004**, *308*, 358-366.

- (12) Bilkei-Gorzo, A.; Abo-Salem, O. M.; Hayallah, A. M.; Michel, K.; Müller, C. E.; Zimmer, A. Adenosine receptor subtype-selective antagonists in inflammation and hyperalgesia. *Naunyn-Schmiedeberg's Arch. Pharmacol.* **2008**, *377*, 65-76.
- (13) Borrmann, T.; Hinz, S.; Bertarelli, D. C. G.; Li, W.; Florin, N. C.; Scheiff, A. B.; Müller, C. E. 1-alkyl-8-(piperazine-1-sulfonyl)phenylxanthines: development and characterization of adenosine A_{2B} receptor antagonists and a new radioligand with subnanomolar affinity and subtype specificity. *J. Med. Chem.* **2009**, *52*, 3994-4006.
- (14) Hayallah, A. M.; Sandoval-Ramírez, J.; Reith, U.; Schobert, U.; Preiss, B.; Schumacher, B.; Daly, J. W.; Müller, C. E. 1,8-disubstituted xanthine derivatives: synthesis of potent A_{2B}-selective adenosine receptor antagonists. *J. Med. Chem.* **2002**, *45*, 1500-1510.
- (15) Yan, L.; Müller, C. E. Preparation, properties, reactions, and adenosine receptor affinities of sulfophenylxanthine nitrophenyl esters: toward the development of sulfonic acid prodrugs with peroral bioavailability. *J. Med. Chem.* **2004**, *47*, 1031-1043.
- (16) Michael, S.; Warstat, C.; Michel, F.; Yan, L.; Müller, C. E.; Nieber, K. Adenosine A_{2A} agonist and A_{2B} antagonist mediate an inhibition of inflammation-induced contractile disturbance of a rat gastrointestinal preparation. *Purinerg. Signal.* **2010**, *6*, 117-124.
- (17) Sorrentino, C.; Miele, L.; Porta, A.; Pinto, A.; Morello, S. Myeloid-derived suppressor cells contribute to A_{2B} adenosine receptor-induced VEGF production and angiogenesis in a mouse melanoma model. *Oncotarget.* **2015**, *6*, 27478-27489.
- (18) Jiang, J.; Seel, C. J.; Temirak, A.; Namasivayam, V.; Arridu, A.; Schabikowski, J.; Baqi, Y.; Hinz, S.; Hockemeyer, J.; Müller, C. E. A_{2B} adenosine receptor antagonists with picomolar potency. *J. Med. Chem.* **2019**, *62*, 4032-4055.
- (19) Yan, L.; Bertarelli, D. C. G.; Hayallah, A. M.; Meyer, H.; Klotz, K.-N.; Müller, C. E. A new synthesis of sulfonamides by aminolysis of p-nitrophenylsulfonates yielding potent and selective adenosine A_{2B} receptor antagonists. *J. Med. Chem.* **2006**, *49*, 4384-4391.
- (20) Alnouri, M. W.; Jepards, S.; Casari, A.; Schiedel, A. C.; Hinz, S.; Müller, C. E. Selectivity is species-dependent: Characterization of standard agonists and antagonists at human, rat, and mouse adenosine receptors. *Purinerg. Signal.* **2015**, *11*, 389-407.
- (21) Basu, S.; Barawkar, D. A.; Ramdas, V.; Waman, Y.; Patel, M.; Panmand, A.; Kumar, S.; Thorat, S.; Bonagiri, R.; Jadhav, D.; Mukhopadhyay, P.; Prasad, V.; Reddy, B. S.; Goswami, A.; Chaturvedi, S.; Menon, S.; Quraishi, A.; Ghosh, I.; Dusange, S.; Paliwal, S.; Kulkarni, A.; Karande, V.; Thakre, R.; Bedse, G.; Rouduri, S.; Gundu, J.; Palle, V. P.; Chugh, A.; Mookhtiar,

K. A. A_{2B} adenosine receptor antagonists: Design, synthesis and biological evaluation of novel xanthine derivatives. *Eur. J. Med. Chem.* **2017**, *127*, 986-996.

(22) Eastwood, P.; Esteve, C.; González, J.; Fonquerna, S.; Aiguadé, J.; Carranco, I.; Doménech, T.; Aparici, M.; Miralpeix, M.; Albertí, J.; Córdoba, M.; Fernández, R.; Pont, M.; Godessart, N.; Prats, N.; Loza, M. I.; Cadavid, M. I.; Nueda, A.; Vidal, B. Discovery of LAS101057: A potent, selective, and orally efficacious A_{2B} adenosine receptor antagonist. *ACS Med. Chem. Lett.* **2011**, *2*, 213-218.

(23) Härter, M.; Kalthof, B.; Delbeck, M.; Lustig, K.; Gerisch, M.; Schulz, S.; Kast, R.; Meibom, D.; Lindner, N. Novel non-xanthine antagonist of the A_{2B} adenosine receptor: From HTS hit to lead structure. *Eur. J. Med. Chem.* **2019**, *163*, 763-778.

(24) Mallo-Abreu, A.; Prieto-Díaz, R.; Jaspers, W.; Azuaje, J.; Majellaro, M.; Velando, C.; García-Mera, X.; Caamaño, O.; Brea, J.; Loza, M. I.; Gutiérrez-de-Terán, H.; Sotelo, E. Nitrogen-walk approach to explore bioisosteric replacements in a series of potent A_{2B} adenosine receptor antagonists. *J. Med. Chem.* **2020**, *63*, 7721-7739.

(25) Gunzner, J. L.; Sutherlin, D. P.; Stanley, M. S.; Bao, L.; Castanedo, G.; Lalonde, R. L.; Wang, S.; Reynolds, M. E.; Savage, S. J.; Malesky, K. Pyridyl inhibitors of hedgehog signalling; WO 2009126863 A2, 2009.

(26) Müller, C. E. General synthesis and properties of 1-monosubstituted xanthines. *Synthesis.* **1993**, *1993*, 125-128.

(27) Lim, C. J.; Kim, N. H.; Park, H. J.; Lee, B. H.; Oh, K.-S.; Yi, K. Y. Synthesis and SAR of 5-aryl-furan-2-carboxamide derivatives as potent urotensin-II receptor antagonists. *Bioorg. Med. Chem. Lett.* **2019**, *29*, 577-580.

(28) Vedantham, P.; Guerra, J. M.; Schoenen, F.; Huang, M.; Gor, P. J.; Georg, G. I.; Wang, J. L.; Neuenswander, B.; Lushington, G. H.; Mitscher, L. A.; Ye, Q.-Z.; Hanson, P. R. Ionic immobilization, diversification, and release: application to the generation of a library of methionine aminopeptidase inhibitors. *J. Comb. Chem.* **2008**, *10*, 185-194.

(29) Klotz, K. N.; Lohse, M. J.; Schwabe, U.; Cristalli, G.; Vittori, S.; Grifantini, M. 2-Chloro-N⁶-[³H]cyclopentyladenosine (3HCCPA) - a high affinity agonist radioligand for A₁ adenosine receptors. *N-S Arch. Pharmacol.* **1989**, *340*, 679-683.

(30) Müller, C. E.; Maurinsh, J.; Sauer, R. Binding of [³H]MSX-2 (3-(3-hydroxypropyl)-7-methyl-8-(*m*-methoxystyryl)-1-propargylxanthine) to rat striatal membranes - a new, selective antagonist radioligand for A_{2A} adenosine receptors. *Eur. J. Pharm. Sci.* **2000**, *10*, 259-265.

(31) Müller, C. E.; Diekmann, M.; Thorand, M.; Ozola, V. [³H]8-Ethyl-4-methyl-2-phenyl-(8*R*)-4,5,7,8-tetrahydro-1*H*-imidazo[2,1-*f*]-purin-5-one ([³H]PSB-11), a novel high-affinity antagonist radioligand for human A₃ adenosine receptors. *Bioorg. Med. Chem. Lett.* **2002**, *12*, 501-503.

(32) Drabczyńska, A.; Müller, C. E.; Karolak-Wojciechowska, J.; Schumacher, B.; Schiedel, A.; Yuzlenko, O.; Kieć-Kononowicz, K. N9-benzyl-substituted 1,3-dimethyl- and 1,3-dipropyl-pyrimido[2,1-*f*]purinediones: synthesis and structure-activity relationships at adenosine A₁ and A_{2A} receptors. *Bioorg. Med. Chem.* **2007**, *15*, 5003-5017.

(33) Köse, M.; Gollos, S.; Karcz, T.; Fiene, A.; Heisig, F.; Behrenswerth, A.; Kieć-Kononowicz, K.; Namasivayam, V.; Müller, C. E. Fluorescent-labeled selective adenosine A_{2B} receptor antagonist enables competition binding assay by flow cytometry. *J. Med. Chem.* **2018**, *61*, 4301-4316.

4.1.8. Supporting information

Exploration of *N*-acetyl-8-(4-piperazine-1-sulfonyl)phenylxanthines as potent and selective adenosine A_{2B} receptor antagonists

Tim Harms,¹ Jörg Hockemeyer,¹ Christin Vielmuth,¹ Sonja Hinz,^{1,2} and Christa E. Müller^{1,*}

¹PharmaCenter Bonn, Pharmaceutical Institute, Pharmaceutical Sciences Bonn (PSB), Pharmaceutical & Medicinal Chemistry, University of Bonn, An der Immenburg 4, 53121, Bonn, Germany.

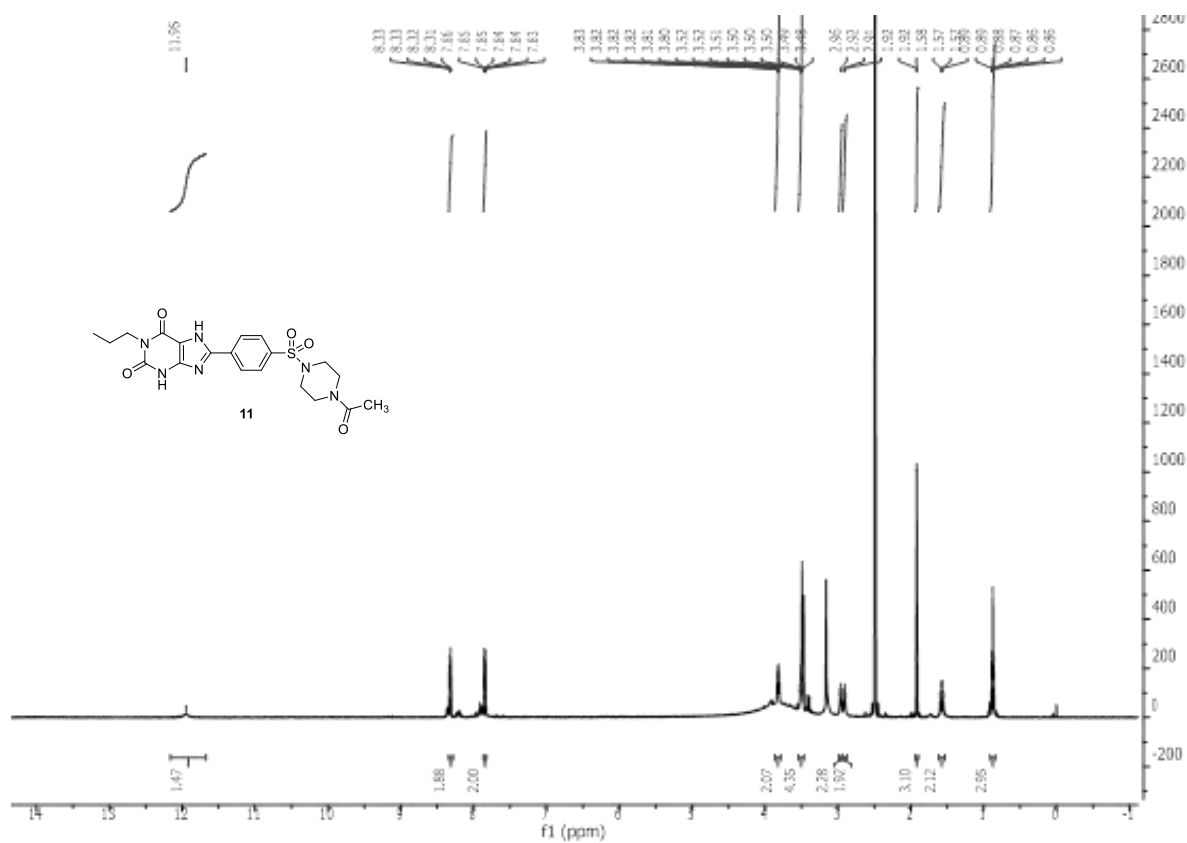
²Institute of Pharmacology and Toxicology, Center for Biomedical Education and Research (ZBAF), School of Medicine, Faculty of Health, University of Witten/Herdecke, D-58453 Witten, Germany.

Email: tim.harms@uni-bonn.de ; christa.mueller@uni-bonn.de

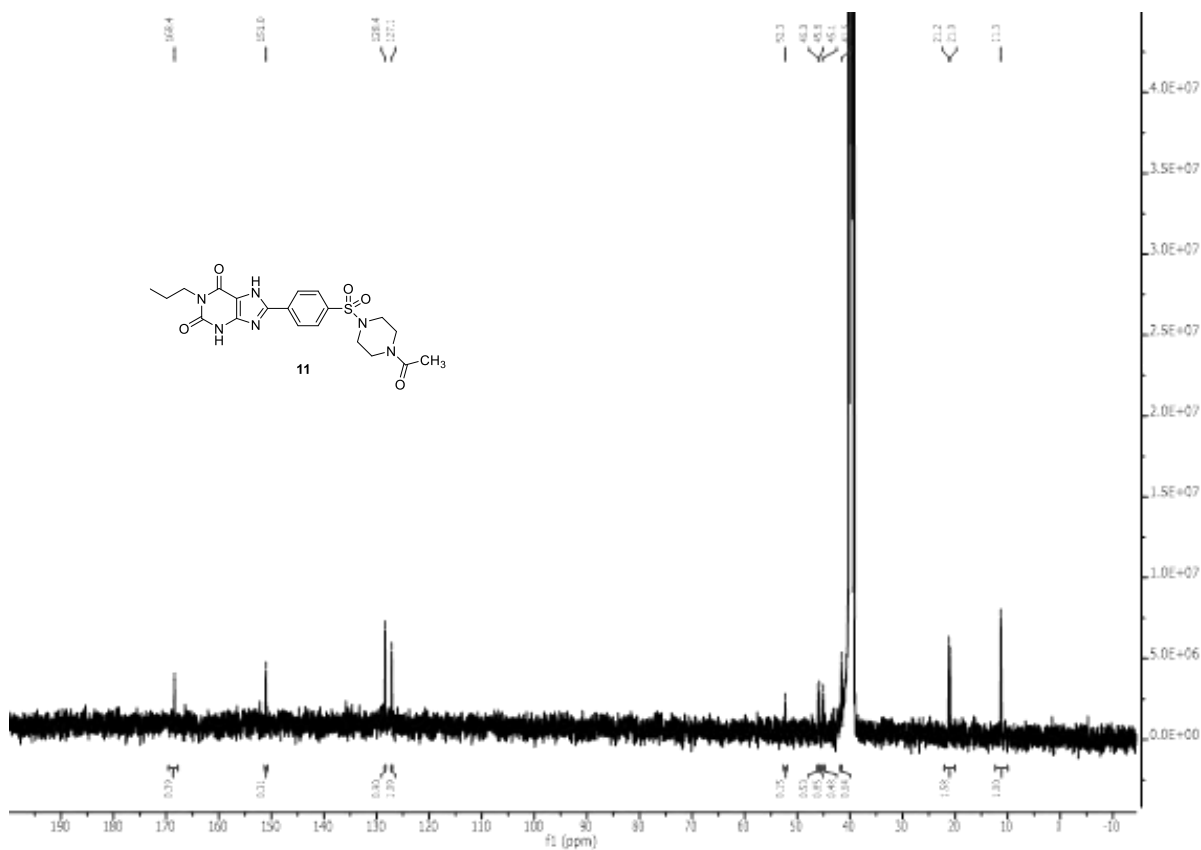
Table of content

S1-S40 - NMR data of compounds **11** and **13-31**

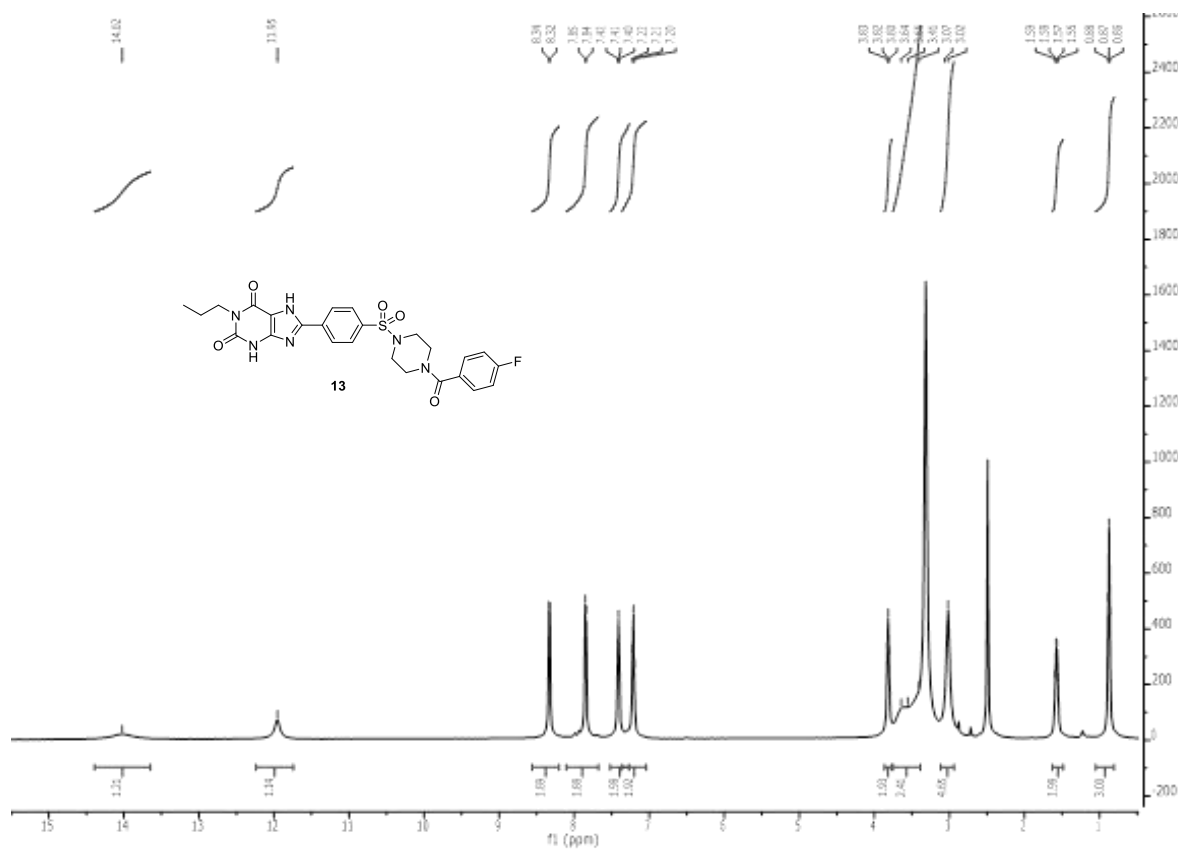
S41-S60 - Mass spectra of compounds **11** and **13-31**



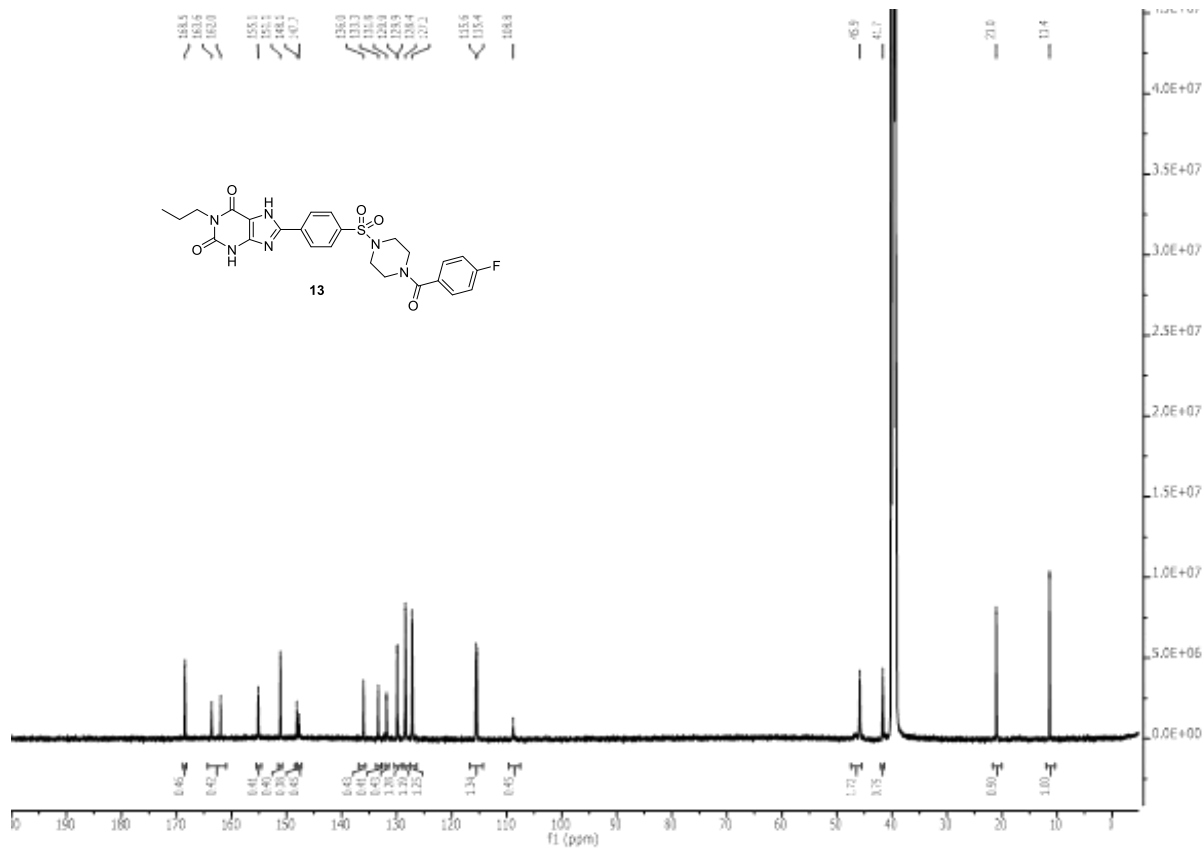
S1. ¹H NMR of compound 11.



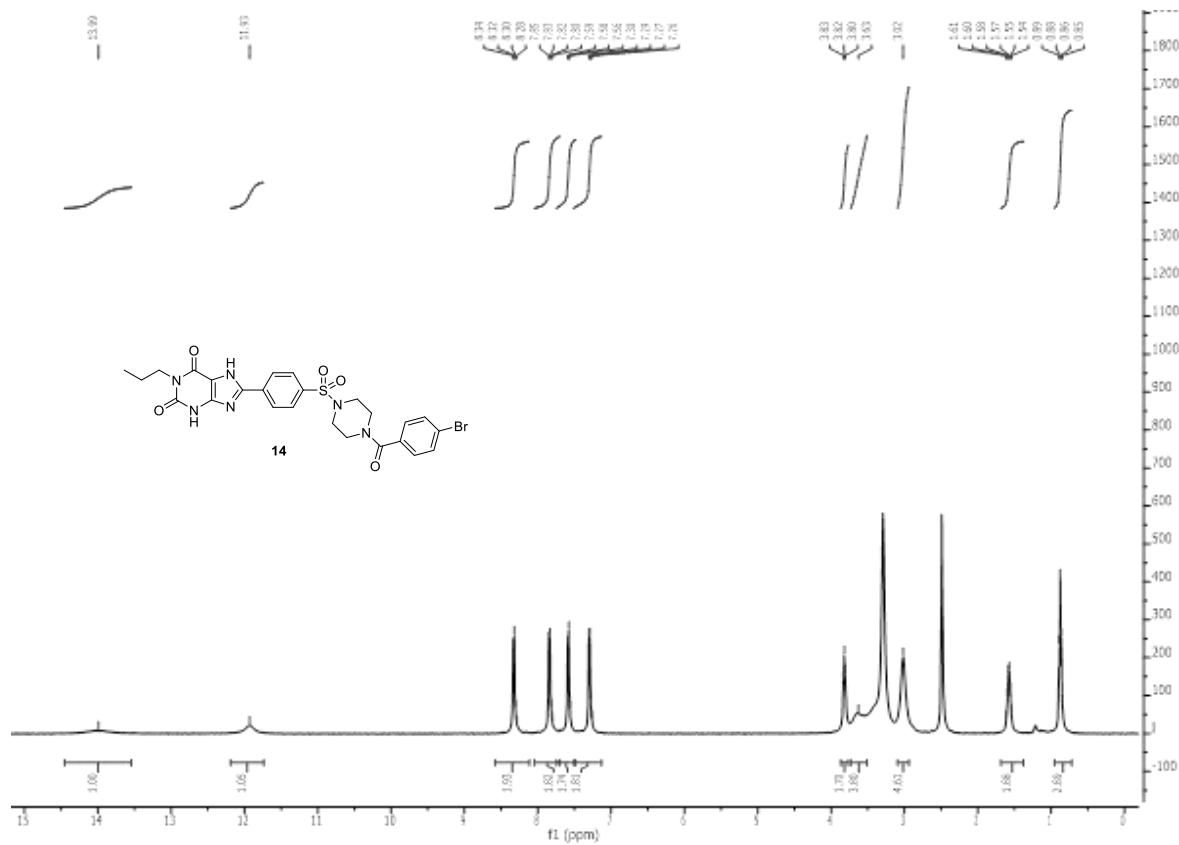
S2. ¹³C NMR of compound 11.



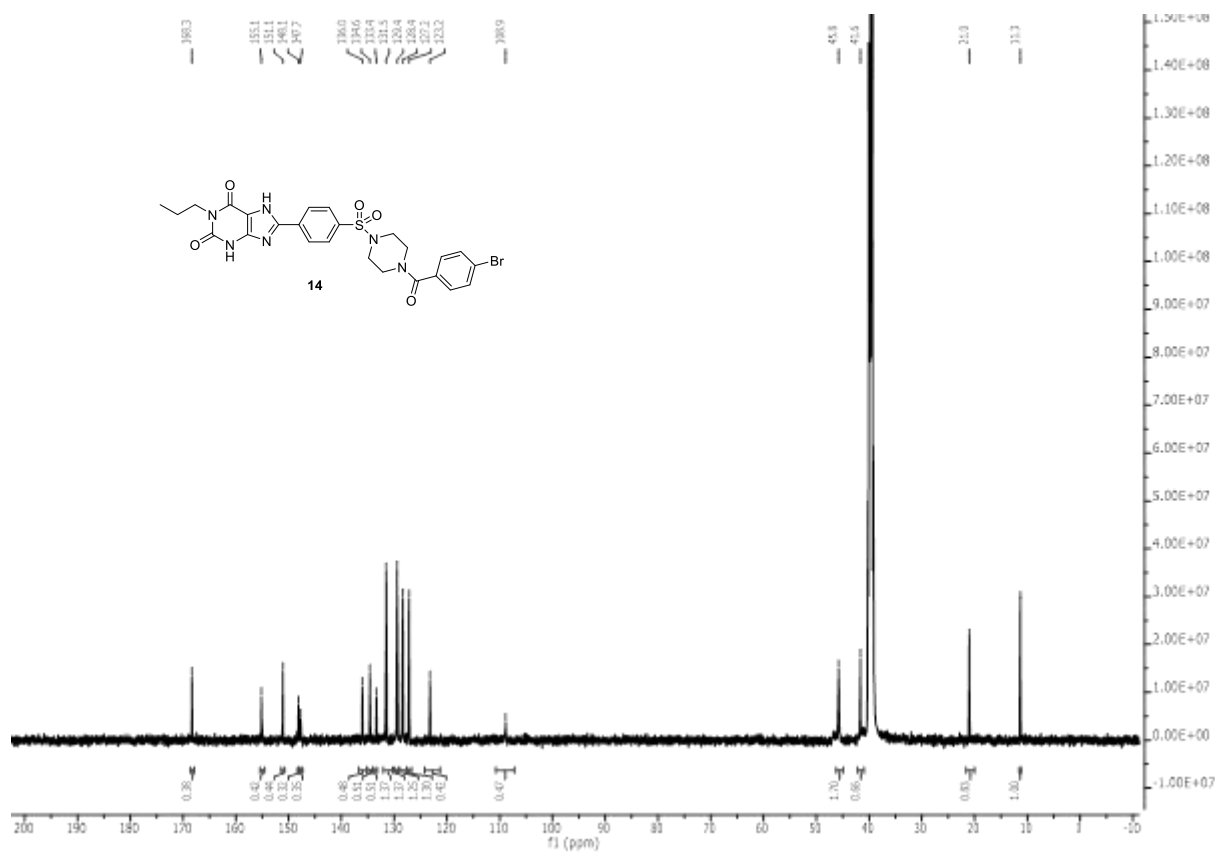
S3. ¹H NMR of compound 13.



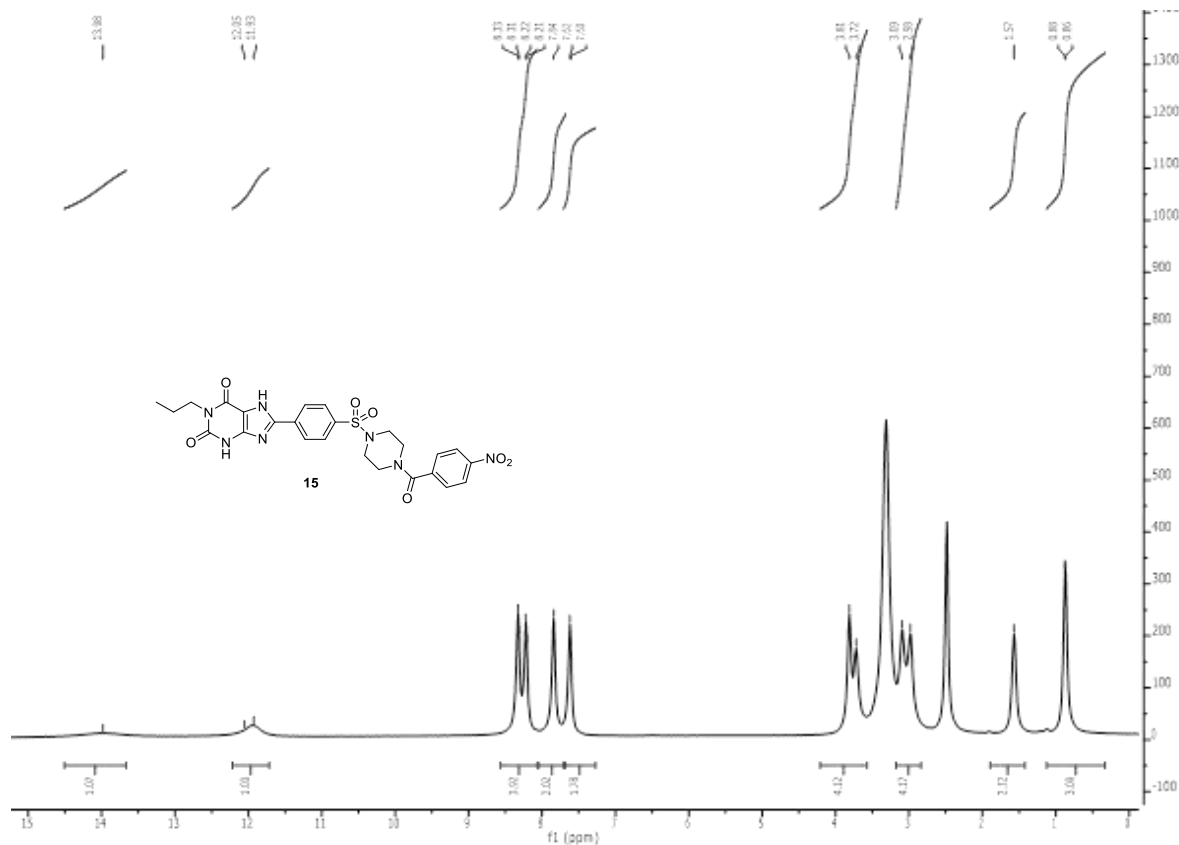
S4. ¹³C NMR of compound 13.



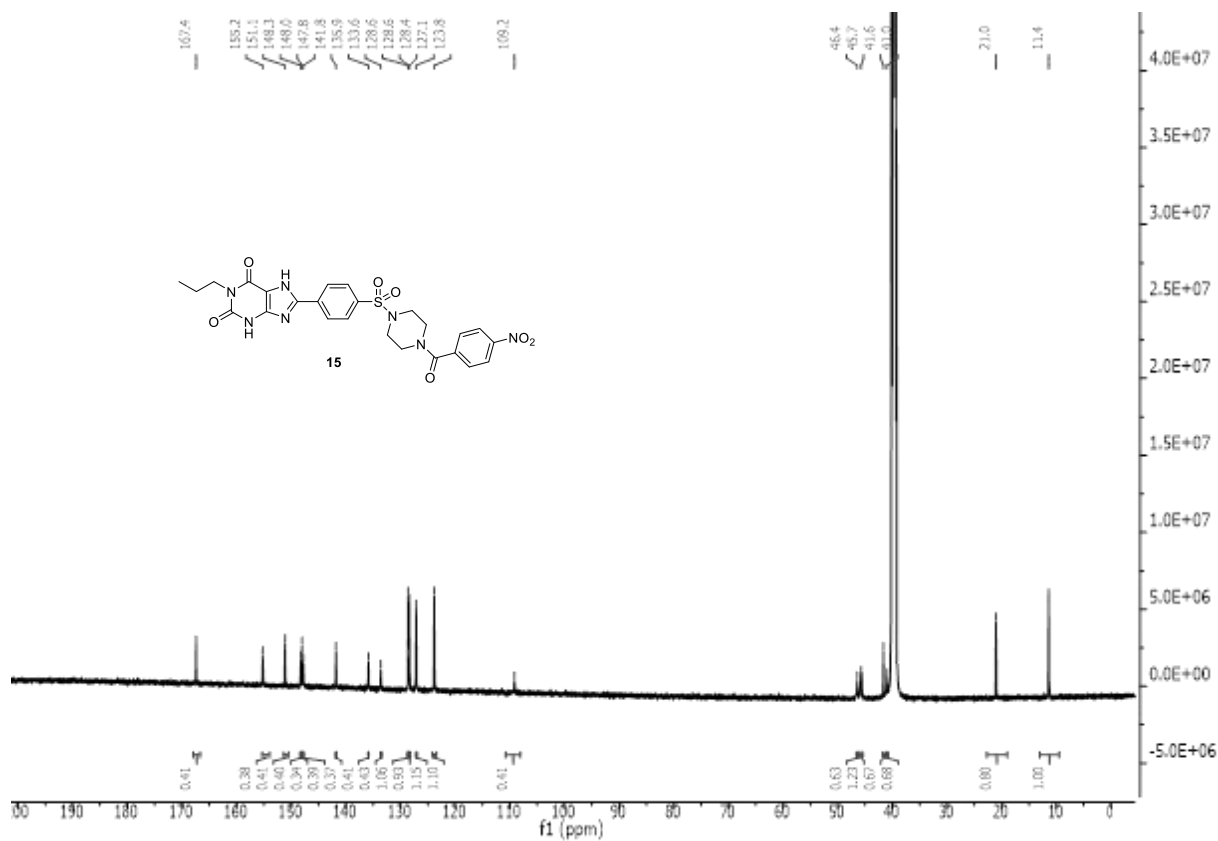
S5. ^1H NMR of compound 14.



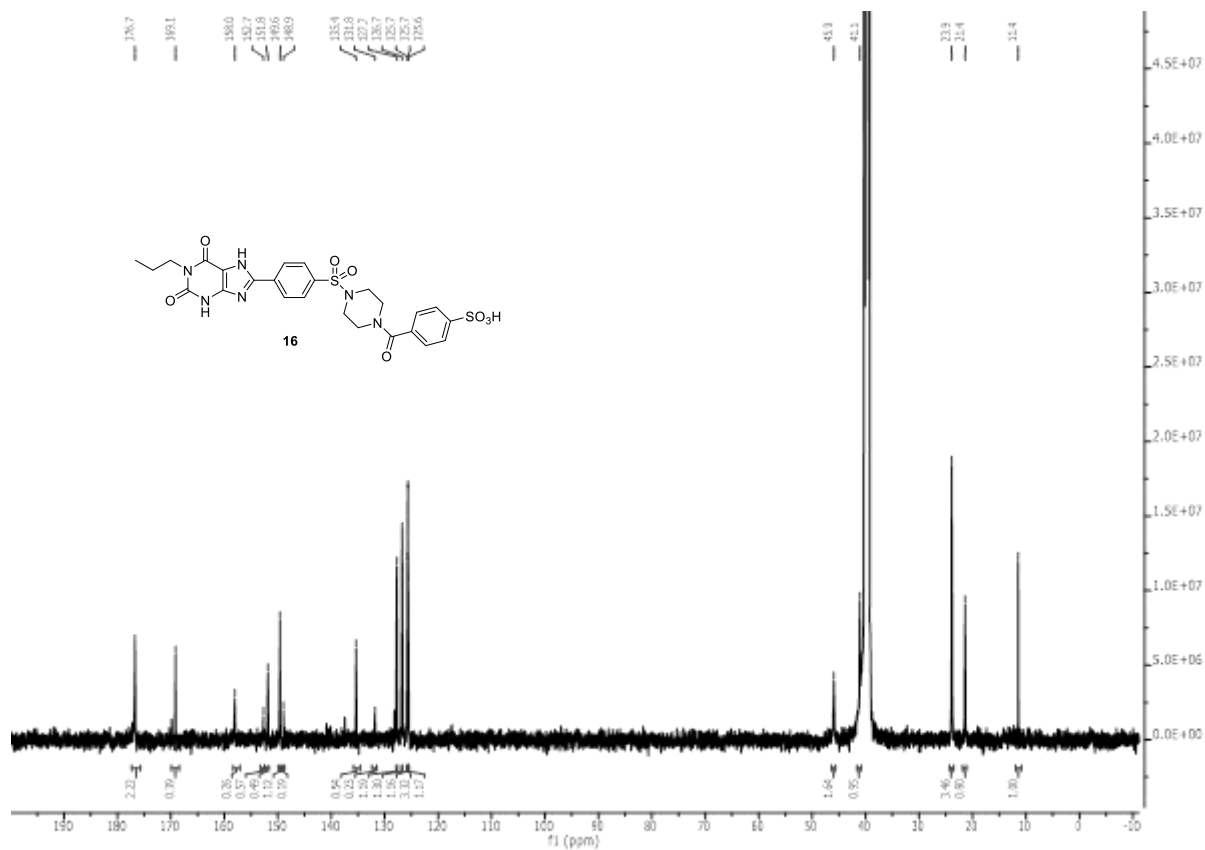
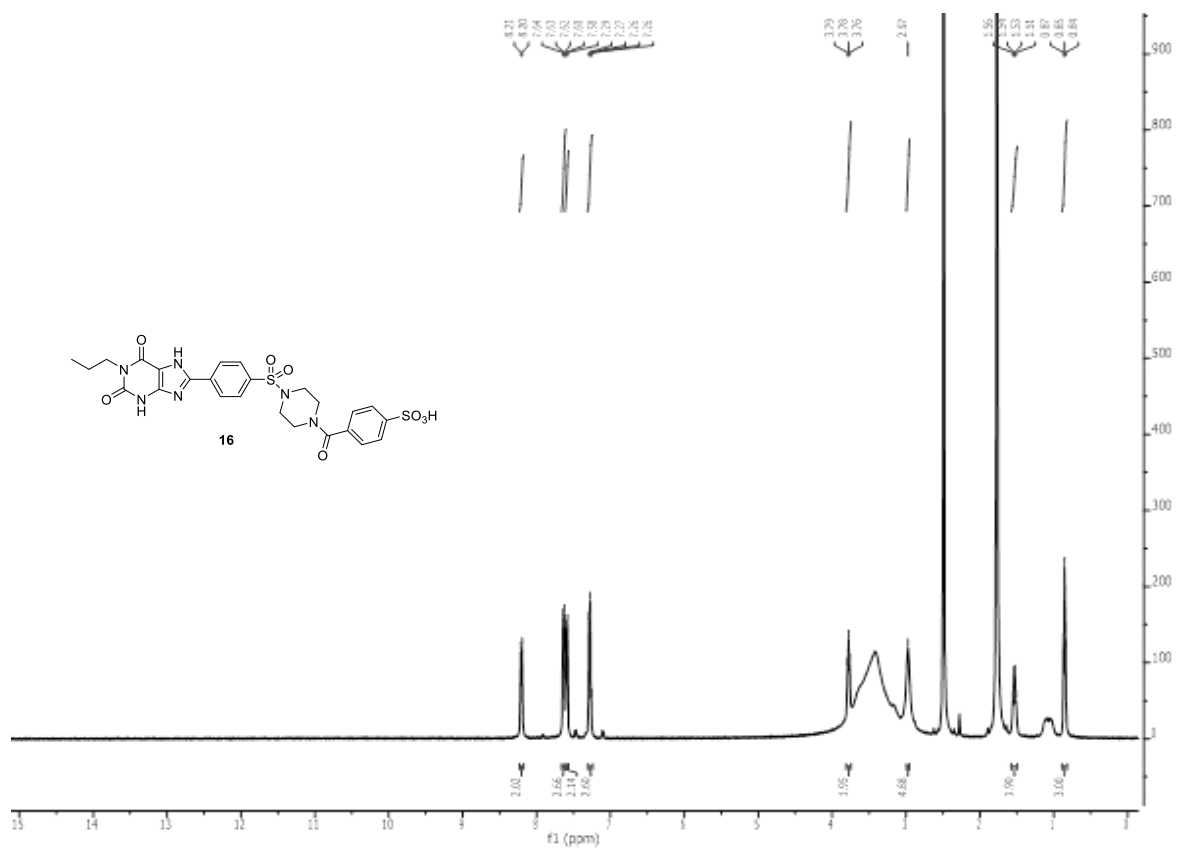
S6. ^{13}C NMR of compound 14.

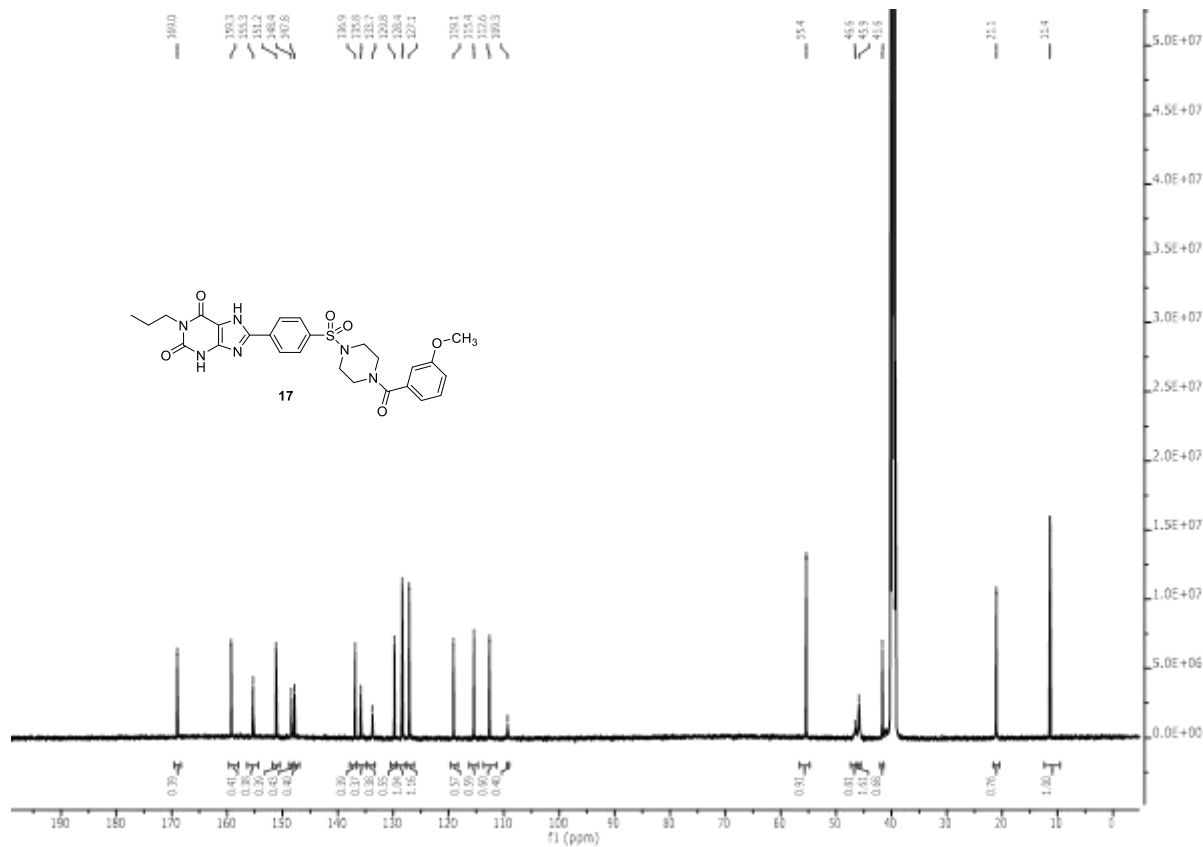
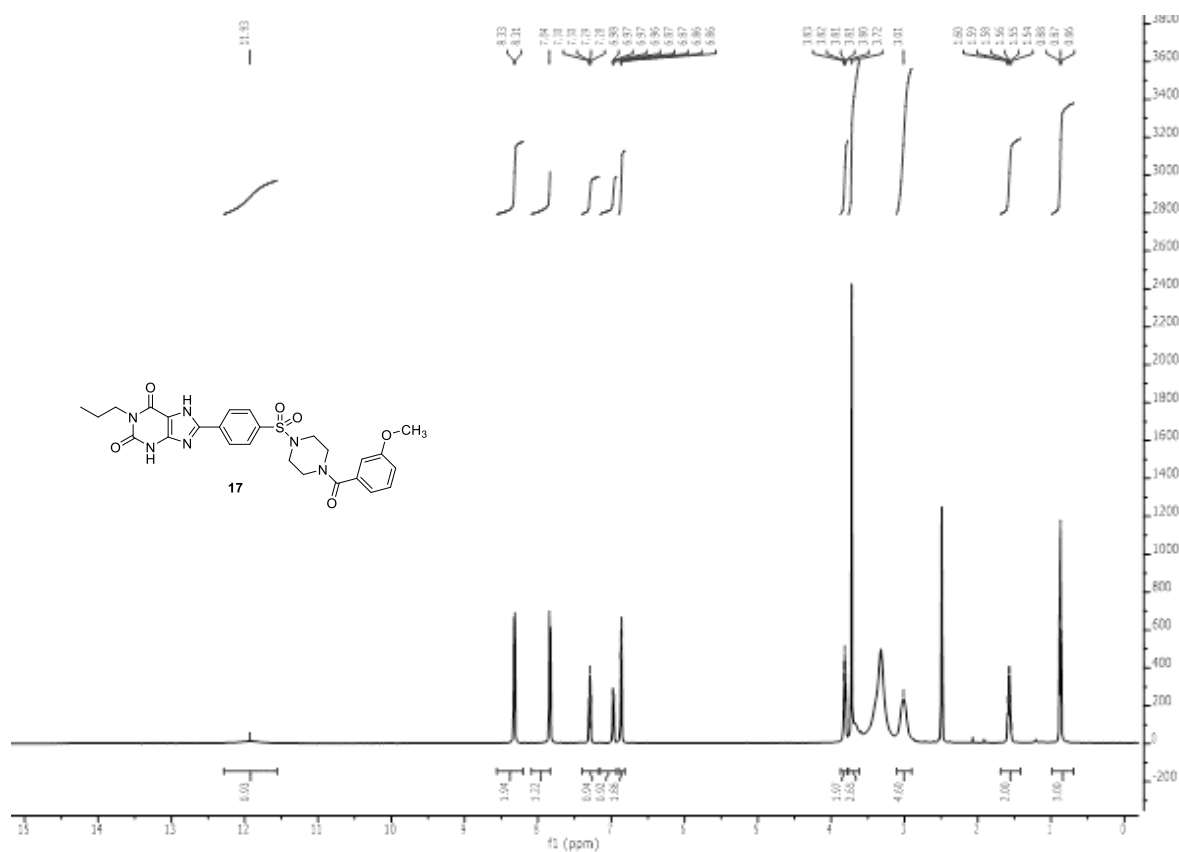


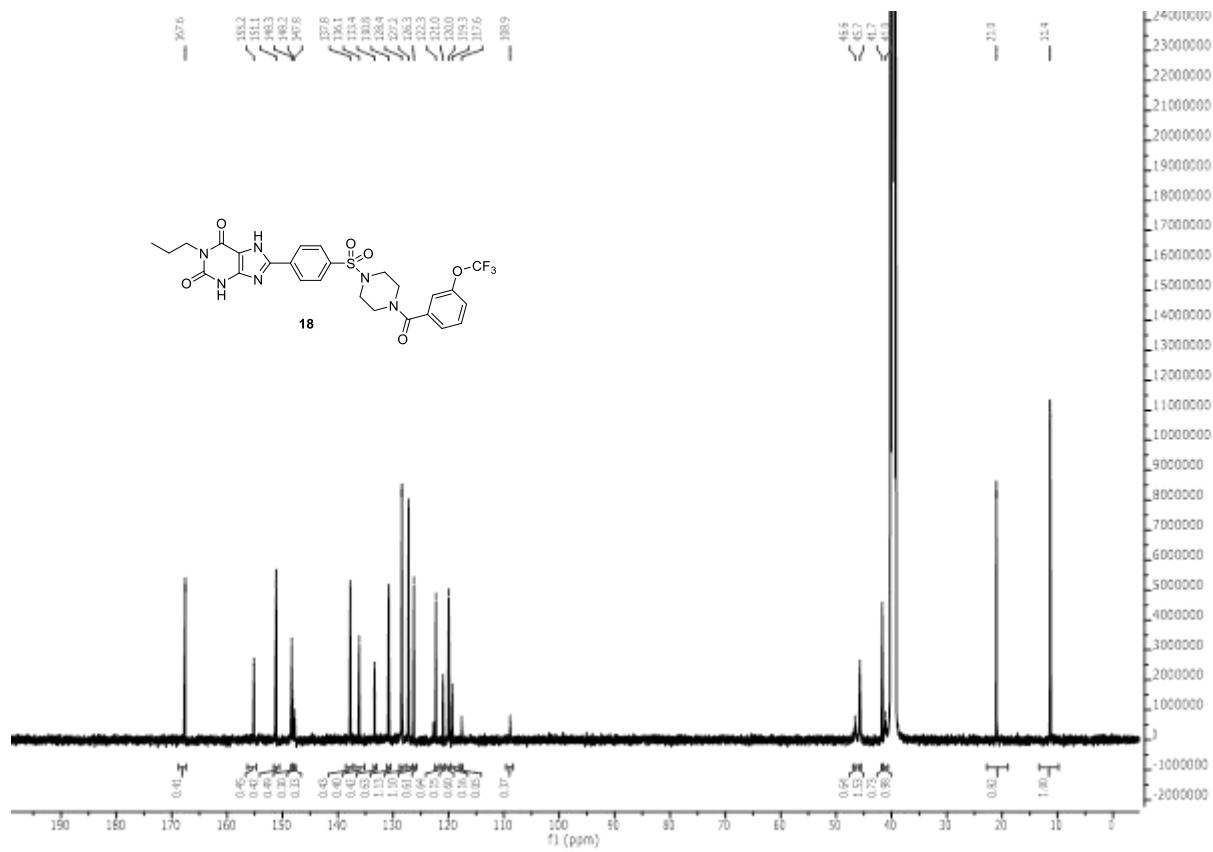
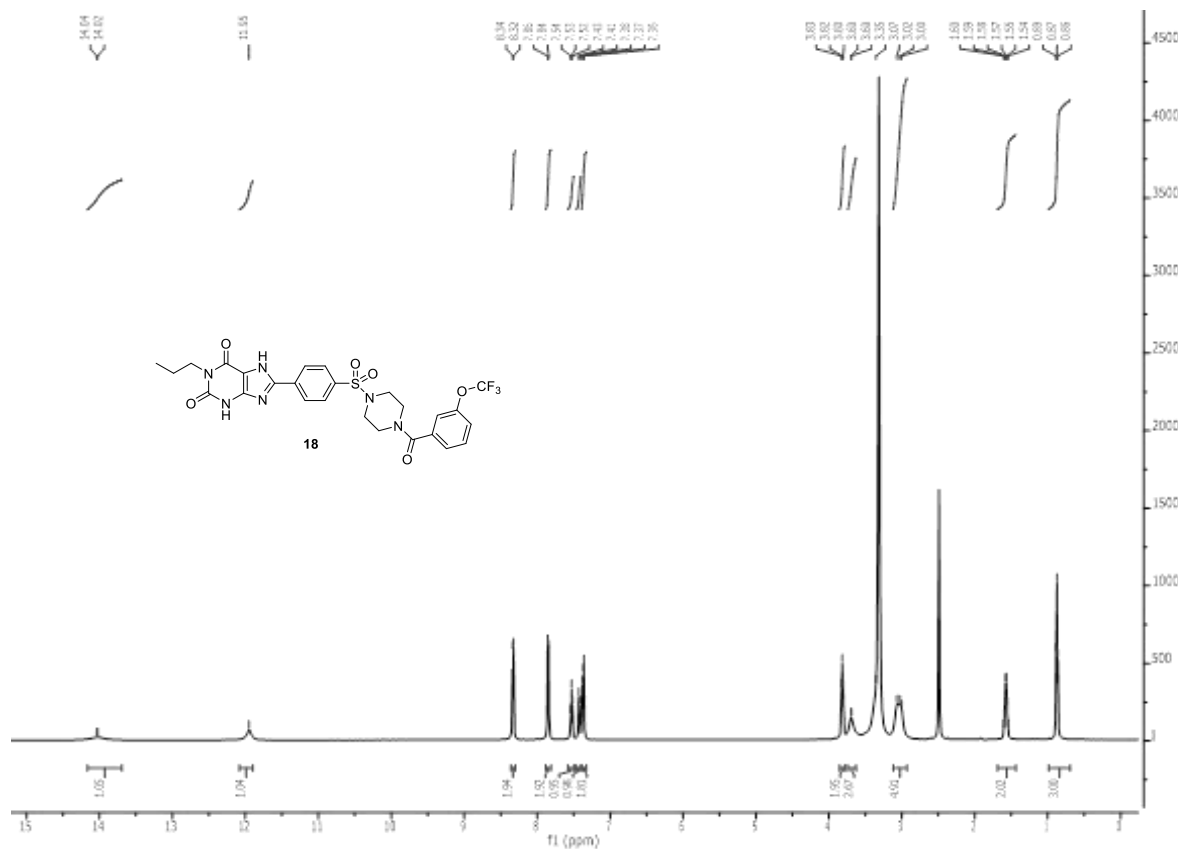
S7. ¹H NMR of compound 15.

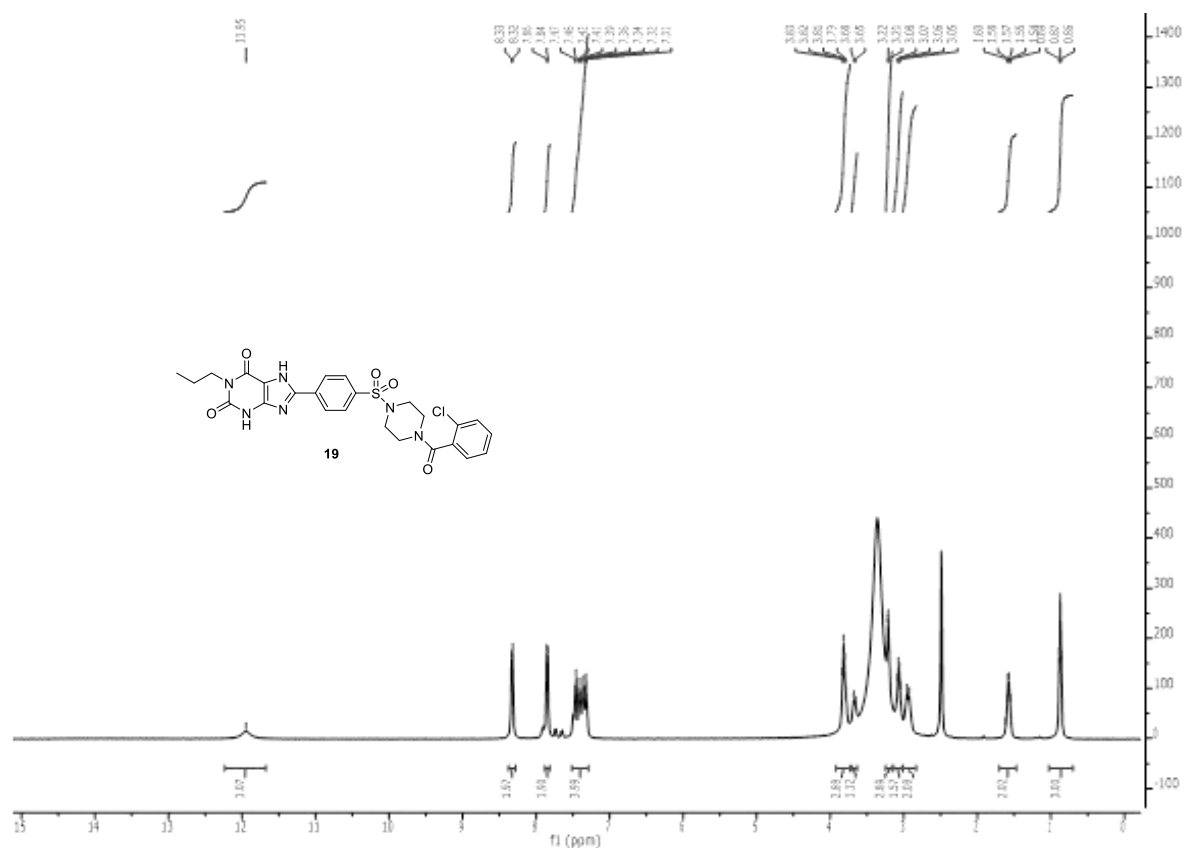


S8. ¹³C NMR of compound 15.

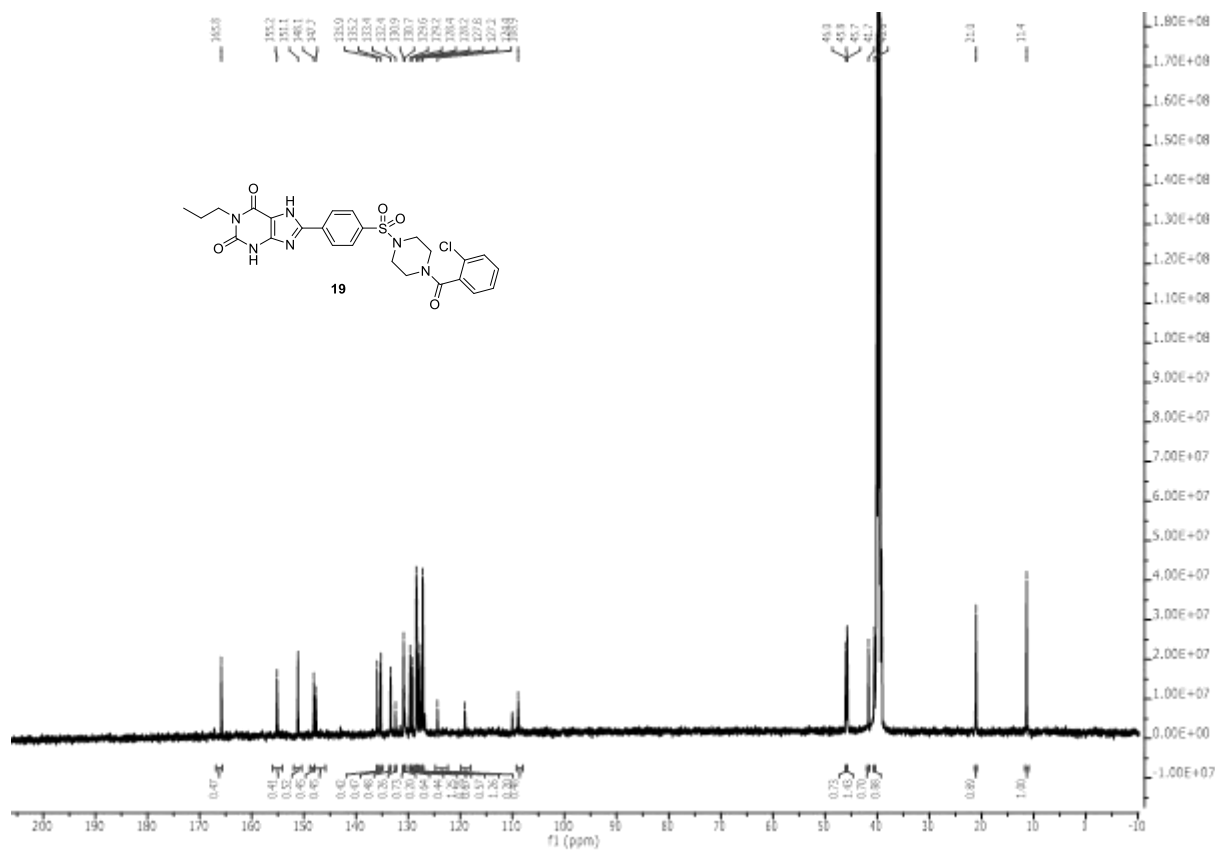




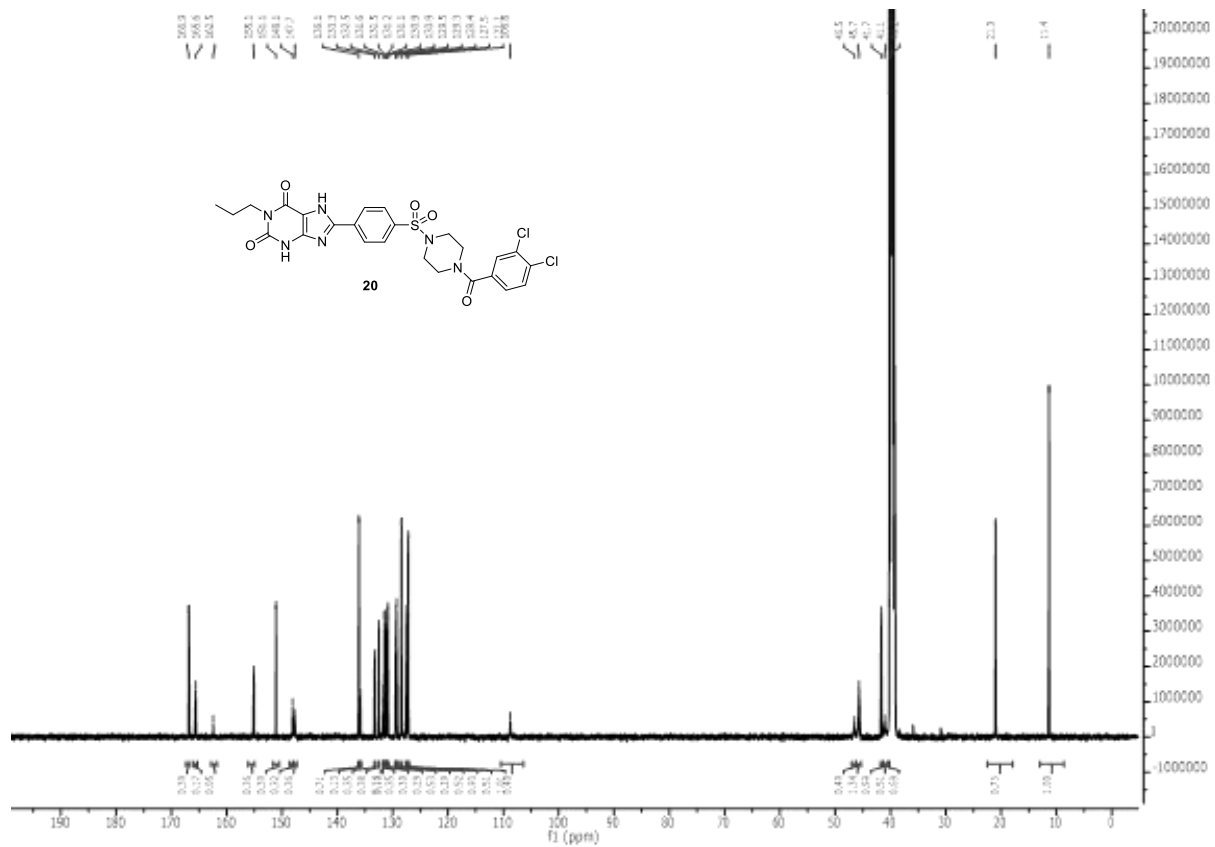
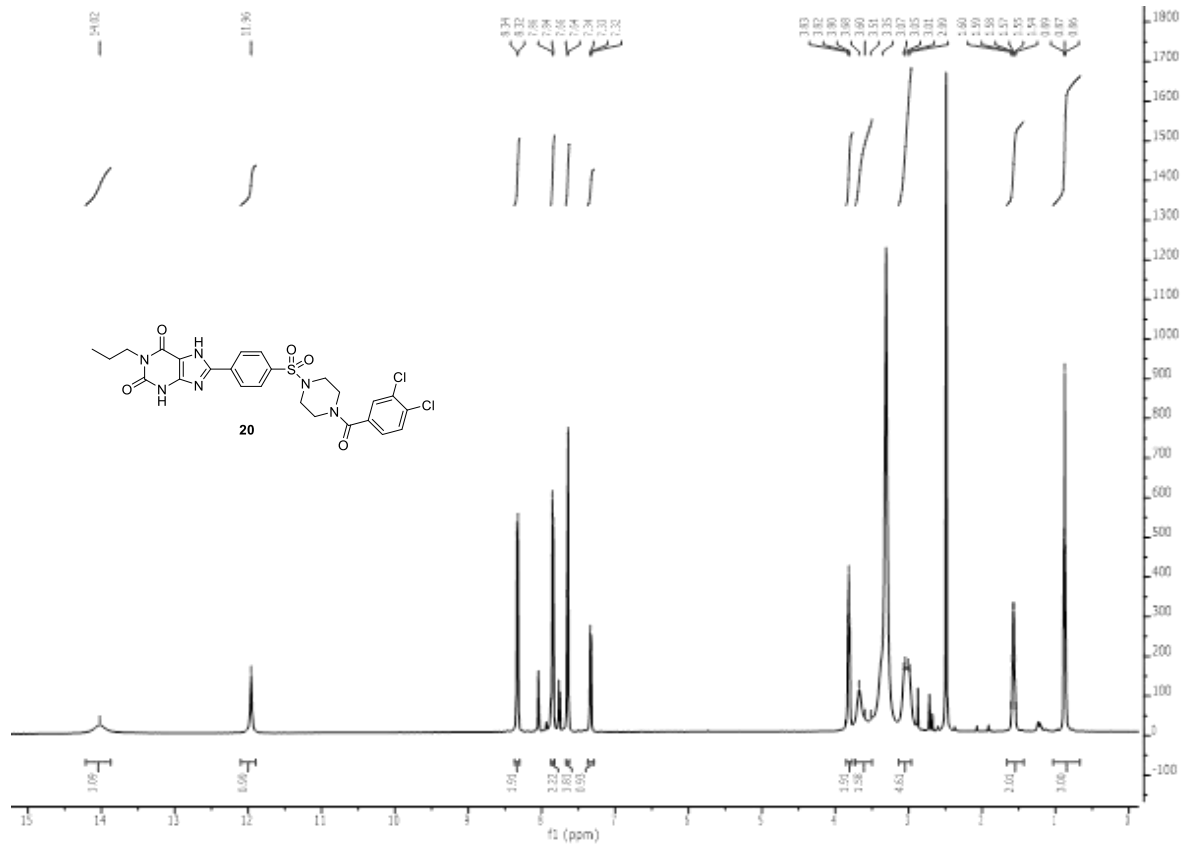


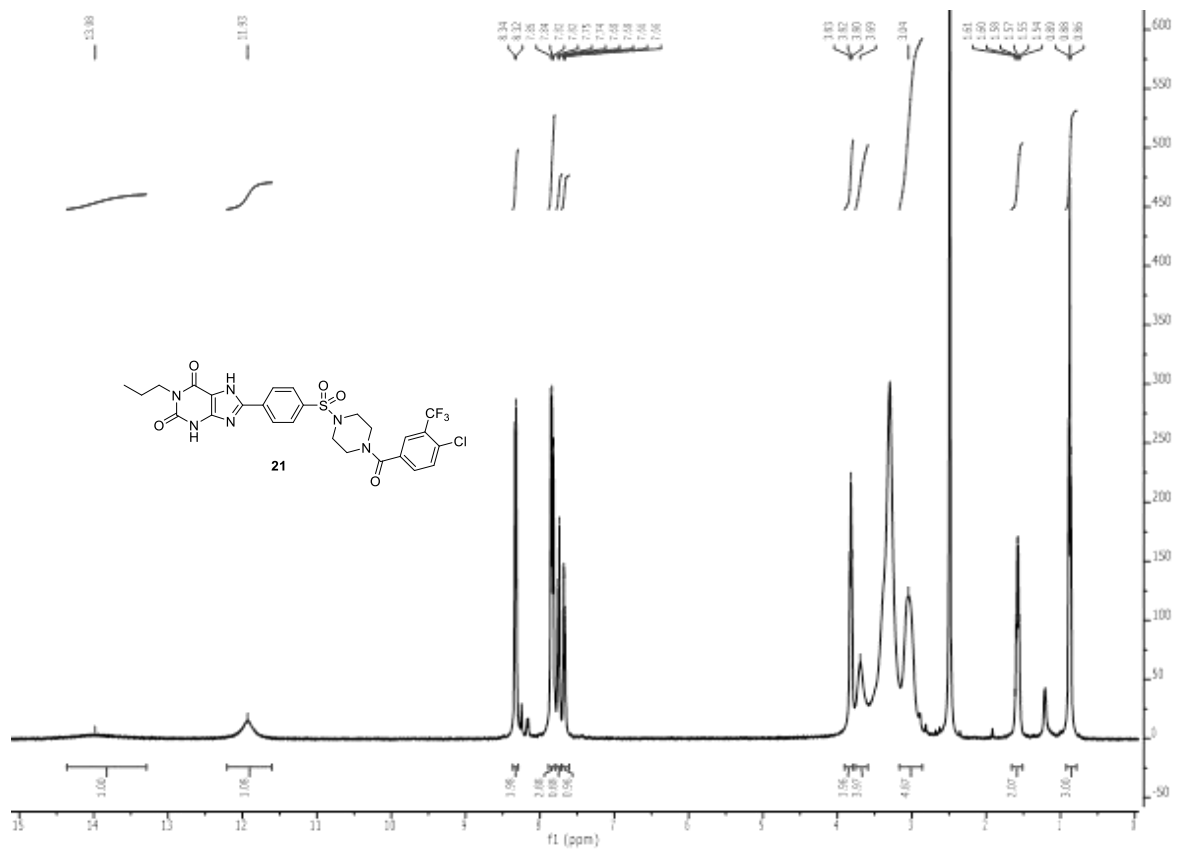


S15. ¹H NMR of compound 19.

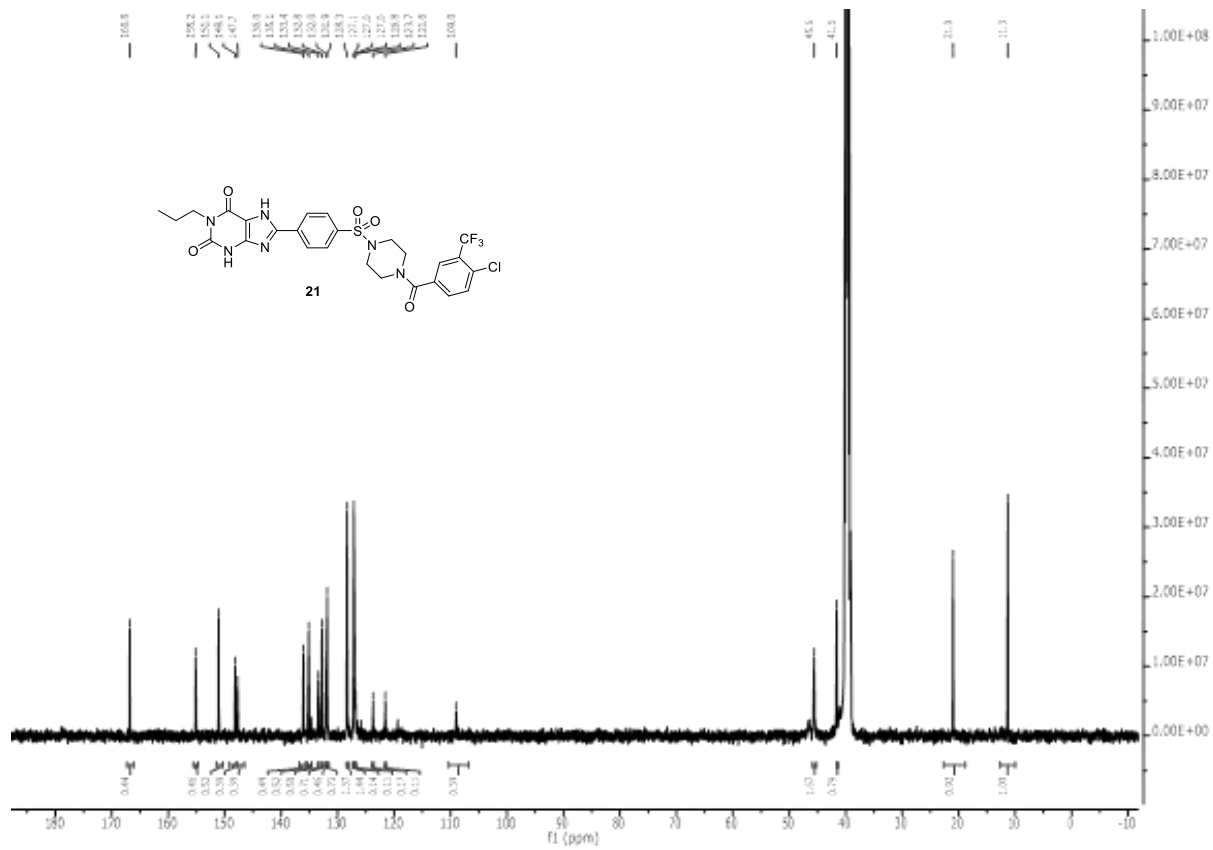


S16. ¹³C NMR of compound 19.

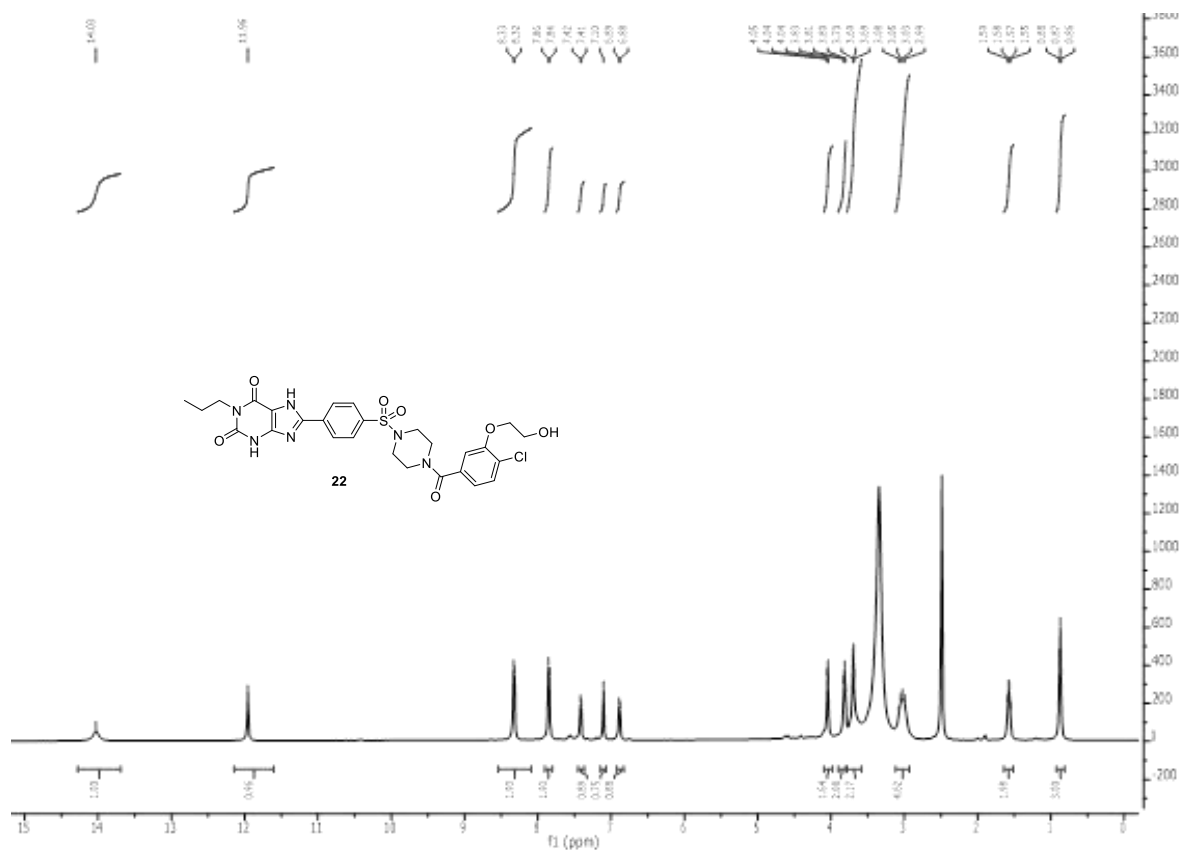




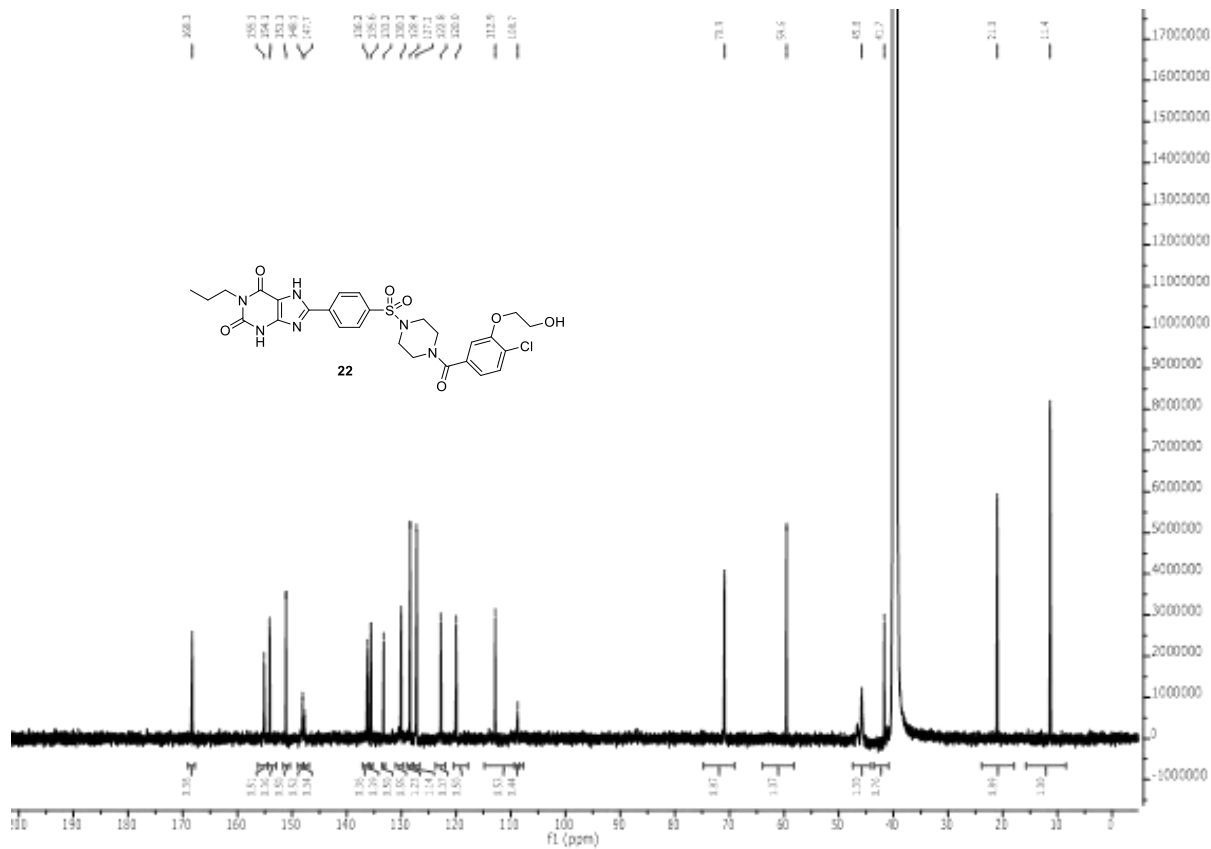
S19. ¹H NMR of compound **21**.



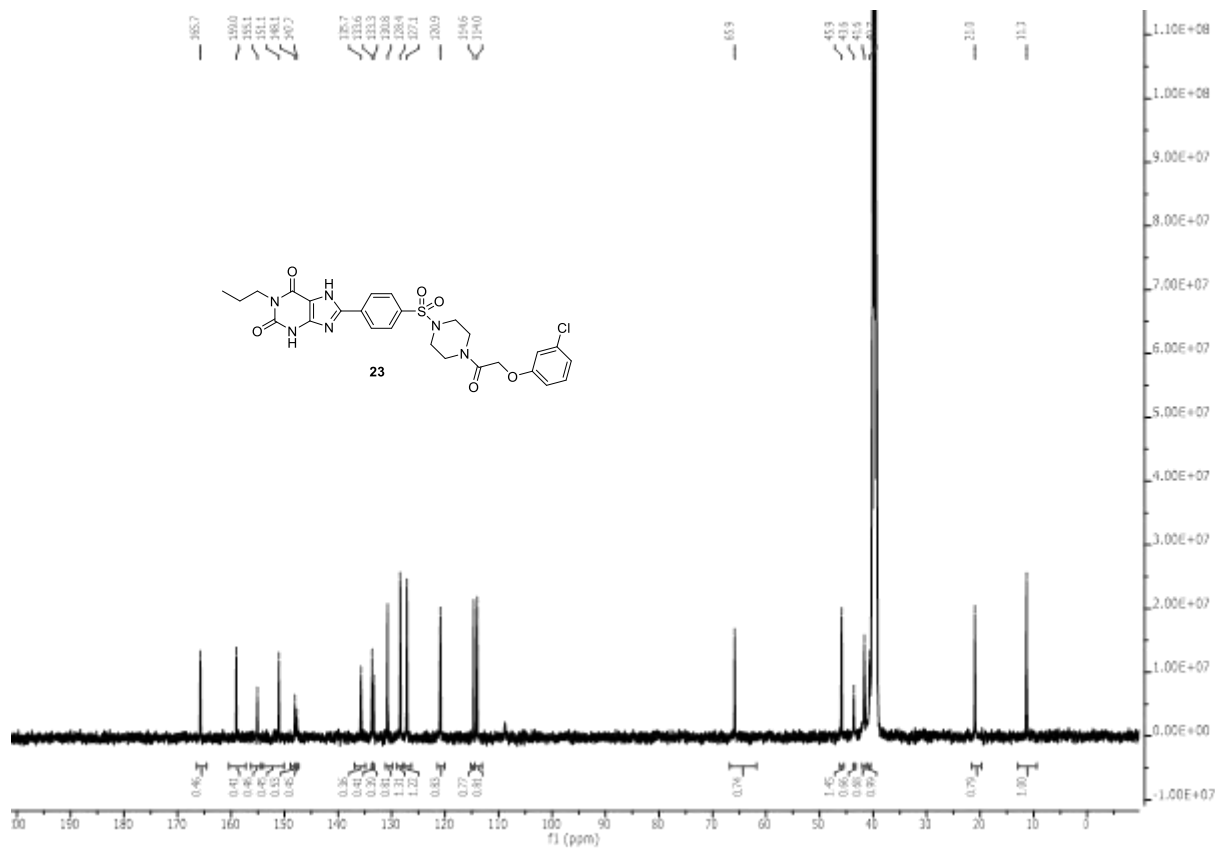
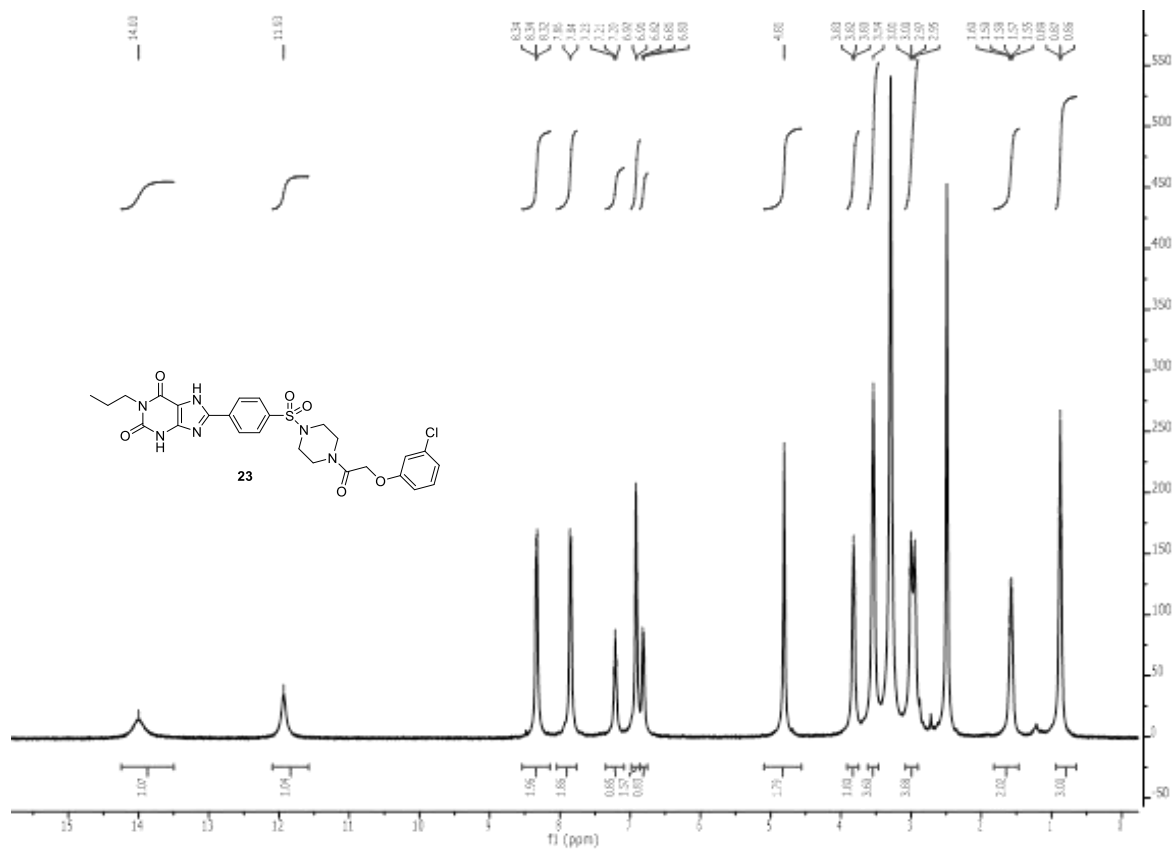
S20. ¹³C NMR of compound **21**.

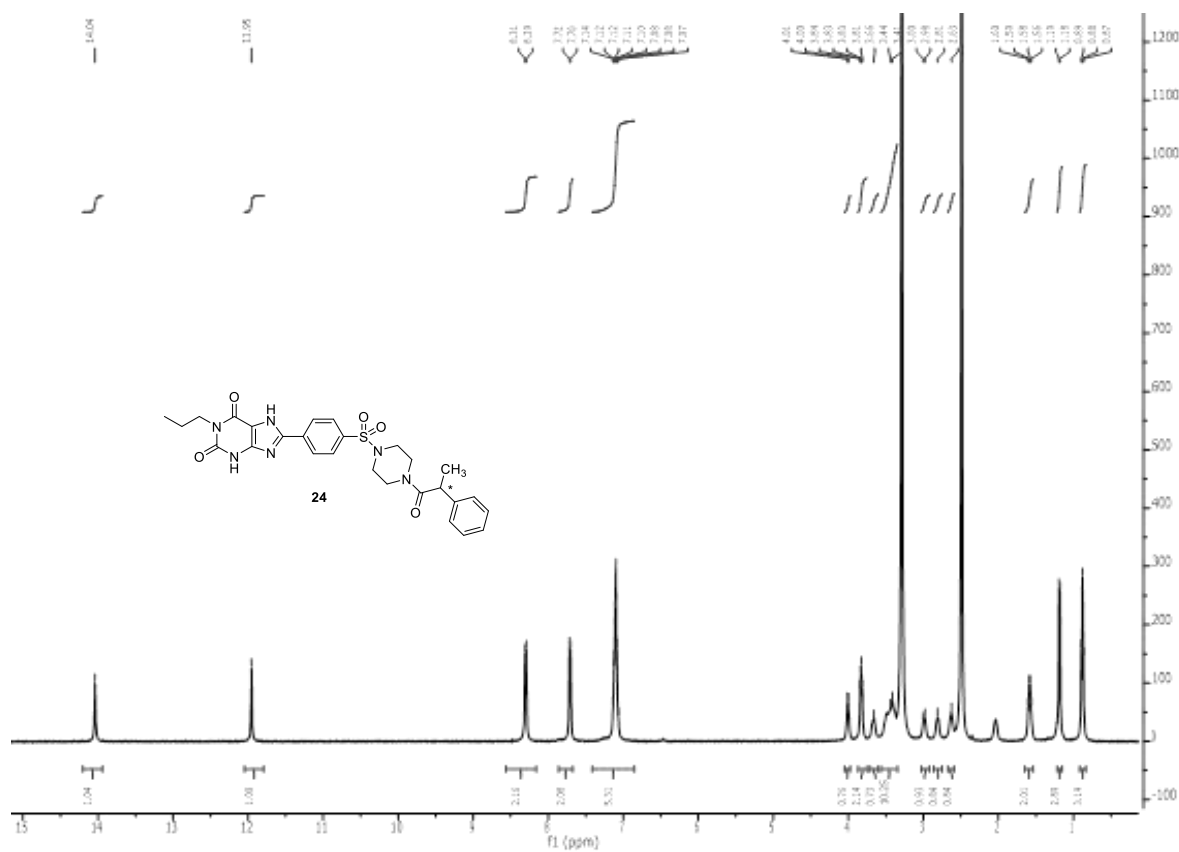


S21. ¹H NMR of compound 22.

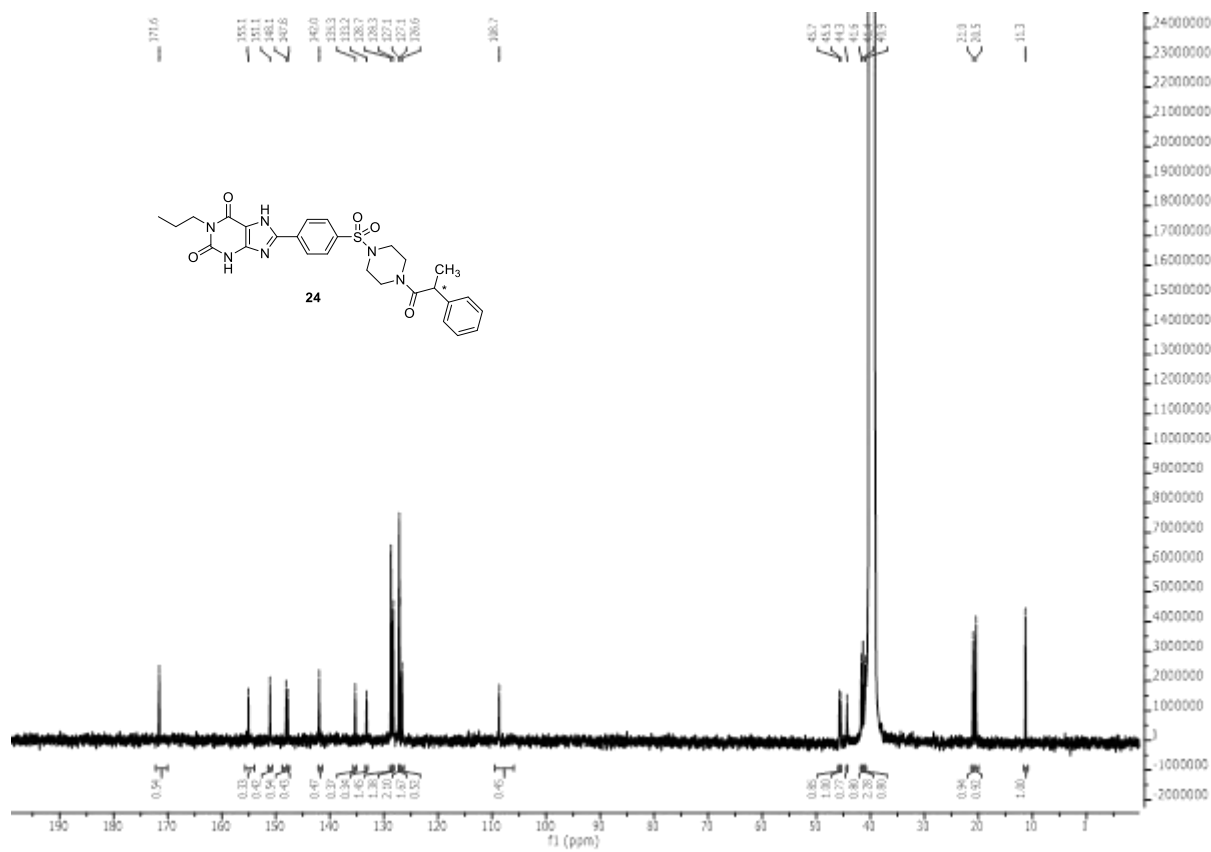


S22. ¹³C NMR of compound 22.

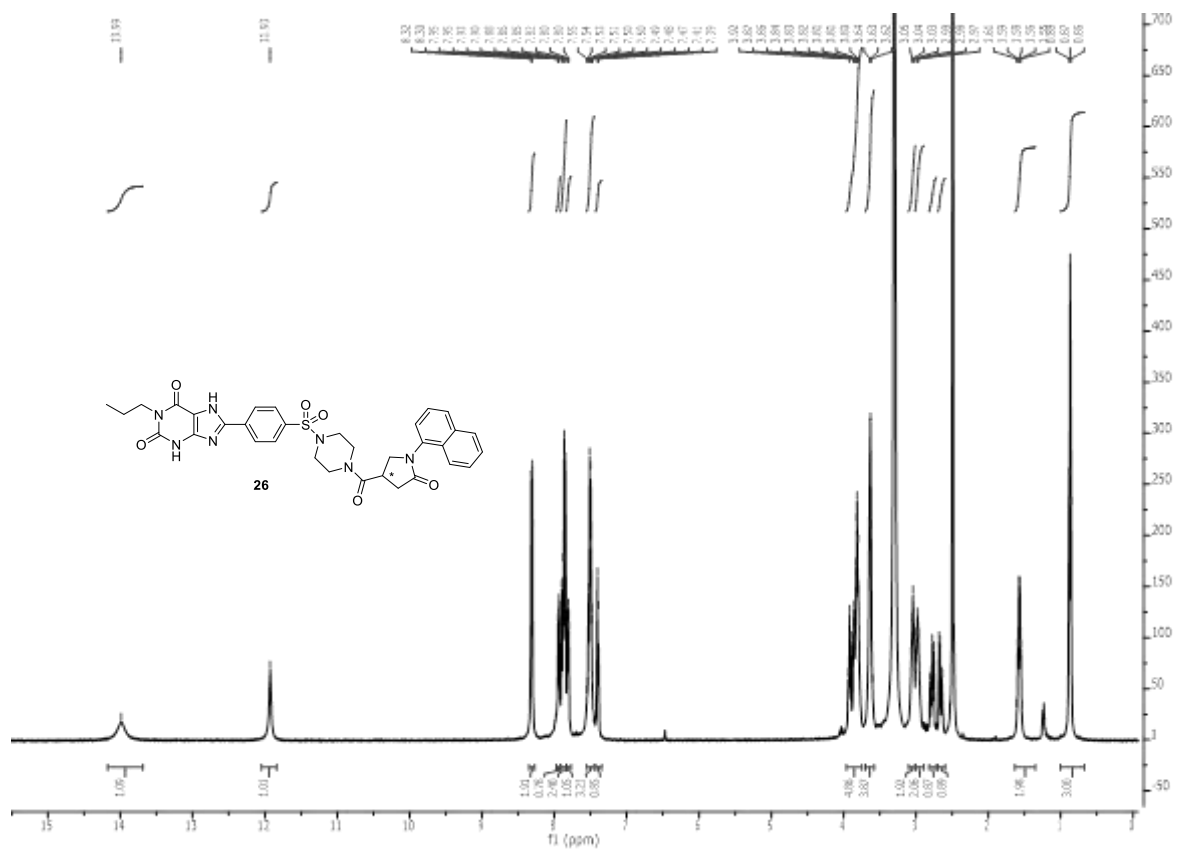




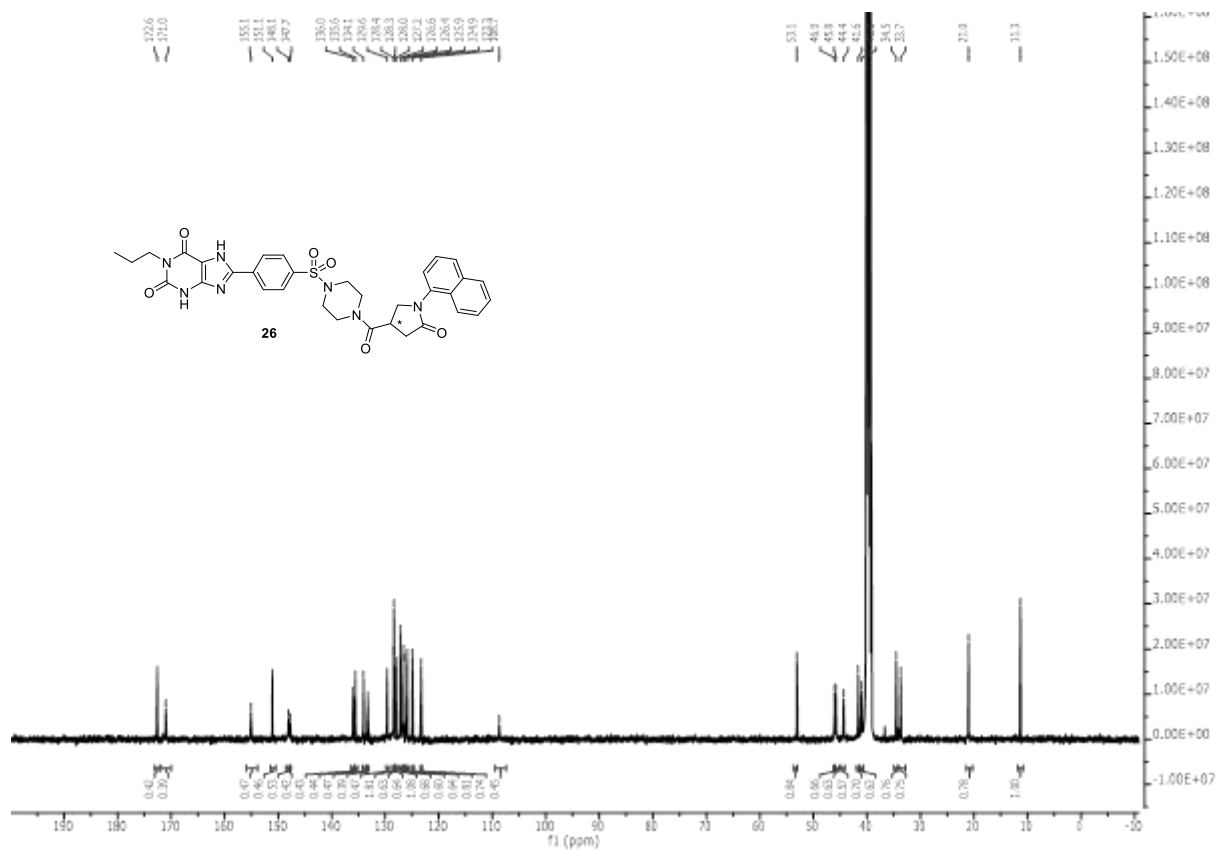
S25. ¹H NMR of compound 24.



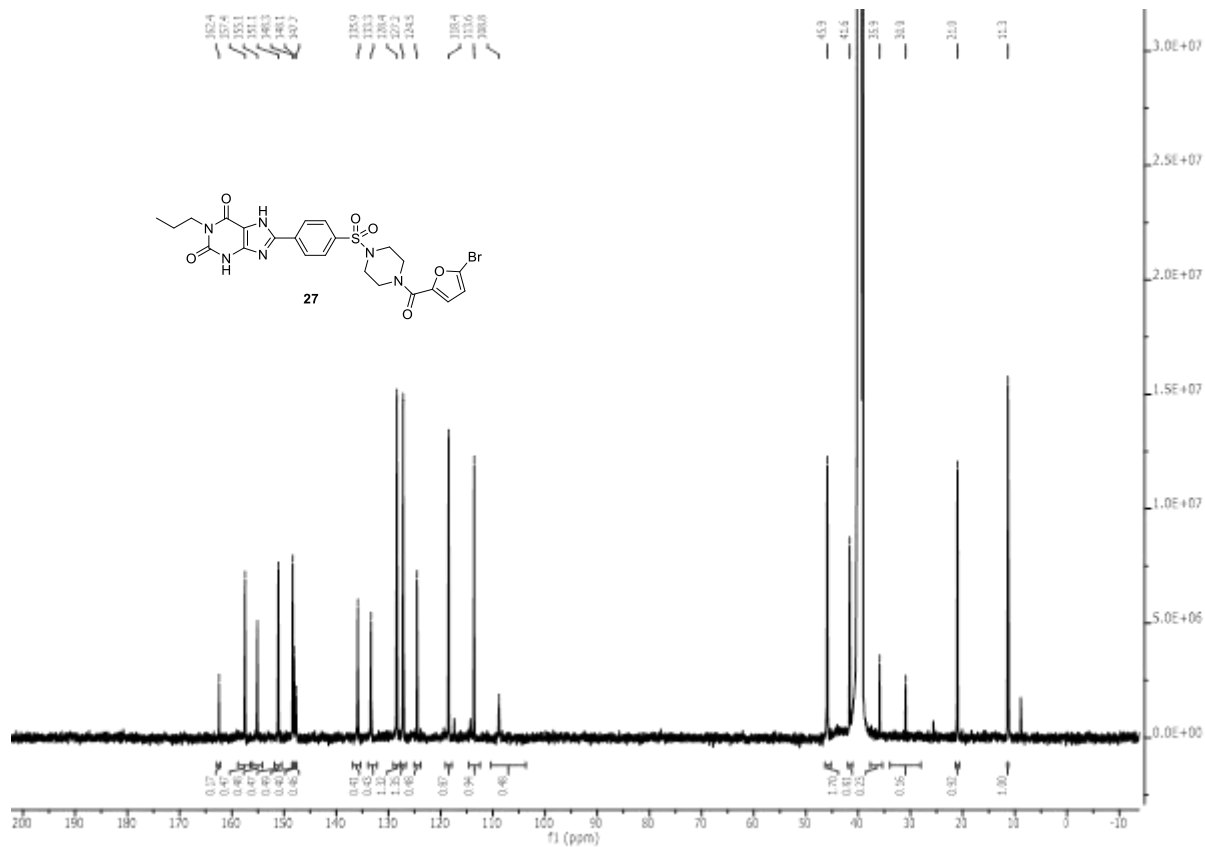
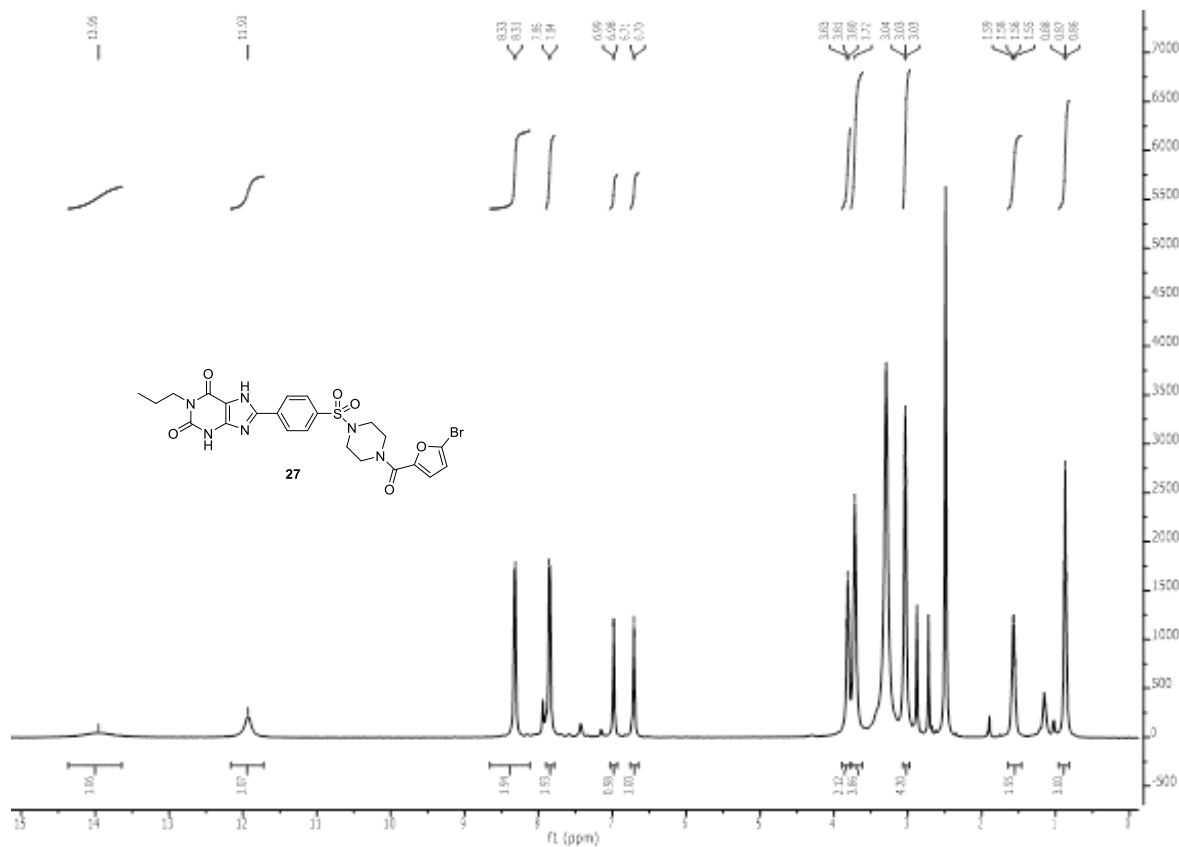
S26. ¹³C NMR of compound 24.

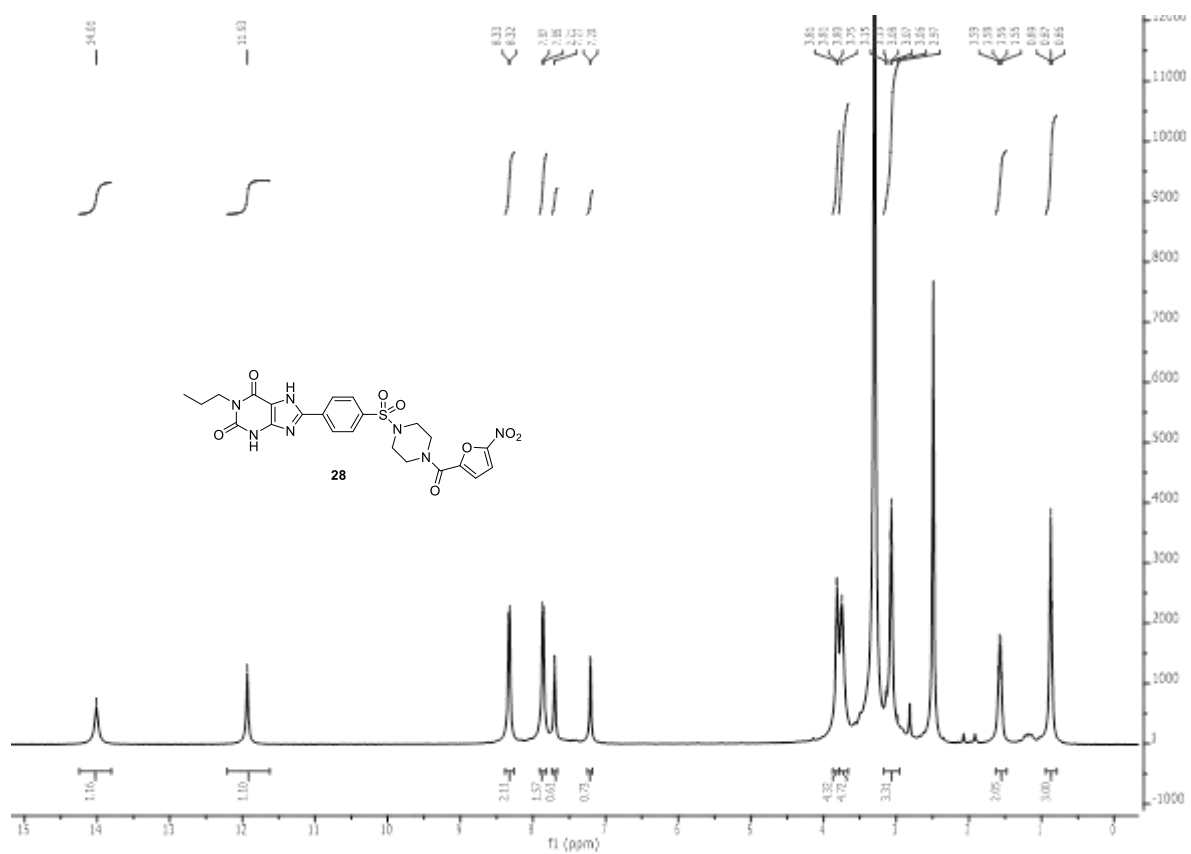


S29. ¹H NMR of compound **26**.

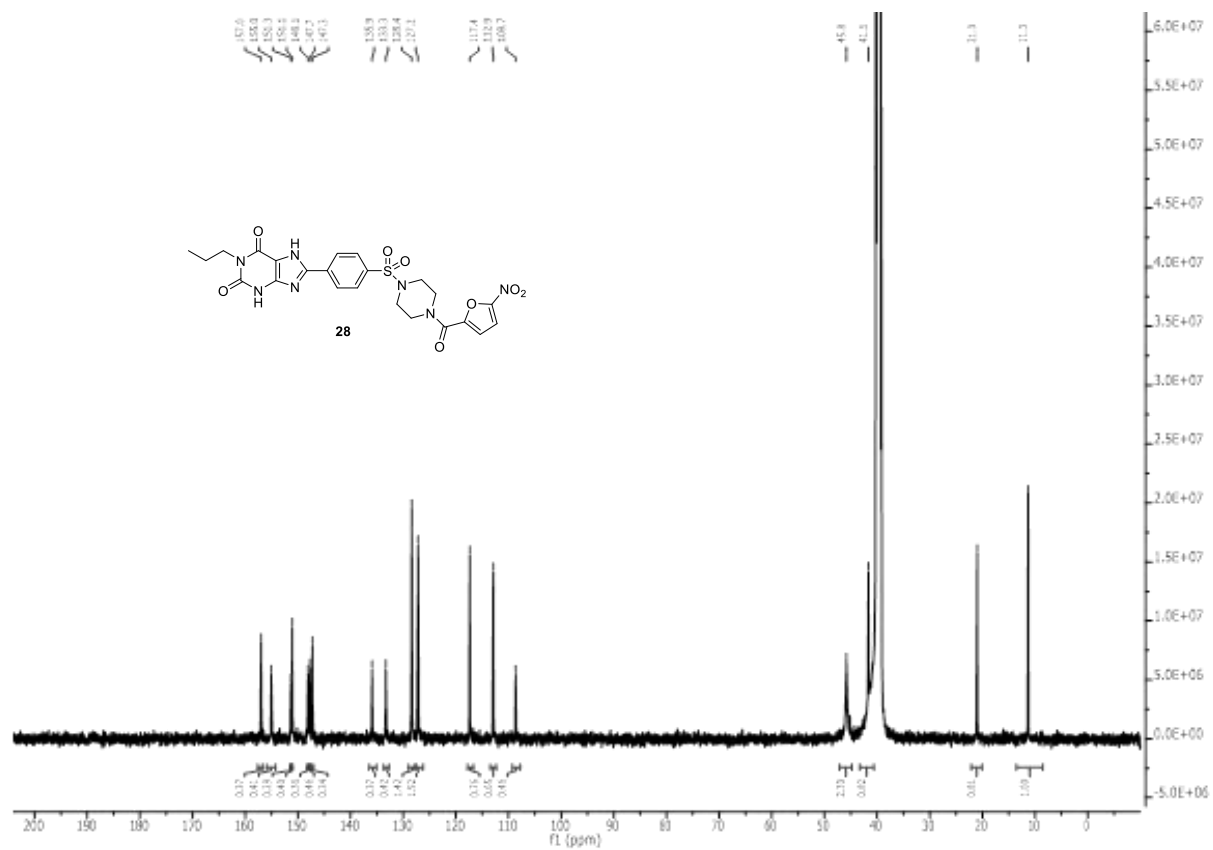


S30. ¹³C NMR of compound **26**.

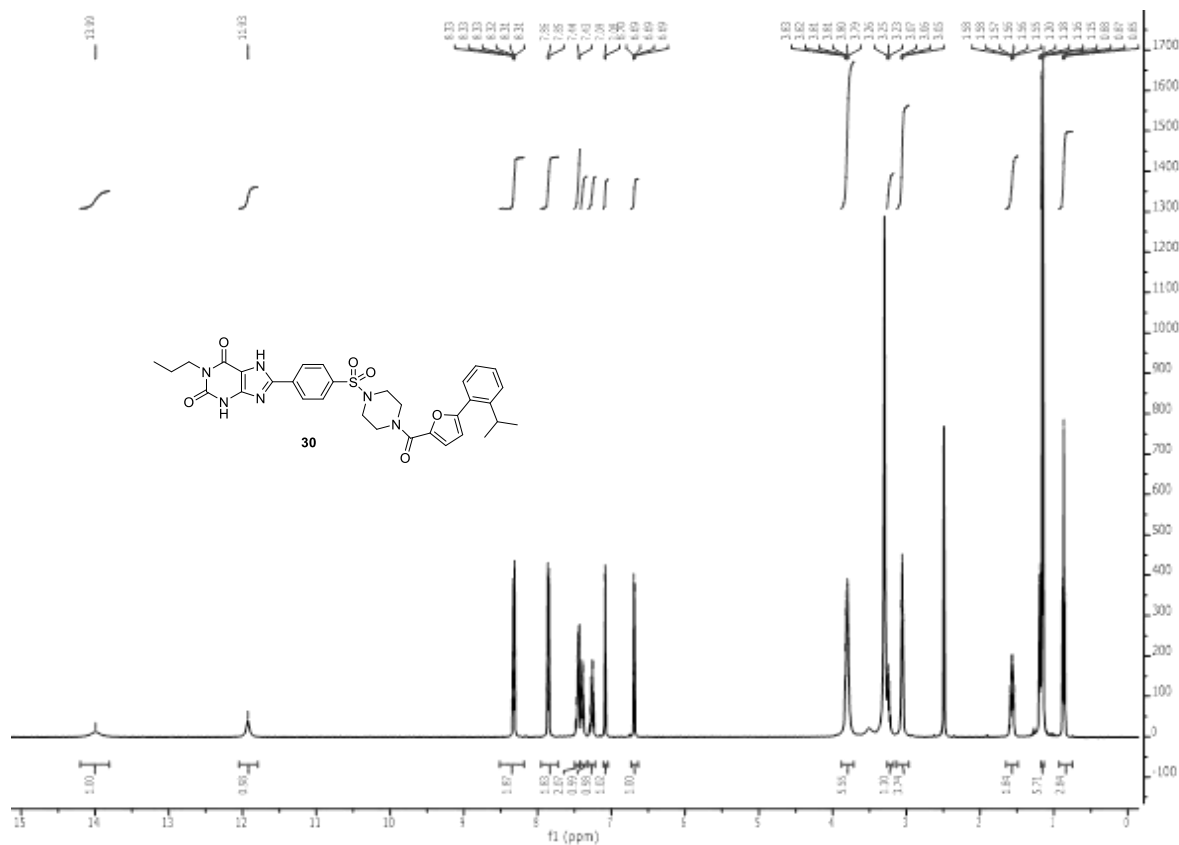




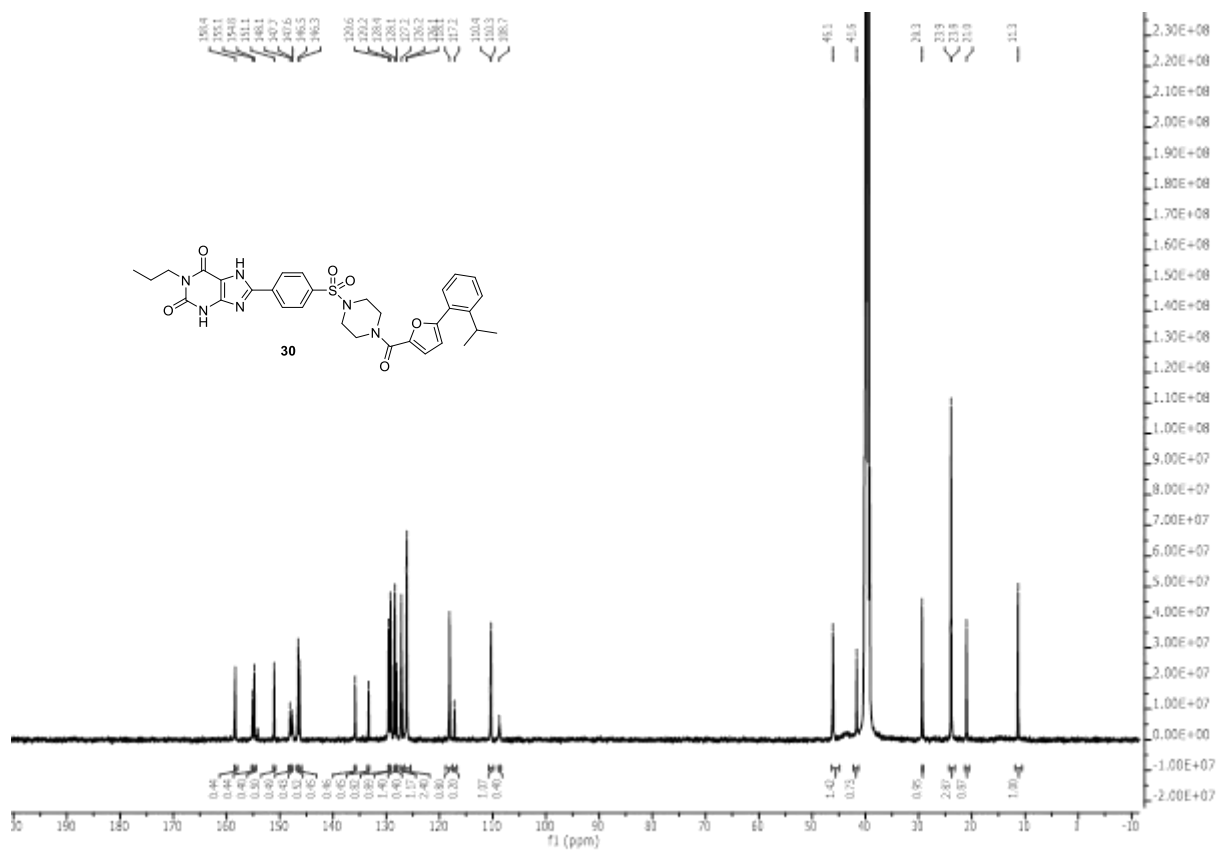
S33. ¹H NMR of compound **28**.



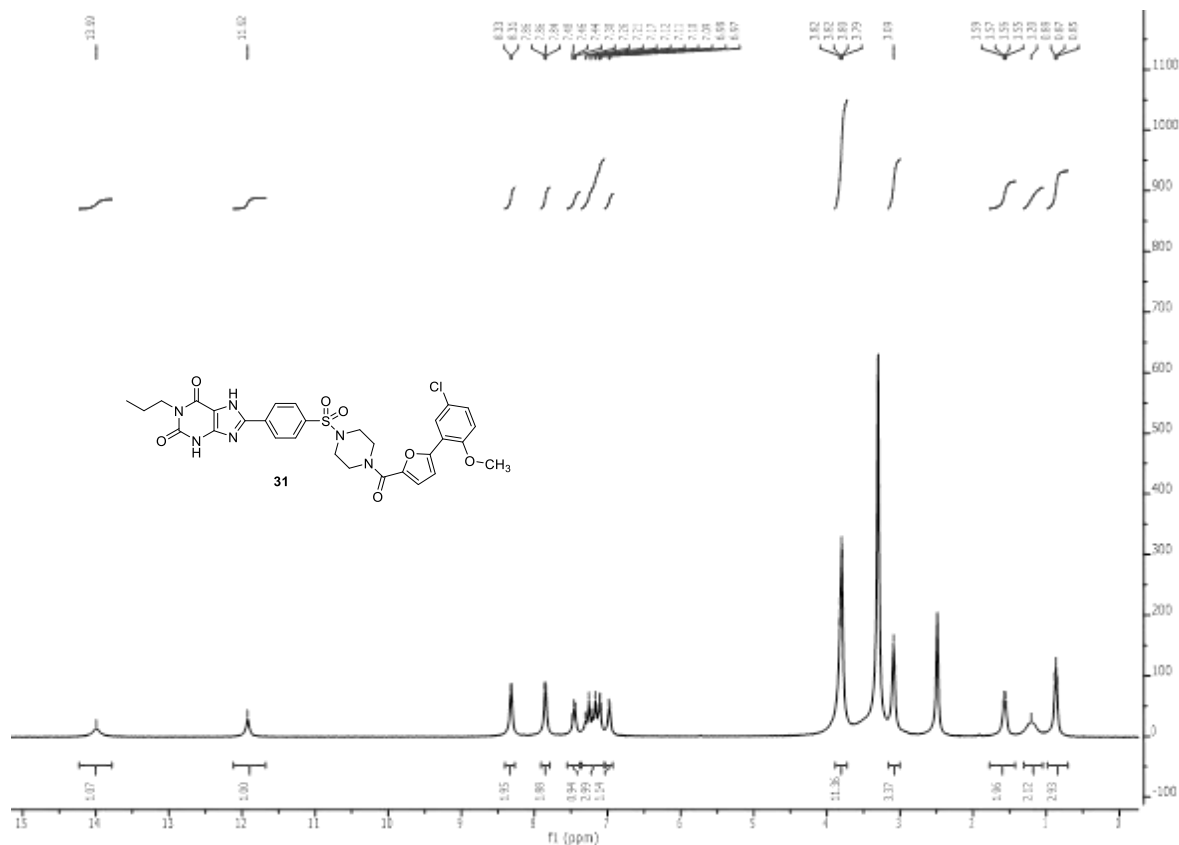
S34. ¹³C NMR of compound **28**.



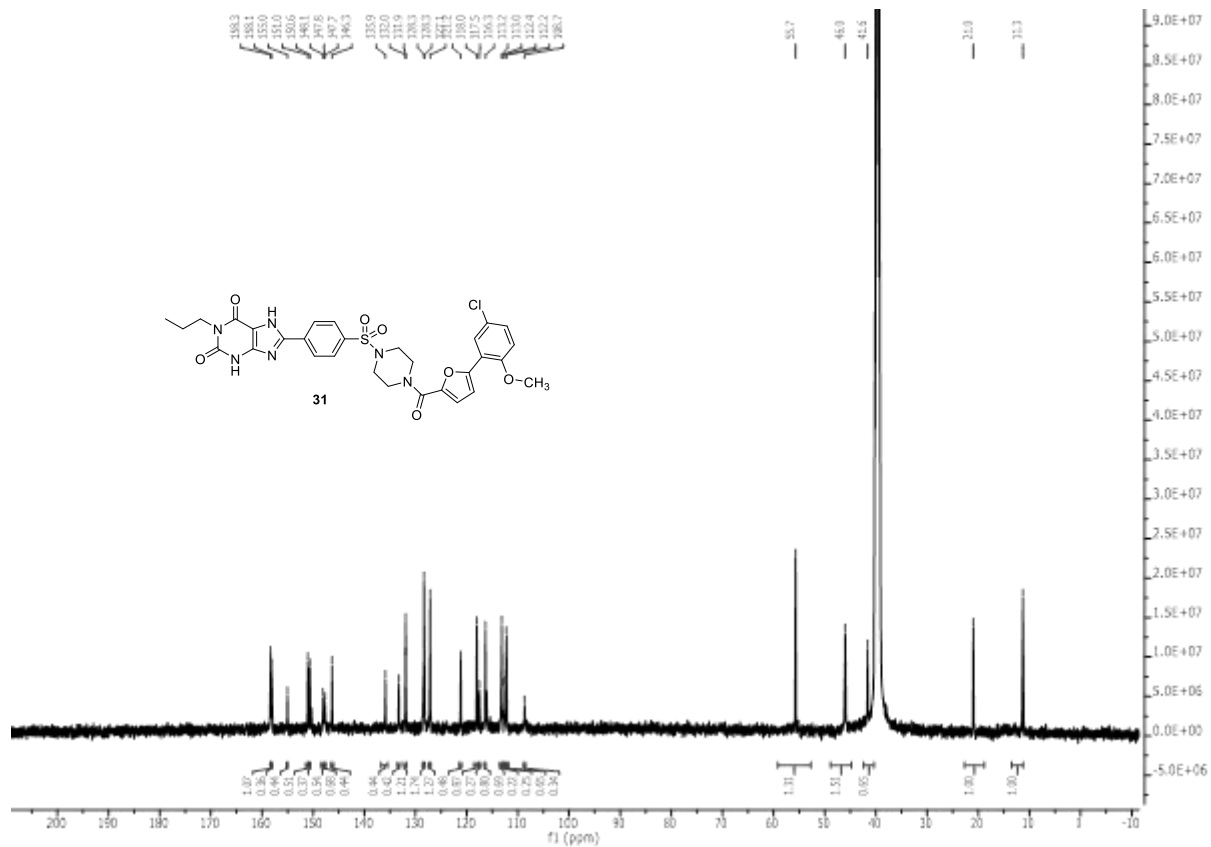
S37. ¹H NMR of compound **30**.



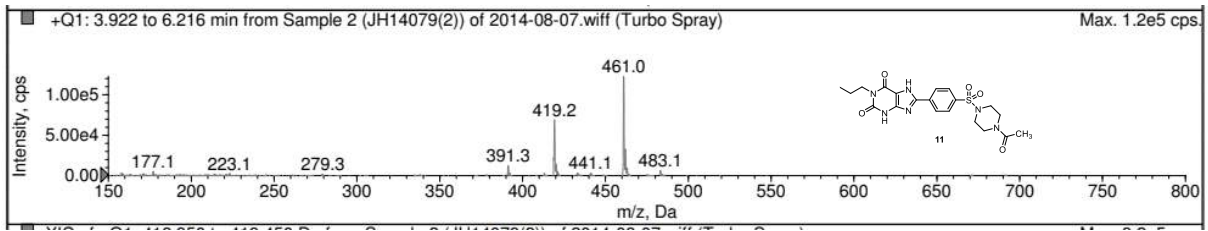
S38. ¹³C NMR of compound **30**.



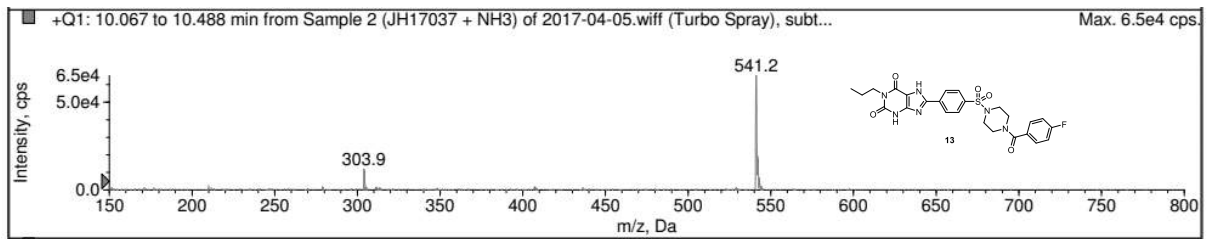
S39. ¹H NMR of compound 31.



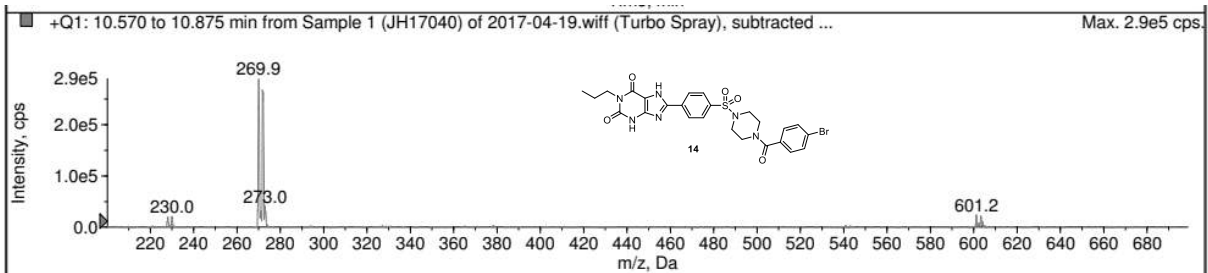
S40. ¹³C NMR of compound 31.



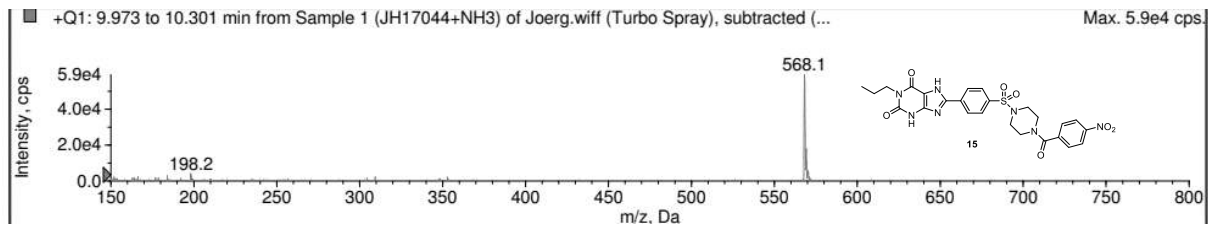
S41. Mass spectrum of compound 11.



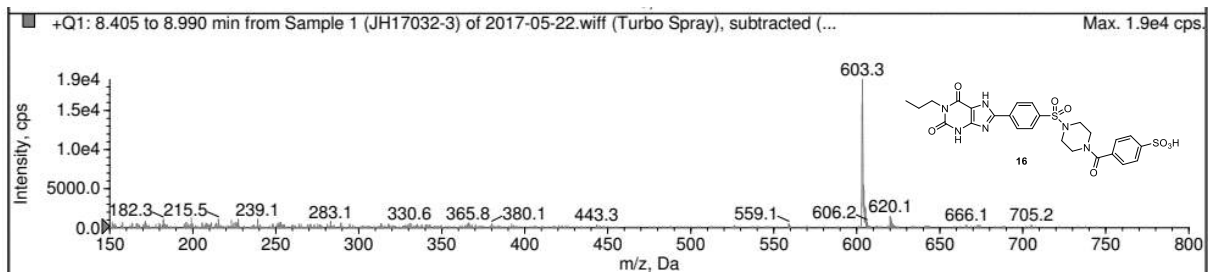
S42. Mass spectrum of compound 13.



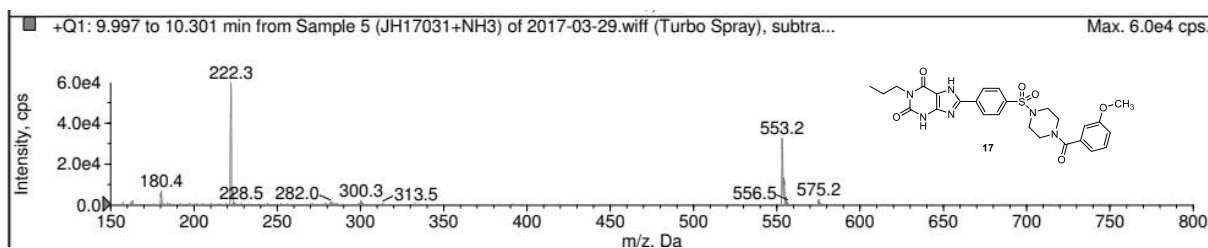
S43. Mass spectrum of compound 14.



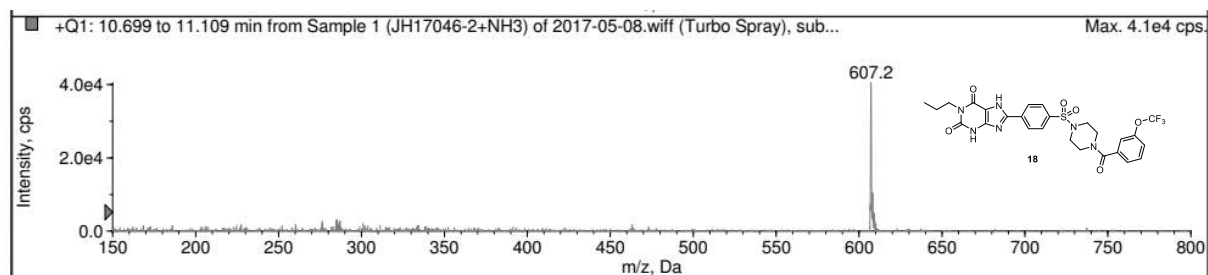
S44. Mass spectrum of compound 15.



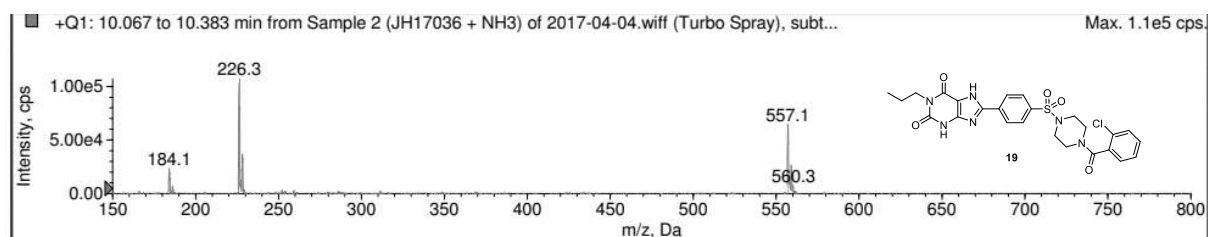
S45. Mass spectrum of compound 16.



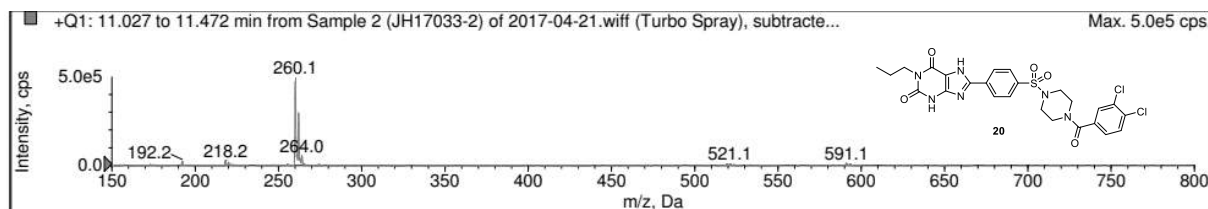
S46. Mass spectrum of compound 17.



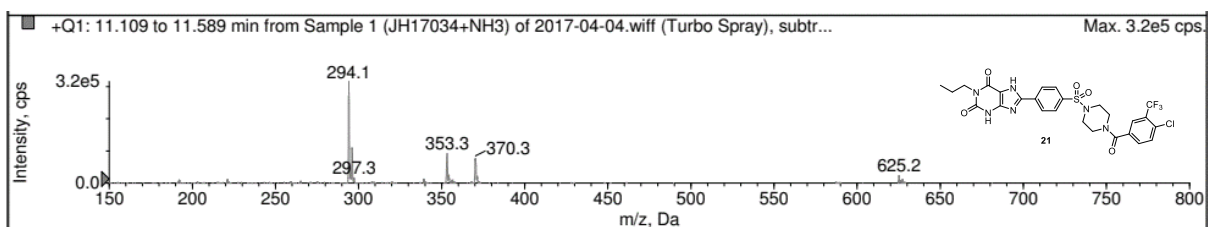
S47. Mass spectrum of compound 18.



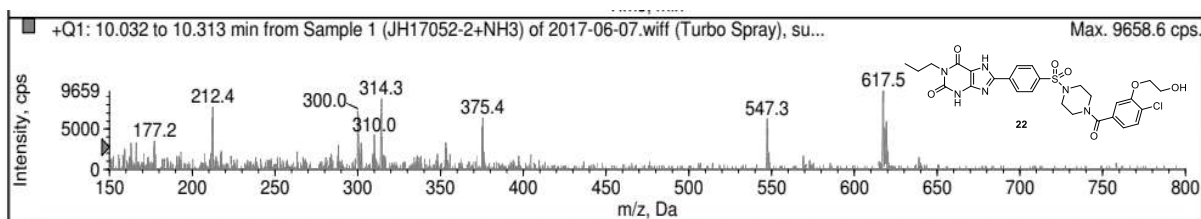
S48. Mass spectrum of compound 19.



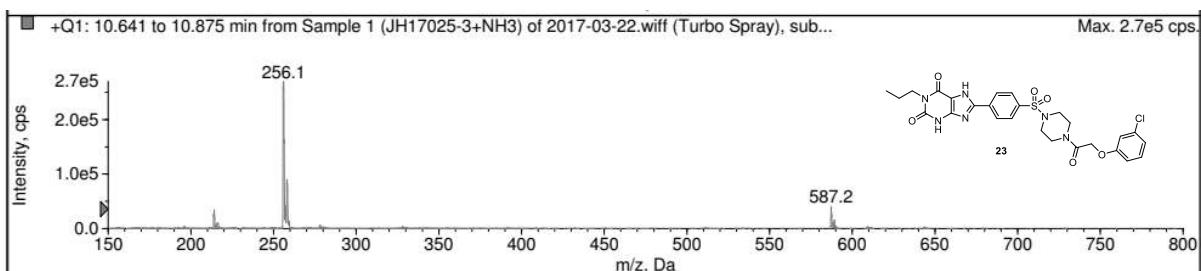
S49. Mass spectrum of compound 20.



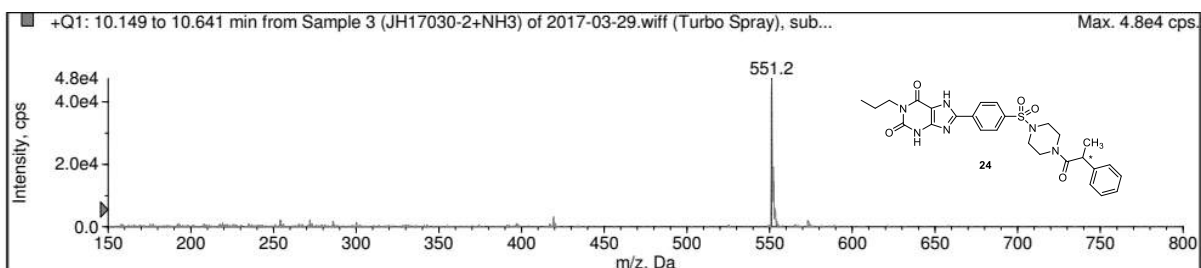
S50. Mass spectrum of compound 21.



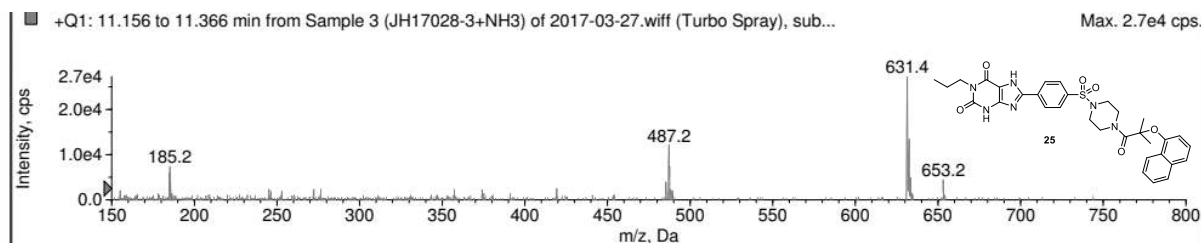
S51. Mass spectrum of compound 22.



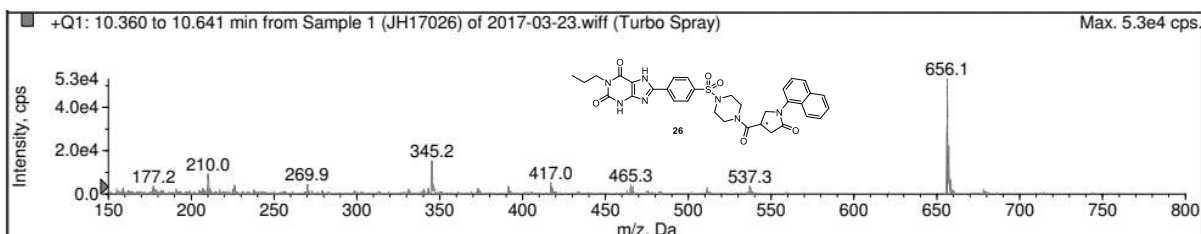
S52. Mass spectrum of compound 23.



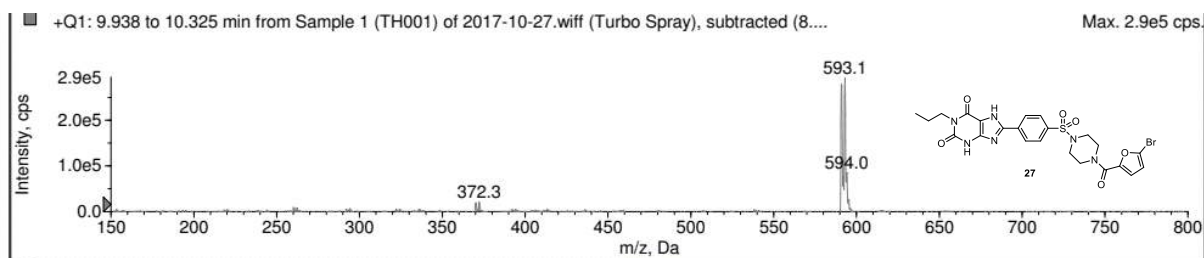
S53. Mass spectrum of compound 24.



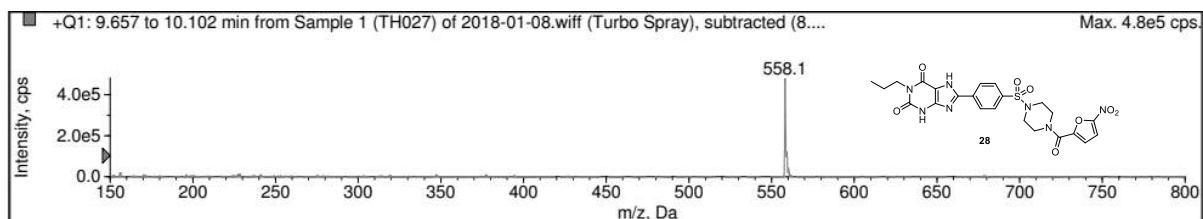
S54. Mass spectrum of compound 25.



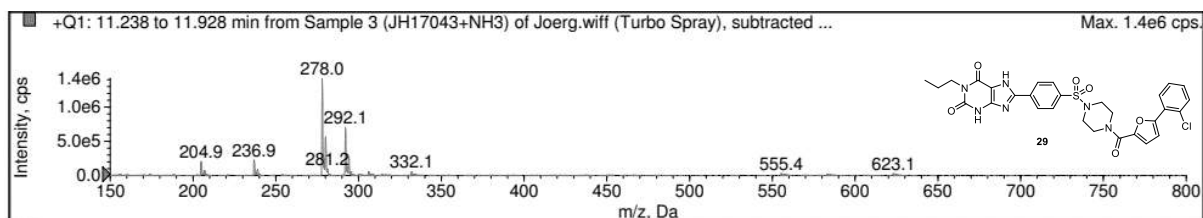
S55. Mass spectrum of compound 26.



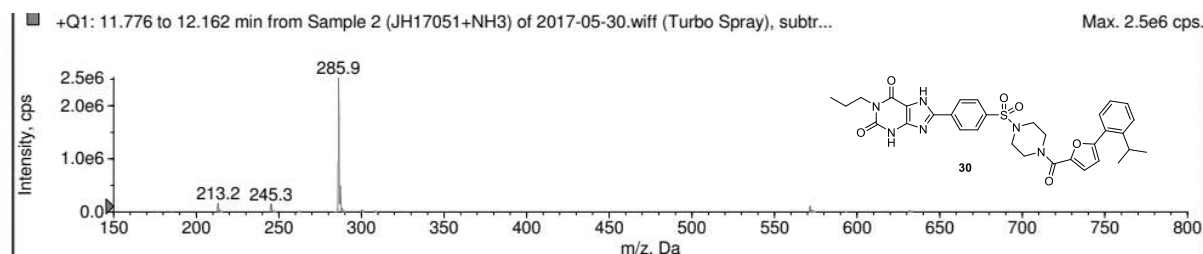
S56. Mass spectrum of compound **27**.



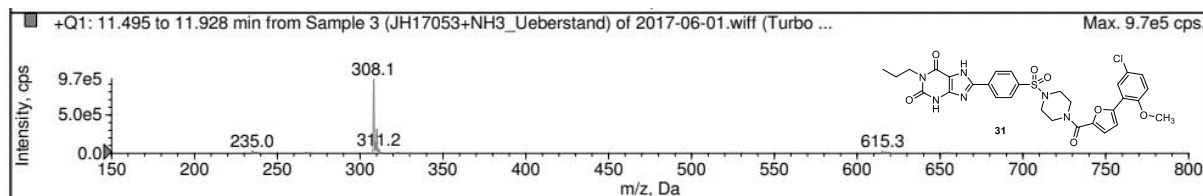
S57. Mass spectrum of compound **28**.



S58. Mass spectrum of compound **29**.



S59. Mass spectrum of compound **30**.



S60. Mass spectrum of compound **31**.

4.2. Part II: Functionalized potent and selective 8-(4-acylpiperazinyl-1-sulfonyl)phenylxanthines providing a platform for fluorescence-labeling of adenosine A_{2B} receptor antagonists

Functionalized potent and selective 8-(4-acylpiperazinyl-1-sulfonyl)phenylxanthines providing a platform for fluorescence-labeling of adenosine A_{2B} receptor antagonists

Tim Harms,¹ Beatriz Büschbell,¹ Christin Vielmuth,¹ Sonja Hinz,^{1,2} Anke C. Schiedel,¹ Jörg Hockemeyer,¹ and Christa E. Müller^{1,*}

¹PharmaCenter Bonn, Pharmaceutical Institute, Pharmaceutical Sciences Bonn (PSB), Pharmaceutical & Medicinal Chemistry, University of Bonn, An der Immenburg 4, 53121, Bonn, Germany.

²Institute of Pharmacology and Toxicology, Center for Biomedical Education and Research (ZBAF), school of Medicine, Faculty of Health, University of Witten/Herdecke, D-58453 Witten, Germany.

4.2.1. Keywords

Cyanine, Fluorophore, A_{2B} Adenosine Receptor, Antagonist, Xanthine

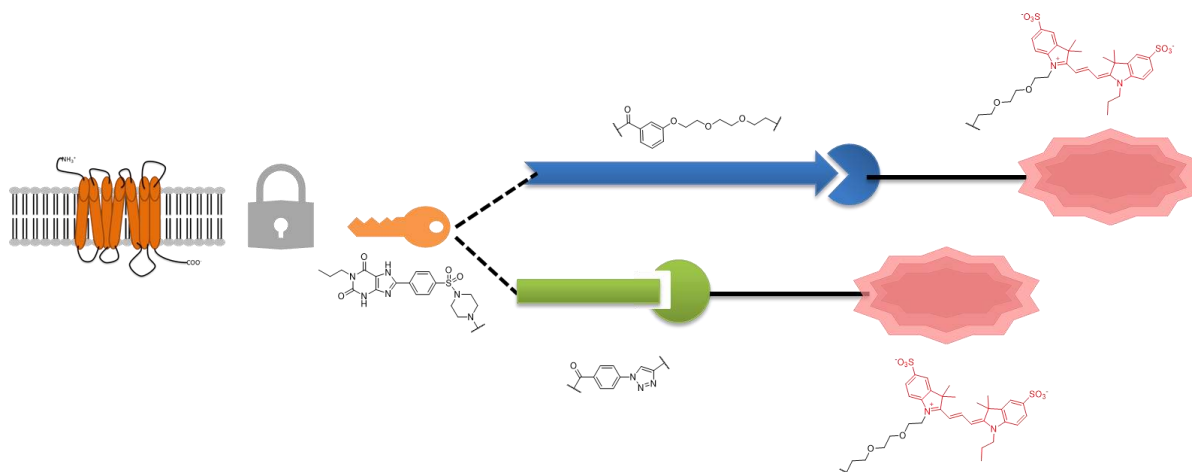
4.2.2. Abstract

Fluorescence-labeled ligands are versatile biological probes for various applications including microscopy, flow cytometry, and ligand binding assays. In this study, we combined antiasthmatic xanthines with water-soluble cyanine fluorophores addressing A_{2B} adenosine receptors (A_{2B}ARs) which have been proposed as novel targets in immuno-oncology. Our approach was to prepare 8-substituted xanthine derivatives bearing different reactive groups as a platform for functionalization with messenger molecules. On this basis, several fluorescent ligands were synthesized. Compounds **39** (PSB-20077) and **40** (PSB-20104) showed good potency (K_i A_{2B}AR 149 nM and 159 nM) combined with receptor subtype selectivity for the A_{2B}AR and were further investigated in confocal microscopy studies, revealing specific binding to the A_{2B}AR. These compounds represent the second generation of potent, selective fluorescent A_{2B}AR ligands and will be used in a variety of applications.

Highlights

- Fluorescent ligand-based biological probes are important tools in pharmacology
- Combining xanthenes with cyanine-dyes results in potent fluorescent-ligands
- Confocal microscopy revealed specific binding

4.2.2.1. Graphical Abstract



4.2.3. Introduction

G protein-coupled receptors (GPCRs) are the largest family of transmembrane proteins in humans and they represent the most important class of drug targets.^{1,2} Adenosine receptors (ARs) belong to the class A, rhodopsin-like subfamily of GPCRs. They are involved in a variety of physiological and pathological processes.^{1,3,4} Four different subtypes exist designated adenosine A₁, A_{2A}, A_{2B} and A₃ receptors.² The A_{2B}AR displays the lowest affinity for adenosine of all four subtypes. Under pathological conditions, such as hypoxia, inflammation and cancer, extracellular adenosine levels can rise up to about 100-fold, and A_{2B}AR expression is concomitantly increased leading to substantial activation of the receptor.^{5,6} This leads to immunosuppressive effects by activation of immune cells, in addition to A_{2A}ARs that are already activated at lower adenosine levels. Adenosine also induces the release of angiogenic cytokines. Moreover, activation of A_{2B}ARs on cancer cells leads to cell proliferation.⁵⁻⁹ In addition, the nucleoside enhances pain responses.¹⁰ Antagonists for the A_{2B}AR have therefore been proposed as immunotherapeutics for cancer with additional direct anti-cancer activity, which is currently evaluated in clinical trials (NCT03274479).¹¹ Further potential applications have been proposed including asthma/bronchial inflammation, diabetes, and Alzheimer's disease. Therefore, significant efforts have been made to develop and investigate appropriate drug molecules targeting the A_{2B}AR.¹²⁻¹⁴

The measurement of receptor-ligand binding affinity is traditionally performed by radioligand binding studies. More recently, fluorescent ligands have gained importance. These approaches include fluorescence polarization (FP),¹⁵ confocal microscopy,¹⁶ fluorescence-correlation spectroscopy (FCS),¹⁷ Förster-resonance-energy transfer (FRET),¹⁸ bioluminescence resonance energy transfer (BRET),¹⁹⁻²¹ fluorescence recovery after photobleaching (FRAP)²² and flow cytometry.^{23;24} Several fluorescent AR ligands, agonists and antagonists, have been described.^{15-20;22-30} Based on the natural product caffeine (**1**), a xanthine derivative that blocks all four AR subtypes, subtype-selective AR antagonists have been developed.³¹ For example, PSB-603 (Figure 1, **2**) is a well-established, highly potent and selective A_{2B} AR antagonist.³² Its tritiated form ($[^3\text{H}]$ PSB-603) is used for radioligand binding studies at the A_{2B} AR.^{33;34}

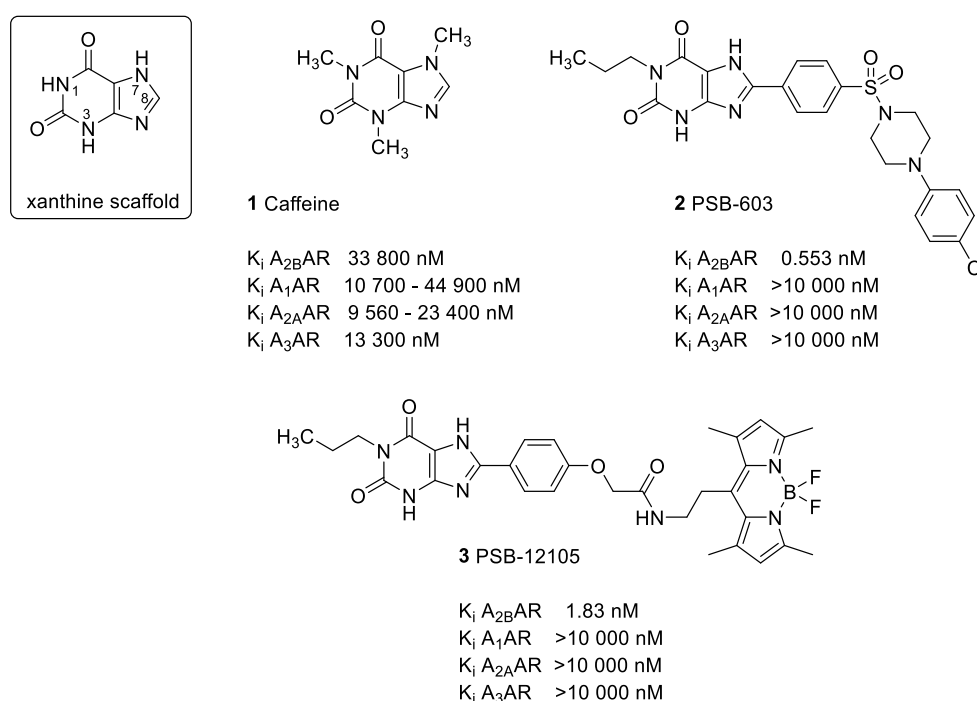


Figure 1. Xanthine derivatives: the natural product caffeine, the A_{2B} -selective AR antagonist PSB-603 and the BODIPY-labeled A_{2B} AR antagonist PSB-12105, K_i values for the human AR subtypes are given.^{10;23;33;35}

Recently, our group reported the first potent and selective fluorescent A_{2B} AR ligands.²³ It was based on a xanthine scaffold and labeled with a borondipyrromethene (BODIPY) dye.³⁶ The best compound of that series, PSB-12105 (see figure 1, **3**), exhibited a K_i value of 1.83 nM at the human A_{2B} AR and was highly selective versus the other AR subtypes. However, linking of the lipophilic BODIPY dye to a scaffold that is notorious for its poor water solubility can lead to solubility problems and high non-specific membrane binding in biological assays.³⁷ In the present study, we significantly expand the toolbox of fluorescent-labeled A_{2B} AR ligands based on previous progress in the design and optimization of A_{2B} AR antagonists.³⁸

4.2.4. Results and discussion

4.2.4.1. Design of fluorescent-labeled 8-(4-acylpiperazine-1-sulfonyl)phenyl-1-propylxanthenes as A_{2B}AR antagonists

Cyanine dyes are fluorescent compounds consisting of conjugated double bond with terminal heterocyclic nitrogen containing rings.^{39;40} Cyanine dyes are appreciated because they offer good water solubility, high stability, sharp fluorescence bands, high sensitivity, and broad versatility.^{40;41} These dyes can be substituted with functional groups on either one or both heterocyclic rings so that they may be chemically conjugated to other functionalized molecules.⁴² A cyanine of the “Cy3”-type (being equipped two sulfonate groups) was chosen as a fluorophore in the present study. One side-chain was a propyl residue since this moiety was reported to enhance the extinction coefficient of cyanine dyes in comparison to a smaller substituent.⁴⁰ The second side-chain was variable bearing diverse linkers and functional groups (see Figure 2). Octanoic acid and an oligoethylenglycole linker being functionalized with a carboxylic acid were suitable moieties to couple the fluorophore to the pharmacophore by amide formation. Moreover, oligoethylenglycole linkers bearing an azide and an ethynyl group were introduced to the fluorophore, this allowed attachment of the dye to the pharmacophore by click reaction.

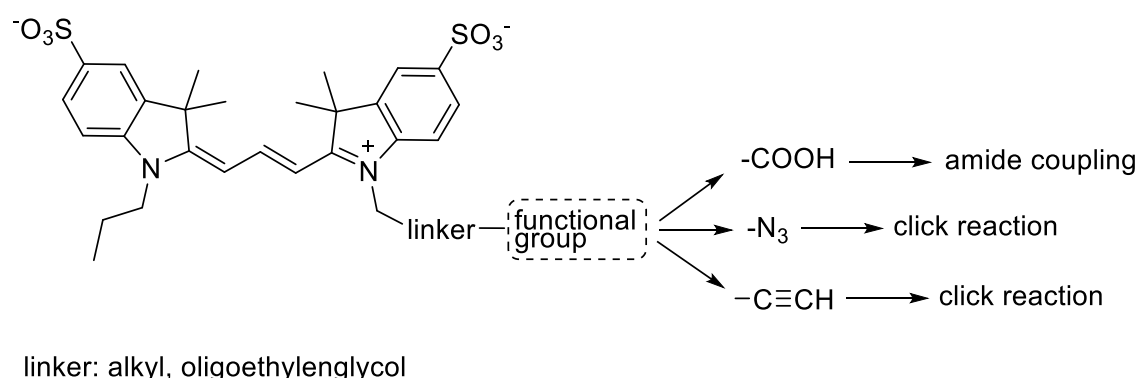


Figure 2. Basic scaffold of selected cyanine dye.

Many xanthine derivatives display low solubility in water, while the very polar Cy3 dye can be expected to increase solubility of the conjugates. Additionally, the high polarity would decrease non-specific membrane binding which is often observed with the lipophilic BODIPY fluorophores.^{23;38} Cyanine dyes of the Cy3 type display an absorption and emission maximum of around 550 nm, making them suitable for a variety of fluorescent probes, including e. g. the NanoBRET technology.²¹ Moreover, cyanine dyes can be easily tuned to obtain derivatives with different wavelengths by simply extending the system of conjugated double bonds connecting the two heterocyclic ring systems.^{39;40}

The benzoyl-substituted 8-(4-benzoylpiperazine-1-sulfonyl)phenyl-1-propylxanthine (**4**)³⁸ was selected as a lead structure for the preparation of fluorescence-labeled A_{2B} AR antagonists (see Figure 3), since it offers an easy and straightforward strategy to introduce a variety of substituents by acylation reaction.

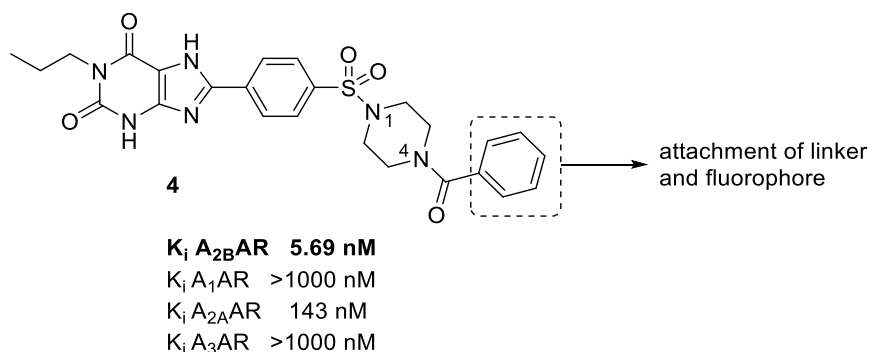


Figure 3. Prototypic lead structure for new fluorescent labeled A_{2B} AR antagonists.³⁸

Based on previous docking studies,³⁸ it was predicted that the benzoyl residue would be oriented towards the extracellular domain of the receptor. Thus, this would be the best position to attach a large fluorophore. Our ultimate goal was to prepare novel fluorescence-labeled probes for the A_{2B} AR. Four benzoic acid derivatives were designed allowing the attachment of a fluorescent dye to the piperazine ring of the potent A_{2B} AR antagonist. These benzoic acid derivatives bear an amino group, an azido group or an ethynyl group, while the functionalized dye was equipped with the required reactive moiety (see Figure 4). Two of these linkage moieties exhibit a functionalized tetraethyleneglycol (TEG) chain to further separate the dye from the antagonist moiety. Polyethyleneglycols are more hydrophilic as compared to alkyl chains, they can be easily functionalized, are often tolerated by biological targets, are non-toxic and the four units of TEG offer an intermediate linker length.^{43;44}

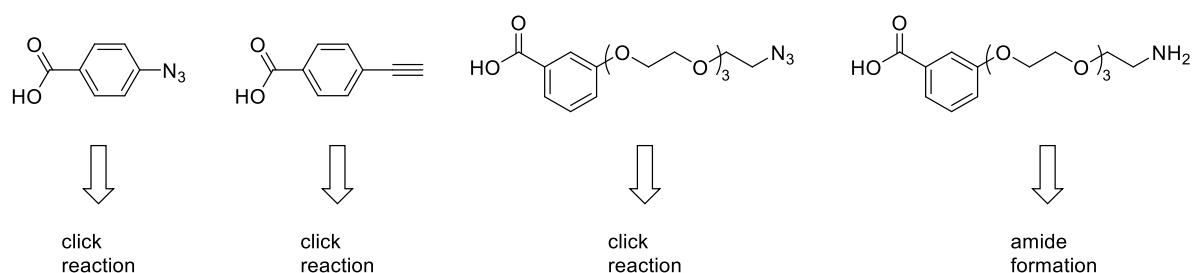
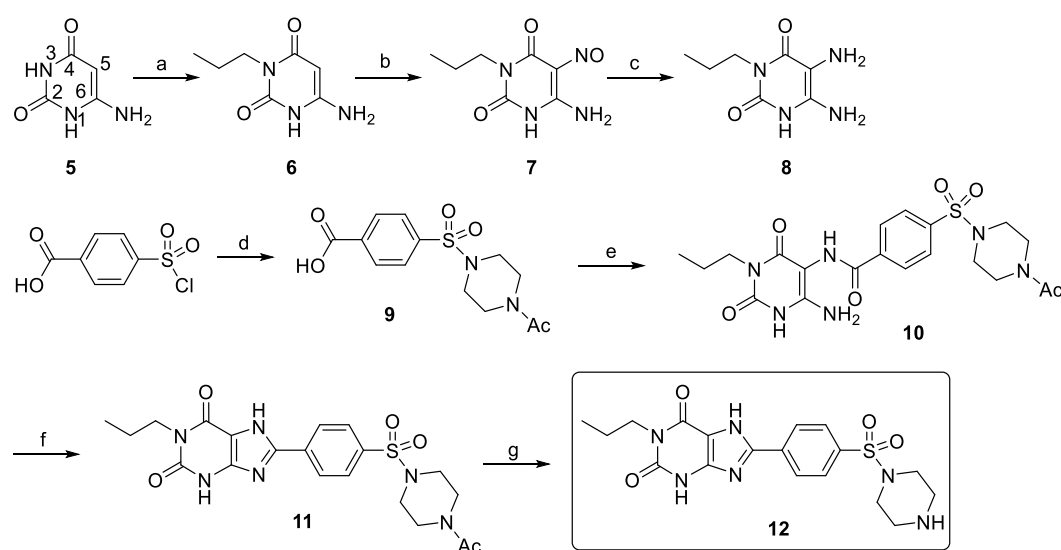


Figure 4. Benzoic acid derivatives bearing conjugatable functional groups.

4.2.4.2. Synthesis of functionalized 8-(4-acylpiperazine-1-sulfonyl)phenyl-1-propylxanthine derivatives

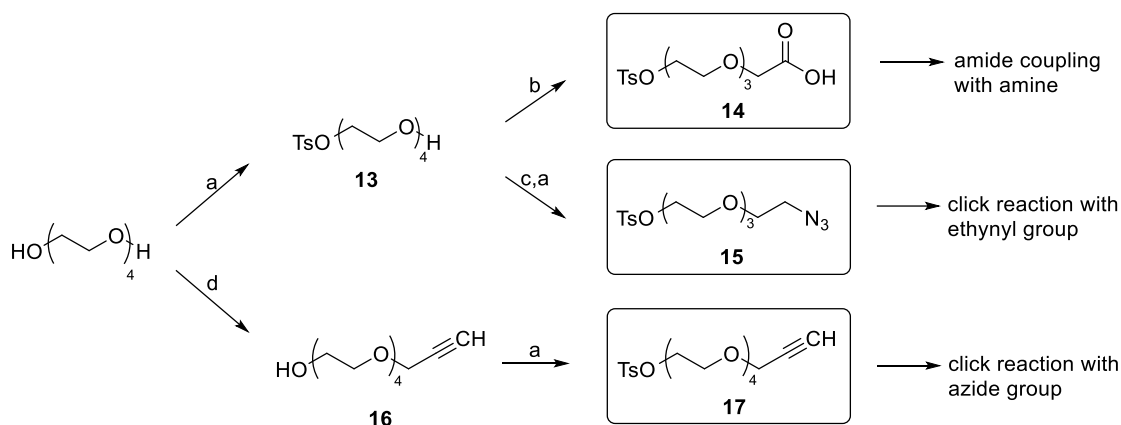
The precursor, 8-(piperazinylsulfonyl)phenyl-1-propylxanthine (**12**), was obtained by reaction of the 4-((acetylpiperazin-1-yl)sulfonyl)benzoic acid (**9**)⁴⁵ with 3-propyl-5,6-diaminouracil (**8**)⁴⁶ yielding intermediate **10**.⁴⁶ Subsequent ring-closure reaction affording **11** was performed using phosphorus pentoxide in *N,N*-dimethylformamide (DMF) at 100 °C as previously described.³⁸ Hydrolysis of **11** with aqueous NaOH solution led to the formation of the new xanthine derivative **12** (see Scheme 1).



Scheme 1. Synthesis of xanthine derivative **12**.

Reaction conditions: (a) (i) hexamethyldisilazane (HMDS), $(\text{NH}_4)_2\text{SO}_4$, reflux for 2 h; (ii) propyl bromide, reflux for 1.5 h; (iii) $\text{Na}_2\text{S}_2\text{O}_3$ in H_2O followed by saturated NaHCO_3 aq. solution at 0 °C; (b) H_2O , conc. HCl, NaNO_2 , 70 °C, 1 h; (c) NH_3 solution (12.5%), $\text{Na}_2\text{S}_2\text{O}_4$, 65 °C, 30 min; (d) 1-*N*-acetylpiperazine, triethylamine (TEA), CH_2Cl_2 , room temperature (rt), 16 h; (e) **8**, 1-ethyl-3-(3-dimethylaminopropyl)carbodiimide hydrochloride (EDC·HCl), methanol (MeOH), rt, 2 h; (f) P_2O_5 , DMF, reflux, 15 min; (g) H_2O / ethanol (EtOH), NaOH, 60 °C, 5 h.^{38;45;46}

Three functionalized TEG-linkers were prepared that exhibited a conjugatable group (carboxylic acid **14**, azide **15** and ethynyl derivative **17**) as well as a reactive leaving group to attach the linker to the fluorescent dye or the pharmacophore (see Scheme 2). The tosyl group was selected as a leaving group as it provides high reactivity and in addition, due to the aromatic group, it renders the compound detectable by thinlayer chromatography (TLC) and high performance liquid chromatography (HPLC).

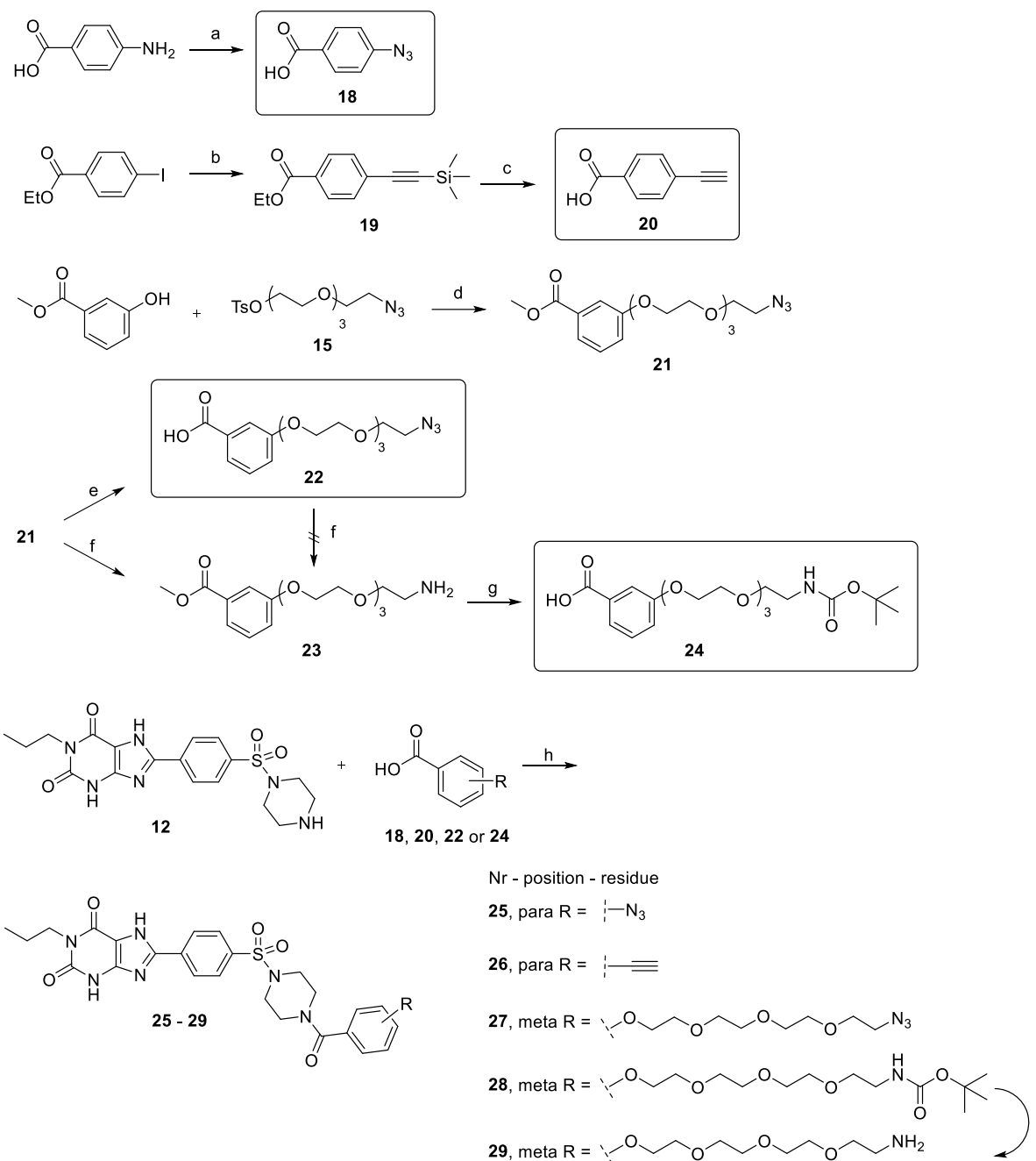


Scheme 2. Synthesis of functionalized linkers.

Reaction conditions: (a) tosyl chloride (TsCl), TEA, CH₂Cl₂, 0 °C to rt, 3 h; (b) CrO₃, acetone, 1.5 M H₂SO₄, 0°C to rt, 16 h; (c) NaN₃, DMF, rt, 16 h; (d) (i) NaH, DMF, 0 °C, 15 min; (ii) propargyl bromide, rt, 6 h.⁴⁷⁻⁴⁹

Two of three linkers were prepared starting from mono-tosylated TEG (**13**). For the preparation of **13**, TsCl (0.3 eq.) was slowly added to TEG in CH₂Cl₂ at 0 °C leading mainly to the mono-tosylated product which was purified by column chromatography. To prepare linker **14**, alcohol **13** was oxidized to the carboxylic acid employing CrO₃ under acidic conditions.⁴⁷ To prepare **15**, alcohol **13** was reacted with NaN₃ to form the corresponding azide, which was subsequently tosylated to obtain linker **15**.⁴⁸ Finally, propargyl bromide was tethered to TEG via Williamson ether synthesis affording **16**, and subsequent tosylation yielded linker **17**.⁴⁹

Four different linker building blocks were synthesized to serve as a connection between the A_{2B}AR antagonist moiety and the fluorescent dye (see Scheme 3). Compound **18** was formed from 4-aminobenzoic acid by a Sandmeyer reaction using NaN₃ (96% yield).⁵⁰ 4-Ethynylbenzoic acid (**20**) was synthesized from ethyl 4-iodobenzoate and trimethylsilyl acetylene using Sonogashira coupling and subsequent basic deprotection of the ester and the trimethylsilyl group (90% overall yield).⁵¹ Nucleophilic substitution reaction between methyl-3-hydroxybenzoate and **15** was performed affording the azide-functionalized linker **21** in excellent yield (95%). This was the basis for the formation of linker **22** and **24**.⁵² In a first sequence, **21** was saponified affording **22**. A Staudinger reaction of **21** led to intermediate **23** which was subsequently Boc-protected and hydrolyzed affording building block **24** in an overall yield of 28% based on **21**.⁵³ Compound **23** could not be obtained directly by Staudinger reaction of **22** because many side products were formed, and purification was therefore difficult.



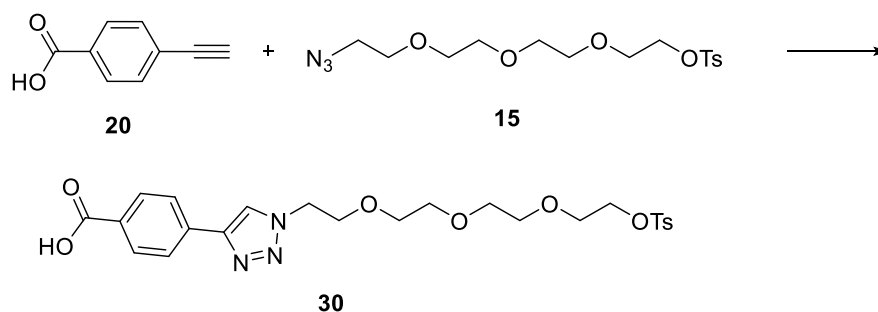
Scheme 3. Synthesis of linker moieties and coupling to xanthines.

Reaction conditions: (a) (i) H_2SO_4 , NaNO_2 , H_2O , $0\text{ }^\circ\text{C}$, 15 min; (ii) NaN_3 , $0\text{ }^\circ\text{C}$, 30 min; (b) $\text{HC}\equiv\text{CSi}(\text{CH}_3)_3$, CuI , $\text{PdCl}_2(\text{PPh}_3)_2$, PPh_3 , DMF , TEA , rt , 16 h; (c) NaOH , H_2O / EtOH , rt , 5 h; (d) K_2CO_3 , DMF , $100\text{ }^\circ\text{C}$, 16 h; (e) LiOH , H_2O / tetrahydrofuran (THF), rt , 16 h; (f) PPh_3 , THF , H_2O , rt , 2 d; (g) Boc_2O (di-tert-butylidicarbonate), NaOH , THF / H_2O , rt , 24 h; (h) 2-(1*H*-benzotriazol-1-yl)-1,1,3,3-tetramethyluronium-hexafluorophosphat (HBTU), TEA , DMF , rt , 2 h; (i) TFA , CH_2Cl_2 , $0\text{ }^\circ\text{C}$ to rt , 4 h.⁵⁰⁻⁵³

The final conjugatable A_{2B}AR antagonists were formed between the piperazine-NH of **12** and the respective modified benzoic acid derivatives (**18**, **20**, **22** and **24**) employing the amide coupling reagent HBTU. Compound **28** was finally deprotected with trifluoroacetic acid (TFA) to afford compound **29** bearing a primary amino group. Product **29** could not be obtained from **27**, presumably due to low solubility of **27** preventing catalytic hydration and Staudinger reaction.

4.2.4.3. Optimization of Huisgen cycloaddition

To find the best reaction conditions for the planned click reaction, several conditions were tested using **15** and **20** as reaction partners affording product **30**. All mixtures were reacted for 16 h, then acidified to pH 4 and extracted with ethyl acetate. The residues of the evaporated organic layers were analyzed by liquid chromatography-mass spectrometry (LC-MS) (see Scheme 4, table 1).



Scheme 4. Synthesis of **30** employing different reaction conditions.

Table 1. Reaction conditions to form **30**.

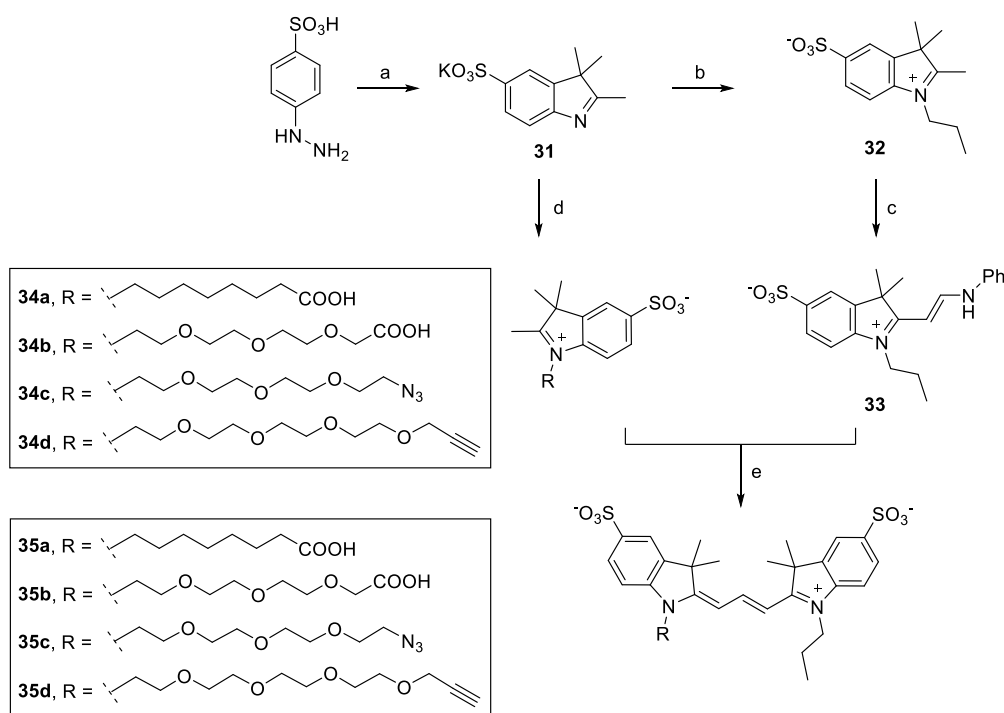
Entry	Copper salt	Base ^a	Solvent	Temp.	Yield
1 ⁵⁴	CuSO ₄ · 5 H ₂ O (0.05 eq.)	NaAsc (0.1 eq.)	H ₂ O/ <i>t</i> BuOH (1:1)	rt	83 %
2 ⁵⁵	CuSO ₄ · 5 H ₂ O (1.2 eq.)	NaAsc (2.5 eq.)	H ₂ O/MeOH (1:1)	rt	90 %
3 ⁵⁶	CuI (0.05 eq.)	TEA	EtOH	reflux	0%
4 ⁵⁷	CuI (0.05 eq.)	TEA	DMF	rt	79%

^aNaAsc, sodium ascorbate; TEA, triethylamine

As a result, only refluxing of the reagents in EtOH failed. All other conditions worked out well, and 79-90 % yields were obtained. As the xanthine derivatives were best soluble in DMF, procedure 4 was chosen.

4.2.4.4. Synthesis of functionalized cyanine fluorophores

Four different linkers were introduced into the Cy3 scaffold, the three aforementioned reactive linkers **14**, **15** and **17**, and octanoic acid as a more classical linker (compound **35a** was commercially available). The functionalized Cy3 fluorophores were synthesized according to a modified literature procedure.^{40;58} 3-Methyl-2-butanone and *p*-hydrazinobenzenesulfonic acid were reacted and subsequently treated with KOH to form the 2,3,3-trimethyl-3*H*-indole-5-sulfonate **31** (see Scheme 5). In a first reaction, **31** was alkylated with 1-propyl iodide yielding **32** and subsequently reacted with *N,N'*-diphenylformamidine to obtain hemi-cyanine **33**.⁴⁰



Scheme 5. Synthesis of functionalized cyanine dyes **35a-35d**.

Reaction conditions: (a) (i) 3-methyl-2-butanon, acetic acid (AcOH) reflux, 4 h; (ii) KOH, MeOH, *n*-propanol (*n*PrOH), rt, 16 h; (b) 1-propyl iodide, reflux, 24 h; (c) *N,N'*-diphenylformamidine, AcOH, reflux, 3 h; (d) (**14**, **15**, **17** or 8-bromooctanoic acid), sulfolane, 130 °C, 16 h; (e) pyridine, Ac₂O, 110 °C, 4 h.^{40;58}

For the introduction of the linker moiety to **31**, several reaction conditions were investigated since reaction conditions described in the literature led to low yields (table **2**, entry 1).⁴⁰ Therefore, **31** was reacted with 8-bromooctanoic acid under a variety of conditions in order to optimize the reaction (see table 2).

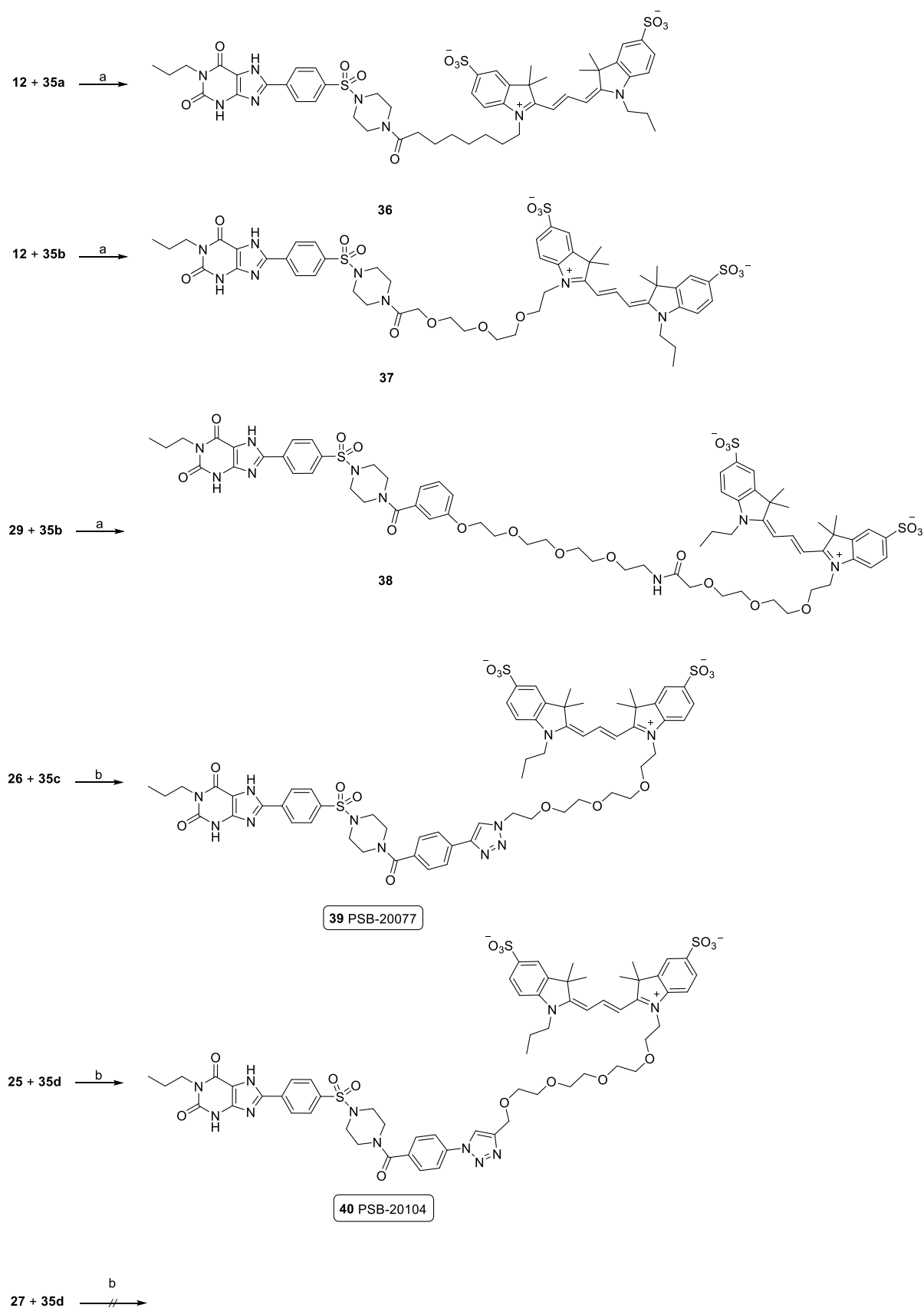
Table 2. Optimization of the reaction conditions to optimize the synthesis of **35a**.

Entry	Solvent	Temp.	Reaction time	Result
1 ⁴⁰	o-Dichloro-benzene	180 °C	12 h	Compound 31 insoluble, 30% product, but much starting material left, formation of side products
2 ⁵⁹	Acetonitrile	120 °C	16 h	Mainly unreacted starting material
3 ⁵⁸	Sulfolane	130 °C	16 h	77% product, no side products
4 ⁶⁰	no	120 °C	16 h	64% product, some side products

All of the reactions were performed in a sealed tube under an argon atmosphere. In contrast to the originally described method 1, the reaction temperature was reduced, acetonitrile and sulfolane were used as solvents, or the reaction was performed in the absence of solvent. All reaction mixtures were subsequently cooled to rt and treated with ethyl acetate to precipitate the product, which was filtered off, dried and analyzed by LC-MS. Sulfolane turned out to be the most suitable solvent for the reaction, presumably because it completely dissolves all reagents. Hence, all reactions involving **14**, **15** and **17** were performed according to this optimized method (Table 2, entry 3). The obtained products were used without further purification. The final reaction step was performed according to literature conditions⁴⁰ leading to the functionalized dyes **35a-35d**.

4.2.4.5. Synthesis of cyanine-labeled A_{2B}AR antagonists

Finally, five different cyanine-labeled A_{2B}AR antagonists were prepared (see Scheme 6). To this end, the established method using HBTU in DMF was utilized to couple **12** directly to **35a** and **35b**, affording **36** and **37**, respectively. Additionally, **35b** was coupled to **29** yielding **38**. Employing the optimized conditions for the click reactions, **26** was reacted with **35c** affording **39** (PSB-20077), and **25** was reacted with **35d** yielding **40** (PSB-20104). While **36** could be obtained in a good isolated yield of 34%, all other reactions led to low isolated yields of 5-6%, mainly because the products were difficult to purify, and unreacted starting material which was present even after extended reaction times, had to be removed. This was presumably due to solubility problems, since all of the cyanine dyes were poorly soluble in DMF. However, the xanthine derivatives displayed low solubility in most other solvents, therefore DMF was used as a compromise. The products were purified by reversed phase column chromatography, and most compounds had to be purified twice, or additionally by normal phase column chromatography. Click reaction between **27** and **35d** was tried but failed, and only starting material was recovered.



Scheme 6. Synthesis of fluorescence-labeled $A_{2B}AR$ antagonists **36-40**.

Reaction conditions: (a) HBTU, TEA, DMF, rt, 2 h. (b) TEA, CuI, DMF, rt, 16 h.⁵⁷

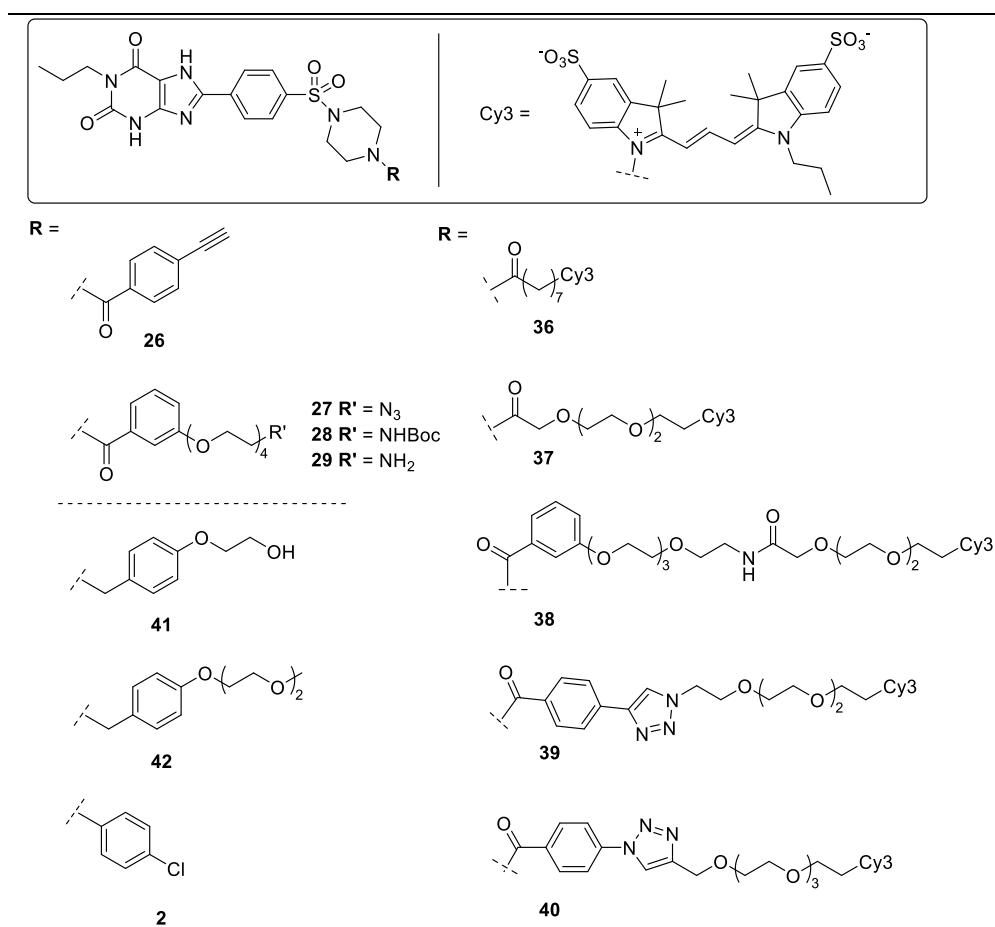
4.2.4.6. Analysis of the products

All of the products were analyzed by LC-MS analysis using a diode array detector, and their purity was confirmed in most cases >95%. Only **36** showed a slightly lower purity of 92%. The structures of the new compounds were validated by ^1H and ^{13}C NMR spectra. The triazole derivatives **39** and **40** were selected for further investigation due to the superior stability of the triazoles in comparison to the amides. The fluorescent properties of **39** and **40** were determined by fluorescence spectroscopy. The absorption maxima were observed at 556 nm and 557 nm, and the emission maxima were determined at 571 nm and 572, respectively. Both compounds showed a Stokes shift of 15 nm (for the absorption and emission spectra, see Figure S1 in the Supporting Information). The fluorescence quantum yields of **39** and **40** were measured in ethanol with rhodamine 6G as a reference compound; they were found to be 0.1 and 0.095, respectively. Such a value is typical for Cy3 cyanine fluorophores.⁶¹

4.2.4.7. Radioligand binding studies

The synthesized 8-(4-acylpiperazine-1-sulfonyl)phenyl-1-propylxanthenes **26-29** and the fluorescent ligands **36-40** were investigated in radioligand binding studies at human A_{2B} ARs versus the antagonist radioligand [^3H]PSB-603^{33;34} (Table 3). To assess the compounds selectivity versus the other AR subtypes, radioligand binding studies at A_1 , A_{2A} , and A_3 ARs were additionally performed using the following radioligands: [^3H]CCPA (for A_1), [^3H]MSX-2 (for A_{2A}), and [^3H]PSB-11 (for A_3). The studies were performed with membrane preparations purchased from Perkin Elmer. The A_{2B} ARs and the A_{2A} ARs originating from human embryonic kidney (HEK-293) cells while the membrane preparations of the A_1 ARs and A_3 ARs were originated from Chinese hamster ovary (CHO) cells. The radioligand-receptor binding assays were performed as previously described.^{23;33;38;62-65} Results are collected in Table 3.

Table 3. Binding affinities of xanthine derivatives at human adenosine receptor subtypes.



Compd.	K _i ± SEM (nM)			
	A _{2B} AR ^a	A ₁ AR ^b	A _{2A} AR ^c	A ₃ AR ^d
26	3.43 ± 0.49	>1000 (22%)	187 ± 59	>1000 (25%)
27	11.3 ± 1.7	>1000 (19%)	>1000 (37%)	>1000 (20%)
28	15.9 ± 1.2	>1000 (17%)	>1000 (30%)	>1000 (32%)
29	39.0 ± 8.5	>1000 (9%)	>1000 (22%)	>1000 (19%)
36	926 ± 289	>1000 (1%)	>1000 (17%)	>1000 (24%)
37	83.8 ± 17.8	>1000 (19%)	>1000 (11%)	>1000 (21%)
38	>1000 (29%)	>1000 (4%)	>1000 (-1%)	>1000 (8%)
39	149 ± 26	>1000 (10%)	>1000 (28%)	≈1000 (56%)
40	159 ± 33	>1000 (6%)	>1000 (36%)	>1000 (35%)
41 ³⁸	12.2 ± 4.0	560 ± 13	241 ± 49	>1000 (17%)
42 ³⁸	7.02 ± 1.1	1010 ± 250	314 ± 73	>1000 (30%)
2 ³²	0.553 ± 0.103	>1000 (10%) ^e	>1000 (7%) ^e	>1000 (10%) ^e

^avs. [³H]PSB-603 (n = 3); ^bvs. [³H]CCPA (n = 3); ^cvs. [³H]MSX-2 (n = 3); ^dvs. [³H]PSB-11 (n = 3)

^einhibition of radioligand binding at 10μM

All TEG-linked 8-(4-benzoylpiperazine-1-sulfonyl)phenyl-1-propylxanthines, **27**, **28** and **29** are potent and selective A_{2B} AR antagonists, displaying K_i values of 11.3 nM, 15.9 nM and 39.0 nM, respectively. They are in the same potency range as the related 8-(4-benzylpiperazine-1-sulfonyl)phenyl-1-propylxanthines **41** and **42** that were recently reported, but exhibit improved selectivity.³⁸ These A_{2B} AR antagonists are of interest with respect to their increased polarity, and due to their terminal functional groups which allow conjugation (**27**, **29**). Ethynylbenzoyl derivative **26** showed high affinity at A_{2B} combined with 55-fold selectivity versus the A_{2A} AR, and 290-fold selectivity versus the A_1 - and A_3 AR subtypes.

The fluorescence-labeled products showed diverse results: compound **36** showed moderate A_{2B} AR affinity ($K_i = 928$ nM). The very polar cyanine moiety is probably too close to the A_{2B} AR pharmacophore. Consequently, connection of the xanthine moiety to the cyanine dye via TEG chain led to increased potency, compound **37** displaying a K_i value of 83.8 nM. Both triazole derivatives, **39** and **40**, displayed similar potency (K_i values of 149 nM and 159 nM, respectively). These compounds are particularly interesting since triazoles are more stable linkers than amides. Fluorescent compound **38** with the longest linker did not show high affinity. All Cy3-labeled xanthine derivatives appeared to display good water solubility.

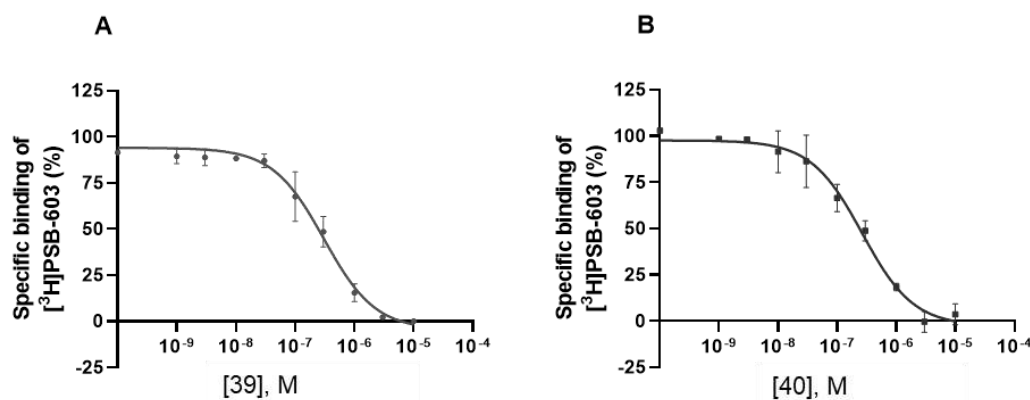


Figure 5. Competition binding experiments. **A.** Competition binding of **39** and **B.** of **40** at membrane preparations of HEK 293 cells recombinantly expressing the human A_{2B} AR versus [³H]PSB-603. Data points represent means \pm SEM of three independent experiments. The following K_i -values were calculated: 149 ± 26 nM (**39** vs. [³H]PSB-603) and 159 ± 33 nM (**40** vs. [³H]PSB-603).

4.2.4.8. Confocal microscopy

The cyanine-labeled $A_{2B}AR$ ligands **39** and **40** were investigated in confocal microscopy studies on CHO cells expressing the human $A_{2B}AR$ (Figure 6 and 7). Incubation with the fluorescent ligands led to the labeling of the cell membrane and parts of the cytosol (Figure 6 and 7, upper panels). When cells were preincubated with the antagonist DPCPX, plasma membrane labeling was decreased (Figure 1 and 2, middle panels). CHO-K1 cells, which did not overexpress $A_{2B}AR$ s (Figure 1 and 2, lower panels) were used as controls. Our results indicated specific binding of **39** and **40** to the $A_{2B}AR$.

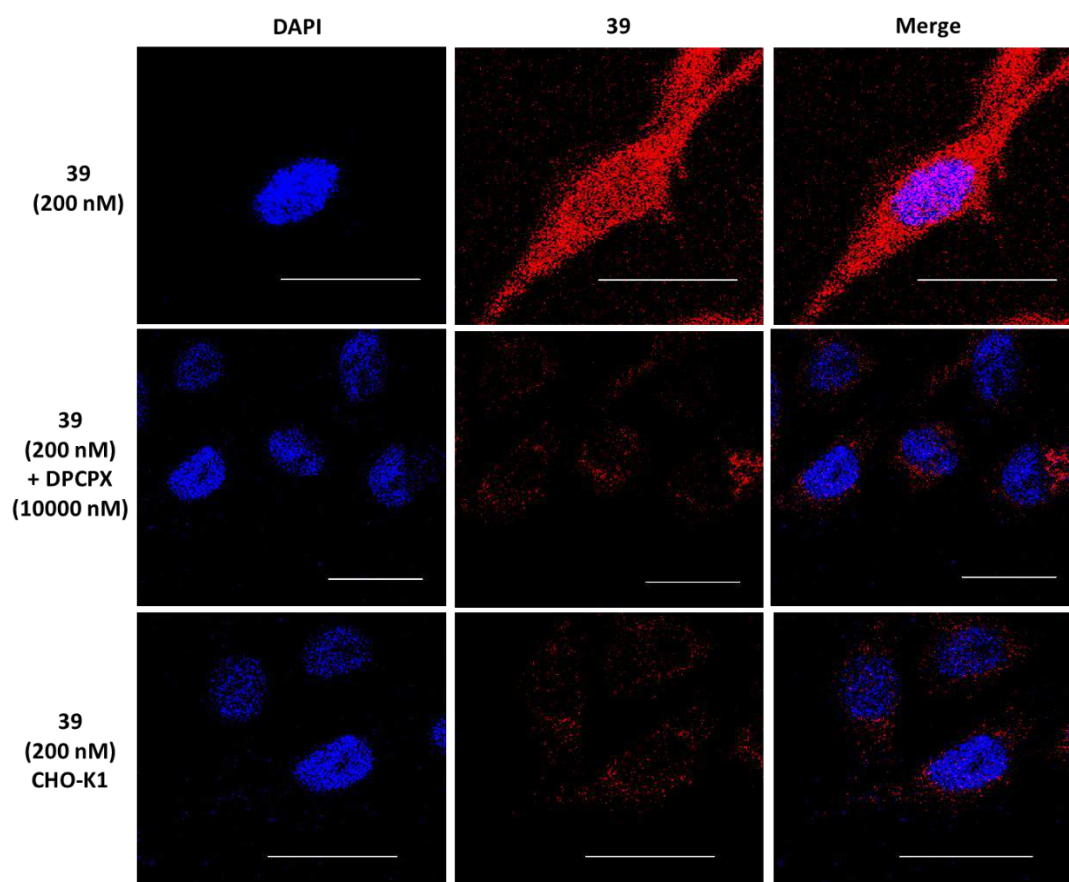


Figure 6. Binding of the cyanine-labeled $A_{2B}AR$ antagonist **39** to CHO cells recombinantly expressing human $A_{2B}AR$ s. Cells were fixed and incubated with 200 nM of **39** and 4',6-diamidino-2-phenylindole (DAPI) (nuclei) for 60 min on ice. Cells expressing the human $A_{2B}AR$ were incubated in the presence or absence of DPCPX (10 μ M) together with **39** under the same conditions (60 min on ice). Scale bar = 20 μ M.

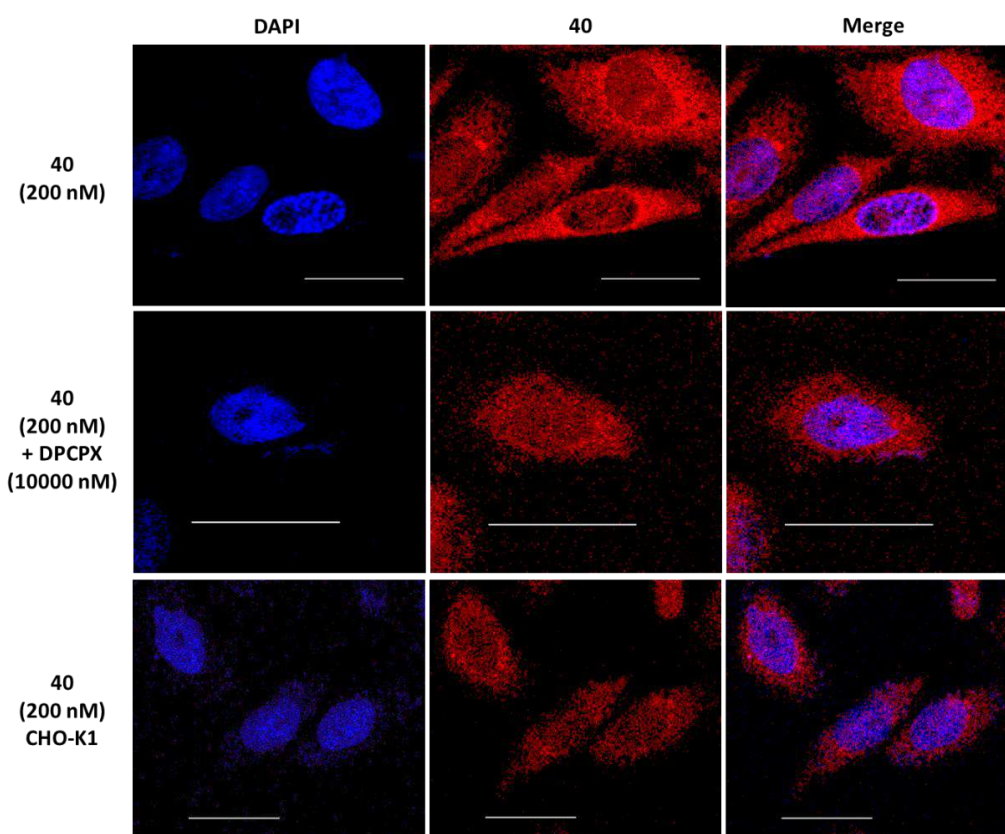


Figure 7. Binding of the cyanine-labeled $A_{2B}AR$ antagonist **40** to CHO cells recombinantly expressing human $A_{2B}AR$ s. Cells were fixed and incubated with 200 nM of **40** and 4',6-diamidino-2-phenylindole (DAPI) (nuclei) for 60 min on ice. Cells expressing the human $A_{2B}AR$ were incubated in the presence or absence of DPCPX (10 μ M) together with **40** under the same conditions (60 min on ice). Scale bar = 20 μ M.

4.2.5. Conclusions

In this study, new potent, selective and conjugatable 8-(4-acylpiperazine-1-sulfonyl)phenyl-1-propylxanthines as $A_{2B}AR$ antagonists were developed. Acylation of **12** was a feasible strategy to introduce a variety of functional groups to the xanthine scaffold. Compound **27** ($K_i A_{2B}AR$ 11.3 nM) and **29** ($K_i A_{2B}AR$ 39.0 nM) are promising antagonists, due to their functional groups, they can be coupled to other labeling molecules to obtain a variety of biological probes. Five cyanine-labeled $A_{2B}AR$ antagonists were synthesized, three of which (**37**, **39** and **40**) showed good affinity for the $A_{2B}AR$. All of the fluorescence-labeled xanthine derivatives are readily soluble in water, since the cyanine fluorophore, bearing sulfonate groups, considerably enhanced water solubility of the generally poorly soluble xanthine derivatives. The fluorescent $A_{2B}AR$ antagonists **39** and **40** were further investigated by confocal microscopy studies and found to specifically bind to the $A_{2B}AR$ recombinantly expressed in the employed cells. In the future, **39** and **40** will be evaluated as pharmacological probes, e.g. for BRET-based binding assays.

4.2.6. Material and methods

4.2.6.1. General methods

Commercially available reagents and solvents (e.g. from ABCR, Acros, Aldrich, Merck, and Sigma) were directly used without further purification or drying. The reaction progress was controlled by TLC on silica gel-coated aluminum sheets (0.2 mm layers, nanosilica gel 60 with fluorescence indicator UV₂₅₄; Merck). Merck silica gel 60 (mesh size 0.040-0.063 mm) was used for column chromatography. Melting points were measured in open capillary tubes employing a Wepa Apotec capillary melting-point apparatus (Wepa) and are uncorrected. The purity of all products was determined by HPLC-UV (Applied Biosystems API 2000 LC-MS/MS, HPLC Agilent 1100) using the following procedure: Compounds were dissolved in a mixture of methanol / H₂O / NH₃ (aq) (1:1:0.1) at a concentration of 0.5 mg/ml. Subsequently, 10 µl of each sample was injected into a Phenomenex Luna C18 HPLC column with a column size of 50 mm × 2.00 mm and a particle size of 3 µm. Chromatography was performed using a gradient of water / methanol (containing 2 mM ammonium acetate) at a flow rate of 250 µl/min from 90:10 to 0:100 over 20 min. A diode array UV detector was used to detect the absorption from 200 to 950 nm. An API 2000 mass spectrometer (electron spray ion source, Applied Biosystems, Darmstadt, Germany) coupled with an Agilent 1100 HPLC system was used to record mass spectra. Mass spectra were recorded on a micrOTOF-Q mass spectrometer (Bruker) with ESI-source coupled with a HPLC Dionex Ultimate 3000 (Thermo Scientific) using flow injection mode. Sample solution was injected to a flow of 0.3 ml/min acetonitrile containing 0.1 % acetic acid or 0.1 % formic acid. Positive or negative full scan MS was observed from 50-1000 m/z. Sodiumacetate or sodiumformiate was used as calibrant. A Bruker Advance 500 MHz NMR spectrometer at 500 MHz (¹H) and at 126 MHz (¹³C) or a 600 MHz NMR spectrometer at 600 MHz (¹H) and 151 MHz (¹³C) was used to collect ¹H and ¹³C NMR data. DMSO-*d*₆ or CDCl₃ was used as solvent. Chemical shifts are reported in parts per million (ppm) in relation to the deuterated solvents, i.e., Chloroform, δ ¹H: 7.26 ppm; ¹³C: 77.36 ppm; DMSO, ¹H: 2.49 ppm; ¹³C: 39.7 ppm. Coupling constants (*J*) are depicted in Hertz, and spin multiplicities are depicted as s (singlet), d (doublet), t (triplet), m (multiplet), or in respective variations.

4.2.6.2. Determination of fluorescent quantum yields

The measurement of fluorescent quantum yields was performed by a F-7000 FL Spectrophotometer (Hitachi). The slit width was 5 nm for both excitation and emission. The concentration of the measured solutions was 0.0025 mM. The quantum yields were calculated by comparing the areas under the curve of the corrected emission spectra and the absorbance at the excitation wavelength with those of a standard solution. The following equation was used to calculate the quantum yields:

$$\Phi_x = \Phi_{st} * \frac{I_x}{I_{st}} * \frac{A_{st}}{A_x} * \frac{\eta_x^2}{\eta_{st}^2}$$

where Φ_{st} is the reported quantum yield of the standard rhodamine 6G ($\Phi = 0.94$ in ethanol), I is the integrated emission spectrum, A is the absorbance at the excitation wavelength, and η is the refractive index of the used solvent. The subscript x denotes the tested substance, st denotes standard.

4.2.6.3. Syntheses

Synthesis of 4-((-acetylpiperazin-1-yl)sulfonyl)-*N*-(6-amino-2,4-dioxo-3-propyl-1,2,3,4-tetrahydropyrimidin-5-yl)benzamide (**10**)^{45;46}

A suspension of 3-propyl-5,6-diaminouracil (**8**) (2.3 g, 12.5 mol), 4-((-acetylpiperazin-1-yl)sulfonyl)benzoic acid (**9**) (3.9 g, 12.5 mmol) and EDC • HCl (3.1 g, 16.3 mol) in MeOH (75 ml) was stirred for 2 h at rt. The product was filtered off under reduced pressure, washed with MeOH (30 ml) and dried at 70°C affording 4.13 g (69%) of a colorless solid. ¹H NMR (500 MHz, DMSO-*d*₆) δ : 10.49 (s, 1H, NH), 9.12 (s, 1H, NH), 8.17 (d, 2H, $J = 8.3$ Hz, C^{H_{arom.}}-H_{arom.}), 7.83 (d, 2H, $J = 8.3$ Hz, C^{H_{arom.}}-H_{arom.}), 6.16 (s, 2H, NH₂), 3.66 (t, 2H, $J = 7.4$ Hz, NCH₂), 3.50 (s, 4H, NCH₂(piperazine)), 2.91 (m NCH₂(piperazine)), 1.92 (s, 3H, NC=OCH₃), 1.50 (q, 2H, $J = 7.4$ Hz, CH₂CH₃), 0.83 (t, 3H, $J = 7.4$ Hz, CH₂CH₃) ppm. ¹³C NMR (126 MHz, DMSO-*d*₆) δ : 168.5 (N^(piperazine)C=OCH₃), 165.3 (NHC=O), 160.7 (C_{6_uracil}), 150.6 (C_{4_uracil}), 150.1 (C_{2_uracil}), 139.0 (C_{arom.}), 137.1 (C_{arom.}), 130.4 (C^{H_{arom.}}-H_{arom.}), 129.1 (C^{H_{arom.}}-H_{arom.}), 127.9 (C^{H_{arom.}}-H_{arom.}), 127.4 (C^{H_{arom.}}-H_{arom.}), 86.7 (C₅), 46.2 (NCH₂), 45.9 (NCH₂(piperazine)) 45.0 (NCH₂(piperazine)), 41.1 (NCH₂(piperazine)), 21.2 (NC=OCH₃), 21.09 (CH₂CH₃), 11.3 (CH₂CH₃) ppm. MS (ESI) (*m/z*): 461.1 [M + H]⁺ Mp.: 194 °C.

Synthesis of 8-(4-((-acetylpiperazin-1-yl)sulfonyl)phenyl)-1-propyl-3,7-dihydro-1*H*-purine-2,6-dione (**11**)³⁸

A solution of **10** (500 mg, 1.05 mmol) in DMF (2 ml) was treated with P₂O₅ (800 mg, 2.8 mmol) and stirred at 100 °C for 15 min. Subsequently, water (20 ml) was added and the precipitated product was filtered under reduced pressure, washed with water (20 ml) and dried at 70°C affording 446 mg (92 %) of a colorless solid. ¹H NMR (500 MHz, DMSO-*d*₆) δ : 10.49 (s br, 1H, NH), 9.12 (s br, 1H, NH), 8.17 (d, 2H, $J = 8.3$ Hz, C^{H_{arom.}}-H_{arom.}), 7.83 (d, 2H, $J = 8.3$ Hz, C^{H_{arom.}}-H_{arom.}), 6.16 (s, 2H, NH₂), 3.66 (t, 2H, $J = 7.4$ Hz, NCH₂), 3.50 (s, 4H, NCH₂(piperazine)₂(piperazine)), 2.91 (d, 4H, $J = 28.9$ Hz, NCH₂(piperazine)₂(piperazine)), 1.92 (s, 3H, NC=OCH₃), 1.50 (q, 2H, $J = 7.4$ Hz, CH₂CH₃), 0.83 (t, 3H, $J = 7.4$ Hz, CH₂CH₃) ppm. ¹³C NMR (126 MHz, DMSO-*d*₆) δ : 168.5 (N^(piperazine)C=OCH₃), 165.3 (NHC=O), 160.7 (C_{6_uracil}), 150.6 (C_{4_uracil}), 150.1 (C_{2_uracil}),

uracil), 139.0 (C_{arom.}), 137.1 (C_{arom.}), 130.4 (C_{arom.}), 129.1 (C_{arom.}), 127.9 (C_{arom.}), 127.4 (C_{arom.}), 86.7 (C_{5_uracil}), 46.2 (N-CH₂), 45.9 (NCH₂(piperazine)₂ (piperazine)), 45.0 (NCH₂(piperazine)₂ (piperazine)), 41.1 (NCH₂(piperazine)₂ (piperazine)), 21.2 (NC=OCH₃), 21.09 (CH₂CH₃), 11.3 (CH₂CH₃) ppm. MS (ESI) (m/z): 419.3 [M + H]⁺.

Synthesis of 8-(4-(piperazine-1-ylsulfonyl)phenyl)-1-propyl-3,7-dihydro-1H-purine-2,6-dione (12)

A solution of **11** (440 mg, 0.96 mmol) in EtOH (15 ml) is treated with 2 M NaOH (15 ml) and heated to 60°C for 5 h. Subsequently, the solution was neutralized with diluted HCl to pH 7. The precipitated product was filtered off under reduced pressure, washed with water (20 ml) dried at 70°C affording 371 mg (93 %) of a colorless solid. ¹H NMR (500 MHz, DMSO-*d*₆) δ: 8.31 (d, 2H, *J* = 8.5 Hz, C_{H_{arom.}}-H_{arom.}), 7.81 (d, 2H, *J* = 8.5 Hz, C_{H_{arom.}}-H_{arom.}), 3.85-3.78 (m, 2H, NCH₂), 2.84 (s, 4H, NCH₂(piperazine)₂ (piperazine)), 2.77-2.72 (m, 4H, NCH₂(piperazine)₂ (piperazine)), 1.57 (h, 2H, *J* = 7.4 Hz, CH₂CH₃), 0.87 (t, 3H, *J* = 7.4 Hz, CH₂CH₃) ppm. no NH-proton not detectable. ¹³C NMR (125 MHz, DMSO-*d*₆) δ: 163.1 (C_{4_xanth.}-xanth.), 155.4 (C_{8_xanth.}-xanth.), 151.2 (C_{2_xanth.}-xanth.), 148.7 (C_{6_xanth.}-xanth.), 147.9 (C_{arom.}), 135.3 (C_{arom.}), 134.0 (C_{arom.}), 128.4 (C_{5_xanth.}-xanth.), 109.8 (C_{H_{arom.}}-H_{arom.}), 46.6 (NCH₂(piperazine)₂ (piperazine)), 44.6 (NCH₂(piperazine)₂ (piperazine)), 41.6 (NCH₂), 21.0 (CH₂CH₃), 11.3 (CH₂CH₃) ppm. MS (ESI) (m/z): 400.3 [M + H]⁺. Mp.: 209-211 °C.

Synthesis of 2-(2-(2-(2-hydroxyethoxy)ethoxy)ethoxy)ethyl-4-methylbenzenesulfonate (13)

To a solution of tetraethyleneglycol (TEG) (21.37g, 110.2 mmol) and TEA (11 ml, 79 mmol) in CH₂Cl₂ (90 ml), tosyl chloride (TsCl) (6 g, 31.5 mmol) in CH₂Cl₂ (60 ml) was added dropwise at 0°C. The solution was allowed to warm up to rt and was stirred for 3 h. The organic solution was washed with saturated NaHCO₃ solution, water and brine (30 ml each), dried over MgSO₄, filtered and the solvent was removed under reduced pressure. The crude product was purified by column chromatography (pure ethyl acetate) to yield 8.5 g (81%) of a colorless oil. MS (ESI) (m/z): 348.7 [M + H]⁺.

Synthesis of 2-(2-(2-(2-(tosyloxy)ethoxy)ethoxy)ethoxy)acetic acid (14)⁴⁷

To a solution of CrO₃ (14.3 g, 143 mmol) in 1.5 M H₂SO₄ (70 ml), **13** (10.44 g, 30 mmol) in acetone (60 ml) was added dropwise at 0°C. The solution was allowed to warm up to rt and was stirred for 16 h. The acetone was removed under reduced pressure. The aqueous solution was extracted with ethyl acetate (3 x 50 ml). The combined organic phases were washed with diluted HCl and brine (50 ml each), dried over MgSO₄, filtered and the solvent was removed under reduced pressure. The crude product was purified by column chromatography (CH₂Cl₂ : MeOH - 9 : 1 + 1% acetic acid) to yield 8.58 g (85%) of a yellowish oil. ¹H NMR (600 MHz, Chloroform-*d*) δ: 7.82-7.76 (m, 2H, C_{H_{arom.}}-H_{arom.}), 7.34 (m, 2H, C_{H_{arom.}}-H_{arom.}), 4.11-4.15

(m, 4H, TsOCH₂/ OCH₂COOH), 3.73 (d, *J* = 5.6 Hz, 2H, OCH₂CH₂O), 3.71-3.65 (m, 4H, OCH₂CH₂O), 3.65-3.58 (m, 4H, OCH₂CH₂O), 2.46-2.42 (m, 3H, CH₃) ppm. ¹³C NMR (151 MHz, Chloroform-*d*) δ: 176.7, 173.5, 144.8, 132.9, 129.8, 127.9, 71.1, 70.5, 70.2, 69.2, 68.8, 21.6, 20.7 ppm. MS (ESI) (*m/z*): 363.0 [M + H]⁺.

Synthesis of 2-(2-(2-(2-azidoethoxy)ethoxy)ethoxy)ethyl 4-methylbenzenesulfonate (15)⁴⁸

A stirred solution of **13** (1.5 g, 4.31 mmol) in DMF (5 ml) was treated with NaN₃ (295 mg, 4.53 mmol) and stirred at rt for 16 h. The resulting suspension was filtered and the solvent was removed under reduced pressure. The crude intermediate was converted to **15** without further purification or identification.

Therefore, the intermediate (4.31 mmol) was dissolved in CH₂Cl₂ (30 ml) and treated with TEA (1.5 ml, 10.78 mmol) and TsCl (1080 mg, 5.6 mmol) at 0°C. The solution was allowed to warm up to rt and was stirred for 16 h. The organic solution was washed with diluted HCl solution, water and brine (30 ml each), dried over MgSO₄, filtered and the solvent was removed under reduced pressure. The crude product was purified by column chromatography (pure CH₂Cl₂ to CH₂Cl₂ : ethyl acetate - 9 : 1) to yield 1.21 g (75%) of a yellowish oil. ¹H NMR (600 MHz, Chloroform-*d*) δ: 7.82-7.77 (m, 2H, C^{H_{arom}}-H_{arom}), 7.36-7.31 (m, 2H, C^{H_{arom}}-H_{arom}), 4.18-4.12 (m, 2H, TsOCH₂), 3.70-3.65 (m, 4H, N₃CH₂CH₂O / CH₂N₃), 3.65-3.61 (m, 4H, OCH₂CH₂O), 3.59 (t, *J* = 1.3 Hz, 4H, OCH₂CH₂O), 3.41-3.35 (m, 2H, TsOCH₂CH₂O), 2.44 (s, 3H, CH₃) ppm. ¹³C NMR (151 MHz, Chloroform-*d*) δ: 144.7, 133.0, 129.8, 128.0, 70.7, 70.6, 70.5, 70.0, 69.2, 68.6, 50.6, 21.6 ppm. MS (ESI) (*m/z*): 374.0 [M + H]⁺.

Synthesis of 3,6,9,12-tetraoxapentadec-14-yn-1-yl 4-methylbenzenesulfonate (17)⁴⁹

A solution of TEG (3 g, 15.15 mmol) in DMF (35 ml) is treated with NaH (60 % in mineral oil, 909 mg, 22.72 mmol) at 0°C and stirred for 15 min. Subsequently, propargyl bromide (3.38 g, 22.7 mmol) in DMF (15 ml) is added dropwise. The solution is stirred at rt for 6 h. The solution is treated with sat. NH₄Cl solution and the aqueous phase is extracted with ethyl acetate (3 x 50 ml). The combined organic phases were dried over MgSO₄, filtered and the solvent was removed under reduced pressure. The crude product was only analyzed by TLC (pure ethyl acetate, KMnO₄ solution was used to visualize the product).

The crude product was dissolved in CH₂Cl₂ (30 ml) and treated with TEA (5 ml) and TsCl (2.88 g, 15.2 mmol) at 0°C. The solution was allowed to warm up to rt and stirred for 6 h. Subsequently, the organic solution was washed with saturated NaHCO₃ solution, water and brine. The organic phase was dried over MgSO₄, filtered and the solvent was removed under reduced pressure. The crude product was purified by column chromatography (pure CH₂Cl₂ to pure ethyl acetate), yielding 1.34 g (23 %) of a brownish oil. ¹H NMR (600 MHz, DMSO-*d*₆) δ:

7.77 (d, $J = 8.3$ Hz, 2H, $C_{\text{H}_{\text{arom}}}-H_{\text{arom}}$), 7.47 (d, $J = 8.1$ Hz, 2H, $C_{\text{H}_{\text{arom}}}-H_{\text{arom}}$), 4.12 (d, $J = 2.4$ Hz, 2H, $\text{CH}_2\text{C}\equiv\text{CH}$), 4.11-4.09 (m, 2H, TsOCH_2), 3.58-3.55 (m, 2H, $\text{OCH}_2\text{CH}_2\text{O}$), 3.54-3.51 (m, 4H, $\text{OCH}_2\text{CH}_2\text{O}$), 3.47 (td, $J = 4.3, 2.5$ Hz, 4H, $\text{OCH}_2\text{CH}_2\text{O}$), 3.44 (s, 4H, $\text{OCH}_2\text{CH}_2\text{O}$), 3.39 (t, $J = 2.4$ Hz, 1H, $\text{C}\equiv\text{CH}$), 2.41 (s, 3H, CH_3) ppm. ^{13}C NMR (151 MHz, $\text{DMSO}-d_6$) δ : 145.0, 132.6, 130.3, 127.8, 80.5, 77.2, 70.1, 69.93, 69.91, 69.8, 69.6, 68.0, 57.6, 21.2 ppm. MS (ESI) (m/z): 387.2 $[\text{M} + \text{H}]^+$.

Synthesis of 4-azidobenzoic acid (**18**)⁵⁰

To a stirred solution of *p*-aminobenzoic acid (137 mg, 1 mmol) in 6 N H_2SO_4 (20 ml), NaNO_2 (83 mg, 1.2 mmol) in 5 ml water was added dropwise at 0°C . The solution was stirred for 15 min. Subsequently, NaN_3 (98 mg, 1.5 mmol) in 5 ml water was added dropwise. After 30 min of stirring at rt, the aqueous solution was extracted with ethyl acetate (3 x 30 ml). The combined organic layers were dried over MgSO_4 and concentrated under reduced pressure. The product was 156 mg (96%) of a brownish solid. ^1H NMR (500 MHz, $\text{DMSO}-d_6$) δ : 12.91 (s, 1H, COOH), 7.98-7.91 (m, 2H, $C_{\text{H}_{\text{arom}}}-H_{\text{arom}}$), 7.23-7.16 (m, 2H, $C_{\text{H}_{\text{arom}}}-H_{\text{arom}}$) ppm. ^{13}C NMR (126 MHz, $\text{DMSO}-d_6$) δ : 166.7 (COOH), 144.1 (C_{arom}), 131.4 (C_{arom}), 127.5 (C_{arom}), 119.3 (C_{arom}) ppm.

Synthesis of 4-ethynylbenzoic acid (**20**)⁵¹

A solution of ethyl 4-iodobenzoate (1.5 g, 5.43 mmol), CuI (207 mg, 1.09 mmol), PPh_3 (285 mg, 1.09 mmol), TEA (2 ml) and ethynyltrimethyl-silane (701 mg, 7.16 mmol) in DMF was gas-flushed with argon for 10 min. Subsequently, $\text{PdCl}_2(\text{PPh}_3)_2$ (381 mg, 0.54 mmol) was added while the solution was still gas-flushed with argon. The flask was sealed and the reaction mixture was stirred 16 h at rt. The solvent was removed under reduced pressure and the residue was treated with saturated NH_4Cl solution. The aqueous solution was extracted with ethyl acetate (3 x 40 ml), the combined organic phases dried over MgSO_4 , filtered and the solvent was removed under reduced pressure. The crude product was purified by column chromatography (ethyl acetate: hexane 1 : 1 to pure ethyl acetate) to yield 1.28 g (95 %) of a yellowish oil (**19**). ^1H NMR (600 MHz, Chloroform-*d*) δ : 7.98-7.93 (m, 2H, $C_{\text{H}_{\text{arom}}}-H_{\text{arom}}$), 7.52-7.47 (m, 2H, $C_{\text{H}_{\text{arom}}}-H_{\text{arom}}$), 4.35 (q, $J = 7.1$ Hz, 2H, CH_2CH_3), 1.37 (t, $J = 7.1$ Hz, 3H, CH_2CH_3), 0.24 (s, 9H, $\text{Si}(\text{CH}_3)_3$) ppm. ^{13}C NMR (151 MHz, Chloroform-*d*) δ : 166.0 (ester), 131.8 (C_{arom}), 129.3 (C_{arom}), 127.6 (C_{arom}), 104.1 (C_{arom}), 97.5 ($\text{C}\equiv\text{C}-\text{TMS}$), 61.1 (CH_2CH_3), 14.3 (CH_2CH_3), -0.2 ($\text{Si}(\text{CH}_3)_3$) ppm. MS (ESI) (m/z): 247.0 $[\text{M} + \text{H}]^+$.

A solution of **19** (1.28 g, 0.52 mmol) in H_2O / EtOH (50 ml) was treated with 5 M NaOH (10 ml) and stirred for 16 h at rt. The aqueous solution was washed with diethyl ether (3 x 30 ml). Subsequently, the solution was acidified with conc. HCl and extracted with ethyl acetate (3 x 30 ml). The combined organic phases were dried over MgSO_4 , filtered off and the solvent was

removed under reduced pressure. The final product was 712 mg (90% overall yield) of a brown solid. ^1H NMR (600 MHz, $\text{DMSO-}d_6$) δ : 13.10 (s, 1H, COOH), 7.96-7.89 (m, 2H, $\text{C}_{\text{H}_{\text{arom}}}\text{-H}_{\text{arom}}$), 7.62-7.55 (m, 2H, $\text{C}_{\text{H}_{\text{arom}}}\text{-H}_{\text{arom}}$), 4.39 (s, 1H, $\text{C}\equiv\text{CH}$) ppm. ^{13}C NMR (151 MHz, $\text{DMSO-}d_6$) δ : 166.8 (COOH), 132.1 (C_{arom}), 131.0 (C_{arom}), 129.5 (C_{arom}), 126.2 (C_{arom}), 83.7 ($\text{C}\equiv\text{CH}$), 82.9 ($\text{C}\equiv\text{CH}$) ppm.⁵¹

Synthesis of methyl 3-(2-(2-(2-(2-azidoethoxy)ethoxy)ethoxy)ethoxy)benzoate (21)⁵²

A solution of methyl-3-hydroxybenzoate (300 mg, 2.17 mmol), **15** (800 mg, 2.17 mmol) and K_2CO_3 (300 mg, 2.17 mmol) in DMF (25 ml) is stirred at 100°C for 16 h. Subsequently, the solvent was removed under reduced pressure and the residue was extracted with sat. NaHCO_3 solution and ethyl acetate (3 x 30 ml). The combined organic solvents were washed with water and brine (30 ml each), dried over MgSO_4 , filtered and the solvent was removed under reduced pressure. The crude product was 733 mg (95%) a brownish oil. ^1H NMR (600 MHz, $\text{DMSO-}d_6$) δ : 7.53 (dt, $J = 7.6, 1.2$ Hz, 1H, $\text{C}_{\text{H}_{\text{arom}}}\text{-H}_{\text{arom}}$), 7.47-7.38 (m, 2H, $\text{C}_{\text{H}_{\text{arom}}}\text{-H}_{\text{arom}}$), 7.23 (ddd, $J = 8.3, 2.7, 1.0$ Hz, 1H, $\text{C}_{\text{H}_{\text{arom}}}\text{-H}_{\text{arom}}$), 4.16-4.11 (m, 2H, CH_2O), 3.84 (s, 3H, OCH_3), 3.77-3.71 (m, 2H, CH_2O), 3.60-3.57 (m, 4H, CH_2O), 3.56 - 3.52 (m, 6H, CH_2O), 3.36 (dd, $J = 5.5, 4.3$ Hz, 2H, CH_2N_3) ppm. MS (ESI) (m/z): 354 [$\text{M} + \text{H}$]⁺.

Synthesis of 3-(2-(2-(2-(2-azidoethoxy)ethoxy)ethoxy)ethoxy)benzoic acid (22)

The crude **21** (733 mg, 2.08 mmol) was dissolved in H_2O / THF (1 : 1, 10 ml), treated with $\text{LiOH} \cdot \text{H}_2\text{O}$ (561 mg, 10.4 mmol) and stirred at rt for 16 h. After complete transformation (controlled by TLC), the reaction mixture was acidified to pH 1 with HCl and extracted with ethyl acetate (3 x 30 ml). The combined organic solvents were washed with water and brine (30 ml each), dried over MgSO_4 , filtered and the solvent was removed under reduced pressure. The crude product was 626 mg (89%) a brownish oil. ^1H NMR (600 MHz, $\text{DMSO-}d_6$) δ : 12.94 (s, 1H, COOH), 7.54-7.49 (m, 1H, $\text{C}_{\text{H}_{\text{arom}}}\text{-H}_{\text{arom}}$), 7.45-7.35 (m, 2H, $\text{C}_{\text{H}_{\text{arom}}}\text{-H}_{\text{arom}}$), 7.19 (dd, $J = 8.2, 2.6$ Hz, 1H, $\text{C}_{\text{H}_{\text{arom}}}\text{-H}_{\text{arom}}$), 4.15-4.10 (m, 2H, CH_2O), 3.77-3.72 (m, 2H, CH_2O), 3.60-3.52 (m, 10H, CH_2O), 3.38-3.35 (m, 2H, CH_2N_3) ppm. ^{13}C NMR (151 MHz, $\text{DMSO-}d_6$) δ : 167.3 (COOH), 158.6 (C_{arom}), 132.4 (C_{arom}), 129.9 (C_{arom}), 121.8 (C_{arom}), 119.6 (C_{arom}), 114.7 (C_{arom}), 70.1 (CH_2O), 70.0 (CH_2O), 67.0 (CH_2O), 69.7 (CH_2O), 69.4 (CH_2O), 69.0 (CH_2O), 67.5 (CH_2O), 50.2 (CH_2N_3) ppm. MS (ESI) (m/z): 340.1 [$\text{M} + \text{H}$]⁺.

Synthesis of methyl 3-(2-(2-(2-(2-aminoethoxy)ethoxy)ethoxy)ethoxy)benzoate (23)⁵³

A solution of **21** (1.95 g, 3.52 mmol) and PPh_3 (1.59 g, 6.08 mmol) in THF (30 ml) was stirred at rt for one day. Subsequently, water (30 ml) was added and the solution was stirred another day at rt. The solvent was evaporated under reduced pressure, the crude product was purified by column Chromatography (ethyl acetate to CH_2Cl_2 / MeOH - 9 : 1) yielding 1.77g of a brown oil. MS (ESI) (m/z): 328.2 [$\text{M} + \text{H}$]⁺.

Synthesis of 3-((2,2-dimethyl-4-oxo-3,8,11,14-tetraoxa-5-azahexadecan-16-yl)oxy)benzoic acid (**24**)

A solution of **23** (1.2 g, 5.06 mmol), Boc₂O (1.65 mg, 7.59 mmol) and LiOH (607 mg, 15.18 mmol) in THF / H₂O (2 : 1, 10 ml) was stirred for 16 h at rt. Subsequently, 900 mg LiOH · H₂O was added to cleave the ester. The solution was stirred for 16 h at rt and subsequently acidified with diluted HCl. The solution was extracted with 3 x 50 ml ethyl acetate, the combined organic phases dried over MgSO₄, filtered and the solvent was removed under reduced pressure. The crude product was purified by column chromatography (ethyl acetate to CH₂Cl₂ / MeOH - 9 : 1) and yielded 739 mg (32 % from **23**) of a brownish oil. ¹H NMR (600 MHz, DMSO-*d*₆) δ: 7.51 (dt, *J* = 7.7, 1.3 Hz, 1H, C^H_{arom}-H_{arom}), 7.45-7.35 (m, 2H, C^H_{arom}-H_{arom}), 7.17 (dd, *J* = 8.2, 2.6 Hz, 1H, C^H_{arom}-H_{arom}), 6.70 (t, *J* = 5.6 Hz, 1H, NHBoc), 4.15-4.10 (m, 2H, PhOCH₂), 3.77-3.72 (m, 2H, CH₂O), 3.58 (dd, *J* = 5.9, 3.6 Hz, 2H, CH₂O), 3.57-3.45 (m, 6H, CH₂O), 3.44-3.33 (t, 2H, CH₂O), 3.04 (q, *J* = 6.0 Hz, 2H, CH₂N), 1.35 (s, 9H, C(CH₃)₃) ppm. MS (ESI) (*m/z*): 413.8 [M + H]⁺.

General procedure A for the formation of 8-(4-acylpiperazine-1-sulfonyl)phenyl-1-propylxanthines (**25-29**)

To a stirred solution of **12** (1 eq.), the corresponding carboxylic acid (1.15 eq.) and TEA (2.5 eq.) in DMF (1 ml), was added HBTU (1.3 eq.). The solution was stirred at rt for 1 h and subsequently treated with water (10 ml). The resulting precipitate was filtered under reduced pressure, washed with water (50 ml) and dried at 70 °C. If necessary, reprecipitation was performed by dissolving the crude compound in a minimum of DMF and subsequent treatment with an excess of water. The solid thus obtained was isolated as described above.

Synthesis of 8-(4-((4-(4-azidobenzoyl)piperazin-1-yl)sulfonyl)phenyl)-1-propyl-3,7-dihydro-1*H*-purine-2,6-dione (**25**)

A mixture of **12** (30 mg, 0.07 mmol), **18** (15 mg, 0.09 mmol), TEA (50 μl, 0.18 mmol) and HBTU (36 mg, 0.9 mmol) in DMF (1 ml) was reacted using the general procedure A. The product **25** was obtained as 30 mg (71 %) of an off-white solid. ¹H NMR (500 MHz, DMSO-*d*₆) δ: 11.80 (s, 1H, NH), 8.29 (d, *J* = 8.2 Hz, 2H, C^H_{arom}-H_{arom}), 7.79 (d, *J* = 8.3 Hz, 2H, C^H_{arom}-H_{arom}), 7.39 (d, *J* = 8.1 Hz, 2H, C^H_{arom}-H_{arom}), 7.11 (d, *J* = 8.1 Hz, 2H, C^H_{arom}-H_{arom}), 3.81 (t, *J* = 7.4 Hz, 2H, NCH₂), 3.60-3.47 (m, 4H, NCH₂ (piperazine)), 3.01 (m, 4H, NCH₂ (piperazine)), 1.56 (p, *J* = 7.7 Hz, 2H, CH₂CH₃), 0.87 (t, *J* = 7.4 Hz, 3H, CH₂CH₃) ppm. Not all NH displayed. ¹³C NMR (126 MHz, DMSO-*d*₆) δ: 168.6 (C=O), 155.9 (C_{4xanth}-xanth), 151.3 (C_{2xanth}-xanth), 149.4 (C_{arom}), 148.2 (C_{8xanth}-xanth), 147.0 (C_{6xanth}-xanth), 134.9 (C_{arom}), 132.0 (C_{arom}), 129.3 (C_{arom}), 128.2 (C_{5xanth}-xanth), 126.7 (C_{arom}), 119.2 (C_{arom}), 45.9 (NCH₂(piperazine)₂(piperazine)), 41.5 (NCH₂), 21.1 (CH₂CH₃), 11.4

(CH₂CH₃) ppm. HPLC-UV (254 nm) ESI-MS, purity: 98.5%. MS (ESI) (m/z): 564.3 [M + H]⁺. Mp.: 298-299 °C.

Synthesis of 8-(4-((4-(4-ethynylbenzoyl)piperazin-1-yl)sulfonyl)phenyl)-1-propyl-3,7-dihydro-1H-purine-2,6-dione (26)

A mixture of **12** (100 mg, 0.24 mmol), **20** (40 mg, 0.28 mmol), TEA (83 µl, 0.6 mmol) and HBTU (118 mg, 0.31 mmol) in DMF (1 ml) was reacted using the general procedure A. The product **26** was obtained as 96 mg (73 %) of an off-white solid. ¹H NMR (500 MHz, DMSO-*d*₆) δ: 11.90 (s, 1H, NH), 8.31 (d, *J* = 8.1 Hz, 2H, C_{H_{arom}}-H_{arom}), 7.81 (d, *J* = 8.1 Hz, 2H, C_{H_{arom}}-H_{arom}), 7.48 (d, *J* = 7.8 Hz, 2H, C_{H_{arom}}-H_{arom}), 7.34 (d, *J* = 7.9 Hz, 2H, C_{H_{arom}}-H_{arom}), 4.26 (s, 1H, C≡CH), 3.81 (t, *J* = 7.7 Hz, 2H, NCH₂), 3.50 (dt, *J* = 9.4, 5.3 Hz, 4H, NCH₂ Piperazine), 3.01 (s, 4H, NCH₂ Piperazine), 1.56 (p, *J* = 7.3 Hz, 2H, CH₂CH₃), 0.87 (t, *J* = 7.5 Hz, 3H, CH₂CH₃) ppm. not all NH protons displayed. ¹³C NMR (126 MHz, DMSO-*d*₆) δ: 168.5 (C=O), 155.7 (C_{4xanth}-xanth), 151.2 (C_{2xanth}-xanth), 149.0 (C_{arom}), 148.0 (C_{8xanth}-xanth), 135.7 (C_{arom}), 135.2 (C_{arom}), 134.7 (C_{arom}), 131.8 (C_{arom}), 128.2 (C_{5xanth}-xanth), 127.6 (C_{arom}), 126.9 (C_{arom}), 123.1 (C_{arom}), 82.9 (C≡CH), 82.2 (C≡CH), 45.8 (NCH_{2(piperazine)2(piperazine)}), 41.5 (NCH₂), 21.1 (CH₂CH₃), 11.4(CH₂CH₃) ppm. HPLC-UV (254 nm) ESI-MS, purity: 95.3 %. MS (ESI) (m/z): 547.3 [M + H]⁺. HRMS (ESI-TOF) m/z: [M + H]⁺ calcd. for C₂₇H₂₆N₆O₅S 547.1758, found 547.1739. Mp.: 302,5-303,5 °C.

Synthesis of 8-(4-((4-(3-(2-(2-(2-azidoethoxy)ethoxy)ethoxy)ethoxy)benzoyl)piperazin-1-yl)sulfonyl)phenyl)-1-propyl-3,7-dihydro-1H-purine-2,6-dione (27)

A mixture of **12** (50 mg, 0.12 mmol), **22** (0,47 mg, 0.137 mmol), TEA (41 µl, 0.3 mmol) and HBTU (60 mg, 0.156 mmol) in DMF (1 ml) was reacted using the general procedure A. The product **27** was obtained as 58 mg (65 %) of a brownish solid. ¹H NMR (600 MHz, DMSO-*d*₆) δ: 14.04 (s, 1H, NH), 11.95 (s, 1H, NH), 8.33 (d, *J* = 8.1 Hz, 2H, C_{H_{arom}}-H_{arom}), 7.85 (d, *J* = 7.9 Hz, 2H, C_{H_{arom}}-H_{arom}), 7.28 (t, *J* = 7.8 Hz, 1H, C_{H_{arom}}-H_{arom}), 6.98 (d, *J* = 8.3 Hz, 1H, C_{H_{arom}}-H_{arom}), 6.86 (d, *J* = 9.0 Hz, 2H, C_{H_{arom}}-H_{arom}), 4.08-4.03 (m, 2H, PhOCH₂), 3.82 (t, *J* = 7.5 Hz, 2H, NCH₂), 3.72-3.60 (m, 4H, CH₂O), 3.58-3.49 (m, 10H, CH₂O), 3.42 (s, 2H, CH₂N₃), 3.01 (s, 4H, NCH₂ Piperazine), 1.57 (h, *J* = 7.7, 7.2 Hz, 2H, CH₂CH₃), 0.87 (t, *J* = 7.3 Hz, 3H, CH₂CH₃) ppm. NCH₂ Piperazine under water peak. ¹³C NMR (151 MHz, DMSO-*d*₆) δ: 169.0 (C=O), 158.5 (C_{arom}), 155.2 (C_{4xanth}xanth), 151.1(C_{2xanth}xanth), 148.2 (C_{8xanth}xanth), 147.8 (C_{6xanth}), 136.9 (C_{arom}), 136.1 (C_{arom}), 133.3 (C_{arom}), 129.8 (C_{arom}), 128.4 (C_{5xanth}xanth), 127.2 (C_{arom}), 119.2 (C_{arom}), 113.1 (C_{arom}), 108.8 (C_{arom}), 70.1 (CH₂O), 67.0 (CH₂O), 67.0 (CH₂O), 69.9 (CH₂O), 69.4 (CH₂O), 69.0 (CH₂O), 67.5 (CH₂O), 50.2 (CH₂N₃), 45.9 (NCH_{2(piperazine)2(piperazine)}), 41.7 (NCH₂), 40.2 (NCH_{2(piperazine)2(piperazine)}), 21.0 (CH₂CH₃), 11.3 (CH₂CH₃) ppm. HPLC-UV (254 nm) ESI-MS, purity: 95.9 %. MS (ESI) (m/z): 740.6 [M + H]⁺. HRMS (ESI-TOF) m/z: [M + H]⁺ calcd. for C₃₃H₄₁N₉O₉S 740.2821, found 740.2802. Mp.: 287-289 °C.

Synthesis of tert-butyl (2-(2-(2-(2-(3-(4-((4-(2,6-dioxo-1-propyl-2,3,6,7-tetrahydro-1H-purin-8-yl)phenyl)sulfonyl)piperazine-1-carbonyl)phenoxy)ethoxy)ethoxy)ethoxy)ethyl)carbamate (28)

A mixture of **12** (100 mg, 0.24 mmol), **24** (110 mg, 0.137 mmol), TEA (80 μ l, 0.6 mmol) and HBTU (118 mg, 0.312 mmol) in DMF (1 ml) was reacted using the general procedure A. The product **28** was obtained as 106 mg (54 %) of a brownish solid. ^1H NMR (500 MHz, DMSO- d_6) δ : 14.00 (s, 1H; NH), 11.93 (s, 1H, NH), 8.36-8.30 (m, 2H, $\text{C}_{\text{H}_{\text{arom}}}-\text{H}_{\text{arom}}$), 7.88-7.82 (m, 2H, $\text{C}_{\text{H}_{\text{arom}}}-\text{H}_{\text{arom}}$), 7.28 (t, $J = 7.8$ Hz, 1H, $\text{C}_{\text{H}_{\text{arom}}}-\text{H}_{\text{arom}}$), 7.04-6.93 (m, 1H, $\text{C}_{\text{H}_{\text{arom}}}-\text{H}_{\text{arom}}$), 6.90-6.85 (m, 2H, $\text{C}_{\text{H}_{\text{arom}}}-\text{H}_{\text{arom}}$), 6.71-6.64 (m, 1H, NHBoc), 4.12-4.03 (m, 2H, PhOCH₂), 3.82 (t, $J = 7.5$ Hz, 2H, CH₂O), 3.70 (t, $J = 4.5$ Hz, 2H CH₂O), 3.58-3.43 (m, 6H, CH₂O), 3.35 (t, $J = 6.0$ Hz, 2H, CH₂O), 3.03 (dd, $J = 13.1, 7.1$ Hz, 6H, CH₂N), 1.58 (q, $J = 7.4$ Hz, 2H, CH₂CH₃), 1.34 (s, 9H, C(CH₃)₃), 0.87 (t, $J = 7.2$ Hz, 3H, CH₂CH₃) ppm. ^{13}C NMR (126 MHz, DMSO- d_6) δ : 169.0 (amide), 158.5 (C_{arom}), 155.7 (C_{Boc}), 155.2 ($\text{C}_4_{\text{xanth-xanth}}$), 151.1 ($\text{C}_2_{\text{xanth-xanth}}$), 148.2 ($\text{C}_8_{\text{xanth-xanth}}$), 147.8 ($\text{C}_6_{\text{xanth-xanth}}$), 136.9 (C_{arom}), 136.1 (C_{arom}), 133.5 (C_{arom}), 129.8 (C_{arom}), 128.4 ($\text{C}_5_{\text{xanth-xanth}}$), 127.2 (C_{arom}), 119.2 (C_{arom}), 116.0 (C_{arom}), 113.1 (C_{arom}), 109.0 (C_{arom}), 77.7 (C(CH₃)₃), 70.1 (OCH₂), 69.9 (OCH₂), 69.9 (OCH₂), 69.7 (OCH₂), 69.3 (OCH₂), 69.0 (OCH₂), 67.5 (OCH₂), 45.9 (NCH₂(piperazine)₂(piperazine)), 41.7 (NCH₂), 28.4 (C(CH₃)₃), 21.0 (CH₂CH₃), 11.4 (CH₂CH₃) ppm. MS (ESI) (m/z): 814.2 [M + H]⁺. HPLC-UV (254 nm) ESI-MS, purity: 95.5 %. HRMS (ESI-TOF) m/z: [M + H]⁺ calcd. for C₃₈H₅₁N₇O₁₁S 814.3440, found 814.3436. Mp.: 277 °C.

Synthesis of 8-(4-((4-(3-(2-(2-(2-(2-aminoethoxy)ethoxy)ethoxy)ethoxy)benzoyl)piperazin-1-yl)sulfonyl)phenyl)-1-propyl-3,7-dihydro-1H-purine-2,6-dione (29)

A suspension of **28** (55 mg, 0.7 mmol) in CH₂Cl₂ (5 ml) is treated with TFA (1 ml) at 0 °C and stirred while warming up to rt. After completion of the reaction (monitored by TLC - CH₂Cl₂ : MeOH - 9:1) the solvent was evaporated under reduce pressure and the residue was suspended in saturated NaHCO₃ solution (10 ml). The product was filtered under reduced pressure and dried at 70°C to yield 41 mg (85 %) of an off-white solid. ^1H NMR (500 MHz, DMSO- d_6) δ : 8.21 (dd, $J = 12.6, 8.4$ Hz, 2H, $\text{C}_{\text{H}_{\text{arom}}}-\text{H}_{\text{arom}}$), 7.68 (t, $J = 9.3$ Hz, 2H, $\text{C}_{\text{H}_{\text{arom}}}-\text{H}_{\text{arom}}$), 7.33-7.24 (m, 1H, $\text{C}_{\text{H}_{\text{arom}}}-\text{H}_{\text{arom}}$), 7.00-6.94 (m, 1H, $\text{C}_{\text{H}_{\text{arom}}}-\text{H}_{\text{arom}}$), 6.89-6.84 (m, 2H, $\text{C}_{\text{H}_{\text{arom}}}-\text{H}_{\text{arom}}$), 4.05 (t, $J = 4.7$ Hz, 2H, PhOCH₂), 3.79 (dd, $J = 9.1, 5.8$ Hz, 2H, NCH₂), 3.68 (dd, $J = 5.7, 3.5$ Hz, 4H, CH₂O / NCH₂), 3.57-3.46 (m, 10H, CH₂O), 2.98-2.86 (m, 4H, NCH₂Piperazine), 1.54 (h, $J = 7.4$ Hz, 2H, CH₂CH₃), 0.86 (t, $J = 7.4$ Hz, 3H, CH₂CH₃) ppm. NH protons not displayed. ^{13}C NMR (126 MHz, DMSO- d_6) δ : 169.0 (amide), 158.4 (C_{arom}), 157.8 (C_{arom}), 152.4 ($\text{C}_4_{\text{xanth-xanth}}$), 151.7 ($\text{C}_2_{\text{xanth-xanth}}$), 149.4 ($\text{C}_8_{\text{xanth-xanth}}$), 139.9 (C_{arom}), 137.0 (C_{arom}), 132.3 (C_{arom}), 129.8 (C_{arom}), 127.9 ($\text{C}_5_{\text{xanth-xanth}}$), 125.9 (d, $J = 16.3$ Hz) (C_{arom}), 119.2 (C_{arom}), 116.4

(C_{arom.}), 116.0 (C_{arom.}), 113.0 (C_{arom.}), 70.1 (OCH₂), 69.9 (OCH₂), 69.8 (OCH₂), 69.0 (OCH₂), 68.2 (OCH₂), 67.5 (OCH₂), 41.2 (NCH₂), 21.4 (CH₂CH₃), 11.4 (CH₂CH₃) ppm. HPLC-UV (254 nm) ESI-MS, purity: 95.0%. MS (ESI) (m/z): 714.2 [M + H]⁺. HRMS (ESI-TOF) m/z: [M + H]⁺ calcd. for C₃₃H₄₃N₇O₉S 714.2916, found 714.2902. Mp.: 316-318 °C.

Synthesis of potassium 2,3,3-trimethyl-3*H*-indole-5-sulfonate (**31**)⁴⁰

A stirred solution of *p*-hydrazinobenzenesulfonic acid (10.0 g, 53.0 mmol) and 3-methyl-2-butanone (17 ml, 160 mmol) in acetic acid (30 ml) was refluxed for 4 h, cooled to rt and filtered under reduced pressure. The obtained solid was washed with ethyl acetate and dried at 70°C to provide the intermediate as a pink solid (8.7 g, 68%). A solution of crude sulfonic acid (8.67 g, 36.2 mmol) in methanol (35 ml) was added drop-wise to a stirred solution of KOH (2.8 g, 50.8 mmol) in *n*-propanol (35 ml). The resulting mixture was stirred over night at rt, filtered under reduced pressure, washed with isopropanol and dried at 70°C to provide the crude potassium salt **31** as a brown solid (8.9 g, 89%). ¹H NMR (600 MHz, D₂O) δ: 7.93 (dt, *J* = 1.8, 0.8 Hz, 1H, CH_{arom.}-H_{arom.}), 7.88-7.83 (m, 1H, CH_{arom.}-H_{arom.}), 7.62 (dd, *J* = 8.1/1.1 Hz, 1H, CH_{arom.}-H_{arom.}), 1.41 (d, *J* = 1.1 Hz, 6H, 2 x CH₃) ppm. The methyl group at the indole position 2 could not (or very poorly) be detected due to an H/D exchange via tautomeric forms. ¹³C NMR (151 MHz, DMSO-*d*₆) δ: 189.0 (C_{indole}), 153.7 (C_{arom.}), 145.32 (C_{arom.}), 145.28 (C_{arom.}), 125.3 (C_{arom.}), 119.3 (C_{arom.}), 118.3 (C_{arom.}), 53.4 (C_{indole}), 22.7 (2 x CH₃), 15.3 (CH₃) ppm. MS (ESI) (m/z): 239.9 [M + H]⁺.

Synthesis of 2,3,3-trimethyl-1-propyl-3*H*-indol-1-ium-5-sulfonate (**32**)⁴⁰

A slurry of **31** (3.3 g, 12 mmol) in 1-iodopropane (18 ml, 25.7 mmol) was refluxed for 24 h, cooled to rt and filtered under reduced pressure. The obtained solid was washed with acetone and dried at 70°C to provide the 3.11 g (92%) of the crude **33** as a pink solid. ¹H NMR (600 MHz, Methanol-*d*₄) δ: 8.16 (d, *J* = 1.6 Hz, 1H, CH_{arom.}-H_{arom.}), 8.07 (dd, *J* = 8.4, 1.7 Hz, 1H, CH_{arom.}-H_{arom.}), 7.98 (d, *J* = 8.4 Hz, 1H, CH_{arom.}-H_{arom.}), 4.63-4.45 (m, 2H, NCH₂), 2.11-1.96 (m, 2H, CH₂CH₃), 1.67 (s, 6H, 2 x CH₃), 1.14 (t, *J* = 7.4 Hz, 3H, CH₂CH₃) ppm. The methyl group at the indole position 2 could not (or very poorly) be detected due to an H/D exchange via tautomeric forms. ¹³C NMR (151 MHz, Methanol-*d*₄) δ: 190.2, 139.0, 137.2, 134.0, 118.9, 117.7, 112.8, 46.7, 21.2, 14.7, 13.5, 13.2, 12.8 ppm (due to the poor quality of the spectrum a reasonable assignment of peaks was not possible). MS (ESI) (m/z): 282.1 [M + H]⁺.

Synthesis of (*E*)-3,3-dimethyl-2-(2-(phenylamino)vinyl)-1-propyl-3*H*-indol-1-ium-5-sulfonate (**33**)⁴⁰

A slurry of crude **32** (2 g, 7.1 mmol) and *N,N'*-diphenylformamidine (1.58 g, 8 mmol) in acetic acid (10 ml) was refluxed for 3 h. After cooling to rt, the crude product was precipitated by adding ethyl acetate (30 ml), filtered under reduced pressure and dried at 70°C. Further

purification was achieved by column chromatography (CH₂Cl₂ / MeOH - 3 : 1 + 2% AcOH). The resulting material was washed with methanol providing product **33** as a 700 mg (23%) of a yellow solid. ¹H NMR (600 MHz, DMSO-*d*₆) δ 8.61 (d, *J* = 10.7 Hz, 1H, =CH), 7.60 (d, *J* = 1.8 Hz, 1H, C^H_{arom}-H_{arom}), 7.54 (dd, *J* = 8.2, 1.7 Hz, 1H, C^H_{arom}-H_{arom}), 7.35 (dd, *J* = 8.4, 7.2 Hz, 2H, C^H_{arom}-H_{arom}), 7.16 (dt, *J* = 8.8, 1.9 Hz, 2H, C^H_{arom}-H_{arom}), 7.15-7.10 (m, 1H, C^H_{arom}-H_{arom}), 7.02 (d, *J* = 8.1 Hz, 1H, C^H_{arom}-H_{arom}), 5.79 (d, *J* = 10.6 Hz, 1H, =CH), 3.80 (t, *J* = 7.2 Hz, 2H, NCH₂), 1.67 (q, *J* = 7.4 Hz, 2H, CH₂CH₃), 1.59 (s, 6H, 2 x CH₃), 0.93 (t, *J* = 7.4 Hz, 3H, CH₂CH₃) ppm. ¹³C NMR (151 MHz, DMSO-*d*₆) δ: 172.6, 155.6, 143.7, 142.4, 138.5, 129.4, 126.0, 124.6, 120.2, 119.7, 107.6, 95.7, 46.9, 44.0, 28.9, 21.5, 19.6, 11.2 ppm. MS (ESI) (*m/z*): 384.9 [M + H]⁺.

Synthesis of 1-(7-carboxyheptyl)-2,3,3-trimethyl-3*H*-indol-1-ium-5-sulfonate (**34a**)⁴⁰

A slurry of **31** (3 g, 10.8 mmol) and 8-bromooctanoic acid (3 g, 13.6 mmol) in *o*-dichlorobenzene (10 ml) was refluxed for 12 h and cooled to rt. Subsequently, the liquid phase was decanted. The residue was recrystallized with 2-propanol (10 ml), filtered under reduced pressure, washed with 2-propanol and dried at 70°C. The resulting material was purified by column chromatography (CH₂Cl₂ / MeOH - 3 : 1 + 2% AcOH) to provide **34a** as a pink solid (2.35 g, 57%). ¹H NMR (600 MHz, DMSO-*d*₆) δ: 7.57-7.29 (m, 2H, C^H_{arom}-H_{arom}), 6.54 (d, *J* = 8.1 Hz, 1H, C^H_{arom}-H_{arom}), 3.88 (dd, *J* = 24.4, 1.9 Hz, 2H, NCH₂), 3.49 (t, *J* = 7.2 Hz, 2H, CH₂COOH), 2.49 (p, *J* = 1.8 Hz, 3H, CH₃), 2.15 (t, *J* = 7.3 Hz, 2H, CH₂), 1.45 (m, 2H, CH₂), 1.31-1.18 (m, 12H, CH₂ and CH₃ groups) ppm. ¹³C NMR (151 MHz, DMSO-*d*₆) δ: 174.8, 160.7, 145.9, 138.8, 136.1, 125.7, 119.7, 104.0, 74.6, 48.8, 43.7, 33.9, 29.9, 28.7, 28.7, 26.4, 25.6, 24.6 ppm. MS (ESI) (*m/z*): 381.9 [M + H]⁺.

Synthesis of 1-(7-carboxyheptyl)-2-((*E*)-3-((*E*)-3,3-dimethyl-1-propyl-5-sulfoindolin-2-ylidene)prop-1-en-1-yl)-3,3-dimethyl-3*H*-indol-1-ium-5-sulfonate (**35a**)⁴⁰

A stirred solution of **34a** (500 mg, 1.3 mmol) and **31** (500 mg, 1.1 mmol) in pyridine / acetic anhydride 1 : 1 (3 ml) was refluxed for 2 h and stirred at rt overnight. The product was precipitated with diethyl ether (30 ml), filtered under reduced pressure and dried at 70°C. The residue was purified by column (CH₂Cl₂ - 3 : 1 + 2% AcOH) several times and at last with RP-gel chromatography (water : acetonitrile 3 : 1) to yield a pink solid (300 mg, 34 %). ¹H NMR (600 MHz, D₂O) δ: 8.42 (t, *J* = 13.4 Hz, 1H, =CH), 7.88-7.84 (m, 2H, C^H_{arom}-H_{arom}), 7.81 (dd, *J* = 8.3, 1.7 Hz, 2H, C^H_{arom}-H_{arom}), 7.31 (t, *J* = 8.2 Hz, 2H, C^H_{arom}-H_{arom}), 6.33 (dd, *J* = 13.4, 7.7 Hz, 2H, =CH), 4.05- 3.96 (m, 4H, NCH₂), 2.12 (t, *J* = 7.5 Hz, 2H, CH₂COOH), 1.78-1.69 (m, 4H), 1.65 (d, *J* = 7.6 Hz, 12H), 1.48 (t, *J* = 7.5 Hz, 2H), 1.30 (td, *J* = 16.0, 7.8 Hz, 4H), 1.23 (q, *J* = 7.3 Hz, 2H), 0.91 (t, *J* = 7.4 Hz, 3H, CH₃) ppm. ¹³C NMR (151 MHz, D₂O) δ: 178.6, 154.5, 147.0, 146.9, 144.2, 142.37, 142.34, 129.53, 129.50, 122.6, 114.35, 114. 45, 106.2, 106.3,

52.1, 48.5, 47.1, 31.4, 31.01, 29.85, 28.95, 29.6, 28.7, 28.6, 13.4 ppm. MS (ESI) (m/z): 673.4 [M + H]⁺.

Synthesis of 1-(2-(2-(2-(carboxymethoxy)ethoxy)ethoxy)ethyl)-2,3,3-trimethyl-3*H*-indol-1-ium-5-sulfonate (**34b**)

A solution of **31** (100 mg, 0.36 mmol) and **14** (156 mg, 0.43 mmol) in sulfolane was stirred under argon atmosphere at 130 °C for 16 h. Subsequently, the solution is cooled down to rt and treated with ethyl acetate. The precipitated product was filtered under reduced pressure and dried at 70 °C. The crude product was converted to **35b** without further purification. MS (ESI) (m/z): 430.1 [M + H]⁺.

Synthesis of 1-(2-(2-(2-(carboxymethoxy)ethoxy)ethoxy)ethyl)-2-((*E*)-3-((*E*)-3,3-dimethyl-1-propyl-5-sulfoindolin-2-ylidene)prop-1-en-1-yl)-3,3-dimethyl-3*H*-indol-1-ium-5-sulfonate (**35b**)⁴⁰

A solution of **33** (138 mg, 0.36 mmol) and crude **34b** (~ 0.36 mmol) in pyridine / Ac₂O is stirred at 110 °C for 4 h. Subsequently, the solution is cooled down to rt and treated with ethyl acetate. The precipitated product is filtered under reduced pressure and dried at 70 °C. The crude product was purified by RP-column chromatography (water : acetonitrile - 7 : 3) and was obtained as 73 mg (28%) of a pink solid. ¹H NMR (500 MHz, DMSO-*d*₆) δ: 8.36 (t, *J* = 7.8 Hz, 1H, =CH), 7.79 (dd, *J* = 8.7, 1.6 Hz, 2H, C^H_{arom}-H_{arom}), 7.67 (dt, *J* = 8.2, 1.8 Hz, 2H, C^H_{arom}-H_{arom}), 7.54-7.48 (m, 1H, C^H_{arom}-H_{arom}), 7.44-7.36 (m, 1H, C^H_{arom}-H_{arom}), 6.63-6.52 (m, 2H, =CH), 4.33 (s, 2H, OCH₂COOH), 4.11 (t, *J* = 7.7 Hz, 2H, NCH₂), 3.88-3.76 (m, 2H, CH₂O), 3.63-3.56 (m, 4H, CH₂O), 3.48-3.41 (m, 4H, CH₂O), 1.74 1.80-1.73 (m, 2H, CH₂CH₃), 1.73-1.64 (m, 12H, CH₃), 0.97 (t, *J* = 7.2 Hz, 3H, CH₂CH₃) ppm. ¹³C NMR (151 MHz, DMSO-*d*₆) δ: 176.1, 150.1, 146.2, 146.1, 145.9, 145.5, 142.4, 142.1, 127.8, 126.6, 119.9, 111.3, 111.0, 110.8, 103.8, 103.3, 78.9, 70.0, 70.0, 69.9, 69.8, 69.7, 69.4, 69.2, 68.8, 60.5, 50.3, 50.1, 49.2, 49.1, 47.1, 27.65, 27.1, 21.1, 11.2, 11.0 ppm. MS (ESI) (m/z): 721.4 [M + H]⁺.

Synthesis of 1-(2-(2-(2-(2-azidoethoxy)ethoxy)ethoxy)ethyl)-2,3,3-trimethyl-3*H*-indol-1-ium-5-sulfonate (**34c**)

A mixture of **31** (100 mg, 0.36 mmol) and **15** (161 mg, 0.43 mmol) in sulfolane (1 ml) was stirred under argon atmosphere at 130 °C for 16 h. Subsequently, the solution is cooled down to rt and treated with ethyl acetate. The precipitated product is filtered under reduced pressure and dried at 70 °C. The crude product was converted to **35c** without further purification. MS (ESI) (m/z): 441.1 [M + H]⁺.

Synthesis of 1-(2-(2-(2-(2-azidoethoxy)ethoxy)ethoxy)ethyl)-2-((E)-3-((E)-3,3-dimethyl-1-propyl-5-sulfoindolin-2-ylidene)prop-1-en-1-yl)-3,3-dimethyl-3*H*-indol-1-ium-5-sulfonate (35c)⁴⁰

A solution of **33** (138 mg, 0.36 mmol) and crude **34c** (~ 0.36 mmol) in pyridine / Ac₂O (1 : 1, 3 ml) is stirred at 110 °C for 4 h. Subsequently, the solution is cooled down to rt and treated with ethyl acetate. The precipitated product is filtered under reduced pressure and dried at 70 °C. The crude product was purified by RP-column chromatography (water : acetonitrile - 7 : 3). The product was obtained as 35 mg (13%) of a pink solid. ¹H NMR (600 MHz, DMSO-*d*₆) δ: 8.62 (t, *J* = 7.8 Hz, 1H, =CH), 7.84-7.76 (m, 2H, C^H_{arom}-H_{arom}), 7.71-7.57 (m, 2H, C^H_{arom}-H_{arom}), 7.42 (dd, *J* = 8.4, 3.2 Hz, 1H, C^H_{arom}-H_{arom}), 7.37 (d, *J* = 8.3 Hz, 1H, C^H_{arom}-H_{arom}), 6.60-6.48 (m, 2H, =CH), 4.79 (d, *J* = 4.9 Hz, 2H, NCH₂), 4.33 (t, *J* = 5.5 Hz, 2H, NCH₂), 4.09 (t, *J* = 7.3 Hz, 2H, CH₂N₃), 3.93-3.88 (m, 2H, OCH₂CH₂O), 3.81 (t, *J* = 5.4 Hz, 2H, OCH₂CH₂O), 3.58-3.55 (m, 2H, OCH₂CH₂O), 3.48-3.38 (m, 2H, OCH₂CH₂O), 3.39-3.35 (m, 2H, OCH₂CH₂O), 3.34-3.30 (m, 2H, OCH₂CH₂O), 1.82-1.72 (m, 2H, CH₂CH₃), 1.70 (s, 12H, CH₃), 0.97 (t, *J* = 7.3 Hz, 3H, CH₃) ppm. ¹³C NMR (151 MHz, DMSO-*d*₆) δ: 175.1, 150.0, 146.0, 146.0, 145.9, 145.4, 142.3, 142.1, 127.9, 126.4, 120.0, 111.3, 111.0, 110.9, 103.7, 103.3, 70.5, 70.02, 70.01, 69.9, 69.8, 69.7, 69.4, 69.3, 68.8, 60.5, 50.2, 50.1, 49.2, 49.1, 49.1, 27.6, 27.6, 20.6, 11.1, 11.1 ppm. MS (ESI) (*m/z*): 732.7 [M + H]⁺.

Synthesis of 2,3,3-trimethyl-1-(3,6,9,12-tetraoxapentadec-14-yn-1-yl)-3*H*-indol-1-ium-5-sulfonate (34d)

A mixture of **31** (200 mg, 0.72 mmol) and **17** (335 mg, 0.87 mmol) in sulfolane (1 ml) was stirred under argon atmosphere at 130 °C for 16 h. Subsequently, the solution was cooled down to rt and treated with ethyl acetate. The precipitated product was filtered under reduced pressure and dried at 70°C. The crude product was 150 mg (46%) of a red solid. The crude product was directly converted to **35d** without further purification. MS (ESI) (*m/z*): 454.4 [M + H]⁺.

Synthesis of 3,6,9,12-tetraoxapentadec-14-yn-1-yl)-2-((E)-3-((E)-3,3-dimethyl-1-propyl-5-sulfoindolin-2-ylidene)prop-1-en-1-yl)-3,3-dimethyl-3*H*-indol-1-ium-5-sulfonate (35d)⁴⁰

A solution of **33** (127 mg, 0.33 mmol) and crude **34d** (150 mg, 0.33 mmol) in pyridine / Ac₂O was stirred at 110 °C for 4h. Subsequently, the solution was cooled down to rt and treated with ethyl acetate. The precipitated product was filtered under reduced pressure and dried at 70 °C. The crude product was purified by RP-column chromatography (water : acetonitrile - 7 : 3). The product was obtained as 67 mg (27%) of a pink solid. ¹H NMR (600 MHz, DMSO-*d*₆) δ: 8.69 (t, *J* = 7.5 Hz, 1H, =CH), 7.89-7.73 (m, 2H, C^H_{arom}-H_{arom}), 7.65-7.51 (m, 2H,

$\text{C}^{\text{H}_{\text{arom}}-\text{H}_{\text{arom}}}$), 7.42 (dd, $J = 8.4, 3.0$ Hz, 1H, $\text{C}^{\text{H}_{\text{arom}}-\text{H}_{\text{arom}}}$), 7.34 (d, $J = 8.1$ Hz, 1H, $\text{C}^{\text{H}_{\text{arom}}-\text{H}_{\text{arom}}}$), 6.69-6.52 (m, 2H, =CH), 4.74 (d, $J = 4.5$ Hz, 2H, NCH₂), 4.31 (t, $J = 5.4$ Hz, 2H, NCH₂), 4.11 (d, $J = 2.4$ Hz, 2H, CH₂C≡CH), 3.93-3.88 (m, 2H, OCH₂CH₂O), 3.81 (t, $J = 5.4$ Hz, 2H, OCH₂CH₂O), 3.58-3.55 (m, 4H, OCH₂CH₂O), 3.48-3.38 (m, 2H, OCH₂CH₂O), 3.39-3.35 (m, 2H, OCH₂CH₂O), 3.34-3.30 (m, 2H, OCH₂CH₂O), 3.25 (t, $J = 2.4$ Hz, 1H, C≡CH), 1.84-1.75 (m, 2H, CH₂CH₃), 1.74 (s, 12H, CH₃), 0.97 (t, $J = 7.3$ Hz, 3H, CH₃) ppm. ¹³C NMR (151 MHz, DMSO-*d*₆) δ: 175.4, 150.2, 146.2, 146.1, 145.7, 145.4, 143.0, 142.3, 128.1, 126.5, 120.2, 111.2, 111.0, 110.8, 103.8, 103.3, 77.0, 70.5, 70.1, 70.0, 69.9, 69.8, 69.7, 69.4, 69.2, 68.9, 59.5, 50.2, 50.1, 49.2, 49.15, 49.11, 27.3, 27.1, 20.6, 11.1, 11.0 ppm. MS (ESI) (*m/z*): 745.5 [M + H]⁺.

Synthesis of 2-((*E*)-3-((*E*)-3,3-dimethyl-1-propyl-5-sulfoindolin-2-ylidene)prop-1-en-1-yl)-1-(8-(4-((4-(2,6-dioxo-1-propyl-2,3,6,7-tetrahydro-1*H*-purin-8-yl)phenyl)sulfonyl)piperazin-1-yl)-8-oxooctyl)-3,3-dimethyl-3*H*-indol-1-ium-5-sulfonate (36)

A stirred solution of **12** (30 mg, 0.072 mmol), **35a** (63 mg, 0.094 mmol) and TEA (25 μl, 0.18 mmol) in DMF (3 ml), was treated with HBTU (36 mg, 0.094 mmol). The solution was stirred for 16 h at rt and then precipitated by diethyl ether (20 ml). The crude product was filtered under reduced pressure, washed with a small amount of diethyl ether and subsequently purified two times by normal column chromatography (CH₂Cl₂ / MeOH, 9 : 1 to 1 : 1) leading to a deep pink solid. To provide enough of the precious product, the procedure was performed two times and the products were combined, affording 26 mg (34%) of a pink solid. ¹H NMR (500 MHz, DMSO-*d*₆) δ: 14.01 (s, 1H, NH), 11.93 (s, 1H, NH), 8.37-8.27 (m, 3H, $\text{C}^{\text{H}_{\text{arom}}-\text{H}_{\text{arom}}}$ / =CH), 7.87-7.82 (m, 2H, $\text{C}^{\text{H}_{\text{arom}}-\text{H}_{\text{arom}}}$), 7.79 (dd, $J = 5.4, 1.6$ Hz, 2H, $\text{C}^{\text{H}_{\text{arom}}-\text{H}_{\text{arom}}}$), 7.66 (dt, $J = 8.3, 6.7, 1.6$ Hz, 2H, $\text{C}^{\text{H}_{\text{arom}}-\text{H}_{\text{arom}}}$), 7.40 (d, $J = 8.3$ Hz, 1H, $\text{C}^{\text{H}_{\text{arom}}-\text{H}_{\text{arom}}}$), 7.35 (d, $J = 8.3$ Hz, 1H, $\text{C}^{\text{H}_{\text{arom}}-\text{H}_{\text{arom}}}$), 6.53-6.41 (m, 2H, =CH), 4.08 (td, $J = 8.3, 7.7, 3.9$ Hz, 4H, NCH₂), 3.84-3.76 (m, 2H, NCH₂), 3.50 (s, 4H, NCH₂ (piperazine)), 2.97-2.84 (m, 4H, NCH₂ (piperazine)), 2.20 (t, $J = 7.4$ Hz, 2H, CH₂COOH), 1.76 (q, $J = 7.4$ Hz, 2H, CH₂), 1.68 (d, $J = 7.0$ Hz, 10H, CH₂), 1.61-1.51 (m, 2H, CH₂), 1.44-1.12 (m, 12H, CH₃), 0.95 (t, $J = 7.4$ Hz, 3H, CH₃), 0.87 (td, $J = 7.4, 2.5$ Hz, 3H, CH₃) ppm. ¹³C NMR (126 MHz, DMSO-*d*₆) δ: 174.5, 174.3, 170.8, 155.3, 151.1, 150.0, 148.3, 147.8, 146.0, 142.1, 141.9, 140.2, 135.5, 128.4, 127.0, 126.4, 120.0, 110.9, 110.8, 103.2, 103.0, 49.1, 46.2, 45.9, 45.4, 44.3, 44.1, 41.6, 32.1, 31.4, 29.1, 28.7, 27.6, 27.5, 27.1, 22.2, 21.0, 20.5, 11.3, 11.1, 9.3 ppm. HPLC-UV (254 nm) ESI-MS, purity: 92%. MS (ESI) (*m/z*): 1074.3 [M + H]⁺. HRMS (ESI-TOF) *m/z*: [M - H]⁻ calcd. for C₅₂H₆₃N₈O₁₁S₃ 1071.3773, found 1071.3778. λ_{max} abs: 554 nm λ_{max} em: 563 nm.

Synthesis of 2-((*E*)-3-((*E*)-3,3-dimethyl-1-propyl-5-sulfoindolin-2-ylidene)prop-1-en-1-yl)-1-(2-(2-(2-(2-(4-((4-(2,6-dioxo-1-propyl-2,3,6,7-tetrahydro-1*H*-purin-8-yl)phenyl)sulfonyl)piperazin-1-yl)-8-oxooctyl)-3,3-dimethyl-3*H*-indol-1-ium-5-sulfonate (36)

piperazin-1-yl)-2-oxoethoxy)ethoxy)ethyl)-3,3-dimethyl-3*H*-indol-1-ium-5-sulfonate (37)

To a stirred solution of **12** (30 mg, 0.072 mmol), **35b** (0,072 mg, 0.072 mmol) and TEA (31µl, 0.18 mmol) in DMF (2 ml), HBTU (36 mg, 0.094 mmol, 1.3 eq.) was added. The solution was stirred at rt for 2 h and subsequently hydrolyzed with water (10 ml). The product was directly purified via RP column Chromatography (water / acetonitrile - 7 : 3) yielding 4,5 mg (6%) of a pink solid. ¹H NMR (600 MHz, DMSO-*d*₆) δ: 10.92 (s, 1H, NH), 8.32 (t, *J* = 13.4 Hz, 1H, =CH), 8.21 (d, *J* = 8.1 Hz, 2H, C^H_{arom.}-H_{arom.}), 7.78 (d, *J* = 12.8 Hz, 2H, C^H_{arom.}-H_{arom.}), 7.65 (dd, *J* = 14.6, 8.2 Hz, 2H, C^H_{arom.}-H_{arom.}), 7.60 (d, *J* = 8.1 Hz, 2H, C^H_{arom.}-H_{arom.}), 7.40 (d, *J* = 8.1 Hz, 1H, C^H_{arom.}-H_{arom.}), 7.34 (d, *J* = 8.6 Hz, 1H, C^H_{arom.}-H_{arom.}), 6.53 (d, *J* = 13.3 Hz, 1H, CH=), 6.48 (d, *J* = 13.3 Hz, 1H, CH=), 4.33-4.25 (m, 2H, NCH₂), 4.13-4.04 (m, 2H, NCH₂), 4.05-3.93 (m, 4H, CH₂O/ OCH₂C=O), 3.75 (dd, *J* = 10.2, 6.0 Hz, 4H, CH₂O), 3.34-3.26 (m, 4H, NCH₂ (piperazine)), 2.87 (s, 4H, NCH₂ (piperazine)), 1.67 (d, *J* = 3.3 Hz, 12H, CH₃), 1.51 (q, *J* = 7.5 Hz, 2H, CH₂CH₃), 1.16 (t, *J* = 7.1 Hz, 2H, CH₂CH₃), 0.92 (t, *J* = 7.2 Hz, 3H, CH₂CH₃), 0.83 (t, *J* = 7.5 Hz, 3H, CH₂CH₃) ppm. ¹³C NMR (151 MHz, DMSO-*d*₆) δ: 175.0, 174.6, 167.5, 155.1, 151.1, 150.0, 148.1, 147.7, 142.3, 140.0, 135.9, 133.3, 128.7, 128.5, 127.3, 127.2, 126.4, 126.3, 119.8, 111.3, 111.0, 108.8, 103.6, 103.3, 70.6, 69.9, 69.9, 69.8, 69.7, 69.7, 69.2, 68.7, 67.4, 60.4, 57.7, 49.1, 49.1, 46.0, 45.9, 45.4, 44.5, 43.8, 43.0, 42.5, 41.7, 27.7, 27.6, 27.6, 24.3, 24.3, 21.0, 20.6, 11.4, 11.1, 8.8 ppm. HPLC-UV (254 nm) ESI-MS, purity: 95%. MS (ESI) (*m/z*): 1121.3 [M + H]⁺. HRMS (ESI-TOF) *m/z*: [M + H]⁺ calcd. for C₅₂H₆₄N₈O₁₄S₃ 1121.3777, found 1121.3778.

Synthesis of 2-((*E*)-3-((*E*)-3,3-dimethyl-1-propyl-5-sulfoindolin-2-ylidene)prop-1-en-1-yl)-1-(23-(3-(4-((4-(2,6-dioxo-1-propyl-2,3,6,7-tetrahydro-1*H*-purin-8-yl)phenyl)sulfonyl)piperazine-1-carbonyl)phenoxy)-11-oxo-3,6,9,15,18,21-hexaoxa-12-azatricosyl)-3,3-dimethyl-3*H*-indol-1-ium-5-sulfonate (38)

To a stirred solution of **29** (60 mg, 0.08 mmol), **35b** (84 mg, 0.9 mmol) and TEA (30 µl, 0.2 mmol) in DMF (3 ml), HBTU (41 mg, 0.11 mmol) was added. The solution was stirred at rt for 2 h and then directly given on a RP column (water / acetonitrile - 3 : 1) to purify the crude product. The product was obtained as 5 mg (5%) of a pink solid. ¹H NMR (500 MHz, DMSO-*d*₆) δ: 8.35 (t, *J* = 13.4 Hz, 1H, =CH), 8.20-8.16 (m, 2H, C^H_{arom.}-H_{arom.}), 7.78 (dd, *J* = 7.5, 1.6 Hz, 2H, C^H_{arom.}-H_{arom.}), 7.66 (ddd, *J* = 8.5, 7.0, 1.6 Hz, 2H, C^H_{arom.}-H_{arom.}), 7.63-7.60 (m, 2H, C^H_{arom.}-H_{arom.}), 7.41 (d, *J* = 8.3 Hz, 1H, C^H_{arom.}-H_{arom.}), 7.36 (d, *J* = 8.4 Hz, 1H, C^H_{arom.}-H_{arom.}), 7.29-7.24 (m, 1H, C^H_{arom.}-H_{arom.}), 6.98-6.94 (m, 1H, C^H_{arom.}-H_{arom.}), 6.87-6.83 (m, 2H, C^H_{arom.}-H_{arom.}), 6.51 (dd, *J* = 25.7, 13.5 Hz, 2H, =CH), 5.38 (s, 1H, NHCO), 4.31 (t, *J* = 5.4 Hz, 2H, PhOCH₂), 4.08 (t, *J* = 7.5 Hz, 2H, CH₂O), 4.04 (dd, *J* = 5.6, 3.6 Hz, 2H, CH₂O), 3.84-3.75 (m, 8H, CH₂O/ NCH₂), 3.70-3.65 (m, 2H), 3.54-3.50 (m, 4H, NCH₂ (piperazine)), 2.96 (s, 4H, NCH₂

(piperazine), 1.79-1.71 (m, 2H, NCH₂), 1.69 (d, *J* = 1.9 Hz, 12H, CH₃), 1.57 - 1.47 (m, 2H, CH₂CH₃), 1.24-1.20 (m, 2H, CH₂CH₃), 0.95 (t, *J* = 7.4 Hz, 3H, CH₂CH₃), 0.87-0.79 (m, 3H, CH₂CH₃) ppm. CH₂O underneath water peak ¹³C NMR (126 MHz, DMSO-*d*₆) δ: 175.1, 174.7, 174.6, 169.4, 169.1, 158.5, 150.1, 146.0, 145.8, 142.4, 142.1, 140.3, 140.0, 136.9, 129.8, 127.7, 126.4, 125.5, 120.0, 119.9, 119.2, 116.1, 112.9, 111.3, 111.0, 103.6, 70.5, 70.3, 70.1, 69.9, 69.9, 69.8, 69.7, 69.0, 67.5, 67.4, 49.2, 49.1, 38.2, 21.4, 20.6, 11.5, 11.1 ppm. HPLC-UV (254 nm) ESI-MS, purity: 95 %. MS (ESI) (*m/z*): 1416.4 [M + H]⁺. HRMS (ESI-TOF) *m/z*: [M + H]⁺ calcd. for C₆₇H₈₅N₉O₁₉S₃, 1416.5197, found 1416.5236.

Synthesis of 2-((*E*)-3-((*E*)-3,3-dimethyl-1-propyl-5-sulfoindolin-2-ylidene)prop-1-en-1-yl)-1-(2-(2-(2-(2-(4-(4-(4-((4-(2,6-dioxo-1-propyl-2,3,6,7-tetrahydro-1*H*-purin-8-yl)phenyl)sulfonyl)piperazine-1-carbonyl)phenyl)-1*H*-1,2,3-triazol-1-yl)ethoxy)ethoxy)ethoxy)ethyl)-3,3-dimethyl-3*H*-indol-1-ium-5-sulfonate (39)

A mixture of **26** (13 mg, 0.024 mmol), **35c** (22 mg, 0.024 mmol), TEA (0.24 mg, 0.024 mmol) and CuI (0.23 mg, 0.001 mmol) was stirred in DMF (1 ml) for 16 h at rt. The crude product was precipitated by addition of ethyl acetate (20 ml) and subsequently purified by RP column chromatography (water / acetonitrile 7 : 3 + 1% TFA) twice, yielding 5 mg (16%) of a pink solid. ¹H NMR (600 MHz, DMSO-*d*₆) δ: 14.05 (s, 1H, NH), 11.97 (s, 1H, NH), 8.58 (s, 1H, triazol), 8.34 (d, *J* = 8.6 Hz, 3H, =CH), 7.85 (dd, *J* = 17.0, 8.0 Hz, 4H, C^{H_{arom}}-H_{arom.}), 7.79 (d, *J* = 8.3 Hz, 2H, C^{H_{arom}}-H_{arom.}), 7.66 (t, *J* = 7.7 Hz, 2H, C^{H_{arom}}-H_{arom.}), 7.41 (d, *J* = 7.9 Hz, 3H, C^{H_{arom}}-H_{arom.}), 7.34 (d, *J* = 8.3 Hz, 1H, C^{H_{arom}}-H_{arom.}), 6.50 (dd, *J* = 25.6, 13.4 Hz, 2H, =CH), 4.56-4.47 (m, 2H, CH₂), 4.32-4.19 (m, 2H, NCH₂), 4.06 (t, *J* = 7.4 Hz, 2H, NCH₂), 3.87-3.68 (m, 8H CH₂O), 3.44 (m, 4H, NCH₂ (piperazine)), 3.08 (m, 4H, NCH₂ (piperazine)), 1.66 (d, *J* = 8.9 Hz, 12H, CH₃), 1.57 (q, *J* = 7.4 Hz, 2H, CH₂CH₃), 1.17 (t, *J* = 7.3 Hz, 2H, CH₂CH₃), 0.94 (t, *J* = 7.3 Hz, 3H, CH₂CH₃), 0.87 (t, *J* = 7.5 Hz, 3H, CH₂CH₃) ppm. CH₂O underneath water peak. ¹³C NMR (151 MHz, DMSO-*d*₆) δ: 175.3, 174.9, 169.4, 158.5, 158.3, 142.7, 142.4, 140.6, 136.4, 134.8, 133.5, 132.6, 128.7, 128.4, 127.5, 126.7, 126.5, 125.4, 122.8, 120.3, 120.1, 111.7, 108.9, 103.9, 103.6, 70.8, 70.2, 70.1, 68.9, 67.6, 50.1, 49.4, 49.4, 46.2, 45.6, 44.8, 41.9, 34.8, 27.92, 27.91, 21.3, 20.8, 11.66, 11.4, 9.0 ppm. HPLC-UV (254 nm) ESI-MS, purity: 95 %. MS (ESI) (*m/z*): 1279.4 [M + H]⁺. HRMS (ESI-TOF) *m/z*: [M + H]⁺ calcd. for C₆₁H₇₁N₁₁O₁₄S₃ 1279.4446, found 1279.4451. λ_{max} abs: 556 nm λ_{max} em: 571 nm

Synthesis of 2-((*E*)-3-((*E*)-3,3-dimethyl-1-propyl-5-sulfoindolin-2-ylidene)prop-1-en-1-yl)-1-(1-(1-(4-(4-((4-(2,6-dioxo-1-propyl-2,3,6,7-tetrahydro-1*H*-purin-8-yl)phenyl)sulfonyl)piperazine-1-carbonyl)phenyl)-1*H*-1,2,3-triazol-4-yl)-2,5,8,11-tetraoxatridecan-13-yl)-3,3-dimethyl-3*H*-indol-1-ium-5-sulfonate (40)

A solution of **25** (23 mg, 0.04 mmol), **35d** (30 mg, 0.04 mmol) TEA (0.4 mg, 0.04 mmol) and CuI (0.46 mg, 0.002 mmol) was stirred in DMF (1 ml) for 16 h at rt. The crude product was

precipitated by addition of ethyl acetate (20 ml) and subsequently purified by RP column chromatography (water / acetonitrile - 7 : 3) twice to yield 3 mg (6%) of a pink solid. ¹H NMR (600 MHz, DMSO-*d*₆) δ 14.05 (s, 1H, NH), 11.96 (s, 1H, NH), 8.83 (s, 1H, triazole), 8.34 (d, *J* = 8.3 Hz, 4H, C^H_{arom.}-H_{arom.}), 7.92 (d, *J* = 8.4 Hz, 1H, CH=), 7.90-7.84 (m, 3H, C^H_{arom.}-H_{arom.}), 7.79 (dd, *J* = 9.1, 1.7 Hz, 2H, C^H_{arom.}-H_{arom.}), 7.65 (ddd, *J* = 7.5, 5.5, 1.7 Hz, 2H, C^H_{arom.}-H_{arom.}), 7.56 (dd, *J* = 8.3, 2.2 Hz, 2H, C^H_{arom.}-H_{arom.}), 7.45-7.34 (m, 2H, C^H_{arom.}-H_{arom.}), 6.53 (d, *J* = 13.3 Hz, 1H, CH=), 6.48 (d, *J* = 13.4 Hz, 1H, CH=), 4.56 (s, 2H, CH₂triazol), 4.31 (q, *J* = 5.7 Hz, 2H, NH₂), 4.07 (t, *J* = 7.6 Hz, 2H, CH₂O), 3.85-3.77 (m, 6H, CH₂O), 3.60-3.53 (m, 2H, CH₂O), 3.49 (ddd, *J* = 11.4, 4.9, 2.7 Hz, 4H, CH₂O), 3.43-3.40 (m, 2H, CH₂O), 3.39 (s, 4H, NCH₂ (piperazine)), 3.05 (s, 4H, NCH₂ (piperazine)), 1.75 (q, *J* = 7.4 Hz, 2H, NCH₂), 1.72-1.64 (m, 12H, CH₃), 1.58 (h, *J* = 7.4 Hz, 4H, CH₂CH₃), 0.95 (t, *J* = 7.4 Hz, 3H, CH₂CH₃), 0.88 (t, *J* = 7.4 Hz, 3H, CH₂CH₃) ppm. ¹³C NMR (151 MHz, DMSO-*d*₆) δ: 175.1, 174.5, 168.3, 155.1, 151.1, 150.0, 147.8, 146.1, 146.0, 145.4, 142.3, 142.0, 140.2, 140.0, 137.4, 136.1, 135.4, 129.0, 128.4, 127.2, 126.2, 122.4, 120.0, 119.9, 111.2, 110.9, 103.6, 103.2, 70.5, 70.0, 70.0, 69.9, 69.8, 69.3, 67.3, 63.5, 49.1, 49.1, 41.7, 34.6, 27.6, 27.6, 21.0, 20.5, 11.4, 11.1 ppm. HPLC-UV (254 nm) ESI-MS, purity: 95%. MS (ESI) (*m/z*): 1308.3 [M + H]⁺. HRMS (ESI-TOF) *m/z*: [M + H]⁺ calcd. for C₆₂H₇₃N₁₁O₁₅S₃ 1308.4523, found 1308.4550. λ_{max} abs: 557 nm λ_{max} em: 572 nm.

4.2.6.4. Biological assays

4.2.6.4.1. Membrane preparations

Membrane preparations of recombinant CHO or HEK cells stably expressing human ARs were performed as previously described^{23;33;38;62-65} or human membranes from ARs were purchased from PerkinElmer (Solingen, Germany).

4.2.6.4.2. Radioligand binding studies

Radioligand binding assays were performed as previously described.^{23;33;62-65} DMSO was used to prepare stock solutions of the tested compounds, 1% was the final concentration of the compounds in the assays. The following radioligands (with their respective concentration, specific activities and incubation times at rt) were used for binding studies at the human A₁-, A_{2A}-, A_{2B}- and A₃AR: [³H]2-Chloro-*N*6-cyclo-pentyladenosine ([³H]CCPA, A₁) (1 nM, 58 Ci/mmol, 90 min), [³H](*E*)-3-(3-hydroxypropyl)-8-(2-(*m*-methoxyphenyl)vinyl)-7-methyl-1-prop-2-ynyl-3,7-dihydropurine-2,6-dione ([³H]MSX-2, A_{2A}) (1 nM, 85 Ci/mmol, 30 min), [³H]8-(4-(4-(4-chlorophenyl)piperazine-1-sulfonyl)phenyl)-1-propyl-3,7-dihydropurine-2,6-dione ([³H]PSB-603, A_{2B}) (0.3 nM, 79 Ci/mmol, 75 min), and [³H]2-phenyl-8-ethyl-4-methyl-(8*R*)-4,5,7,8-tetrahydro-1*H*-imidazo[2.1-*j*]purin-5-one ([³H]PSB-11, A₃) (1 nM, 28 Ci/mmol, 45 min), respectively. To remove endogenous adenosine, the membrane preparations were preincubated for 10 - 15 min with 2 μl/ml adenosine deaminase (ADA). For the A₁-, A_{2A}- and

A₃AR the assays were performed in a mixture of 200 µl of 50 mM TRIS buffer (pH 7.4), 4 µl of the respective test compound in DMSO, 100 µl of membrane preparation, and 100 µl of the corresponding radioligand, resulting in a total volume of 404 µl. The assays for the A_{2B}AR were performed in a mixture of 790 µl of the 50 mM TRIS buffer (pH 7.4), 10 µl of the test compound in DMSO, 100 µl of membrane preparation, and 100 µl of the radioligand, resulting in a total volume of 1000 µl. Nonspecific binding was investigated employing the following substances: 2-Chloroadenosine (CADO) (10 µM) for the A₁AR, 9-chloro-2-(2-furyl)[1,2,4]triazolo[1,5-c]quinazolin-5-amine (CGS15943) (10 µM) for the A_{2A}AR, DPCPX (10 µM) for the A_{2B}AR, and (*R*)-N⁶-phenylisopropyladenosine (R-PIA) (100 µM) for the A₃AR. Filtration through Whatman GF/B glass fiber filters using a Brandel harvester (Brandel) determined the incubation. For the A₁-, A_{2A}-, and A₃AR assays, the filters were rinsed four times (3 - 4 ml each) with cold 50 mM Tris-HCl buffer (pH 7.4). For the A_{2B}AR assay, the 50 mM Tris-HCl buffer (pH 7.4) additionally contained 0.1 % bovine serum albumin (BSA) to reduce non-specific binding. Subsequently, the filters were transferred to scintillation vials followed by incubation for 9 h with 2.5 ml of scintillation cocktail (Triskem). Subsequent counting was performed in a liquid scintillation counter (Tricarb 2810TR, counting efficiency ~ 53%). Each assay was performed in three independent experiments.

K_i values were calculated using the following equation:

$$K_i = \frac{IC_{50}}{1 + \frac{L}{K_d}}$$

IC₅₀ represents the average inhibitory concentration of the test substance while L is the concentration of the radioligand and K_d is the affinity of the radioligand to the receptor.

4.2.6.4.3. Confocal Imaging

Confocal microscopy was performed as described in Köse et al.²³ CHO cells stably expressing human recombinant A_{2B}ARs were seeded at 5×10^4 [d1]cells in 6-well plates (Sarstedt) and were grown over night on sterile coverslips to approximately 80% confluency before imaging. For negative control, CHO-K1 wildtype cells were seeded and grown under the same conditions. Cells were washed three times with phosphate buffered saline (PBS) + 1% bovine serum albumin -(BSA) and fixed for 20 min at -20 °C with 50 : 50 methanol acetone solution. Then cells were washed twice with PBS and stained with DAPI (1 : 10,000) for 5 min in the dark. The cells were subsequently washed twice with PSB + 1% BSA and incubated for 60 min on ice with 100 µl of PSB-20077 (200 nM) or PSB-20104 (200 nM), respectively. The cyanine-labeled A_{2B}AR antagonists had been dissolved in DMSO and diluted in OptimMEM medium.

The same procedure was performed with addition of 10 μ M DPCPX for incubation. Then, the cells were washed twice with PBS and mounted using Fluoromount™ aqueous mounting medium (Sigma-Aldrich) and stored in the dark at 4°C. A Nikon A1 spectral confocal microscope operating with an argon laser and the NIS Element Advanced Research software 4.0 were used for image acquisition and analysis. A 543 nm laser [d2] was used for the excitation of **39** and **40** and the emission (552-617 nm) was detected using a bandpass filter of 550/20 nm (Nikon). [PP3] Corresponding images were taken using identical settings (laser power, detector offset, and gain). The experiment was repeated twice or thrice and at least ten squares (60x objective) were imaged for each sample. Representative images are shown.

4.2.7. References

- (1) Fredholm, B. B.; IJzerman, A. P.; Jacobson, K. A.; Linden, J.; Müller, C. E. International union of basic and clinical pharmacology. LXXXI. Nomenclature and classification of adenosine receptors - an update. *Pharmacol. Rev.* **2011**, *63*, 1-34.
- (2) Fredholm, B. B.; IJzerman, A. P.; Jacobson, K. A.; Klotz, K. N.; Linden, J. International union of pharmacology. XXV. Nomenclature and classification of adenosine receptors. *Pharmacol. Rev.* **2001**, *53*, 527-552.
- (3) Chen, J.-F.; Eltzschig, H. K.; Fredholm, B. B. Adenosine receptors as drug targets - what are the challenges? *Nat. Rev. Drug Discov.* **2013**, *12*, 265-286.
- (4) Müller, C. E.; Jacobson, K. A. Recent developments in adenosine receptor ligands and their potential as novel drugs. *Biochim. Biophys. Acta.* **2011**, *1808*, 1290-1308.
- (5) Müller, C. E.; Baqi, Y.; Namasivayam, V. Agonists and antagonists for purinergic receptors. In *Pelegrín (Hg.) 2020 -Purinergic Signaling*; pp. 45-64.
- (6) Allard, D.; Turcotte, M.; Stagg, J. Targeting A₂ adenosine receptors in cancer. *Immunol. Cell Biol.* **2017**, *95*, 333-339.
- (7) Hinz, S.; Navarro, G.; Borroto-Escuela, D.; Seibt, B. F.; Ammon, Y.-C.; Filippo, E. de; Danish, A.; Lacher, S. K.; Červinková, B.; Rafehi, M.; Fuxe, K.; Schiedel, A. C.; Franco, R.; Müller, C. E. Adenosine A_{2A} receptor ligand recognition and signaling is blocked by A_{2B} receptors. *Oncotarget.* **2018**, *9*, 13593-13611.
- (8) Ham, J.; Rees, D. A. The adenosine A_{2B} receptor: its role in inflammation. *Endocr. Metab. Immune Disord. Drug Targets.* **2008**, *8*, 244-254.
- (9) Haskó, G.; Csóka, B.; Németh, Z. H.; Vizi, E. S.; Pacher, P. A_{2B} adenosine receptors in immunity and inflammation. *Trends immunol.* **2009**, *30*, 263-270.

- (10) Abo-Salem, O. M.; Hayallah, A. M.; Bilkei-Gorzo, A.; Filipek, B.; Zimmer, A.; Müller, C. E. Antinociceptive effects of novel A_{2B} adenosine receptor antagonists. *J. Pharmacol. Exp. Ther.* **2004**, *308*, 358-366.
- (11) ClinicalTrials.gov [Internet]. Bethesda (MD): National Library of Medicine (US). 2000 Feb 29 -. Identifier NCT03274479, Phase I Trial of PBF-1129 in Patients With Advanced Non-Small Cell Lung Cancer (NSCLC); cited 2021 July 13 (2017, September 7); Available from: <https://clinicaltrials.gov/ct2/show/NCT03274479?term=a2b+adenosine+receptor+antagonist&draw=2&rank=2> (about 4 screens).
- (12) Jacobson, K. A.; Gao, Z.-G. Adenosine receptors as therapeutic targets. *Nat. Rev. Drug Discov.* **2006**, *5*, 247-264.
- (13) Kasama, H.; Sakamoto, Y.; Kasamatsu, A.; Okamoto, A.; Koyama, T.; Minakawa, Y.; Ogawara, K.; Yokoe, H.; Shiiba, M.; Tanzawa, H.; Uzawa, K. Adenosine A_{2B} receptor promotes progression of human oral cancer. *BMC Cancer.* **2015**, *15*, 563.
- (14) Haskó, G.; Linden, J.; Cronstein, B.; Pacher, P. Adenosine receptors: therapeutic aspects for inflammatory and immune diseases. *Nat. Rev. Drug Discov.* **2008**, *7*, 759-770.
- (15) Kecskés, M.; Kumar, T. S.; Yoo, L.; Gao, Z.-G.; Jacobson, K. A. Novel Alexa Fluor-488 labeled antagonist of the A_{2A} adenosine receptor: Application to a fluorescence polarization-based receptor binding assay. *Biochem. Pharmacol.* **2010**, *80*, 506-511.
- (16) Baker, J. G.; Hall, I. P.; Hill, S. J. Pharmacology and direct visualisation of BODIPY-TMR-CGP: a long-acting fluorescent beta₂-adrenoceptor agonist. *Br. J. Pharmacol.* **2003**, *139*, 232-242.
- (17) Middleton, R. J.; Briddon, S. J.; Cordeaux, Y.; Yates, A. S.; Dale, C. L.; George, M. W.; Baker, J. G.; Hill, S. J.; Kellam, B. New fluorescent adenosine A₁-receptor agonists that allow quantification of ligand-receptor interactions in microdomains of single living cells. *J. Med. Chem.* **2007**, *50*, 782-793.
- (18) Fernández-Dueñas, V.; Gómez-Soler, M.; Jacobson, K. A.; Kumar, S. T.; Fuxe, K.; Borroto-Escuela, D. O.; Ciruela, F. Molecular determinants of A_{2A}R-D₂R allosterism: role of the intracellular loop 3 of the D₂R. *J. Neurochem.* **2012**, *123*, 373-384.
- (19) Stoddart, L. A.; Johnstone, E. K. M.; Wheal, A. J.; Goulding, J.; Robers, M. B.; Machleidt, T.; Wood, K. V.; Hill, S. J.; Pflieger, K. D. G. Application of BRET to monitor ligand binding to GPCRs. *Nat. Methods.* **2015**, *12*, 661-663.

- (20) Bouzo-Lorenzo, M.; Stoddart, L. A.; Xia, L.; IJzerman, A. P.; Heitman, L. H.; Briddon, S. J.; Hill, S. J. A live cell NanoBRET binding assay allows the study of ligand-binding kinetics to the adenosine A₃ receptor. *Purinerg. Signal.* **2019**, *15*, 139-153.
- (21) Hall, M. P.; Unch, J.; Binkowski, B. F.; Valley, M. P.; Butler, B. L.; Wood, M. G.; Otto, P.; Zimmerman, K.; Vidugiris, G.; Machleidt, T.; Robers, M. B.; Benink, H. A.; Eggers, C. T.; Slater, M. R.; Meisenheimer, P. L.; Klaubert, D. H.; Fan, F.; Encell, L. P.; Wood, K. V. Engineered luciferase reporter from a deep sea shrimp utilizing a novel imidazopyrazinone substrate. *ACS Chem. Biol.* **2012**, *7*, 1848-1857.
- (22) Lalo, U.; Allsopp, R. C.; Mahaut-Smith, M. P.; Evans, R. J. P2X₁ receptor mobility and trafficking; regulation by receptor insertion and activation. *J. Neurochem.* **2010**, *113*, 1177-1187.
- (23) Köse, M.; Gollos, S.; Karcz, T.; Fiene, A.; Heisig, F.; Behrenswerth, A.; Kieć-Kononowicz, K.; Namasivayam, V.; Müller, C. E. Fluorescent-labeled selective adenosine A_{2B} receptor antagonist enables competition binding assay by flow cytometry. *J. Med. Chem.* **2018**, *61*, 4301-4316.
- (24) Kozma, E.; Kumar, T. S.; Federico, S.; Phan, K.; Balasubramanian, R.; Gao, Z.-G.; Paoletta, S.; Moro, S.; Spalluto, G.; Jacobson, K. A. Novel fluorescent antagonist as a molecular probe in A₃ adenosine receptor binding assays using flow cytometry. *Biochem. Pharmacol.* **2012**, *83*, 1552-1561.
- (25) Comeo, E.; Kindon, N. D.; Soave, M.; Stoddart, L. A.; Kilpatrick, L. E.; Scammells, P. J.; Hill, S. J.; Kellam, B. Subtype-selective fluorescent ligands as pharmacological research tools for the human adenosine A_{2A} receptor. *J. Med. Chem.* **2020**, *63*, 2656-2672.
- (26) Briddon, S. J.; Middleton, R. J.; Cordeaux, Y.; Flavin, F. M.; Weinstein, J. A.; George, M. W.; Kellam, B.; Hill, S. J. Quantitative analysis of the formation and diffusion of A₁-adenosine receptor-antagonist complexes in single living cells. *Proc. Natl. Acad. Sci. U. S. A.* **2004**, *101*, 4673-4678.
- (27) Kumar, T. S.; Mishra, S.; Deflorian, F.; Yoo, L. S.; Phan, K.; Kecskés, M.; Szabo, A.; Shinkre, B.; Gao, Z.-G.; Trenkle, W.; Jacobson, K. A. Molecular probes for the A_{2A} adenosine receptor based on a pyrazolo-4,3-*e*1,2,4-triazolo1,5-cpyrimidin-5-amine scaffold. *Bioorg. Med. Chem. Lett.* **2011**, *21*, 2740-2745.
- (28) Federico, S.; Margiotta, E.; Moro, S.; Kozma, E.; Gao, Z.-G.; Jacobson, K. A.; Spalluto, G. Conjugable A₃ adenosine receptor antagonists for the development of functionalized ligands and their use in fluorescent probes. *Eur. J. Med. Chem.* **2020**, *186*, 111886.

- (29) Ciruela, F.; Fernández-Dueñas, V.; Jacobson, K. A. Lighting up G protein-coupled purinergic receptors with engineered fluorescent ligands. *Neuropharmacology*. **2015**, *98*, 58-67.
- (30) Ciruela, F.; Jacobson, K. A.; Fernández-Dueñas, V. Portraying G protein-coupled receptors with fluorescent ligands. *ACS Chem. Biol.* **2014**, *9*, 1918-1928.
- (31) Müller, C. E.; Scior, T. Adenosine receptors and their modulators. *Pharm. Acta Helv.* **1993**, *68*, 77-111.
- (32) Yan, L.; Bertarelli, D. C. G.; Hayallah, A. M.; Meyer, H.; Klotz, K.-N.; Müller, C. E. A new synthesis of sulfonamides by aminolysis of *p*-nitrophenylsulfonates yielding potent and selective adenosine A_{2B} receptor antagonists. *J. Med. Chem.* **2006**, *49*, 4384-4391.
- (33) Borrmann, T.; Hinz, S.; Bertarelli, D. C. G.; Li, W.; Florin, N. C.; Scheiff, A. B.; Müller, C. E. 1-alkyl-8-(piperazine-1-sulfonyl)phenylxanthines: development and characterization of adenosine A_{2B} receptor antagonists and a new radioligand with subnanomolar affinity and subtype specificity. *J. Med. Chem.* **2009**, *52*, 3994-4006.
- (34) Hinz, S.; Lacher, S. K.; Seibt, B. F.; Müller, C. E. BAY60-6583 acts as a partial agonist at adenosine A_{2B} receptors. *J. Pharm. Exp. Ther.* **2014**, *349*, 427-436.
- (35) Jacobson, K. A.; IJzerman, A. P.; Linden, J. 1,3-dialkylxanthine derivatives having high potency as antagonists at human A_{2B} adenosine receptors. *Drug Dev. Res.* **1999**, *47*, 45-53.
- (36) Heisig, F.; Gollos, S.; Freudenthal, S. J.; El-Tayeb, A.; Iqbal, J.; Müller, C. E. Synthesis of BODIPY derivatives substituted with various bioconjugatable linker groups: a construction kit for fluorescent labeling of receptor ligands. *J. Fluoresc.* **2014**, *24*, 213-230.
- (37) Kowada, T.; Maeda, H.; Kikuchi, K. BODIPY-based probes for the fluorescence imaging of biomolecules in living cells. *Chem. Soc. Rev.* **2015**, *44*, 4953-4972.
- (38) Jiang, J.; Seel, C. J.; Temirak, A.; Namasivayam, V.; Arridu, A.; Schabikowski, J.; Baqi, Y.; Hinz, S.; Hockemeyer, J.; Müller, C. E. A_{2B} adenosine receptor antagonists with picomolar potency. *J. Med. Chem.* **2019**, *62*, 4032-4055.
- (39) Mishra, A.; Behera, R. K.; Behera, P. K.; Mishra, B. K.; Behera, G. B. Cyanines during the 1990s: A Review. *Chem. Rev.* **2000**, *100*, 1973-2012.
- (40) Park, J. W.; Kim, Y.; Lee, K.-J.; Kim, D. J. Novel cyanine dyes with vinylsulfone group for labeling biomolecules. *Bioconjugate Chem.* **2012**, *23*, 350-362.
- (41) Mujumdar, R. B.; Ernst, L. A.; Mujumdar, S. R.; Waggoner, A. S. Cyanine dye labeling reagents containing isothiocyanate groups. *Cytometry*. **1989**, *10*, 11-19.

- (42) Wolf, N.; Kersting, L.; Herok, C.; Mihm, C.; Seibel, J. High-yielding water-soluble asymmetric cyanine dyes for labeling applications. *J. Org. Chem.* **2020**, *85*, 9751-9760.
- (43) Banerjee, S. S.; Aher, N.; Patil, R.; Khandare, J. Poly(ethylene glycol)-prodrug conjugates: Concept, design, and applications. *J. Drug Deliv.* **2012**, *2012*, 103973.
- (44) Veronese, F. M.; Pasut, G. PEGylation, successful approach to drug delivery. *Drug Discov. Today.* **2005**, *10*, 1451-1458.
- (45) Gunzner, J. L.; Sutherlin, D. P.; Stanley, M. S.; Bao, L.; Castanedo, G.; Lalonde, R. L.; Wang, S.; Reynolds, M. E.; Savage, S. J.; Malesky, K. Pyridyl inhibitors of hedgehog signalling; WO 2009126863 A2, 2009.
- (46) Müller, C. E. General synthesis and properties of 1-monosubstituted xanthines. *Synthesis.* **1993**, *1993*, 125-128.
- (47) Ghidini, A.; Steunenberg, P.; Murtola, M.; Strömberg, R. Synthesis of PNA oligoether conjugates. *Molecules.* **2014**, *19*, 3135-3148.
- (48) Edward Semple, J.; Sullivan, B.; Vojkovsky, T.; Sill, K. N. Synthesis and facile end-group quantification of functionalized PEG azides. *J. Polym. Sci. Part A.* **2016**, *54*, 2888-2895.
- (49) Entract, G. M.; Bryden, F.; Domarkas, J.; Savoie, H.; Allott, L.; Archibald, S. J.; Cawthorne, C.; Boyle, R. W. Development of PDT/PET theranostics: synthesis and biological evaluation of an (18)F-radiolabeled water-soluble porphyrin. *Mol. Pharm.* **2015**, *12*, 4414-4423.
- (50) Wu, X.; Hu, L. Design and synthesis of peptide conjugates of phosphoramidate mustard as prodrugs activated by prostate-specific antigen. *Bioorgan. Med. Chem.* **2016**, *24*, 2697-2706.
- (51) Frei, R.; Breitbach, A. S.; Blackwell, H. E. Expedient construction of small molecule macroarrays via sequential palladium- and copper-mediated reactions and their ex situ biological testing. *Chem. Sci.* **2012**, *3*, 1555-1561.
- (52) Chopra, P.; Logun, M. T.; White, E. M.; Lu, W.; Locklin, J.; Karumbaiah, L.; Boons, G.-J. Fully synthetic heparan sulfate-based neural tissue construct that maintains the undifferentiated state of neural stem cells. *ACS Chem. Biol.* **2019**, *14*, 1921-1929.
- (53) Feng, C.; Gonzalez-Alvarez, M. J.; Song, Y.; Li, I.; Zhao, G.; Molev, G.; Guerin, G.; Walker, G.; Scholes, G. D.; Manners, I.; Winnik, M. A. Synthesis, self-assembly and photophysical properties of oligo(2,5-dihexyloxy-1,4-phenylene vinylene)-block-poly(ethylene glycol). *Soft Matter.* **2014**, *10*, 8875-8887.

- (54) Rostovtsev, V. V.; Green, L. G.; Fokin, V. V.; Sharpless, K. B. A stepwise Huisgen cycloaddition process: copper(I)-catalyzed regioselective "ligation" of azides and terminal alkynes. *Angew. Chem.* **2002**, *41*, 2596-2599.
- (55) dos Santos, J. A.; Reis Corrales, R. C. N.; Pavan, F. R.; Leite, C. Q. F.; Paula Dias, R. M. de; da Silva, A. D. Synthesis and antitubercular evaluation of new 1,2,3-triazole derivatives of carbohydrates. *Mediterr. J. Chem.* **2012**, *1*, 282-288.
- (56) Sivaev, I. B.; Kulikova, N. Y.; Nizhnik, E. A.; Vichuzhanin, M. V.; Starikova, Z. A.; Semioshkin, A. A.; Bregadze, V. I. Practical synthesis of 1,4-dioxane derivative of the closedodecaborate anion and its ring opening with acetylenic alkoxides. *J. Organomet. Chem.* **2008**, *693*, 519-525.
- (57) Bai, S.; Li, S.; Xu, J.; Peng, X.; Sai, K.; Chu, W.; Tu, Z.; Zeng, C.; Mach, R. H. Synthesis and structure-activity relationship studies of conformationally flexible tetrahydroisoquinolinyl triazole carboxamide and triazole substituted benzamide analogues as σ_2 receptor ligands. *J. Med. Chem.* **2014**, *57*, 4239-4251.
- (58) Blanchard, S. C.; Altman, R.; Warren, J. D.; Zhou, Z. Cyanine fluorescent dyes with triplet-state quenching groups, WO 2013109859, 2004.
- (59) Rungta, P.; Bandera, Y. P.; Roeder, R. D.; Li, Y.; Baldwin, W. S.; Sharma, D.; Sehorn, M. G.; Luzinov, I.; Foulger, S. H. Selective imaging and killing of cancer cells with protein-activated near-infrared fluorescing nanoparticles. *Macromol. Biosci.* **2011**, *11*, 927-937.
- (60) Lin, Y.; Sun, L.; Zeng, F.; Wu, S. An unsymmetrical squaraine-based activatable probe for imaging lymphatic metastasis by responding to tumor hypoxia with MSOT and aggregation-enhanced fluorescent imaging. *Chemistry - A European Journal.* **2019**, *25*, 16740-16747.
- (61) Mujumdar, R. B.; Ernst, L. A.; Mujumdar, S. R.; Lewis, C. J.; Waggoner, A. S. Cyanine dye labeling reagents: sulfoindocyanine succinimidyl esters. *Bioconjugate Chem.* **1993**, *4*, 105-111.
- (62) Alnouri, M. W.; Jepards, S.; Casari, A.; Schiedel, A. C.; Hinz, S.; Müller, C. E. Selectivity is species-dependent: Characterization of standard agonists and antagonists at human, rat, and mouse adenosine receptors. *Purinerg. Signal.* **2015**, *11*, 389-407.
- (63) Klotz, K. N.; Hessling, J.; Hegler, J.; Owman, C.; Kull, B.; Fredholm, B. B.; Lohse, M. J. Comparative pharmacology of human adenosine receptor subtypes - characterization of stably transfected receptors in CHO cells. *Naunyn-Schmiedeberg's Arch. Pharmacol.* **1998**, *357*, 1-9.

(64) Weyler, S.; Fülle, F.; Diekmann, M.; Schumacher, B.; Hinz, S.; Klotz, K.-N.; Müller, C. E. Improving potency, selectivity, and water solubility of adenosine A₁ receptor antagonists: xanthines modified at position 3 and related pyrimido[1,2,3-cd]purinediones. *ChemMedChem*. **2006**, *1*, 891-902.

(65) Drabczyńska, A.; Müller, C. E.; Karolak-Wojciechowska, J.; Schumacher, B.; Schiedel, A.; Yuzlenko, O.; Kieć-Kononowicz, K. N⁹-benzyl-substituted 1,3-dimethyl- and 1,3-dipropyl-pyrimido[2,1-f]purinediones: synthesis and structure-activity relationships at adenosine A₁ and A_{2A} receptors. *Bioorg. Med. Chem.* **2007**, *15*, 5003-5017.

4.2.8. Supporting Information

Functionalized potent and selective 8-(4-acylpiperazinyl-1-sulfonyl)phenylxanthines providing a platform for fluorescence-labeling of adenosine A_{2B} receptor antagonists

Tim Harms,¹ Beatriz Büschbell,¹ Christin Vielmuth,¹ Sonja Hinz,^{1,2} Anke C. Schiedel,¹ Jörg Hockemeyer,¹ and Christa E. Müller^{1,*}

¹PharmaCenter Bonn, Pharmaceutical Institute, Pharmaceutical Sciences Bonn (PSB), Pharmaceutical & Medicinal Chemistry, University of Bonn, An der Immenburg 4, 53121, Bonn, Germany.

²Institute of Pharmacology and Toxicology, Center for Biomedical Education and Research (ZBAF), school of Medicine, Faculty of Health, University of Witten/Herdecke, D-58453 Witten, Germany.

Table of content

1. **S1.** Fluorescence spectra of **39** and **40**
2. **S2. - S10.** NMR data for selected key compounds
3. **S11. - S19.** Radioligand receptor binding experiments at adenosine receptor subtypes

1. Fluorescence spectra of **39** and **40**

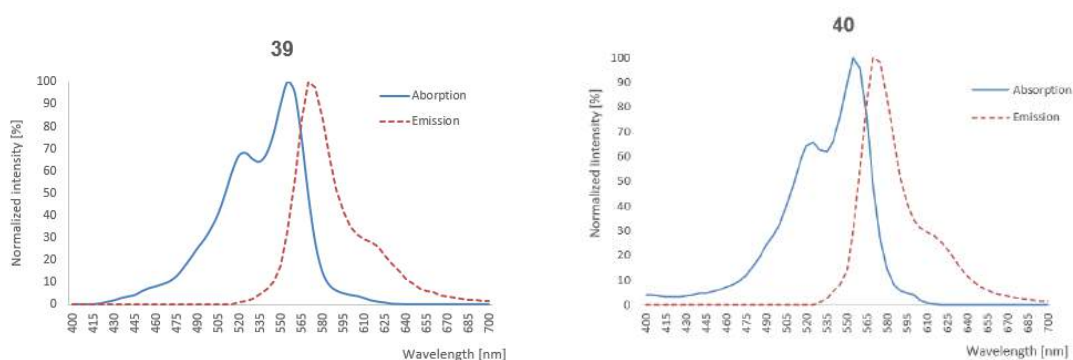


Figure S1. Absorption and emission spectra of **39** and **40**

Table S1. Spectral properties of **39** and **40**

Compound	Absorption λ (nm)	Emission λ (nm)	Stokes' Shift (nm)	Φ
39	556	571	15	0.095
40	557	572	15	0.10

2. NMR data for selected key compounds

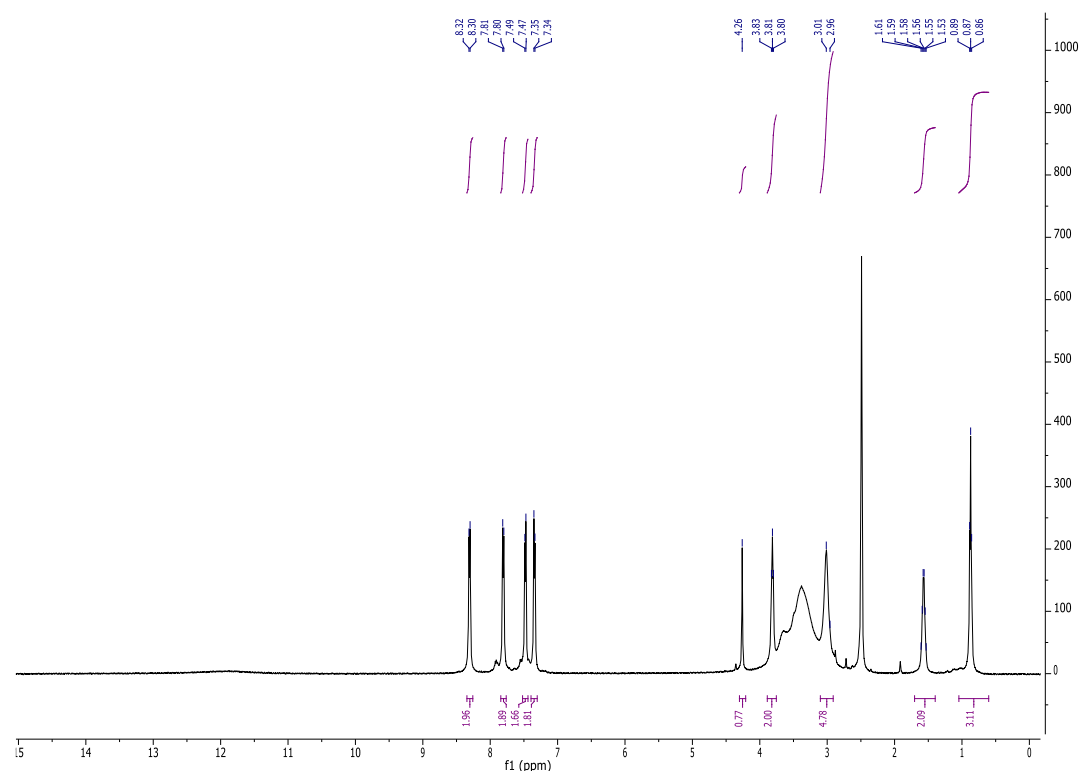


Figure S2. ^1H NMR (600 MHz) spectra ($\text{DMSO}-d_6$) of 8-(4-((4-(4-ethynylbenzoyl)piperazin-1-yl)sulfonyl)phenyl)-1-propyl-3,7-dihydro-1*H*-purine-2,6-dione (**27**)

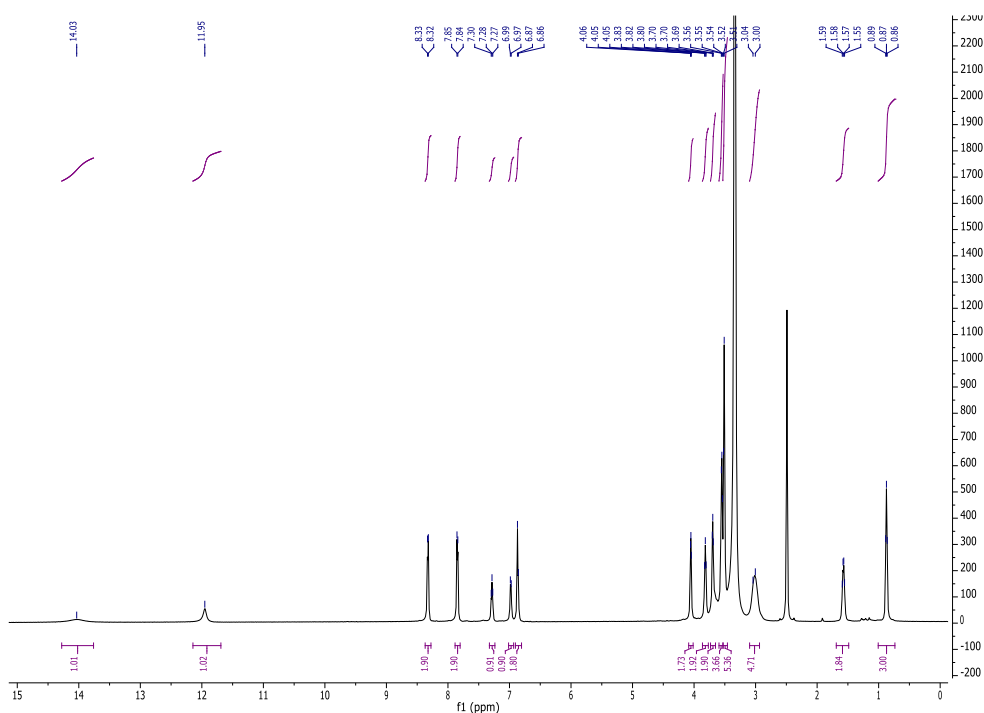


Figure S3. ^1H NMR (600 MHz) spectra ($\text{DMSO-}d_6$) of 8-(4-((4-(3-(2-(2-(2-azidoethoxy)ethoxy)ethoxy)ethoxy)benzoyl) piperazin-1-yl)sulfonyl)phenyl)-1-propyl-3,7-dihydro-1*H*-purine-2,6-dione (**28**)

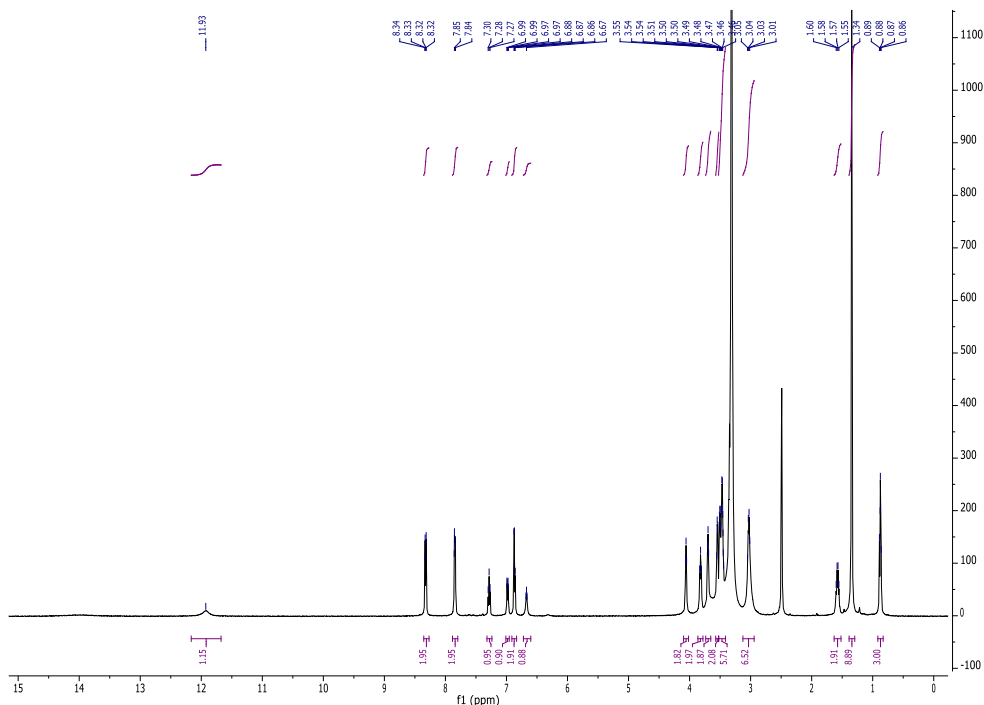


Figure S4. ^1H NMR (600 MHz) spectra ($\text{DMSO-}d_6$) of *tert*-butyl (2-(2-(2-(2-(3-(4-((4-(2,6-dioxo-1-propyl-2,3,6,7-tetrahydro-1*H*-purin-8-yl)phenyl)sulfonyl)piperazine-1-carbonyl)phenoxy)ethoxy)ethoxy)ethoxy)ethyl)carbamate (**29**)

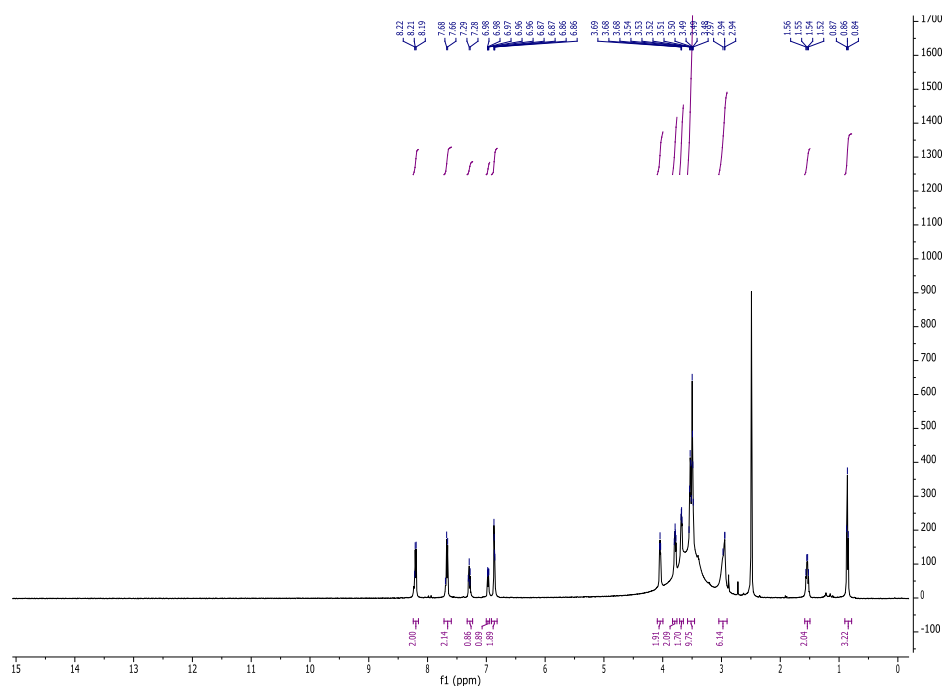


Figure S5. ¹H NMR (600 MHz) spectra (DMSO-d₆) of 8-(4-((4-(3-(2-(2-(2-(2-aminoethoxy)ethoxy)ethoxy)ethoxy)benzoyl)piperazin-1-yl)sulfonyl)phenyl)-1-propyl-3,7-dihydro-1*H*-purine-2,6-dione (**30**)

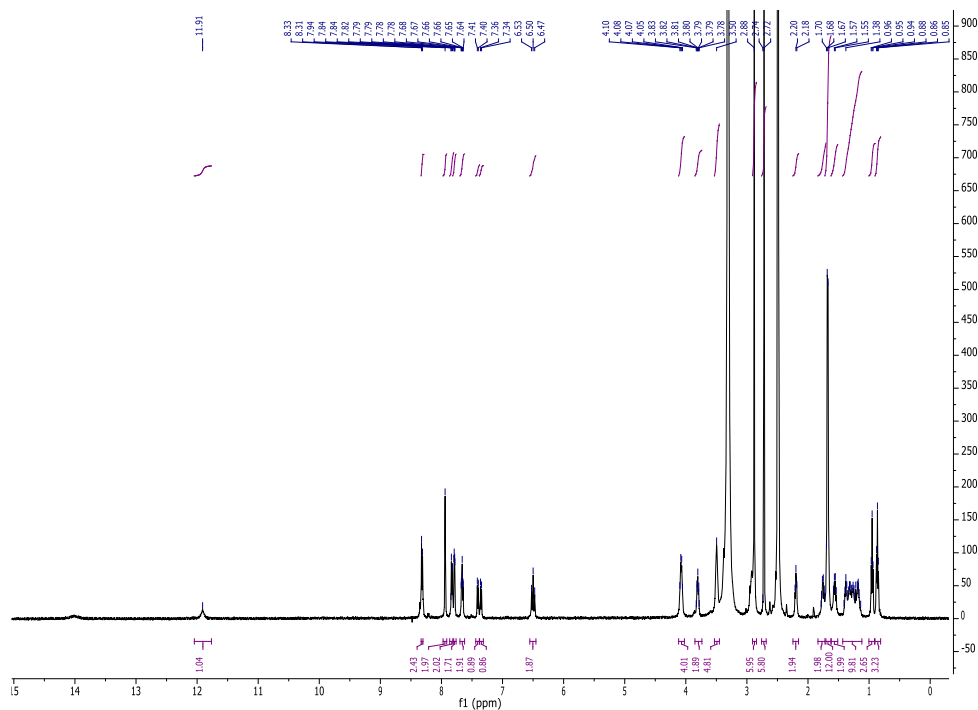


Figure S6. ¹H NMR (600 MHz) spectra (DMSO-d₆) of 2-(((*E*)-3-((*E*)-3,3-dimethyl-1-propyl-5-sulfoindolin-2-ylidene)prop-1-en-1-yl)-1-(8-(4-((4-(2,6-dioxo-1-propyl-2,3,6,7-tetrahydro-1*H*-purin-8-yl)phenyl)sulfonyl)piperazin-1-yl)-8-oxooctyl)-3,3-dimethyl-3*H*-indol-1-ium-5-sulfonate (**37**)

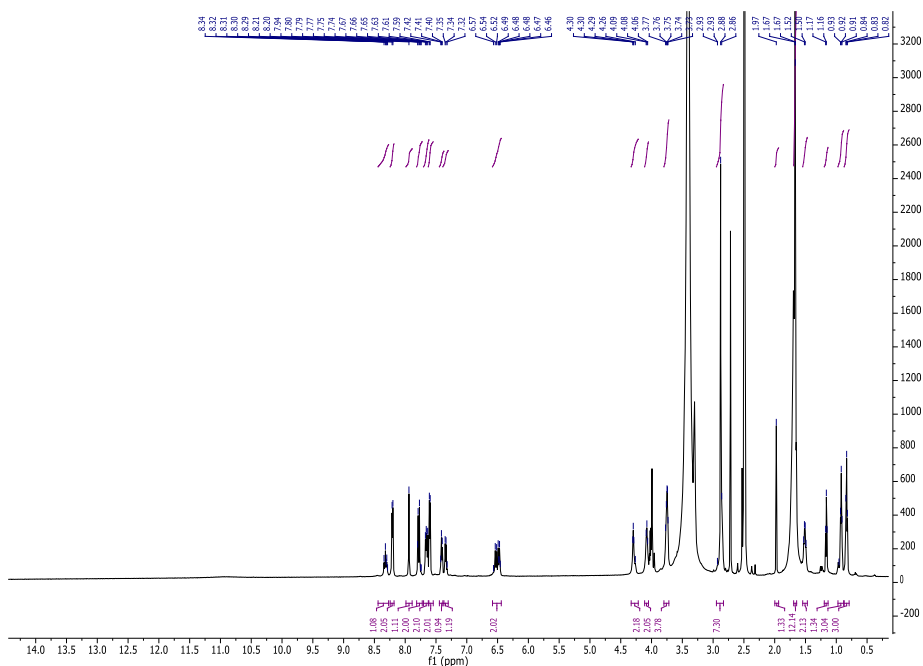


Figure S7. ^1H NMR (600 MHz) spectra ($\text{DMSO-}d_6$) of 2-((*E*)-3-((*E*)-3,3-dimethyl-1-propyl-5-sulfoindolin-2-ylidene)prop-1-en-1-yl)-1-(2-(2-(2-(2-(4-((4-(2,6-dioxo-1-propyl-2,3,6,7-tetrahydro-1*H*-purin-8-yl)phenyl)sulfonyl)piperazin-1-yl)-2-oxoethoxy)ethoxy)ethoxy)ethyl)-3,3-dimethyl-3*H*-indol-1-ium-5-sulfonate (**38**)

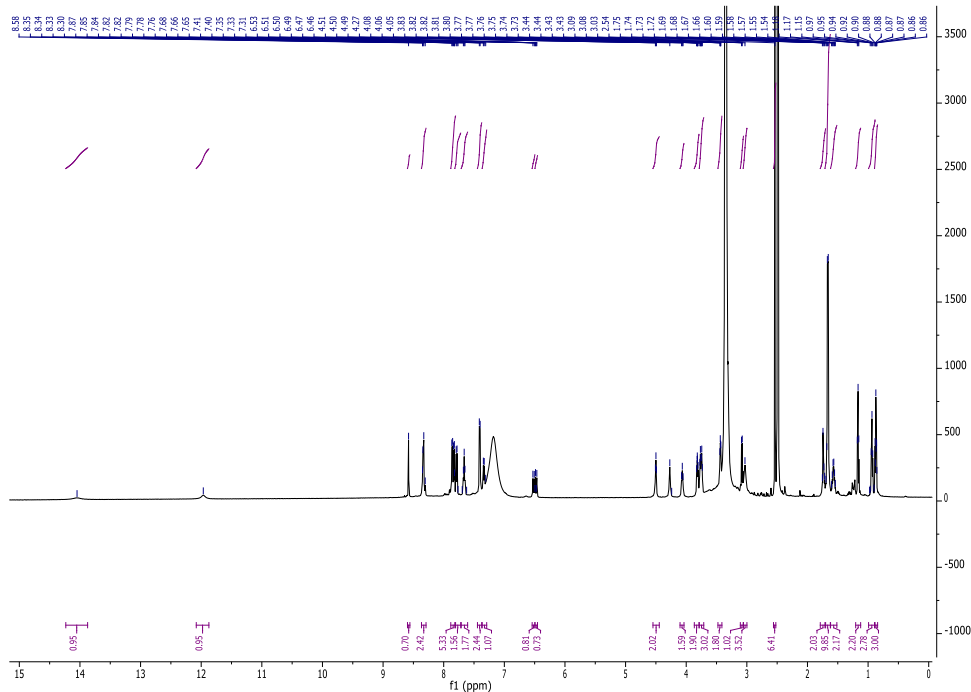


Figure S8. ^1H NMR (600 MHz) spectra ($\text{DMSO-}d_6$) of 2-((*E*)-3-((*E*)-3,3-dimethyl-1-propyl-5-sulfoindolin-2-ylidene)prop-1-en-1-yl)-1-(2-(2-(2-(2-(4-(4-(4-((4-(2,6-dioxo-1-propyl-2,3,6,7-tetrahydro-1*H*-purin-8-yl)phenyl)sulfonyl)piperazine-1-carbonyl)phenyl)-1*H*-1,2,3-triazol-1-yl)ethoxy)ethoxy)ethoxy)ethyl)-3,3-dimethyl-3*H*-indol-1-ium-5-sulfonate (**39**)

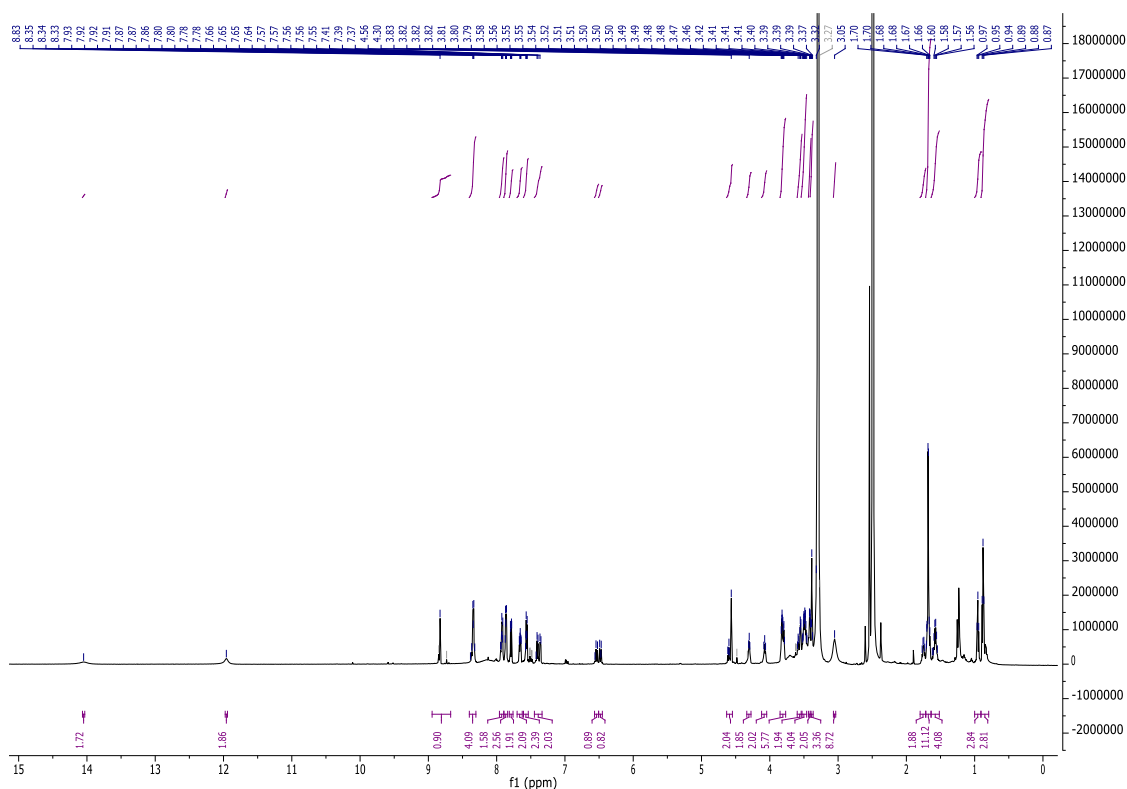


Figure S9. ^1H NMR (600 MHz) spectra ($\text{DMSO-}d_6$) of 2-((*E*)-3-((*E*)-3,3-dimethyl-1-propyl-5-sulfoindolin-2-ylidene)prop-1-en-1-yl)-1-(1-(1-(4-(4-((4-(2,6-dioxo-1-propyl-2,3,6,7-tetrahydro-1*H*-purin-8-yl)phenyl)sulfonyl)piperazine-1-carbonyl)phenyl)-1*H*-1,2,3-triazol-4-yl)-2,5,8,11-tetraoxatridecan-13-yl)-3,3-dimethyl-3*H*-indol-1-ium-5-sulfonate (**40**)

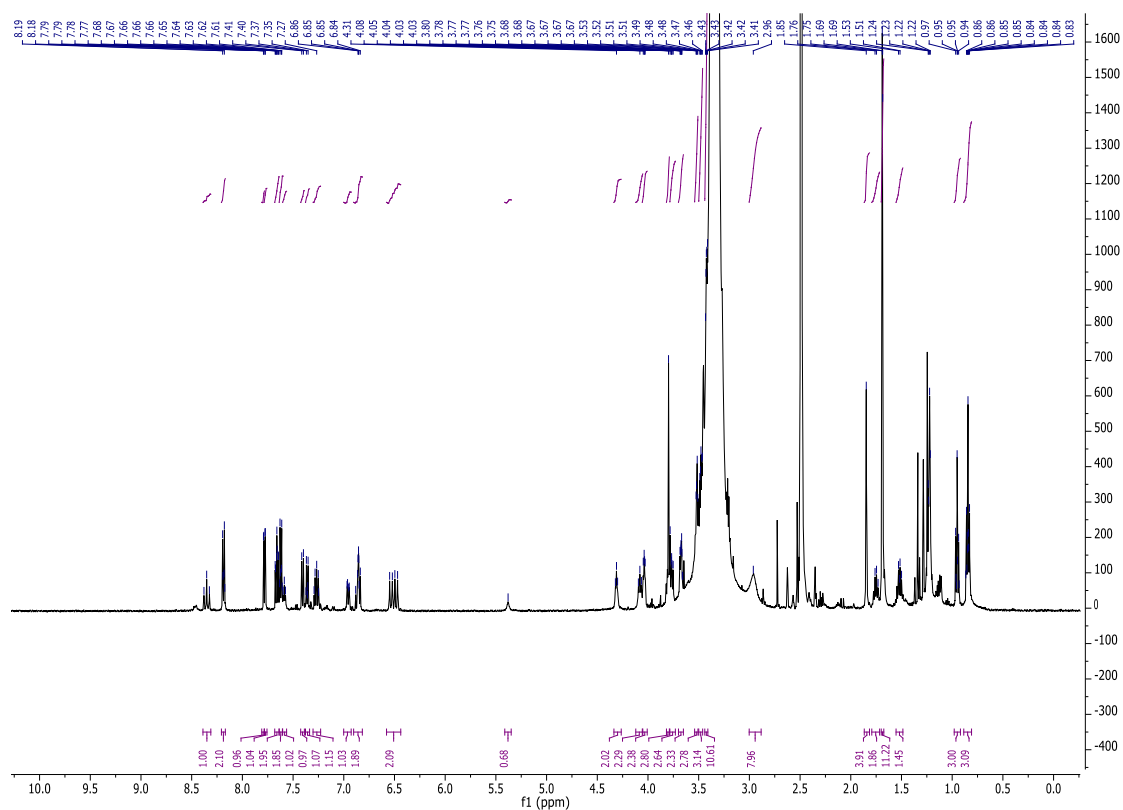


Figure S10. ¹H NMR (600 MHz) spectra (DMSO-*d*₆) of 2-((*E*)-3-((*E*)-3,3-dimethyl-1-propyl-5-sulfoindolin-2-ylidene)prop-1-en-1-yl)-1-(23-(3-(4-((4-(2,6-dioxo-1-propyl-2,3,6,7-tetrahydro-1*H*-purin-8-yl)phenyl)sulfonyl)piperazine-1-carbonyl)phenoxy)-11-oxo-3,6,9,15,18,21-hexaoxa-12-azatricosyl)-3,3-dimethyl-3*H*-indol-1-ium-5-sulfonate (**41**)

3. Radioligand receptor binding experiments at adenosine receptor subtypes

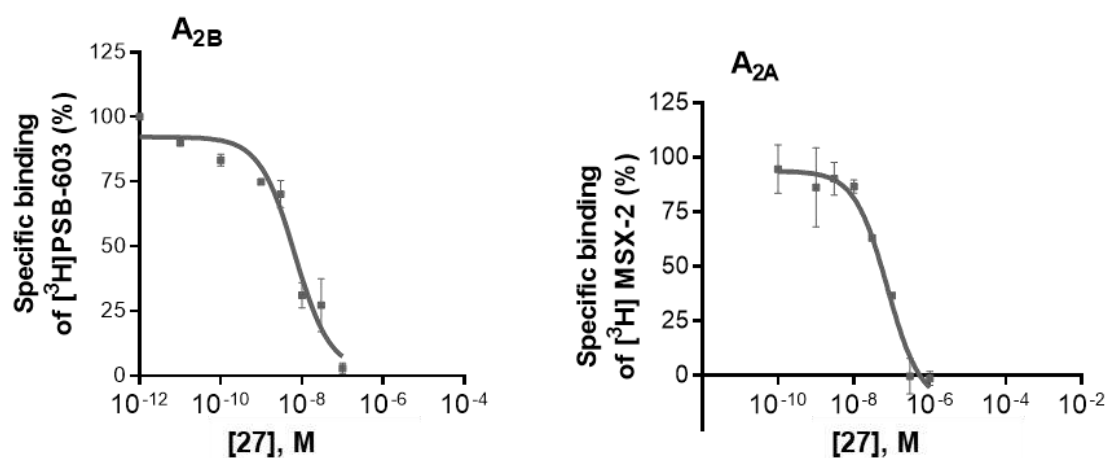


Figure S11. Radioligand-receptor binding experiments at the human $A_{2B}AR$ and $A_{2A}AR$ of 8-((4-(4-ethynylbenzoyl)piperazin-1-yl)sulfonyl)phenyl)-1-propyl-3,7-dihydro-1*H*-purine-2,6-dione (**27**)

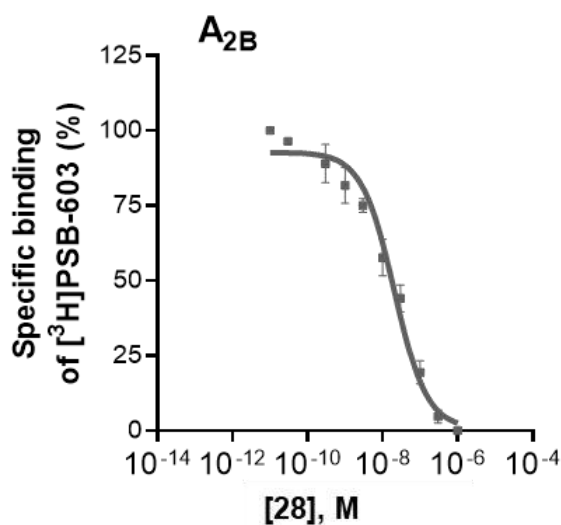


Figure S12. Radioligand-receptor binding experiments at the human $A_{2B}AR$ of 8-(4-((4-(3-(2-(2-(2-azidoethoxy)ethoxy)ethoxy)ethoxy)benzoyl)piperazin-1-yl)sulfonyl)phenyl)-1-propyl-3,7-dihydro-1*H*-purine-2,6-dione (**28**)

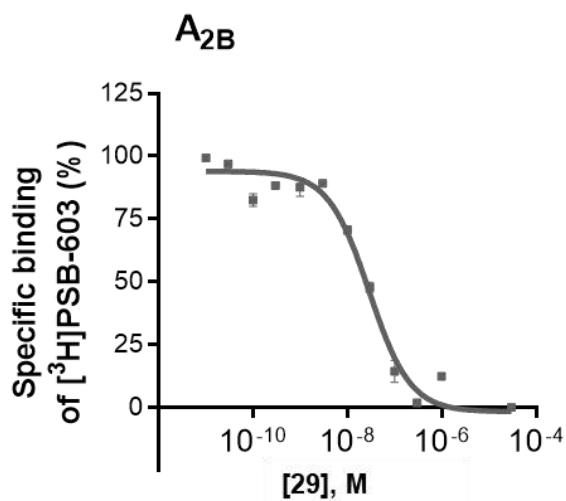


Figure S13. Radioligand-receptor binding experiments at the human A_{2B}AR of *tert*-butyl (2-(2-(2-(2-(3-(4-((4-(2,6-dioxo-1-propyl-2,3,6,7-tetrahydro-1*H*-purin-8-yl)phenyl)sulfonyl)piperazine-1-carbonyl)phenoxy)ethoxy)ethoxy)ethoxy)ethyl)carbamate (**29**)

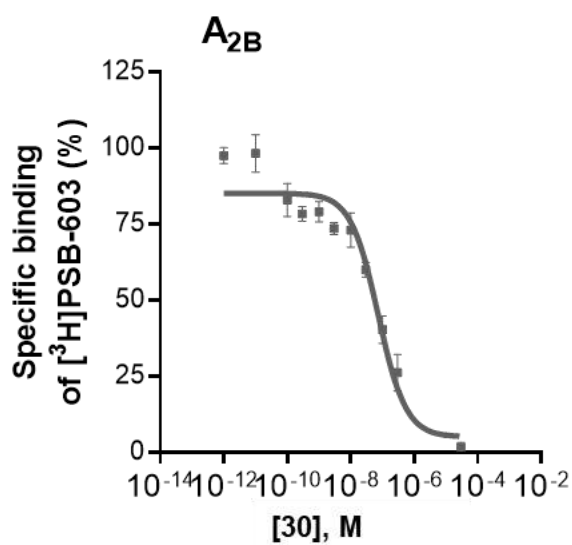


Figure S14. Radioligand-receptor binding experiments at the human A_{2B}AR of 8-(4-((4-(3-(2-(2-(2-(2-aminoethoxy)ethoxy)ethoxy)ethoxy)benzoyl)piperazin-1-yl)sulfonyl)phenyl)-1-propyl-3,7-dihydro-1*H*-purine-2,6-dione (**30**)

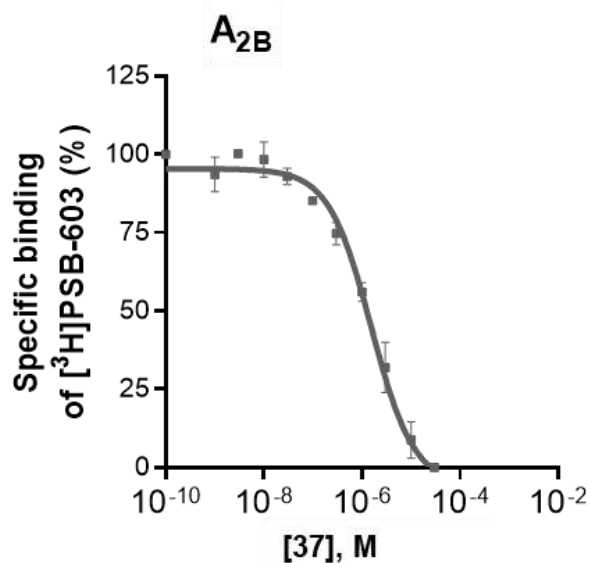


Figure S15. Radioligand-receptor binding experiments at the human A₂BAR of 2-((*E*)-3-((*E*)-3,3-dimethyl-1-propyl-5-sulfoindolin-2-ylidene)prop-1-en-1-yl)-1-(8-(4-((4-(2,6-dioxo-1-propyl-2,3,6,7-tetrahydro-1*H*-purin-8-yl)phenyl)sulfonyl)piperazin-1-yl)-8-oxooctyl)-3,3-dimethyl-3*H*-indol-1-ium-5-sulfonate (**37**)

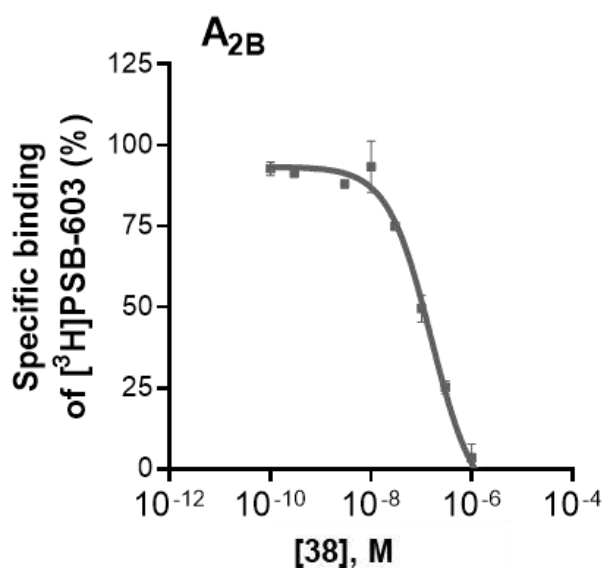


Figure S16. Radioligand-receptor binding experiments at the human A₂BAR of 2-((*E*)-3-((*E*)-3,3-dimethyl-1-propyl-5-sulfoindolin-2-ylidene)prop-1-en-1-yl)-1-(2-(2-(2-(2-(4-((4-(2,6-dioxo-1-propyl-2,3,6,7-tetrahydro-1*H*-purin-8-yl)phenyl)sulfonyl)piperazin-1-yl)-2-oxoethoxy)ethoxy)ethoxy)ethyl)-3,3-dimethyl-3*H*-indol-1-ium-5-sulfonate (**38**)

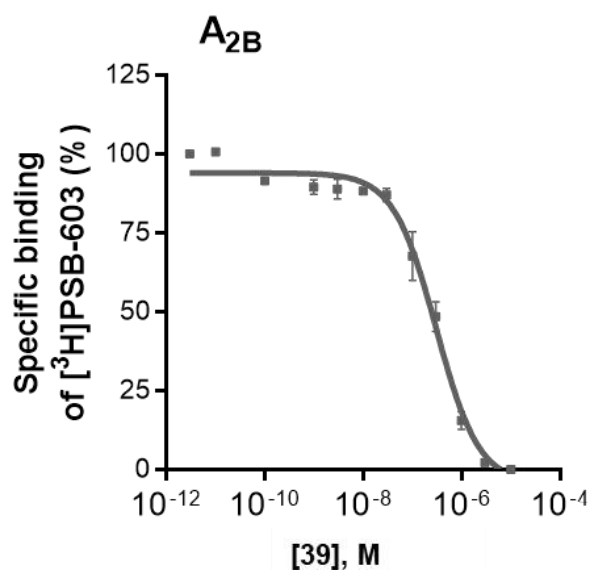


Figure S17. Radioligand-receptor binding experiments at the human A_{2B}AR of 2-((*E*)-3-((*E*)-3,3-dimethyl-1-propyl-5-sulfoindolin-2-ylidene)prop-1-en-1-yl)-1-(2-(2-(2-(2-(4-(4-(4-((4-(2,6-dioxo-1-propyl-2,3,6,7-tetrahydro-1*H*-purin-8-yl)phenyl)sulfonyl)piperazine-1-carbonyl)phenyl)-1*H*-1,2,3-triazol-1-yl)ethoxy)ethoxy)ethoxy)ethyl)-3,3-dimethyl-3*H*-indol-1-ium-5-sulfonate (**39**)

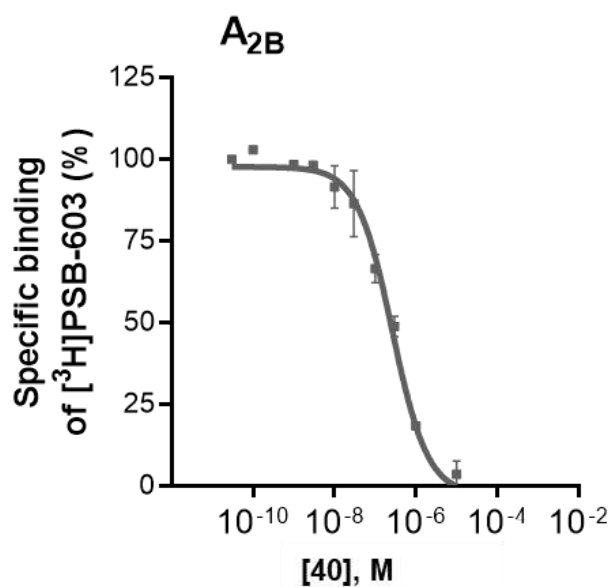


Figure S18. Radioligand-receptor binding experiments at the human A_{2B}AR of 2-((*E*)-3-((*E*)-3,3-dimethyl-1-propyl-5-sulfoindolin-2-ylidene)prop-1-en-1-yl)-1-(1-(1-(4-(4-((4-(2,6-dioxo-1-propyl-2,3,6,7-tetrahydro-1*H*-purin-8-yl)phenyl)sulfonyl)piperazine-1-carbonyl)phenyl)-1*H*-1,2,3-triazol-4-yl)-2,5,8,11-tetraoxatridecan-13-yl)-3,3-dimethyl-3*H*-indol-1-ium-5-sulfonate (**40**)

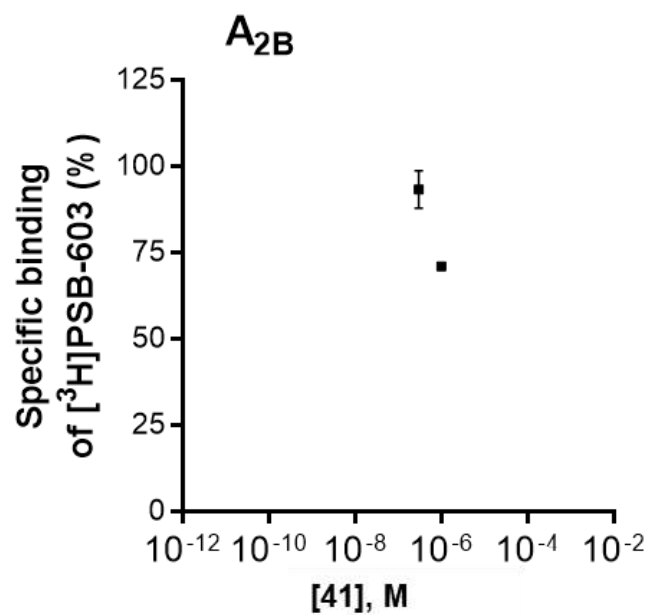


Figure S19. Radioligand-receptor binding experiments at the human $A_{2B}AR$ of 2-((*E*)-3-((*E*)-3,3-dimethyl-1-propyl-5-sulfoindolin-2-ylidene)prop-1-en-1-yl)-1-(23-(3-(4-((4-(2,6-dioxo-1-propyl-2,3,6,7-tetrahydro-1*H*-purin-8-yl)phenyl)sulfonyl)piperazine-1-carbonyl)phenoxy)-11-oxo-3,6,9,15,18,21-hexaoxa-12-azatricosyl)-3,3-dimethyl-3*H*-indol-1-ium-5-sulfonate (**41**)

4.3. Part III: Synthesis of 3-amino-*N*-benzyl-1-phenyl-1*H*-pyrazole-4-carboxamides as A_{2A}AR antagonists

4.3.1. SAR analysis of 5-aminotriazoles as A_{2A}AR antagonists based on computational studies

The A_{2A}AR has recently been cocrystallized with the antagonist Cmpd-1 (**I**) bound to the A_{2A}AR subtype.¹ The published X-ray structures were used as a basis for molecular modeling in order to elucidate the SARs and to optimize the scaffold. Figure 1 depicts important interactions between the ligand and the protein's amino acid residues: The 5-amino group of the triazole forms an important hydrogen bond with Glu169 and the amide oxygen of Asn253. In addition, Asn253 forms a hydrogen bond with the N1 nitrogen atom of the triazole ring. Aromatic π - π stacking was observed for Phe168 in ECL2 with the aminotriazole ring (cf. Figure 1A). The abovementioned amino acid residues are known to interact with other A_{2A}AR ligands in further reported A_{2A}AR cocrystal structures as well. Both the 3-methylphenyl and aminotriazole ring bind within the orthosteric pocket of the A_{2A}AR, which is defined by the space that is occupied by the natural ligand adenosine.² Figure 1B shows an allosteric site. The 2-methoxyphenyl ring is located in a compact pocket formed by eight surrounding amino acid residues. Tyr9 and Tyr271 form the key aromatic interactions, shielding the ligand from solvent exposure.

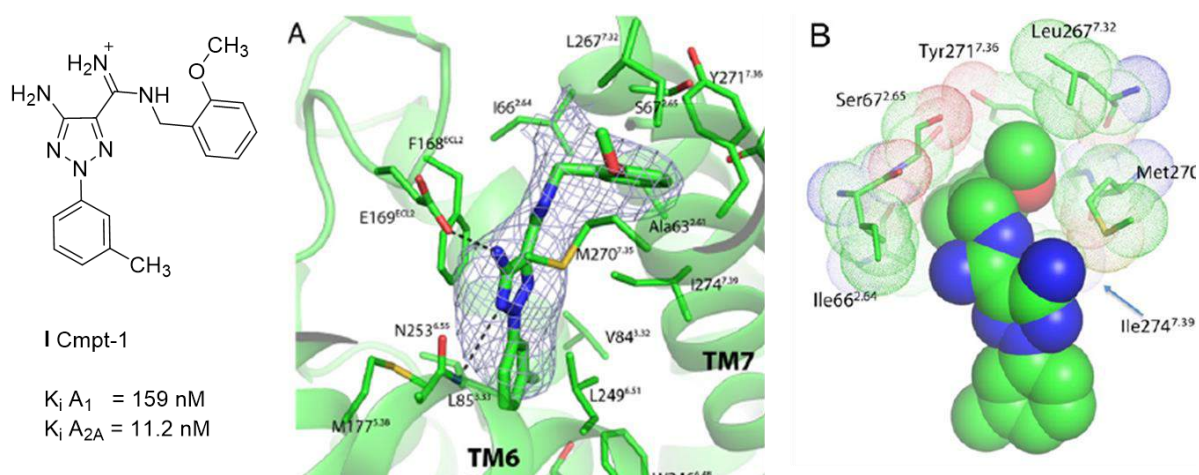


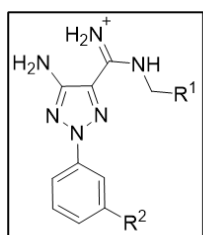
Figure 1. Structure of Cmpd-1 (**I**) and biological data. **A:** Binding pocket of Cmpd-1, the side chains of amino acid residues within 4 Å of the ligand are shown in stick representation. Hydrogen bonding interactions are depicted by dashed lines. **B:** Cmpd-1 is shown in sphere representation, and residues are shown in stick representation, with the contact residues' van der Waals radii depicted as dots.¹

Analogues of Cmpd-1 with methoxy groups in the *meta*- and *para*- position revealed that the potency drops dramatically (**II**, *m*-methoxyphenyl $K_i A_{2A} = 159 \text{ nM}$; **III**, *p*-methoxyphenyl $K_i A_{2A} = 1259 \text{ nM}$) when the position of the methoxy group is altered (see Table 1). Apparently, the

protein pocket leaves only limited space for accommodating a methoxy group on the phenyl ring in another than the *ortho*-position as a conformational effect on the position of the benzyl ring. Leu267 and Met270 of the A_{2A}AR form contacts with the *ortho*-methoxy group; its removal resulted in a decrease in A_{2A}AR affinity and a loss of A_{2A}AR / A₁AR selectivity (**IV**, K_i A_{2A} = 126 nM; K_i A₁ = 79 nM). Since the native ligand adenosine and many reported ligands do not extend to this pocket, this sub-pocket was designated as an allosteric site.¹

Table 1. Binding properties of Cmpd-1 and analogues to the A_{2A} and A₁ adenosine receptors.¹

Compound	R ¹	R ²	K _i A _{2A} AR	K _i A ₁ AR
I	<i>o</i> -Methoxyphenyl	Methyl	10.0 nM	159 nM
II	<i>m</i> -Methoxyphenyl	Methyl	159 nM	251 nM
III	<i>p</i> -Methoxyphenyl	Methyl	1259 nM	251 nM
IV	Phenyl	H	126 nM	79 nM
V	Cyclopropyl	Methyl	1585 nM	1000 nM



In 2018, Jaiteh et al. docked a library with 5.4 million molecules to crystal structures of the A_{2A}AR and MAO-B. Twenty-four compounds that were among the highest ranked ones for both targets were evaluated experimentally, resulting in the discovery of four dual-acting ligands. Interestingly, the most potent structure was also a 5-aminotriazole derivative (**VI**).³ It exhibited nanomolar potency for the A_{2A}AR (K_i = 19 nM) and MAO-B (IC₅₀ = 100 nM).

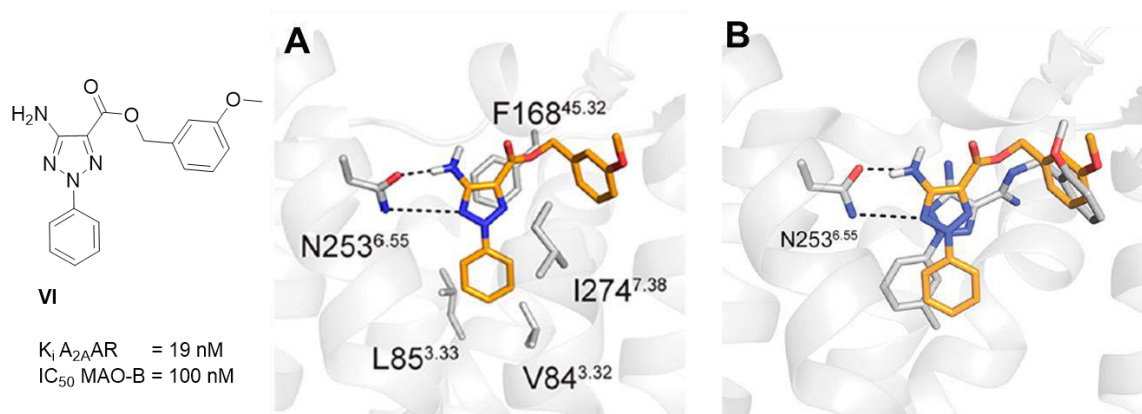


Figure 2. Biological data and structure of **VI**. **A:** Predicted binding mode of compound **VI** to the A_{2A}AR, key binding site residues and the ligand are shown in stick representation. Hydrogen bonds are shown as black dashed lines. **B:** Comparison of the predicted binding mode of compound **VI** to a crystal structure of Cmpd-1 (**I**) from Sun et al. in complex with the A_{2A}AR. The dual-target ligand **VI** is shown in stick representation with orange colored carbon atoms. The cocrystallized antagonist Cmpd-1 is depicted in sticks with gray carbon atoms. The A_{2A}AR is depicted in gray cartoon representation. Hydrogen bonds are shown as black dashed lines.³

As a matter of fact, 5-aminotriazoles have been discovered as antagonist for the $A_{2A}AR$ by different approaches (virtual screening vs. design and synthesis). The virtual prediction led to very similar results as the crystallization of Sun et al. Again, Asn253 stood out as a very important amino acid due to the strong hydrogen bonds its residue can form with the amino group and the N1 nitrogen atom of the triazole ring. Figure 2 **B** illustrates simulated binding modes of **VI** and Cmpd-1. This illustration might suggest, that substituents at the “southern” phenyl region could alter the binding mode of the antagonists. This might explain why the *meta*-methoxyphenyl moiety of **VI** is tolerated by the receptor whereas compound **II** showed comparably low affinity: Since **VI** has more space in the “southern” part of the molecule, it could form a different rotamer and fit into the protein in a slightly different binding mode than **I**. Hence, an unsubstituted phenyl ring at the triazole nitrogen atom might “allow” the benzylamine moiety to bear bigger substituents. The illustration in Figure 2**B** also suggests, that, depending on the size of the substituents at both phenyl rings, or the nature of the linker moiety (ester / amidine), the benzylamine moiety might exert different binding modes.

All these findings show, that a scaffold based on 3-aminopyrazoles for the $A_{2A}AR$ may be promising since all important interactions with the protein would be retained. A better chemical accessibility and the innovation of this undescribed scaffold are additional advantages. Pyrrole derivatives or a switched pyrazole (3-aminopyrrole / 4-aminopyrazole) as $A_{2A}AR$ antagonists do not seem reasonable as the important interaction with Asn253 would then be missing.

4.3.2. Compound design

4.3.2.1. Design of 3-amino-*N*-benzyl-1-phenyl-1*H*-pyrazole-4-carboxamides on the basis of triazoles

In literature three unsubstituted 5-aminotriazole derivatives are reported connecting a 5-amino-2-phenyl-1,2,3-triazoles with a benzyl moiety via different conjunctions, namely an imidine (**IV**), an ester (**VII**) and an amide (**VIII**).^{1:3} The imidine derivative showed the least affinity for the $A_{2A}AR$ ($K_i = 126$ nM), presumably because of its positive charge at physiologic pH value (cf. Figure 3). Moreover, the imidine structure is difficult to synthesize and its pharmacokinetic properties such as oral bioavailability are expected to be unfavorable. The ester and the amide derivatives exhibited similar affinities at the $A_{2A}AR$, however, due to its higher stability, the amide structure is more favorable. Based on these findings, our new scaffold was based on amide as a linker between the pyrazole core and the benzyl moiety.

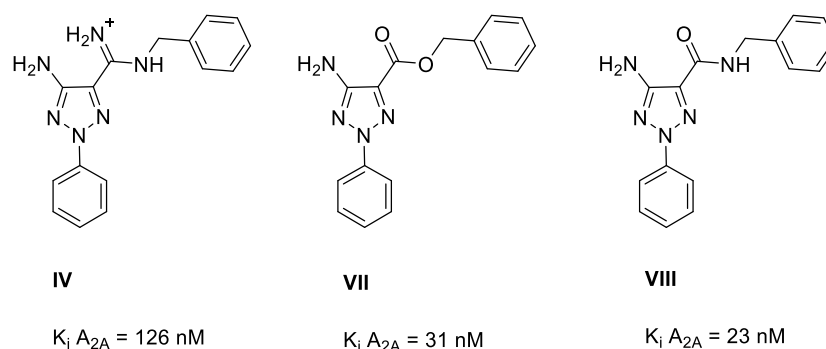


Figure 3. Aminotriazole derivatives with different conjunctions and their affinities for the $A_{2A}AR$.^{1;3}

On the basis of the reported triazoles, 6 different moieties were carefully selected for the new N1 position of the pyrazole: 3,4-difluorobenzyl, 3-hydroxybenzyl, 4-hydroxybenzyl, 1*H*-indazol-5-yl, and 1*H*-pyrazole-5-yl as well as an unsubstituted phenyl residue. Since the synthesis of the hydroxybenzyl derivatives involves the corresponding methoxy derivatives, those will be isolated and tested as well, leading to 8 different residues altogether. The benzyl moiety was planned to be explored with different (mostly) *ortho*-substituted benzylamines with small residues like halogens or (alkylated) OH groups (cf. Figure 4). Also, cyclic structures like aminoindane were planned to be explored.

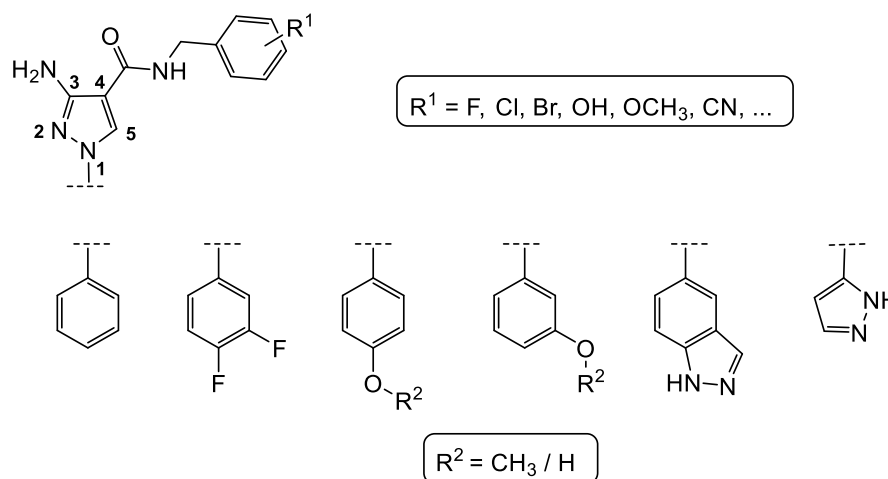


Figure 4. Overview of designed 3-amino-*N*-benzyl-1-phenyl-1*H*-pyrazole-4-carboxamides.

Many of the reported triazoles were substituted with benzyl moieties at the position 4 of the triazole. To investigate the importance of the methylene linker, slightly different building blocks were additionally planned for that position: phenylhydrazine and *O*-phenylhydroxylamine.

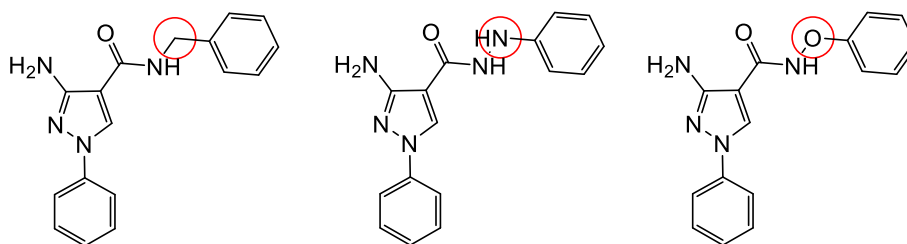


Figure 5. Planned structures with altered benzylamine moieties.

Also, an entirely unsubstituted compound was planned to be prepared. This compound is a neutral point to compare the influences of substituents and also the importance of a methylene linker.

4.3.2.2. Substitution of position 5 of aminopyrazoles

Crystal structure analysis of aminotriazoles cocrystallized with the $A_{2A}AR$ indicate that free space at position 5 of the pyrazole core might be available (cf. Figure 6, red circle).¹ Small residues including a methyl group or halogens were planned as substituents at position 5 to explore a possible binding pocket.

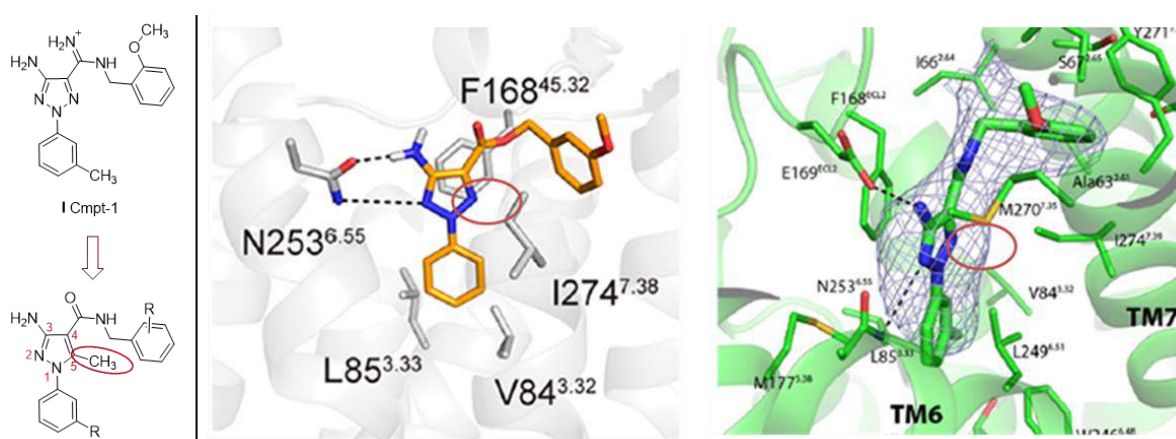


Figure 6. Crystal structures of Cmpd-1 (I) in the $A_{2A}AR$ and suggested new structure.^{1,3}

Moreover, the crystal structure suggests, that the 3-amino group, being important for receptor interaction, should be closer to the amino acid residues E169 and N253. This could be probed with hydrazine structure or a CH_2NH_2 group at position 3 of the pyrazole ring (cf. Scheme 7).

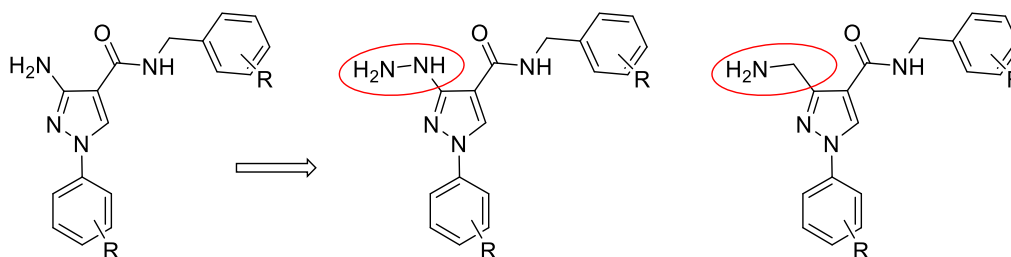
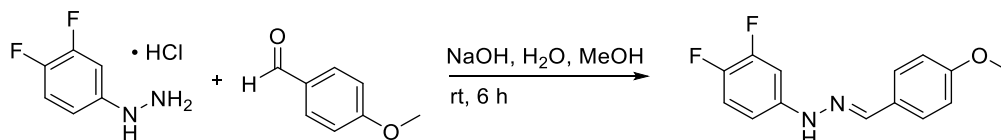


Figure 7. Planned structures with altered 3-amino group.

4.3.3. Synthesis of 3-amino-*N*-benzyl-1-phenyl-1*H*-pyrazole-4-carboxamides

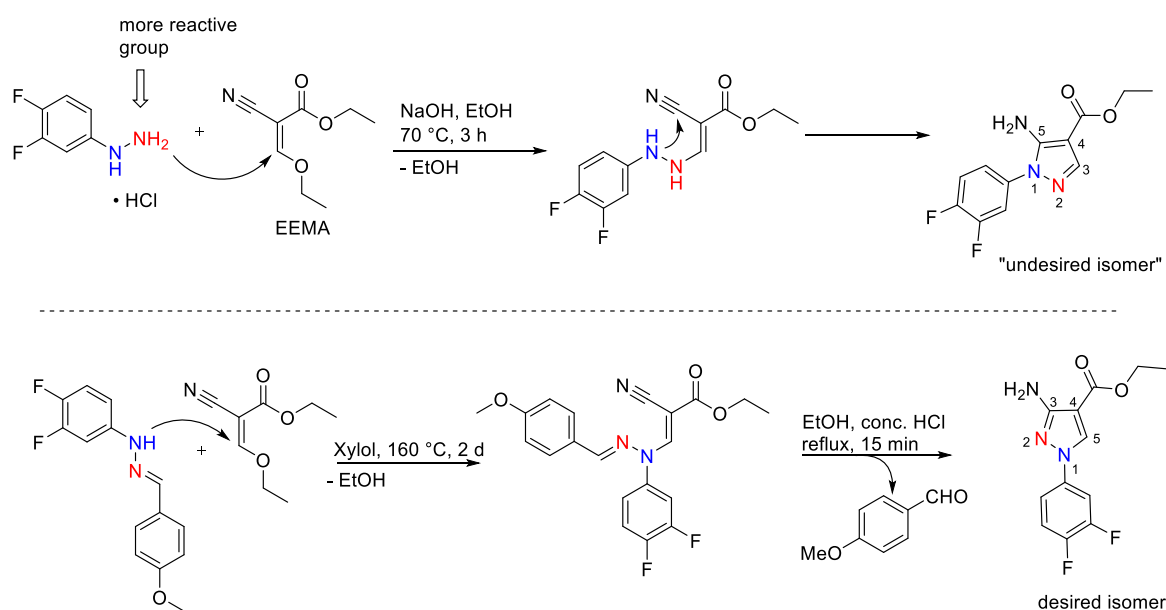
4.3.3.1. Synthesis towards 3-amino-*N*-benzyl-1-phenyl-1*H*-pyrazole-4-carboxamides based on phenylhydrazines

The synthetic route towards 3-amino-*N*-benzyl-1-phenyl-1*H*-pyrazole-4-carboxamides, as described in literature, starts with a phenylhydrazine forming an imine with a simple aromatic aldehyde like benzaldehyde or anisaldehyde.⁴ 3,4-Difluorophenylhydrazine was initially selected as starting material due to its availability.



Scheme 1. Planned synthesis of (*E*)-1-phenyl-2-(4-methoxybenzylidene)hydrazine derivative.

The imine serves as a protection group. Without that protection, the next reaction step would lead to an undesired isomer or, depending on the synthetic conditions, to a mixture of isomers (cf. Scheme 2).⁵



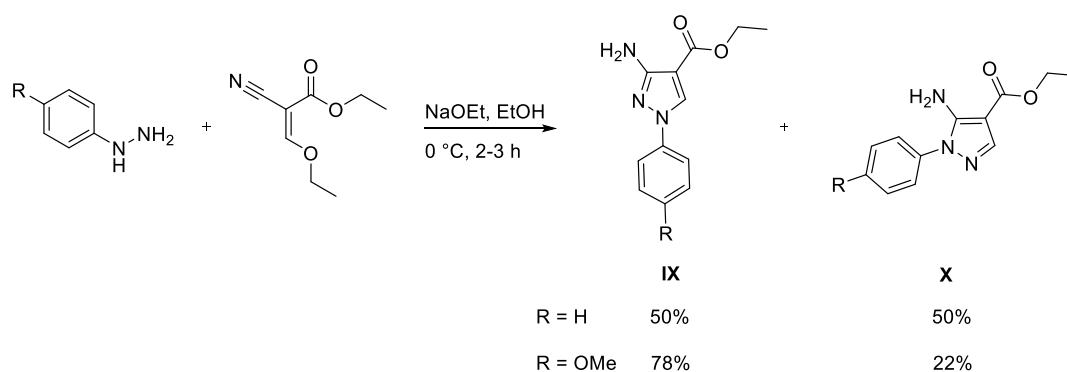
Scheme 2. Reaction mechanism of the formation of the undesired ethyl 5-amino-1-phenyl-1*H*-pyrazole-4-carboxylate and the desired ethyl 3-amino-1-phenyl-1*H*-pyrazole-4-carboxylate, respectively.

Due to steric hindrance and the higher reactivity, the NH₂ group of the respective phenylhydrazine (highlighted in red in Scheme 2) would perform a nucleophilic attack at the reactive position of the ethyl(ethoxymethylene)cyanoacetate (EEMA), eliminating EtOH as a leaving group. Subsequent nucleophilic addition of the remaining NH of the hydrazine at the

cyano group would finally lead to an undesired ethyl 5-amino-1-phenyl-1*H*-pyrazole-4-carboxylate (cf. Scheme 2, top).⁵ Two derivatives of that isomer were planned to be synthesized and tested in order to explore this isomeric scaffold, although these isomers could not be expected to be active. A comparison of the spectral properties of both isomers can be utilized to confirm the identity of the desired isomer.

Employing the protection group strategy, only the NH of the respective phenylhydrazine is able to react with EEMA (blue highlighted in Scheme 2). Due to steric hindrance and lower reactivity, the reaction conditions need to be much harsher. While the undesired isomer is formed after 3 h at 70 °C or longer reaction time at rt, the intermediate of the desired isomer is only formed at very high temperature and after a long reaction time (2-3 days at 160 °C). Subsequent heating in EtOH with conc. aqueous HCl solution leads to a deprotection of the hydrazine's amino group via hydrolysis of the imine. Finally, the nucleophilic addition of the free amino group at the cyano group forms the desired ethyl 3-amino-1-phenyl-1*H*-pyrazole-4-carboxylate.^{4,6}

Other procedures for the preparation of 3-aminopyrazoles have been described.⁵ They did not exploit the above-mentioned protection group strategy. Instead, they used very basic conditions (2 eq. NaOEt over 45 min, 3 h stirring at 0°C). This method was described to be faster and cheaper as compared to the protection group strategy. However, the described syntheses using phenylhydrazine and 4-methoxyphenylhydrazine as examples led to the formation of isomers (**IX**, 50 : 50 and **X** 78 : 22, respectively). Separating the corresponding isomers would be difficult, so this method is unfeasible for the current project.

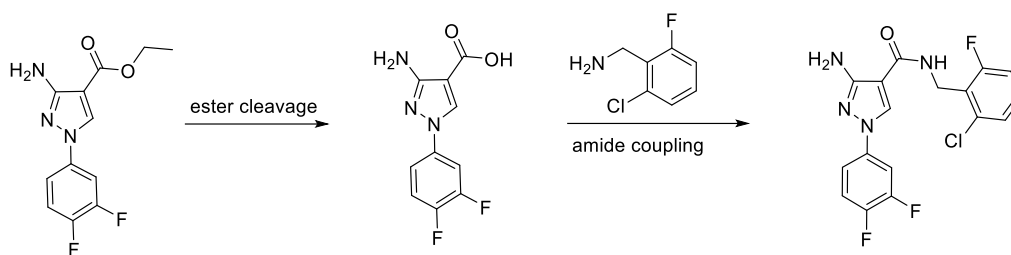


Scheme 3. Synthesis of aminopyrazole isomers.⁵

A simple method to synthesize 3-amino-1-(phenyl)-1*H*-pyrazole derivatives starting from unprotected phenylhydrazines was described by Jia, H. et. al.⁷ in 2020 and in a patent from 2017.⁸ This method was studied in order to avoid the tedious alternative route using protection group techniques. The method suggested that heating the respective phenylhydrazine and EEMA with sodium acetate in a water / AcOH mixture at 130°C for 1 h would lead to the desired 3-amino-1-phenyl-1*H*-pyrazole-4-carboxylate.^{7,8} However, an analysis including TLC, HPLC-

UV/Vis, and NMR spectroscopy (see section 4.3.4.2) confirmed that the undesired ethyl 5-amino-1-phenyl-1*H*-pyrazole-4-carboxylate was formed instead. These findings show that the published and even patented procedures cannot be reproduced and that the protection group strategy is still the method of choice, despite its inconvenience.

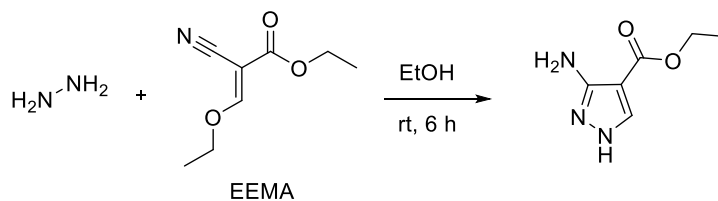
The formation of the respective ethyl 3-amino-1-phenyl-1*H*-pyrazole-4-carboxylate is supposed to be followed by basic hydrolysis of the ester and subsequent amide coupling reaction with different benzylamines to form the amide at position 4 of the pyrazole. Scheme 4 illustrates the reactions with 2-chloro-6-fluorobenzylamine as an example.



Scheme 4. Planned synthetic route to form 3-amino-*N*-benzyl-1-phenyl-1*H*-pyrazole-4-carboxamides.

4.3.3.2 Planned synthesis of 3-amino-*N*-benzyl-1-phenyl-1*H*-pyrazole-4-carboxamides using coupling reactions

As another attempt, the synthesis of 3-amino-*N*-benzyl-1-phenyl-1*H*-pyrazole-4-carboxamides could start with the preparation of ethyl 3-amino-1*H*-pyrazole-4-carboxylate followed by copper-catalyzed coupling reactions (cf. Scheme 5).⁵



Scheme 5. Synthesis of ethyl 3-amino-1*H*-pyrazole-4-carboxylate.⁵

The unprotected 3-aminopyrazole (literature reported the emergence of side products and isomers for the unprotected molecule)⁴ or NH₂-protected derivatives could be used for coupling reactions of the Ullmann type using aryl halides and copper catalysis. Such copper-mediated reactions have been widely used for the formation of natural products and drug molecules in the past.⁹ Although many studies have been made in this field, the exact mechanism is not yet fully understood.^{10;11} One common theory for amination of aryl halides is that the Cu(I)-halide (being in complex with two ligands) and the deprotonated amine form a complex in the first step (cf. Figure 8). The oxidative addition of an aryl halide leads to a Cu(III) species complexing

the two ligands, the halide, the amine and the aromatic moiety. A reductive elimination yields the desired arylamine while the copper catalyst is regenerated. The reacting amines can be aliphatic amines or NH-containing heterocyclic structures.^{10;11}

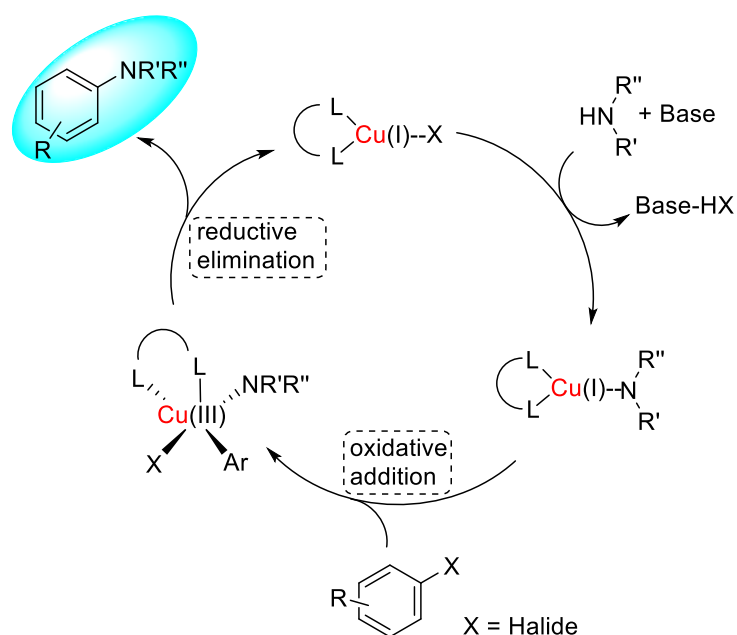
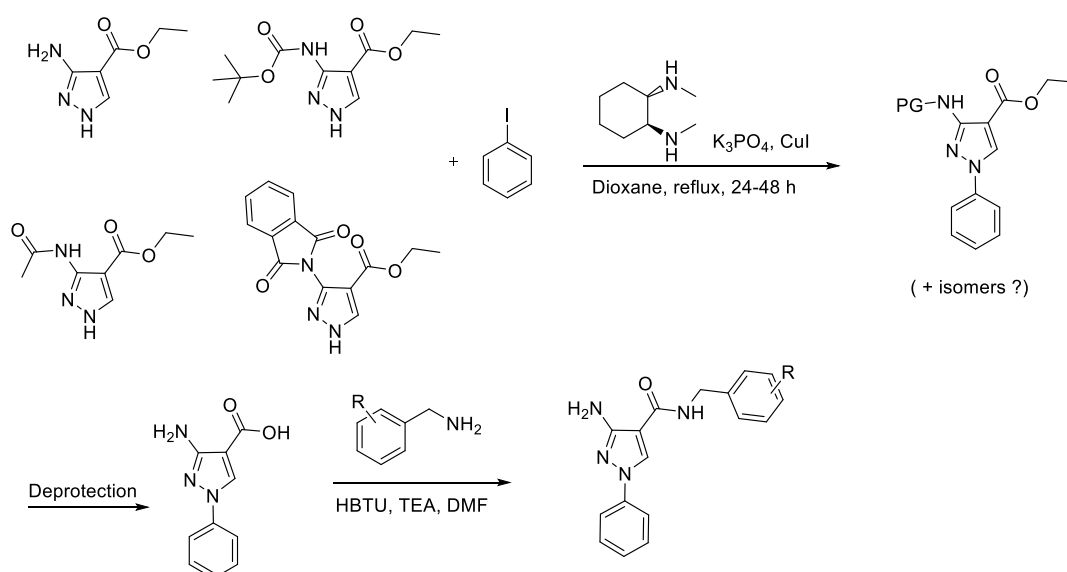


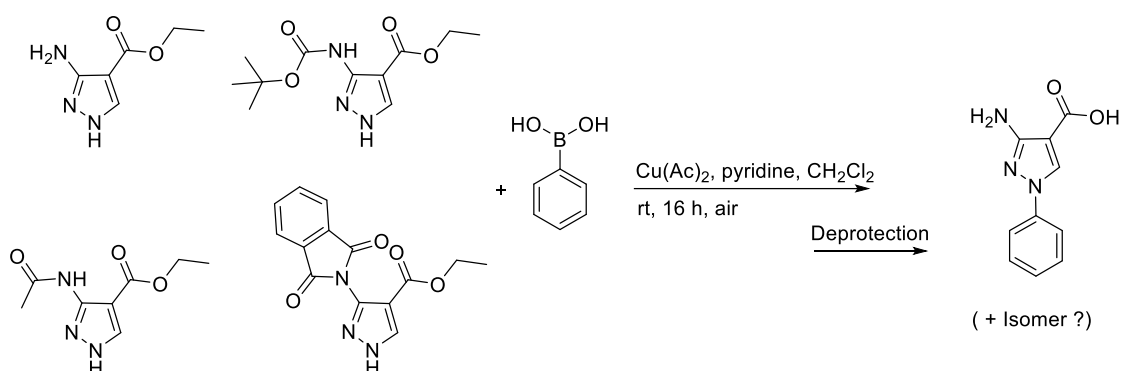
Figure 8. Catalytic cycle of copper(I) catalyst during Ullmann amination reaction.^{10;11}

Scheme 6 illustrates different protected 3-aminopyrazoles and the described reaction conditions with iodobenzene as an example. As illustrated, the procedure includes a Cu(I) salt, a base and a bidentate ligand, and fairly harsh reaction conditions.^{4;12} A subsequent deprotection of the amino group and the carboxylic acid (possibly in one reaction step) would lead to a building block that can be coupled with different benzylamines.



Scheme 6. Possible synthetic route for the synthesis of 3-amino-1-phenyl-1H-pyrazole-4-carboxylic acid employing an Ullmann reaction and protection groups.

A different reaction type - the Chan-Lam-coupling reaction - could use (protected) 3-aminopyrazoles and boronic acids under copper catalysis to form similar intermediates as illustrated in Scheme 7.¹³ The conditions for this reaction type are much milder as compared with the Ullmann coupling reaction. The reaction takes place at rt and under air making the reaction much more feasible. However, more copper (1.5 eq., in this case in form of $\text{Cu}(\text{Ac})_2$) is required, making the reaction less ecofriendly.¹³ An excess of pyridine serves as ligands for the $\text{Cu}(\text{II})$ ion. The obtained intermediates could finally result in the respective 3-amino-1-phenyl-1*H*-pyrazole-4-carboxylic acid after deprotection steps, similar to the reactions in Scheme 6.



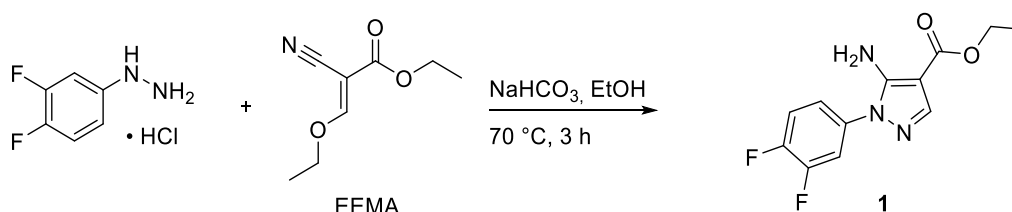
Scheme 7. Possible synthetic route to form 3-amino-1-phenyl-1*H*-pyrazole-4-carboxylic acid employing boronic acid coupling and protection groups.

These synthetic routes involving coupling reactions are particularly interesting if the phenyl moiety at the 1-position of the pyrazole is not available or the corresponding phenylhydrazine cannot be prepared.

4.3.4. Synthesis

4.3.4.1. Synthesis of 5-amino-*N*-benzyl-1-(3,4-difluorophenyl)-1*H*-pyrazole-4-carboxamide derivatives

The synthesis of the undesired isomer was straightforward. 3,4-Difluorophenylhydrazine hydrochloride and EEMA were heated in EtOH in the presence of a base (NaHCO_3).⁵ The product could be isolated via column chromatography and was obtained in 68% yield.



Scheme 8. Synthesis of compound 1.⁵

A 2D-Noesy NMR spectrum revealed an interaction between the amino-group (5.27 ppm) and *ortho*-protons of the 3,4-difluorophenyl moiety (7.23 ppm). No interaction between the proton of C3 of the pyrazole and any other H atom could be observed.

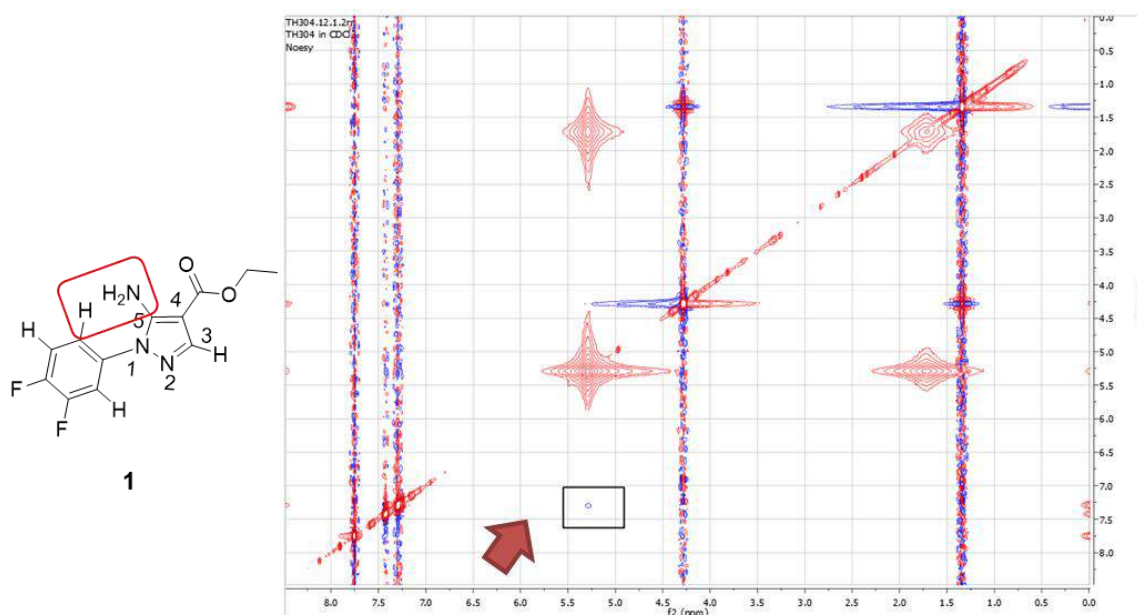
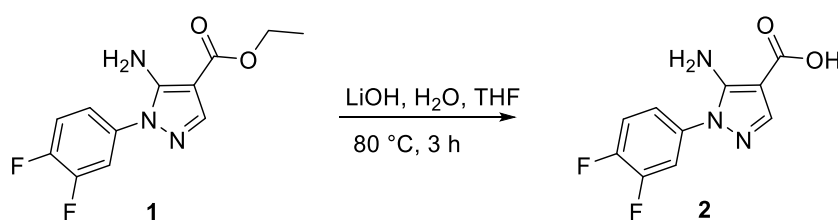


Figure 9. 2D-Noesy NMR spectrum of **1**; the red arrow points at the described interaction.

Subsequent saponification leading to compound **2** required surprisingly harsh conditions. Normally, 5 equivalents of LiOH hydrate at rt in a THF / water mixture are sufficient to cleave ethyl esters. In this case, however, 80 °C (and 3 h reaction time) were required for the conversion to the free carboxylic acid. Subsequent acidification to pH 3 and extraction with CH₂Cl₂ led to the desired compound **2** in 79% yield and 97 % purity.



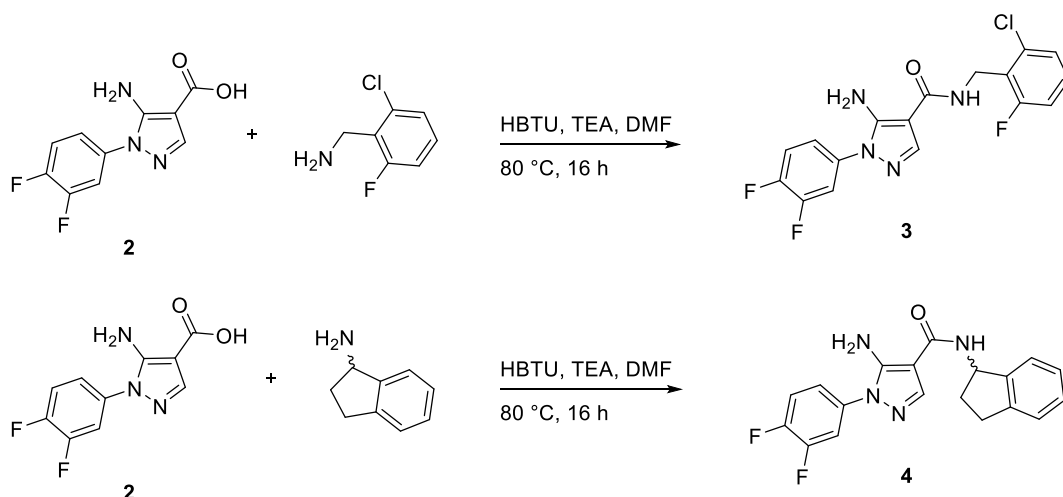
Scheme 9. Synthesis of compound **2**.

Finally, the carboxylic acid **2** could be used to explore the reaction conditions for the final amide formation. Different coupling reagents and reaction conditions were tested with 2-chloro-6-fluorobenzylamine as amine. In any case, 1.3 equivalents of amine and 1.5 equivalents of triethylamine (TEA) as a base were employed.

- Using T3P (propanephosphonic acid anhydride, 1.5 equivalents) in CH₂Cl₂ at rt led to side-products. TLC-MS analysis showed that **2** was consumed but no product was found; some unreacted amine was left.

- A reaction with BOP reagent (benzotriazolyl-oxy-tris(dimethylamino)-phosphonium hexafluorophosphate, 1.5 eq.) in THF as a solvent at rt also led to side products and unreacted starting material; no product mass could be found by TLC-MS.
- Refluxing of **2** with 1.5 equivalents of SOCl₂ in toluene was supposed to convert it to the corresponding carboxylic acid chloride. TLC analysis showed that this first step was already accompanied by the formation of side products. After removing of the solvents under reduced pressure, the crude mixture was dissolved in CH₂Cl₂ and treated with TEA and 2-chloro-6-fluorobenzylamine at rt. This method actually resulted in the formation of the desired product, however, too many side products made the method uneconomic.
- Finally, using HBTU (2-(1*H*-benzotriazol-1-yl)-1,1,3,3-tetramethyluronium-hexafluorophosphat, 1.5 eq.) in DMF led to good results. At rt, a small amount of product could be found in TLC-MS analysis after 8 h reaction time. The biggest spot, however, was found for the intermediate product formed by **2** and the benzotriazol of the HBTU reagent. This led to the assumption, that this intermediate is simply not reactive enough. This was also observed during saponification which required heating. Thus, the reaction mixture was heated to 80 °C for 16 h, finally leading to a suitable amount of product that could be isolated by column chromatography (CH₂Cl₂/ MeOH - 95 : 5).

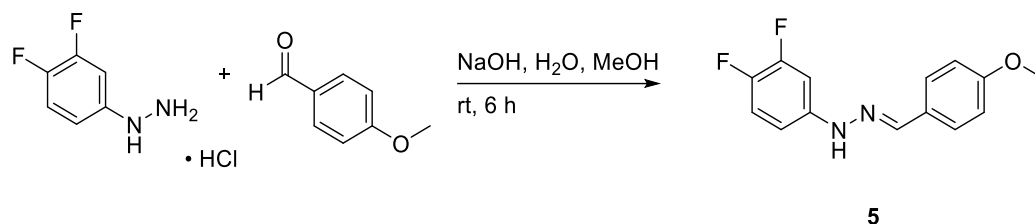
With a yield of 50% and 93% purity, this method was chosen to be the synthetic route for future reactions. Scheme 10 illustrates the successful reaction conditions. The same method was used to form **4**. The products **3** and **4** were submitted to biological testing to explore the biological activity of this isomer.



Scheme 10. Synthesis of compounds **3** and **4**.

4.3.4.2. Establishment of a general synthesis of 3-amino-*N*-benzyl-1-phenyl-1*H*-pyrazole-4-carboxamide derivatives

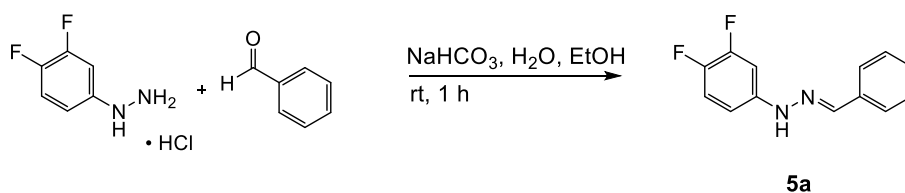
The first reaction step towards the 3-amino-*N*-benzyl-1-(3,4-difluorophenyl)-1*H*-pyrazole-4-carboxamide scaffold was the protection of the required phenylhydrazine (**5**). Therefore, a method from literature was used that suggested a MeOH / water mixture (8 : 2) as solvent and NaOH to neutralize the hydrochloride (cf. Scheme 11). Due to its supposedly high reactivity, anisaldehyde was chosen as reagent.⁴



Scheme 11. Synthesis of compound **5**.⁴

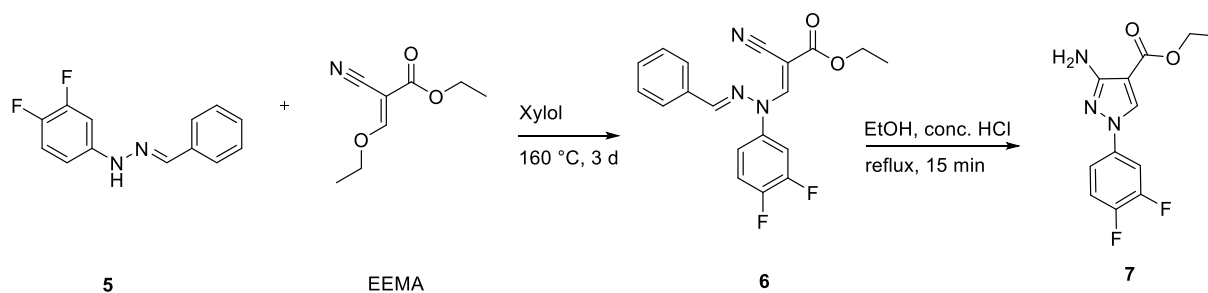
This method turned out to be disadvantageous; it resulted in side products and unreacted starting material that required purification via column chromatography (petrol ether / ethyl acetate - 8 : 2).

A different approach using NaHCO₃ as a base and a mixture of EtOH / water (1 : 1) as solvent, and benzaldehyde was used in a second trial.⁶ These conditions resulted in a high yield (97%) and purity (95%). After precipitation, the product was simply filtered and washed with water and EtOH.



Scheme 12. Synthesis of compound **5a**.⁶

In the next reaction step, the protected phenylhydrazine **5a** was reacted with EEMA at 160 °C in xylene. After three days, the reaction mixture was analyzed by TLC; the intermediate **6** could be found in obviously high purity according to analysis by TLC-MS. The crude intermediate was treated with conc. HCl and EtOH (1 : 2) and refluxed for 15 min. This reaction step led to many side products, even unprotected 3,4-difluorophenylhydrazine was detected by LC-MS.



Scheme 13. Synthesis of compound **7**.^{5,6}

Purification using column chromatography (CH₂Cl₂/ MeOH - 98 : 2) led to the desired product **7** in low yield (29%, 85% purity). However, this yield is still nearly twice as high as described in the literature for similar derivatives (15%).^{5,6}

A 2D-Noesy NMR analysis of **7** revealed an interaction between the proton of C5 (8.05 ppm) of the pyrazole and two of the aromatic protons in *ortho*-position of the 3,4-difluorophenyl moiety (7.48 / 7.30 ppm). No interaction between the amino-group and the 3,4-difluorophenyl moiety could be observed. This analysis proved the formation of the desired isomer and showed that the protection group strategy had been successful.

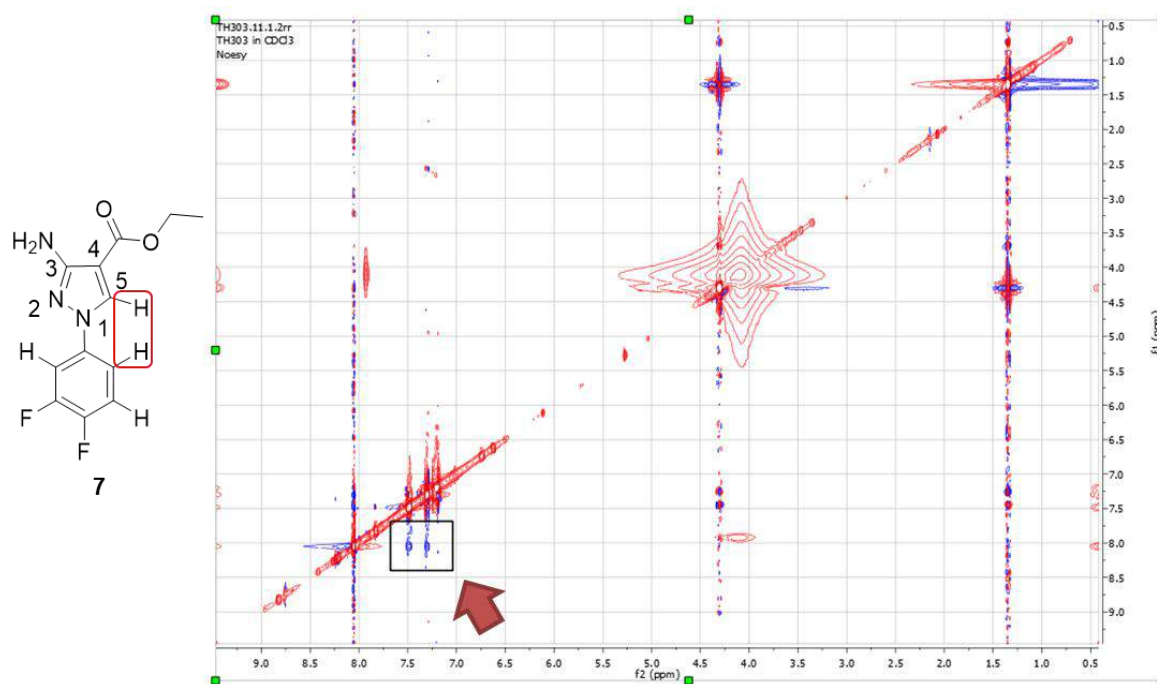


Figure 10. 2D-Noesy NMR analysis of **7**; the red arrow points at the described interaction.

Fortunately, the different isomers **1** and **7** gave very different UV/Vis spectra in the LC-MS analysis (performed by a DAD detector) so that both compounds and other comparable isomers could be distinguished by that method (cf. Figure 11).

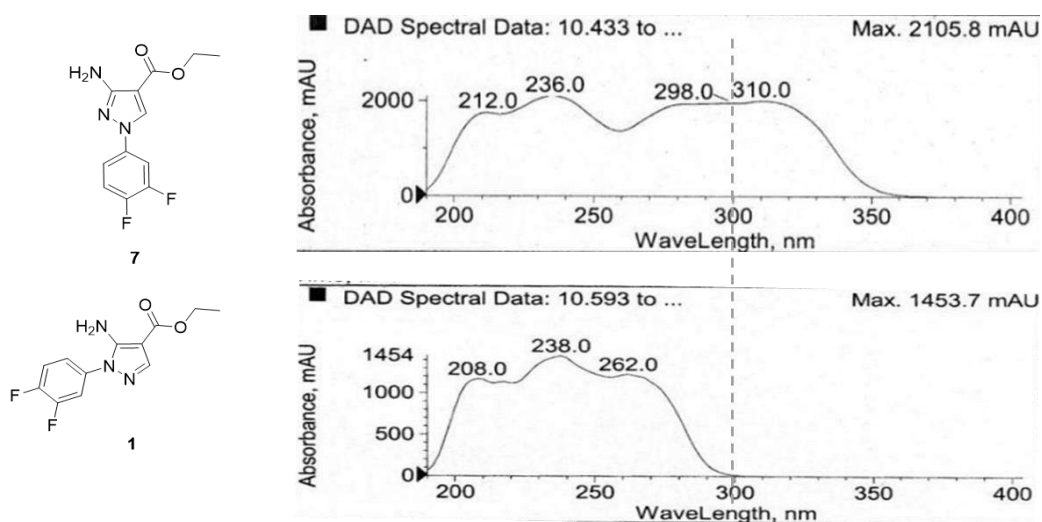
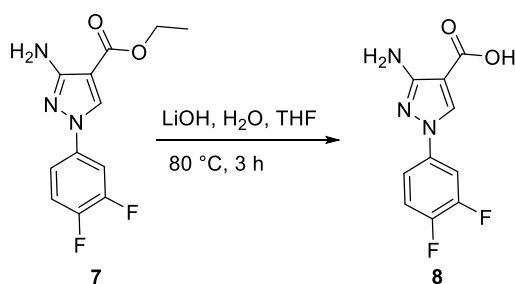


Figure 11. UV/Vis spectra of **7** and **1** using an HPLC-UV(DAD).

While the ethyl 5-amino-1-phenyl-1*H*-pyrazole-4-carboxylate **1** does not absorb light at around 300 nm, the ethyl 3-amino-1-phenyl-1*H*-pyrazole-4-carboxylate **7** displayed strong absorption at 300 nm and an absorption maximum at 310 nm. Furthermore, the desired isomer showed strong blue fluorescence under UV light while the undesired isomer was not fluorescent at all. These spectral properties have been reported in the literature for comparable 2-phenyl-1,2,3-triazole derivatives which also showed fluorescent properties.¹⁴ Hence, it was possible to differentiate the isomers via TLC-UV analysis as well.

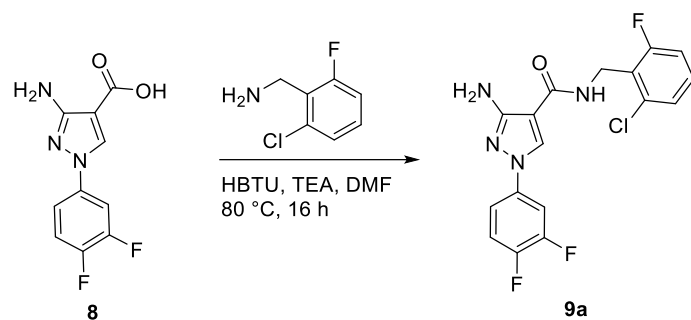
Subsequent saponification was performed as established for **1** but led to a lower yield (52%, purity: 87%).



Scheme 14. Synthesis of compound **8**.

Maybe the extraction step led to a loss of product. It might be a better method to neutralize the reaction mixture and directly purify the crude carboxylic acid via RP-HPLC. This might lead to better yields, but adds an additional purification step.

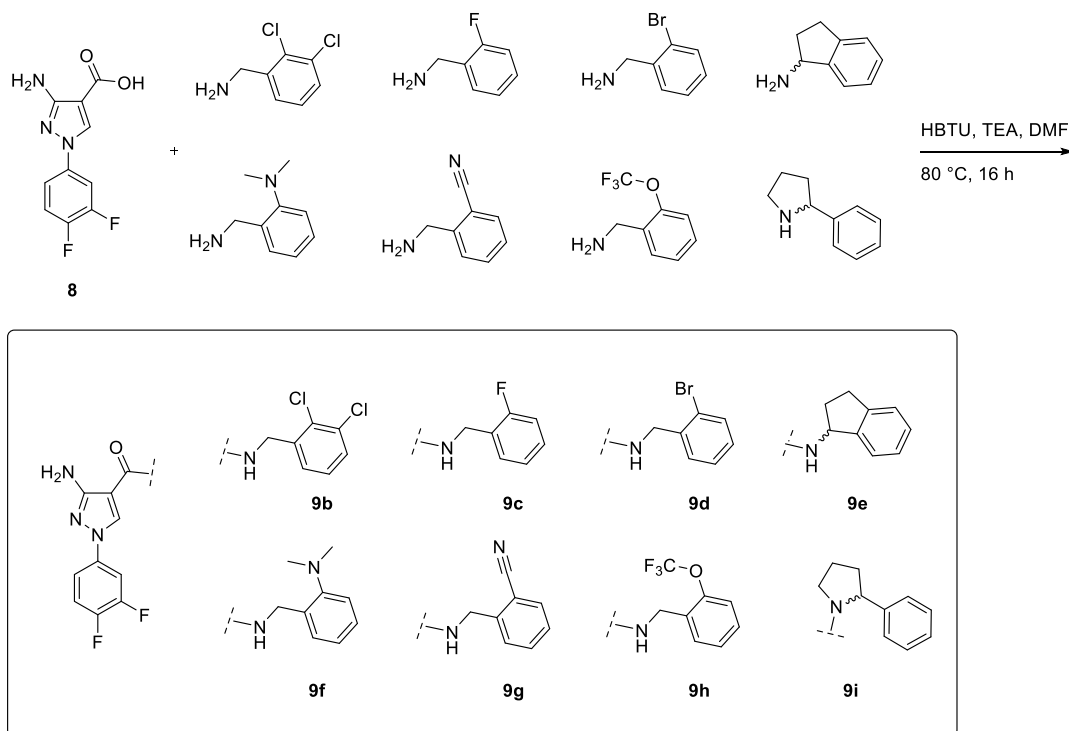
The previously established amide formation employing HBTU was applied for **8** and 2-chloro-6-fluorobenzylamine to form **9a**. The yield was much lower (22%) as compared to the formation of **3**, but the product could be isolated in high purity (95%) using RP-HPLC (10 to 100% MeOH) and a subsequent column chromatography on normal phase (CH₂Cl₂/ MeOH - 95 : 5).



Scheme 15. Synthesis route of compound **9a**.

4.3.4.3. Synthesis of 3-amino-*N*-benzyl-1-(3,4-difluorophenyl)-1*H*-pyrazole-4-carboxamide derivatives

With a suitable synthetic route at hand, the carboxylic acid **8** was bound to several benzylamides to form the illustrated final compounds (Scheme 16). On the basis of the reported aminotriazoles, several benzylamines were chosen to form different 3-amino-*N*-benzyl-1-phenyl-1*H*-pyrazole-4-carboxamide derivatives (cf. Scheme 4). Most of those selected benzylamines were *ortho*-substituted with small residues. Two special amines were chosen in order to investigate if rigid conformations at the benzylamine moiety are accepted by the receptor: 2-aminoindane (**9e**) and 2-phenylpyrrolidine (**9i**), both exhibiting a benzylamine structure but being integrated to different five-membered rings.



Scheme 16. Synthesis of 3-amino-*N*-benzyl-1-(3,4-difluorophenyl)-1*H*-pyrazole-4-carboxamides **9b-9i**.

Table 1. Selected experimental data of derivatives **9a-9i**.

<i>Compd.</i>	<i>Yield</i>	<i>Purity</i>	<i>MW</i>	<i>Mp.</i>
9a	22%	95%	379.9	198 °C
9b	8%	85%	397.0	178 °C
9c	20%	99%	346.0	154 °C
9d	21%	94%	408.1	171 °C
9e	22%	95%	354.1	192 °C
9f	9%	80%	371.1	166 °C
9g	20%	97%	353.1	198 °C
9h	13%	80%	412.0	175 °C
9i	52%	95%	367.8	188 °C

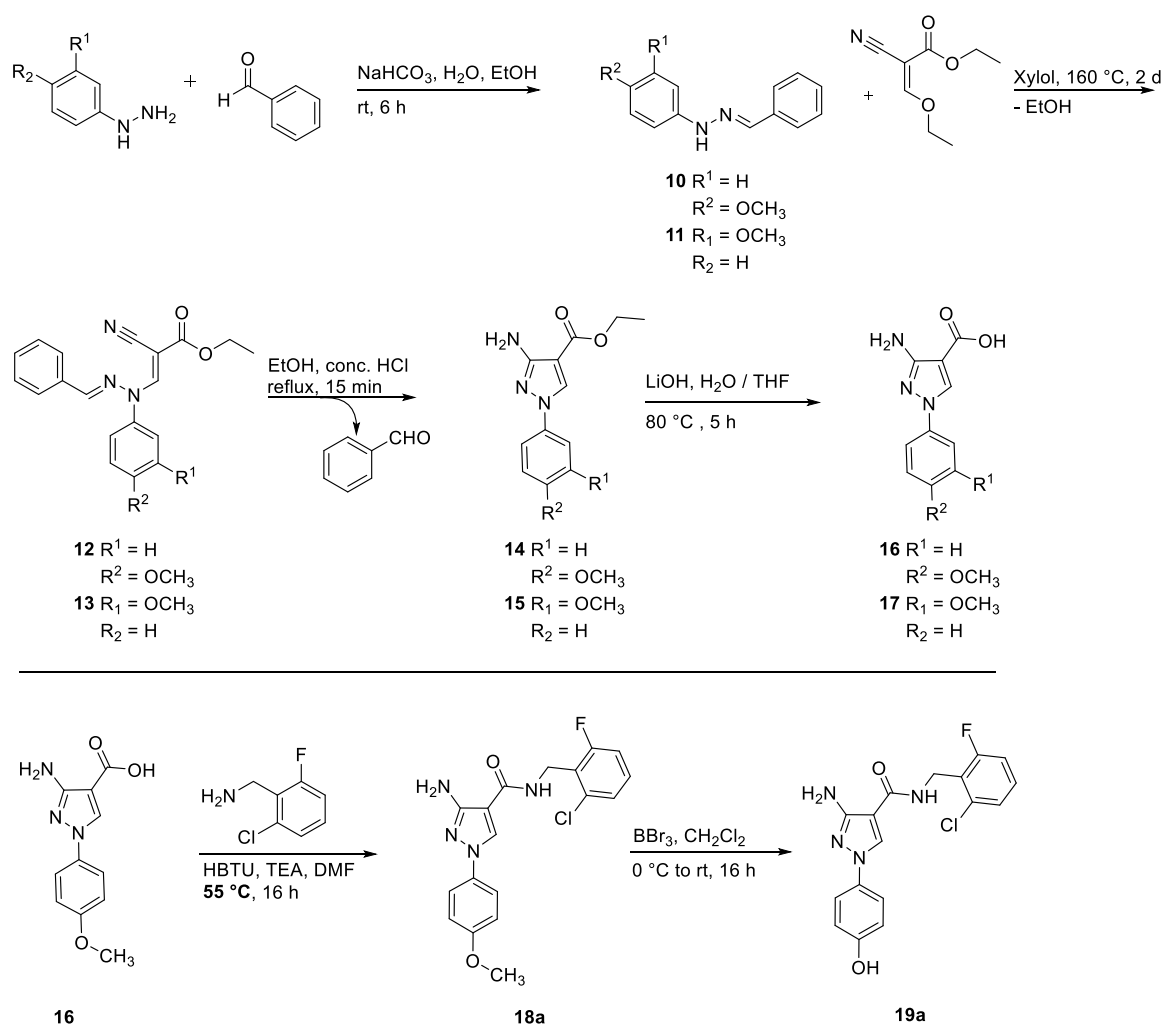
Most products were isolated in very low yields (8 - 21%). Only **9i** was obtained in a satisfactory yield of 52%. As it turned out, most of the employed benzylamines were very old and partly decomposed, which could be seen during TLC analysis of the reaction mixtures when the benzylamines were used as references. The utilization of pure benzylamines should result in better yields. To isolate the final products in sufficient purity, each one had to be purified by at least one run of RP-HPLC and one run of normal phase column chromatography.

4.3.4.4. Synthesis of 3-amino-*N*-benzyl-1-(3-hydroxyphenyl)-1*H*-pyrazole-4-carboxamides and 3-amino-*N*-benzyl-1-(4-hydroxyphenyl)-1*H*-pyrazole-4-carboxamides

All compounds were prepared according to the established method. The appropriate hydrazines (4-methoxyphenylhydrazine hydrochloride or 3-methoxyphenylhydrazine hydrochloride, respectively) were protected by imine formation with benzaldehyde. The imines (**10** and **11**) were reacted with EEMA under harsh reaction conditions to form intermediates **12** and **13**. Subsequent deprotection under acidic conditions followed by an addition reaction led to the desired ethyl 3-amino-1-phenyl-1*H*-pyrazole-4-carboxylates **14** and **15**.⁴⁻⁶ The ester was saponified to afford the corresponding carboxylic acid **16** and **17** that was subsequently used to form several different amides.

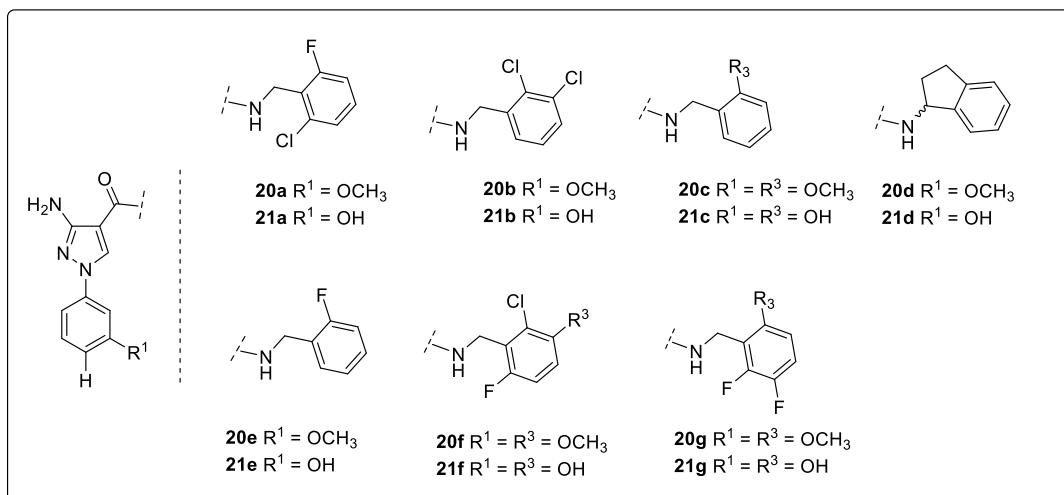
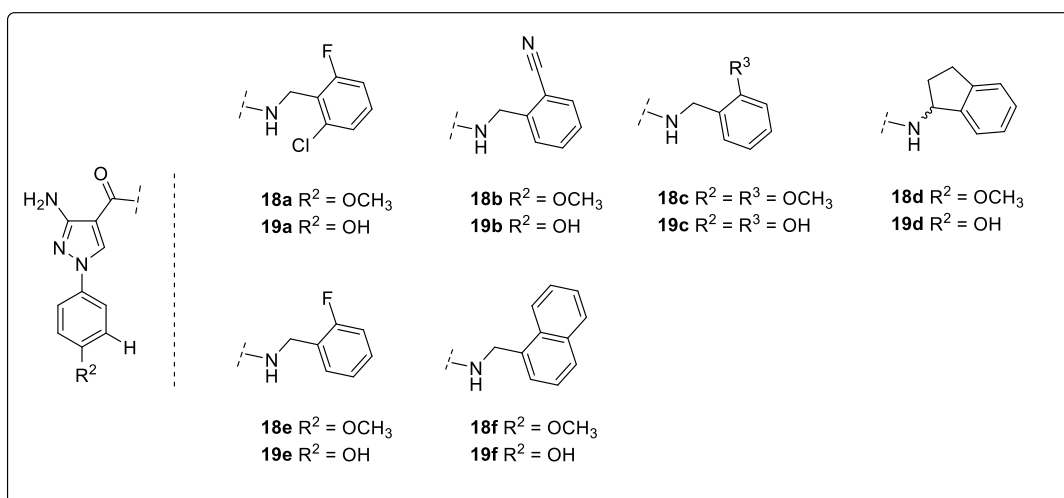
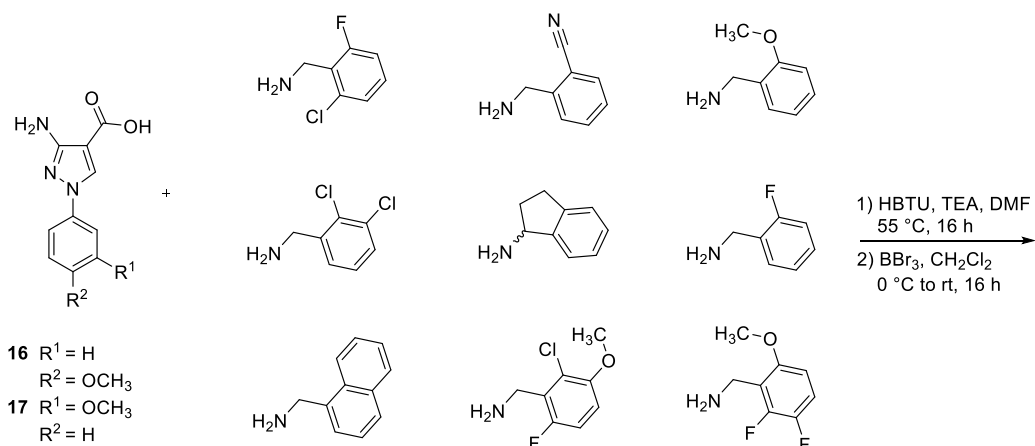
It is noteworthy, that the reaction conditions for the amide formation were improved: the reaction temperature was lowered from 80 to 55 °C, this still led to the desired product but the reaction is accompanied by less formation of side products. The last reaction step for the compound family was the deprotection of the methoxy group at the phenyl ring at the N1-position to afford the corresponding hydroxyphenyl moiety. This was done using BBr₃ in CH₂Cl₂. Scheme 17 illustrates the general synthetic route leading to the formation of the 3-amino-1-phenyl-1*H*-pyrazole-4-carboxylic acids **16** and **17** as well as a reaction to form a 3-

amino-*N*-benzyl-1-(4-methoxyphenyl)-1*H*-pyrazole-4-carboxamide (**18a**) and the subsequent deprotection to a 3-amino-*N*-benzyl-1-(4-hydroxyphenyl)-1*H*-pyrazole-4-carboxamide (**19a**) as an example.



Scheme 17. General synthetic route to form 3-amino-*N*-benzyl-1-(4-hydroxyphenyl)-1*H*-pyrazole-4-carboxamides; syntheses of **18a** and **19a** as examples.

Scheme 18 illustrates all used benzylamines and final products. Both methoxy- and hydroxyphenyl-derivatives were isolated and submitted to biological testing. For all reactions that yielded methoxy derivatives the yield of the derivative was calculated for the isolated amount of product that was submitted to biological testing. In most cases, impure methoxy derivatives were used for the subsequent demethylation step, these amounts were not considered for the calculation of the yield.



Scheme 18. Synthesis of 3-amino-*N*-benzyl-1-(4-hydroxyphenyl)-1*H*-pyrazole-4-carboxamides **19a-19f** and 3-amino-*N*-benzyl-1-(3-hydroxyphenyl)-1*H*-pyrazole-4-carboxamides **21a-21g**.

Table 2. Selected experimental data of derivatives **18a-18f**, **19a-19f**, **20a-20g** and **21a-21g**.

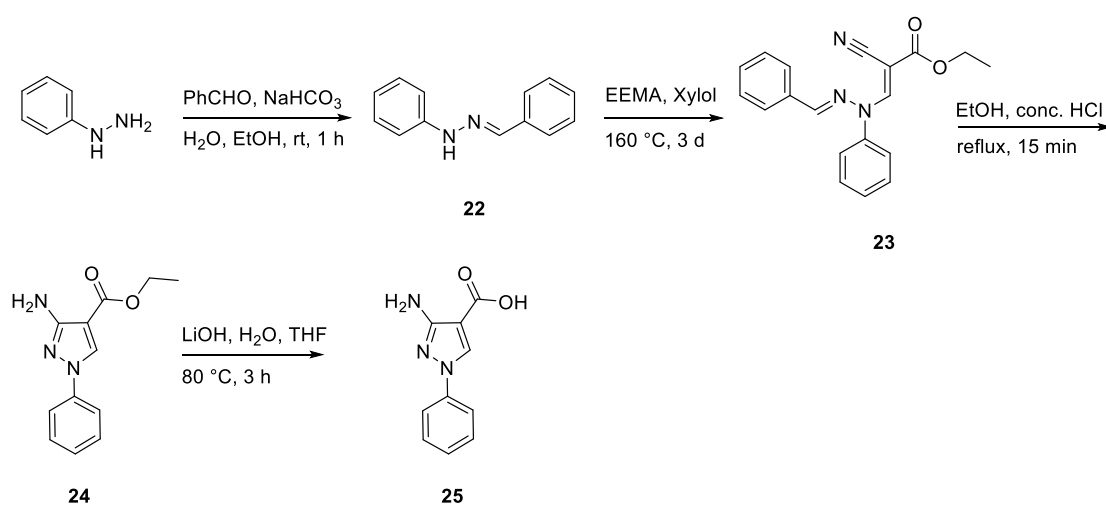
<i>Compd.</i>	<i>Yield</i>	<i>Purity</i>	<i>MW</i>	<i>Mp.</i>
18a	23%	96%	373.9	178 °C
19a	55%	98%	359.9	195 °C
18b	49%	98%	347.0	147 °C
19b	15%	98%	333.0	153 °C
18c	18%	98%	352.0	137 °C
19c	32%	96%	324.2	155 °C
18d	69%	96%	348.0	177 °C
19d	16%	95%	334.1	180 °C
18e	31%	96%	340.2	171 °C
19e	60%	98%	326.1	179 °C
18f	41%	93%	372.1	201 °C
19f	24%	96%	358.2	213 °C
20a	35%	99%	373.9	185 °C
21a	31%	98%	359.9	179 °C
20b	13%	89%	390.1	189 °C
21b	56%	96%	376.2	191 °C
20c	18%	95%	352.1	188 °C
21c	56%	98%	324.2	195 °C
20d	3%	96%	348.0	194 °C
21d	9%	94%	334.1	196 °C
20e	3%	94%	340.2	187 °C
21e	69%	97%	326.1	190 °C
20f	4%	96%	404.2	200 °C
21f	76%	94%	376.2	204 °C
20g	14%	96%	388.3	192 °C
21g	35%	97%	360.2	199 °C

The amide formation gave moderate to low yields because the methoxy derivatives were hard to purify and often needed at least two runs of column chromatography, one on a normal column and one run on a flash RP-HPLC column. The impure fractions obtained from column chromatography were used for the deprotection step. The resulting more polar products could be isolated more easily. If the benzylamine moiety exhibited a methoxy group as well, both methoxy groups were demethylated; this was the case for **19c**, **21c**, **21f** and **21g**. Although the

attempt would have been interesting, no compounds that exhibited one methoxy and one hydroxyphenyl structure were prepared due to synthetic complexity. Not all combinations of carboxylic acids and benzylamines were isolated due to purification issues or because intermediate biological testing results suggested that particular combinations are not tolerated by the $A_{2A}AR$. The building blocks 2-chloro-6-fluoro-3-methoxybenzylamine and 2,3-difluoro-6-methoxybenzylamine were used to explore, if the $A_{2A}AR$ would also tolerate tri-substituted derivatives.

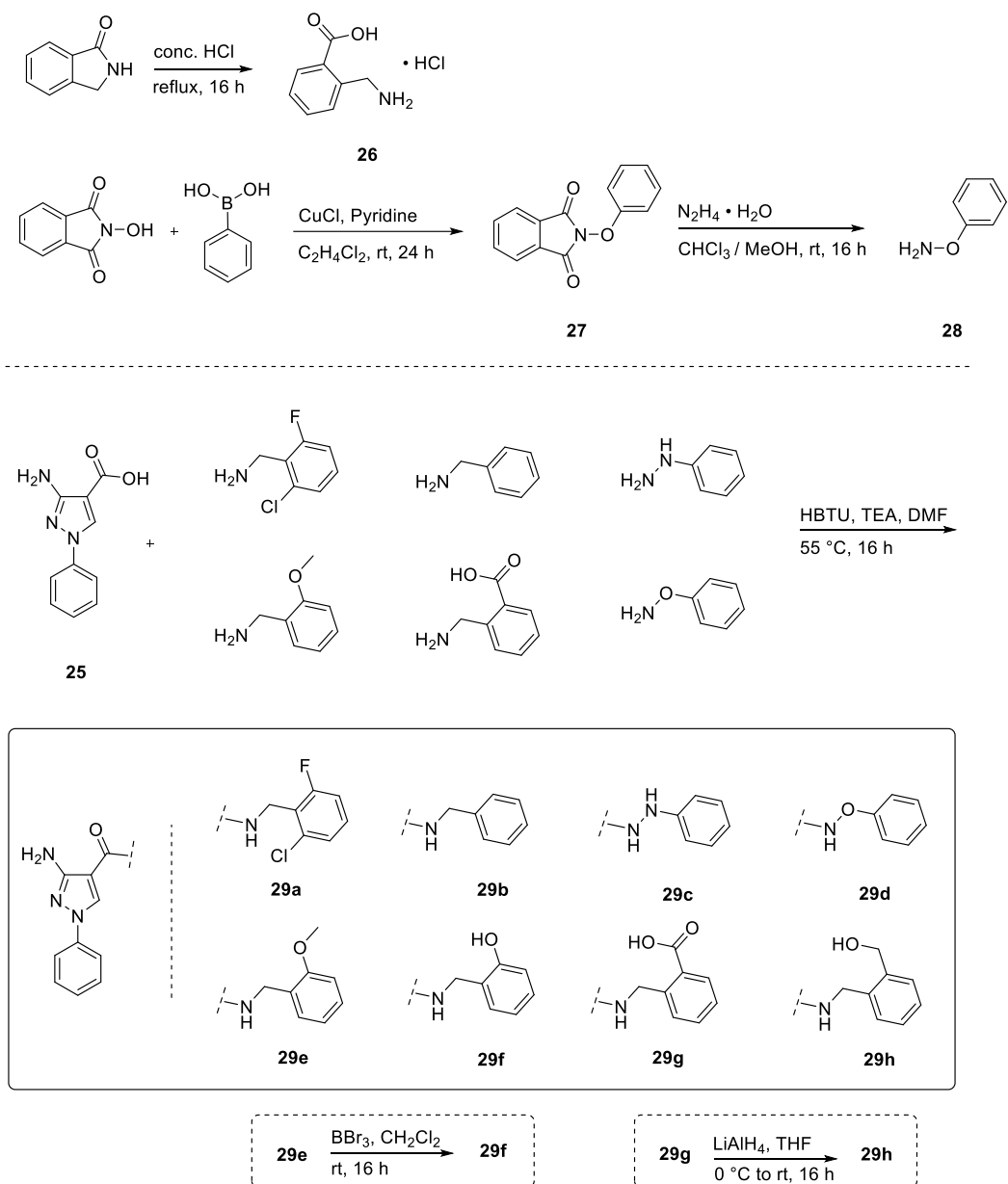
4.3.4.5. Synthesis of 3-amino-*N*-benzyl-1-phenyl-1*H*-pyrazole-4-carboxamide

The compounds illustrated in Schemes 19 and 20 were prepared by employing the abovementioned methods, starting from phenylhydrazine.



Scheme 19. Synthesis of 3-amino-*N*-benzyl-1-phenyl-1*H*-pyrazole-4-carboxylic acid **25**.

It is noteworthy, that the reactions towards carboxylic acid **25** and subsequent reactions involving **25** were more feasible than reactions involving other building blocks. Apparently, the substituents on the phenyl ring at the N1-position influence the reactivity, or the resulting reaction mixtures involving **25** were easier to purify. Carboxylic acid **25** was coupled to a variety of amines using the established method.



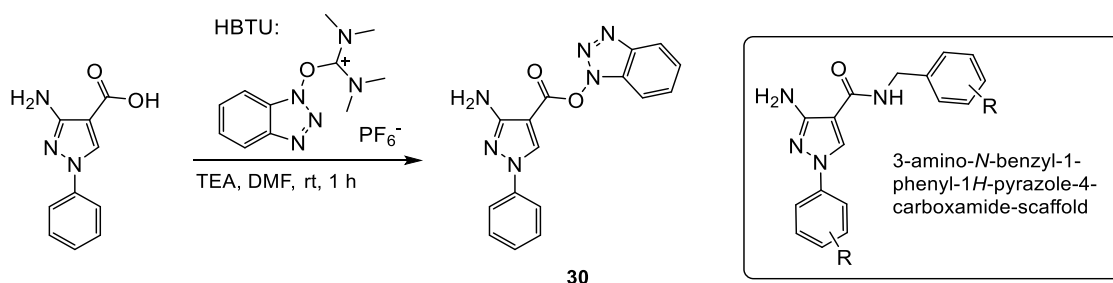
Scheme 20. Synthesis of 3-amino-*N*-benzyl-1-phenyl-1*H*-pyrazole-4-carboxamides **29a-29h**.

Table 3. Selected experimental data of derivatives **29a-29h**.

<i>Compd.</i>	<i>Yield</i>	<i>Purity</i>	<i>MW</i>	<i>Mp.</i>
29a	17%	98%	344.1	160 °C
29b	8%	95%	292.1	151 °C
29c	71%	88%	293.0	177 °C
29d	18%	96%	294.1	165 °C
29e	8%	94%	322.3	163 °C
29f	65%	95%	308.2	175 °C
29g	17%	98%	336.0	223 °C
29h	52%	96%	322.3	197 °C

The methoxy derivative **29e** was subsequently demethylated to **29f** using BBr_3 as described before. Using phenylhydrazine instead of benzylamine was possible and resulted in higher yield (**29c**, 71%) than the reaction with benzylamine (**29b**, 8%). Building block **28**, illustrated in Scheme 20, was prepared by a Chan-Lam-coupling reaction of phenylboronic acid with *N*-hydroxyphthalimide to form **27** which was subsequently deprotected using hydrazine.¹⁵ The amide coupling reaction proceeded similar as for the corresponding benzylamine in moderate yield. The building block **26** was prepared by an acidic hydrolysis of 1-isoindolinone (cf. Scheme 20). The reaction procedure to prepare **29g** was slightly different from the typical conditions: While usually all reagents were mixed at the same time, in this case, all reagents, except for **26**, were mixed, and only one equivalent HBTU was used. These conditions ensured that only the carboxylic acid of **25** would be activated. If the carboxylic acid of **26** would have been activated by the coupling reagent, it would directly react back to 1-isoindolinone. Part of **26** was subsequently reduced using LiAlH_4 in THF to obtain **29h** in good yield.

During the first test reactions, the coupling reagent HBTU was used at rt. This, however, led only to the intermediate **30** that was supposed to react with an amine to form an amide (cf. Scheme 21). The structure of this intermediate interestingly resembles the structure of the given scaffold, the benzotriazolol mimicking the benzylamine moiety of the 3-amino-*N*-benzyl-1-phenyl-1*H*-pyrazole-4-carboxamide.

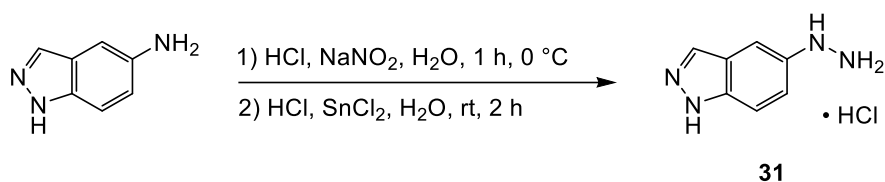


Scheme 21. Synthesis of compound **30**, and general 3-amino-*N*-benzyl-1-phenyl-1*H*-pyrazole-4-carboxamide-scaffold.

To explore if the $\text{A}_{2\text{A}}\text{AR}$ would also tolerate a rigid, bicyclic structures like a benzotriazolyl residue instead of the benzylamine moiety, intermediate **30** was isolated during the reactions of the 3-amino-*N*-benzyl-1-phenyl-1*H*-pyrazole-4-carboxamide family and purified using PR-HPLC (91% purity). During these processes the compound seemed to be stable. Since this compound is still a reactive intermediate, it might react with the receptor, e.g. with the amino group of a lysine, and lead to an irreversible inhibition of the receptor.

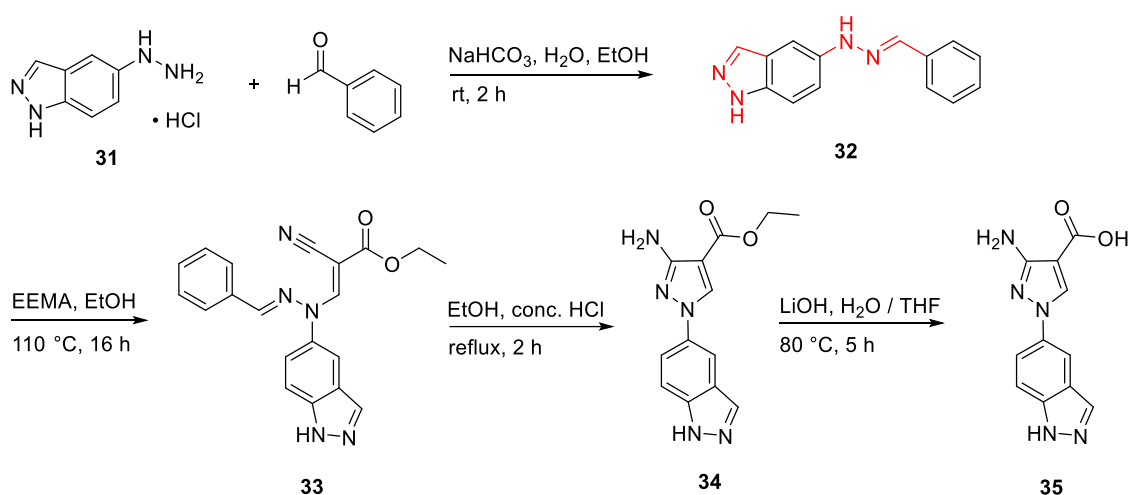
4.3.4.6. Synthesis of 3-amino-*N*-benzyl-1-(1*H*-indazol-5-yl)-1*H*-pyrazole-4-carboxamides

For the formation of 3-amino-*N*-benzyl-1-(1*H*-indazol-5-yl)-1*H*-pyrazole-4-carboxamides the synthetic route started with the preparation of 5-hydrazinyl-1*H*-indazole hydrochloride (**31**) since this compound was not commercially available.



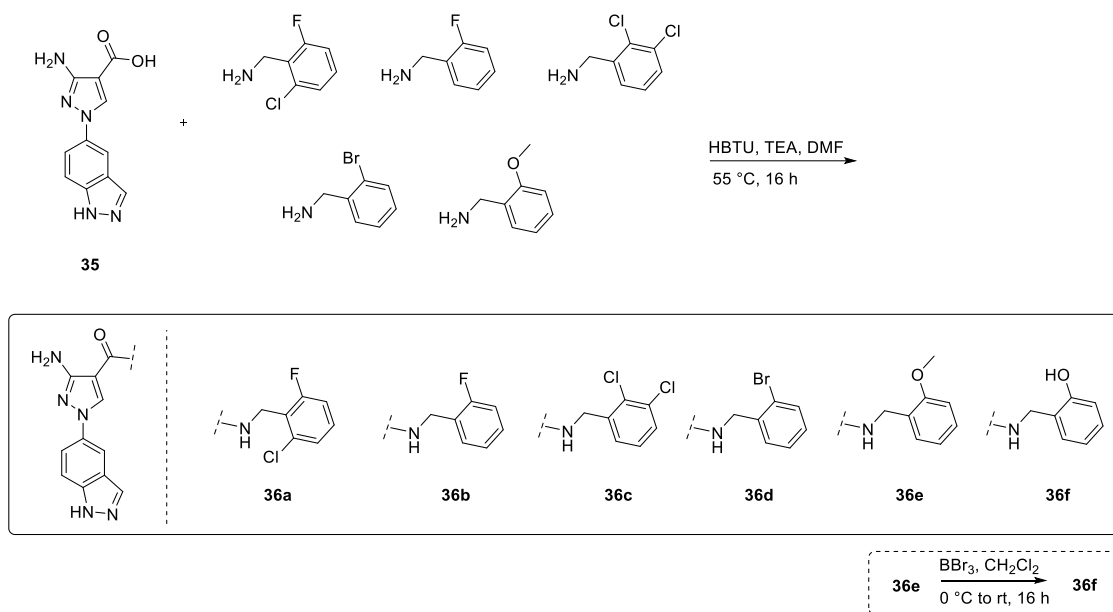
Scheme 22. Synthesis of compound **31**.¹⁶

Hydrazine derivative **31** could be obtained by diazotation and subsequent reduction of 1*H*-indazol-5-ylamine (cf. Scheme 22).¹⁶ The yield of this reaction was poor since the product hardly precipitated from the reaction mixture. The subsequent steps of the synthetic route proceeded as previously described with a few adjustments (cf. Scheme 23).



Scheme 23. Synthesis of compound **35**.

Notably, the 1*H*-indazol-5-yl residue led to a few problems during the synthesis. The protected intermediate **32** was much more reactive than the previous derivatives so that the reaction conditions of the substitution reaction with EEMA needed to be less harsh; 110 °C in EtOH for 16 h in a pressure tube was sufficient to consume all of **32**. For unknown reasons, heating at 170 °C (as applied for the other derivatives) instantly led to the formation of the undesired isomer. Another problem was that **32** exhibited two similar hydrazone-like moieties (highlighted in red in Scheme 23) that could both react with EEMA. TLC-MS analysis of the reaction mixture revealed that this actually happened. Conveniently, the intermediate **33** was readily separatable from the other side products via column chromatography. The subsequent steps of the synthesis were performed as established yielding **35** in low yield.



Scheme 24. Synthesis of 3-amino-*N*-benzyl-1-(1*H*-indazol-5-yl)-1*H*-pyrazole-4-carboxamides **36a-36f**.

Table 4. Selected experimental data of derivatives **36a-36f**.

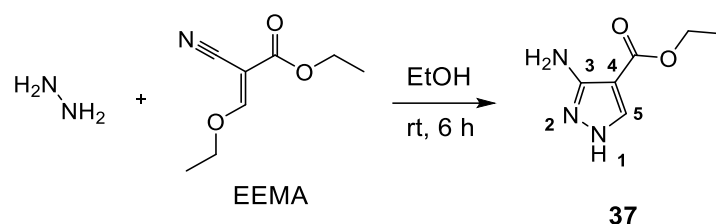
<i>Compd.</i>	<i>Yield</i>	<i>Purity</i>	<i>MW</i>	<i>Mp.</i>
36a	67%	96%	384.3	188 °C
36b	48%	96%	350.1	174 °C
36c	10%	96%	400.1	167 °C
36d	81%	93%	410.1	211 °C
36e	4%	94%	362.1	203 °C
36f	10%	95%	348.1	216 °C

The compounds illustrated in Scheme 24 were all prepared by employing the established methods. Most of the isolated yields were bad due to isolation problems, only **36a** could be obtained in a satisfactory yield of 67%. The methoxy derivative **36e** was subsequently demethylated using BBr_3 as described before.

4.3.4.7. Coupling reactions including amino-protection strategies of ethyl 3-amino-1*H*-pyrazole-4-carboxylate (**37**)

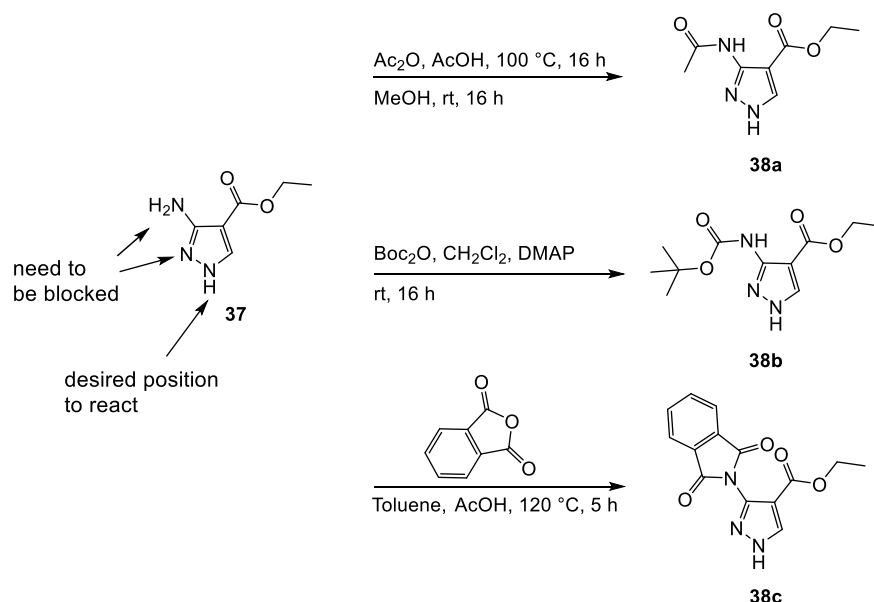
Synthetic procedures starting with substituted phenylhydrazines were sophisticated and resulted in low yields. However, this method unmistakably led to the desired isomer. This method made variation of the phenyl moiety at the N1-position difficult since the building block is introduced at the very beginning of the synthetic route. Coupling reactions, fusing ethyl 3-amino-1*H*-pyrazole-4-carboxylate (**37**) to a respective phenyl moiety, would make the variation

of this moiety more feasible. The synthetic route started with the preparation of **37** which was easily formed from EEMA and hydrazine hydrate, reacting in EtOH at rt in good yield.⁴



Scheme 25. Synthesis of compound **37**.⁴

Compound **37** exhibits three possibly reactive nitrogen atoms, but only N1 was desired to react. One approach was to protect the amino group in position 3 and thereby also block N2 sterically. Therefore, acetylation (**38a**),¹² a *tert*-butyloxycarbonyl (Boc) protection group (**38b**) and the formation of a phthalimide (**38c**)¹⁷ were tried using the illustrated conditions (cf. Scheme 26).

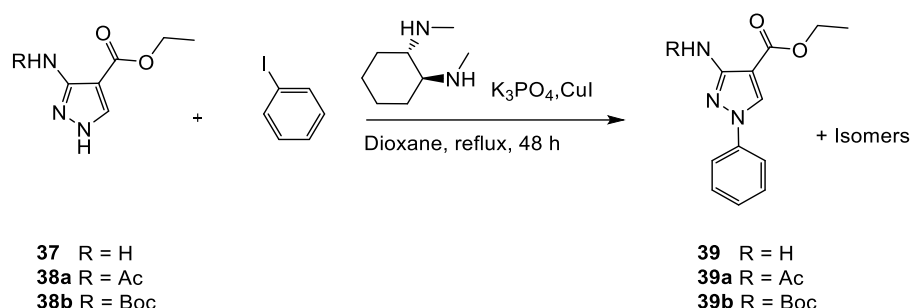


Scheme 26. Synthesis of compounds **38a**, **38b** and **38c**.^{12;17}

Acetylation of **37** followed a remarkable procedure described in the literature.¹² Using common acetylation reagents (like acetic acid chloride or acetic acid anhydride) resulted in an unselective (multiple) alkylation of **37**. However, if this crude mixture was dissolved in MeOH and left standing over night. **38a** was formed in moderate yield. Apparently, MeOH formed esters with all acetyl groups except for the desired NHAc group. Column chromatography was necessary to isolate **38a** in sufficient purity. The obtained NMR data coincided with literature. The Boc-protection of **37** proceeded with an isolated yield of only 12%, and side products formed during the reaction. Maybe heating would have led to better yields since the amino group of 3-aminopyrazoles is just as unreactive as the carbonyl function. Also, the selectivity of this reaction is questionable. The phthalimide **38c** was formed by heating of **37** with phthalic

anhydride in toluene under acid catalysis.¹⁷ The product could be isolated by column chromatography (CH₂Cl₂/ MeOH - 95 : 5) with a moderate yield (54%).

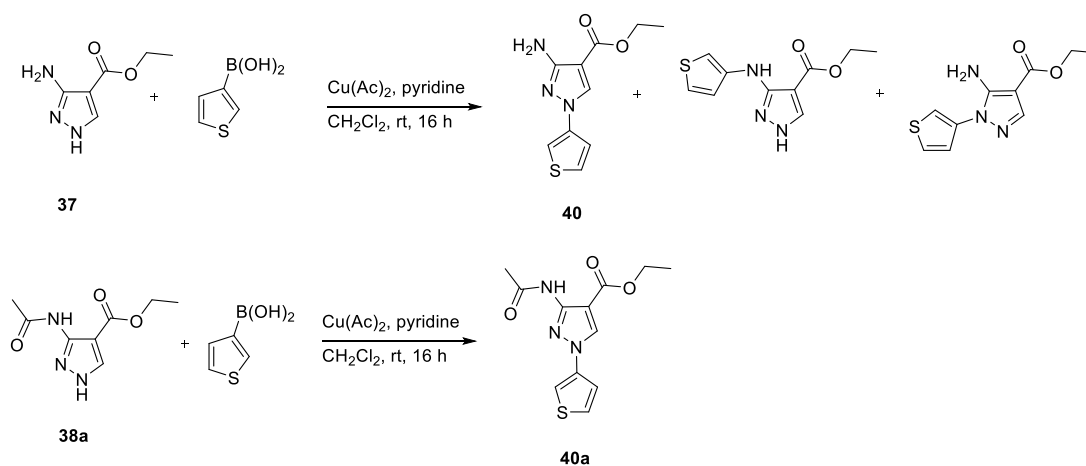
An Ullmann reaction was performed using **37**, **38a** and **38b** and iodobenzene as coupling partner (cf. Scheme 27).⁴



Scheme 27. Tried synthesis of compounds **39-39b**.⁴

Unexpectedly, the unprotected compound **37** gave the best results. After an extraction and subsequent purification via column chromatography (CH₂Cl₂/ MeOH - 98 : 2), the product could be isolated with 29% yield and 89% purity (the other 11% being the undesired isomer). The reaction of **38a** resulted in a mixture of unreacted starting material, deprotected **37**, deprotected product **39** and the desired product **39a**. Seemingly, the K₃PO₄ partly cleaved the acetate, suggesting that acetylation is not a good protection strategy for this reaction. Also, literature suggests that the NHAc could also be coupled to phenyl halide, so this reaction strategy was discarded.⁴ Reaction of **39b** also resulted in a mixture of protected and unprotected products, as well as and starting material; this strategy was also not suitable.

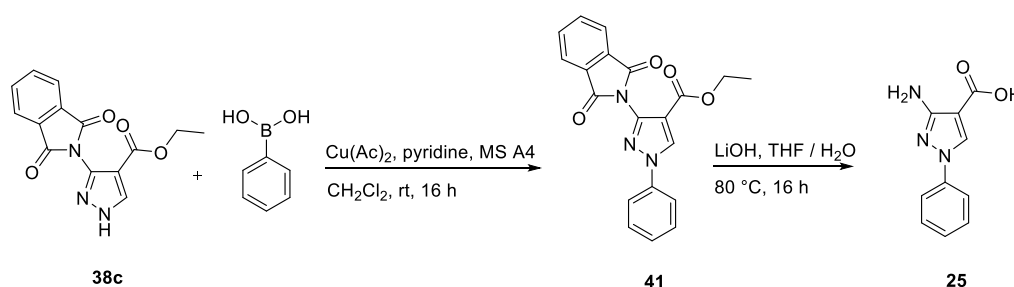
A different way to couple ethyl 3-amino-1*H*-pyrazole-4-carboxylate (derivatives) to an aromatic ring is the Chan-Lam-coupling reaction. Therefore, **37** and **38a** were reacted with 3-thienylboronic acid as test reactions using copper catalysis (cf. Scheme 28).¹³



Scheme 28. Attempts to synthesize compound **40**.¹³

It was possible to identify two isomers of **40** from the reaction based on **37** (55% and 25% in LC-MS analysis). However, the UV/Vis spectra suggested that the desired isomer was the minor component of 25%, and the peaks of the chromatogram as well as different TLC analyses showed that a separation of these isomers would be very hard. Using **38a** did not lead to better results; too many side products were observed and also deacetylated products so that this procedure was discarded as well.

A more successful reaction was performed between **38c** and phenylboronic acid (cf. Scheme 29).

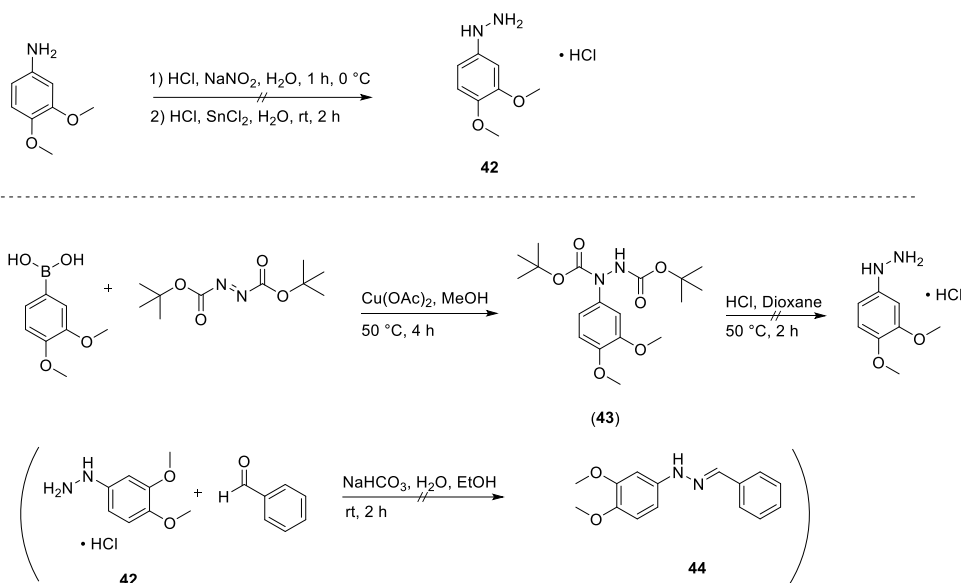


Scheme 29. Synthesis of **41** and **25**.¹³

This reaction resulted in only one isomer that could be isolated in moderate yield and good purity. Together with the unprotected **24**, the intermediate **41** was heated with an excess of LiOH, cleaving both phthalimide and ester to form **25**. The success of this reaction indicates that a phthalimide is a suitable protection group for **37** and that phenylboronic acid was a more reactive boronic acid for Chan-Lam-coupling reactions as compared to 3-thienylboronic acid.

4.3.4.8. Synthesis of 3-amino-*N*-benzyl-1-(3,4-dihydroxyphenyl)-1*H*-pyrazole-4-carboxamides

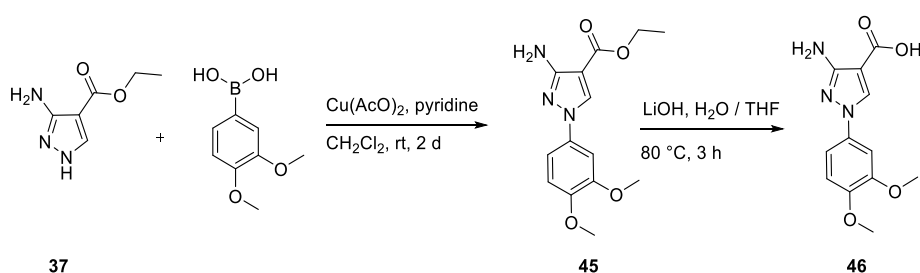
Since many 3-amino-*N*-benzyl-1-(hydroxyphenyl)-1*H*-pyrazole-4-carboxamide derivatives showed good biological activity in initial studies, it was an obvious idea to prepare a 3,4-dihydroxyphenyl derivative. This attempt, however, turned out to be much more difficult than preparing the corresponding 3-amino-*N*-benzyl-1-(4-hydroxyphenyl)-1*H*-pyrazole-4-carboxamides and 3-amino-*N*-benzyl-1-(3-hydroxyphenyl)-1*H*-pyrazole-4-carboxamides. Surprisingly, (3,4-dimethoxyphenyl)hydrazine or the respective hydrochloride were both not commercially available. As indicated in Scheme 30, two different reactions were tested to prepare this compound, both did not succeed.



Scheme 30. Attempted synthesis of compound **44**.^{16,18}

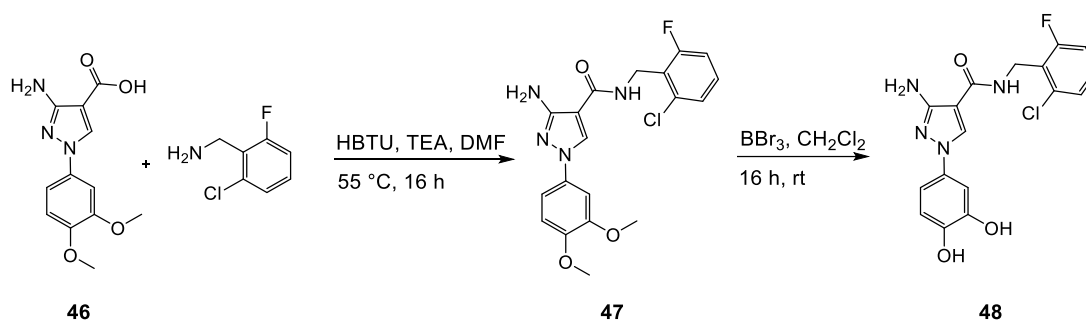
The first and obvious attempt was a classic diazotization of the aniline utilizing NaNO₂, followed by a reduction of the diazonium salt using SnCl₂ under strongly acidic conditions.¹⁶ These conditions were feasible for the formation of **32**, however, in two trials, only the starting material 3,4-dimethoxyaniline could be recovered. An entirely different approach to form a phenylhydrazines was a coupling reaction that employs a phenylboronic acid and di-*tert*-butyl azodicarboxylate. Under copper(II) catalysis, the respective di-*tert*-butyl-phenylhydrazine-1,2-dicarboxylate (**43**) was supposed to be formed as an intermediate. These compounds can be deprotected under acidic conditions in analogy to the deprotection of a Boc-protection group.¹⁸ Using the conditions illustrated in Scheme 30, a less polar product (TLC-analysis) was obtained. This intermediate was treated with HCl in dioxane. TLC analysis showed a product that was much more polar than the intermediate, however, LC-MS and NMR analysis did not unambiguously confirm the desired structure. Finally, the assumed phenylhydrazine was tried to be reacted with benzaldehyde to form the respective imine (**44**). Such imines are usually very stable and could be readily isolated and analyzed. In this case, however, no correct mass could be found, so this strategy was discarded.

Conveniently, the Chan-Lan-coupling reaction could be employed as illustrated in Scheme 31.



Scheme 31. Synthesis of compound **46** exploiting Chan-Lan conditions.¹³

(3,4-Dimethoxyphenyl)boronic acid was commercially available. The unprotected pyrazole **37** was reacted with two equivalents of the boronic acid under Cu(II) catalysis. Two days of stirring under air in CH₂Cl₂ led to a mixture of isomers and side products. The mixture was directly purified by column chromatography (CH₂Cl₂/ MeOH - 95 : 5). The crude, still impure product **45** was identified by TLC-MS ([M + H]⁺ = 292) and directly hydrolyzed by treating the material with LiOH in THF / H₂O (1 : 1) and stirring this mixture at 80 °C for 3 h. The obtained mixture was neutralized and purified by column chromatography (CH₂Cl₂/ MeOH - 9 : 1). The desired carboxylic acid was obtained in very low yield (6% based on **37**) but in high purity (89%) and without formation of the undesired isomer.

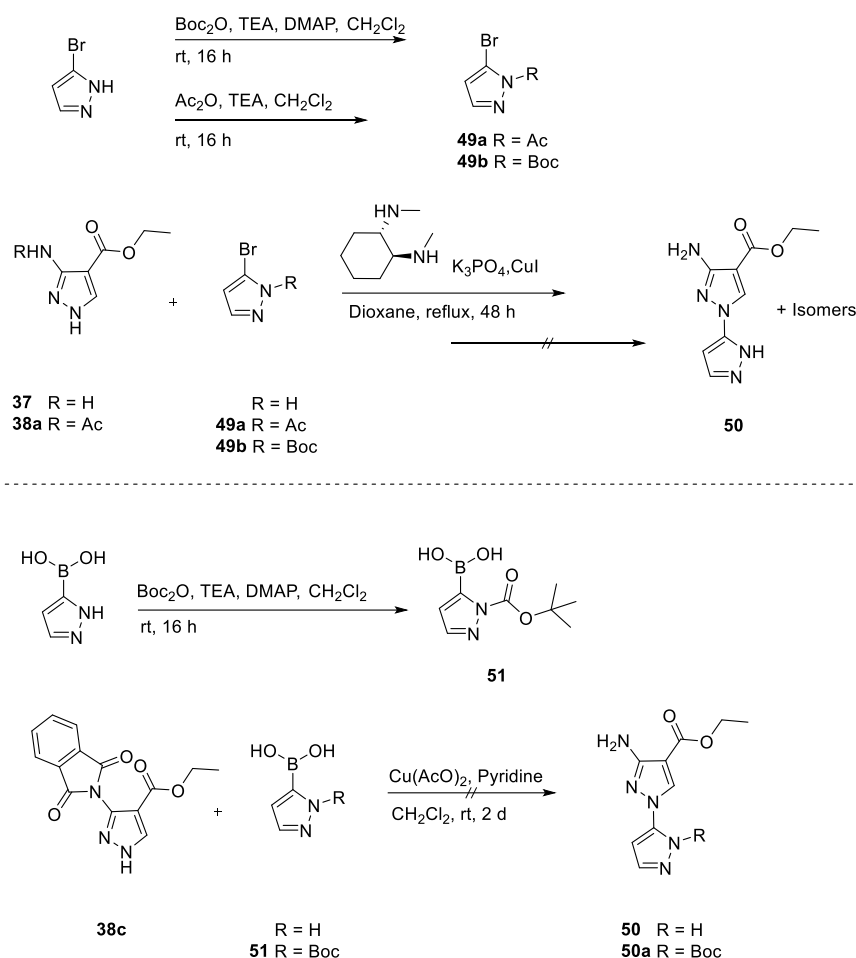


Scheme 32. Synthesis of **48**.

Scheme 32 illustrates the final steps of the formation of **48**, being the only compound bearing a 3,4-dihydroxyphenyl residue at N1 thus far. The conditions for these reactions followed the aforementioned procedures, and the final product was obtained in high yield (83% for the amide coupling and 66% for the deprotection step).

4.3.4.9. Attempted preparation of 3-amino-*N*-benzyl-2'-*H*-[1,3'-bipyrazole]-4-carboxamides

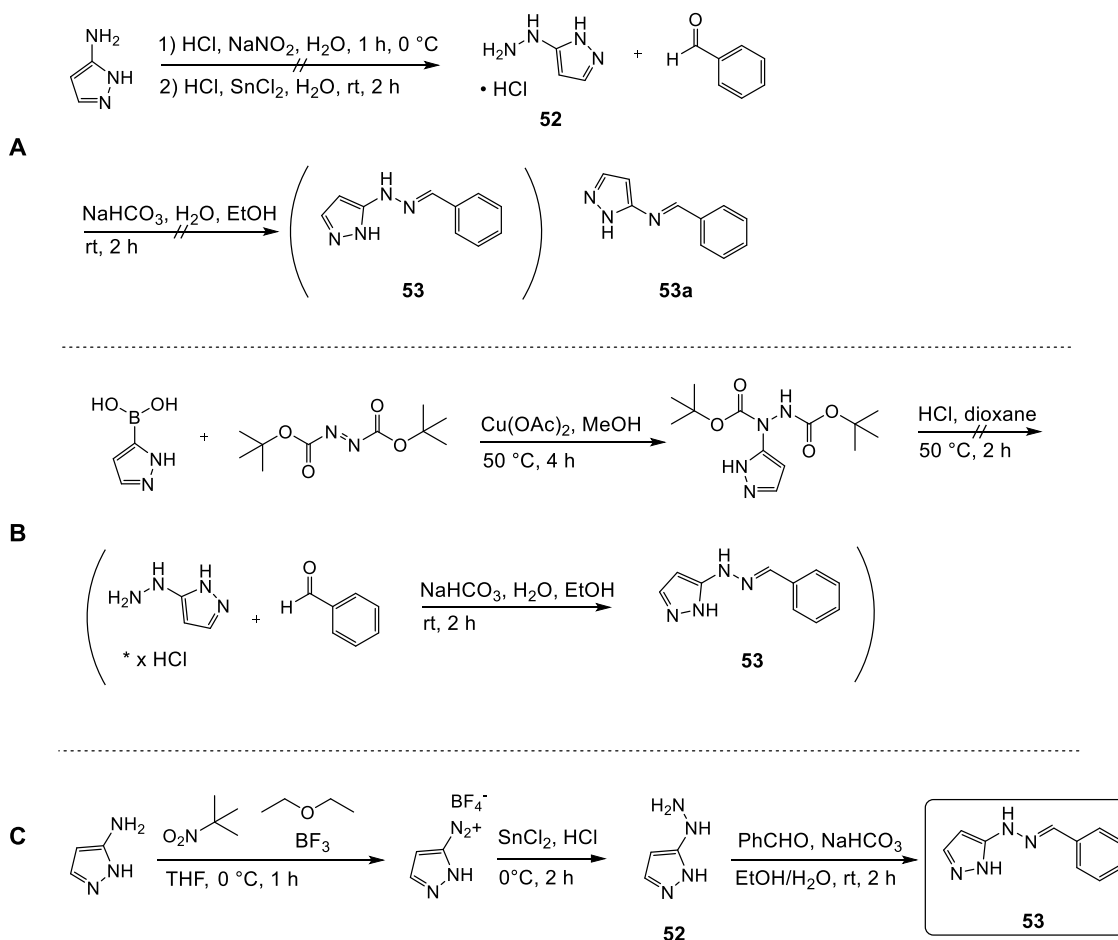
Several attempts were made to synthesize 3-amino-*N*-benzyl-2'-*H*-[1,3'-bipyrazole]-4-carboxamides, however, no final product could be obtained. 3-Hydrazinyl-1*H*-pyrazole or its hydrochloride were not commercially available, and its preparation starting from the 5-amino-1*H*-pyrazole is not described in literature and could initially not be obtained. Therefore, the aforementioned coupling reaction methods were pursued to form the intermediate ethyl 3-amino-2'-*H*-[1,3'-bipyrazole]-4-carboxylate (**50**) (see Scheme 33).



Scheme 33. Attempted synthesis of compound **50**.^{4,13}

Several protected and unprotected building blocks were tried to be reacted with one another as illustrated in Scheme 33. The coupling partners 5-bromo-1*H*-pyrazole and (1*H*-pyrazol-5-yl)boronic acid could be readily protected with an acetate or a boc-group by employing standard conditions. The Chan-Lam reactions between **37** or **38a** and the protected **51** and the unprotected (1*H*-pyrazol-5-yl)boronic acid yielded only unreacted starting material and side products. The boronic acid was particularly difficult to handle since it was seemingly insoluble in all employed solvents (water, EtOH, DMF, DMSO, CH₂Cl₂) and it could not be detected under UV-light for TLC analysis. Also, its mass was not detected in the mass spectral analysis. The reactions involving 5-bromo-1*H*-pyrazole yielded several (side) products and unreacted starting material. The desired product **50** was detected in small amounts (by LC-MS), but numerous side products made an isolation impossible. Cleavage of the protection groups was observed. The 5-bromo-1*H*-pyrazole derivatives were difficult to detect.

Since coupling reactions were not feasible, the preparation of 5-hydrazinyl-1*H*-pyrazole was tried although no appropriate method had been described in the literature.



Scheme 34. Synthesis of compound **53**.^{16,18,19}

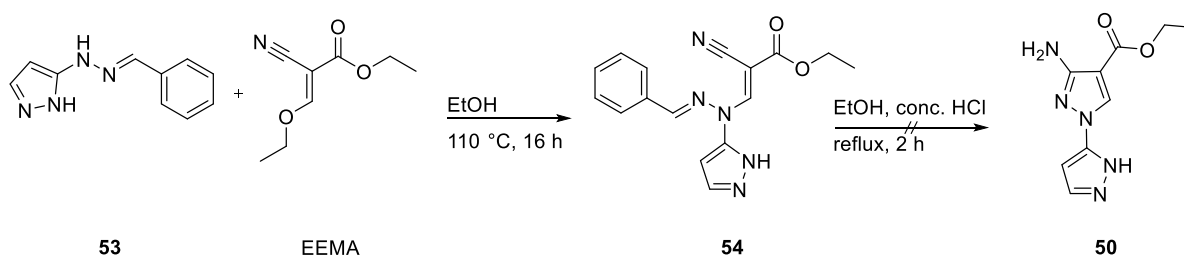
Scheme 34 shows three synthetic approaches to form the desired intermediate **53**. The obvious attempt was to form the diazonium salt and reduce it using SnCl_2 under acidic conditions (method **A**). This method worked out for the formation of **32** (Scheme 23), but in case of **52**, similarly to 3,4-dimethoxyaniline, only unreacted starting material could be obtained. This was proven by a subsequent imine formation with benzaldehyde since the mass of the undesired imine **53a** was clearly found in TLC-MS analysis.

Similar to the aforementioned trials to form the di-*tert*-butyl-phenylhydrazine-1,2-dicarboxylate of 3,4-methoxyaniline, the same reaction was tried with (1*H*-pyrazol-5-yl)boronic acid and di-*tert*-butyl azodicarboxylate (Scheme 34**B**). The supposed intermediate was deprotected under acidic conditions and the resulting product was reacted with benzaldehyde in order to produce the imine for analysis. However, the expected mass was not detectable.

In a final approach, the synthesis of intermediate **52** started with the formation of the diazonium salt of 5-amino-1*H*-pyrazole. However, not the classical method using NaNO_2 in concentrated aqueous HCl solution was utilized, but a different one, i.e. formation of the diazonium ion in THF with BF_3 -diethyletherate and *tert.* butylnitrite.¹⁹ The resulting salt (1*H*-pyrazole-5-diazonium tetrafluoroborate) precipitated upon treatment with diethyl ether and could be

obtained very easily in high yield (95%) and purity (one spot on TLC). Moreover, this salt was stable and could be stored. Also, it was detectable under UV light by TLC and by TLC-MS, making it easier to handle. The diazonium tetrafluoroborate could be readily reduced to the corresponding hydrazine derivate **52** by stirring it with SnCl₂ in concentrated HCl solution at 0 °C. The resulting solid was collected by filtration under reduced pressure. Since only a very small amount of solid could be isolated, the filtrate was neutralized with NaOH, and the resulting mixture of Sn salts and the product were isolated by filtration. This mixture was suspended in H₂O / EtOH and treated with NaHCO₃ until a pH value of approximately 9 was reached, then benzaldehyde was added to the mixture in order to form the imine **53** directly in the crude mixture. After 2 h of stirring, the mixture was treated with ethyl acetate, and the product could be extracted. Subsequent column chromatography afforded the desired imine in good yield (71% based on 5-amino-1*H*-pyrazole) and purity (91%). This method was much more convenient and effective than employing NaNO₂ for the formation of the diazonium salt so that this method would be the method of choice for future reactions of this kind.

Unfortunately, the subsequent reaction steps affording the desired 3-amino-2'*H*[1,3'-bipyrazole]-4-carboxylate **50** did not work as planned.

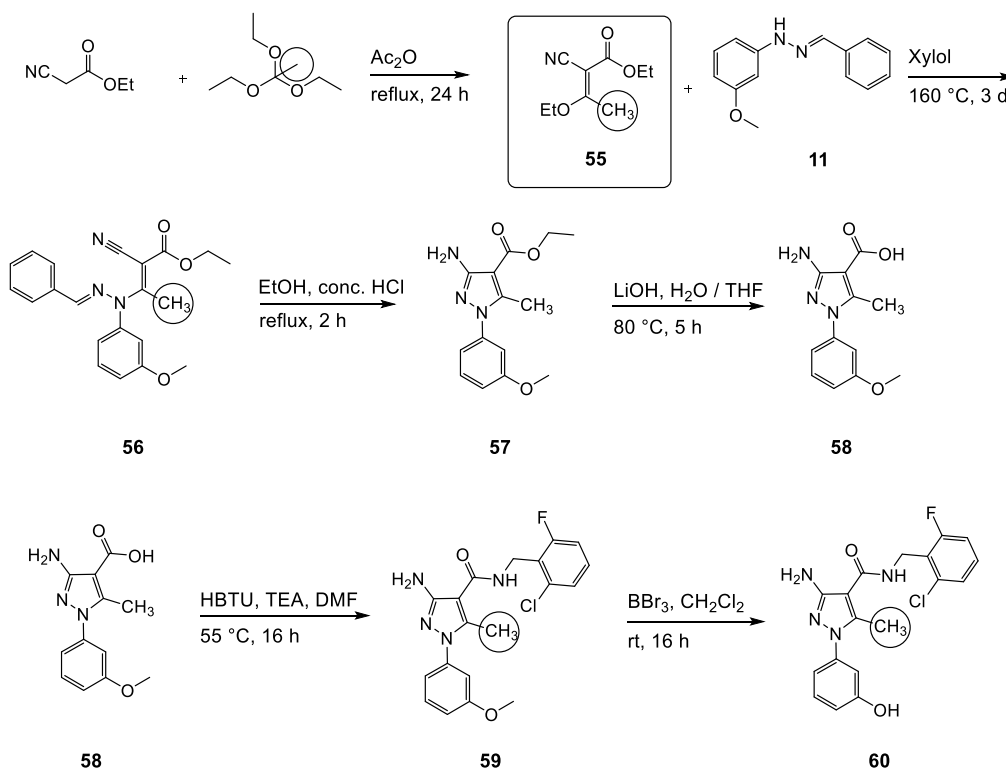


Scheme 35. Attempted synthesis of compound **50**.

As illustrated in Scheme 35, compound **53** could be reacted with EEMA to form intermediate **54** as detected by both TLC-MS and LC-MS. However, the subsequent deprotection step failed. A lot of unreacted starting material could be observed, as well as unidentifiable side products. Maybe the pyrazole ring of **50** was protonated or destroyed under the acidic conditions. The reaction conditions for this step need to be reconsidered and optimized in the future.

4.3.4.10. Introduction of a methyl group in pyrazole position 5: Synthesis of 3-amino-*N*-(2-chloro-6-fluorobenzyl)-1-(3-hydroxyphenyl)-5-methyl-1*H*-pyrazole-4-carboxamide

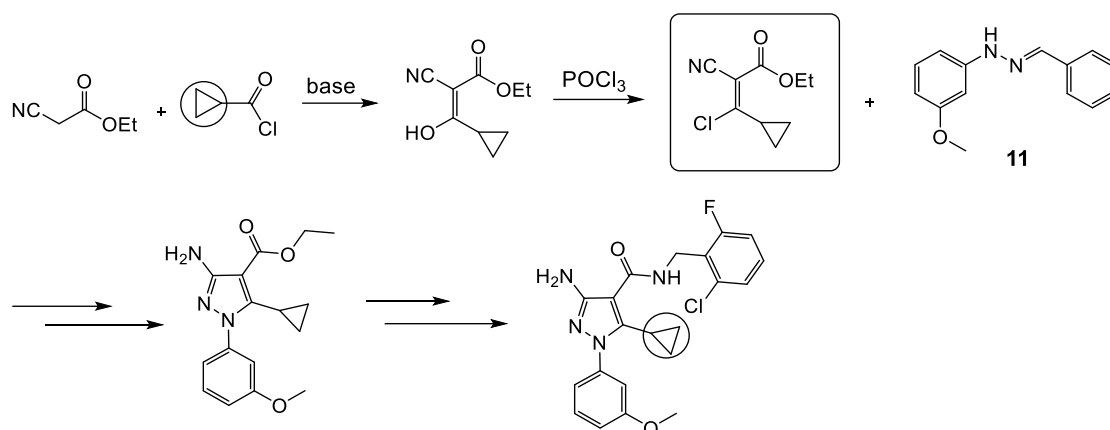
To introduce a methyl group into the pyrazole core of the scaffold, the substituent needed to be introduced at the very beginning of the synthesis. A reaction between ethyl cyanoacetate and triethyl orthoacetate in Ac₂O under reflux conditions yielded the methyl-substituted building block **55** in good yield. This compound will replace the unfunctionalized EEMA in the subsequent reaction steps (cf. Scheme 36).²⁰



Scheme 36. Synthesis of 3-amino-*N*-(2-chloro-6-fluorobenzyl)-1-(3-hydroxyphenyl)-5-methyl-1*H*-pyrazole-4-carboxamide **60**.²⁰

The subsequent steps of the synthetic route, as illustrated in Scheme 36, followed the established method. No noteworthy changes were observed, and yields were comparable to the corresponding unsubstituted analogues. *Meta*-methoxyphenyl- (and the corresponding hydroxyphenyl-) substituents were chosen for the N1-position since interim test results showed good biological values for this moiety. 2-Chloro-6-fluorobenzylamine was chosen as benzylamine because all testing results suggested that this building block was the best one for this moiety. As a result, **59** and **60** could be isolated as new methylated derivatives.

Introducing other alkyl moiety into the 5-position of the pyrazole core is theoretically possible using the appropriate acid chloride as a starting compound.²⁰ Scheme 37 illustrates a possible synthetic route for the introduction of a cyclopropyl residue at position 5 as an example.

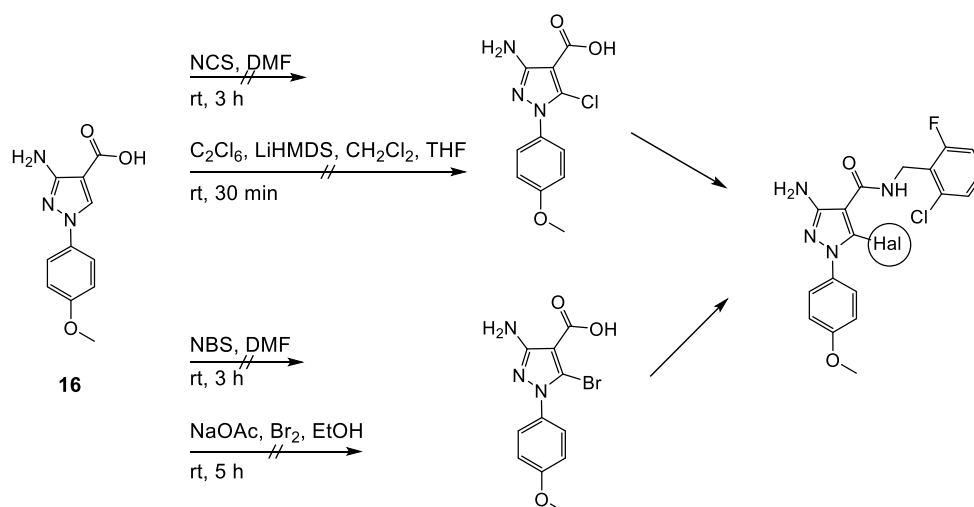


Scheme 37. Possible introduction of an alkyl substituent at position 5 of the pyrazole core.

Therefore, an appropriate carboxylic acid chloride would be reacted with ethyl cyanoacetate, and a subsequent chlorination would provide the activated building block. In this case, chlorine would be the leaving group for the substitution reaction instead of the ethanolate residue that is usually used when EEMA is the reagent.²⁰ The subsequent reaction steps would be performed according to the established procedures.

4.3.4.11. Functionalization of the pyrazole position 5: Introduction of halogen atoms

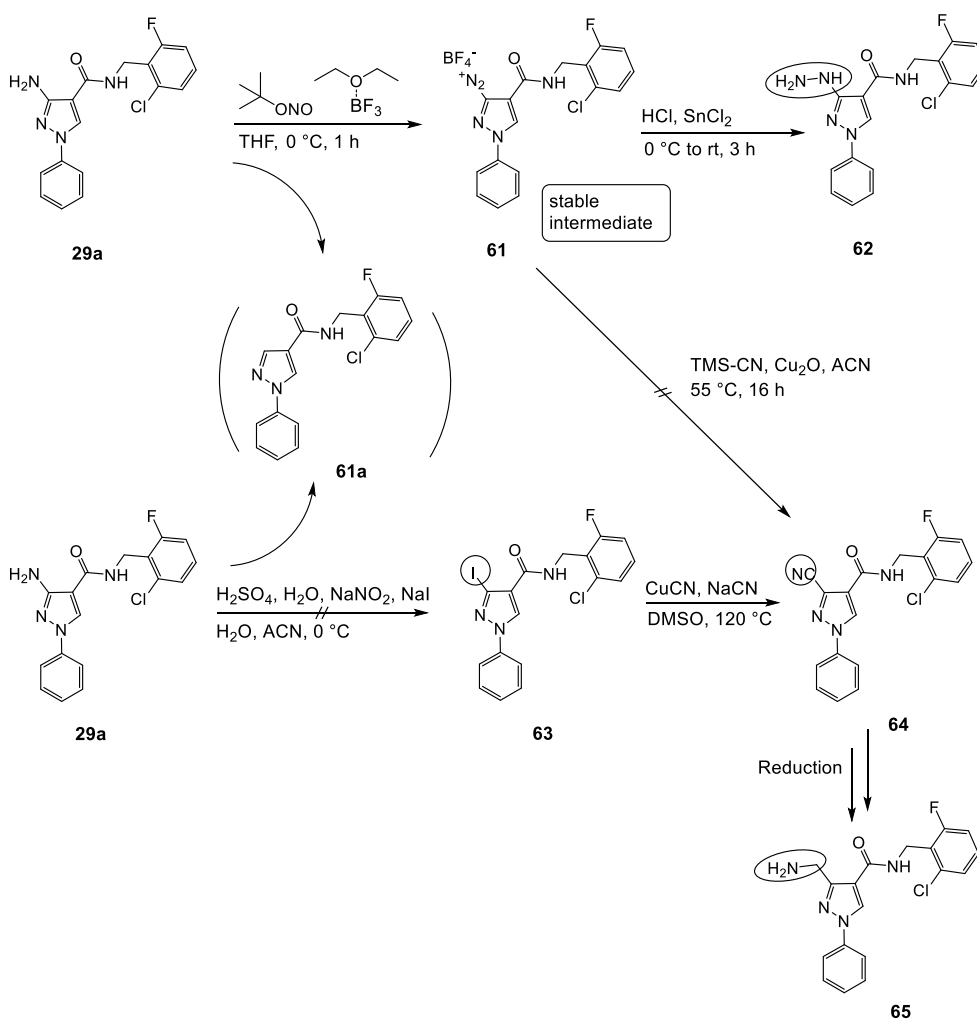
Trials were made to substitute position 5 of the pyrazole core with halogen atoms. Scheme 38 illustrates the attempted conditions. Starting from the carboxylic acid **16**, different reagents were tested to form the desired halogenated product. A chlorination was tried employing *N*-chlorosuccinimide (NCS)²¹ in DMF or C_2Cl_6 in the presence of lithium hexamethyldisilazide (LiHMDS) in THF.²² Bromination of **16** was tried using *N*-bromosuccinimide (NBS) in DMF²³ and Br_2 in EtOH.²⁴ However, all of the trials resulted in complex mixtures not containing the desired products. Maybe the application of the ester **15** would have been more successful.



Scheme 38. Attempted syntheses of **16** halogen derivative.²¹⁻²⁴

4.3.4.12. Modification of the pyrazole position 3: Alteration of the amino group

To change the amino group at position 3 of the pyrazole, two different attempts were made. Scheme 39 illustrates the tried or planned reaction steps. Compound **29a** was chosen as a prototype. The 2-chloro-6-fluorobenzylamine was always the best residue for the amide moiety in biological testing, and the unsubstituted phenyl ring at the N1-position had no functional groups that might interfere with the reactions. Hence, **29a** was resynthesized in a bigger scale.



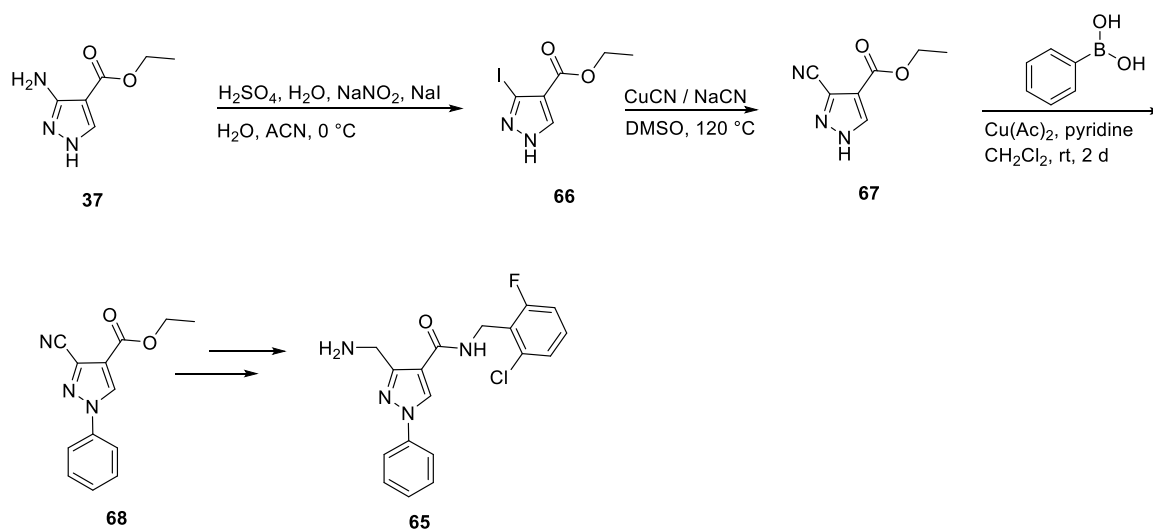
Scheme 39. Attempted syntheses of compounds **62** and **65**.^{5,19,25}

In a first approach, the 3-amino group of **29a** was converted into a stable diazonium tetrafluoroborate utilizing the abovementioned procedure (cf. Scheme 39).¹⁹ Therefore, **29a** was dissolved in cold THF and treated with BF_3 -diethyletherate and *tert.* butylnitrite. The diazonium tetrafluoroborate salt (**61**) precipitated after diethyl ether was added to the reaction mixture. The intermediate could be detected by TLC-MS ($m/z = 356$ $[\text{M} + \text{H}]^+$), the mass corresponding to the diazonium ion R-N_2^+ without the BF_4^- counterion. Besides, the deaminated side product **61a** could be identified by TLC-MS. This compound remained in the mother liquor after filtration. As indicated in Scheme 39, the intermediate **61** was added to a mixture of

concentrated aqueous HCl solution and 2 equivalents of SnCl₂ in order to reduce the diazonium salt to the corresponding hydrazine (**62**). TLC-MS analysis of the reaction mixture indicated the correct mass for the hydrazine beneath other side products. The crude product was collected by filtration and tried to be purified by RP column chromatography. Unfortunately, the product could not be detected among the fractions isolated from the column, indicating that the compound was not stable or it was lost otherwise during the purification process. Since the procedure seemed to be generally feasible, a second attempt should be made in the future. Another purification process could be chosen, e.g. a normal phase column chromatography might offer more control over the purification progress and the destiny of the product.

The second concept was a Sandmeyer reaction converting the respective amino group into a diazonium salt using NaNO₂ in sulfuric acid, followed by subsequent iodination using NaI.⁵ This reaction was not feasible, supposedly due to solubility problems. Compound **29a** was insoluble in the medium, and not even a homogenous suspension was obtained. Mostly starting material and the supposedly deaminated side product (**61a**) were detected by LC-MS analysis of the isolated solid.

A future approach could be iodination of **37** since it might be better soluble in the reaction medium than **29a** (cf. Scheme 40).



Scheme 40. Suggested synthetic route towards compound **65**.^{5,25}

The intermediate **66** might be converted to the respective nitrile derivative **67** by heating with CN⁻ ions.²⁵ A subsequent Chan-Lam-coupling reaction could introduce the phenyl ring at the N1-position of the pyrazole ring (**68**). Ester saponification, amide coupling reaction and subsequent reduction of the nitrile could successively lead to the desired product **65**.

4.3.5. Reactivity of 3-aminopyrazole derivatives

During this project, the lack of reactivity of the amino group as well as the carbonyl group of the pyrazole derivatives (be it the ester, carboxylic acid or amide) was observed. This phenomenon can be explained by an intramolecular hydrogen bond that is formed between the amino group and the carbonyl function (cf. Figure 12.) This very stable interaction needs energy (e.g. heating at 80 °C) to be broken and to allow the separated functional groups to react.

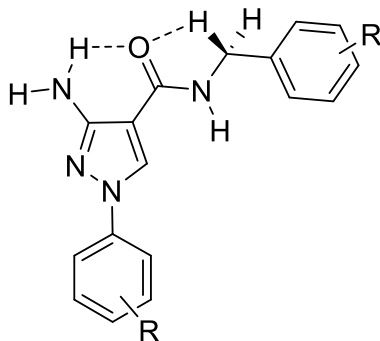
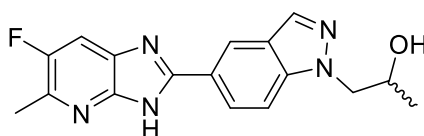


Figure 12. Intramolecular hydrogen bond of 3-aminopyrazoles.

4.3.6. Resynthesis of 1-(5-(6-fluoro-5-methyl-3*H*-imidazo[4,5-*b*]pyridine-2-yl)-1*H*-indazol-1-yl)propan-2-ol (PZB00712006)

The goal of a small, independent project was the resynthesis of the compound **69** (PZB00712006) in order to provide it for further biological and structural studies. This compound was particularly interesting due to good dual activity at the A_{2A}AR and the MAO-B (cf. Figure 13).⁴³



69, PZB 00712006

$K_i A_1 = 763 \text{ nM}$

$K_i A_{2A} = 70 \text{ nM}$

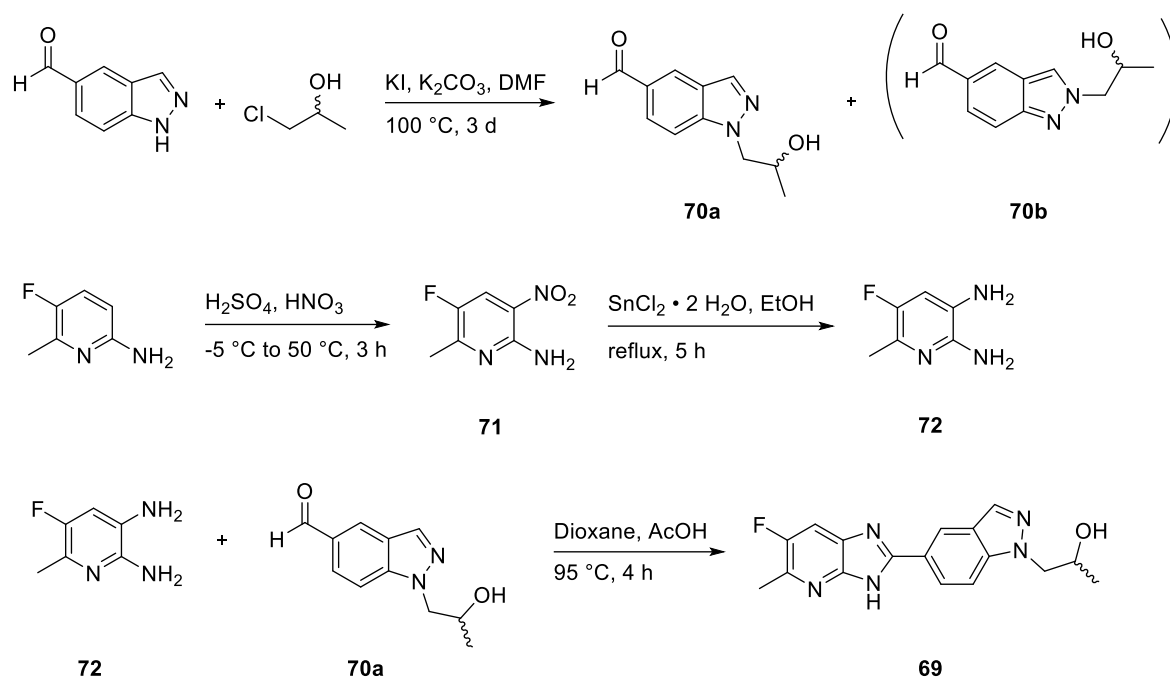
$K_i A_{2B} = 174 \text{ nM}$

$K_i A_3 = 186 \text{ nM}$

$IC_{50} \text{ MAO-B} = 118 \text{ nM}$

Figure 13. Structure and potencies of **69** (PZB00712006) at the human AR subtypes and the human MAO-B.⁴³

The first reaction step was the most problematic one: the reaction between 1*H*-indazole-5-carbaldehyde and 1-chloro-2-propanol naturally led to the formation of regioisomers that were difficult to isolate and to identify (cf. Scheme 41). Purification via column chromatography (CH₂Cl₂ / MeOH - 95 : 5) led to a small amount of relatively pure product **70a**. The desired isomer could be identified by reference to previous NMR spectra and NMR prediction.



Scheme 41. Synthesis of 1-(5-(6-fluoro-5-methyl-3*H*-imidazo[4,5-*b*]pyridin-2-yl)-1*H*-indazol-1-yl)propan-2-ol (**69**, PZB00712006).⁴³

The preparation of the required diamine **72** was straightforward. The nitration of 2-amino-5-fluoro-6-methylpyridine and the subsequent reduction using SnCl₂ were feasible. Column chromatography led to the desired intermediate **72** in good yield (cf. Scheme 41). Finally, the formation of the desired compound was performed under acid catalysis. The resulting reaction mixture was purified by column chromatography (CH₂Cl₂ / MeOH - 95 : 5) on normal phase followed by an additional purification by RP HPLC (10 to 100% MeOH). The desired compound **69** (PZB00712006) was obtained in low isolated yield but very good purity. Analytic data matched with those of a previously prepared sample.⁴³

18a	H	OCH ₃	2-chloro-6-fluoro-benzylamine	>1000 (34%)	577 ± 54	>1000 (31%)	908 ± 226	1.7
19a	H	OH	2-chloro-6-fluoro-benzylamine	>1000 (31%)	29.2 ± 5.1	154 ± 22	>1000 (20%)	34.3
18b	H	OCH ₃	2-cyanobenzylamine	>1000 (23%)	>1000 (34%)	>1000 (29%)	234 ± 36	-
19b	H	OH	2-cyanobenzylamine	>1000 (13%)	313 ± 57	>1000 (46%)	>1000 (15%)	3.2
18c	H	OCH ₃	2-methoxybenzylamine	>1000 (18%)	>1000 (14%)	>1000 (20%)	851 ± 53	-
19c	H	OH	2-hydroxybenzylamine	>1000 (34%)	39.4 ± 7.1	144 ± 48	>1000 (-7%)	25.4
18d	H	OCH ₃	1-aminoindane	>1000 (20%)	>1000 (15%)	>1000 (-3%)	>1000 (21%)	-
19d	H	OH	1-aminoindane	367 ± 107	675 ± 302	>1000 (12%)	>1000 (-6%)	-
18e	H	OCH ₃	2-fluorobenzylamine	>1000 (38%)	473 ± 109	>1000 (41%)	>1000 (48%)	2.1
19e	H	OH	2-fluorobenzylamine	538 ± 61	37.4 ± 9.5	146 ± 33	>1000 (25%)	14.4
18f	H	OCH ₃	1-naphthylmethylamine	257 ± 140	506 ± 150	>1000 (29%)	>1000 (26%)	-
19f	H	OH	1-naphthylmethylamine	131 ± 12	103 ± 45	>1000 (34%)	>1000 (3%)	1.3
20a	OCH ₃	H	2-chloro-6-fluoro-benzylamine	271 ± 41	24.1 ± 9.4	186 ± 11	448 ± 86	11.2
21a	OH	H	2-chloro-6-fluoro-benzylamine	>1000 (19%)	23.4 ± 6.0	266 ± 44	>1000 (34%)	42.8
20b	OCH ₃	H	2,3-dichlorobenzylamine	296 ± 6	47.2 ± 13.6	>1000 (29%)	>1000 (44%)	6.3
21b	OH	H	2,3-dichlorobenzylamine	1100 ± 210	12.9 ± 2.8	>1000 (34%)	>1000 (34%)	85.3
20c	OCH ₃	H	2-methoxybenzylamine	>1000 (15%)	178 ± 31	>1000 (2%)	>1000 (41%)	5.6
21c	OH	H	2-hydroxybenzylamine	>1000 (29%)	15.4 ± 4.7	170 ± 73	>1000 (16%)	65.0
20d	OCH ₃	H	1-aminoindane	224 ± 78	40.1 ± 11.9	>1000 (20%)	>1000 (28%)	5.6
21d	OH	H	1-aminoindane	>1000 (18%)	>1000 (32%)	>1000 (28%)	>1000 (32%)	-
20e	OCH ₃	H	2-fluorobenzylamine	433 ± 126	55.1 ± 7.9	434 ± 61	883 ± 135	7.9
21e	OH	H	2-fluorobenzylamine	>1000 (28%)	15.3 ± 2.9	156 ± 23	>1000 (20%)	65.4
20f	OCH ₃	H	2-chloro-6-fluoro-3-methoxybenzylamine	312 ± 99	84.8 ± 19.3	>1000 (33%)	>1000 (45%)	3.7
21f	OH	H	2-chloro-6-fluoro-3-hydroxybenzylamine	>1000 (4%)	174 ± 35	89.3 ± 18.8	>1000 (27%)	5.8
20g	OCH ₃	H	2,3-difluoro-6-methoxybenzylamine	411 ± 116	218 ± 39	>1000 (9%)	357 ± 7	1.9

21g	OH	H	2,3-difluoro-6-hydroxybenzylamine	193 ± 68	5.41 ± 0.86	36.9 ± 7.2	>1000 (30%)	35.7
29a	H	H	2-chloro-6-fluoro-benzylamine	210 ± 44	19.7 ± 7.5	226 ± 46	>1000 (31%)	10.7
29b	H	H	benzylamine	493 ± 244	493 ± 244	>1000 (34%)	>1000 (40%)	3.5
29c	H	H	phenylhydrazine	>1000 (31%)	256 ± 23	>1000 (31%)	328 ± 134	3.9
29d	H	H	O-phenylhydroxylamine	281 ± 24	745 ± 114	>1000 (22%)	>1000 (35%)	2.6
29e	H	H	2-methoxybenzylamine	>1000 (32%)	81.1 ± 2.4	>1000 (39%)	>1000 (23%)	12.3
29f	H	H	2-hydroxybenzylamine	87.3 ± 24.0	8.03 ± 2.17	60.1 ± 6.2	>1000 (32%)	10.9
29g	H	H	2-carboxylbenzylamine	>1000 (27%)	>1000 (-4%)	>1000 (5%)	>1000 (9%)	-
29h	H	H	2-(hydroxymethyl)-benzylamine	>1000 (20%)	138 ± 30	>1000 (35%)	>1000 (6%)	7.2
30	H	H	hydroxybenzotriazol	529 ± 74	>1000 (34%)	>1000 (10%)	>1000 (-2%)	-
36a			2-chloro-6-fluoro-benzylamine	328 ± 71	5.07 ± 0.37	31.9 ± 2.1	>1000 (19%)	64.7
36b			2-fluorobenzylamine	555 ± 77	15.3 ± 1.3	62.5 ± 17.6	>1000 (5%)	36.3
36c			2,3-dichlorobenzylamine	235 ± 70	12.1 ± 0.5	569 ± 182	>1000 (8%)	19.4
36d			2-bromobenzylamine	452 ± 74	33.4 ± 10.2	338 ± 85	>1000 (14%)	13.5
36e			2-methoxybenzylamine	>1000 (24%)	68.2 ± 3.9	>1000 (27%)	>1000 (29%)	14.7
36f			2-hydroxybenzylamine	119 ± 10	39.2 ± 2.2	46.8 ± 13.5	>1000 (24%)	3.0
48	OH	OH	2-chloro-6-fluoro-benzylamine	>1000 (16%)	432 ± 43	>1000 (22%)	>1000 (15%)	2.3
59	OCH ₃	H	2-chloro-6-fluoro-benzylamine	>1000 (4%)	331 ± 75	>1000 (33%)	538 ± 62	3.0
60	OH	H	2-chloro-6-fluoro-benzylamine	863 ± 62	157 ± 13	>1000 (22%)	>1000 (26%)	5.5

^avs. [³H]CCPA (n = 3); ^bvs. [³H]MSX-2 (n = 3); ^cvs. [³H]PSB-603 (n = 3); ^dvs. [³H]PSB-11 (n = 3);
^eK_i A₁AR / K_i A_{2A}AR

4.3.7.2. Analysis of structure-activity relationship of 3-amino-*N*-benzyl-1-phenyl-1*H*-pyrazole-4-carboxamides focused on the A_{2A}AR

The most interesting molecules with regard to A_{2A} affinity and A₁ selectivity are depicted in Figure 14:

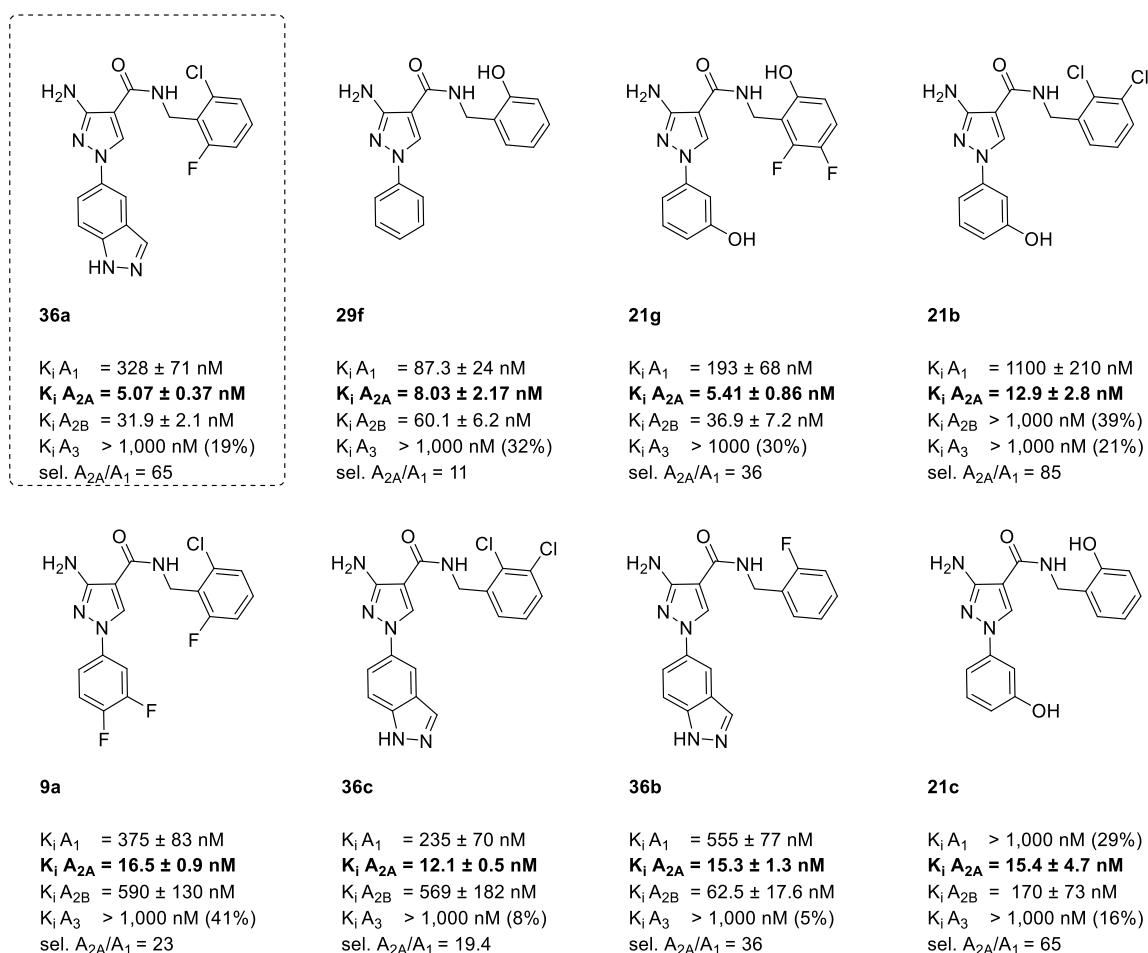


Figure 14. AR affinities of compounds **36a**, **29f**, **21g**, **21b**, **9a**, **36c**, **36b** and **21c**, inhibition at 1 μM in % is displayed for some receptors.

The best A_{2A} antagonist of this series by far turned out to be **36a** with an excellent K_i value of 5.07 nM at the A_{2A}AR and a good 65-fold selectivity towards the A₁AR. The compound was also very potent at the A_{2B}AR (making it a dual acting antagonists) and selective towards A₃. Moreover, **29f** and **21g** displayed K_i values of <10 nM for the A_{2A}AR but were not as selective. The most selective compound among the scaffold was **21b** with an 85-fold selectivity towards the A₁AR, it additionally displayed a K_i value in low nanomolar range. The derivatives **9a**, **36c**, **36b** and **21c** showed high affinity for the A_{2A}AR as well. Some compounds might even be more selective, but the affinity for the A₁AR still needs to be determined. Nearly all *meta*-hydroxyphenyl derivatives (**21a**, **21b**, **21c**, **21e** and **21g**) showed no noteworthy activity at A₁, making them the most selective series of this scaffold. Compound **21g** was an exception (K_i A₁ = 193 nM) but showed still some selectivity (36-fold).

The A_{2A} -affinity of 3-amino-*N*-benzyl-1-phenyl-1*H*-pyrazole-4-carboxamides is depending on both varied moieties: the phenyl ring at N1 and the benzylamine. Seemingly, the A_{2A} AR only tolerates one “large” residue like a methoxy group. 2-Methoxybenzylamine was not well tolerated when the N1-phenyl ring also exhibited a methoxy group (see **18c** and **20c**) but it showed high potency when an unsubstituted phenyl ring was attached to at N1 (e. g. **29e**, $K_i A_{2A} = 81$ nM). On the other hand, the entirely unsubstituted compound **29b** displayed only moderate affinity ($K_i A_{2A} = 142$ nM) and low selectivity versus, revealing that a lack of substituents is disadvantageous as well. Hence, a very specific substitution pattern of the scaffold and a particular molecular size is necessary to perfectly fit into the receptor binding pocket.

The comprehensive data suggests that 2-chloro-6-fluorobenzylamine is by far the best benzylamine. The building blocks 2,3-dichlorobenzylamine, 2-fluorobenzylamine and 2-hydroxybenzylamine also showed results in the same range. 2-Methoxybenzylamine was a successful building block in compounds **29e** and **36e**. Compound **20d**, bearing 1-aminoindane at the amide position showed high affinity but its hydroxyphenyl analogue **21d** was surprisingly inactive at all ARs. All other 1-aminoindane derivatives showed no or poor potency.

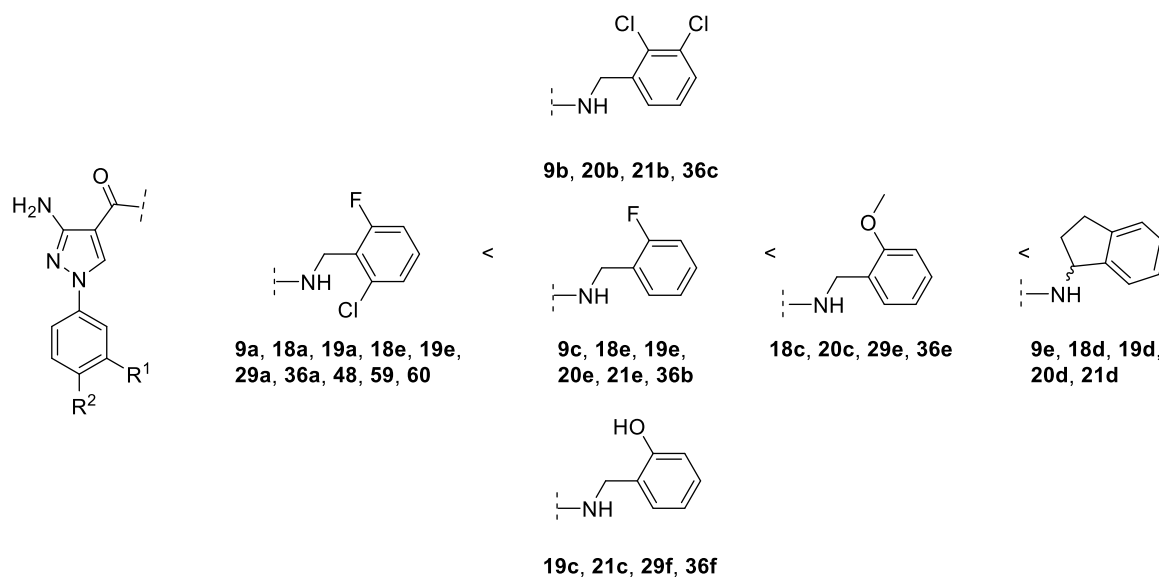


Figure 15. SARs of benzylamine substitution of 3-amino-*N*-benzyl-1-phenyl-1*H*-pyrazole-4-carboxamides.

For the N1-phenyl moiety, the indazole residue was the best by far; all compounds of this family (**36a-36f**) exhibited K_i values in the low nanomolar range, one of them, namely **36a**, even below 10 nM. The hydroxyphenyl derivatives were more potent than the corresponding methoxy derivatives. The *meta*-substituted residues were superior to the *para*-substituted analogues (cf. Figure 16). Derivatives of the phenyl-substituted compounds showed in part high A_{2A} affinity but lacked selectivity.

Compound **48**, bearing a 3,4-dihydroxyphenyl residue at N1 showed only very poor potency at the A_{2A}AR (K_i A_{2A} = 432 nM) although the molecule was also equipped with the beneficial 2-chloro-6-fluorobenzylamine moiety. Two OH groups might be too space-demanding or too polar to be tolerated by the receptor.

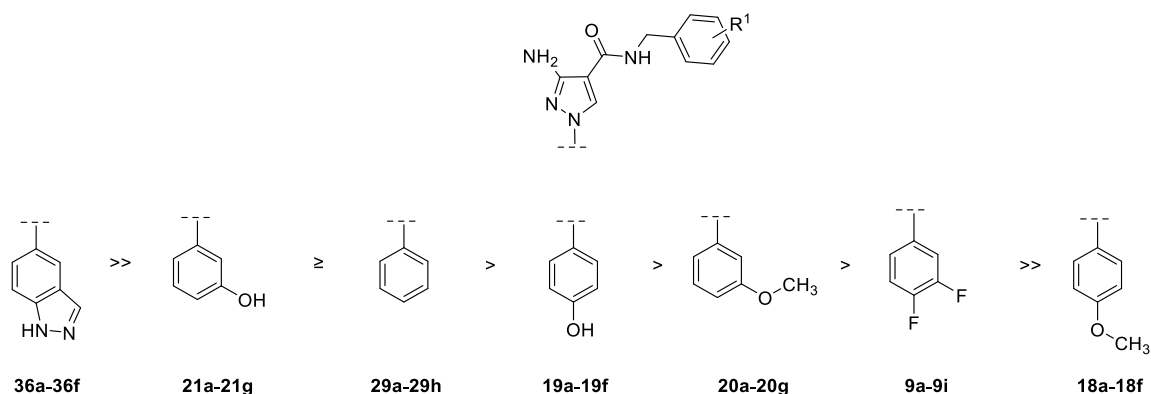


Figure 16. SARs of phenyl substitution at position N1 of 3-amino-*N*-benzyl-1-phenyl-1*H*-pyrazole-4-carboxamides.

Especially the very promising 3-amino-*N*-benzyl-1-(3-hydroxyphenyl)-1*H*-pyrazole-4-carboxamides show high selectivity towards the A₁AR combined with high potency for the A_{2A}AR. Conspicuously, nearly all 2-chloro-6-fluorobenzylamine derivatives (except for **18a**) circle around a K_i value of approximately 20 nM at the A_{2A}AR while all other derivatives exhibit greater variance. Apparently, the “northern” part of the molecule, especially when 2-chloro-6-fluorobenzylamine is present, is the part that fits quiet well into the receptor allowing little flexibility while the phenyl ring at the N1-position is a more variable moiety.

Most of the compounds showed high selectivity towards the A₃AR, exhibiting K_i values of >1000 nM. Only compounds **18b**, **20a**, **20g**, **29c** and **59** showed some A₃-affinity activity in the high nanomolar range.

The methylene linker in the benzylamine moiety was already the best possible linker; a change from benzylamine (**29b**, K_i A_{2A} = 142 nM) to phenylhydrazine (**29c**, K_i A_{2A} = 256 nM) or *O*-phenylhydroxylamine (**29d**, K_i A_{2A} = 745 nM) was disadvantageous (cf. Figure 17). The heteroatom presumably changes the orientation of the phenyl ring within the protein, or the receptor just does not tolerate a polar moiety at this particular position.

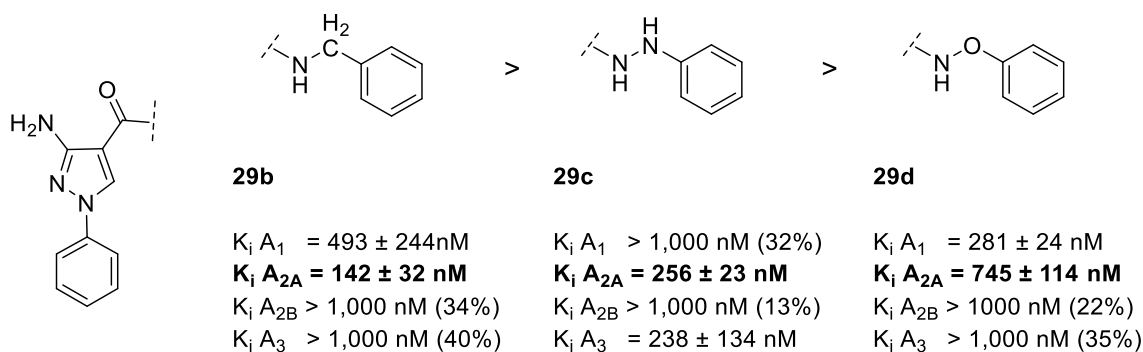


Figure 17. AR affinities of compounds **29b**, **29c** and **29d**; inhibition at 1 μM in % is displayed for some receptors.

The introduction of a 2-phenylpyrrolidine moiety, that can be found in compound **9i**, led to a complete loss of potency at any AR subtype. The position of the phenyl ring is too much altered by the central pyrrolidine ring. The building block 2-aminoindane (being found in **9e**, **18d**, **19d**, **20d**, **21d**) showed elusive results: high A_{2A} -affinity was only observed in combination with the *meta*-methoxy phenyl ring at the N1-position (**20d**, $K_i A_{2A} = 40.1 \text{ nM}$). All other derivatives showed no or only unsatisfactory affinity towards A_{2A} , making this building block unsuitable to be recommended for more derivatives. Seemingly, a freely rotatable, benzylamine moiety (substituents at the phenyl ring are advantageous) is needed for high affinity to the A_{2A} AR.

Compound **30**, which was a reaction intermediate with a similar structure as the final products, did not show any noteworthy affinity for the ARs (only poor affinity to A_1). It was either unstable or the receptors did not tolerate the hydroxybenzotriazole moiety.

Methylation of the pyrazole core turned out to be disadvantageous. Compounds **59** and **60** showed lower affinity for the A_{2A} AR than their analogues **20a** and **21a** (cf. Figure 18).

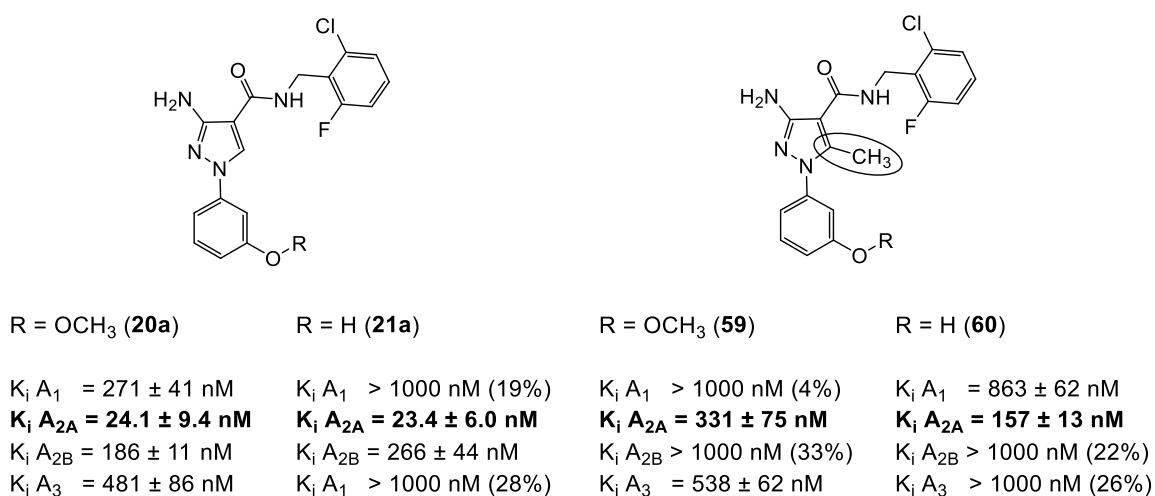


Figure 18. AR affinities of compounds **20a**, **21a**, **59** and **60**, inhibition at 1 μM in % is displayed and some receptors.

Maybe the methyl group at the 5-position of the pyrazole leads to a steric clash with the proton in the *ortho*-position of the N1 phenyl moiety (cf. Figure 19). Crystal structures suggest a coplanar arrangement of the triazole ring and the phenyl ring when bound to the A_{2A}AR.^{1,3} A steric clash preventing a coplanar conformation could lead to decreased potency. That might be the reason why all 3-amino-*N*-benzyl-1-phenyl-1*H*-pyrazole-4-carboxamides exhibit lower potency at the A_{2A}AR than the reported 5-amino-*N*-benzyl-1-phenyl-1*H*-pyrazole-4-carboxamides: The proton at the 5-position of the aminopyrazole might still cause a minor steric clash with the *ortho*-protons of the N1 phenyl ring and thus interfere with a coplanar conformation of both rings. On the other hand, a 5-amino-*N*-benzyl-4-carboxamido-2-phenyl-1,2,3-triazole has no space-demanding substituent at the discussed positions, both rings can occupy any conformation.^{14,36} In this light, any substitution of position 5 (the introduction of halides was also tried) seems disadvantageous.

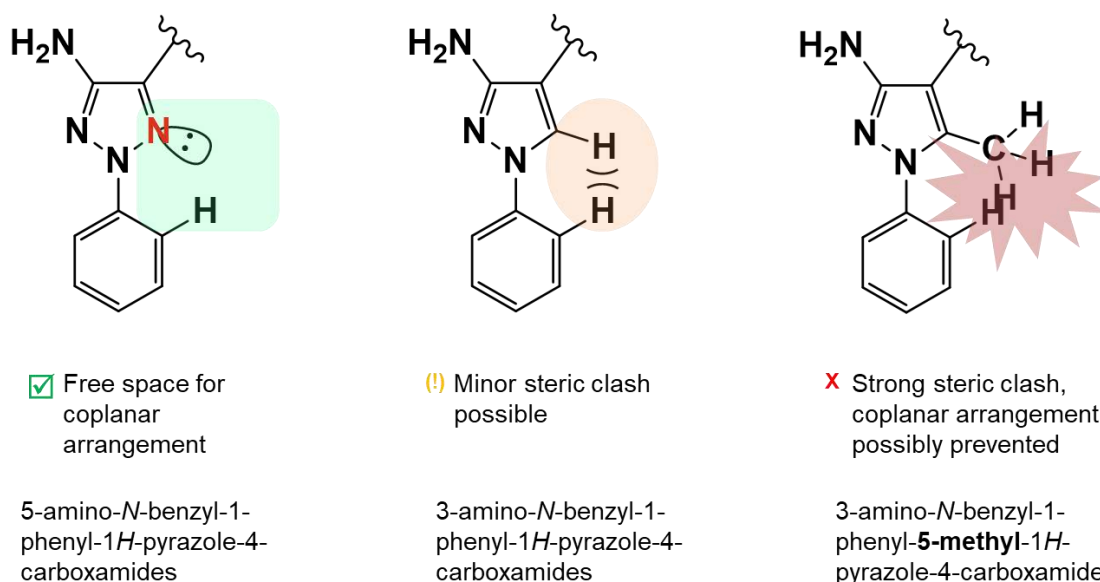
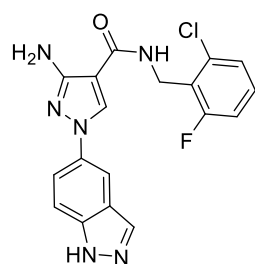


Figure 19. Steric situation of 5-amino-*N*-benzyl-4-carboxamido-2-phenyl-1,2,3-triazoles, 3-amino-*N*-benzyl-1-phenyl-1*H*-pyrazole-4-carboxamides and 3-amino-*N*-benzyl-1-phenyl-5-methyl-1*H*-pyrazole-4-carboxamides.

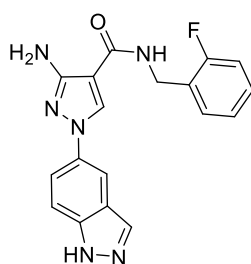
4.3.7.3. Analysis of structure-activity relationship of 3-amino-*N*-benzyl-1-phenyl-1*H*-pyrazole-4-carboxamides focused on the A_{2B}AR

18 compounds revealed some affinity for the A_{2B}AR, often around 10-fold weaker as compared to the A_{2A}AR. Still, this could offer the opportunity for dual antagonists. The most active compound was **29a** with a K_i value of 31.9 nM for the A_{2B}AR. Figure 20 shows selected compounds that exhibit particularly low A_{2A}/A_{2B}-selectivity. Derivative **21f** displayed higher affinity for the A_{2B}AR than for the A_{2A}AR and **29f** showed high affinity for the A₁-, A_{2A}- and A_{2B}AR.



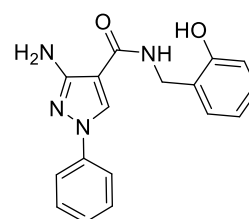
36a

$K_i A_1 = 328 \pm 71$ nM
 $K_i A_{2A} = 5.07 \pm 0.37$ nM
 $K_i A_{2B} = 31.9 \pm 2.1$ nM
 $K_i A_3 > 1,000$ nM (19%)
 sel. $A_{2A}/A_{2B} = 6$



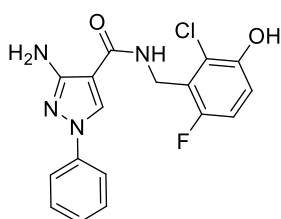
36b

$K_i A_1 = 555 \pm 77$ nM
 $K_i A_{2A} = 15.3 \pm 1.3$ nM
 $K_i A_{2B} = 62.5 \pm 17.6$ nM
 $K_i A_3 > 1,000$ nM (5%)
 sel. $A_{2A}/A_{2B} = 4$



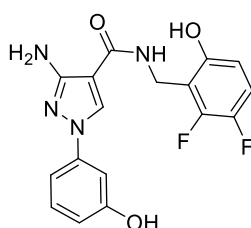
29f

$K_i A_1 = 87.3 \pm 24$ nM
 $K_i A_{2A} = 8.03 \pm 2.17$ nM
 $K_i A_{2B} = 60.1 \pm 6.2$ nM
 $K_i A_3 > 1,000$ nM (32%)
 sel. $A_{2A}/A_{2B} = 7$



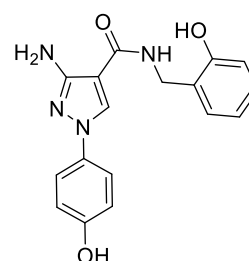
21f

$K_i A_1 > 1,000$ nM (4%)
 $K_i A_{2A} = 174 \pm 35$ nM
 $K_i A_{2B} = 89.3 \pm 18.8$ nM
 $K_i A_3 > 1,000$ nM (27%)
 sel. $A_{2A}/A_{2B} = 2$



21g

$K_i A_1 = 193 \pm 68$ nM
 $K_i A_{2A} = 5.41 \pm 0.86$ nM
 $K_i A_{2B} = 36.9 \pm 7.2$ nM
 $K_i A_3 > 1000$ (30%)
 sel. $A_{2A}/A_{2B} = 7$



19c

$K_i A_1 > 1,000$ nM (34%)
 $K_i A_{2A} = 39.4 \pm 7.1$ nM
 $K_i A_{2B} = 144 \pm 48$ nM
 $K_i A_3 > 1,000$ nM (-7%)
 sel. $A_{2A}/A_{2B} = 4$

Figure 20. AR affinities of compounds **36a**, **36b**, **39f**, **21f**, **21g** and **19c**, inhibition at 1 μ M in % is displayed for some receptors.

An SAR analysis of the 3-amino-*N*-benzyl-1-phenyl-1*H*-pyrazole-4-carboxamides with regard to A_{2B} affinity reveals that large residues like the methoxy group were not well tolerated at both phenyl moieties. A comparison of the analogues **29b**, **29f** and **29e** reveals that only **29f** (2-hydroxybenzylamine) showed good A_{2B} -affinity but with low selectivity ($K_i A_{2A} = 60.1$ nM). No substitution (**29b**, benzylamine) or a too large substituent (**29e**, 2-methoxybenzylamine) resulted in a loss of potency at the A_{2B} AR. Either the A_{2B} AR only accepts a polar residue at that position or there is a very particular space demand to perfectly interact with the receptor. Another interesting example are compounds **36b** (2-fluorobenzylamine, $K_i A_{2A} = 62.5$ nM), **36d** (2-bromobenzylamine, $K_i A_{2A} = 338$ nM) and **36e** (2-methoxybenzylamine, $K_i A_{2A} > 1,000$ nM): The A_{2B} -affinity decreases drastically with increasing size of the *ortho*-substituent of the benzylamine moiety. The potency indeed seems to be depending on the space demand of the substituents since all three substituents are lipophilic, and a fluorine atom and an OH group are of comparable size.

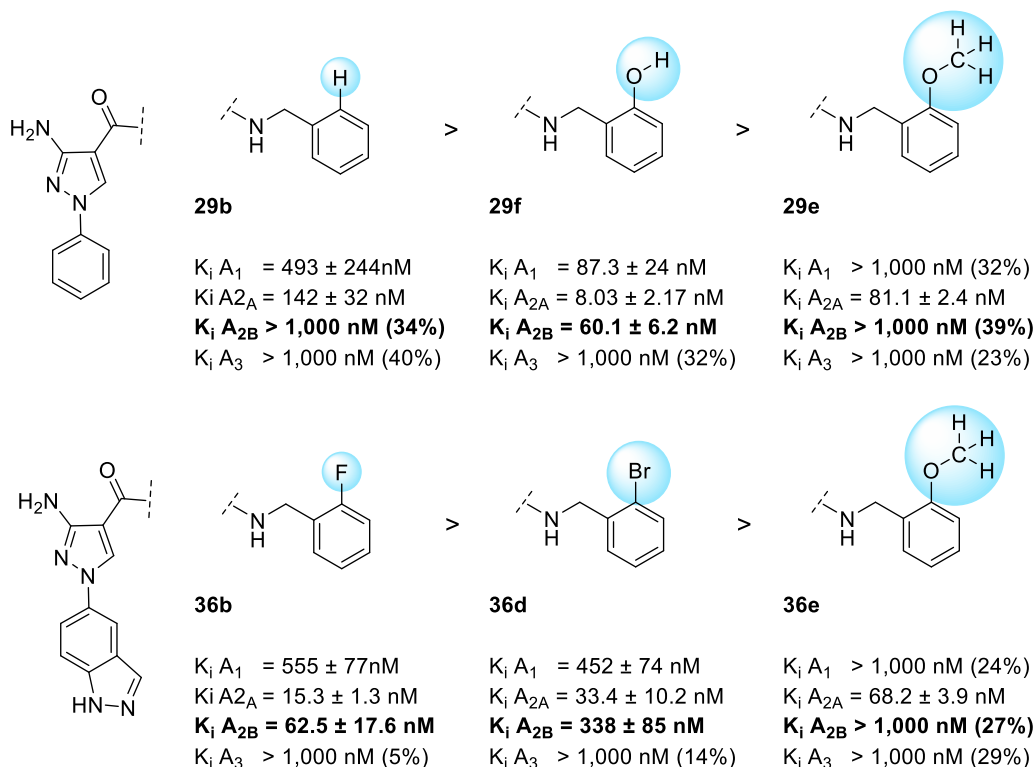


Figure 21. AR affinities of compounds **29b**, **29f** and **29e** as well as **36b**, **36d**, **36e** inhibition at 1 μM in % is displayed for some receptors.

The 5-amino-*N*-benzyl-1-phenyl-1*H*-pyrazole-4-carboxamides **3** and **4**, that were synthesized to find out if phenyl rings at N2 would be tolerated as well, did not show any noteworthy affinity at any AR. These findings correspond with our expectation from the computational approaches in the literature^{1;3} and the SAR conclusions of our studies. Thus, this scaffold will not be further explored.

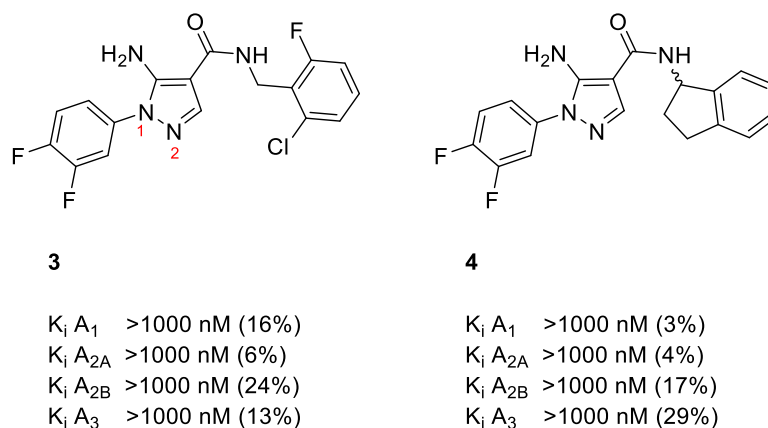


Figure 22. AR affinities of 5-amino-*N*-benzyl-1-(3,4-difluorophenyl)-1*H*-pyrazole-4-carboxamide derivatives **3** and **4**, inhibition at 1 μM in % is displayed.

4.3.7.4. Physicochemical properties

4.3.7.4.1. Water solubility and lipophilicity

Physicochemical properties like water solubility are important parameters for drug development. Sufficient solubility is required for injection-, eye drop- or inhalation solutions, and it influences oral bioavailability.³⁷ A wide variety of potent compounds is practically useless because a lack of solubility limits their utility as biological probes or as drugs. In order to compare our new 3-amino-*N*-benzyl-1-phenyl-1*H*-pyrazole-4-carboxamide scaffold with the scaffold of 5-amino-*N*-benzyl-4-carboxamido-2-phenyl-1,2,3-triazoles,^{1,3} selected compounds were subjected to measurement of their physicochemical properties. Therefore, compound **73** (PSB-11202) was synthesized as an analogue of **9a** according to the literature.³⁸

The kinetic solubility of a molecule is the maximal solubility of the fastest precipitating species of this compound. In most procedures, the respective compound is solved in DMSO, this stock solution is given into an aqueous puffer solution and the supernatant is evaluated via HPLC analysis after a specific time passed. It is noteworthy that these values strongly depend on time and the specifics of used machines and procedures. Accordingly, results should only be compared within a particular testing system.³⁹ The kinetic solubilities of **9a** (PSB-20310) and **73** (PSB-11202)³⁸ were measured by an extern company (Pharmacelsus, Saarbrücken, Germany). The results are illustrated in Table 6 along with additional data:

Table 6. Selected physicochemical parameters of **9a** and triazole derivative **73**.

Compound	9a	73
Molecular weight	380,76	381,74
Kinetic solubility ^a	34.9 μ M	3.16 μ M
R _f ^b	0.14	0.59
Melting point	198 °C	141 °C
Log P ^c	3.85	3.89
tPSA ^c	70.7 Å ²	83.0 Å ²

^aCompounds were dissolved in DMSO to obtain a 20 mM stock solution then diluted with PBS buffer (pH 7.4), followed by vigorous shaking (1.5 h) and centrifugation (3 min). ^beluent: (CH₂Cl₂ / ethyl acetate - 95 : 5). ^cvalues were calculated with ChemDraw Professional 15.0.

As a result, 3-amino-*N*-benzyl-1-phenyl-1*H*-pyrazole-4-carboxamide **9a** showed reasonably high solubility of 34.9 μM in the assay. This is 11-fold better than the solubility of the corresponding triazole which only displayed a solubility of 3.16 μM . Moreover, the two compounds were analyzed and compared with regard to their properties by TLC probes. In the solvent-system CH_2Cl_2 / ethyl acetate - 95 : 5, **9a** showed an R_f value of 0.14 while **73** showed an R_f value of 0.59. This indicates, that the pyrazole derivative is more polar than the corresponding triazole. Also, a comparison of the melting points (198 $^\circ\text{C}$ for **9a** and 141 $^\circ\text{C}$ for **73**) indicates different physicochemical properties for the two scaffolds, despite their chemical resemblance. The log P value (*n*-octanol-water partition coefficient) and the tPSA (topological polar surface area) are further parameter to evaluate the lipophilicity of molecules. With (calculated) log P values of 3.85 and 3.89, the two compounds seem quite similar. Compounds that display log P values in that range are considered as rather lipophilic.⁴⁰ Naturally, the (calculated) tPSA values (70.72 \AA^2 for **9a** and 83.08 \AA^2 for **73**) differ a bit more since the triazole has an additional heteroatom. Compounds with a tPSA below 90 \AA^2 are expected to be able to cross the blood brain barrier.⁴¹ In summary, compound **9a** has overall suitable drug-like properties. In theory, it is lipophilic enough to pass biomembranes but it is soluble enough to be used in *in vivo* or *in vitro* studies.

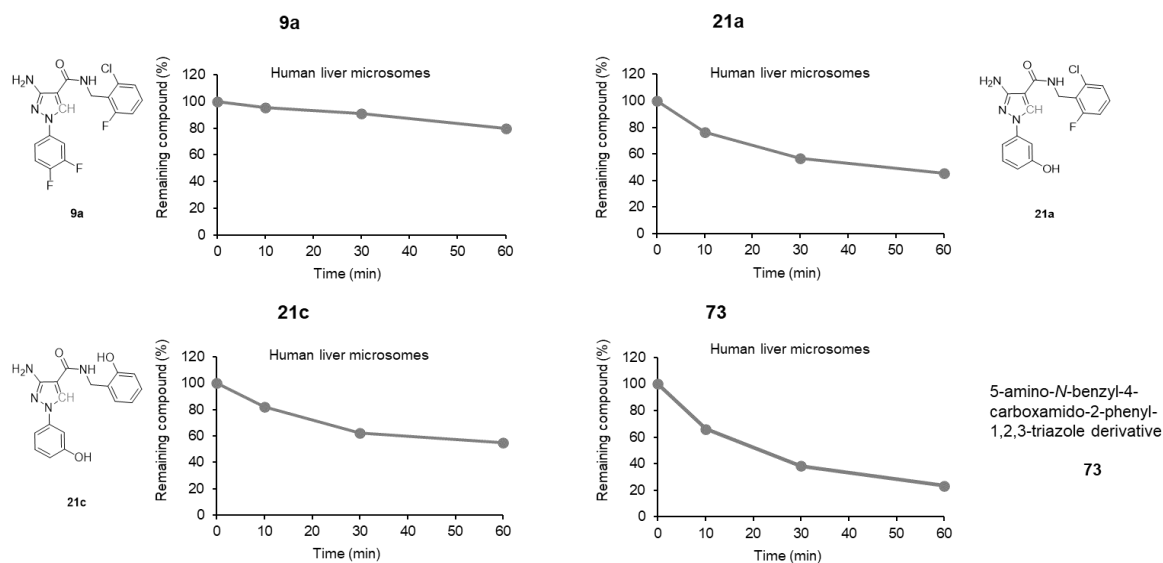
4.3.7.4.2. Metabolic stability analysis

When it comes to *in vivo* studies or to an actual clinical use of a drug molecule, pharmacokinetic parameters including the basic processes of absorption, distribution, metabolism, and excretion (ADME) are important. Especially the metabolic stability, that refers to the susceptibility of compounds to biotransformation and is measured in human liver microsomes, is an important parameter for drug design. The metabolic stability of **9a**, **21a**, **21c** and **73** was measured by an external company (Pharmacelsus, Saarbrücken, Germany).

Table 7. Metabolic stability of **9a**, **21a**, **21c** and **73**.

Compound	9a	21a	21c	73
$t_{1/2}$ (min)	192.5	55.5	70.7	29.4
Metabolic stability (CL_{int}) ($\mu\text{l}/\text{min}/\text{mg}$ protein) ^a	7.2	25.0	19.6	47.2
CL'_{int} (ml/min/kg)	9.7	33.7	26.4	63.7
E_h^b	0.32	0.62	0.56	0.75
% E_h	31.6	61.6	55.7	75.2

^aperformed using human liver microsomes at 0.5 mg/ml. The remaining amount of substance was measured by HPLC analysis after 10, 30 and 60 minutes. ^bhepatic excretion.

**Figure 23.** Microsomal stability profile of **9a**, **21a**, **21c** and **73** measured by HPLC.

As a result, all three 3-amino-*N*-benzyl-1-phenyl-1*H*-pyrazole-4-carboxamides **9a**, **21a** and **21c** were metabolically more stable than the respective 5-amino-*N*-benzyl-4-carboxamido-2-phenyl-1,2,3-triazole **73**. Especially the analogues **9a** and **73** displayed a large difference in their half-lives, the triazole decomposed 6.5-fold faster than the pyrazole **9a**. With a $t_{1/2}$ of 193 min, **9a** was also the most stable compound among the pyrazoles. Bisphenol **21c** is even a bit more stable than monophenol **21a**. The overall polarity and the resulting properties such as protein binding (not measured) might influence metabolic stability.⁴² These results are encouraging, indicating that the 3-amino-*N*-benzyl-1-phenyl-1*H*-pyrazole-4-carboxamides could be developed as drugs with sufficient metabolic stability.

4.3.7.4.3. Thermostability assay at the A_{2A}AR

Thermostability assays are a useful method to identify ligands that stabilize a GPCR and could be suitable for X-ray crystallography studies. In our group, several antagonists were tested in thermostability studies using a thermostabilized A_{2A}AR harboring a single point mutation. A procedure that employed the thiol-specific fluorescent dye *N*-[4-(7-diethylamino-4-methyl-3-coumarinyl)phenyl]maleimide (CPM) was used.^{43;44} The melting temperature (and thus the degree of stability) of the protein is determined (cf. Figure 24). A ligand with high residence time stabilizes the protein and would accordingly be helpful for crystallization. One of the compounds was **36a** (see Figure 24, blue), which had exhibited the highest binding affinity among the series of 3-amino-*N*-benzyl-1-phenyl-1*H*-pyrazole-4-carboxamides (K_i human A_{2B}AR = 5.07 nM). However, **36a** did not enhance the thermostability of the protein, and the melting temperature was comparable to the control in the absence of ligands (black). Hence, **36a** would not stabilize the GPCR during crystallization. This is in contrast to its high binding affinity. However, the A_{2B}AR is already quite stable without ligands by nature, and the employed protein was a stabilized protein and not the wildtype receptor protein.⁴³

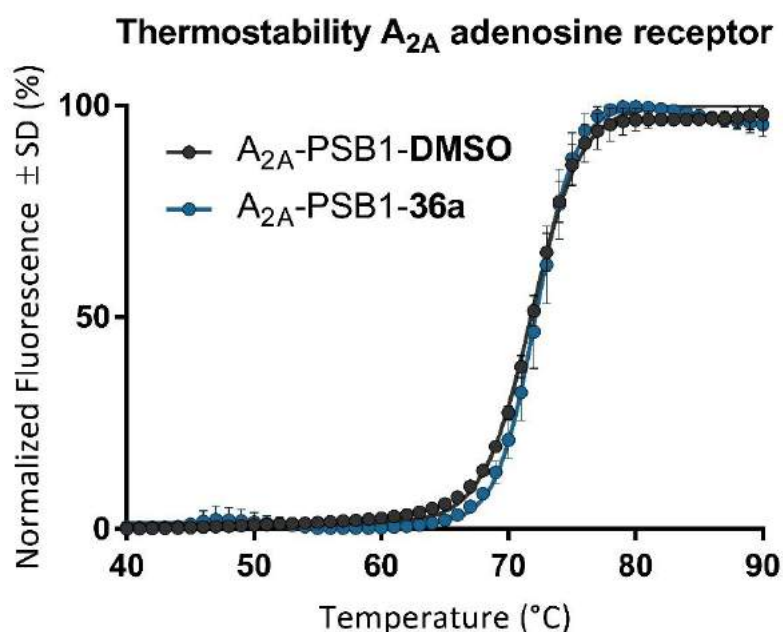


Figure 24. Thermostability experiment of **36a** (in blue) in comparison with DMSO as control (black).^{43;44}

4.3.8. Summary and outlook

The A_{2A}AR is an important drug target since it is involved in severe diseases including inflammation, cancer, Parkinson's disease and Alzheimer disease.⁴⁵ Although numerous agonists and antagonists have been described, only few of them are actually in clinical use or evaluated in preclinical studies.

In the course of this project, different synthetic routes to prepare 3-amino-*N*-benzyl-1-phenyl-1*H*-pyrazole-4-carboxamide derivatives have been successfully explored and used. Starting from (substituted) phenylhydrazines, a protection group strategy led to the selective formation of the desired isomer of 3-aminopyrazoles in moderate yields. However, the yield was twice as high as described in the literature.⁴⁻⁶ Depending on the availability of the building blocks, aromatic halides or arylboronic acids can be coupled to the aminopyrazole core **37** using Ullmann or Chan-Lam reactions in order to obtain the desired 3-amino-*N*-benzyl-1-phenyl-1*H*-pyrazole-4-carboxamide derivatives.^{4;13} With **38c**, a suitable *N*-protected building block was identified as a basis for these procedures.

The established methods of synthesis were applied to prepare a compound library of 53 new compounds of the scaffold. Figure 25 illustrates all planned substituents for the N1-position of the pyrazole core. 7 of the 8 planned substituents could be realized combined with various substituted benzylamide residues in position 4. In case of the 3,4-dihydroxyphenyl residue, only one product was prepared. A pyrazole residue at N1 could not yet be introduced into the scaffold. Furthermore, 2 compounds of the wrong and inactive isomer 5-amino-*N*-benzyl-1-(3,4-difluorophenyl)-1*H*-pyrazole-4-carboxamide were prepared and tested.

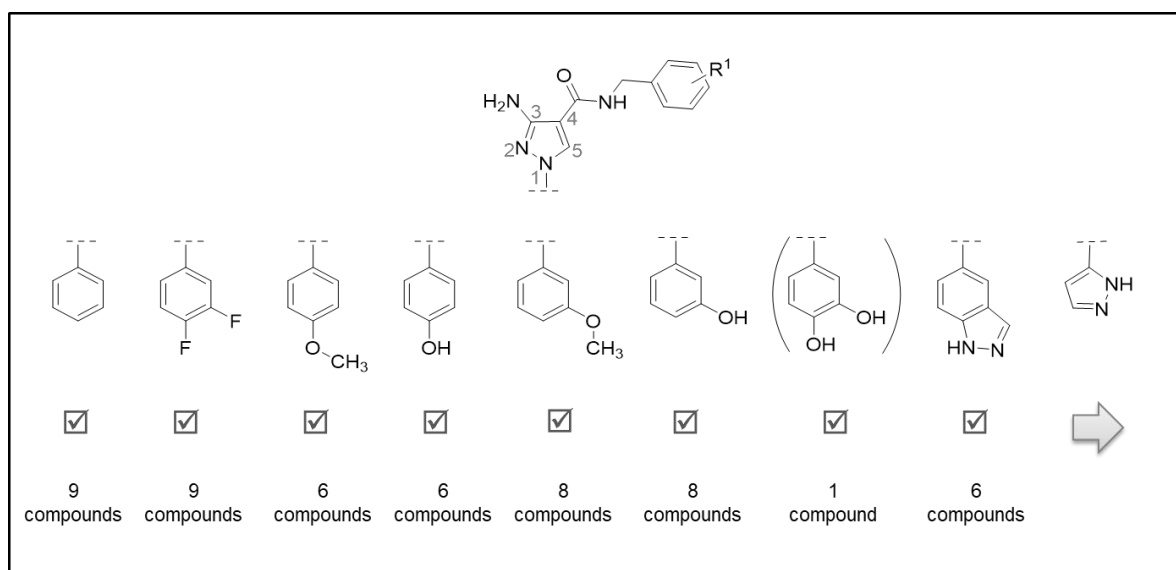


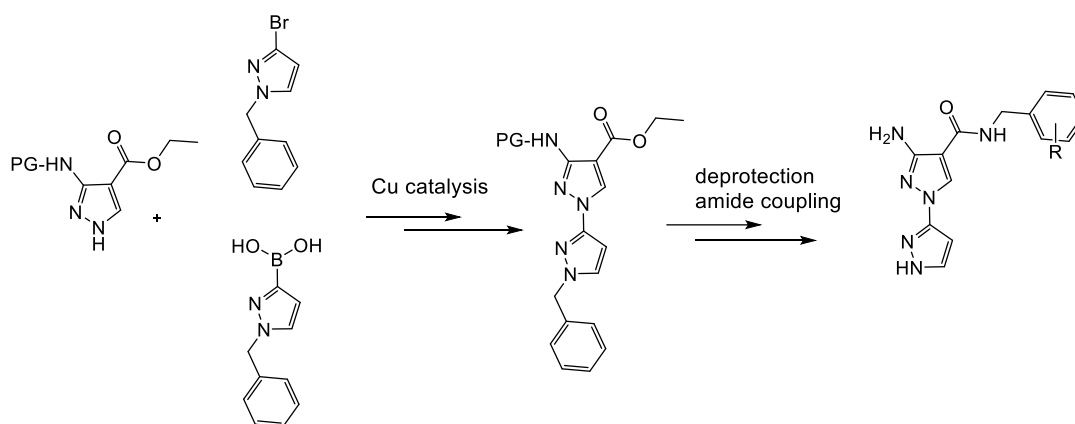
Figure 25. Overview of all synthesized residues for the N1-position of the 3-amino-*N*-benzyl-1-phenyl-1*H*-pyrazole-4-carboxamide scaffold.

As a highlight, the difficultly accessible 1*H*-indazol-5-yl residue could be introduced into the scaffold at the N1-position, and six compounds bearing that promising moiety could be synthesized. Also, two compounds that exhibit a slightly different scaffold were prepared: the 3-amino-*N*-(2-chloro-6-fluorobenzyl)-1-phenyl-5-methyl-1*H*-pyrazole-4-carboxamides **59** and **60** display a methyl group at position 5 of the pyrazole ring. However, the alkylation of this position turned out to result in a less potent derivatives as compared to the parent compounds **20a** and **21a** (cf. Figure 17). Further modifications of that position are thus not recommended. A modification of the 3-amino group could not be implemented and needs to be investigated in the future.

Compound **36a** ($K_i A_{2A}$ 5.07 nM) is the most potent A_{2A} AR antagonist of the 3-amino-*N*-benzyl-1-phenyl-1*H*-pyrazole-4-carboxamide scaffold that was prepared. More than that, it showed good A_{2B} affinity ($K_i A_{2B}$ 31.9 nM) and selectivity versus A_1 ($K_i A_1$ 328 nM, 65-fold selective). Our results prove that switching the scaffold from aminotriazole to aminopyrazole was successful.

Furthermore, a DMPK study of **9a** and **73** indicated, that the physicochemical properties (especially the water solubility) of the 3-amino-*N*-benzyl-1-phenyl-1*H*-pyrazole-4-carboxamides might be superior to those of the corresponding aminotriazoles.

The desired residue pyrazole could not yet be introduced into the N1-position. All previously tried coupling reactions between **37** / **38c** and the respective 5-bromo-1*H*-pyrazole and (1*H*-pyrazol-5-yl)boronic acid gave unsatisfactory results. One of the reasons could be the utilization of inappropriate protection groups. A benzyl group might result in better properties (cf. Scheme 42). Moreover, the compounds could be detected by UV light in TLC analysis. The coupling reaction under Cu-catalysis would be followed by deprotection and amide coupling to yield the final 3-amino-*N*-benzyl-2'*H*-[1,3'-bipyrazole]-4-carboxamides.



Scheme 42. Suggested synthesis of 3-amino-*N*-benzyl-2'*H*-[1,3'-bipyrazole]-4-carboxamides.

Beside the substituent at the N1-position of the pyrazole core, a variety of other moieties could be investigated in the future. Figure 26 illustrates several suggestions.

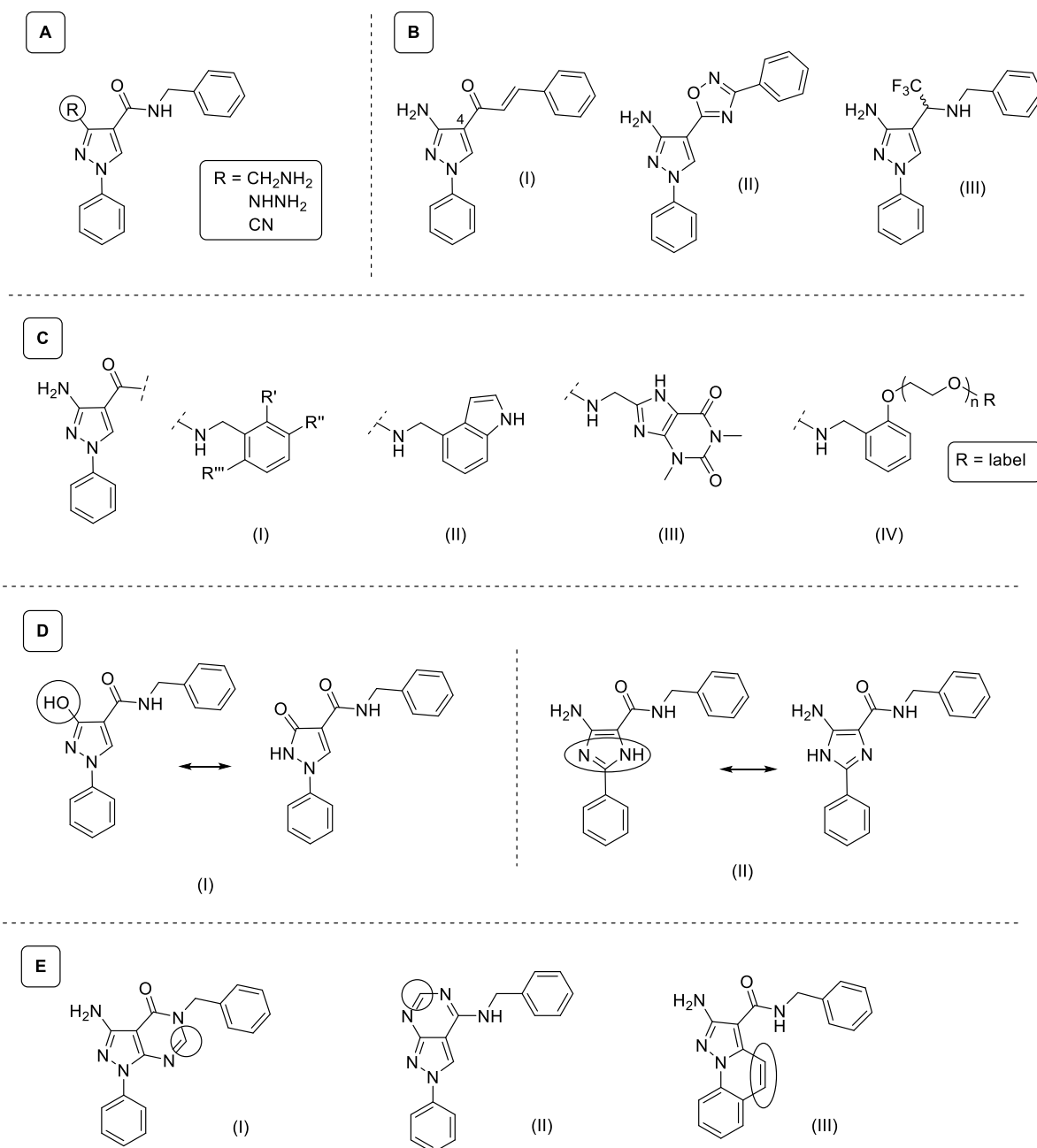


Figure 26. Examples of modified pyrazole scaffolds for the future.

A: Since the modification of the 3-amino group could not be implemented, this moiety still needs to be explored.

B: Beside esters, amidines and amides,^{1,3} other linker structures like bioisosteres of amides could be tested for position 4. Figure 26B illustrates an α,β -unsaturated ketone (B-I), a 1,2,4-oxadiazole (B-II) and trifluoroethylamine (B-III) as examples for a bioisosteric exchange of the amide structure. While binding angles and steric demand are comparable to the parent

compound, potency, lipophilicity, toxicity and metabolic fate might be altered. Bioisosterism is furthermore an opportunity to create new intellectual property.

C: Until this point, mostly substituted benzylamines (and in two cases 1-naphthylmethylamine) were used as building blocks for the amide moiety. Like already done with compounds **21f**, **21g** and their derivatives, more combinations of established substituents could be used to prepare compounds that bear di- or tri-substituted benzylamine moieties (C-I). The good biological activity of the 2,3-dichlorobenzylamine- and 2,3-difluoro-6-hydroxybenzylamine moiety suggest that the A_{2A} AR still has sub-pockets at that position. Hence, bicyclic heterocycles like indoles and other residues of comparable size might be interesting building blocks (C-II). Small bioactive compounds like xanthine derivatives could be introduced at the amide moiety as well (C-III). They are sterically not too demanding and it is a common pharmaceutical approach to combine two drug molecules to address more than one protein or to direct a drug molecule to a particular target in the body.⁴⁶ This approach however is much more complicated and needs to be carefully considered. Moreover, the benzylamine moiety might be a possible position to attach a longer linker like polyethyleneglycols (C-IV). The terminus of the linker might be coupled with a fluorophore or another label.

D: Furthermore, the core structure itself, the pyrazole, could be modified. The introduction of a different H-bond donor like a hydroxyl group at the 3-position of the pyrazole ring (D-I) is conceivable. However, the introduction of a hydroxyl group would probably not lead to the desired effect based on the lactam-lactim tautomerism. Here, the carbonyl group at the 3-position of the lactam structure would not act as a hydrogen bond donor, but as a hydrogen bond acceptor. Also, an imidazole could be a possible core structure for the scaffold (D-II). The presumable tautomerism of the NH proton of the imidazole might be disadvantageous, however, it might also offer a new kind of interaction towards the receptor. While the N2 of the pyrazole can only act as an H-bond acceptor, the NH of the imidazole could act as an H-donor. Since the amino acid Asn253 of the A_{2A} AR is the possible interaction partner,^{1:3} this exchange of interaction could be beneficial as the amide function of the amino acid might interact with both moieties.

E: It is a common approach in medicinal chemistry to rigidify compounds by the formation of cyclic structures. Less rotatable bonds in the drug molecule improve the chance of the molecule to interact with the target protein in the bioactive conformation. Furthermore, the drug molecule becomes less promiscuous since a rigid molecule has fewer active conformations and might thus address less targets.⁴⁷ Figure 26E illustrates possible position for a ring formation.

All of these possible future modifications need to be carefully considered since many approaches require an entirely new synthetic pathway and the possible gain needs to justify the effort.

4.3.9. Experimental Part

4.3.9.1 General methods

The general methods were the same as in script 4.1. and 4.2..

4.3.9.2. Synthesis

General procedure A. This procedure has been applied to the preparation of **3,4** and **9a-9i**. A solution of the respective carboxylic acid **2** of **8**, the appropriate benzylamine, HBTU and TEA in DMF (3 ml) were stirred at 80 °C for 16 h. Subsequently, the mixture was treated with water and extracted with CH₂Cl₂ (3 x 20 ml), the combined organic layers were dried over MgSO₄, filtered off and the solvent was evaporated under reduced pressure. The residue was purified via column chromatography (CH₂Cl₂/ MeOH - 98 : 2). Additionally, still impure products were purified via flash RP-HPLC (10 to 100% MeOH).

General procedure B. This procedure has been applied to the preparation of **18a-18f**, **20a-20g**, **29a-29e**, **36a-36e**, **47** and **59**. A solution of respective carboxylic acid **16**, **17**, **25**, **35**, **46** or **58**, the appropriate benzylamine, HBTU and TEA in DMF (1 ml) were stirred at 55 °C for 16 h. Subsequently, the mixture was treated with water and extracted with CH₂Cl₂ (3 x 20 ml), the combined organic layers were dried over MgSO₄, filtered off and the solvent was evaporated under reduced pressure. The residue was purified via column chromatography (CH₂Cl₂/ MeOH - 98 : 2). Additionally, still impure products were purified via flash RP-HPLC (10 to 100% MeOH).

General procedure C. This procedure has been applied to the preparation of **19a-19f**, **21a-21g**, **29f**, **36f**, **48** and **60**. A solution of the respective methoxy derivative in CH₂Cl₂ was treated with a 1M solution of BBr₃ in CH₂Cl₂ (5 eq.) and stirred at rt for 16 h. Subsequently, the mixture was treated with water and extracted with ethyl acetate (3 x 20 ml), the combined organic layers were dried over MgSO₄, filtered off and the solvent was evaporated under reduced pressure. The residue was purified via column chromatography (CH₂Cl₂/ MeOH - 9 : 1) and/or via flash RP-HPLC (10 to 100% MeOH).

4.3.9.2.1. Synthesis of 5-amino-*N*-benzyl-1-(3,4-difluorophenyl)-1*H*-pyrazole-4-carboxamide

Synthesis of ethyl 5-amino-1-(3,4-difluorophenyl)-1*H*-pyrazole-4-carboxylate (**1**)⁴

A solution of 3,4-difluorophenylhydrazine hydrochloride (250 mg, 1.39 mmol), ethyl(ethoxymethylene)cyanoacetate (EEMA) (235 mg, 1.39 mmol) and NaHCO₃ (117 mg, 1.39 mmol) in EtOH (3 ml) was stirred at 70 °C for 3 h. Subsequently, the solvent was removed under reduced pressure and the residue was purified via column chromatography (CH₂Cl₂ / MeOH - 98 : 2). The product **1** was obtained as 251 mg (68%) of a yellow solid. ¹H NMR (600 MHz, Chloroform-*d*) δ: 7.75 (s, 1H, CH_{pyrazole}), 7.44-7.39 (m, 1H, CH_{arom.}), 7.32-7.23 (m, 2H, CH_{arom.}), 5.27 (s, 2H, NH₂), 4.28 (q, *J* = 7.1 Hz, 2H, CH₂CH₃), 1.34 (t, *J* = 7.1 Hz, 3H, CH₂CH₃) ppm. ¹³C NMR (151 MHz, Chloroform-*d*) δ: 164.37 (ester), 150.56 (dd, ¹*J*_{CF} = 251.8, 13.5 Hz), 149.7 (dd, ¹*J*_{CF} = 251.0, 12.2 Hz), 140.9, 133.8 (dd, ³*J*_{CF} = 7.9, 3.6 Hz), 119.7 (dd, ³*J*_{CF} = 6.5, 3.7 Hz), 118.2 (d, ²*J*_{CF} = 18.7 Hz), 113.7 (d, ²*J*_{CF} = 20.2 Hz), 96.6, 59.8, 14.3 ppm. HPLC-UV (254 nm) ESI-MS, purity: 81%. LC-MS (m/z): 267.8 [M + H]⁺. Mp.: 121 °C.

Synthesis of 5-amino-1-(3,4-difluorophenyl)-1*H*-pyrazole-4-carboxylic acid (**2**)

A solution of **2** (240 mg, 0.89 mmol) and LiOH monohydrate (189 mg, 4.5 mmol) in water / THF (1 : 1, 5 ml) was stirred at 80 °C for 3 h. Subsequently, the solution was treated with water and the pH value was adjusted to 3 using AcOH. This mixture was extracted with ethyl acetate (3 x 30 ml), the combined organic layers were dried over MgSO₄, filtered and the solvent was evaporated under reduced pressure. The residue was dissolved in a small amount of ethyl acetate and then precipitated with heptane. The solid was filtered and dried at 70 °C. The product was obtained as 169 mg (79%) of a colorless solid. ¹H NMR (600 MHz, DMSO-*d*₆) δ: 12.09 (s, 1H, COOH), 7.67 (s, 1H, CH_{pyrazole}), 7.67-7.62 (m, 1H, CH_{arom.}), 7.62-7.56 (m, 1H, CH_{arom.}), 7.42-7.38 (m, 1H, CH_{arom.}), 6.39 (s, 2H, NH₂) ppm. ¹³C NMR (151 MHz, DMSO-*d*₆) δ: 190.8, 164.6, 150.4, 148.6 (dd, ¹*J*_{CF} = 232.2, 12.8 Hz), 149.4 (dd, ¹*J*_{CF} = 248.7, 14.5 Hz), 132.0, 127.9, 117.4, 114.2, 107.6, 102.0, 55.6, 55.3 ppm. HPLC-UV (254 nm) ESI-MS, purity: 97%. LC-MS (m/z): 239.7 [M + H]⁺.

Synthesis of 5-amino-*N*-(2-chloro-6-fluorobenzyl)-1-(3,4-difluorophenyl)-1*H*-pyrazole-4-carboxamide (**3**)

A solution of **2** (40 mg, 0.17 mmol), 2-chloro-6-fluorobenzylamine (28 mg, 0.175 mmol), HBTU (84 mg, 0.22 mmol) and TEA (33 mg, 0.25 mmol) in DMF (3 ml) was reacted according to general procedure A. The product **3** was obtained as 32 mg (50%) of a colorless solid. ¹H NMR (600 MHz, Chloroform-*d*) δ: 7.54 (s, 1H, CH_{pyrazole}), 7.41 (t, *J* = 8.8 Hz, 1H, CH_{arom.}), 7.25-7.18 (m, 2H, CH_{arom.}), 7.22 (m, 2H, CH_{arom.}), 7.02 (t, *J* = 8.8 Hz, 1H, CH_{arom.}), 6.01-5.89 (m, 1H, NH), 5.52 (s, 2H, NH₂), 4.75 (d, *J* = 5.8 Hz, 2H, NHCH₂Ar) ppm. ¹³C NMR (151 MHz, Chloroform-*d*)

δ : 163.8, 162.5, 160.8, 151.0 (dd, $^1J_{CF} = 126.1, 13.1$ Hz), 149.3 (dd, $^1J_{CF} = 125.0, 13.0$ Hz), 137.4, 135.5 (d, $^3J_{CF} = 5.1$ Hz), 134.0, 129.8 (d, $^3J_{CF} = 9.5$ Hz), 125.5, 123.9 (d, $^2J_{CF} = 17.9$ Hz), 119.6, 118.2 (d, $^2J_{CF} = 18.4$ Hz), 114.5 (d, $^2J_{CF} = 23.0$ Hz), 113.7 (d, $^2J_{CF} = 20.0$ Hz), 98.1, 34.4 (d, $^4J_{CF} = 4.1$ Hz) ppm. HPLC-UV (254 nm) ESI-MS, purity: 93%. LC-MS (m/z): 380.9 [M + H]⁺. Mp.: 170 °C.

Synthesis of 5-amino-1-(3,4-difluorophenyl)-N-(2,3-dihydro-1H-inden-1-yl)-1H-pyrazole-4-carboxamide (4)

A solution of **2** (20 mg, 0.08 mmol), 1-aminoindane hydrochloride (21 mg, 0.12 mmol), HBTU (48 mg, 0.12 mmol) and DIPEA (33 mg, 0.25 mmol) in DMF (3 ml) was reacted according to general procedure A. The product **4** was obtained as 16 mg (57%) of a colorless solid. ¹H NMR (600 MHz, Chloroform-*d*) δ : 7.51 (s, 1H, CH_{pyrazole}), 7.44 (ddd, $J = 10.0, 6.9, 2.4$ Hz, 1H, CH_{arom.}), 7.35-7.20 (m, 6H, CH_{arom.}), 5.79 (d, $J = 8.5$ Hz, 1H, NH), 5.64 (q, $J = 7.8$ Hz, 1H, CH_{indane}), 5.57 (s, 2H, NH₂), 3.08-2.97 (m, 1H, CH_{2 indane}), 2.95-2.86 (m, 1H, CH_{2 indane}), 2.69-2.61 (m, 1H, CH_{2 indane}), 1.96-1.85 (m, 1H, CH_{2 indane}) ppm. ¹³C NMR (151 MHz, Chloroform-*d*) δ : 164.1, 151.42 (d, $^2J_{CF} = 13.5$ Hz), 150.6 (dd, $^1J_{CF} = 249.8, 13.2$ Hz, C_{arom.}), 148.9 (dd, $^1J_{CF} = 248.7, 12.8$ Hz, C_{arom.}), 143.5, 143.2, 137.4, 134.1 (dd, $^3J_{CF} = 8.0, 3.6$ Hz), 128.1, 126.8, 124.9, 124.1, 119.6 (dd, $^3J_{CF} = 6.6, 3.6$ Hz), 118.2 (d, $^2J_{CF} = 18.3$ Hz), 113.6 (d, $^2J_{CF} = 20.2$ Hz), 98.2, 54.2, 34.30, 30.3 ppm. HPLC-UV (254 nm) ESI-MS, purity: 98%. LC-MS (m/z): 355.0 [M + H]⁺. Mp.: 169 °C.

4.3.9.2.2. Synthesis of 3-amino-N-benzyl-1-(3,4-difluorophenyl)-1H-pyrazole-4-carboxamide derivatives

Synthesis of (E)-1-(3,4-difluorophenyl)-2-(4-methoxybenzylidene)hydrazine (5)⁵

A solution of 3,4-difluorophenylhydrazine hydrochloride (3000 mg, 16.7 mmol), anisaldehyde (2514 mg, 19 mmol) and NaOH (680 mg, 17 mmol) in MeOH (50 ml) and water (10 ml) was stirred at rt for 6 h. Subsequently, the solvent was removed under reduced pressure and the residue was purified via column chromatography (petrol ether / ethyl acetate - 8 : 2). The product **5** was obtained as 957 mg (25%) of a brown solid. LC-MS (m/z): 232.9 [M + H]⁺.

Ethyl 3-amino-1-(3,4-difluorophenyl)-1H-pyrazole-4-carboxylate (7)5

A solution of **5** (915 mg, 3.94 mmol) and EEMA (666 mg, 3.94 mmol) in xylol (2 ml) was stirred at 160 °C for 3 days. The solvent was evaporated and the intermediate **6** was identified via TLC-MS (356 [M + H]⁺). The crude substances were dissolved in EtOH (3 ml) and treated with conc. HCl (1.4 ml). This mixture was refluxed for 15 min at 100 °C. The solution was basified to pH 9 with saturated NaHCO₃ solution and extracted with CH₂Cl₂ (3 x 20 ml), the combined organic layers were dried over MgSO₄, filtered and the solvent was evaporated under reduced

pressure. Subsequently, the solvent was removed under reduced pressure and the residue was purified via flash column chromatography (CH₂Cl₂ / MeOH - 100 to 98 : 2). The product **7** was obtained as 300 mg (29%) of a yellow solid. ¹H NMR (600 MHz, Chloroform-*d*) δ: 8.05 (s, 1H, CH_{pyrazole}), 7.48 (ddd, *J* = 11.2, 6.9, 2.7 Hz, 1H, CH_{arom.}), 7.30 (dddd, *J* = 9.0, 3.9, 2.5, 1.5 Hz, 1H, CH_{arom.}), 7.28-7.16 (m, 1H, CH_{arom.}), 4.30 (q, *J* = 7.1 Hz, 2H, CH₂CH₃), 4.09 (s, 2H, NH), 1.35 (t, *J* = 7.1 Hz, 3H, CH₂CH₃) ppm. ¹³C NMR (151 MHz, Chloroform-*d*) δ: 163.7, 156.7, 151.4 (dd, ¹*J*_{CF} = 249.4, 13.7 Hz), 149.0 (dd, ¹*J*_{CF} = 247.8, 12.8 Hz), 135.6 (d, ³*J*_{CF} = 7.9 Hz), 129.7, 117.9 (d, ²*J*_{CF} = 18.7 Hz), 114.0 (dd, ³*J*_{CF} = 6.4, 3.7 Hz), 108.7 (d, ²*J*_{CF} = 22.0 Hz), 102.4, 60.3, 14.4 ppm. HPLC-UV (254 nm) ESI-MS, purity: 85%. LC-MS (m/z): 267.8 [M + H]⁺. Mp.: 140 °C.

Synthesis of 3-amino-1-(3,4-difluorophenyl)-1*H*-pyrazole-4-carboxylic acid (**8**)

A solution of **7** (290 mg, 1.09 mmol) and LiOH monohydrate (228 mg, 5.43 mmol) in water / THF (1 : 1, 5 ml) was stirred at 80 °C for 3 h. Subsequently, the solution was treated with water and the pH value was adjusted to 3 using AcOH. This mixture was extracted with ethyl acetate (3 x 30 ml), the combined organic layers were dried over MgSO₄, filtered and the solvent was evaporated under reduced pressure. The residue was dissolved in a small amount of ethyl acetate and then crystallized with heptane. The solid was filtered and dried at 70 °C. The product was obtained as 136 mg (52%) of a colorless solid. ¹H NMR (600 MHz, DMSO-*d*₆) δ: 8.70 (s, 1H, CH_{pyrazole}), 7.93-7.80 (m, 1H, CH_{arom.}), 7.68-7.60 (m, 1H, CH_{arom.}), 7.5-7.46 (m, 1H, CH_{arom.}), 5.78-5.55 (m, 2H, NH₂) ppm. ¹³C NMR (151 MHz, DMSO) δ: 165.2, 157.4, 149.7 (dd, ¹*J*_{CF} = 247.1, 12.4 Hz), 148.2 (dd, ¹*J*_{CF} = 250.3, 12.6 Hz), 136.1 (d, ³*J*_{CF} = 8.7 Hz), 131.2, 118.3 (d, ²*J*_{CF} = 18.3 Hz), 114.3 (dd, ³*J*_{CF} = 6.6, 3.4 Hz), 107.5 (d, ²*J*_{CF} = 22.1 Hz), 102.5 ppm. HPLC-UV (254 nm) ESI-MS, purity: 87%. LC-MS (m/z): 239.7 [M + H]⁺.

Synthesis of 3-amino-*N*-(2-chloro-6-fluorobenzyl)-1-(3,4-difluorophenyl)-1*H*-pyrazole-4-carboxamide (**9a**)

A solution of **8** (30 mg, 0.13 mmol), 2-chloro-6-fluorobenzylamine (24 mg, 0.15 mmol), HBTU (68 mg, 0.18 mmol) and TEA (33 mg, 0.25 mmol) in DMF (3 ml) was reacted according to general procedure A. The product **9a** was obtained as 11 mg (22%) of a colorless solid. ¹H NMR (600 MHz, Chloroform-*d*) δ: 7.85 (s, 1H, CH_{pyrazole}), 7.43 (ddd, *J* = 11.1, 6.9, 2.6 Hz, 1H, CH_{arom.}), 7.28-7.12 (m, 4H, CH_{arom.}), 7.01 (d, *J* = 8.2 Hz, 1H, CH_{arom.}), 6.18 (t, *J* = 5.7 Hz, 1H, NH), 4.99-4.77 (m, 2H, NH₂), 4.74 (d, *J* = 5.5 Hz, 2H, NHCH₂Ar) ppm. ¹³C NMR (151 MHz, Chloroform-*d*) δ: 163.2 (C=O), 161.6 (d, ¹*J*_{CF} = 250.1 Hz, C_{arom.}), 156.7 (C₃ pyrazole), 150.4 (dd, ¹*J*_{CF} = 249.4, 13.7 Hz, C_{arom.}), 148.6 (dd, ¹*J*_{CF} = 248.1, 12.6 Hz, C_{arom.}), 135.8 (dd, ⁴*J*_{CF} = 8.0, 3.2 Hz, C_{arom.}), 135.5 (d, ³*J*_{CF} = 5.3 Hz, C_{arom.}), 129.8 (d, ³*J*_{CF} = 9.6 Hz), 125.8 (C₅ pyrazole), 125.5 (d, ⁴*J*_{CF} = 3.7 Hz, C_{arom.}), 123.8 (d, ²*J*_{CF} = 17.8 Hz, C_{arom.}), 117.9 (d, ²*J*_{CF} = 18.6 Hz, C_{arom.}), 114.5 (d, ²*J*_{CF} = 22.9 Hz, C_{arom.}), 113.8 (dd, ⁴*J*_{CF} = 8.0, 3.2 Hz, C_{arom.}), 108.4 (d, ²*J*_{CF} = 21.9 Hz), 105.1

(C₄ pyrazole) , 34.6 (d, ³J_{CF} = 4.1 Hz, NHCH₂Ar) ppm. HPLC-UV (254 nm) ESI-MS, purity: 95%. LC-MS (m/z): 380.9 [M + H]⁺. Mp.: 198 °C.

Synthesis of 3-amino-*N*-(2,3-dichlorobenzyl)-1-(3,4-difluorophenyl)-1*H*-pyrazole-4-carboxamide (**9b**)

A solution of **8** (30 mg, 0.13 mmol), 2,3-dichlorobenzylamine (30 mg, 0.17 mmol), HBTU (68 mg, 0.18 mmol) and TEA (32 mg, 0.32 mmol) in DMF (3 ml) was reacted according to general procedure A. The product **9b** was obtained as 4.3 mg (8%) of a colorless solid. ¹H NMR (600 MHz, Chloroform-*d*) δ: 8.51 (s, 1H, NH), 7.94 (s, 1H, CH_{pyrazole}), 7.37-7.30 (m, 1H, CH_{arom.}), 7.21-7.14 (m, 3H, CH_{arom.}), 7.07-6.98 (m, 2H, CH_{arom.}), 4.57-4.33 (m, 2H, NHCH₂Ar) ppm. NH₂ not displayed. ¹³C NMR (151 MHz, Chloroform-*d*) δ: 150.4 (dd, ¹J_{CF} = 249.4, 13.7 Hz, C_{arom.}), 148.6 (dd, ¹J_{CF} = 248.1, 12.6 Hz, C_{arom.}), 146.9 (d, ²J_{CF} = 12.4 Hz, C_{arom.}), 138.4, 135.7 (d, ³J_{CF} = 7.6 Hz, C_{arom.}), 132.4, 130.0, 128.8, 127.6, 126.9 (d, ⁴J_{CF} = 5.3 Hz, C_{arom.}), 117.4 (d, ²J_{CF} = 18.5 Hz, C_{arom.}), 113.1 (d, ³J_{CF} = 5.7 Hz, C_{arom.}), 107.4 (d, ²J_{CF} = 21.9 Hz, C_{arom.}), 40.8 ppm. HPLC-UV (254 nm) ESI-MS, purity: 85%. LC-MS (m/z): 397.0 [M + H]⁺. Mp.: 178 °C.

Synthesis of 3-amino-1-(3,4-difluorophenyl)-*N*-(2-fluorobenzyl)-1*H*-pyrazole-4-carboxamide (**9c**)

A solution of **8** (30 mg, 0.13 mmol), 2-fluorobenzylamine (21 mg, 0.17 mmol), HBTU (68 mg, 0.18 mmol) and TEA (32 mg, 0.32 mmol) in DMF (3 ml) was reacted according to general procedure A. The product **9c** was obtained as 9 mg (20%) of a colorless solid. ¹H NMR (600 MHz, Chloroform-*d*) δ: 8.07 (s, 1H, CH_{pyrazole}), 7.43 (ddd, *J* = 11.3, 7.0, 2.5 Hz, 1H, CH_{arom.}), 7.37 (td, *J* = 7.6, 2.0 Hz, 1H, CH_{arom.}), 7.27-7.20 (m, 2H, CH_{arom.}), 7.18-7.12 (m, 1H, CH_{arom.}), 7.08 (td, *J* = 7.5, 1.3 Hz, 1H, CH_{arom.}), 7.01 (ddd, *J* = 9.7, 8.3, 1.2 Hz, 1H, CH_{arom.}), 6.54 (s, 1H, NH), 4.58 (d, *J* = 5.3 Hz, 2H, NHCH₂Ar) ppm. NH₂ not displayed. ¹³C NMR (151 MHz, Chloroform-*d*) δ: 163.47, 161.83, 160.20, 156.36, 151.34 (d, *J* = 13.6 Hz), 150.4 (dd, ¹J_{CF} = 249.4, 13.7 Hz, C_{arom.}), 148.6 (dd, ¹J_{CF} = 248.1, 12.6 Hz, C_{arom.}), 147.8 (d, *J* = 12.8 Hz, C_{arom.}), 135.6 (dd, *J* = 8.1, 3.2 Hz, C_{arom.}), 130.3 (d, *J* = 4.2 Hz, C_{arom.}), 129.4 (d, *J* = 8.2 Hz, C_{arom.}), 126.3, 125.2 (d, *J* = 14.8 Hz, C_{arom.}), 124.4 (d, *J* = 3.6 Hz, C_{arom.}), 117.9 (d, *J* = 18.6 Hz, C_{arom.}), 115.4 (d, ²J_{CF} = 21.2 Hz, C_{arom.}), 113.8 (dd, ⁴J_{CF} = 8.0, 3.2 Hz, C_{arom.}), 108.4 (d, ²J_{CF} = 21.8 Hz), 104.9, 37.3 (d, ⁴J_{CF} = 3.9 Hz) ppm. HPLC-UV (254 nm) ESI-MS, purity: 99%. LC-MS (m/z): 347 [M + H]⁺. Mp.: 154 °C.

Synthesis of 3-amino-*N*-(2-bromobenzyl)-1-(3,4-difluorophenyl)-1*H*-pyrazole-4-carboxamide (**9d**)

A solution of **8** (30 mg, 0.13 mmol), 2-bromobenzylamine (32 mg, 0.17 mmol), HBTU (68 mg, 0.18 mmol) and TEA (32 mg, 0.32 mmol) in DMF (3 ml) was reacted according to general procedure A. The product **9d** was obtained as 11 mg (21%) of a colorless solid. ¹H NMR (600

MHz, Chloroform-*d*) δ : 7.99 (s, 1H, CH_{pyrazole}), 7.53 (d, $J = 7.9$, 1H, CH_{arom.}), 7.48-7.40 (m, 2H, CH_{arom.}), 7.29-7.24 (m, 2H, CH_{arom.}), 7.21-7.10 (m, 2H, CH_{arom.}), 6.49 (s, 1H NH), 4.61 (d, $J = 5.4$ Hz, 2H, NHCH₂Ar) ppm. NH₂ not displayed. ¹³C NMR (151 MHz, Chloroform-*d*) δ : 163.4, 156.3, 150.4 (dd, ¹ $J_{CF} = 249.4$, 13.7 Hz, C_{arom.}), 148.6 (dd, ¹ $J_{CF} = 248.1$, 12.6 Hz, C_{arom.}), 137.2, 135.6, 132.8, 130.5, 129.3, 127.8, 126.2, 123.7, 117.9 (d, ² $J_{CF} = 18.6$ Hz), 113.9 (dd, ⁴ $J_{CF} = 8.0$, 3.2 Hz, C_{arom.}), 108.5 (d, ² $J_{CF} = 21.9$ Hz, C_{arom.}), 105.1, 43.6 ppm. HPLC-UV (254 nm) ESI-MS, purity: 94%. LC-MS (m/z): 409.1 [M + H]⁺. Mp.: 171 °C.

Synthesis of 3-amino-1-(3,4-difluorophenyl)-*N*-(2,3-dihydro-1*H*-inden-1-yl)-1*H*-pyrazole-4-carboxamide (**9e**)

A solution of **8** (30 mg, 0.13 mmol), 2-aminoindane hydrochloride (32 mg, 0.19 mmol), HBTU (68 mg, 0.18 mmol) and TEA (50 mg, 0.5 mmol) in DMF (3 ml) was reacted according to general procedure A. The product **9b** was obtained as 29 mg (22%) of a colorless solid. ¹H NMR (600 MHz, Chloroform-*d*) δ : 7.86 (s, 1H, CH_{pyrazole}), 7.51-7.38 (m, 1H, CH_{arom.}), 7.32 (d, $J = 7.2$ Hz, 1H, CH_{arom.}), 7.28-7.10 (m, 5H, CH_{arom.}), 6.01 (d, $J = 8.0$ Hz, 1H, NH), 5.61 (q, $J = 7.4$ Hz, 1H, CH_{indane}), 3.61 (s br, 2H, HN₂), 3.06-2.96 (m, 1H, CH_{2 indane}), 2.95-2.84 (m, 1H, CH_{2 indane}), 2.71-2.56 (m, 1H, CH_{2 indane}), 1.96-1.82 (m, 1H, CH_{2 indane}) ppm. ¹³C NMR (151 MHz, Chloroform-*d*) δ : 163.4, 156.8, 150.2 (dd, ¹ $J_{CF} = 249.6$, 13.8 Hz, C_{arom.}), 148.6 (dd, ¹ $J_{CF} = 249.1$, 12.8 Hz, C_{arom.}), 143.6, 143.0, 135.8 (d, ³ $J_{CF} = 7.7$ Hz), 128.2, 126.8, 125.7, 124.9, 124.1, 117.9 (d, ² $J_{CF} = 18.6$ Hz), 114.2 - 113.1, 108.4 (d, ² $J_{CF} = 22.0$ Hz), 105.1, 54.5, 34.2 (NHCH₂Ar), 30.29 ppm. HPLC-UV (254 nm) ESI-MS, purity: 95%. LC-MS (m/z): 355.1 [M + H]⁺. Mp.: 192,5 °C.

Synthesis of 3-amino-1-(3,4-difluorophenyl)-*N*-(2-(dimethylamino)benzyl)-1*H*-pyrazole-4-carboxamide (**9f**)

A solution of **8** (30 mg, 0.13 mmol), 2-(*N,N*-dimethyl)benzylamine (26 mg, 0.17 mmol), HBTU (68 mg, 0.18 mmol) and TEA (32 mg, 0.32 mmol) in DMF (3 ml) was reacted according to general procedure A. The product **9f** was obtained as 4.5 mg (9%) of a colorless solid. ¹H NMR (600 MHz, Chloroform-*d*) δ : 7.93 - 7.68 (s, 1H, CH_{pyrazole}), 7.44 (d, $J = 7.8$ Hz, 2H, CH_{arom.}), 7.24 (s, 2H, CH_{arom.}), 7.17 (q, $J = 9.0$ Hz, 2H, CH_{arom.}), 6.30 (s, 1H, NH), 4.67 (d, $J = 5.4$ Hz, 2H, NHCH₂Ar), 2.91-2.50 (s, 6H, N(CH₃)₂) ppm. NH₂ not displayed. ¹³C NMR (151 MHz, Chloroform-*d*) δ : 156.7, 156.0, 151.4 (d, ² $J_{CF} = 13.5$ Hz), 150.4 (dd, ¹ $J_{CF} = 249.4$, 13.7 Hz, C_{arom.}), 148.6 (dd, ¹ $J_{CF} = 248.1$, 12.6 Hz, C_{arom.}), 147.7 (d, ³ $J_{CF} = 12.6$ Hz), 135.9 (d, ³ $J_{CF} = 8.2$ Hz), 132.0, 128.6, 119.6, 117.9 (d, ² $J_{CF} = 18.6$ Hz), 113.85 - 112.5, 108.3 (d, ² $J_{CF} = 22.0$ Hz), 40.5, 29.7 ppm. HPLC-UV (254 nm) ESI-MS, purity: 80%. LC-MS (m/z): 372.1 [M + H]⁺. Mp.: 166 °C.

Synthesis of 3-amino-*N*-(2-cyanobenzyl)-1-(3,4-difluorophenyl)-1*H*-pyrazole-4-carboxamide (**9g**)

A solution of **8** (30 mg, 0.13 mmol), 2-cyanobenzylamine hydrochloride (29 mg, 0.17 mmol), HBTU (68 mg, 0.18 mmol) and TEA (32 mg, 0.32 mmol) in DMF (3 ml) was reacted according to general procedure A. The product **9g** was obtained as 9 mg (20%) of a colorless solid. ¹H NMR (600 MHz, DMSO-*d*₆) δ: 8.92 (s, 1H, CH_{pyrazole}), 8.75 (t, *J* = 5.8 Hz, 1H, NH), 7.82 (dd, *J* = 7.8, 1.4 Hz, 1H, CH_{arom.}), 7.69 (td, *J* = 7.7, 1.4 Hz, 1H, CH_{arom.}), 7.66-7.61 (m, 1H, CH_{arom.}), 7.60-7.53 (m, 2H, CH_{arom.}), 7.48-7.41 (m, 2H, CH_{arom.}), 4.59 (d, *J* = 5.6 Hz, 2H, NHCH₂Ar) ppm. NH₂ not displayed. ¹³C NMR (151 MHz, DMSO-*d*₆) δ: 163.8, 157.2, 149.8 (dd, ¹*J*_{CF} = 245.9, 13.6 Hz), 147.2 (dd, ¹*J*_{CF} = 244.4, 13.0 Hz), 143.2, 136.3 (d, ³*J*_{CF} = 8.4 Hz), 133.5, 132.9, 128.6, 128.5, 127.9, 118.6 (d, ²*J*_{CF} = 18.4 Hz), 117.5 (C≡N), 113.7 (dd, ³*J*_{CF} = 6.5, 3.3 Hz), 110.6, 107.1 (d, ²*J*_{CF} = 21.9 Hz), 104.3, 30.8 ppm. HPLC-UV (254 nm) ESI-MS, purity: 97%. LC-MS (m/z): 354.1 [M + H]⁺. Mp.: 198 °C.

Synthesis of 3-amino-1-(3,4-difluorophenyl)-*N*-(2-(trifluoromethoxy)benzyl)-1*H*-pyrazole-4-carboxamide (**9h**)

A solution of **8** (30 mg, 0.13 mmol), 2-(trifluoromethoxy)benzylamine (25 mg, 0.17 mmol), HBTU (68 mg, 0.18 mmol) and TEA (32 mg, 0.32 mmol) in DMF (3 ml) was reacted according to general procedure A. The product **9h** was obtained as 7 mg (13%) of a colorless solid. ¹H NMR (600 MHz, Chloroform-*d*) δ: 8.08 (d, *J* = 4.1 Hz, 1H, CH_{pyrazole}), 7.50-7.42 (m, 2H, CH_{arom.}), 7.34-7.20 (m, 4H, CH_{arom.}), 7.16 (q, *J* = 8.9 Hz, 1H, CH_{arom.}), 6.51 (s, 1H, NH), 4.61 (d, *J* = 5.4 Hz, 2H, NHCH₂Ar) ppm. NH₂ not displayed. ¹³C NMR (151 MHz, Chloroform-*d*) δ: 163.4, 156.3, 150.4 (dd, ¹*J*_{CF} = 249.4, 13.7 Hz, C_{arom.}), 148.6 (dd, ¹*J*_{CF} = 248.1, 12.6 Hz, C_{arom.}), 137.2, 135.6, 132.8, 130.5, 129.3, 127.8, 126.2 (q, ¹*J*_{CF} = 244.1), 123.7, 117.9 (d, ²*J*_{CF} = 18.6 Hz), 113.9 (dd, ⁴*J*_{CF} = 8.0, 3.2 Hz, C_{arom.}), 108.4 (d, ²*J*_{CF} = 21.9 Hz), 105.1, 43.6 ppm. HPLC-UV (254 nm) ESI-MS, purity: 80%. LC-MS (m/z): 413.0 [M + H]⁺. Mp.: 175 °C.

Synthesis of (3-amino-1-(3,4-difluorophenyl)-1*H*-pyrazol-4-yl)(2-phenylpyrrolidin-1-yl)methanone (**9i**)

A solution of **8** (30 mg, 0.13 mmol), 2-phenylpyrrolidine (25 mg, 0.17 mmol), HBTU (68 mg, 0.18 mmol) and TEA (32 mg, 0.32 mmol) in DMF (3 ml) was reacted according to general procedure A. The product **9i** was obtained as 25 mg (52%) of a colorless solid. ¹H NMR (600 MHz, DMSO-*d*₆) δ: 8.68 (s, 1H, CH_{pyrazole}), 7.97-7.87 (m, 1H, CH_{arom.}), 7.67 (d, *J* = 8.9 Hz, 1H, CH_{arom.}), 7.61-7.46 (m, 1H, CH_{arom.}), 7.29 (t, *J* = 7.5 Hz, 2H, CH_{arom.}), 7.24-7.12 (m, 3H, CH_{arom.}), 5.23 (s, 1H, NCHAr), 4.12-4.05 (m, 1H, CH_{pyrrolidine}), 3.87 (q, *J* = 8.2, 7.8 Hz, 1H, CH_{pyrrolidine}), 3.59 (s, 2H, NH₂), 2.29 (s, 1H, CH_{pyrrolidine}), 1.95 (s, 2H, CH_{pyrrolidine}), 1.74 (s, 1H, CH_{pyrrolidine})

ppm. ^{13}C NMR (151 MHz, DMSO- d_6) δ : 163.0, 158.4, 149.7 (dd, $^1J_{\text{CF}} = 245.2$, 13.5 Hz), 147.1 (dd, $^1J_{\text{CF}} = 243.9$, 12.6 Hz), 144.2, 136.3, 128.7, 128.2, 126.4, 125.5, 118.3 (d, $^2J_{\text{CF}} = 18.2$ Hz), 114.2, 107.3 (d, $^2J_{\text{CF}} = 22.4$ Hz), 104.1, 60.9, 49.1, 33.8, 24.2 ppm. HPLC-UV (254 nm) ESI-MS, purity: 95%. LC-MS (m/z): 368.8 [M + H] $^+$. Mp.: 188 °C.

4.3.9.2.3. Synthesis of 3-amino-*N*-benzyl-1-(4-hydroxyphenyl)-1*H*-pyrazole-4-carboxamide derivatives

Synthesis of (*E*)-1-benzylidene-2-(4-methoxyphenyl)hydrazine (**10**)⁵

A solution of 4-methoxyphenylhydrazine hydrochloride (10 g, 57 mmol) in H₂O / EtOH (80 ml) was treated with NaHCO₃ (6.7 g, 80 mmol) at rt and stirred for 30 min until the solution was clear. Benzaldehyde (7.25 g, 68 mmol) was added and the resulting suspension was stirred for 2 h at rt. Subsequently, the precipitate was filtered off under reduced pressure and washed with water and EtOH and dried at 60 °C, yielding the desired product **10** as 12.2 g (94%) of a colorless solid. HPLC-UV (254 nm) ESI-MS, purity: 94%. LC-MS (m/z): 227.0 [M + H] $^+$.

Synthesis of ethyl-3-amino-1-(4-methoxyphenyl)-1*H*-pyrazole-4-carboxylate (**14**)⁵

A mixture of **10** (5 g, 22 mmol) and EEMA (3.74 g, 22 mmol) in xylol (5 ml) was stirred at 160 °C for 3 d in a sealed tube. The intermediate **12** could be detected via TLC-MS (MW = 349). The crude mixture was dissolved in EtOH (35 ml) and conc. HCl (1.7 ml) and refluxed for 2 h. The mixture was treated with saturated NaHCO₃ solution until pH 9 and subsequently extracted with CH₂Cl₂ (3 x 50 ml), the combined organic layers were dried over MgSO₄, filtered off and the solvent was evaporated under reduced pressure. The crude product **14** was purified via column chromatography (CH₂Cl₂ / MeOH - 98 : 2) and was obtained as 3,85 g (64%) of a dark brown oil that was directly use for the next reaction step. ^1H NMR (600 MHz, Chloroform- d) δ : 8.00 (s, 1H, CH_{pyrazole}), 7.55-7.45 (m, 2H, CH_{arom.}), 6.95-6.88 (m, 2H, CH_{arom.}), 5.20-5.16 (m, 2H, NH₂), 4.28 (p, $J = 7.2$ Hz, 2H, CH₂CH₃), 3.81 (d, $J = 11.5$ Hz, 3H, OCH₃), 1.45-1.24 (m, 3H, CH₂CH₃) ppm. LC-MS (m/z): 261.8 [M + H] $^+$.

Synthesis of 3-amino-1-(4-methoxyphenyl)-1*H*-pyrazole-4-carboxylic acid (**16**)

A solution of **14** (3.58 g, 13.75 mmol) and LiOH monohydrate (2.88 g, 68.75 mmol) in water / THF (1:1, 40 ml) was stirred for 16 h at 80 °C. Subsequently, the reaction mixture was cooled to rt and then extracted with ethyl acetate. The aqueous solution was acidified to pH 2 with acetic acid and the precipitated product was collected by filtration. The crude product was purified by flash RP-HPLC (water / MeOH - 10 to 100%). The product **16** was obtained 1.78 g (56%) as a beige powdery solid. ^1H NMR (500 MHz, DMSO- d_6) δ : 8.51 (s, 1H, CH_{pyrazole}), 7.72-7.64 (m, 2H, CH_{arom.}), 7.03-6.95 (m, 2H, CH_{arom.}), 5.54 (s, 2H, NH₂), 3.77 (d, $J = 0.8$ Hz, 3H,

OCH₃) ppm. ¹³C NMR (126 MHz, DMSO-*d*₆) δ: 165.3, 157.5, 157.2, 132.9, 129.9, 119.5, 114.6, 101.1, 55.5 ppm. HPLC-UV (254 nm) ESI-MS, purity: 97%. LC-MS (m/z): 234.0 [M + H]⁺.

Synthesis of 3-amino-*N*-(2-chloro-6-fluorobenzyl)-1-(4-methoxyphenyl)-1*H*-pyrazole-4-carboxamide (18a)

A solution of **16** (75 mg, 0.29 mmol), 2-chloro-6-fluorobenzylamine (68 mg, 0.43 mmol), HBTU (143 mg, 0.38 mmol) and TEA (44 mg, 0.43 mmol) in DMF (1 ml) was reacted according to general procedure B. The product **18a** was obtained as 25 mg (23%) of a beige solid. ¹H NMR (600 MHz, DMSO-*d*₆) δ: 8.62 (s, 1H, CH_{pyrazole}), 8.02 (t, *J* = 5.0 Hz, 1H, NH), 7.53-7.44 (m, 2H, CH_{arom.}), 7.40 (td, *J* = 8.2, 5.9 Hz, 1H, CH_{arom.}), 7.36-7.34 (m, 1H, CH_{arom.}), 7.25 (ddd, *J* = 9.5, 8.2, 1.2 Hz, 1H, CH_{arom.}), 7.04-6.93 (m, 2H CH_{arom.}), 4.54 (dd, *J* = 4.9, 1.6 Hz, 2H, NHCH₂Ar), 3.76 (s, 3H, OCH₃) ppm. NH₂ not displayed. ¹³C NMR (151 MHz, DMSO-*d*₆) δ: 163.6, 162.4, 160.8, 157.2 (d, ²*J*_{CF} = 20.8 Hz), 135.1 (d, *J* = 5.6 Hz), 133.1, 130.3 (d, ³*J*_{CF} = 9.7 Hz), 127.2, 125.6 (d, ⁴*J*_{CF} = 3.3 Hz), 124.1 (d, ²*J*_{CF} = 18.0 Hz), 118.9, 114.8, 114.6, 102.8, 55.5, 34.3 (d, ³*J*_{CF} = 9.7 Hz) ppm. HPLC-UV (254 nm) ESI-MS, purity: 96%. LC-MS (m/z): 374.9[M + H]⁺. Mp.: 178 °C.

Synthesis of 3-amino-*N*-(2-chloro-6-fluorobenzyl)-1-(4-hydroxyphenyl)-1*H*-pyrazole-4-carboxamide (19a)

A solution of **18a** (17 mg, 0.05 mmol) was reacted according to general procedure C. The product **19a** was obtained as 10 mg (55%) of a colorless solid. ¹H NMR (600 MHz, Methanol-*d*₄) δ: 8.34 (s, 1H, CH_{pyrazole}), 7.44-7.41 (m, 2H, CH_{arom.}), 7.38 (td, *J* = 8.2, 5.9 Hz, 1H, CH_{arom.}), 7.34-7.31 (m, 1H, CH_{arom.}), 7.16 (ddd, *J* = 9.4, 8.1, 1.2 Hz, 1H, CH_{arom.}), 6.90-6.84 (m, 2H, CH_{arom.}), 4.72 (d, *J* = 1.9 Hz, 2H, NHCH₂Ar) ppm. NH₂ not displayed. ¹³C NMR (151 MHz, Methanol-*d*₄) δ: 166.5, 164.5, 162.8, 158.8, 157.9, 137.2 (d, ⁴*J*_{CF} = 5.1 Hz), 133.7, 131.4 (d, ³*J*_{CF} = 9.7 Hz), 129.2, 126.9 (d, ⁴*J*_{CF} = 3.7 Hz), 125.3, 121.9, 117.1, 115.6 (d, ²*J*_{CF} = 22.7 Hz), 104.2, 35.8 (d, ⁴*J*_{CF} = 4.4 Hz) ppm. HPLC-UV (254 nm) ESI-MS, purity: 98%. LC-MS (m/z): 360.9 [M + H]⁺. Mp.: 195 °C.

Synthesis of 3-amino-*N*-(2-cyanobenzyl)-1-(4-methoxyphenyl)-1*H*-pyrazole-4-carboxamide (18b)

A solution of **16** (75 mg, 0.29 mmol), 2-cyanobenzylamine hydrochloride (58 mg, 0.43 mmol), HBTU (143 mg, 0.38 mmol) and TEA (44 mg, 0.43 mmol) in DMF (1 ml) was reacted according to general procedure B. The product **18b** was obtained as 49 mg (49%) of a beige solid. ¹H NMR (600 MHz, Chloroform-*d*) δ: 7.90-7.80 (s, 1H, CH_{pyrazole}), 7.24 (dd, *J* = 7.9, 4.5 Hz, 1H, CH_{arom.}), 7.19-7.11 (m, 2H, CH_{arom.}), 7.06 (td, *J* = 6.1, 3.1 Hz, 2H, CH_{arom.}), 6.99-6.92 (m, 1H, CH_{arom.}), 6.53 (td, *J* = 6.4, 6.0, 3.1 Hz, 2H, CH_{arom.}), 4.33-4.21 (m, 2H, NHCH₂Ar), 3.46-3.34 (m, 3H, OCH₃) ppm. NH₂ not displayed. ¹³C NMR (151 MHz, Chloroform-*d*) δ: 164.3, 158.2, 155.6,

142.5, 133.1, 133.0, 132.7, 132.6, 132.6, 132.5, 128.7, 127.6, 120.2, 120.2, 117.4, 114.4, 110.8, 103.3, 55.3, 41.0 ppm. HPLC-UV (254 nm) ESI-MS, purity: 98%. LC-MS (m/z): 348.0 [M + H]⁺. Mp.: 147 °C.

Synthesis of 3-amino-N-(2-cyanobenzyl)-1-(4-hydroxyphenyl)-1H-pyrazole-4-carboxamide (19b)

A solution of **18b** (34 mg, 0.1 mmol) was reacted according to general procedure C. The product **19b** was obtained as 5 mg (15%) of a colorless solid. ¹H NMR (600 MHz, Methanol-*d*₄) δ: 8.35 (s, 1H, CH_{pyrazole}), 7.77 (dd, *J* = 7.8, 1.3 Hz, 1H, CH_{arom.}), 7.69 (td, *J* = 7.7, 1.3 Hz, 1H, CH_{arom.}), 7.61 (d, *J* = 7.9 Hz, 1H, CH_{arom.}), 7.50-7.44 (m, 3H, CH_{arom.}), 6.91-6.85 (m, 2H, CH_{arom.}), 4.75 (s, 2H, NHCH₂Ar) ppm. NH₂ not displayed. ¹³C NMR (151 MHz, MeOD) δ: 166.9, 158.9, 144.4, 134.6, 134.3, 133.4, 129.8, 129.3, 129.2, 129.1, 122.0, 118.6, 117.4, 112.7, 104.1, 42.4 ppm. HPLC-UV (254 nm) ESI-MS, purity: 98%. LC-MS (m/z): 334.0 [M + H]⁺. Mp.: 153 °C.

Synthesis of 3-amino-N-(2-methoxybenzyl)-1-(4-methoxyphenyl)-1H-pyrazole-4-carboxamide (18c)

A solution of **16** (75 mg, 0.29 mmol), 2-methoxybenzylamine (59 mg, 0.43 mmol), HBTU (143 mg, 0.38 mmol) and TEA (44 mg, 0.43 mmol) in DMF (1 ml) was reacted according to general procedure B. The product **18c** was obtained as 18 mg (18%) of a colorless solid. ¹H NMR (600 MHz, Chloroform-*d*) δ: 7.97 (s, 1H, CH_{pyrazole}), 7.42 (d, 2H, CH_{arom.}), 7.30 (d, 1H, CH_{arom.}), 7.28 - 7.17 (m, 1H, CH_{arom.}), 6.92 - 6.81 (m, 4H, CH_{arom.}), 6.56 (s, 1H, NH), 4.53 (d, *J* = 4.5 Hz, 2H, NHCH₂Ar), 3.84 (s, 3H, OCH₃), 3.78 (s, 3H, OCH₃) ppm. NH₂ not displayed. ¹³C NMR (151 MHz, Chloroform-*d*) δ: 163.4, 158.4, 157.5, 155.5, 132.1, 129.7, 128.9, 126.6, 126.2, 120.7, 120.3, 114.6, 110.3, 103.8, 55.6, 55.4, 38.9 ppm. HPLC-UV (254 nm) ESI-MS, purity: 98%. LC-MS (m/z): 353.0 [M + H]⁺. Mp.: 137 °C.

Synthesis of 3-amino-N-(2-hydroxybenzyl)-1-(4-hydroxyphenyl)-1H-pyrazole-4-carboxamide (19c)

A solution of **18c** (64 mg, 0.18 mmol) was reacted according to general procedure C. The product **19c** was obtained as 18.6 mg (32%) of a colorless solid. ¹H NMR (600 MHz, Methanol-*d*₄) δ: 8.70 (s, 1H, CH_{pyrazole}), 7.65-7.51 (m, 2H, CH_{arom.}), 7.28 (dd, *J* = 7.5, 1.6 Hz, 1H, CH_{arom.}), 7.15 (td, *J* = 7.7, 1.6 Hz, 1H, CH_{arom.}), 7.00-6.91 (m, 2H, CH_{arom.}), 6.89-6.77 (m, 2H, CH_{arom.}), 4.56 (s, 2H, NHCH₂Ar) ppm. NH₂ not displayed. ¹³C NMR (151 MHz, Methanol-*d*₄) δ: 164.3, 159.3, 156.9, 145.8, 132.6, 130.9, 130.8, 130.1, 126.0, 122.8, 122.7, 120.9, 117.4, 116.9, 110.1, 40.0 ppm. HPLC-UV (254 nm) ESI-MS, purity: 96%. LC-MS (m/z): 325.2 [M + H]⁺. Mp.: 155 °C.

Synthesis of 3-amino-*N*-(2,3-dihydro-1*H*-inden-1-yl)-1-(4-methoxyphenyl)-1*H*-pyrazole-4-carboxamide (**18d**)

A solution of **16** (75 mg, 0.29 mmol), 1-aminoindane hydrochloride (73 mg, 0.43 mmol), HBTU (143 mg, 0.38 mmol) and TEA (44 mg, 0.43 mmol) in DMF (1 ml) was reacted according to general procedure B. The product **18d** was obtained as 70 mg (69%) of a colorless solid. ¹H NMR (600 MHz, Chloroform-*d*) δ: 7.82 (s, 1H, CH_{pyrazole}), 7.48-7.42 (m, 2H, CH_{arom.}), 7.34 (d, *J* = 7.2 Hz, 1H, CH_{arom.}), 7.25 (d, *J* = 1.5 Hz, 1H, CH_{arom.}), 7.23-7.18 (m, 2H, CH_{arom.}), 6.90 (d, *J* = 8.5 Hz, 2H, CH_{arom.}), 6.00 (d, *J* = 8.1 Hz, 1H, NH), 5.63 (q, *J* = 7.6 Hz, 1H, CH_{indane}), 3.80 (s, 3H, OCH₃), 3.01 (ddd, *J* = 16.1, 8.7, 4.0 Hz, 1H, CH_{2 indane}), 2.90 (dt, *J* = 16.0, 8.0 Hz, 1H, CH_{2 indane}), 2.65 (dtd, *J* = 12.2, 7.9, 4.0 Hz, 1H, CH_{2 indane}), 1.90 (dq, *J* = 13.0, 7.9 Hz, 1H, CH_{2 indane}) ppm. NH₂ not displayed. ¹³C NMR (151 MHz, Chloroform-*d*) δ: 163.7, 158.3, 156.3, 143.6, 143.2, 132.9, 128.1, 126.8, 125.6, 124.9, 124.2, 124.2, 120.3, 120.2, 114.6, 114.6, 103.9, 55.6, 54.4, 34.2, 34.2, 30.3 ppm. HPLC-UV (254 nm) ESI-MS, purity: 96%. LC-MS (*m/z*): 349.0 [M + H]⁺. Mp.: 177 °C.

Synthesis of 3-amino-*N*-(2,3-dihydro-1*H*-inden-1-yl)-1-(4-hydroxyphenyl)-1*H*-pyrazole-4-carboxamide (**19d**)

A solution of **18d** (70 mg, 0.2 mmol) was reacted according to general procedure C. The product **19d** was obtained as 11 mg (16%) of a colorless solid. ¹H NMR (600 MHz, Methanol-*d*₄) δ: 8.32 (s, 1H, CH_{pyrazole}), 7.41-7.37 (m, 2H, CH_{arom.}), 7.29 (d, *J* = 7.1 Hz, 1H, CH_{arom.}), 7.26-7.15 (m, 3H, CH_{arom.}), 6.86 - 6.79 (m, 2H, CH_{arom.}), 5.56 (t, *J* = 7.7 Hz, 1H, NH), 4.59 (s, 2H, NH₂), 3.03 (ddd, *J* = 15.9, 8.8, 3.6 Hz, 1H, CH_{indane}), 2.88 (dt, *J* = 16.3, 8.4 Hz, 1H, CH_{indane}), 2.55 (dtd, *J* = 11.7, 7.9, 3.5 Hz, 1H, CH_{indane}), 1.95 (dq, *J* = 12.6, 8.4 Hz, 1H, CH_{indane}) ppm. ¹³C NMR (151 MHz, Methanol-*d*₄) δ: 166.3, 158.6, 157.6, 144.7, 144.5, 133.5, 128.8, 128.7, 127.7, 125.7, 125.1, 121.6, 116.9, 104.2, 55.4, 34.6, 31.1 ppm. HPLC-UV (254 nm) ESI-MS, purity: 95%. LC-MS (*m/z*): 335.1 [M + H]⁺. Mp.: 180 °C.

Synthesis of 3-amino-*N*-(2-fluorobenzyl)-1-(4-methoxyphenyl)-1*H*-pyrazole-4-carboxamide (**18e**)

A solution of **16** (75 mg, 0.29 mmol), 2-fluorobenzylamine (60 mg, 0.48 mmol), HBTU (183 mg, 0.48 mmol) and TEA (98 mg, 0.96 mmol) in DMF (1 ml) was reacted according to general procedure B. The product **18e** was obtained as 33.3 mg (31%) of a beige solid. ¹H NMR (600 MHz, Chloroform-*d*) δ: 7.93 (s, 1H, CH_{pyrazole}), 7.45 - 7.42 (m, 2H, CH_{arom.}), 7.39 (td, *J* = 7.6, 1.8 Hz, 1H, CH_{arom.}), 7.27-7.22 (m, 1H, CH_{arom.}), 7.09 (td, *J* = 7.5, 1.2 Hz, 1H, CH_{arom.}), 7.03 (ddd, *J* = 9.7, 8.3, 1.1 Hz, 1H, CH_{arom.}), 6.90-6.86 (m, 2H, CH_{arom.}), 6.37 (d, *J* = 7.0 Hz, 1H, NH), 4.60 (d, *J* = 5.7 Hz, 2H, NHCH₂Ar), 3.79 (s, 3H, OCH₃) ppm. NH₂ not displayed. ¹³C NMR (151 MHz, Chloroform-*d*) δ: 163.6, 161.1 (d, ¹*J*_{CF} = 246.0 Hz), 158.4, 155.9, 132.4, 130.4 (d, ³*J*_{CF} =

4.2 Hz), 129.3, 126.3, 125.3 (d, $^2J_{CF} = 13.8$ Hz), 124.4, 120.3, 115.4 (d, $^2J_{CF} = 21.3$ Hz), 114.6, 103.7, 55.5, 37.2 (d, $^4J_{CF} = 3.8$ Hz) ppm. HPLC-UV (254 nm) ESI-MS, purity: 96%. LC-MS (m/z): 341.2 [M + H]⁺. Mp.: 171 °C.

Synthesis of 3-amino-*N*-(2-fluorobenzyl)-1-(4-hydroxyphenyl)-1*H*-pyrazole-4-carboxamide (19e)

A solution of **18e** (25 mg, 0.07 mmol) was reacted according to general procedure C. The product **19e** was obtained as 13.8 mg (60%) of a colorless solid. ¹H NMR (600 MHz, Methanol-*d*₄) δ: 8.35 (s, 1H, CH_{pyrazole}), 7.48-7.41 (m, 3H, CH_{arom.}), 7.33 (tdd, $J = 7.4, 5.3, 1.8$ Hz, 1H, CH_{arom.}), 7.18 (td, $J = 7.5, 1.2$ Hz, 1H, CH_{arom.}), 7.12 (ddd, $J = 10.3, 8.2, 1.1$ Hz, 1H, CH_{arom.}), 6.92-6.86 (m, 2H, CH_{arom.}), 4.61 (s, 2H, NHCH₂Ar) ppm. NH₂ not displayed. ¹³C NMR (151 MHz, Methanol-*d*₄) δ: 166.8, 162.5 (d, $^1J_{CF} = 244.1$ Hz), 158.8, 157.9, 133.7, 131.1, 130.4 (d, $^3J_{CF} = 8.3$ Hz), 129.1, 127.4 (d, $^2J_{CF} = 15.0$ Hz), 125.6 (d, $^4J_{CF} J = 3.8$ Hz), 122.0, 117.2, 116.4 (d, $^2J_{CF} = 22.5$ Hz), 104.4, 37.7 (d, $^3J_{CF} = 4.7$ Hz) ppm. HPLC-UV (254 nm) ESI-MS, purity: 98%. LC-MS (m/z): 327.1 [M + H]⁺. Mp.: 179 °C.

Synthesis of 3-amino-*N*-(2-methoxybenzyl)-1-(4-methoxyphenyl)-1*H*-pyrazole-4-carboxamide (18f)

A solution of **16** (75 mg, 0.29 mmol), 1-naphthylmethylamine (68 mg, 0.43 mmol), HBTU (163 mg, 0.38 mmol) and TEA (88 mg, 0.87 mmol) in DMF (1 ml) was reacted according to general procedure B. The product **18f** was obtained as 45 mg (41%) of a colorless solid. ¹H NMR (600 MHz, Chloroform-*d*) δ: 7.97 (d, $J = 8.4$ Hz, 1H, CH_{arom.}), 7.95 (s, 1H, CH_{pyrazole}), 7.77 (dd, $J = 7.9, 1.5$ Hz, 1H, CH_{arom.}), 7.70 (d, $J = 8.2$ Hz, 1H, CH_{arom.}), 7.45-7.40 (m, 1H, CH_{arom.}), 7.40-7.37 (m, 2H, CH_{arom.}), 7.33 (dd, $J = 8.3, 7.0$ Hz, 1H, CH_{arom.}), 7.30 (dd, $J = 9.6, 2.7$ Hz, 2H, CH_{arom.}), 6.79 (dd, $J = 9.6, 3.0$ Hz, 2H, CH_{arom.}), 4.88 (s, 2H, NHCH₂Ar), 3.69 (s, 3H, OCH₃) ppm. NH₂ not displayed. ¹³C NMR (151 MHz, Chloroform-*d*) δ: 164.1, 158.0, 156.5, 133.6, 133.4, 132.8, 131.3, 128.6, 128.5, 128.3, 128.2, 126.9, 126.9, 126.4, 126.2, 125.7, 125.2, 123.3, 123.2, 120.1, 114.4, 103.4, 55.3, 41.0 ppm. HPLC-UV (254 nm) ESI-MS, purity: 93%. LC-MS (m/z): 373.2 [M + H]⁺. Mp.: 201 °C.

Synthesis of 3-amino-1-(4-hydroxyphenyl)-*N*-(naphthalen-1-ylmethyl)-1*H*-pyrazole-4-carboxamide (19f)

A solution of **18f** (43 mg, 0.18 mmol) was reacted according to general procedure C. The product **19f** was obtained as 10.5 mg (24%) of a colorless solid. ¹H NMR (600 MHz, Methanol-*d*₄) δ: 8.33 (s, 1H, CH_{pyrazole}), 8.16 (d, $J = 8.4$ Hz, 1H, CH_{arom.}), 7.96-7.89 (m, 1H, CH_{arom.}), 7.85 (d, $J = 8.2$ Hz, 1H, CH_{arom.}), 7.62-7.51 (m, 3H, CH_{arom.}), 7.49 (dd, $J = 8.2, 7.0$ Hz, 1H, CH_{arom.}), 7.45-7.36 (m, 2H, CH_{arom.}), 6.90-6.82 (m, 2H, CH_{arom.}), 5.03 (s, 2H, NHCH₂Ar) ppm. NH₂ not displayed. ¹³C NMR (151 MHz, Methanol-*d*₄) δ: 166.6, 158.9, 135.7, 135.5, 133.7, 133.1, 130.0,

129.5, 129.1, 127.7, 127.2, 127.2, 126.7, 124.8, 121.9, 117.2, 104.5, 42.2 ppm. HPLC-UV (254 nm) ESI-MS, purity: 96%. LC-MS (m/z): 359.2 [M + H]⁺. Mp.: 213 °C.

4.3.9.2.4. Synthesis of 3-amino-*N*-benzyl-1-(3-hydroxyphenyl)-1*H*-pyrazole-4-carboxamide derivatives

Synthesis of (*E*)-1-benzylidene-2-(3-methoxyphenyl)hydrazine (**11**)⁵

A solution of 3-methoxyphenylhydrazine hydrochloride (10 g, 57 mmol) in H₂O / EtOH (80 ml) was treated with NaHCO₃ (6.7 g, 80 mmol) at rt and stirred for 30 min until the solution was clear. Benzaldehyde (7.25 g, 68 mmol) was added and the resulting suspension was stirred for 2 h at rt. Subsequently, the precipitate was filtered off under reduced pressure and washed with water and EtOH and dried at 60 °C, yielding the desired product **11** as 12.5 g (97%) of a colorless solid. HPLC-UV (254 nm) ESI-MS, purity: 92%. LC-MS (m/z): 227.0 [M + H]⁺.

Synthesis of ethyl-3-amino-1-(3-methoxyphenyl)-1*H*-pyrazole-4-carboxylate (**15**)⁵

A mixture of **11** (5 g, 22 mmol) and EEMA (3.74 g, 22 mmol) in xylol (5 ml) was stirred at 160 °C for 3 d in a sealed tube. The intermediate could be detected via TLC-MS (MW = 349). The crude mixture was dissolved in EtOH (35 ml) and conc. HCl (1.7 ml) and refluxed for 2 h. The mixture was treated with saturated NaHCO₃ solution until pH 9 and subsequently extracted with CH₂Cl₂ (3 x 50 ml), the combined organic layers were dried over MgSO₄, filtered and the solvent was evaporated under reduced pressure. The crude product **15** was purified via column chromatography (CH₂Cl₂ / MeOH - 98 : 2) and was obtained as 4.13 g (72%) of a dark brown oil that was directly use for the next reaction step. ¹H NMR (600 MHz, Chloroform-*d*) δ: 8.11 (s, 1H, CH_{pyrazole}), 7.29 (t, *J* = 8.2 Hz, 1H, CH_{arom.}), 7.19 (t, *J* = 2.3 Hz, 1H, CH_{arom.}), 7.15-7.10 (m, 1H, CH_{arom.}), 6.82-6.76 (m, 1H, CH_{arom.}), 4.30 (q, *J* = 7.1 Hz, 2H, CH₂CH₃), 3.83 (s, 3H, OCH₃), 1.35 (t, *J* = 7.1 Hz, 3H, CH₂CH₃) ppm. NH₂ not displayed. LC-MS (m/z): 261.8 [M + H]⁺.

Synthesis of 3-amino-1-(3-methoxyphenyl)-1*H*-pyrazole-4-carboxylic acid (**17**)

A solution of **15** (4.13 g, 15.81 mmol) and LiOH monohydrate (3.32 g, 79.1 mmol) in water / THF (1:1, 40 ml) was stirred for 16 h at 80 °C. Subsequently, the reaction mixture was cooled to rt and then extracted with ethyl acetate. The aqueous solution was acidified to pH 2 with acetic acid and the precipitated product was collected with filtration. The crude product was purified via flash RP-HPLC (water / MeOH - 10 to 100%). The product **17** was obtained 966 mg (26%) as a beige powdery solid. ¹H NMR (500 MHz, DMSO-*d*₆) δ 8.68 (s, 1H, CH_{pyrazole}), 7.40-7.28 (m, 3H, CH_{arom.}), 6.80 (ddd, *J* = 7.9, 2.5, 1.2 Hz, 1H, CH_{arom.}), 5.61 (s, 2H, NH₂), 3.80 (s, 3H, OCH₃) ppm. ¹³C NMR (126 MHz, DMSO-*d*₆) δ: 165.3, 160.2, 157.1, 140.4, 130.8, 130.3, 111.9, 110.0, 103.4, 101.8, 55.5 ppm. HPLC-UV (254 nm) ESI-MS, purity: 93%. LC-MS (m/z): 233.9 [M + H]⁺.

Synthesis of 3-amino-*N*-(2-chloro-6-fluorobenzyl)-1-(3-methoxyphenyl)-1*H*-pyrazole-4-carboxamide (**20a**)

A solution of **17** (75 mg, 0.29 mmol), 2-chloro-6-fluorobenzylamine (68 mg, 0.43 mmol), HBTU (143 mg, 0.38 mmol) and TEA (44 mg, 0.43 mmol) in DMF (1 ml) was reacted according to procedure B. The product **20a** was obtained as 38 mg (35%) of a colorless solid. ¹H NMR (600 MHz, Chloroform-*d*) δ: 7.91 (s, 1H, CH_{pyrazole}), 7.30-7.11 (m, 4H, CH_{arom.}), 7.07 (d, *J* = 8.0 Hz, 1H, CH_{arom.}), 7.04-6.98 (m, 1H, CH_{arom.}), 6.76 (dd, *J* = 8.6, 2.5 Hz, 1H, CH_{arom.}), 6.23-6.09 (m, 1H, NH), 4.75 (d, *J* = 5.4 Hz, 2H, NHCH₂Ar), 3.82 (s, 3H, OCH₃) ppm. NH₂ not displayed. ¹³C NMR (151 MHz, Chloroform-*d*) δ: 163.4, 162.4, 160.8, 160.5, 156.3, 140.4, 135.5 (d, ³*J*_{CF} = 6.3 Hz), 130.2, 129.7 (d, ³*J*_{CF} = 10.4 Hz), 125.9, 125.4 (d, ⁴*J*_{CF} = 4.4 Hz), 123.8 (d, ²*J*_{CF} = 18.3 Hz), 114.4 (d, ²*J*_{CF} = 23.2 Hz), 112.2, 110.3, 104.4, 55.5, 34.5 (d, ⁴*J*_{CF} = 5.2 Hz) ppm. HPLC-UV (254 nm) ESI-MS, purity: 99%. LC-MS (m/z): 374.9 [M + H]⁺. Mp.: 185 °C.

Synthesis of 3-amino-*N*-(2-chloro-6-fluorobenzyl)-1-(3-hydroxyphenyl)-1*H*-pyrazole-4-carboxamide (**21a**)

A solution of **20a** (20 mg, 0.05 mmol) was reacted according to procedure C. The product **21a** was obtained as 5.5 mg (31%) of a colorless solid. ¹H NMR (600 MHz, Methanol-*d*₄) δ 8.48 (s, 1H, CH_{pyrazole}), 7.40-7.31 (m, 2H, CH_{arom.}), 7.25 (t, *J* = 8.1 Hz, 1H, CH_{arom.}), 7.17 (ddd, *J* = 9.5, 8.2, 1.3 Hz, 1H, CH_{arom.}), 7.11-7.03 (m, 2H, CH_{arom.}), 6.72 (dd, *J* = 8.2, 2.3 Hz, 1H, CH_{arom.}), 4.73 (d, *J* = 1.6 Hz, 2H, NHCH₂Ar) ppm. NH₂ not displayed. ¹³C NMR (151 MHz, Methanol-*d*₄) δ: 166.4, 162.8, 160.1, 158.9, 142.2, 137.3, 131.6, 131.5 (d, ³*J*_{CF} = 10.0 Hz), 129.3, 126.9, 125.2 (d, ²*J*_{CF} = 18.3 Hz), 115.6 (d, ²*J*_{CF} = 23.0 Hz), 114.6, 110.5, 107.2, 104.9, 35.9 (d, ⁴*J*_{CF} = 4.9 Hz) ppm. HPLC-UV (254 nm) ESI-MS, purity: 98%. LC-MS (m/z): 360.9 [M + H]⁺. Mp.: 179 °C.

Synthesis of 3-amino-*N*-(2,3-dichlorobenzyl)-1-(3-methoxyphenyl)-1*H*-pyrazole-4-carboxamide (**20b**)

A solution of **17** (75 mg, 0.29 mmol), 2,3-dichlorobenzylamine (75 mg, 0.43 mmol), HBTU (143 mg, 0.38 mmol) and TEA (44 mg, 0.43 mmol) in DMF (1 ml) was reacted according to procedure B. The product **20b** was obtained as 14.4 mg (13%) of a colorless solid. ¹H NMR (600 MHz, Chloroform-*d*) δ: 7.98 (s, 1H, CH_{pyrazole}), 7.38 (dd, *J* = 8.0, 1.5 Hz, 1H, CH_{arom.}), 7.35 (dd, *J* = 7.7, 1.6 Hz, 1H, CH_{arom.}), 7.27 (t, *J* = 8.2 Hz, 1H, CH_{arom.}), 7.19-7.13 (m, 2H, CH_{arom.}), 7.11-7.04 (m, 1H, CH_{arom.}), 6.78 (dd, *J* = 8.2, 2.4 Hz, 1H, CH_{arom.}), 6.42 (t, *J* = 6.2 Hz, 1H, NH), 4.66 (d, *J* = 5.9 Hz, 2H, NHCH₂Ar), 3.82 (s, 3H, OCH₃) ppm. NH₂ not displayed. ¹³C NMR (151 MHz, Chloroform-*d*) δ: 163.8, 160.6, 156.3, 140.3, 138.1, 133.3, 131.8, 130.2, 129.7, 128.3, 127.6, 126.1, 112.4, 110.4, 104.5, 104.4, 55.5, 41.8 ppm. HPLC-UV (254 nm) ESI-MS, purity: 89%. LC-MS (m/z): 391.1 [M + H]⁺. Mp.: 189 °C.

Synthesis of 3-amino-*N*-(2,3-dichlorobenzyl)-1-(3-hydroxyphenyl)-1*H*-pyrazole-4-carboxamide (**21b**)

A solution of **20a** (10 mg, 0.03 mmol) was reacted according to procedure C. The product **21b** was obtained as 31 mg (56%) of a colorless solid. ¹H NMR (600 MHz, Chloroform-*d*) δ: 7.96 (s, 1H, CH_{pyrazole}), 7.37 (dd, *J* = 19.5, 7.8 Hz, 3H, CH_{arom.}), 7.18 (t, *J* = 7.9 Hz, 1H, CH_{arom.}), 7.12-7.02 (m, 2H, CH_{arom.}), 6.71 (d, *J* = 8.0 Hz, 1H, CH_{arom.}), 6.40 (s, 1H, NH), 4.67 (d, *J* = 5.9 Hz, 2H, NHCH₂Ar) ppm. NH₂ not displayed. ¹³C NMR (151 MHz, Chloroform-*d*) δ: 163.8, 160.6, 156.3, 140.3, 138.1, 133.3, 131.8, 130.2, 129.7, 128.3, 127.6, 126.1, 112.4, 110.4, 104.5, 104.4, 41.8 ppm. HPLC-UV (254 nm) ESI-MS, purity: 96%. LC-MS (*m/z*): 377.2 [M + H]⁺. Mp.: 191 °C.

Synthesis of 3-amino-*N*-(2-methoxybenzyl)-1-(3-methoxyphenyl)-1*H*-pyrazole-4-carboxamide (**20c**)

A solution of **17** (75 mg, 0.29 mmol), 2-methoxybenzylamine (59 mg, 0.43 mmol), HBTU (143 mg, 0.38 mmol) and TEA (44 mg, 0.43 mmol) in DMF (1 ml) was reacted according to procedure B. The product **20c** was obtained as 11 mg (18%) of a colorless solid. ¹H NMR (600 MHz, Chloroform-*d*) δ 7.96 (s, 1H, CH_{pyrazole}), 7.30 (dd, *J* = 7.5, 1.7 Hz, 1H, CH_{arom.}), 7.27-7.22 (m, 2H, CH_{arom.}), 7.14 (t, *J* = 2.2 Hz, 1H, CH_{arom.}), 7.06 (dd, *J* = 8.2, 2.0 Hz, 1H, CH_{arom.}), 6.93-6.83 (m, 2H, CH_{arom.}), 6.90 (td, *J* = 7.4, 1.1 Hz, 1H, CH_{arom.}), 6.45-6.40 (m, 1H, NH), 4.54 (d, *J* = 5.6 Hz, 2H, NHCH₂Ar), 3.84 (s, 3H, OCH₃), 3.81 (s, 3H, OCH₃) ppm. NH₂ not displayed. ¹³C NMR (151 MHz, Chloroform-*d*) δ: 163.6, 160.5, 157.5, 156.3, 140.3, 130.2, 129.8, 128.9, 126.2, 126.1, 120.7, 112.2, 110.4, 110.3, 104.7, 104.4, 55.5, 55.4, 39.0 ppm. HPLC-UV (254 nm) ESI-MS, purity: 95%. LC-MS (*m/z*): 353.1 [M + H]⁺. Mp.: 188 °C.

Synthesis of 3-amino-*N*-(2-hydroxybenzyl)-1-(3-hydroxyphenyl)-1*H*-pyrazole-4-carboxamide (**21c**)

A solution of **20c** (60 mg, 0.18 mmol) was reacted according to procedure C. The product **21c** was obtained as 31 mg (56%) of a colorless solid. ¹H NMR (600 MHz, Methanol-*d*₄) δ 7.61 (s, 1H, CH_{pyrazole}), 6.45 - 6.36 (m, 2H, CH_{arom.}), 6.29 (td, *J* = 7.7, 1.7 Hz, 1H, CH_{arom.}), 6.26 (t, *J* = 2.2 Hz, 1H, CH_{arom.}), 6.23 (ddd, *J* = 8.0, 2.1, 0.9 Hz, 1H, CH_{arom.}), 6.01-5.95 (m, 2H, CH_{arom.}), 5.87 (ddd, *J* = 8.2, 2.4, 0.9 Hz, 1H, CH_{arom.}), 3.65 (s, 2H, NHCH₂Ar) ppm. NH₂ not displayed. ¹³C NMR (151 MHz, Methanol-*d*₄) δ: 157.5, 149.3, 147.3, 132.6, 122.0, 121.3, 119.6, 116.9, 111.3, 107.4, 105.1, 101.0, 97.6, 95.5, 30.3 ppm. HPLC-UV (254 nm) ESI-MS, purity: 98%. LC-MS (*m/z*): 325.2 [M + H]⁺. Mp.: 195 °C.

Synthesis of 3-amino-*N*-(2,3-dihydro-1*H*-inden-1-yl)-1-(3-methoxyphenyl)-1*H*-pyrazole-4-carboxamide (**20d**)

A solution of **17** (75 mg, 0.29 mmol), 1-aminoindane hydrochloride (73 mg, 0.43 mmol), HBTU (143 mg, 0.38 mmol) and TEA (44 mg, 0.43 mmol) in DMF (1 ml) was reacted according to procedure B. The product **20d** was obtained as 3.4 mg (3%) of a colorless solid. ¹H NMR (600 MHz, Chloroform-*d*) δ: 8.22 (s, 1H, CH_{pyrazole}), 7.30 (d, *J* = 7.3 Hz, 1H, CH_{arom.}), 7.27-7.21 (m, 1H, CH_{arom.}), 7.20 (m, 2H, CH_{arom.}), 7.16 (dd, *J* = 7.6, 4.1 Hz, 1H, CH_{arom.}), 7.12 (t, *J* = 2.2 Hz, 1H, CH_{arom.}), 7.05 (dd, *J* = 7.9, 2.1 Hz, 1H, CH_{arom.}), 6.76 (dd, *J* = 8.2, 2.4 Hz, 1H, CH_{arom.}), 6.53 (d, *J* = 8.3 Hz, 1H, NH), 5.57 (q, *J* = 7.7 Hz, 1H, CH_{indane}), 4.61 (s, 2H, NH₂), 3.79 (s, 3H, OCH₃), 2.97 (ddd, *J* = 15.9, 8.8, 4.0 Hz, 1H, CH_{2 indane}), 2.84 (dt, *J* = 16.0, 8.1 Hz, 1H, CH_{2 indane}), 2.57 (ddt, *J* = 15.8, 7.9, 3.9 Hz, 1H, CH_{2 indane}), 2.00-1.91 (m, 1H, CH_{2 indane}) ppm. ¹³C NMR (151 MHz, CDCl₃) δ: 163.2, 160.6, 155.6, 143.5, 143.1, 139.2, 130.3, 128.0, 127.2, 126.7, 124.8, 124.2, 112.9, 110.2, 104.2, 103.9, 55.6, 54.5, 33.8, 30.3 ppm. HPLC-UV (254 nm) ESI-MS, purity: 96%. LC-MS (*m/z*): 349.0 [M + H]⁺. Mp.: 194 °C.

Synthesis of 3-amino-*N*-(2,3-dihydro-1*H*-inden-1-yl)-1-(3-hydroxyphenyl)-1*H*-pyrazole-4-carboxamide (**21d**)

A solution of **20d** (87 mg, 0.25 mmol) was reacted according to procedure C. The product **21d** was obtained as 7.7 mg (9%) of a colorless solid. ¹H NMR (600 MHz, Methanol-*d*₄) δ: 8.53 (s, 1H, CH_{pyrazole}), 7.43 (d, *J* = 7.3 Hz, 1H, CH_{arom.}), 7.31-7.26 (m, 2H, CH_{arom.}), 7.26-7.18 (m, 3H, CH_{arom.}), 7.17 (dd, *J* = 8.1, 2.0 Hz, 1H, CH_{arom.}), 6.75 (dd, *J* = 8.1, 2.3 Hz, 1H, CH_{arom.}), 5.34 (t, *J* = 7.1 Hz, 1H, CH_{indane}), 3.09-3.02 (m, 1H, CH_{2 indane}), 2.95-2.88 (m, 1H, CH_{2 indane}), 2.73 (dq, *J* = 11.7, 3.7 Hz, 1H, CH_{2 indane}), 1.96 (dq, *J* = 12.6, 8.0 Hz, 1H, CH_{2 indane}) ppm. NH₂ not displayed. ¹³C NMR (151 MHz, Methanol-*d*₄) δ: 169.4, 160.0, 159.5, 146.3, 144.8, 142.5, 131.6, 129.7, 129.0, 127.8, 126.0, 125.4, 114.5, 110.5, 107.3, 104.1, 59.8, 36.0, 31.3 ppm. HPLC-UV (254 nm) ESI-MS, purity: 94%. LC-MS (*m/z*): 335.1 [M + H]⁺. Mp.: 196 °C.

Synthesis of 3-amino-*N*-(2-fluorobenzyl)-1-(3-methoxyphenyl)-1*H*-pyrazole-4-carboxamide (**20e**)

A solution of **17** (75 mg, 0.29 mmol), 2-fluorobenzylamine (60 mg, 0.48 mmol), HBTU (183 mg, 0.48 mmol) and TEA (98 mg, 0.96 mmol) in DMF (1 ml) was reacted according to procedure B. The product **20e** was obtained as 3.6 mg (3%) of a colorless solid. ¹H NMR (600 MHz, Chloroform-*d*) δ: 8.01 (s, 1H, CH_{pyrazole}), 7.38 (td, *J* = 7.7, 1.7 Hz, 1H, CH_{arom.}), 7.27-7.22 (m, 2H, CH_{arom.}), 7.16-7.13 (m, 1H, CH_{arom.}), 7.11-7.05 (m, 2H, CH_{arom.}), 7.05-7.01 (m, 1H, CH_{arom.}), 6.76 (dd, *J* = 8.2, 2.2 Hz, 1H, CH_{arom.}), 6.34 (s, 1H, NH), 4.60 (d, *J* = 5.3 Hz, 2H, NHCH₂Ar), 3.81 (s, 3H, OCH₃) ppm. NH₂ not displayed. ¹³C NMR (151 MHz, Chloroform-*d*) δ: 163.8, 161.1 (d, ¹*J*_{CF} = 246.0 Hz), 160.6, 156.2, 140.1, 130.4 (d, ³*J*_{CF} = 5.1 Hz), 130.2, 129.4 (d, ³*J*_{CF} = 8.8

Hz), 126.2, 125.3 (d, $^2J_{CF} = 15.1$ Hz), 124.4 (d, $^4J_{CF} = 4.1$ Hz), 115.4 (d, $^2J_{CF} = 21.5$ Hz), 112.5, 110.3, 104.4, 55.5, 37.3 (d, $^3J_{CF} = 5.1$ Hz) ppm. HPLC-UV (254 nm) ESI-MS, purity: 94%. LC-MS (m/z): 341.2 [M + H]⁺. Mp.: 187 °C.

Synthesis of 3-amino-*N*-(2-fluorobenzyl)-1-(3-hydroxyphenyl)-1*H*-pyrazole-4-carboxamide (**21e**)

A solution of **20e** (25 mg, 0.07 mmol) was reacted according to procedure C. The product **21e** was obtained as 16 mg (69%) of a colorless solid. ¹H NMR (600 MHz, Methanol-*d*₄) δ: 8.50 (s, 1H, CH_{pyrazole}), 7.45 (td, *J* = 7.7, 1.7 Hz, 1H, CH_{arom.}), 7.37-7.30 (m, 1H, CH_{arom.}), 7.28 (t, *J* = 8.1 Hz, 1H, CH_{arom.}), 7.19 (td, *J* = 7.6, 1.2 Hz, 1H, CH_{arom.}), 7.15-7.08 (m, 3H, CH_{arom.}), 6.74 (ddd, *J* = 8.2, 2.3, 0.9 Hz, 1H, CH_{arom.}), 4.62 (s, 2H NHCH₂Ar) ppm. NH₂ not displayed. ¹³C NMR (151 MHz, Methanol-*d*₄) δ: 166.5, 163.3, 160.9 (d, $^1J_{CF} = 244.2$ Hz), 158.4, 142.2, 131.7, 130.4 (d, $^3J_{CF} = 8.2$ Hz), 129.2, 127.3 (d, $^2J_{CF} = 15.3$ Hz), 125.6 (d, $^4J_{CF} = 2.9$ Hz), 116.4 (d, $^2J_{CF} = 21.4$ Hz), 114.8, 110.6, 107.2, 105.3, 36.6 (d, $^3J_{CF} = 5.2$ Hz) ppm. HPLC-UV (254 nm) ESI-MS, purity: 97%. LC-MS (m/z): 327.1 [M + H]⁺. Mp.: 190 °C.

Synthesis of 3-amino-*N*-(2-chloro-6-fluoro-3-methoxybenzyl)-1-(3-methoxyphenyl)-1*H*-pyrazole-4-carboxamide (**20f**)

A solution of **17** (75 mg, 0.29 mmol), 2-chloro-6-fluoro-3-methoxybenzylamine (90 mg, 0.48 mmol), HBTU (183 mg, 0.48 mmol) and TEA (98 mg, 0.96 mmol) in DMF (1 ml) was reacted according to procedure B. The product **20f** was obtained as 4.54 mg (4%) of a colorless solid. ¹H NMR (600 MHz, Chloroform-*d*) δ: 7.91 (s, 1H, CH_{pyrazole}), 7.26 (t, *J* = 8.2 Hz, 1H, CH_{arom.}), 7.14 (t, *J* = 2.3 Hz, 1H, CH_{arom.}), 7.07 (dd, *J* = 8.0, 2.0 Hz, 1H, CH_{arom.}), 6.98 (t, *J* = 8.9 Hz, 1H, CH_{arom.}), 6.84 (dd, *J* = 9.1, 4.7 Hz, 1H, CH_{arom.}), 6.76 (dd, *J* = 8.2, 2.4 Hz, 1H, CH_{arom.}), 6.21 (t, *J* = 5.3 Hz, 1H, NH), 4.76 (dd, *J* = 5.7, 1.7 Hz, 2H, NHCH₂Ar), 3.86 (s, 3H, OCH₃), 3.82 (s, 3H, OCH₃) ppm. NH₂ not displayed. ¹³C NMR (151 MHz, Chloroform-*d*) δ: 163.4, 160.5, 156.3, 155.4 (d, $^1J_{CF} = 242.7$ Hz), 151.9, 140.4, 130.1, 125.9, 124.9 (d, $^2J_{CF} = 19.0$ Hz), 123.6 (d, $^3J_{CF} = 5.4$ Hz), 113.9 (d, $^2J_{CF} = 23.8$ Hz), 112.3, 111.7 (d, $^3J_{CF} = 9.1$ Hz), 110.3, 104.4, 56.7, 55.5, 34.8 (d, $^4J_{CF} = 3.7$ Hz) ppm. HPLC-UV (254 nm) ESI-MS, purity: 96%. LC-MS (m/z): 405.2 [M + H]⁺. Mp.: 200 °C.

Synthesis of 3-amino-*N*-(2-chloro-6-fluoro-3-hydroxybenzyl)-1-(3-hydroxyphenyl)-1*H*-pyrazole-4-carboxamide (**21f**)

A solution of **20f** (35 mg, 0.086 mmol) was reacted according to procedure C. The product **21f** was obtained as 25 mg (76%) of a colorless solid. ¹H NMR (600 MHz, Methanol-*d*₄) δ: 8.50 (s, 1H, CH_{pyrazole}), 7.19 (t, *J* = 8.1 Hz, 1H, CH_{arom.}), 7.00 (t, *J* = 2.3 Hz, 1H, CH_{arom.}), 6.95 (ddd, *J* = 8.1, 2.1, 0.9 Hz, 1H, CH_{arom.}), 6.80 (t, *J* = 9.2 Hz, 1H, CH_{arom.}), 6.72 (dd, *J* = 9.1, 5.3 Hz, 1H, CH_{arom.}), 6.67 (ddd, *J* = 8.2, 2.4, 0.9 Hz, 1H, CH_{arom.}), 4.66 (d, *J* = 2.0 Hz, 2H, NHCH₂Ar) ppm.

NH₂ not displayed. ¹³C NMR (151 MHz, Methanol-*d*₄) δ: 180.7, 166.5, 161.8, 160.0, 158.8 (d, ¹J_{CF} = 247.4 Hz), 142.2, 131.3, 129.4, 125.1, 123.4 (d, ²J_{CF} = 17.4 Hz), 119.7 (d, ³J_{CF} = 8.2 Hz), 116.2, 114.6 (d, ²J_{CF} = 23.2 Hz), 108.9, 108.2, 104.9, 37.0 (d, ⁴J_{CF} = 4.1 Hz) ppm. HPLC-UV (254 nm) ESI-MS, purity: 94%. LC-MS (m/z): 377.2 [M + H]⁺. Mp.: 204 °C.

Synthesis of 3-amino-*N*-(2,3-difluoro-6-methoxybenzyl)-1-(3-methoxyphenyl)-1*H*-pyrazole-4-carboxamide (20g)

A solution of **17** (75 mg, 0.29 mmol), 2,3-difluoro-6-methoxybenzylamine (83 mg, 0.48 mmol), HBTU (183 mg, 0.48 mmol) and TEA (98 mg, 0.96 mmol) in DMF (1 ml) was reacted according to procedure B. The product **20g** was obtained as 17 mg (14%) of a colorless solid. ¹H NMR (600 MHz, Chloroform-*d*) δ: 7.88 (s, 1H, CH_{pyrazole}), 7.13-6.89 (m, 2H, CH_{arom.} / NH), 7.05 (dt, *J* = 19.1, 9.0 Hz, 2H, CH_{arom.}), 6.76 (d, *J* = 8.3 Hz, 1H, CH_{arom.}), 6.63-6.48 (m, 1H, CH_{arom.}), 6.19 (s, 1H, CH_{arom.}), 4.66 (s, 2H, NHCH₂Ar), 3.86 (s, 3H, OCH₃), 3.83 (s, 3H, OCH₃) ppm. NH₂ not displayed. ¹³C NMR (151 MHz, Chloroform-*d*) δ: 163.4, 160.5, 156.4, 154.2 (d, ⁴J_{CF} = 4.6 Hz), 149.2 (dd, ¹J_{CF} = 247.2 Hz, 15.7 Hz), 145.4 (d, ¹J_{CF} = 251.0 Hz, 16.8 Hz) 140.4, 130.1, 125.8, 115.87 (d, ²J_{CF} = 15.7 Hz), 115.7 (d, ²J_{CF} = 20.4 Hz), 112.2, 110.3, 105.5, 104.7, 104.5, 56.3, 55.5, 31.8 ppm. HPLC-UV (254 nm) ESI-MS, purity: 96%. LC-MS (m/z): 389.3 [M + H]⁺. Mp.: 192 °C.

Synthesis of 3-amino-*N*-(2,3-difluoro-6-hydroxybenzyl)-1-(3-hydroxyphenyl)-1*H*-pyrazole-4-carboxamide (21g)

A solution of **20g** (12 mg, 0.03 mmol) was reacted according to procedure C. The product **21g** was obtained as 3.7 mg (35%) of a colorless solid. ¹H NMR (600 MHz, Methanol-*d*₄) δ: 8.48 (s, 1H, CH_{pyrazole}), 7.27 (t, *J* = 8.1 Hz, 1H, CH_{arom.}), 7.11 (t, *J* = 2.2 Hz, 1H, CH_{arom.}), 7.10-7.04 (m, 2H, CH_{arom.}), 6.73 (dd, *J* = 8.0, 2.3 Hz, 1H, CH_{arom.}), 6.66 (ddd, *J* = 9.2, 3.9, 1.9 Hz, 1H, CH_{arom.}), 4.56 (d, *J* = 1.8 Hz, 2H, NHCH₂Ar) ppm. NH₂ not displayed. ¹³C NMR (151 MHz, Methanol-*d*₄) δ: 167.58, 160.07, 158.92, 154.34, 150.83 (dd, ¹J_{CF} = 245.4, 13.8 Hz), 145.79 (dd, ¹J_{CF} = 237.2, 13.4 Hz), 142.13, 131.65, 129.45, 117.64 (d, ²J_{CF} = 18.3 Hz), 116.35 (d, ²J_{CF} = 14.0 Hz), 114.77, 112.78 (t, ³J_{CF} = 4.7 Hz), 110.61, 107.22, 104.52, 33.21 (d, ⁴J_{CF} = 5.0 Hz) ppm. HPLC-UV (254 nm) ESI-MS, purity: 97%. LC-MS (m/z): 361.2 [M + H]⁺. Mp.: 199 °C.

4.3.9.2.5. Synthesis of 3-amino-*N*-benzyl-1-phenyl-1*H*-pyrazole-4-carboxamide derivatives

Synthesis of (*E*)-1-benzylidene-2-phenylhydrazine (22**)⁵**

A solution of phenylhydrazine (3 g, 27.7 mmol) in H₂O / EtOH (80 ml) was treated with NaHCO₃ (1 g, 11.9 mmol) at rt and stirred for 30 min until the solution was clear. Benzaldehyde (3.5 g, 33.3 mmol) was added and the resulting suspension was stirred for 2 h at rt. Subsequently,

the precipitate was filtered under reduced pressure and washed with water and EtOH and dried at 60°C, yielding the desired product **22** as 4.925 g (91%) of a colorless solid. The mass was determined via TLC-MS, (m/z): 197.0 [M + H]⁺.

Synthesis of ethyl-3-amino-1-phenyl-1*H*-pyrazole-4-carboxylate (**24**)⁵

A mixture of **22** (4.925 g, 25 mmol) and EEMA (5.5 g, 33 mmol) in xylol (5 ml) was stirred at 160 °C for 3 d in a sealed tube. The intermediate **23** could be detected via TLC-MS ((m/z): 319.0 [M + H]⁺). The crude mixture was dissolved in EtOH (35 ml) and conc. HCl (1.7 ml) and was refluxed for 2 h. The mixture was treated with saturated NaHCO₃ solution until pH 9 and subsequently extracted with CH₂Cl₂ (3 x 50 ml), the combined organic layers were dried over MgSO₄, filtered and the solvent was evaporated under reduced pressure. The crude product **24** was purified by column chromatography (CH₂Cl₂ / MeOH - 98 : 2) and was obtained as 3,85 g (64%) of a dark brown oil that was directly use for the next reaction step. The mass was determined via TLC-MS (m/z): 232 [M + H]⁺.

Synthesis of 3-amino-1-phenyl-1*H*-pyrazole-4-carboxylic acid (**25**)

A mixture of crude **24** in H₂O / THF (1 : 1 - 30 ml) was treated with LiOH monohydrate (518 mg, 138.5 mmol) and heated at 80 °C for 5 h. Subsequently, the mixture was treated with ethyl acetate (3 x 30 ml) and extracted. The organic phase was discarded and the aqueous phase was acidified with diluted HCl. The resulting precipitated solid was filtered and dried under vacuum, yielding 2.57 g (51% based on **22**) of a brown solid. ¹H NMR (600 MHz, DMSO-*d*₆) δ: 12.41 (s, 1H, COOH), 8.65 (s, 1H, CH_{pyrazole}), 7.77 (d, *J* = 8.0 Hz, 2H, CH_{arom.}), 7.43 (t, *J* = 7.7 Hz, 2H, CH_{arom.}), 7.23 (t, *J* = 7.4 Hz, 1H, CH_{arom.}), 5.52 (s, 2H, NH₂) ppm. ¹³C NMR (151 MHz, DMSO-*d*₆) δ: 165.3, 157.27, 139.2, 130.5, 129.5, 125.9, 117.9, 101.8 ppm. HPLC-UV (254 nm) ESI-MS, purity: 80%. LC-MS (m/z): 203.2 [M + H]⁺.

Synthesis of 3-amino-*N*-(2-chloro-6-fluorobenzyl)-1-phenyl-1*H*-pyrazole-4-carboxamide (**29a**)

A solution of **25** (22 mg, 0.1 mmol), 2-chloro-6-fluorobenzylamine (25 mg, 0.15 mmol), HBTU (53 mg, 0.14 mmol) and TEA (22 mg, 0.22 mmol) in DMF (1 ml) was reacted according to procedure B. The product **29a** was obtained as 6.5 mg (17%) of a beige solid. ¹H NMR (600 MHz, Chloroform-*d*) δ: 8.36 (s, 1H, CH_{pyrazole}), 7.57-7.47 (m, 2H, CH_{arom.}), 7.37 (t, *J* = 7.3 Hz, 2H, CH_{arom.}), 7.27-7.24 (m, 1H, CH_{arom.}), 7.21-7.14 (m, 3H, CH_{arom.}), 6.99 (t, *J* = 8.1 Hz, 1H, CH_{arom.}), 6.86 (s, 1H, CH_{arom.}), 6.36 (d, *J* = 21.7 Hz, 2H, NH₂), 4.74-4.69 (m, 2H, NHCH₂Ar) ppm. ¹³C NMR (151 MHz, Chloroform-*d*) δ: 162.5, 160.9, 135.6, 129.9, 129.61, 127.5, 125.5, 123.6, 119.3, 118.5, 114.4 (d, ²*J*_{CF} = 22.7 Hz), 34.68 ppm. HPLC-UV (254 nm) ESI-MS, purity: 98%. LC-MS (m/z): 345.1 [M + H]⁺. Mp.: 160 °C.

Synthesis of 3-amino-*N*-benzyl-1-phenyl-1*H*-pyrazole-4-carboxamide (**29b**)

A solution of **25** (100 mg, 0.49 mmol), benzylamine (79 mg, 0.74 mmol), HBTU (284 mg, 0.74 mmol) and TEA (151 mg, 0.15 mmol) in DMF (1 ml) was reacted according to procedure B. The product **29b** was obtained as 12 mg (8%) of a colorless solid. ¹H NMR (500 MHz, Chloroform-*d*) δ: 8.18 (s, 1H, CH_{pyrazole}), 7.52-7.48 (m, 2H, CH_{arom.}), 7.37-7.29 (m, 6H, CH_{arom.}), 7.30-7.18 (m, 2H, CH_{arom.}), 6.60 (s, 1H, NH), 4.57-4.51 (m, 2H, NHCH₂Ar) ppm. NH₂ not displayed. ¹³C NMR (126 MHz, Chloroform-*d*) δ: 163.2, 155.6, 138.3, 129.7, 128.8, 127.9, 127.6, 127.0, 126.9, 118.4, 104.0, 43.3 ppm. HPLC-UV (254 nm) ESI-MS, purity: 95%. LC-MS (m/z): 293.1 [M + H]⁺. Mp.: 151 °C.

Synthesis of 3-amino-*N*,1-diphenyl-1*H*-pyrazole-4-carbohydrazide (**29c**)

A solution of **25** (100 mg, 0.49 mmol), phenylhydrazine (80 mg, 0.74 mmol), HBTU (284 mg, 0.74 mmol) and TEA (151 mg, 0.15 mmol) in DMF (1 ml) was reacted according to procedure B. The product **29c** was obtained as 102 mg (71%) of a colorless solid. ¹H NMR (500 MHz, DMSO-*d*₆) δ: 9.77 (s, 1H, NH), 8.82 (s, 1H, CH_{pyrazole}), 7.78 (s, 1H, NH), 7.67-7.61 (m, 2H, CH_{arom.}), 7.52-7.45 (m, 2H, CH_{arom.}), 7.26 (t, *J* = 7.5 Hz, 1H, CH_{arom.}), 7.18-7.10 (m, 2H, CH_{arom.}), 6.82-6.75 (m, 2H, CH_{arom.}), 6.70 (tt, *J* = 7.1, 1.1 Hz, 1H, CH_{arom.}), 5.68 (s, 2H, NH₂), 2.68 (s, 1H, NH) ppm. ¹³C NMR (126 MHz, DMSO-*d*₆) δ: 164.1, 157.4, 149.9, 139.4, 129.7, 128.8, 127.3, 125.8, 118.7, 117.5, 112.4, 101.9 ppm. HPLC-UV (254 nm) ESI-MS, purity: 88%. LC-MS (m/z): 294 [M + H]⁺. Mp.: 177 °C.

Synthesis of *O*-phenylhydroxylamine (**28**)¹⁵

A suspension of *N*-hydroxyphthalimide (500 mg, 3.07 mmol), phenyl boronic acid (742 mg, 6.14 mmol), CuCl (303 mg, 3.07 mmol) and pyridine (266 mg, 3.38 mmol) in dichloroethane (3 ml) was stirred at rt for 24 h. The crude mixture was directly purified via column chromatography (CH₂Cl₂/ MeOH - 95 : 5). The crude intermediate **27** (TLC-MS analysis: (m/z): 239.9 [M + H]⁺) was treated with hydrazine monohydrate in chloroform / MeOH (9 : 1). The mixture was filtrated and the filtrate was purified via column chromatography (pure dichloromethane). The product **28** was obtained as 250 mg (74% based on *N*-hydroxyphthalimide) of a beige oil. HPLC-UV (254 nm) ESI-MS, purity: 95%. LC-MS (m/z): 109.8 [M + H]⁺.

Synthesis of 3-amino-*N*-phenoxy-1-phenyl-1*H*-pyrazole-4-carboxamide (**29d**)

A solution of **25** (100 mg, 0.49 mmol), **27** (80 mg, 0.74 mmol), HBTU (280 mg, 0.74 mmol) and TEA (149 mg, 1.47 mmol) in DMF (2 ml) was reacted according to procedure B. The product **29d** was obtained as 26 mg (18%) of a colorless solid. ¹H NMR (600 MHz, DMSO-*d*₆) δ: 11.82 (s, 1H, NH), 8.64 (s, 1H, CH_{pyrazole}), 7.69-7.64 (m, 2H, CH_{arom.}), 7.51-7.42 (m, 2H, CH_{arom.}),

7.37-7.30 (m, 2H, CH_{arom.}), 7.27 (t, *J* = 7.4 Hz, 1H, CH_{arom.}), 7.11 (d, *J* = 8.1 Hz, 2H, CH_{arom.}), 7.06-7.00 (m, 1H, CH_{arom.}), 5.71 (s, 2H, NH₂) ppm. ¹³C NMR (151 MHz, DMSO-*d*₆) δ: 163.6, 160.1, 157.5, 139.2, 129.8, 129.6, 127.5, 126.0, 122.5, 117.8, 113.2, 100.1 ppm. HPLC-UV (254 nm) ESI-MS, purity: 96%. LC-MS (*m/z*): 295.1 [M + H]⁺. Mp.: 165 °C.

Synthesis of 3-amino-*N*-(2-methoxybenzyl)-1-phenyl-1*H*-pyrazole-4-carboxamide (**29e**)

A solution of **25** (100 mg, 0.49 mmol), 2-methoxybenzylamine (101 mg, 0.74 mmol), HBTU (284 mg, 0.74 mmol) and TEA (151 mg, 0.15 mmol) in DMF (1 ml) was reacted according to procedure B. The product **29e** was obtained as 13 mg (8%) of a colorless solid. ¹H NMR (600 MHz, Chloroform-*d*) δ: 7.99 (s, 1H, CH_{pyrazole}), 7.51 (d, *J* = 8.0 Hz, 2H, CH_{arom.}), 7.35 (t, *J* = 7.8 Hz, 2H, CH_{arom.}), 7.29 (dd, *J* = 7.6, 1.7 Hz, 1H, CH_{arom.}), 7.26-7.16 (m, 2H, CH_{arom.}), 6.89 (t, *J* = 7.4 Hz, 1H, CH_{arom.}), 6.85 (d, *J* = 8.2 Hz, 1H, CH_{arom.}), 6.55-6.51 (m, 1H, NH), 4.54 (d, *J* = 5.6 Hz, 2H, NHCH₂Ar), 3.83 (s, 3H, OCH₃) ppm. NH₂ not displayed. ¹³C NMR (151 MHz, Chloroform-*d*) δ: 169.7, 163.7, 160.8, 157.5, 156.4, 139.2, 129.8, 129.6, 129.4, 128.8, 126.3, 126.2, 125.9, 120.7, 118.3, 110.3, 110.2, 55.3, 38.9 ppm. HPLC-UV (254 nm) ESI-MS, purity: 94%. LC-MS (*m/z*): 323.3 [M + H]⁺. Mp.: 163 °C.

Synthesis of 3-amino-*N*-(2-hydroxybenzyl)-1-phenyl-1*H*-pyrazole-4-carboxamide (**29f**)

A solution of **29e** (97 mg, 0.3 mmol) was reacted according to procedure C. The product **29f** was obtained as 60 mg (65%) of a colorless solid. ¹H NMR (600 MHz, Methanol-*d*₄) δ: 8.54 (s, 1H, CH_{pyrazole}), 7.67 (dd, *J* = 8.4, 1.5 Hz, 2H, CH_{arom.}), 7.49 (dd, *J* = 8.5, 7.3 Hz, 2H, CH_{arom.}), 7.35-7.28 (m, 1H, CH_{arom.}), 7.26 (dd, *J* = 7.9, 1.6 Hz, 1H, CH_{arom.}), 7.15 (td, *J* = 7.7, 1.6 Hz, 1H, CH_{arom.}), 6.84 (t, *J* = 7.1 Hz, 2H, CH_{arom.}), 4.52 (s, 2H, NHCH₂Ar) ppm. NH₂ not displayed. ¹³C NMR (151 MHz, Methanol-*d*₄) δ: 166.9, 158.2, 156.9, 141.0, 130.9, 130.1, 129.3, 127.8, 126.4, 120.9, 119.8, 117.0, 105.6, 40.0 ppm. HPLC-UV (254 nm) ESI-MS, purity: 95%. LC-MS (*m/z*): 309.2 [M + H]⁺. Mp.: 175 °C.

Synthesis of 2-(aminomethyl)benzoic acid hydrochloride (**26**)

1-Isoindolinone (300 mg, 2.2 mmol) was refluxed in conc. HCl (5 ml) for 16 h. The product **26** was isolated by filtration and yielded 221 mg (67%) of a white solid. LC-MS (*m/z*): 173.21 [M + H]⁺.

Synthesis of 2-((3-amino-1-phenyl-1*H*-pyrazole-4-carboxamido)methyl)benzoic acid (**29g**)

A solution of **25** (100 mg, 0.49 mmol), HBTU (183 mg, 0.48 mmol) and TEA (98 mg, 0.96 mmol) in DMF (1 ml) were stirred at 55 °C for 2 h. The mixture was then treated with **26** (81 mg, 0.54 mmol) and stirred for 16 h at 55 °C. Subsequently, the mixture was treated with diluted HCl and extracted with CH₂Cl₂ (3 x 20 ml), the combined organic layers were dried over MgSO₄,

filtered and the solvent was evaporated under reduced pressure. The residue was purified via column chromatography (CH₂Cl₂ / MeOH - 9 : 1). Additionally, the still impure product was purified via flash RP-HPLC (10 to 100% MeOH). The product **29g** was obtained as 28 mg (17%) of a colorless solid. ¹H NMR (600 MHz, DMSO-*d*₆) δ: 13.00 (s, 1H, COOH), 8.83 (s, 1H, CH_{pyrazole}), 8.37 (t, *J* = 6.0 Hz, 1H, CH_{arom.}), 7.87 (dd, *J* = 7.8, 1.4 Hz, 1H, CH_{arom.}), 7.64-7.60 (m, 2H, CH_{arom.}), 7.54 (td, *J* = 7.6, 1.5 Hz, 1H, CH_{arom.}), 7.49-7.44 (m, 3H, CH_{arom.}), 7.36 (td, *J* = 7.5, 1.3 Hz, 1H, CH_{arom.}), 7.26-7.21 (m, 1H, NH), 5.68 (s, 2H, NH₂), 4.77 (d, *J* = 5.9 Hz, 2H, NHCH₂Ar) ppm. ¹³C NMR (151 MHz, DMSO-*d*₆) δ: 168.5, 164.0, 157.3, 140.9, 139.4, 132.1, 130.5, 129.7, 129.7, 128.0, 127.5, 126.9, 125.6, 117.4, 103.9, 59.9 ppm. HPLC-UV (254 nm) ESI-MS, purity: 98%. LC-MS (*m/z*): 337.0 [M + H]⁺. Mp.: 223 °C.

Synthesis of 3-amino-*N*-(2-(hydroxymethyl)benzyl)-1-phenyl-1*H*-pyrazole-4-carboxamide (29h)

A solution of **29g** (10 mg, 0.03 mmol) in THF (5 ml) was treated with LiAlH₄ (2 mg, 0.05 mmol) at 0 °C and was then allowed to warm up to rt. This mixture was stirred at rt for 24 h. Subsequently, the mixture was treated with diluted HCl and extracted with ethyl acetate (3 x 20 ml), the combined organic layers were dried over MgSO₄, filtered and the solvent was evaporated under reduced pressure. The residue was purified by flash RP-HPLC (10 to 100% MeOH). The product **29h** was obtained as 5 mg (52%) of a colorless solid. ¹H NMR (600 MHz, Methanol-*d*₄) δ: 8.61 (s, 1H, CH_{pyrazole}), 7.72 - 7.68 (m, 2H, CH_{arom.}), 7.54-7.49 (m, 2H, CH_{arom.}), 7.47-7.44 (m, 1H, CH_{arom.}), 7.44 - 7.41 (m, 1H, CH_{arom.}), 7.35 (t, *J* = 7.4 Hz, 1H, CH_{arom.}), 7.34-7.30 (m, 2H, CH_{arom.}), 4.79 (s, 2H, NHCH₂Ar), 4.68 (s, 2H, CH₂OH) ppm. NH₂ not displayed. ¹³C NMR (151 MHz, Methanol-*d*₄) δ: 165.7, 155.5, 140.9, 140.5, 138.1, 131.0, 130.0, 129.9, 129.5, 129.3, 128.9, 128.2, 120.0, 107.0, 63.4, 41.4 ppm. HPLC-UV (254 nm) ESI-MS, purity: 96%. LC-MS (*m/z*): 323.3 [M + H]⁺. Mp.: 197 °C.

4.3.9.2.6. Synthesis of 3-amino-*N*-benzyl-1-(1*H*-indazol-5-yl)-1*H*-pyrazole-4-carboxamide derivatives

Synthesis of 5-hydrazinyl-1*H*-indazole hydrochloride (31)¹⁶

To a solution of 1*H*-indazol-5-ylamine (5 g, 38 mmol) in conc. HCl (12.5 ml) was added an aqueous solution (12.5 ml) of NaNO₂ (4.75 g, 38 mmol) at 0 °C and the resulting mixture was stirred for 1h. A solution of SnCl₂ · 2H₂O (22.5 g, 74 mmol) in conc. HCl (17.5 ml), pre-cooled to 0 °C, was then added. The reaction solution was stirred for 2 h at rt. The precipitate was filtered and washed with ether to yield **31** as a yellow solid, which was used for the next reaction without further purification. LC-MS (*m/z*): 148.9 [M + H]⁺.

Synthesis of (*E*)-5-(2-benzylidenehydrazinyl)-1*H*-indazole (**32**)⁵

A solution of **31** (5.8 g, 31 mmol) in H₂O / EtOH (80 ml) was treated with NaHCO₃ (3.9 g, 80 mmol) at rt and stirred for 30 min until the solution was clear. Benzaldehyde (3.67 g, 35 mmol) was added and the resulting suspension was stirred for 2 h at rt. Subsequently, the precipitate was filtered under reduced pressure and washed thoroughly with water and EtOH and dried under reduced pressure, yielding the desired product **32** as 6.6 g (90%) of a colorless solid. ¹H NMR (600 MHz, DMSO-*d*₆) δ: 12.76 (s, 1H, NH), 10.26 (s, 1H, NH), 7.89 (s, 1H, =CH), 7.86 (s, 1H, =CH), 7.66 - 7.62 (m, 2H, CH_{arom.}), 7.42 (d, *J* = 8.9 Hz, 1H, CH_{arom.}), 7.37 (t, *J* = 7.7 Hz, 2H, CH_{arom.}), 7.33 (d, *J* = 1.9 Hz, 1H, CH_{arom.}), 7.28-7.24 (m, 1H, CH_{arom.}), 7.18 (dd, *J* = 8.9, 2.0 Hz, 1H, CH_{arom.}) ppm. ¹³C NMR (151 MHz, DMSO-*d*₆) δ: 139.7, 136.3, 135.9, 135.6, 132.6, 128.8, 127.8, 125.6, 123.8, 115.4, 110.8, 99.6 ppm. HPLC-UV (254 nm) ESI-MS, purity: 88%. LC-MS (*m/z*): 236.9 [M + H]⁺.

Synthesis of ethyl-3-amino-1-(1*H*-indazol-5-yl)-1*H*-pyrazole-4-carboxylate (**34**)

A solution of **32** (2.17 g, 6.12 mmol) and EEMA (2.17 g, 12.8 mmol) in EtOH (20 ml) was heated at 110 °C for 16 h. Subsequently, the solvent was removed and the intermediate **33** was isolated by column chromatography (100% CH₂Cl₂ to CH₂Cl₂ / MeOH - 9 : 1) and characterized by TLC-MS ((*m/z*): 360.1 [M + H]⁺). The crude intermediate was dissolved in EtOH (15 ml) and conc. HCl (1.7 ml) and refluxed for 2 h. The mixture was treated with saturated NaHCO₃ solution until pH 9 and subsequently extracted with CH₂Cl₂ (3 x 50 ml), the combined organic layers were dried over MgSO₄, filtered off and the solvent was evaporated under reduced pressure. The crude product **34** was purified via column chromatography (CH₂Cl₂ / MeOH - 95 : 5) and was obtained as 347 mg (21% based on **32**) of a brown oil that was directly use for the next reaction step. ¹H NMR (600 MHz, DMSO-*d*₆) δ: 13.16 (s, 1H, NH), 8.65 (s, 1H, CH_{pyrazole}), 8.12 (d, *J* = 1.9 Hz, 1H, CH_{arom.}), 8.10 (t, *J* = 1.3 Hz, 1H, CH_{arom.}), 7.84 (dd, *J* = 9.0, 2.1 Hz, 1H, CH_{arom.}), 7.59 (dt, *J* = 8.9, 0.9 Hz, 1H, CH_{arom.}), 5.61 (s, 2H, NH₂), 4.23 (q, *J* = 7.1 Hz, 2H, CH₂), 1.29 (t, *J* = 7.1 Hz, 3H, CH₃) ppm. HPLC-UV (254 nm) ESI-MS, purity: 86%. LC-MS (*m/z*): 271.8 [M + H]⁺.

Synthesis of 3-amino-1-(1*H*-indazol-5-yl)-1*H*-pyrazole-4-carboxylic acid (**35**)

A mixture of **34** (347 mg, 1.28 mmol) and LiOH monohydrate (270 mg, 6.4 mmol) was stirred in H₂O / THF (1 : 1) at 70 °C for 3 h. Subsequently, the mixture was treated with ethyl acetate (3 x 30 ml) and extracted. The organic phase was discarded and the aqueous phase was acidified with diluted HCl. The resulting precipitated solid was filtered off and dried under vacuum, yielding 236 mg (76%) of a brown solid. ¹H NMR (600 MHz, DMSO-*d*₆) δ: 13.17 (s, 1H, NH), 8.59 (s, 1H, CH_{pyrazole}), 8.09 (s, 1H, =CH), 8.08 (d, *J* = 2.0 Hz, 1H, CH_{arom.}), 7.81 (dd,

$J = 9.0, 2.1$ Hz, 1H, CH_{arom.}), 7.59 (d, $J = 9.0$ Hz, 1H, CH_{arom.}), 5.57 (s, 2H, NH₂) ppm. HPLC-UV (254 nm) ESI-MS, purity: 88%. LC-MS (m/z): 244.2 [M + H]⁺.

Synthesis of 3-amino-*N*-(2-chloro-6-fluorobenzyl)-1-(1*H*-indazol-5-yl)-1*H*-pyrazole-4-carboxamide (36a)

A solution of **35** (50 mg, 0.21 mmol), 2-chloro-6-fluorobenzylamine (48 mg, 0.32 mmol), HBTU (121 mg, 0.32 mmol) and TEA (63 mg, 0.63 mmol) in DMF (1 ml) was reacted according to procedure B. The product **36a** was obtained as 54 mg (67%) of a beige solid. ¹H NMR (600 MHz, DMSO-*d*₆) δ: 13.19 (s, 1H, NH), 8.75 (s, 1H, CH_{pyrazole}), 8.10 (s, 1H, =CH), 8.06 (t, $J = 5.0$ Hz, 1H, CH_{arom.}), 7.91 (t, $J = 1.4$ Hz, 1H, CH_{arom.}), 7.67-7.59 (m, 2H, CH_{arom.} / NH), 7.42-7.38 (m, 1H, CH_{arom.}), 7.36 (d, $J = 8.0$ Hz, 1H, CH_{arom.}), 7.26 (ddd, $J = 9.5, 8.2, 1.3$ Hz, 1H, CH_{arom.}), 4.55 (dd, $J = 5.1, 1.6$ Hz, 2H, NHCH₂Ar) ppm. NH₂ not displayed. ¹³C NMR (151 MHz, DMSO-*d*₆) δ: 163.6, 161.6 (d, ¹ $J_{CF} = 249.2$ Hz), 156.8, 138.3, 135.1, 133.9, 133.3, 130.4, 127.8, 125.6 (d, ⁴ $J_{CF} = 3.3$ Hz), 124.1, 122.9, 117.9, 114.7 (d, ² $J_{CF} = 21.9$ Hz), 111.3, 108.7, 103.1, 34.3 (d, ⁴ $J_{CF} = 3.9$ Hz) ppm. HPLC-UV (254 nm) ESI-MS, purity: 96%. LC-MS (m/z): 385.3 [M + H]⁺. Mp.: 188 °C.

Synthesis of 3-amino-*N*-(2-fluorobenzyl)-1-(1*H*-indazol-5-yl)-1*H*-pyrazole-4-carboxamide (36b)

A solution of **35** (30 mg, 0.12 mmol), 2-fluorobenzylamine (23 mg, 0.18 mmol), HBTU (68 mg, 0.18 mmol) and TEA (37 mg, 0.36 mmol) in DMF (1 ml) was reacted according to procedure B. The product **36b** was obtained as 20 mg (48%) of a beige solid. ¹H NMR (600 MHz, DMSO-*d*₆) δ: 13.22 (s, 1H, NH), 8.82 (s, 1H, CH_{pyrazole}), 8.44 (t, $J = 5.7$ Hz, 1H, CH_{arom.}), 8.14 (t, $J = 5.5$ Hz, 1H, CH_{arom.}), 7.94 (s, 1H, =CH), 7.66-7.62 (m, 1H, CH_{arom.}), 7.48 (t, $J = 7.6$ Hz, 1H, CH_{arom.}), 7.43-7.37 (m, 1H, CH_{arom.}), 7.34-7.28 (m, 1H, CH_{arom.}), 7.26-7.20 (m, 1H, CH_{arom.}), 7.20-7.08 (m, 1H, NH), 4.47 (d, $J = 5.7$ Hz, 2H, NHCH₂Ar) ppm. NH₂ not displayed. ¹³C NMR (151 MHz, DMSO-*d*₆) δ: 164.0, 160.4 (d, ¹ $J_{CF} = 245.7$ Hz), 157.1, 130.7 (d, ⁴ $J_{CF} = 4.1$ Hz), 130.4 (d, ³ $J_{CF} = 8.1$ Hz), 129.9, 129.1 (d, ³ $J_{CF} = 7.8$ Hz), 127.8, 126.5 (d, ³ $J_{CF} = 14.8$ Hz), 124.8, 124.5, 117.9, 115.7 (d, ² $J_{CF} = 21.0$ Hz), 115.2 (d, ² $J_{CF} = 21.0$ Hz), 108.7, 103.2, 42.4 (d, ³ $J_{CF} = 3.6$ Hz) ppm. HPLC-UV (254 nm) ESI-MS, purity: 96%. LC-MS (m/z): 351.1 [M + H]⁺. Mp.: 174 °C.

Synthesis of 3-amino-*N*-(2,3-dichlorobenzyl)-1-(1*H*-indazol-5-yl)-1*H*-pyrazole-4-carboxamide (36c)

A solution of **35** (30 mg, 0.12 mmol), 2,3-dichlorobenzylamine (32 mg, 0.18 mmol), HBTU (68 mg, 0.18 mmol) and TEA (37 mg, 0.36 mmol) in DMF (1 ml) was reacted according to procedure B. The product **36c** was obtained as 5 mg (10%) of a beige solid. ¹H NMR (600 MHz, Methanol-*d*₄) δ: 8.72 (s, 1H, CH_{pyrazole}), 8.19 (s, 1H, =CH), 8.12 (d, $J = 2.0$ Hz, 1H, CH_{arom.}),

7.81 (dd, $J = 9.0, 2.1$ Hz, 1H, CH_{arom.}), 7.73 (d, $J = 9.0$ Hz, 1H, CH_{arom.}), 7.51 (dd, $J = 8.0, 1.5$ Hz, 1H, CH_{arom.}), 7.45 (dd, $J = 7.8, 1.5$ Hz, 1H, CH_{arom.}), 7.33 (t, $J = 7.9$ Hz, 1H, CH_{arom.}), 4.71 (s, 2H, NHCH₂Ar) ppm. NH₂ not displayed. ¹³C NMR (151 MHz Methanol-*d*₄) δ : 165.3, 140.9, 140.1, 135.7, 134.9, 134.4, 132.6, 130.7, 130.5, 129.1, 128.8, 124.6, 121.2, 112.8, 112.7, 42.7 ppm. HPLC-UV (254 nm) ESI-MS, purity: 96%. LC-MS (m/z): 401.1 [M + H]⁺. Mp.: 167 °C.

Synthesis of 3-amino-*N*-(2-bromobenzyl)-1-(1*H*-indazol-5-yl)-1*H*-pyrazole-4-carboxamide (36d)

A solution of **35** (30 mg, 0.12 mmol), 2-bromobenzylamine (33 mg, 0.18 mmol), HBTU (68 mg, 0.18 mmol) and TEA (37 mg, 0.36 mmol) in DMF (1 ml) was reacted according to procedure B. The product **36d** was obtained as 40 mg (81%) of a beige solid. ¹H NMR (600 MHz, Methanol-*d*₄) δ : 8.55 (s, 1H, CH_{pyrazole}), 8.15 (s, 1H, =CH), 8.03 (d, $J = 1.9$ Hz, 1H, CH_{arom.}), 7.76 (dd, $J = 9.0, 2.1$ Hz, 1H, CH_{arom.}), 7.68 (d, $J = 9.0$ Hz, 1H, CH_{arom.}), 7.63 (dd, $J = 8.0, 1.2$ Hz, 1H, CH_{arom.}), 7.46 (dd, $J = 7.7, 1.7$ Hz, 1H, CH_{arom.}), 7.39 (td, $J = 7.5, 1.2$ Hz, 1H, CH_{arom.}), 7.26-7.20 (m, 1H, CH_{arom.}), 4.65 (s, 2H, NHCH₂Ar) ppm. NH₂ not displayed. ¹³C NMR (151 MHz, Methanol-*d*₄) δ : 166.8, 159.1, 139.3, 135.7, 135.4, 134.1, 130.4, 130.3, 129.7, 129.1, 124.7, 124.4, 121.1, 112.5, 112.0, 105.6, 104.8, 44.5 ppm. HPLC-UV (254 nm) ESI-MS, purity: 93%. LC-MS (m/z): 411.1 [M + H]⁺. Mp.: 211 °C.

Synthesis of 3-amino-1-(1*H*-indazol-5-yl)-*N*-(2-methoxybenzyl)-1*H*-pyrazole-4-carboxamide (36e)

A solution of **35** (57 mg, 0.23 mmol), 2-methoxybenzylamine (48 mg, 0.35 mmol), HBTU (133 mg, 0.35 mmol) and TEA (133 mg, 0.35 mmol) in DMF (1 ml) was reacted according to procedure B. The product **36e** was obtained as 3.1 mg (4%) of a colorless solid. ¹H NMR (600 MHz, Methanol-*d*₄) δ : 8.79 (s, 1H, CH_{pyrazole}), 8.26 (s, 1H, =CH), 8.13 (d, $J = 2.0$ Hz, 1H, CH_{arom.}), 7.83 (dd, $J = 9.0, 2.0$ Hz, 1H, CH_{arom.}), 7.73 (d, $J = 9.0$ Hz, 1H, CH_{arom.}), 7.35 (dd, $J = 7.5, 1.7$ Hz, 1H, CH_{arom.}), 7.31 (td, $J = 7.9, 1.6$ Hz, 1H, CH_{arom.}), 7.02 (d, $J = 8.1$ Hz, 1H, CH_{arom.}), 6.96 (t, $J = 7.4$ Hz, 1H, CH_{arom.}), 4.60 (s, 2H, NHCH₂Ar), 3.92 (s, 3H, OCH₃) ppm. NH₂ not displayed. ¹³C NMR (151 MHz, Methanol-*d*₄) δ : 159.1, 134.8, 130.6, 130.0, 130.0, 127.7, 121.7, 121.2, 113.1, 113.0, 111.7, 109.4, 56.1, 39.6 ppm. HPLC-UV (254 nm) ESI-MS, purity: 94%. LC-MS (m/z): 363.2 [M + H]⁺. Mp.: 203 °C.

Synthesis of 3-amino-*N*-(2-hydroxybenzyl)-1-(1*H*-indazol-5-yl)-1*H*-pyrazole-4-carboxamide (36f)

A solution of **36e** (43 mg, 0.12 mmol) was reacted according to procedure C. The product **36f** was obtained as 4.2 mg (10%) of a colorless solid. ¹H NMR (600 MHz, Methanol-*d*₄) δ: 8.85 (s, 1H, CH_{pyrazole}), 8.25 (s, 1H, =CH), 8.17 (d, *J* = 2.1 Hz, 1H, CH_{arom.}), 7.85 (dd, *J* = 9.0, 2.1 Hz, 1H, CH_{arom.}), 7.76 (d, *J* = 8.9 Hz, 1H, CH_{arom.}), 7.30 (dd, *J* = 7.4, 1.7 Hz, 1H, CH_{arom.}), 7.16 (td, *J* = 7.8, 1.7 Hz, 1H, CH_{arom.}), 6.85 (t, *J* = 7.6 Hz, 2H, CH_{arom.}), 4.59 (s, 2H, NHCH₂Ar) ppm. NH₂ not displayed. ¹³C NMR (151 MHz, MeOD) δ: 154.6, 147.3, 125.0, 121.7, 121.3, 120.6, 116.3, 111.8, 111.3, 107.2, 103.8, 103.5, 101.4, 30.4 ppm. HPLC-UV (254 nm) ESI-MS, purity: 95%. LC-MS (*m/z*): 349.1 [M + H]⁺. Mp.: 216 °C.

4.3.9.2.7. Synthesis of *N*-protected 3-aminopyrazoles and subsequent cross coupling

Synthesis of ethyl 3-amino-1*H*-pyrazole-4-carboxylate (**37**)⁴

A solution of hydrazine hydrate (473 mg, 8.3 mmol) and ethyl(ethoxymethylene)cyanoacetate (EEMA) (2000 mg, 11.83 mmol) in EtOH (20 ml) was stirred at rt for 6 h. Subsequently, the solvent was removed under reduced pressure and the residue was purified by column chromatography (pure ethyl acetate). The product **37** was obtained as 590 mg (32%) of a yellow solid. ¹H NMR (600 MHz, Chloroform-*d*) δ: 7.70 (s, 1H, CH_{pyrazole}), 6.64 (s, 2H, NH₂), 4.25 (q, *J* = 7.1 Hz, 2H, CH₂CH₃), 1.31 (t, *J* = 7.1 Hz, 3H, CH₂CH₃). ¹³C NMR (151 MHz, Chloroform-*d*) δ: 164.4 (ester), 153.7 (C₃), 136.0 (C₅), 97.8 (C₄), 59.8 (CH₂CH₃), 14.4 (CH₂CH₃). LC-MS (*m/z*): 115.8 [M + H]⁺. Mp.: 102 °C.

Synthesis of ethyl 3-acetamido-1*H*-pyrazole-4-carboxylate (**38a**)¹²

A solution of **37** (240 mg, 1.54 mmol) and Ac₂O (631 mg, 6.2 mmol) in AcOH (1 ml) was stirred at 100 °C for 16 h. Subsequently, the mixture was treated with saturated NaHCO₃ solution and extracted with CH₂Cl₂ (3 x 20 ml), the combined organic layers were dried over MgSO₄, filtered and the solvent was evaporated under reduced pressure. The crude product was dissolved in 1 ml of ethyl acetate and then treated with 30 ml of *n*-heptane to crystallize the product. The crude product was dissolved in MeOH and left for 24 h. This led to a cleavage of undesired acetyl groups. The product was obtained as 139 mg (46%) of a beige solid. ¹H NMR (600 MHz, Chloroform-*d*) δ: 9.57 (s, 1H, NHAc), 7.77 (s, 1H, CH_{pyrazole}), 4.30 (q, *J* = 7.1 Hz, 2H, CH₂CH₃), 2.26 (s, 3H, COCH₃), 1.35 (t, *J* = 7.1 Hz, 3H, CH₂CH₃) ppm. ¹³C NMR (151 MHz, Chloroform-*d*) δ: 169.3, 164.6, 143.0, 138.9, 98.0, 60.5, 23.7, 14.3 ppm. HPLC-UV (254 nm) ESI-MS, purity: 94%. LC-MS (*m/z*): 179.8 [M + H]⁺. Mp.: 109 °C.

Synthesis of ethyl 3-((tert-butoxycarbonyl)amino)-1H-pyrazole-4-carboxylate (**38b**)

A solution of **37** (200 mg, 1.29 mmol) and Boc₂O (562 mg, 2.58 mmol) in CH₂Cl₂ (3 ml) was stirred over night at rt. Subsequently, the solvent was removed under reduced pressure and the residue was purified via column chromatography (CH₂Cl₂ / MeOH - 98 : 2). The product **38b** was obtained as 40 mg (12%) of a colorless solid. HPLC-UV (254 nm) ESI-MS, purity: 93%. LC-MS (m/z): 255.8 [M + H]⁺.

Synthesis of 3-(1,3-dioxisoindolin-2-yl)-1H-pyrazole-4-carboxylic acid (**38c**)¹⁷

A stirred solution of **38c** (1.42 g, 9.17 mmol), phthalic anhydride (1.36 g, 9.17 mmol) and AcOH (1.5 ml) in toluol (5 ml) was heated at 100 °C for 5 h. Subsequently, the solvent was removed under reduced pressure and the residue was purified by column chromatography (CH₂Cl₂ / MeOH - 95 : 5). The product **38c** was obtained as 1.41 g (51%) of a colorless solid. ¹H NMR (600 MHz, Chloroform-*d*) δ: 8.16 (s, 1H, CH_{pyrazole}), 7.95 (dd, *J* = 5.5, 3.0 Hz, 2H, CH_{arom.}), 7.82-7.74 (*J* = 5.5, 3.0 Hz, 2H, CH_{arom.}), 4.13 (q, *J* = 7.1 Hz, 2H, CH₂CH₃), 1.07 (t, *J* = 7.1 Hz, 3H, CH₂CH₃) ppm. ¹³C NMR (151 MHz, Chloroform-*d*) δ: 166.8, 161.4, 140.6, 134.6, 134.4, 132.0, 132.0, 124.0, 110.7, 60.5, 13.9 ppm. HPLC-UV (254 nm) ESI-MS, purity: 95%. LC-MS (m/z): 286.3 [M + H]⁺.

Syntheses of 1H-acetyl-3-bromopyrazole (**49a**)

A solution of 3-bromo-1H-pyrazole (500 mg, 3.4 mmol), Ac₂O (416 mg, 4.08 mmol), TEA (516 mg, 5.1 mmol) and DMAP (42 mg, 0.34 mmol) in CH₂Cl₂ (4 ml) was stirred at rt for 18 h. Subsequently, the mixture was treated with water and extracted with CH₂Cl₂ (3 x 20 ml), the combined organic layers were dried over MgSO₄, filtered and the solvent was evaporated under reduced pressure. The product **49a** was obtained as 539 mg (84%) of a colorless solid. Mass was found in ASAP-MS: 190 [M + H]⁺. ¹H NMR (600 MHz, Chloroform-*d*) δ: 8.13 (d, *J* = 2.8 Hz, 1H, CH_{arom.}), 6.45 (d, *J* = 2.8 Hz, 1H, CH_{arom.}), 2.67 (s, 3H, CH₃) ppm. ¹³C NMR (151 MHz, Chloroform-*d*) δ: 168.4, 132.1, 129.7, 113.1, 21.5 ppm.

Synthesis of 1H-(tert-butoxycarbonyl)-3-bromopyrazol (**49b**)

A mixture of 3-bromo-1H-pyrazole (5 g, 34.2 mmol), Boc₂O (8.96 g, 41.1 mmol), TEA (5.18 g, 51.3 mmol) and DMAP (catalytic amount) in CH₂Cl₂ (50 ml) was stirred at rt for 16 h. Subsequently, the mixture was treated with diluted HCl and extracted. The organic phase was furthermore washed with water and saturated NaCl solution, dried over MgSO₄, filtered and the solvent was evaporated under reduced pressure. The product **49b** was obtained as 7.41 g (88%) of yellow oil that eventually crystallized. ¹H NMR (600 MHz, Chloroform-*d*) δ: 7.96 (d, *J* = 2.8 Hz, 1H, C₅ pyrazole), 6.39 (d, *J* = 2.8 Hz, 1H, C₄ pyrazole), 1.62 (s, 9H, C(CH₃)₃) ppm. HPLC-UV (254 nm) ESI-MS, purity: 98%. LC-MS (m/z): 246.7 [M + H]⁺.

Synthesis of 3-amino-1-(3,4-dimethoxyphenyl)-1*H*-pyrazole-4-carboxylic acid (**46**)¹³

A solution of **37** (500 mg, 3.23 mmol), (3,4-dimethoxyphenyl)boronic acid (1174 mg, 6.45 mmol) Cu(AcO)₂ (876 mg, 4.85 mmol) and pyridine (1020 mg, 12.9 mmol) in CH₂Cl₂ (5 ml) was stirred for 2 days in an open flask. Subsequently, the mixture was directly purified via column chromatography (CH₂Cl₂ / MeOH - 95 : 5). The crude, still impure product **45** (approximately 160 mg) was directly saponificated by treating the material with LiOH monohydrate (16 mg, 2.7 mmol) in THF / H₂O (1 : 1) and stirring this mixture at 80 °C for 3 h. The mixture was neutralized and purified via column chromatography (CH₂Cl₂ / MeOH - 9 : 1). The product **46** was obtained as 50 mg (6% based on **37**) of a beige solid. HPLC-UV (254 nm) ESI-MS, purity: 89%. LC-MS (m/z): 264.0 [M + H]⁺.

Synthesis of 3-amino-*N*-(2-chloro-6-fluorobenzyl)-1-(3,4-dimethoxyphenyl)-1*H*-pyrazole-4-carboxamide (**47**)

A solution of **46** (50 mg, 0.19 mmol), 2-chloro-6-fluorobenzylamine (45 mg, 0.28 mmol), HBTU (106 mg, 0.28 mmol) and TEA (58 mg, 0.57 mmol) in DMF (2 ml) was reacted according to procedure B. The product **47** was obtained as 64 mg (83%) of a colorless solid. ¹H NMR (600 MHz, Chloroform-*d*) δ: 7.83 (s, 1H, CH_{pyrazole}), 7.23 - 7.18 (m, 2H, CH_{arom.}), 7.17 (d, *J* = 2.5 Hz, 1H, CH_{arom.}), 7.04 - 7.00 (m, 1H, CH_{arom.}), 6.99 (dd, *J* = 8.6, 2.6 Hz, 1H, CH_{arom.}), 6.83 (d, *J* = 8.7 Hz, 1H, CH_{arom.}), 6.20 - 6.07 (m, 1H, NH), 4.76 (dd, *J* = 5.7, 1.6 Hz, 2H, NHCH₂Ar), 3.91 (s, 3H, OCH₃), 3.87 (s, 3H, OCH₃) ppm. NH₂ not displayed. ¹³C NMR (151 MHz, Chloroform-*d*) δ: 163.4, 161.6 (d, ¹*J*_{CF} = 250.1 Hz), 156.2, 149.6, 147.6, 135.5 (d, ³*J*_{CF} = 5.5 Hz), 133., 129.7 (d, ³*J*_{CF} = 9.5 Hz), 125.9, 125.5 (d, ⁴*J*_{CF} = 3.4 Hz), 123.9 (d, ²*J*_{CF} = 17.9 Hz), 114.5 (d, ²*J*_{CF} = 22.4 Hz), 111.2, 110.3, 103.9, 103.7, 56.1 (d, ³*J*_{CF} = 5.5 Hz), 34.5 ppm. HPLC-UV (254 nm) ESI-MS, purity: 97%. LC-MS (m/z): 405.3 [M + H]⁺.

Synthesis of 3-amino-*N*-(2-chloro-6-fluorobenzyl)-1-(3,4-dihydroxyphenyl)-1*H*-pyrazole-4-carboxamide (**48**)

A solution of **47** (64 mg, 0.16 mmol) was reacted according to procedure C. The product **48** was obtained as 37 mg (66%) of a brownish solid. ¹H NMR (600 MHz, DMSO-*d*₆) δ: 9.21 (s, 1H, OH), 8.99 (s, 1H, OH), 8.51 (s, 1H, CH_{pyrazole}), 7.99 (t, *J* = 5.0 Hz, 1H, NH), 7.42 - 7.37 (m, 1H, CH_{arom.}), 7.34 (d, *J* = 8.1 Hz, 1H, CH_{arom.}), 7.24 (t, *J* = 8.8 Hz, 1H, CH_{arom.}), 7.01 (d, *J* = 2.5 Hz, 1H, CH_{arom.}), 6.80 (dd, *J* = 8.5, 2.6 Hz, 1H, CH_{arom.}), 6.74 (d, *J* = 8.6 Hz, 1H, CH_{arom.}), 5.58 (s, 2H, NH₂), 4.52 (d, *J* = 4.4 Hz, 2H, NHCH₂Ar). ¹³C NMR (151 MHz, DMSO-*d*₆) δ: 163.7, 161.6 (d, ¹*J*_{CF} = 249.0 Hz), 156.9, 145.9, 143.7, 135.1 (d, ³*J*_{CF} = 5.6 Hz), 132.1, 130.3 (d, ³*J*_{CF} = 9.7 Hz), 126.9, 125.6 (d, ⁴*J*_{CF} = 3.3 Hz), 124.2 (d, ²*J*_{CF} = 17.6 Hz), 115.9, 114.7 (d, ²*J*_{CF} = 22.1 Hz), 108.4, 106.3, 102.4, 34.3 (d, ⁴*J*_{CF} = 3.9 Hz). HPLC-UV (254 nm) ESI-MS, purity: 96%. LC-MS (m/z): 377.1 [M + H]⁺. Mp.: 231 °C.

Synthesis of (*E*)-5-(2-benzylidenehydrazinyl)-1*H*-pyrazole (**53**)¹⁹

A mixture of 3-amino-1*H*-pyrazole (3 g, 36.15 mmol) and BF₃ - etherate (10.2 g, 72.3 mmol) in dry THF (50 ml) was treated with *tert.* butylnitrit (7.44 g, 72.3 mmol) at 0 °C and stirred for 2 h. Subsequently, the mixture was treated with diethyl ether and the resulting solid was collected with filtration under reduced pressure. The intermediate **52** was obtained as 6.29 g (95%) of a beige solid. ¹H NMR (500 MHz, DMSO-*d*₆) δ: 8.40 (d, *J* = 2.8 Hz, 1H), 7.78 (d, *J* = 2.8 Hz, 1H).

The intermediate diazonium salt (6.91 g, 37.9 mmol) was given to a solution of SnCl₂ (14.35g, 76 mmol) in conc. HCl (15 ml) at 0 °C and this mixture was stirred for 2 h at rt. The resulting solid was collected by filtration under reduced pressure. Since only a very small amount of solid could be isolated, the filtrate was neutralized with NaOH pellets and the resulting mixture of Sn-salts and product was isolated with filtration. This mixture was suspended in H₂O / EtOH (250 ml) and treated with NaHCO₃ until a pH value of approximately 9 was reached, then benzaldehyde (4.98 g, 47 mmol) was given to the mixture. After 2 h of stirring, the mixture was treated with ethyl acetate and the aqueous phase was extracted with ethyl acetate (3 x 50 ml). The combined organic layers were dried over MgSO₄, filtered and the solvent was evaporated under reduced pressure. The residue was purified via column chromatography (CH₂Cl₂/MeOH - 9:1). The product **53** was obtained as 4.77 g (71%) of a brownish solid. ¹H NMR (500 MHz, DMSO-*d*₆) δ: 11.98 (s, 1H, NH), 10.24 (s, 1H, CH=), 7.86 (s, 1H, CH_{arom.}), 7.60 - 7.54 (m, 2H, CH_{arom.}), 7.48 (d, *J* = 2.0 Hz, 1H, CH_{arom.}), 7.34 (td, *J* = 7.7, 1.4 Hz, 2H, CH_{arom.}), 7.28 - 7.22 (m, 1H, CH_{arom.}), 5.99 - 5.78 (m, 1H, NH) ppm. HPLC-UV (254 nm) ESI-MS, purity: 91%. LC-MS (m/z): 186.8 [M + H]⁺.

Synthesis of ethyl(ethoxymethylene)-4-methyl-cyanoacetate (**55**)²⁰

A mixture of ethyl cyanoacetate (3.48 g, 0.03 mol), triethylorthoacetate (5 g, 0.03 mol) and Ac₂O (10 ml) were refluxed for 24 h. Subsequently, the mixture was cooled to rt and treated with heptane. The resulting precipitate was filtered under reduced pressure and washed with heptane. The product **55** was obtained as 1.1 g (23 %) of a white solid. ¹H NMR (600 MHz, Chloroform-*d*) δ: 4.25 (q, *J* = 7.0 Hz, 2H, CH₂), 4.20 (q, *J* = 7.1 Hz, 2H, CH₂), 2.58 (s, 3H, CH₃), 1.41 (t, *J* = 7.0 Hz, 3H, CH₃), 1.29 (t, *J* = 7.1 Hz, 3H, CH₃) ppm. ¹³C NMR (151 MHz, CDCl₃) δ: 183.8, 115.1, 85.8, 65.9, 15.6, 14.8, 14.2 ppm. ASAP (m/z): 184 [M + H]⁺.

Synthesis of ethyl-3-amino-1-(3-methoxyphenyl)-5-methyl-1*H*-pyrazole-4-carboxylate (**57**)⁵

A mixture of **11** (309 g, 1.37 mmol) and **55** (250 mg g, 1.37 mmol) in xylol (2 ml) was stirred at 160°C for 3 d in a sealed tube. The intermediate could be detected via TLC-MS (MW = 363). The crude mixture was treated with EtOH / conc. HCl (2 : 1, 10 ml) and refluxed for 5 h. The

reaction mixture was neutralized with NaOH solution and extracted with ethyl acetate (3 x 30 ml). The crude product was 350 mg of a brown solid. LC-MS (m/z): 276.0 [M + H]⁺.

Synthesis of 3-amino-1-(3-methoxyphenyl)-5-methyl-1H-pyrazole-4-carboxylic acid (58)

The impure **57** was stirred with 274 mg (6,85 mmol) of LiOH monohydrate in THF / H₂O (1:1, 20 ml) at 80 for 5 h. Subsequently, the reaction mixture was cooled to rt and then extracted with ethyl acetate. The aqueous solution was acidified to pH 2 with acetic acid and the precipitated product was collected with filtration. The crude product was purified via flash RP-HPLC (water / MeOH - 10 to 100%). The product **58** was obtained as 30,3 mg (9%, based on **11**). ¹H NMR (500 MHz, DMSO-*d*₆) δ: 7.48 (td, *J* = 7.6, 1.2 Hz, 1H, CH_{arom.}), 7.38 (dd, *J* = 8.4, 7.3 Hz, 1H, CH_{arom.}), 7.04 - 6.99 (m, 1H, CH_{arom.}), 6.98 - 6.92 (m, 1H, CH_{arom.}), 3.78 (d, *J* = 1.1 Hz, 3H, CH₃), 2.43 (d, *J* = 1.1 Hz, 3H, OCH₃) ppm. NH₂ not displayed. ¹³C NMR (126 MHz, DMSO) δ: 166.2, 159.8, 156.9, 142.8, 140.1, 128.7, 117.2, 113.6, 110.8, 55.6, 12.8 ppm. HPLC-UV (254 nm) ESI-MS, purity: 87%. LC-MS (m/z): 247.9 [M + H]⁺.

Synthesis of 3-amino-N-(2-chloro-6-fluorobenzyl)-1-(3-methoxyphenyl)-5-methyl-1H-pyrazole-4-carboxamide (59)

A solution of **58** (30 mg, 0.12 mmol), 2-chloro-6-fluorobenzylamine (28 mg, 0.18 mmol), HBTU (68 mg, 0.18 mmol) and TEA (36 mg, 0.36 mmol) in DMF (1 ml) was reacted according to procedure B. The product **59** was obtained as 13 mg (28%) of a brownish solid. ¹H NMR (600 MHz, Chloroform-*d*) δ: 7.31 (t, *J* = 8.4 Hz, 1H, CH_{arom.}), 7.23 - 7.18 (m, 2H, CH_{arom.}), 7.02 (ddd, *J* = 9.3, 7.3, 2.1 Hz, 1H, CH_{arom.}), 6.92 - 6.86 (m, 3H, CH_{arom.}), 6.62 (t, *J* = 5.9 Hz, 1H, NH), 4.76 (dd, *J* = 5.7, 1.5 Hz, 2H, NHCH₂Ar), 3.80 (s, 3H, CH₃), 2.46 (s, 3H, CH₃) ppm. NH₂ not displayed. ¹³C NMR (151 MHz, Chloroform-*d*) δ: 164.1, 161.5 (d, ¹*J*_{CF} = 250.7 Hz), 160.1, 154.1, 140.4, 139.4, 135.3 (d, ³*J*_{CF} = 5.4 Hz), 129.8, 129.6 (d, ³*J*_{CF} = 9.9 Hz), 125.5 (d, ⁴*J*_{CF} = 3.6 Hz), 124.3, 117.5, 114.5 (d, ²*J*_{CF} = 22.5 Hz), 114.2, 111.1, 103.2, 55.5, 34.4 (d, ⁴*J*_{CF} = 4.1 Hz), 12.7 ppm. HPLC-UV (254 nm) ESI-MS, purity: 95%. LC-MS (m/z): 389.3 [M + H]⁺. Mp.: 180°C.

Synthesis of 3-amino-N-(2-chloro-6-fluorobenzyl)-1-(3-hydroxyphenyl)-5-methyl-1H-pyrazole-4-carboxamide (60)

A solution of **59** (10 mg, 0.05 mmol) was reacted according to procedure C. The product **60** was obtained as 8.7 mg (89%) of a brownish solid. ¹H NMR (600 MHz, Methanol-*d*₄) δ: 7.40 - 7.32 (m, 3H, CH_{arom.}), 7.17 (ddd, *J* = 9.6, 8.2, 1.3 Hz, 1H, CH_{arom.}), 6.94 - 6.87 (m, 2H, CH_{arom.}), 6.86 (t, *J* = 2.2 Hz, 1H, CH_{arom.}), 4.77 (d, *J* = 1.4 Hz, 2H, NHCH₂Ar), 2.41 (s, 3H, CH₃). NH₂ not displayed. ¹³C NMR (151 MHz, Methanol-*d*₄) δ: 166.4, 163.4 (d, ¹*J*_{CF} = 249.1 Hz), 159.8, 154.3, 142.9, 140.6, 136.9 (d, ³*J*_{CF} = 5.3 Hz), 131.5, 126.9, 125.4 (d, ²*J*_{CF} = 17.5 Hz), 117.9, 117.1,

115.7 (d, $^2J_{CF} = 23.5$ Hz), 114.2, 111.1, 105.2, 36.0 (d, $^4J_{CF} = 4.2$ Hz), 12.8 ppm. HPLC-UV (254 nm) ESI-MS, purity: 94%. LC-MS (m/z): 375.1 [M + H]⁺. Mp.: 193 °C.

Synthesis of 1-(2-hydroxypropyl)-1H-indazole-5-carbaldehyde (70a)

A solution of 1H-indazole-5-carbaldehyde (2000 mg, 13.7 mmol), 1-chloro-2-propanol (1562 mg, 16.4 mol) and K₂CO₃ (2263 mg, 16.4 mmol) in DMF (5 ml) was stirred at 100 °C for 3 d. Subsequently, the mixture was treated with water and extracted with CH₂Cl₂ (3 x 20 ml), the combined organic layers were dried over MgSO₄, filtered off and evaporated under reduced pressure. The crude mixture was purified via column chromatography product was purified via column chromatography (CH₂Cl₂ / MeOH - 95 : 5). The product **70a** was obtained as 160 mg of a yellow oil. ¹H NMR (600 MHz, Chloroform-*d*) δ: 9.99 (s, 1H, CHO), 8.23-8.20 (m, 1H, CH_{arom.}), 8.15 (d, $J = 1.0$ Hz, 1H, CH_{arom.}), 7.91 (dd, $J = 8.8, 1.5$ Hz, 1H, CH_{arom.}), 7.51 (d, $J = 8.8$ Hz, 1H, CH_{arom.}), 4.39 (dd, $J = 13.7, 2.8$ Hz, 1H, CH₂), 4.33 (ddd, $J = 7.8, 6.2, 2.9$ Hz, 1H, CH_{OH}), 4.27 (dd, $J = 13.7, 7.7$ Hz, 1H, CH₂), 1.26 (d, $J = 6.3$ Hz, 3H, CH₃). ¹³C NMR (151 MHz, Chloroform-*d*) δ: 191.4 (CHO), 142.5 (C_{arom.}), 135.6 (C_{arom.}), 130.6 (C_{arom.}), 127.6 (C_{arom.}), 125.5 (C_{arom.}), 123.4 (C_{arom.}), 110.1 (C_{arom.}), 67.2 (CHOH), 55.6 (CH₂), 20.5 (CH₃). HPLC-UV (254 nm) ESI-MS, purity: 73%. LC-MS (m/z): 204.7 [M + H]⁺.

Synthesis of 5-fluoro-6-methylpyridine-2,3-diamine (72)⁴³

A mixture of 2-amino-5-fluoro-6-methylpyridine (1.26 g, 10 mmol) in conc H₂SO₄ (25 ml) was treated with fuming HNO₃ (0.6 ml) at 0 °C. The reaction mixture was heated up to 50 °C and stirred for 3 h. Subsequently, the mixture was poured into ice (150 g) neutralized with aqueous ammonia solution (25%) and extracted with ethyl acetate (3 x 50 ml), the combined organic layers were dried over MgSO₄, filtered and evaporated under reduced pressure. The product **71** was obtained as 860 mg (50%) of a brown solid. ¹H NMR (600 MHz, Chloroform-*d*) δ: 8.07 (d, $J = 8.4$ Hz, 1H, CH_{arom.}), 6.61 (s, 2H, NH₂), 2.44 (d, $J = 2.8$ Hz, 3H, CH₃).

A mixture of **71** (860 mg, 5.03 mmol) and SnCl₂ • 2 H₂O (3395 mg, 15 mmol) in EtOH (20 ml) was stirred at 80 °C for 5 h. Subsequently, the mixture was treated with 2N NaOH solution and extracted with CH₂Cl₂ (3 x 50 ml), the combined organic layers were dried over MgSO₄, filtered and evaporated under reduced pressure. The crude product was purified via column chromatography using pure ethyl acetate, yielding **72** as 860 mg (50%) of a brown solid. ¹H NMR (600 MHz, Chloroform-*d*) δ: 6.65 (d, $J = 9.6$ Hz, 1H, CH_{arom.}), 4.15 (s, 2H, NH₂), 3.35 (s, 2H, NH₂), 2.26 (d, $J = 2.9$ Hz, 3H, CH₃). HPLC-UV (254 nm) ESI-MS, purity: 95%. LC-MS (m/z): 141.8 [M + H]⁺.

Synthesis of 1-(5-(6-fluoro-5-methyl-3H-imidazo[4,5-b]pyridin-2-yl)-1H-indazol-1-yl)propan-2-ol (**69**)⁴³

A solution of **70a** (160 mg, 0.78 mmol) and **72** (100 mg, 0.71 mmol) in dioxane / AcOH (1 : 1, 2 ml) was stirred at 95 °C for 4 h. Subsequently, the solvent was removed under reduced pressure and the residue was purified by column chromatography (pure ethyl acetate). The crude product was further purified via flash RP-HPLC (10 to 100% MeOH). The product **69** was obtained as 77 mg (33%) of a colorless solid. ¹H NMR (600 MHz, DMSO-*d*₆) δ: 13.45 (s, 1H, NH), 8.62-8.55 (m, 1H, CH_{arom.}), 8.27-8.16 (m, 2H, CH_{arom.}), 7.90-7.79 (m, 2H, CH_{arom.}), 4.89 (m, *J* = 5.2, 2.8 Hz, 1H, OH), 4.39-4.29 (m, 2H, CH₂), 4.14-4.05 (m, 1H, CH_{OH}), 2.52 (d, *J* = 3.3 Hz, 3H, CH₃), 1.09 (d, *J* = 6.4 Hz, 3H, CH₃). ¹³C NMR (126 MHz, DMSO-*d*₆) δ: 155.3, 154.4, 153.4, 140.8, 139.7 (d, ²*J*_{CF} = 20.4 Hz), 133.9, 124.6, 123.6, 122.2, 119.7, 111.1, 65.9, 56.0, 21.1, 18.2. HPLC-UV (254 nm) ESI-MS, purity: 96%. LC-MS (m/z): 326.0 [M + H]⁺.

4.3.10. References

- (1) Sun, B.; Bachhawat, P.; Chu, M. L.-H.; Wood, M.; Ceska, T.; Sands, Z. A.; Mercier, J.; Lebon, F.; Kobilka, T. S.; Kobilka, B. K. Crystal structure of the adenosine A_{2A} receptor bound to an antagonist reveals a potential allosteric pocket. *P. Natl. Acad. Sci. U.S.A.* **2017**, *114*, 2066-2071.
- (2) Lebon, G.; Warne, T.; Edwards, P. C.; Bennett, K.; Langmead, C. J.; Leslie, A. G. W.; Tate, C. G. Agonist-bound adenosine A_{2A} receptor structures reveal common features of GPCR activation. *Nature.* **2011**, *474*, 521-525.
- (3) Jaiteh, M.; Zeifman, A.; Saarinen, M.; Svenningsson, P.; Brea, J.; Loza, M. I.; Carlsson, J. Docking screens for dual inhibitors of disparate drug targets for Parkinson's Disease. *J. Med. Chem.* **2018**, *61*, 5269-5278.
- (4) Deprez-Poulain, R.; Cousaert, N.; Toto, P.; Willand, N.; Deprez, B. Application of Ullmann and Ullmann-Finkelstein reactions for the synthesis of *N*-aryl-*N*-(1*H*-pyrazol-3-yl) acetamide or *N*-(1-aryl-1*H*-pyrazol-3-yl) acetamide derivatives and pharmacological evaluation. *Eur. J. Med. Chem.* **2011**, *46*, 3867-3876.
- (5) Fandrick, D. R.; Sanyal, S.; Kaloko, J.; Mulder, J. A.; Wang, Y.; Wu, L.; Lee, H.; Roschangar, F.; Hoffmann, M.; Senanayake, C. H. A Michael equilibration model to control site selectivity in the condensation toward aminopyrazoles. *Org. Lett.* **2015**, *17*, 2964-2967.
- (6) Christian Breuer. Synthesis and structure-activity relationships of triazole derivatives with a dual mode of action as potential novel therapeutics for Parkinson's disease, Master Thesis, Bonn, 2011.

- (7) Jia, H.; Yu, J.; Du, X.; Cherukupalli, S.; Zhan, P.; Liu, X. Design, diversity-oriented synthesis and biological evaluation of novel heterocycle derivatives as non-nucleoside HBV capsid protein inhibitors. *Eur. J. Med. Chem.* **2020**, *202*, 112495.
- (8) Jefson, Martin, R.; Lowe, John, A.; Dey, F.; Bergmann, A.; Schoop, A.; Fuller, Nathan: „HETERO-HALO INHIBITORS OF HISTONE DEACETYLASE”, WO 2017/007756 A1, 2016.
- (9) Evano, G.; Blanchard, N.; Toumi, M. Copper-mediated coupling reactions and their applications in natural products and designed biomolecules synthesis. *Chem. Rev.* **2008**, *108*, 3054-3131.
- (10) Sung, S.; Braddock, D. C.; Armstrong, A.; Brennan, C.; Sale, D.; White, A. J. P.; Davies, R. P. Synthesis, characterization and reactivity of copper(I) amide complexes and studies on their role in the modified Ullmann amination reaction. *Chem. Eur. J.* **2015**, *21*, 7179-7192.
- (11) Sperotto, E.; van Klink, G. P. M.; van Koten, G.; Vries, J. G. de. The mechanism of the modified Ullmann reaction. *Dalton Trans.* **2010**, *39*, 10338-10351.
- (12) Kusakiewicz, D. The synthesis, structure and properties of *N*-acetylated derivatives of ethyl 3-amino-1*H*-pyrazole-4-carboxylate. *Chem. Pharm. Bull.* **2007**, *55*, 747-752.
- (13) Lam, P.; Clark, C.; Saubern, S.; Adams, J.; Michael P Winters, Dominic M.T, Chan, A.C. New aryl/heteroaryl C-N bond cross-coupling reactions via arylboronic acid/cupric acetate arylation. *Tetrahedron Lett.* **1998**, *39*, 2941-2944.
- (14) Lai, Q.; Liu, Q.; He, Y.; Zhao, K.; Wei, C.; Wojtas, L.; Shi, X.; Song, Z. Triazole-imidazole (TA-IM) derivatives as ultrafast fluorescent probes for selective Ag⁺ detection. *Org. Biomol. Chem.* **2018**, *16*, 7801-7805.
- (15) Johnson, S. M.; Petrassi, H. M.; Palaninathan, S. K.; Mohamedmohaideen, N. N.; Purkey, H. E.; Nichols, C.; Chiang, K. P.; Walkup, T.; Sacchettini, J. C.; Sharpless, K. B.; Kelly, J. W. Bisaryloxime ethers as potent inhibitors of transthyretin amyloid fibril formation. *J. Med. Chem.* **2005**, *48*, 1576-1587.
- (16) Wang, X.; Chen, Y.-F.; Yan, W.; Cao, L.-L.; Ye, Y.-H. Synthesis and biological evaluation of benzimidazole phenylhydrazone derivatives as antifungal agents against phytopathogenic fungi. *Molecules.* **2016**, *21*.
- (17) Nasr, E. E.; Mostafa, A. S.; El-Sayed, M. A. A.; Massoud, M. A. M. Design, synthesis, and docking study of new quinoline derivatives as antitumor agents. *Arch. Pharm.* **2019**, *352*, 1800355.
- (18) Graaff, C. de; Bensch, L.; Boersma, S. J.; Cioc, R. C.; van Lint, M. J.; Janssen, E.; Turner, N. J.; Orru, R. V. A.; Ruijter, E. Asymmetric synthesis of tetracyclic pyrroloindolines and

constrained tryptamines by a switchable cascade reaction. *Angew. Chem. Int. Edit.* **2015**, *54*, 14133-14136.

(19) Abrams, J. N.; Chi, B. K. Gold(I)-catalyzed cross-coupling reactions of arenediazonium salts with alkynoic acids. *Russ. J. Org. Chem.* **2020**, *56*, 1236-1244.

(20) C.Sundarla; G. L. Atmaram; Khairatkar-Joshi N.; Kumar S.; Mukhopadhyay I.; S. D. Manish. Substituted bicyclic heterocyclic compounds as NADPH oxidase inhibitors, WO 002018203298A1, 2018.

(21) Jin, B.; Dong, Q.; Hung, Gene. Preparation of oxoisoquinoliny pyrazolecarboxamides as PI3 kinase inhibitors and uses thereof. WO 2019028395, 2019.

(22) Li, P.; Zheng, H.; Zhao, J.; Wennogle, Lawrence P., Preparation of imidazopyrazolopyrimidinones as PDE1 inhibitors useful in therapy. WO 2016022893 A1, 2016.

(23) Chen, X.; Gao, Y.; Kong, Norman Xianglong. Preparation of alkynyl-substituted heterocyclic compounds as FGFR inhibitors. US 20190210997, 2019.

(24) Mahesh Kumar, P.; Siva Kumar, K.; Meda, C. L. T.; Rajeshwar Reddy, G.; Mohakhud, P. K.; Mukkanti, K.; Rama Krishna, G.; Malla Reddy, C.; Rambabu, D.; Shiva Kumar, K.; Krishna Priya, K.; Chennubhotla, K. S.; Banote, R. K.; Kulkarni, P.; Parsa, K. V. L.; Pal, M. (Pd/C-mediated) coupling-iodocyclization-coupling strategy in discovery of novel PDE4 inhibitors: a new synthesis of pyrazolopyrimidines. *Med. Chem. Commun.* **2012**, *3*, 667.

(25) McDonald, A.; Qian, Shawn, Preparation of heterocyclic compounds for inhibiting plasma kallikrein, WO2018011628A1, 2017.

(26) Klotz, K. N.; Lohse, M. J.; Schwabe, U.; Cristalli, G.; Vittori, S.; Grifantini, M. 2-Chloro-N6-[³H]cyclopentyladenosine (3HCCPA) - a high affinity agonist radioligand for A₁ adenosine receptors. *N-S Arch. Pharmacol.* **1989**, *340*, 679-683.

(27) Müller, C. E.; Maurinsh, J.; Sauer, R. Binding of ³HMSX-2 (3-(3-hydroxypropyl)-7-methyl-8-(*m*-methoxystyryl)-1-propargylxanthine) to rat striatal membranes - a new, selective antagonist radioligand for A_{2A} adenosine receptors. *Eur. J. Pharm. Sci.* **2000**, *10*, 259-265.

(28) Borrmann, T.; Hinz, S.; Bertarelli, D. C. G.; Li, W.; Florin, N. C.; Scheiff, A. B.; Müller, C. E. 1-alkyl-8-(piperazine-1-sulfonyl)phenylxanthines: development and characterization of adenosine A_{2B} receptor antagonists and a new radioligand with subnanomolar affinity and subtype specificity. *J. Med. Chem.* **2009**, *52*, 3994-4006.

(29) Müller, C. E.; Diekmann, M.; Thorand, M.; Ozola, V. [³H]8-Ethyl-4-methyl-2-phenyl-(8*R*)-4,5,7,8-tetrahydro-1*H*-imidazo[2,1-*l*]-purin-5-one ([³H]PSB-11), a novel high-affinity antagonist radioligand for human A₃ adenosine receptors. *Bioorg. Med. Chem. Lett.* **2002**, *12*, 501-503.

- (30) Alnouri, M. W.; Jepards, S.; Casari, A.; Schiedel, A. C.; Hinz, S.; Müller, C. E. Selectivity is species-dependent: Characterization of standard agonists and antagonists at human, rat, and mouse adenosine receptors. *Purinerg. Signal.* **2015**, *11*, 389-407.
- (31) Klotz, K. N.; Hessling, J.; Hegler, J.; Owman, C.; Kull, B.; Fredholm, B. B.; Lohse, M. J. Comparative pharmacology of human adenosine receptor subtypes - characterization of stably transfected receptors in CHO cells. *Naunyn-Schmiedeberg's Arch. Pharmacol.* **1998**, *357*, 1-9.
- (32) Weyler, S.; Fülle, F.; Diekmann, M.; Schumacher, B.; Hinz, S.; Klotz, K.-N.; Müller, C. E. Improving potency, selectivity, and water solubility of adenosine A₁ receptor antagonists: xanthines modified at position 3 and related pyrimido1,2,3-cdpurinediones. *ChemMedChem.* **2006**, *1*, 891-902.
- (33) Drabczyńska, A.; Müller, C. E.; Karolak-Wojciechowska, J.; Schumacher, B.; Schiedel, A.; Yuzlenko, O.; Kieć-Kononowicz, K. N9-benzyl-substituted 1,3-dimethyl- and 1,3-dipropyl-pyrimido[2,1-f]purinediones: synthesis and structure-activity relationships at adenosine A₁ and A_{2A} receptors. *Bioorg. Med. Chem.* **2007**, *15*, 5003-5017.
- (34) Köse, M.; Gollos, S.; Karcz, T.; Fiene, A.; Heisig, F.; Behrenswerth, A.; Kieć-Kononowicz, K.; Namasivayam, V.; Müller, C. E. Fluorescent-labeled selective adenosine A_{2B} receptor antagonist enables competition binding assay by flow cytometry. *J. Med. Chem.* **2018**, *61*, 4301-4316.
- (35) Jiang, J.; Seel, C. J.; Temirak, A.; Namasivayam, V.; Arridu, A.; Schabikowski, J.; Baqi, Y.; Hinz, S.; Hockemeyer, J.; Müller, C. E. A_{2B} adenosine receptor antagonists with picomolar potency. *J. Med. Chem.* **2019**, *62*, 4032-4055.
- (36) Damljanović, I.; Čolović, M.; Vukićević, M.; Manojlović, D.; Radulović, N.; Wurst, K.; Laus, G.; Ratković, Z.; Joksović, M.; Vukićević, R. D. Synthesis, spectral characterization and electrochemical properties of 1H-3-(*o*-, *m*- and *p*-ferrocenylphenyl)-1-phenylpyrazole-4-carboxaldehydes. *J. Organomet. Chem.* **2009**, *694*, 1575-1580.
- (37) Sanches, B. M. A.; Ferreira, E. I. Is prodrug design an approach to increase water solubility? *Int. J. Pharm.* **2019**, *568*, 118498.
- (38) Al-Zaydi, K. M.; Borik, R. M.; Elnagdi, M. H. Arylhydrazononitriles as precursors to 2-substituted 1,2,3-triazoles and 4-amino-5-cyano-pyrazole derivatives utilizing microwave and ultrasound irradiation. *Green Chem. Lett. Rev.* **2012**, *5*, 241-250.
- (39) Sou, T.; Bergström, C. A. S. Automated assays for thermodynamic (equilibrium) solubility determination. *Drug Discov. Today: Technologies.* **2018**, *27*, 11-19.

- (40) Leo, A.; Hansch, C.; Elkins, D. Partition coefficients and their uses. *Chem. Rev.* **1971**, *71*, 525-616.
- (41) Hitchcock, S. A.; Pennington, L. D. Structure-brain exposure relationships. *J. Med. Chem.* **2006**, *49*, 7559-7583.
- (42) Buscher, B.; Laakso, S.; Mascher, H.; Pusecker, K.; Doig, M.; Dillen, L.; Wagner-Redeker, W.; Pfeifer, T.; Delrat, P.; Timmerman, P. Bioanalysis for plasma protein binding studies in drug discovery and drug development: views and recommendations of the European Bioanalysis Forum. *Bioanalysis*. **2014**, *6*, 673-682.
- (43) Unpublished data from Müller group.
- (44) Alexandrov, A. I.; Mileni, M.; Chien, E. Y. T.; Hanson, M. A.; Stevens, R. C. Microscale fluorescent thermal stability assay for membrane proteins. *Structure*. **2008**, *16*, 351-359.
- (45) Al-Attaqchi, O. H. A.; Attimarad, M.; Venugopala, K. N.; Nair, A.; Al-Attaqchi, N. H. A. Adenosine A_{2A} receptor as a potential drug target - current status and future perspectives. *Curr. Pharm. Design*. **2019**, *25*, 2716-2740.
- (46) Patel, T. K.; Adhikari, N.; Amin, S. A.; Biswas, S.; Jha, T.; Ghosh, B. Small molecule drug conjugates (SMDCs): an emerging strategy for anticancer drug design and discovery. *New J. Chem.* **2021**, *45*, 5291-5321.
- (47) Verlinde, C. L.; Hol, W. G. J. Structure-based drug design: progress, results and challenges. *Structure*. **1994**, *2*, 577-587.

4.4. Part IV: Synthesis of 2,4,6,8-tetrasubstituted pyrimido[5,4-d]pyrimidines as MRGPRX3 agonists

4.4.1. Dipyridamole and derivatives

Dipyridamole (also known as Persantin) is a well-established drug that arose in the early 1960s as a coronary vasodilator for peripheral arterial disease and coronary artery disease as the drug inhibits phosphodiesterases (PDE). Additionally, it is used as antithrombotic agent. It inhibits the uptake of adenosine and thereby increases the extracellular adenosine concentration.^{1,2} More recently, the application of dipyridamole was suggested for the treatment of various ocular conditions such as ocular hypertension, glaucoma, inflammatory eye disorders, retinal vascular disorder, pterygia, and dry eye disease in strongly diluted eye drop solution.³ Studies suggested the use of dipyridamole derivatives as inhibitors of multidrug resistance to antitumor agents.^{4,5} Some time ago, dipyridamole was found to possess antiviral properties, this was recently re-examined in the context of the SARS Covid-19 pandemic, also with regard to symptom reduction.⁶⁻⁸ Figure 1 summarizes the activity of dipyridamole at its common targets.

human equilibrative Nucleoside Transporters (ENT) inhibition:

human ENT 1 IC_{50} = 15.1 nM

human ENT 2 IC_{50} = 308 nM

human ENT 4 IC_{50} = 2,797 nM

Phosphodiesterase (PDE) inhibition:

human PDE 1 IC_{50} = 45,000 nM

human PDE 2 IC_{50} = 4,000 nM

human PDE 3 IC_{50} = 43,000 nM

human PDE 4 IC_{50} = 500 nM

human PDE 5 IC_{50} = 574 nM

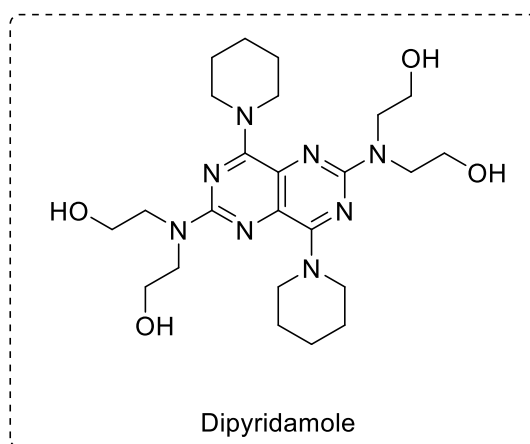
human PDE 6 K_i = 125 nM

human PDE 7 K_i = 600 nM

human PDE 8 K_i = 9,000 nM

human PDE 10 K_i = 1,000 nM

human PDE 11 K_i = 400 nM

**Gamma-aminobutyric acid receptor subunit alpha-1:**

rat K_i = 87.9 nM

Inhibition of 3H -thymidine uptake into L1210 leukemia cells via nucleoside transporters:

1 μ M dipyridamole: Inhibition 80%, IC_{50} = 0.34 μ M

10 μ M dipyridamole: Inhibition 99%

Suppression of HCoV-19 replication:

EC_{50} = 100 nM

Figure 1. Activity of dipyridamole at its common targets.⁸⁻¹⁵

On the basis of dipyridamole, derivatives with a 2,4,6,8-tetrasubstituted pyrimido[5,4-*d*]pyrimidine scaffold were synthesized. That scaffold is particularly interesting for medicinal chemists due to its resemblance to bioactive purines. In 2001, Northen et al. prepared many compounds belonging to this class bearing various substitution patterns. Selected compounds were tested as inhibitors of the cyclin-dependent kinase 1 complex (cyclin B/CDK1) but none of the compounds showed significant activity.¹⁶ Nonetheless, this provides a good introduction into the chemistry of 2,4,6,8-tetrasubstituted pyrimido[5,4-*d*]pyrimidines and their preparation.

In a publication from Curtin et al., 2,4,6,8-tetrasubstituted pyrimido[5,4-*d*]pyrimidine-based nucleoside transport inhibitors were described as modulators of antitumor drugs. Analogues of dipyridamole were synthesized and evaluated as inhibitors of 3H -thymidine uptake into L1210 leukemia cells in the presence and absence of 5 mg/mL α_1 -acid glycoprotein (AGP). Compounds with potency similar to that of dipyridamole were identified but none of them was superior to dipyridamole.¹⁰

In 2007, Lin and Buolamwini performed the synthesis of potent dipyrnidamole analogues as equilibrative nucleoside transporter 1 inhibitors and evaluated the compounds via flow cytometric. As a result, 2,6-bis(diethanolamino)-4,8-diheptamethyleneiminopyrimido[5,4-*d*]pyrimidine was found to be more potent than the parent compound with a K_i value of 0.49 nM compared to a K_i value of 308 nM for dipyrnidamole.¹⁷

4.4.2. Compound design

As a starting point, dipyrnidamole derivatives with different substitution patterns were to be synthesized using the established building blocks piperidine, diethanolamine, ethanolamine and ammonia. New derivatives with a defined ABBA or AABB substitution pattern were to be prepared and tested at the MRGPRX3. Figure 2 illustrated several examples.

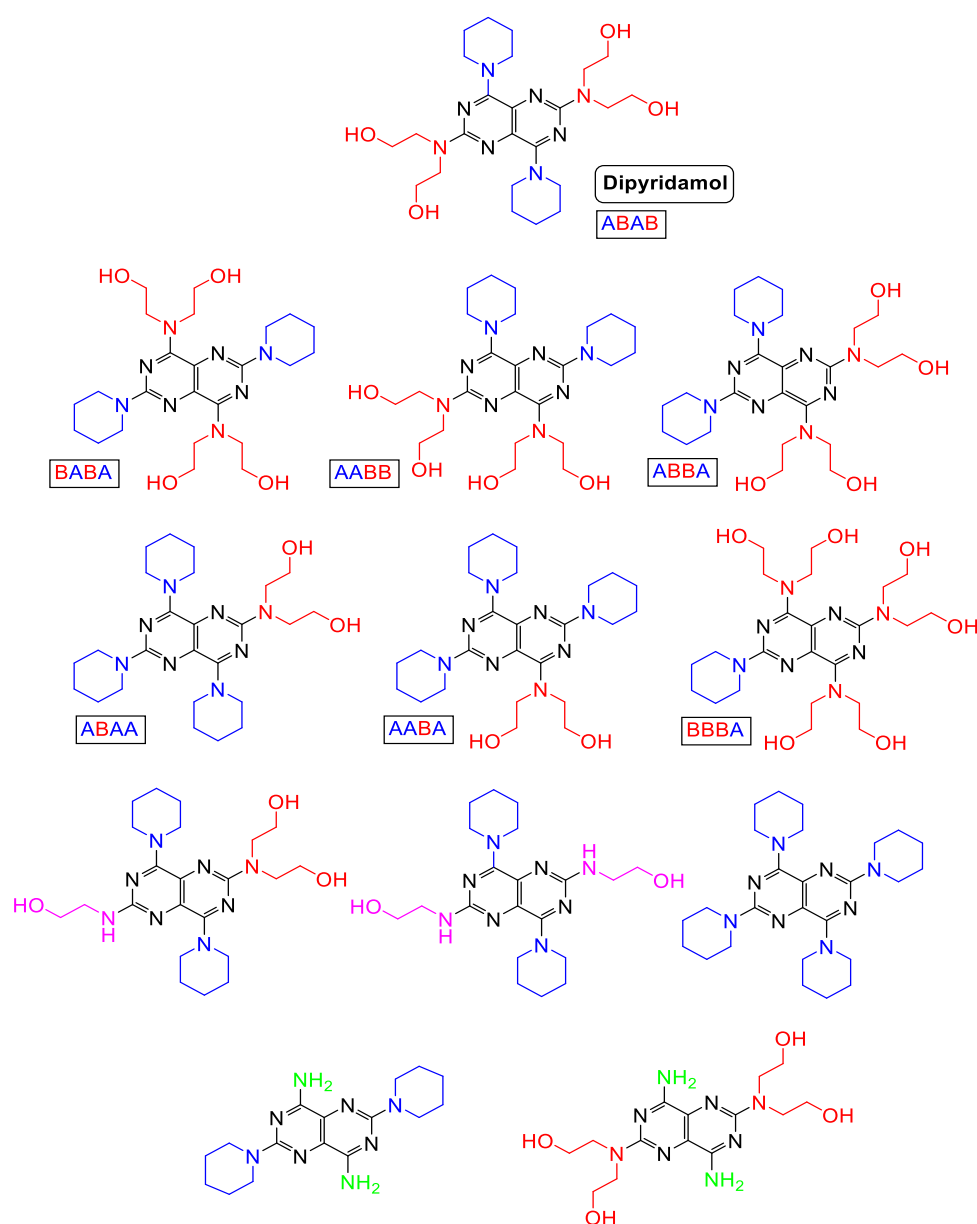


Figure 2. Examples for dipyrnidamole derivatives, to be synthesized as MRGPRX3 agonists.

As soon as biological test results suggest the superiority of particular substituents or substitution patterns, new compounds will be designed according to the new findings. To avoid random compound design in the future, 2 or 3 carefully selected residues will be kept constant while one or two positions will be modified.

Furthermore, related compound classes such as purines and pyrimidines decorated with the established substituents, were to be explored (cf. Figure 3).

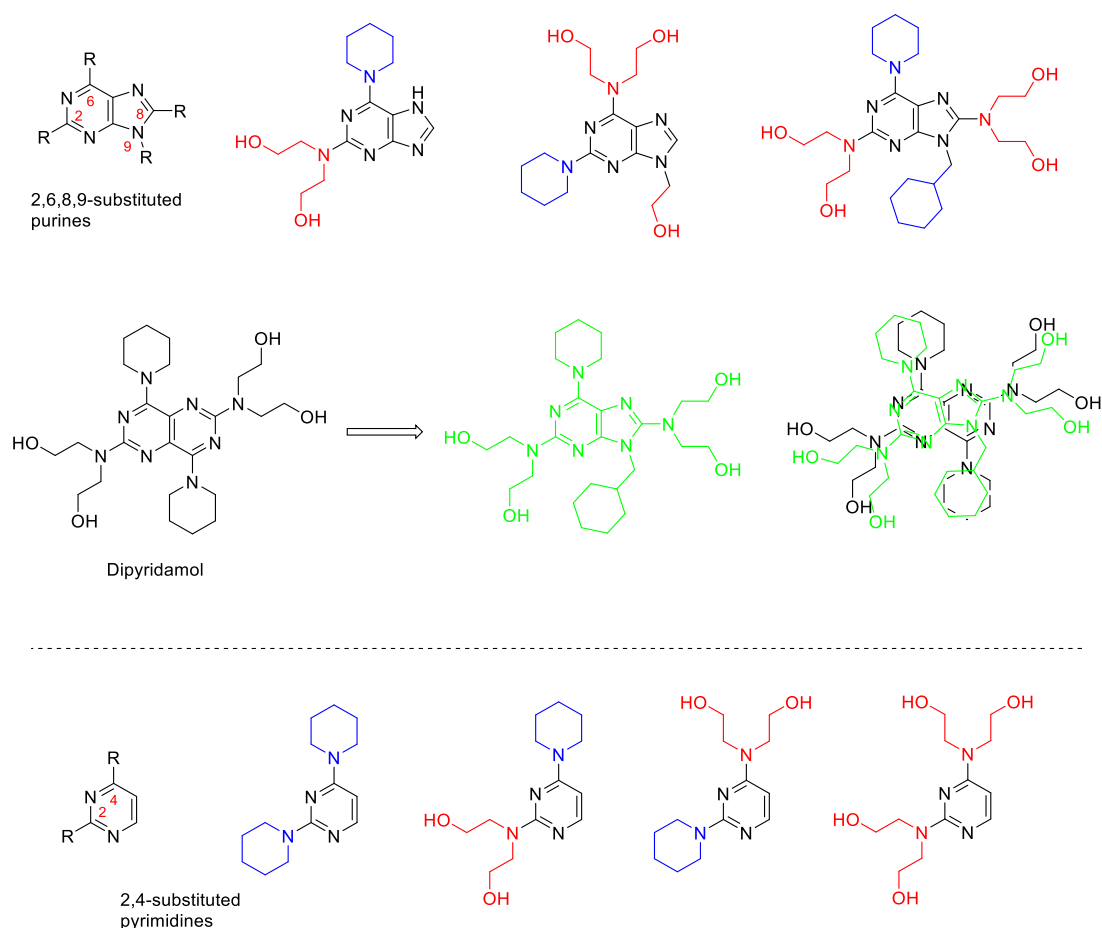


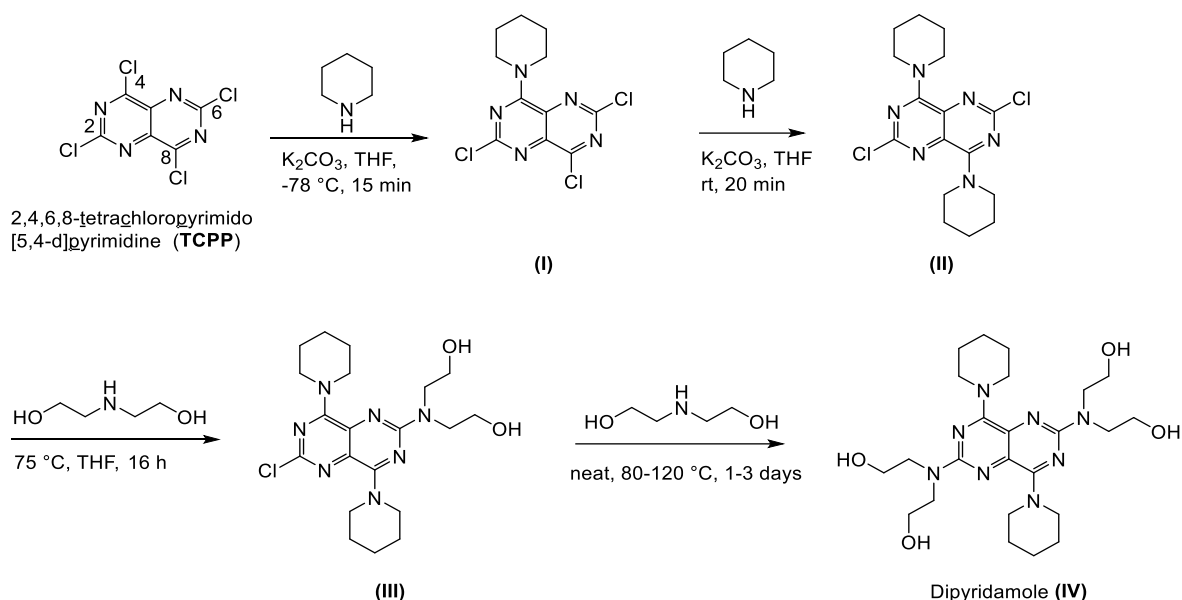
Figure 3. Examples for planned purine and pyrimidine derivatives.

Purines are common structures in biology and are structurally closely related to the pyrimido[5,4-*d*]pyrimidine scaffold, thus we plan to investigate derivatives of this compound family. Purines offer several positions for substitution. The residues found in dipyridamole were planned to be introduced into the purine scaffold, hence, 2,6-disubstituted, 2,6,9-trisubstituted and 2,6,8,9-tetrasubstituted purines were planned to be synthesized.

Additionally, disubstituted pyrimidines were to be synthesized. The pyrimidines represent “half” of the 2,4,6,8-tetrasubstituted pyrimido[5,4-*d*]pyrimidines. Investigation of these structures will show, if the entire pyrimido[5,4-*d*]pyrimidines scaffold plus substituents is needed for activity at MRGPRX3 or if only a part of the structure would be sufficient.

4.4.2.1 Synthesis of 2,4,6,8-tetrasubstituted pyrimido[5,4-d]pyrimidines

The synthesis of dipyriddyamole and corresponding derivatives is straightforward in theory, the commercially available 2,4,6,8-tetrachloropyrimido[5,4-d]pyrimidine (TCPP) is the classical precursor for 2,4,6,8-tetrasubstituted pyrimido[5,4-d]pyrimidines. The nature of TCPP allows the successive substitute of the chlorine atoms with nucleophiles, such as amines. The chlorine atoms at the positions 4 and 8 are much more reactive towards nucleophiles than those in positions 2 and 6. The observed regioselectivity relates to the ability to delocalize the negative charge arising from attack of a nucleophile at C2/C6 or C4/C8 during the reaction. A nucleophilic attack at C4/C8 results in a transition state with a negative charge on nitrogen N3 or N7. This charge can be delocalized into an adjacent C=N bond, whereas attack at C2/C6 does not permit this stabilizing interaction.¹⁶

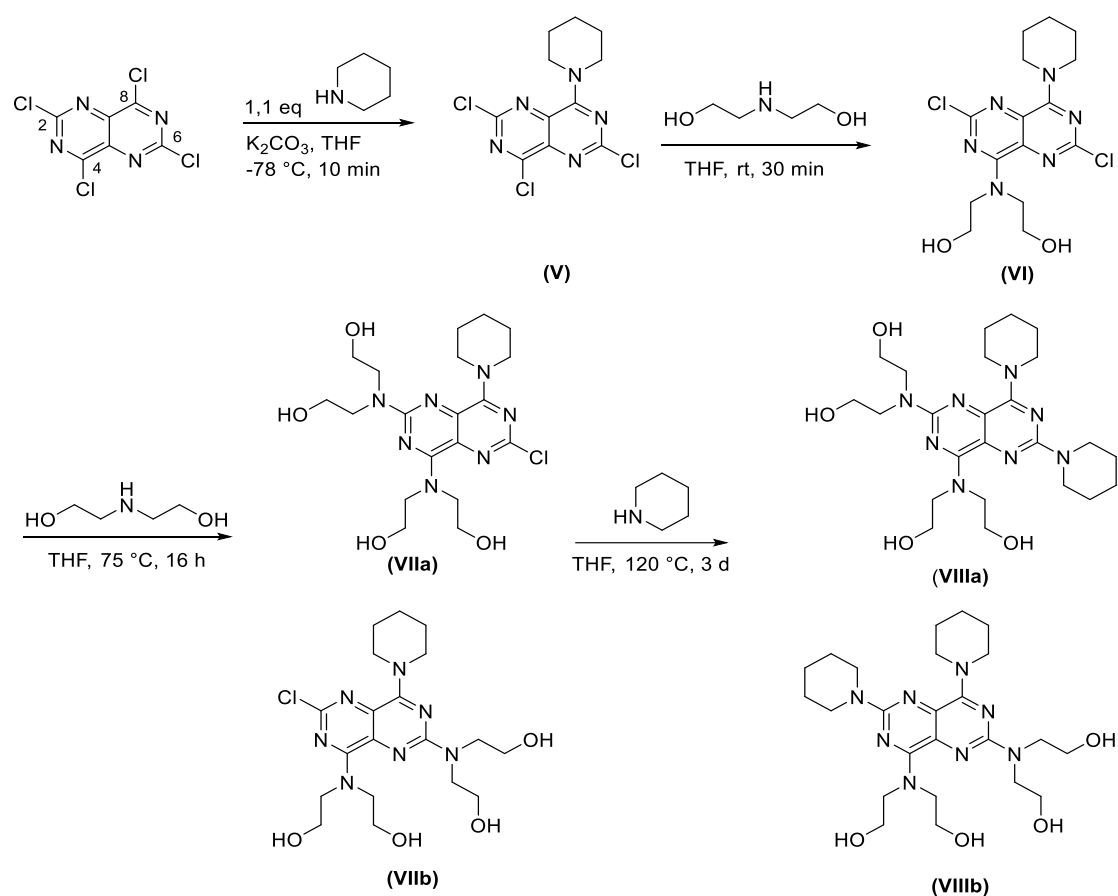


Scheme 1. Synthesis of dipyriddyamole as an example for symmetrical 2,4,6,8-tetrasubstituted pyrimido[5,4-d]pyrimidines derivatives.¹⁶

Scheme 1 illustrates the reaction conditions to gradually substitute the scaffold with nucleophiles, for dipyriddyamole as an example. A mono-substitution of TCPP (**I**) requires very low temperatures (-78 °C) and careful addition of the nucleophile (1.1 equivalents). Too high temperatures or too much reagent will result in di-substitution. The second substitution can be readily performed at room temperature (**II**). If the identical nucleophile is introduced at C4 and C8 at the same time, the first step can be skipped and an excess of nucleophile can directly react yielding the disubstituted intermediate at rt. Access of reagent does normally not lead to a third substitution. In both cases a base to neutralize the released HCl is added. For the third substitution, an excess of the respective nucleophile is heated with precursor (**II**) at elevated temperatures (75 °C) for 16 h yielding (**III**). The last reaction step requires very harsh conditions. The desired nucleophile is heated with (**III**) at 120 °C for several days. A large

excess of the reagent is needed which is often used as solvent to obtain **(IV)**. Again, the third step can be bypassed if the substitution pattern is symmetrical at C2 and C6. These conditions can traditionally be used for substitution patterns like ABAB or ABAC.¹⁶

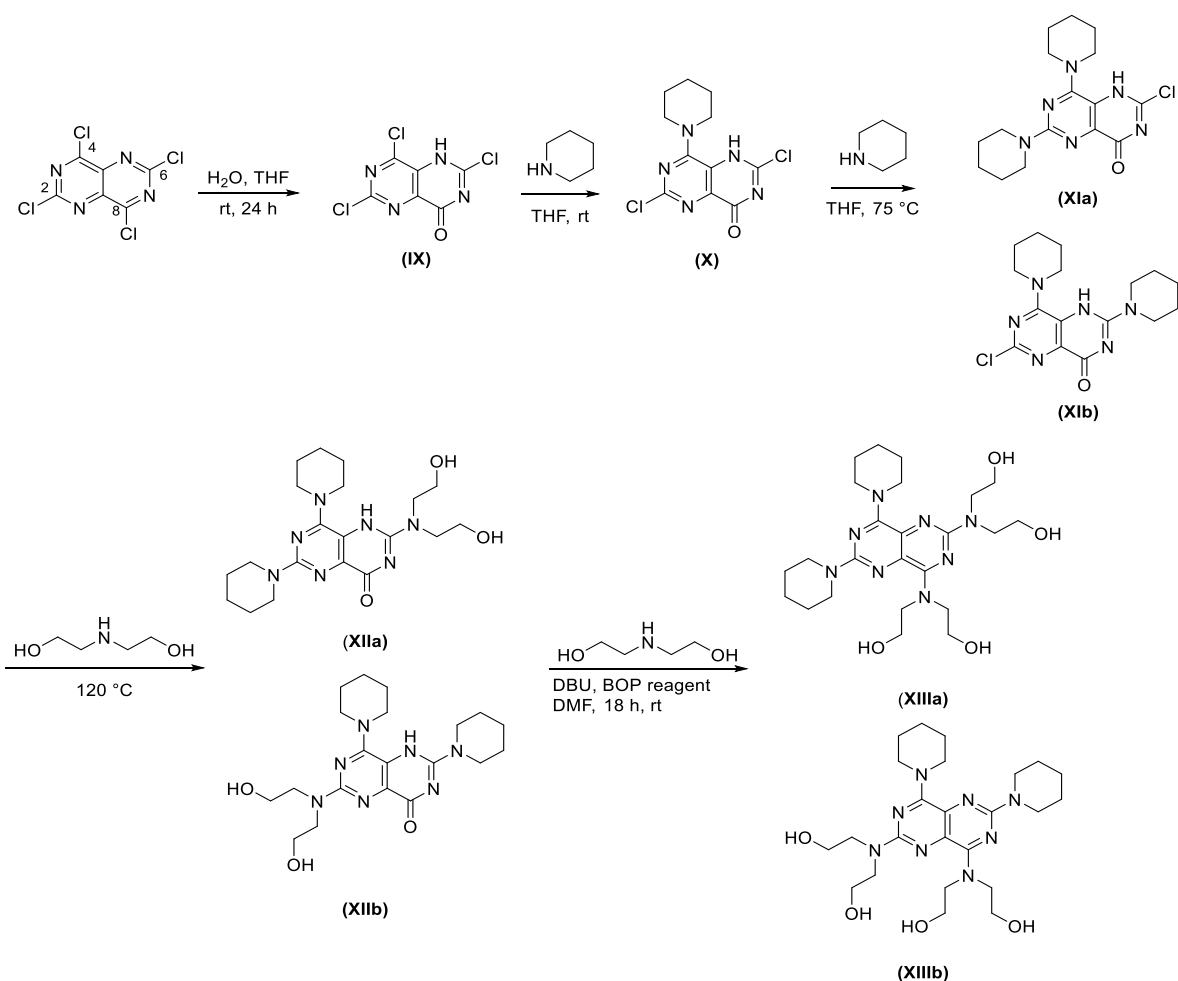
An appropriate method to prepare 2,4,6,8-tetrasubstituted pyrimido[5,4-*d*]pyrimidines that exhibit an AABB, an ABBA, or even an ABCD substitution pattern still needs to be investigated. As shown in Scheme 2, it is possible to prepare 2,4,6,8-tetrasubstituted pyrimido[5,4-*d*]pyrimidines with such substitution patterns, however, the emergence of regioisomers is an issue that needs to be overcome.¹⁶



Scheme 2. Synthesis route of 2,4,6,8-tetrasubstituted pyrimido[5,4-*d*]pyrimidines with an AABB or ABBA substitution pattern.

The illustrated examples **(VIIIa)** and **(VIIIb)** will hardly be separable with satisfying yields as their properties are very similar. Thus, it would be more favorable to have a selective synthetic route, or to separate isomers at a point when they possess more divergent properties.

One idea could be to initially hydrolyze one of the chlorine atoms at the 4/8 position (**IX**) and subsequently introduce a nucleophile to the other reactive position (**X**). This would yield a compound that is not symmetric anymore (cf. Scheme 3).



Scheme 3. Suggested synthetic route for AABB- or ABBA-substituted 2,4,6,8-tetrasubstituted pyrimido[5,4-*d*]pyrimidines using a hydrolyzed intermediate.

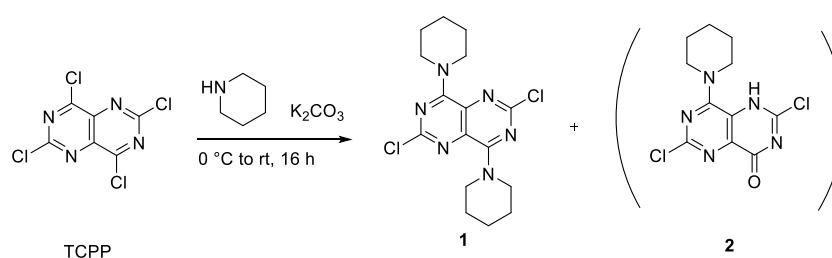
In the best case, a selective substitution of one of the chlorine atoms might be possible since they are not 100% equal anymore, yielding **(XIa)** and **(XIb)**. If this is not possible, the arising isomers might be better separable and characterizable than the isomers **(XIIa)**/**(XIIb)**, or **(XIIIa)**/**(XIIIb)**, respectively. In literature, only few reports describe reactions involving mono-hydrolyzed 2,4,6,8-tetrasubstituted pyrimido[5,4-*d*]pyrimidines.¹⁸ Those publications only describe substitutions that are symmetrical to some degree. The suggested synthetic pathway has not been described yet. In a fourth step, the last chlorine would be substituted to obtain **(XIIa)** and **(XIIb)**. Finally, a coupling reaction using the last nucleophile, BOP reagent (benzotriazolylxytris(dimethylamino)-phosphonium hexafluorophosphate) and DBU (1,8-diazabicyclo[5.4.0]undec-7-ene) as a base is supposed to lead to the final compounds **(XIIIa)** and **(XIIIb)**.^{18;19}

4.4.3. Synthesis

4.4.3.1. Synthesis of AAAB-substituted pyrimido[5,4-*d*]pyrimidine derivatives bearing traditional substituents

In order to explore the structure activity relationship of 2,4,6,8-tetrasubstituted pyrimido[5,4-*d*]pyrimidines at the MRGPRX3 receptor in a structured way, the established substituents (piperidine and diethanolamine) were introduced to the scaffold in different substitution patterns. One approach was to introduce 3 identical residues and one single residue.

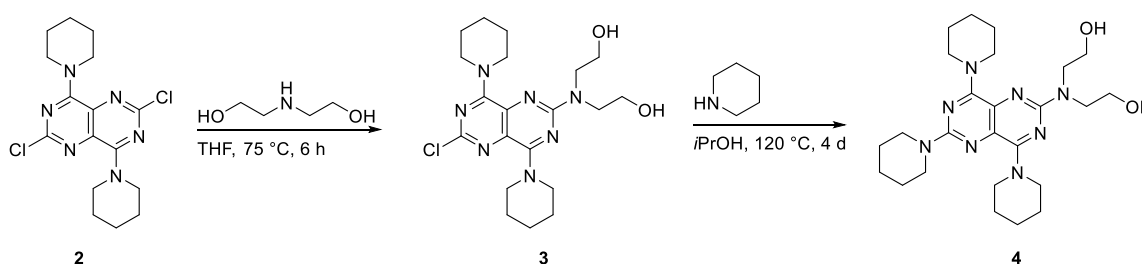
To prepare the precursor 4,8-bis(piperazine)-2,6-dichloropyrimido[5,4-*d*]pyrimidine (**1**) and its derivatives, the reported methods were used (cf. Scheme 4).^{10;16;17}



Scheme 4. Synthesis of **1**.

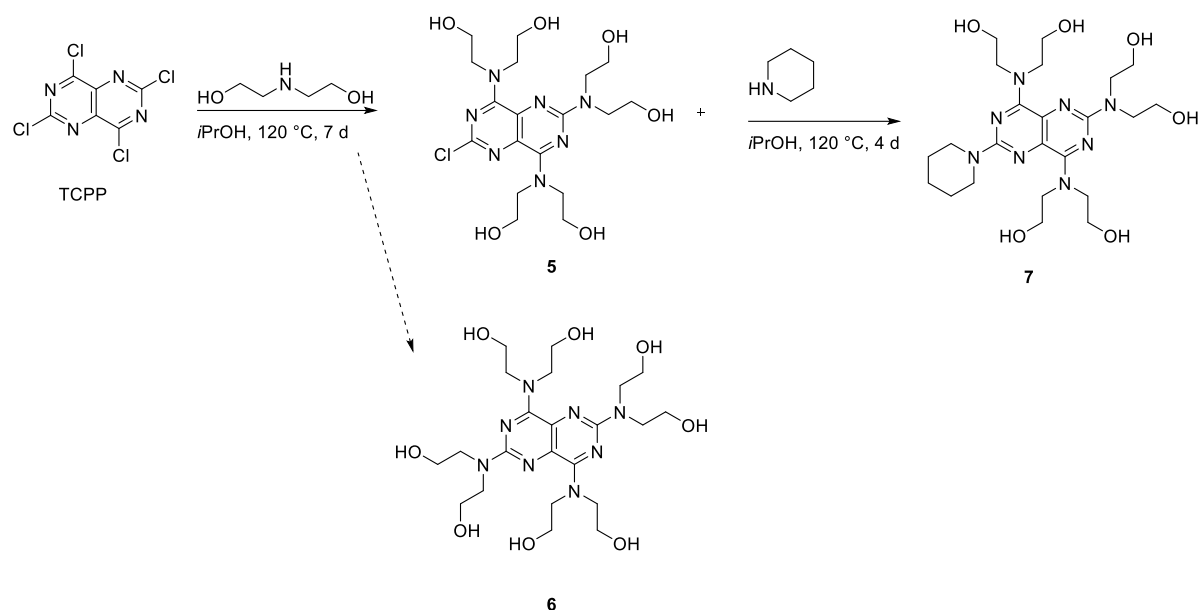
Therefore, TCPP was treated with 2.5 equivalents of piperidine at 0 °C in THF. This reaction mixture was allowed to warm up to rt and was stirred at rt for 16 h. TLC-MS analysis suggested the emergence of **2** as an undesired side product, showing that TCPP is prone to hydrolyzation, even if dry solvents are used. Yet, the desired product **1** could be obtained in good yield (66%).

Subsequently, **1** was reacted with diethanolamine using the reported method¹⁶ to prepare the trisubstituted pyrimido[5,4-*d*]pyrimidine derivative **3** in good yield (77%) (cf. Scheme 5). Since starting material remained unreacted, the product had to be isolated by column chromatography (petrol ether / ethyl acetate - 1 : 1). However, longer reaction times are not necessarily beneficial as unknown side products and small amounts of tetrasubstituted pyrimido[5,4-*d*]pyrimidine derivatives can arise. In a subsequent reaction, the final product **4** was obtained by reacting **3** with piperidine at elevated temperature for 4 days. The product could be obtained in an excellent yield of 90%.



Scheme 5. Synthesis of **4**.

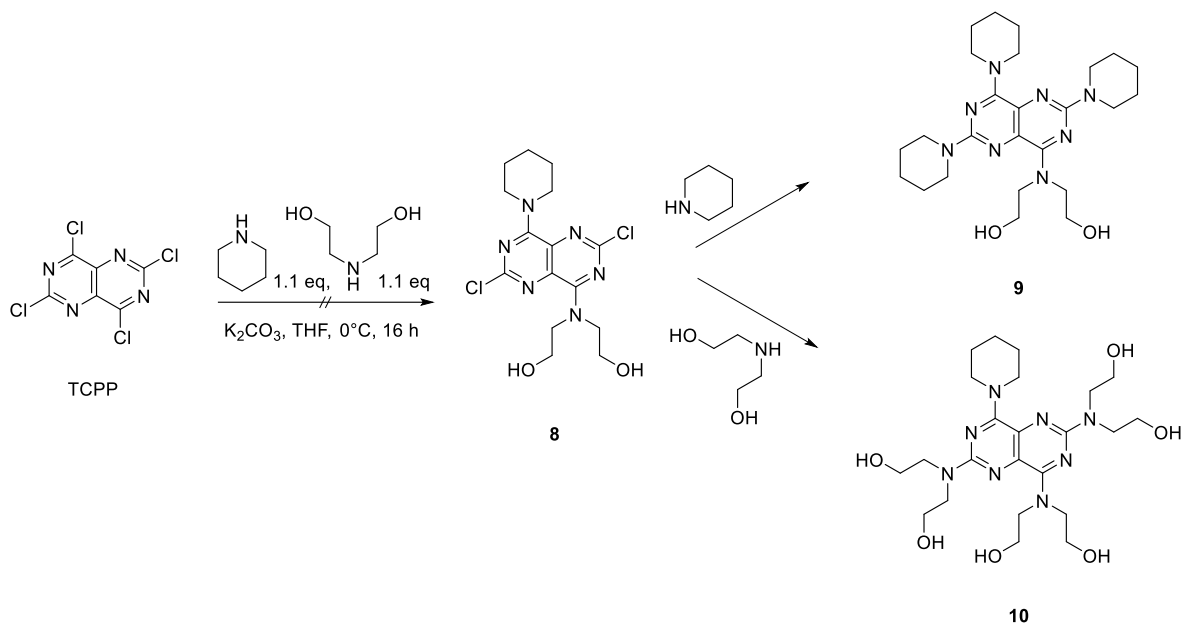
The reaction illustrated in Scheme 6 was performed to prepare the tetrasubstituted pyrimido[5,4-*d*]pyrimidine **6** bearing four diethanolamine units. Therefore, TCPP was heated with a large excess of diethanolamine at 120 °C for a week. Even after 7 days of harsh reaction conditions, the trisubstituted derivative **5** was obtained in satisfactory yield (49%) and purity (70%). **6** could be isolated in sufficient purity (94%) but low yield (11%). However, LC-MS analysis was not perfectly clear due to tailing of the compound in the chromatogram and a large injection peak. Additionally, NMR analysis was not possible due to solubility problems. Nevertheless, the compound was submitted to biological testing.



Scheme 6. Synthesis of **6** and **7**.

The impure side product **5**, however, was subsequently used to form product **7** by reaction with piperidine. Purification by column chromatography (CH₂Cl₂/ MeOH - 9 : 1) led to the final product in moderate yield (27% over two steps).

Several trials were made to form the key compound **8** (cf. Scheme 7). This compound would allow a straightforward synthesis of the final products **9** and **10**.



Scheme 7. Attempted synthesis of **8**.

None of those trials, however, led to the formation of the desired product. In one of the first trials, TCPP was simultaneously treated with piperidine and diethanolamine (1.1 equivalents each) at 0 °C in THF in the presence of K_2CO_3 . In two further trials, the amines were consecutively added. Therefore, TCPP and K_2CO_3 were suspended in THF at 0 °C and an amine (e.g. piperidine) was added. After 15 min, the second amine (e.g. diethanolamine) was added, and the mixture was stirred for 1 hour at rt. LC-MS analysis of all trials revealed that no product was formed; they resulted in a complex mixture of unknown side products as well as **1** (2 x piperidine) and **2** (1 x piperidine, 1 x Oxygen). No mass indicated that diethanolamine had reacted with TCPP. The addition of a molecular sieve to the reaction mixture, or working under vacuum or an argon atmosphere might solve the problem of hydrolysis leading to the formation of **2**. Heating of the reaction mixture might enhance the reactivity of the weak nucleophile diethanolamine.

The trials described in this chapter yielded the three final compounds **4**, **6** and **7** as well as the important intermediates **1**, **3**.

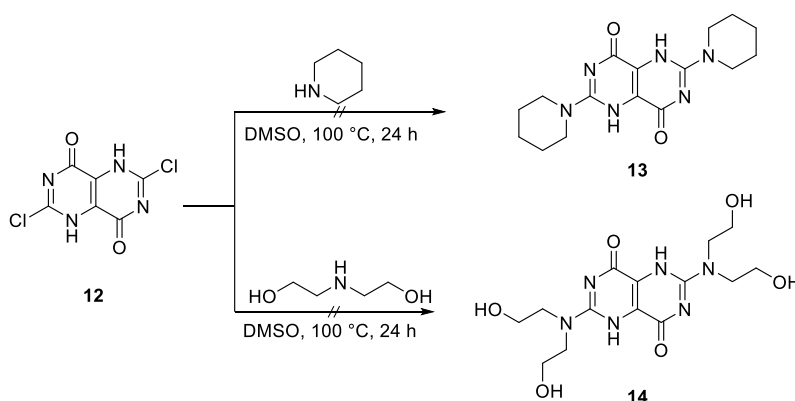
4.4.3.2. Synthesis of pyrimido[5,4-*d*]pyrimidine derivatives closely related to dipyrnidamole

In order to prepare compounds with the special substitution pattern AABB and ABBA, the abovementioned approach towards unsymmetric derivatives by mono-hydrolysis of TCPP was tried.¹⁸ The first trials were attempts to selectively hydrolyze one chlorine atom at C4/C8 leading to the formerly undesired side product **11**. Table 5 illustrates the tested conditions; each reaction was performed at rt with a small amount of TCPP for 16 h.

Table 1. Tried conditions to hydrolyze TCPP.

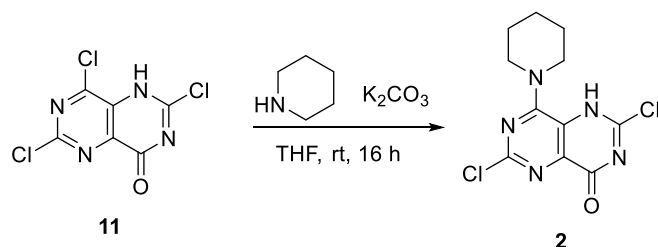
Entry	Solvents	Base	Result
1	H ₂ O / THF	-	Desired product 11 (85%)
2	H ₂ O / THF	KOH	Side product 12
3	H ₂ O / THF	NaOH	Side product 12
4	H ₂ O / THF	NaOH / Bu ₄ NOH	Side product 12
5	H ₂ O / acetone	-	Desired product 11 (91%)

Simple stirring of TCPP in an aqueous mixture of THF or acetone (1 : 1) for 16 h results in the desired product 2,6,8-trichloropyrimido[5,4-*d*]pyrimidin-4(1*H*)-one (**11**) in excellent yield (91%).¹⁸ This product is the basis for all compounds described in this chapter. The addition of a base results in the undesired side product **12**. This side product was only tested for reactivity towards the established substituents piperidine and diethanolamine (cf. Scheme 8).



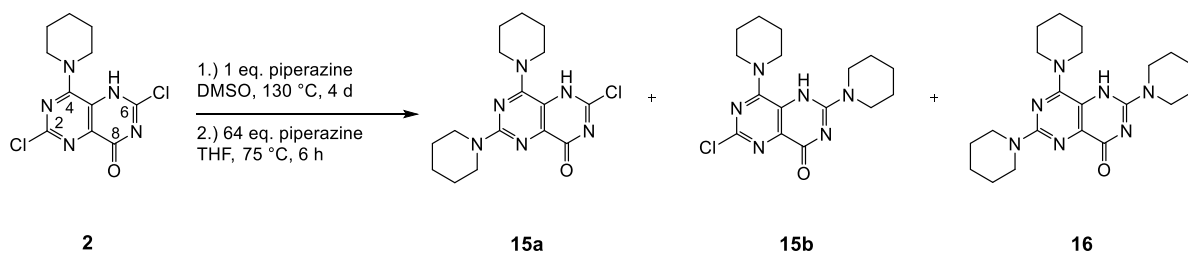
Scheme 8. Test reactions of **12** with selected nucleophiles.

As it turned out, no desired product could be found. Hence, the di-hydrolyzed intermediate does not appear to be suitable for the planned synthesis. As expected, the mono-hydrolyzed intermediate **11** could be easily converted into **2**.¹⁸ Overnight stirring at rt with piperidine led to the desired product in very good yield (87%, cf. Scheme 9).



Scheme 9. Synthesis of **2**.

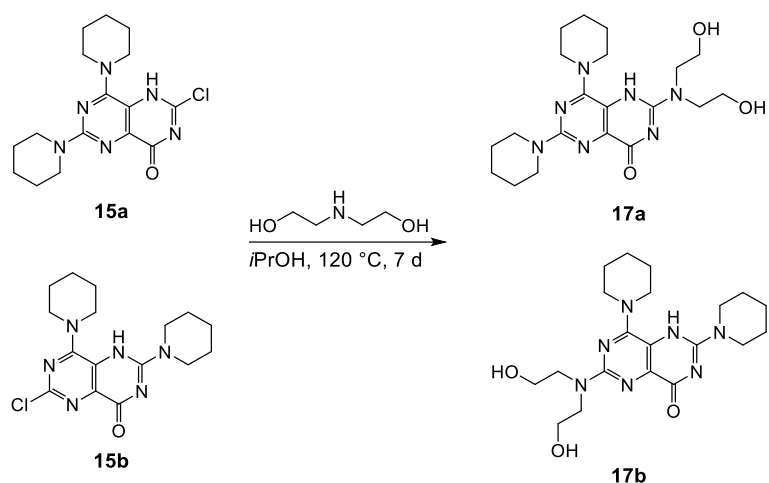
Compound **2** was the basis for several further reactions. Starting from **2**, two different methods to form a pyrimido[5,4-*d*]pyrimidin-4(1*H*)-one that bears an oxygen in the 8-position and two piperidine residues in position 4 and at C2 or C6 were investigated (cf. Scheme 10).



Scheme 10. Reactions of **2** with nucleophiles.

The first method, using only 1 equivalent of piperazine to make sure that not both chlorine atoms could be replaced, a high temperature was needed for complete transformation of **2**. As a result, only one isomer could be isolated (**15a** or **15b**). However, it was not possible to identify which one it was. In the second trial, a reported method¹⁶ for mono-substitution in position 2/6 was tried, using and a huge excess of amine but with milder reaction conditions. In this case, both isomers were formed (approximately 1 : 1) and could be separated using column chromatography. Both methods also yielded **16** as an undesired side product. The two isomers **15a** and **15b** are hardly distinguishable by NMR but the UV-spectra obtained by LC-DAD-UV-MS showed very different spectral properties.

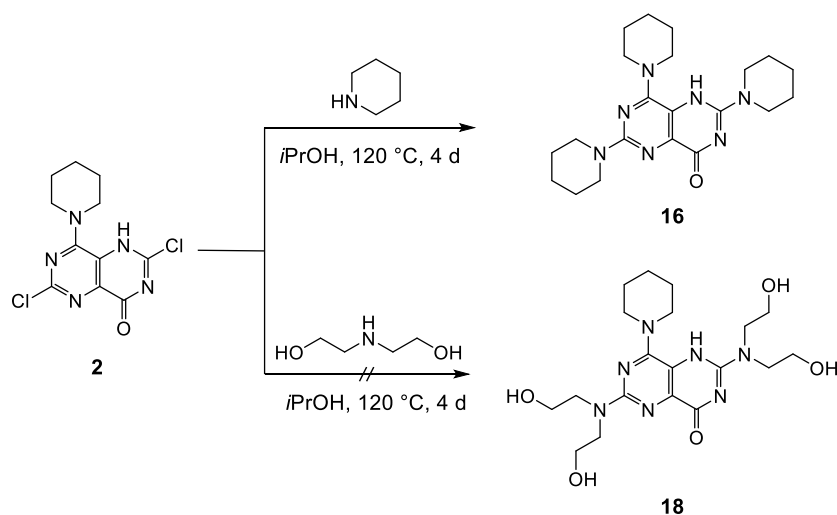
In the next step, the last chlorine atom was supposed to be replaced by diethanolamine to form the isomers **17a** and **17b** as illustrated in Scheme 11.



Scheme 11. Synthesis of the isomers **17a** and **17b**.

Although these reactions should have been feasible in theory, the reaction resulted in complex mixtures of unconverted starting material and unidentified side products. The expected product mass, however, could be detected by LC-MS in small amounts. Since this synthetic approach did not seem to be practicable altogether, and the isomers were not clearly recognizable by NMR, these attempts to prepare 2,4,6,8-tetrasubstituted pyrimido[5,4-*d*]pyrimidines with a substitution pattern AABB and ABBA were stopped.

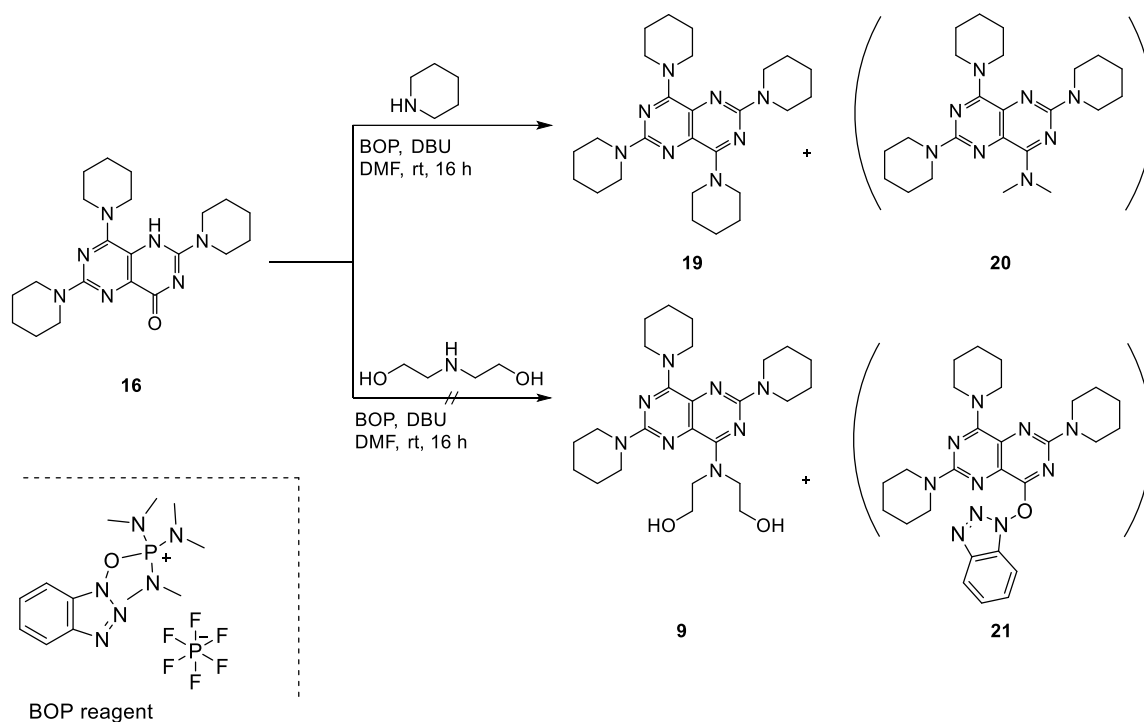
In order to further investigate the potential of compound **2** as a basis for further synthesis, more reactions were performed. Both chlorine atoms of **2** were supposed to be substituted by another piperidine unit or diethanolamine to form **16** and **18**, respectively (cf. Scheme 12).



Scheme 12. Synthesis of **16** and **18**.

Therefore, **2** was heated with the appropriate amine at 120 °C for 4 days. As a result, **16** could be isolated in satisfactory yield (58%). The compound was submitted to biological testing. The formation of **18**, however, could not be observed at all.

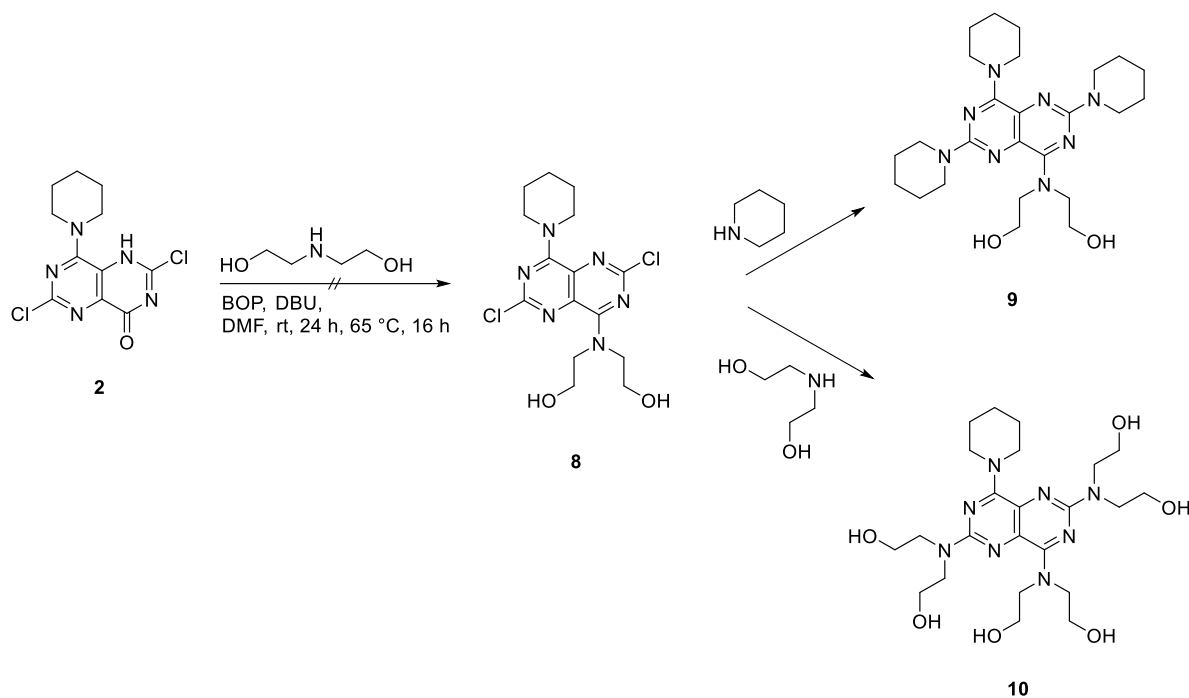
According to literature, cyclic amides and urea structures are supposed to be accessible for nucleophilic attacks using the coupling reagents BOP in combination with the base 1,8-diazabicyclo[5.4.0]undec-7-en (DBU), yielding the respective amidine or guanidine derivative (see Scheme 13).¹⁹ Compound **16** was used to investigate this coupling reaction using piperidine and diethanolamine as nucleophiles.



Scheme 13. Reactions of **16** towards **9** and **19** using BOP reagent.¹⁹

The reaction using piperidine as a nucleophile was successful, LC-MS analysis showed the formation of the desired product. The reaction was, however, accompanied by the formation of side products, and the product could not be isolated in high purity. Side product **20** was observed by LC-MS analysis. Presumably, dimethylamine originating from the BOP reagent reacted with **16**. However, a proof of principle was achieved: the suggested reaction condition could be used to introduce new nucleophile at the cyclic amide moiety employing the coupling reagent BOP.¹⁹ Diethanolamine, on the other hand, did not perform well as a nucleophile. A lot of starting material was left, and undesired side products were formed. Heating of the reaction mixture led to a complete disappearance of the starting material but also led to more side products. TLC-MS analysis revealed the formation of the intermediate **21**, supporting the idea that diethanolamine is not suitable as a nucleophile for this type of reaction.

In another trial, the same reaction type was tested to form **8** from **2** using the abovementioned reaction conditions. In this case, a complex mixture of unknown products was obtained (cf. Scheme 14). Hence, this method to form 4,8-disubstituted pyrimido[5,4-*d*]pyrimidines was discarded. Compound **8** would have been an interesting intermediate to form the desired compounds **9** and **10**.



Scheme 14. Attempted synthesis of **8** as a precursor for **9** and **10**.

Altogether, hydrolysis of one chlorine atom and subsequent coupling of nucleophiles using BOP reagent only works for very specific conditions and thus cannot be recommended in general.

4.4.3.3. Synthesis of 4,8-bis(piperazinyl)-2,6-dichloropyrimido[5,4-*d*]pyrimidine-derivatives

It is a common approach in medicinal chemistry to replace a certain residue with similar structures to investigate the importance of particular features of a substituent. In order to investigate further possible residues at R² and R⁴, moieties replacing diethanolamine are planned to be introduced at this position (cf. Figure 6).

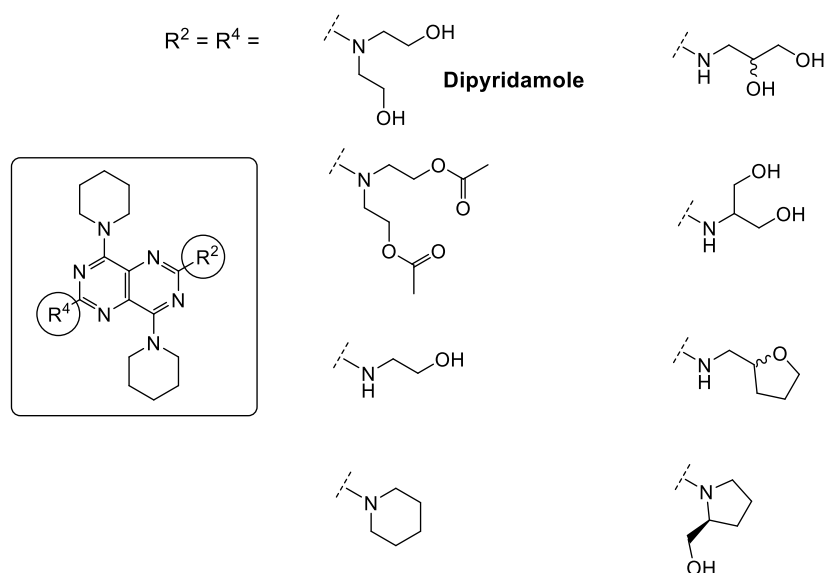
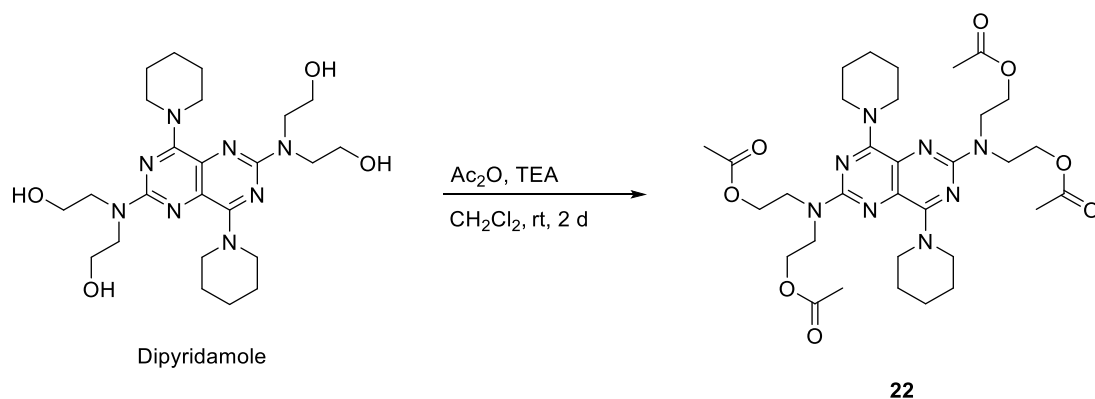


Figure 4. Planned structures with different residues at position 2 and 4.

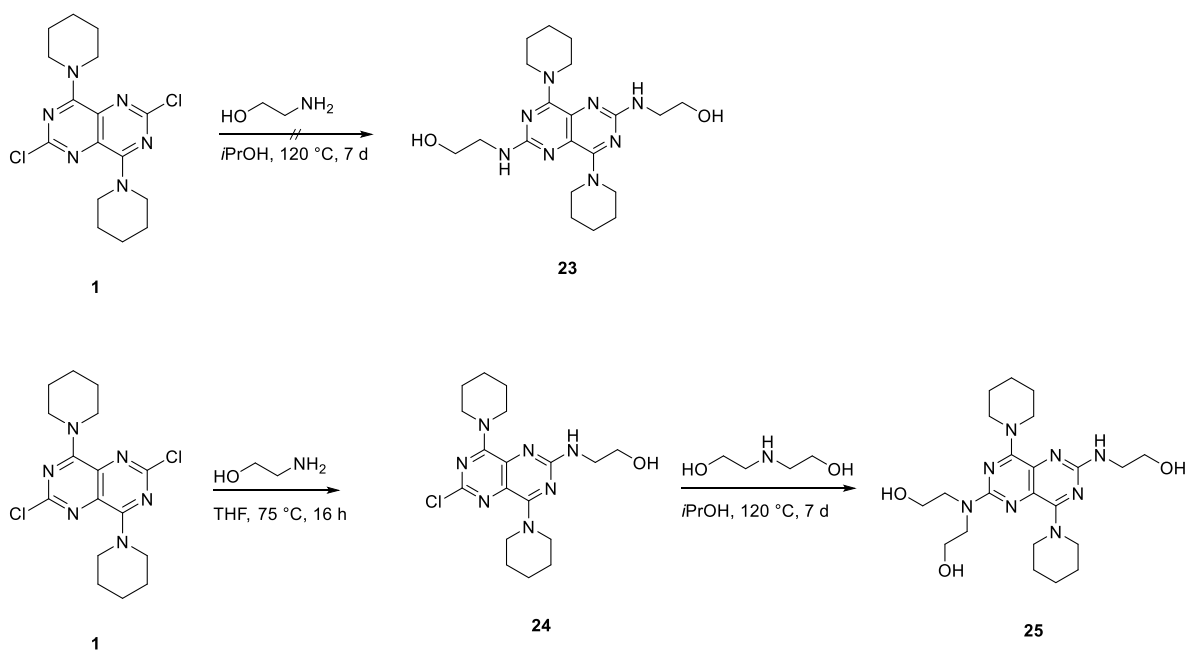
Acetylation of the diethanolamine residue might indicate whether free OH groups are necessary and how much space is required for binding to the target protein (**22**).¹⁷ Ethanolamine would be “half” of diethanolamine and might indicate if actually 2 ethanol moieties are needed at this position for biological activity at MRGPRX3 (**23**). Substitution of the pyrimido[5,4-*d*]pyrimidines core with 4 piperidine rings (**19**) would show if OH groups are necessary or if a lipophilic residue would also be tolerated. The residues 3-amino-1,2-propanediol (**24**) and 2-amino-1,3-propanediol (**25**) harbor two OH groups that are differently arranged in comparison to diethanolamine. 2-Tetrahydrofurylamine (**26**) and *L*-prolinol (**27**) contain an oxygen atom with two carbon atoms between the nitrogen atom, similar to diethanolamine, but are less flexible.

For the preparation of **22**, dipyridamole was synthesized according to literature. Dipyridamole was treated with Ac₂O and TEA as a base in CH₂Cl₂ and was stirred for 2 days at rt (cf. Scheme 15). After purification by RP-HPLC, the desired compound was obtained in satisfactory yield (54%).¹⁷



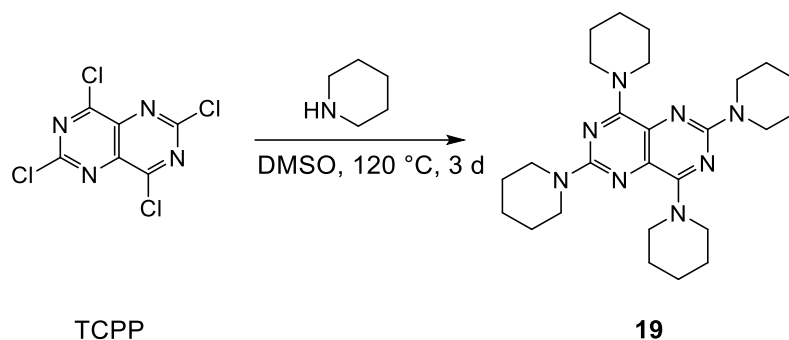
Scheme 15. Synthesis of **22**.

The synthesis of **23** turned out to be infeasible using the reported methods.^{10;16;17} Heating of **1** with a large excess of ethanolamine at 120 °C for 7 days did not result in the formation of the desired product. However, the tri-substituted intermediate **24** could be found in the reaction mixture beneath many side products. In another approach, **24** was prepared utilizing milder conditions that usually led to a substitution of the “third” chlorine: Heating of **1** at 75 °C for 16 h with an excess of ethanolamine in THF led to the formation of **24** in high yield (92%) and without the formation of any side products. Since product **23** was not directly accessible, diethanolamine was reacted with **24** under the same conditions that were employed for the attempted formation of **23**. This time, heating of **24** with an excess of diethanolamine led to the formation of **25** in moderate yield (34%). This compound was not initially planned to be synthesized, yet, the compound would give interesting insight into the SAR, thus it was submitted to biological evaluation.



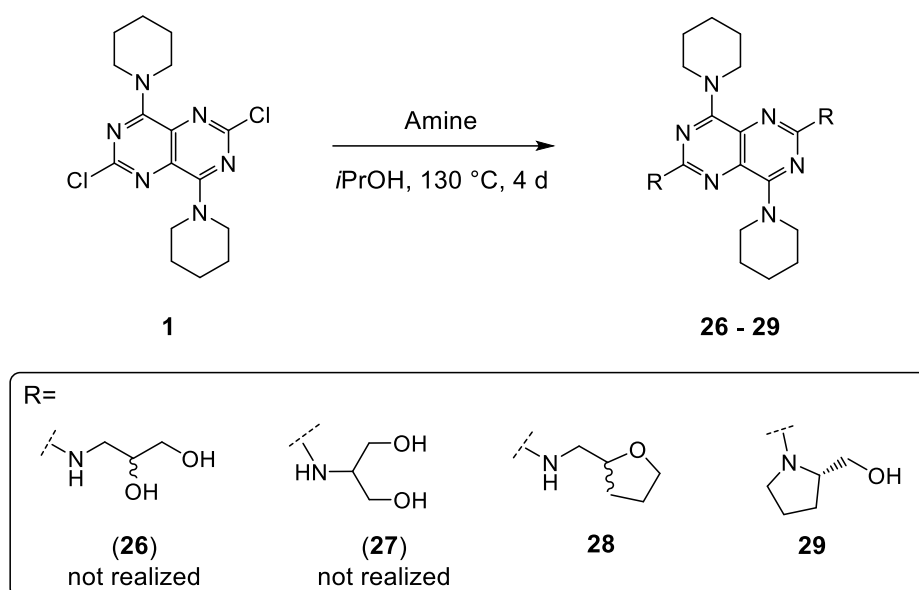
Scheme 16. Attempted synthesis of **23** and synthesis of **25**.

The formation of **19** was comparably easy, TCPPP was heated with an excess of piperidine for 3 days at 120 °C in DMSO (cf. Scheme 17). Subsequently, the mixture was treated with water, and the precipitated product was filtered off under reduced pressure yielding 52% of **19**.



Scheme 17. Synthesis of **19**.

To synthesize the desired compounds **26** to **29**, illustrated in Scheme 18, the established method was used.^{10;16;17} An excess of the required amine (3-amino-1,2-propanediol for **26**, 2-amino-1,3-propanediol for **27**, 2-tetrahydrofurylamine for **28** and L-prolinole for **29**) was heated with **1** for 4 days at 120 °C in *i*PrOH. Only **28** and **29** could be isolated, while the preparation of **26** and **27** was accompanied by too many side products.

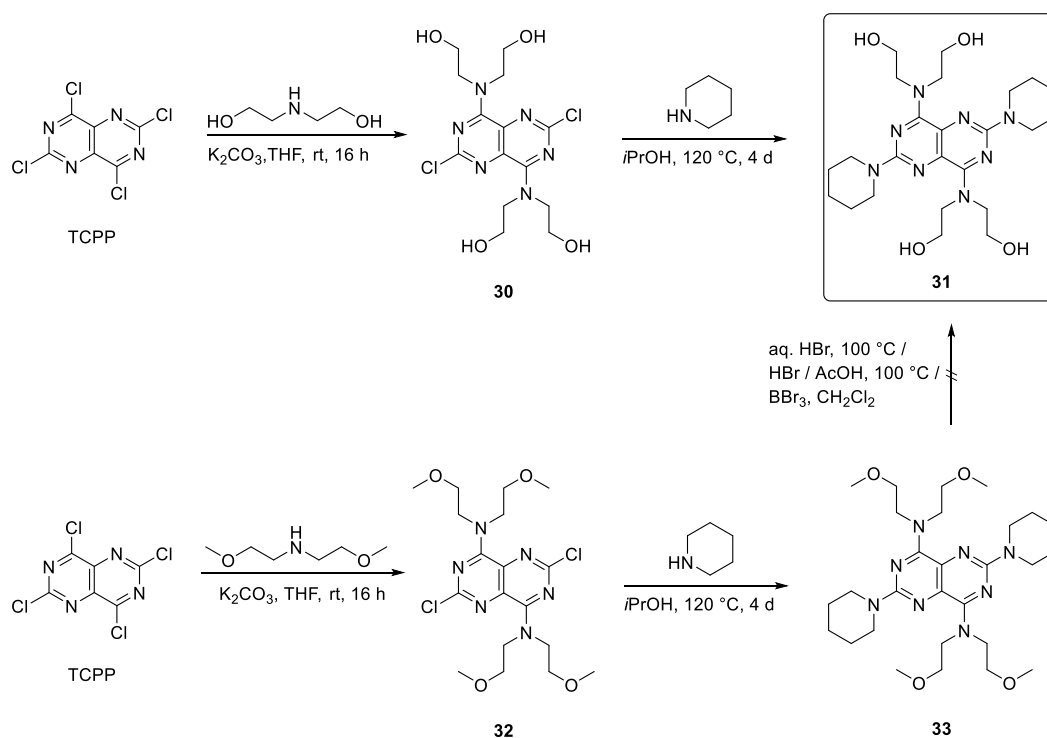


Scheme 18. Attempted synthesis of **26** and **27** and synthesis of **28** und **29**.

4.4.3.4. Synthesis of 4,8-bis(2-dihydroxyethylamino)-2,6-dichloropyrimido[5,4-d]pyrimidine derivatives

An obvious idea for SAR exploration is to simply switch the position of the dipyrindamole substituents on the pyrimido[5,4-d]pyrimidine scaffold. This means that diethanolamine would be introduced at C4 and C8 while C2 and C6 would be substituted with piperidine.

Therefore, **30** was prepared utilizing the reported method (cf. Scheme 19). Additionally, molecular sieve was added to the reaction mixture. During the overall project, it could be observed that reactions that involve diethanolamine often resulted in undesired hydrolysis products. The reason might be the hygroscopicity of the very polar diethanolamine. Compared to the preparation of other 4,8-di-substituted pyrimido[5,4-d]pyrimidine derivatives, such as **1**, the yield of **30** was lower (48%) since many side products were formed. The product could be isolated in good purity (LC-MS: 88%) and was directly used for the next reaction step.



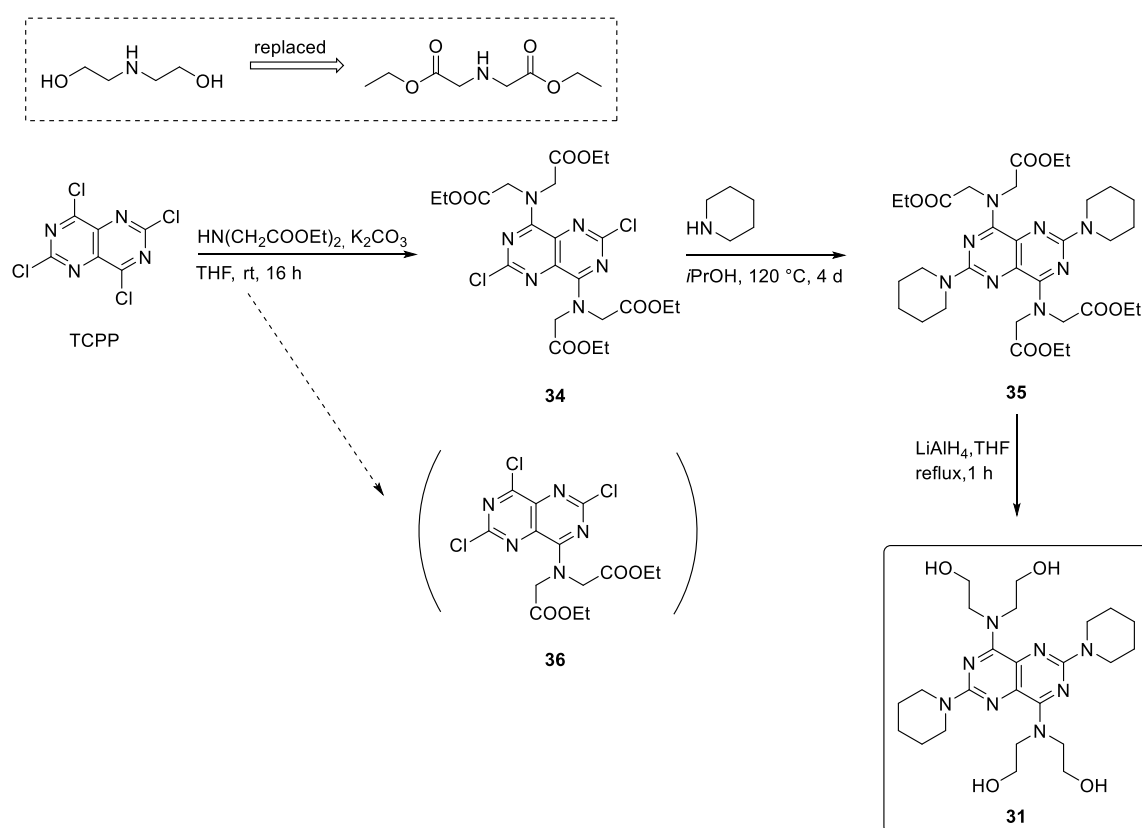
Scheme 19. Synthesis of **31** and **33**, and attempted demethylation of **33**.

In a subsequent reaction, piperidine was introduced to **30** forming the final product **31** using the established method. Purification by column chromatography (CH₂Cl₂/ MeOH - 9 : 1) led to the final product in moderate yield (26%).

Since many reactions involving diethanolamine did not work particularly well, trials were made using bis(2-methoxyethyl)amine as amine to replace diethanolamine. A subsequent cleaving reaction of the methyl ether group was supposed to lead to the free alcohols. Biological testing of the methoxy derivatives would also be interesting for SAR analysis. Product **31** was tried to

be prepared by this method. The formation of **32** was much easier and faster compared to the formation of **30** (using the same method), no side products were observed and the yield was excellent (99%). Also, the preparation of **33** by reacting **32** with piperidine turned out to be very feasible (96% yield). In both cases, no chromatographic purification was necessary; both products **32** and **33** were obtained in high purity by simple precipitation with water (LC-MS: 97% and 98%, respectively). The cleaving of the methoxy groups, however, was not possible with the tested conditions. A small amount of **33** was heated at 100 °C in conc. HBr and HBr in AcOH, respectively. Alternatively, BBr₃ in CH₂Cl₂ was tried. A molecule with the mass of **13** was found which might indicate hydrolysis at C4/C8. This would overlap with observations reported in literature.²⁰ Bis(2-methoxyethyl)amine is still an interesting building block for SAR exploration but the present approaches were stopped. Product **33** was submitted to biological testing.

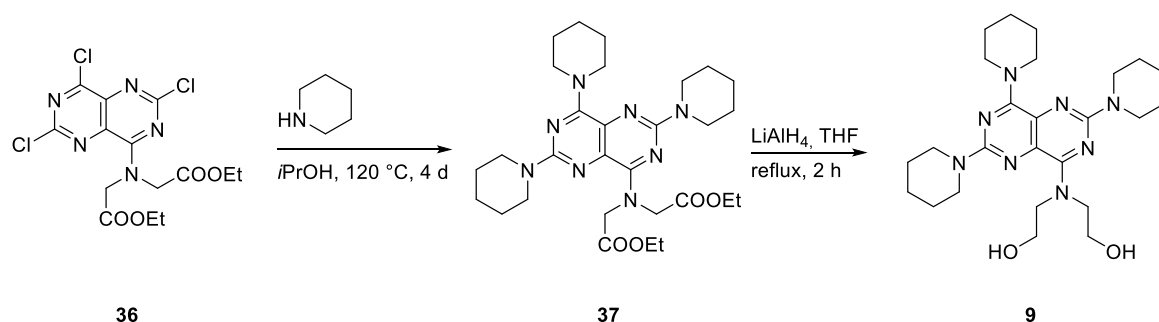
To avoid the disadvantageous properties of diethanolamine, another building block was explored to be used for synthesis to replace diethanolamine in critical reactions: diethyl iminodiacetate. This moiety was introduced to the pyrimido[5,4-*d*]pyrimidine core and subsequently reduced to the corresponding diethanolamine derivative. For example, **31** was much easier producible by this method (cf. Scheme 20).



Scheme 20. Synthetic route with diethyl iminodiacetate replacing diethanolamine and subsequent reduction to **31**.

To this end, TCPP was treated with 2 equivalents of diethyl iminodiacetate and K_2CO_3 in THF at rt. Beside the desired intermediate **34**, the mono-substituted side product **36** was formed. Compound **34** could be isolated in good yield (74%) and purity (95%), while the side product was isolated in low purity but was used for further reactions. A subsequent reaction with piperidine (using the established method) readily afforded **35** in good yield (89%). LC-MS analysis revealed that part of the product consisted of the isopropyl ester due to transesterification. The ester was reduced during the next step. To do so, **35** was refluxed with $LiAlH_4$ in THF for 1 h. Compound **31** could be easily obtained via purification by column chromatography, proving that diethyl iminodiacetate is indeed a suitable replacement regarding diethanolamine for reactions on the basis of TCPP.

The undesired side product **36** was then used to prepare the formerly inaccessible compound **9** (see Scheme 21). The impure substance was heated with an excess of piperidine leading to the intermediate **37** which was directly reduced to the final compound. Purification by column chromatography finally led to the desired product **9** in high purity (95%).

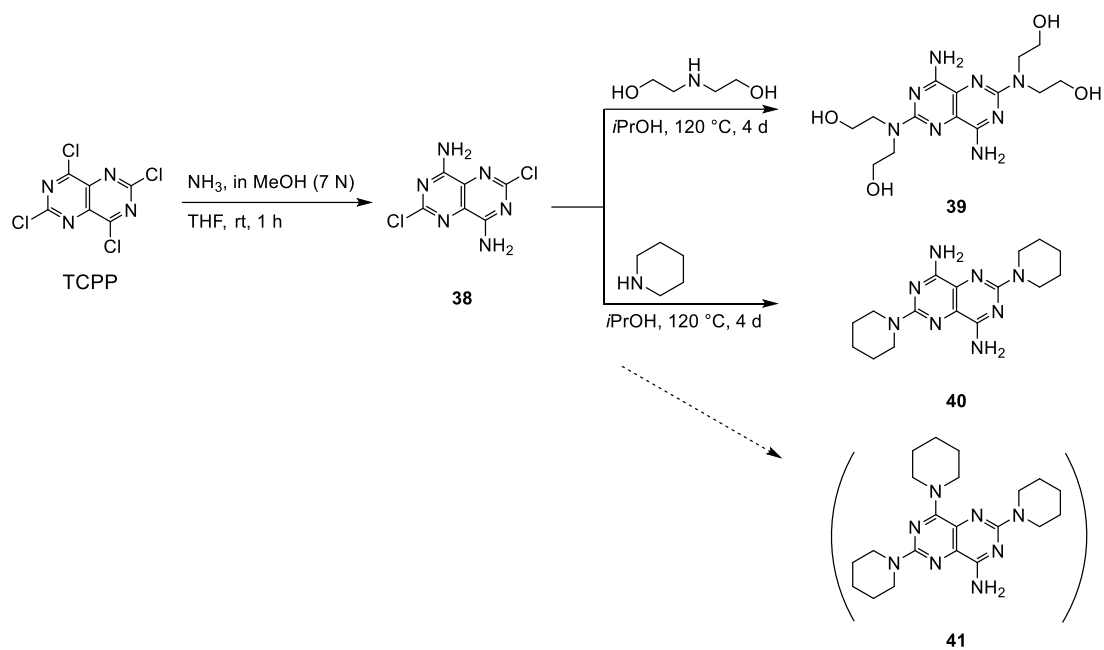


Scheme 21. Synthesis of **9** using the side product **36**.

4.4.3.5. Synthesis of 4,8-bis(amino)-2,6-dichloropyrimido[5,4-d]pyrimidine-derivatives

One approach towards SAR exploration was to reduce the size of specific moieties of the lead structure. In this trial, the residues at C4 and C8 were supposed to be reduced to simple NH_2 groups in order to probe the necessary size of substituents at C4/C8.

While the introduction of amino groups in the 2/6-position of the pyrimido[5,4-d]pyrimidine scaffold was reported to be very difficult, they can be easily introduced at C4/C8.²⁰ Therefore, ammonia, (7 N) dissolved in MeOH, was added to a solution of TCPP in THF at rt to prepare **38**. The solvent was subsequently removed under reduced pressure, and the residue was suspended in water and filtered off. The desired compound was obtained in excellent yield (95%). As illustrated in Scheme 22, **38** was subsequently used to prepare **39** and **40** by reacting the compound with diethanolamine or piperidine employing the established method.^{10;16;17} Purification by column chromatography (CH_2Cl_2 / MeOH - 9 : 1) led to the final products that were obtained in good yield (63% each).



Scheme 22. Synthesis of **39** and **40**.

Interestingly, all three compounds bearing free amino groups in the 4/8 position suffer from solubility problems in all used solvents, although one would expect that less lipophilic structures would enhance the solubility at least in polar solvents. During the synthesis of **40**, the side product **41** was isolated but not fully characterized. Nevertheless, it was submitted to biological testing anyway.

4.4.3.6. Synthesis of 4,6,8-tripiperidinopyrimido[5,4-d]pyrimidine derivatives (variation of R²)

Interim results showed, that compound **4** was comparably potent (EC₅₀ 28 μM) as dipyridamole and is thus an interesting starting point for further modification. Therefore, 3 substituents (at C4, C6 and C8) will be kept constant as piperidine and the fourth position will be varied with various carefully selected moieties. Especially polar moieties would be interesting since the overall scaffold is very lipophilic and might suffer from low solubility in water. Figure 5 illustrates all planned residues for the R² moiety.

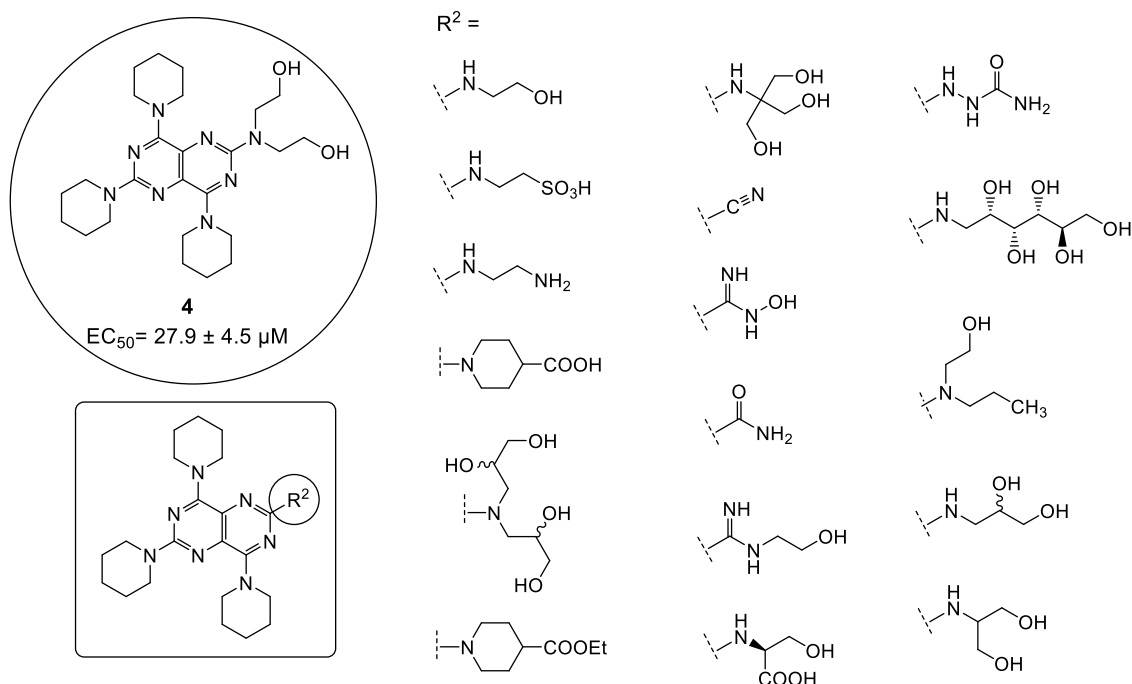
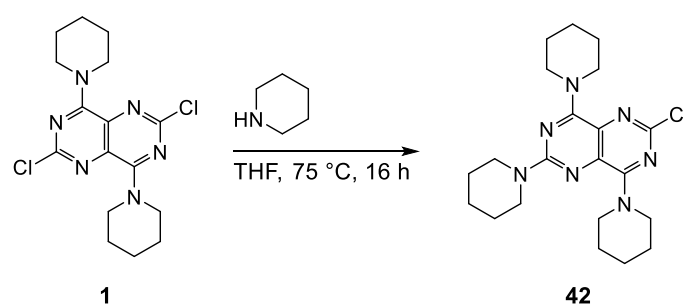


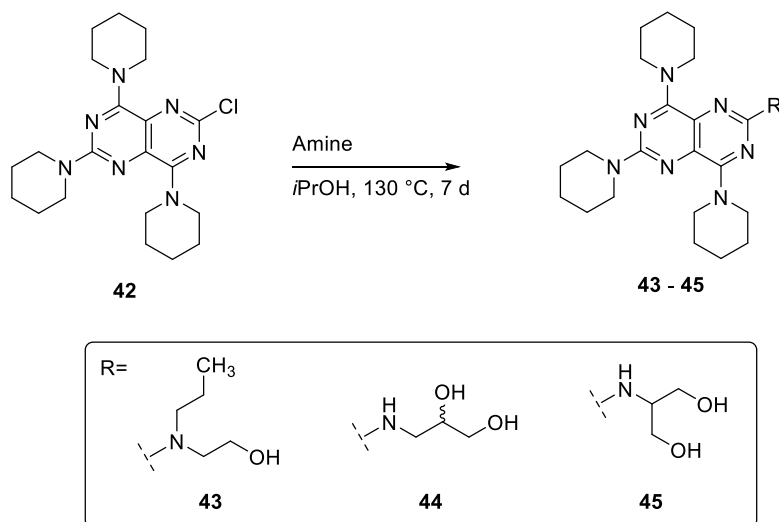
Figure 5. Planned structures: 4,6,8-tripiperidinopyrimido[5,4-d]pyrimidine derivatives with varied residues at R²

Initially, compound **42** that exhibits the 3 piperidine residues in the desired positions, and a chlorine atom at position 2 that can be substituted by various nucleophiles (cf. Scheme 23), was to be prepared.



Scheme 23. Synthesis of **42**.

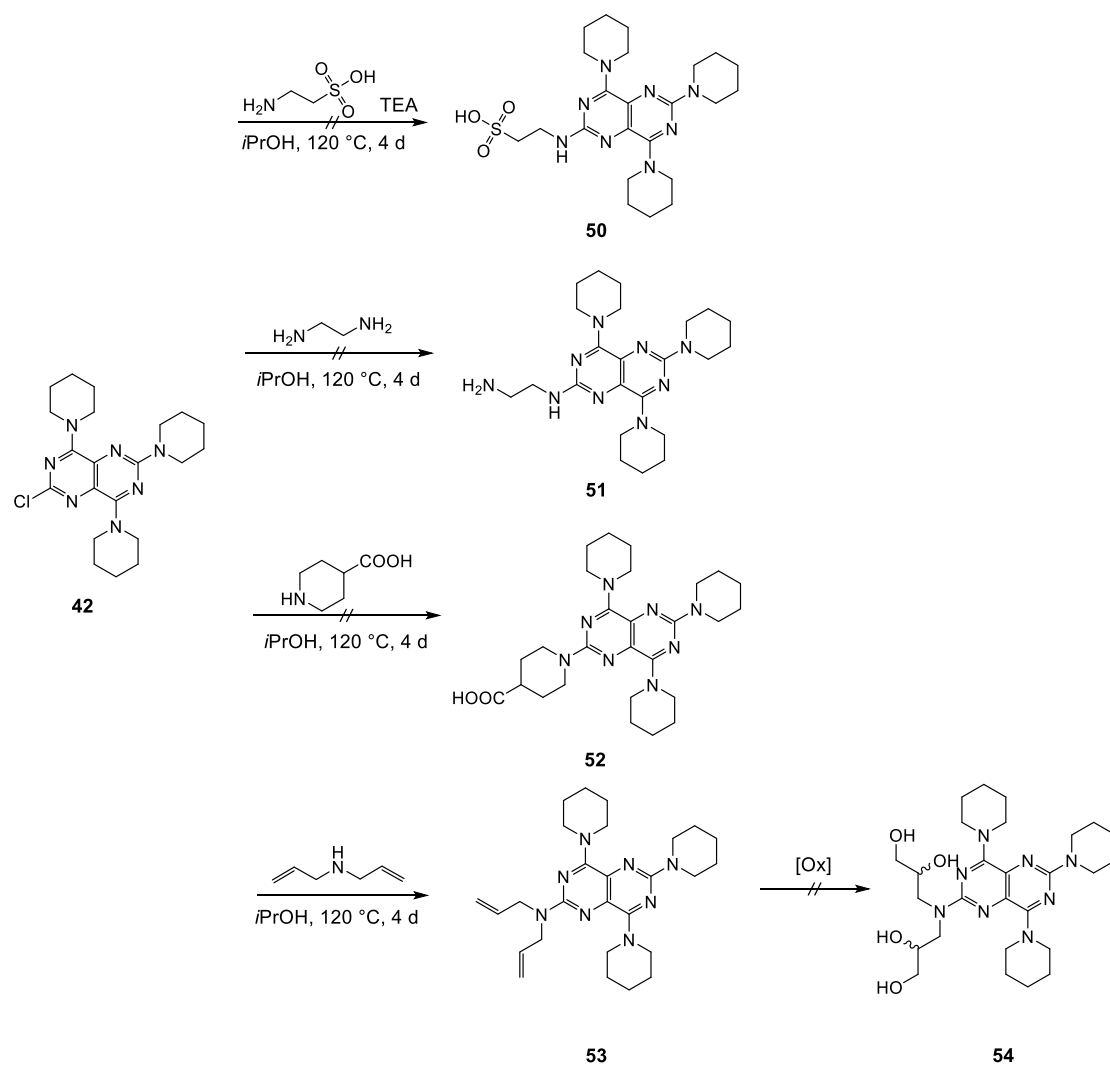
The reaction was performed employing the established method. The product was purified by column chromatography and could be isolated in excellent yield (96%) and purity (93%). Most of the chosen amines were tried to be reacted with **42**. However, this attempt did not work out for all reagents. Scheme 24 illustrates the successful trials.



Scheme 24. Synthesis of **43**, **44** and **45**.

The amines *N*-propylethanolamine, 3-aminopropane-1,2-diol and 2-aminopropane-1,3-diol could be reacted with **42** utilizing the standard procedure.^{10;16;17} The reactions led to the products **43** (35%), **44** (15%) and **45** (24%) in low to moderate yields. The compounds could all be purified by column chromatography (CH₂Cl₂ / MeOH - 9 : 1).

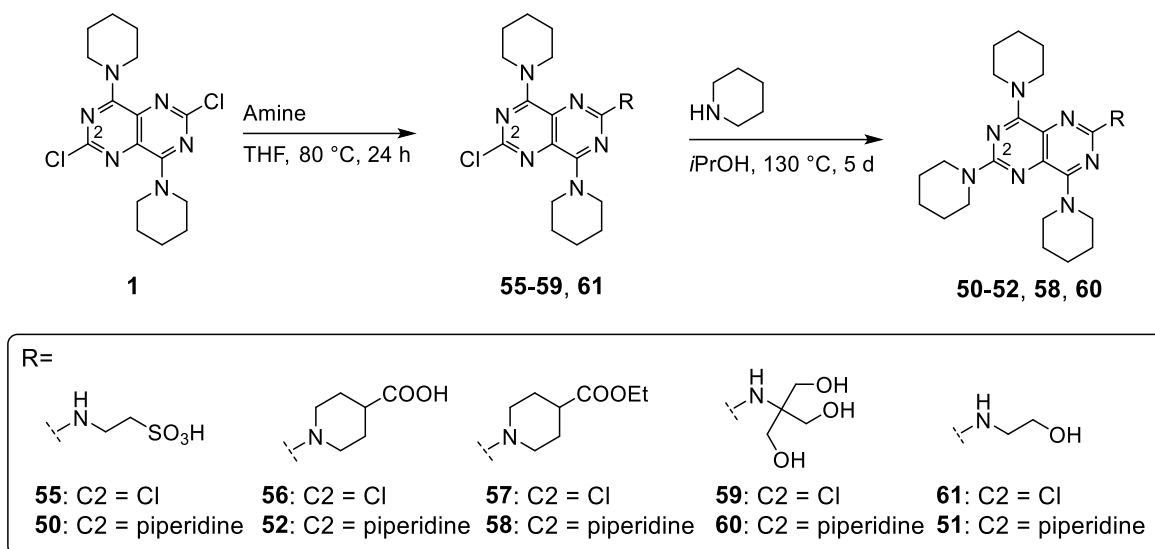
The formation of **46** was readily possible with **42** as a starting point since the cyanide ion is a suitable nucleophile even for the difficult fourth substitution step (58% yield). DMSO was utilized as a solvent due to limited solubility of the precursor (cf. Scheme 25).²¹



Scheme 26. Attempted synthesis of **50-54**.

In case of **53**, the product could be obtained; a subsequent epoxidation using MCPBA resulted in numerous side products, none of them being the desired intermediate or final product.

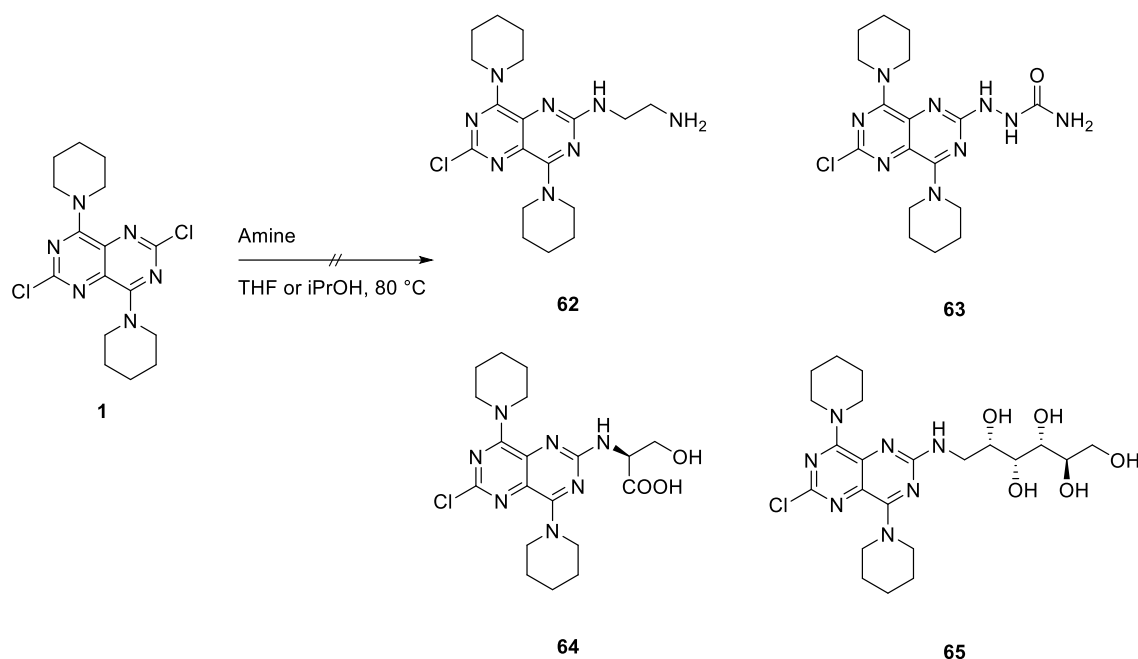
In order to obtain the desired products, the new polar moiety is firstly introduced as the third substituent, starting from **1**. This step is easier for less nucleophilic amines. Subsequently, piperidine will be introduced as a final substituent. The reaction with piperidine as a fourth substituent has proven to be feasible.



Scheme 27. Synthesis of **50-52** and **55-61**.

In case of **50** (taurine), **52** (4-piperidinecarboxylic acid), **58** (4-piperidinecarboxylic acid ethyl ester), **60** (tris(hydroxymethyl)aminomethane) and **51** (ethanolamine) the altered synthetic route starting from **1** worked out well. The reaction of **1** with an excess of the respective amine in THF at moderate temperature (80 °C) led to the trisubstituted intermediates **55-59** and **61** illustrated in Scheme 27. These intermediates were subsequently reacted with an excess of piperidine. Elevated temperature (130 °C at least) and a long reaction time of up to 5 days led to the final products in moderate yields. Extraction and column chromatography was needed to isolate the desired compounds **50-52**, **58** and **60**.

However not all reactions using that route were successful. In case of the planned compounds **62-65**, the reactions failed (cf. Scheme 28). The reagents *L*-serine, *D*-glucamine and semi carbazide were poorly soluble in THF and *i*PrOH and thus unreactive while reaction with ethylenediamine led to many side products.



Scheme 28. Attempted synthetic attempts to prepare **62-65**.

4.4.3.7. Attempted syntheses of 2-[bis(2-hydroxyethyl)amino]-4,8-di(piperidin-1-yl)pyrimido[5,4-*d*]pyrimidin derivatives (variation of R⁴)

On the basis of intermediate test results, **4** was selected to be further modified (see 4.4.3.6.). The idea was to leave three substituents of the molecule constant and to vary one substituent. Three products were planned with R² being the polar residue diethanolamine, R¹ and R³ being piperidine combined with different lipophilic residues for R⁴:

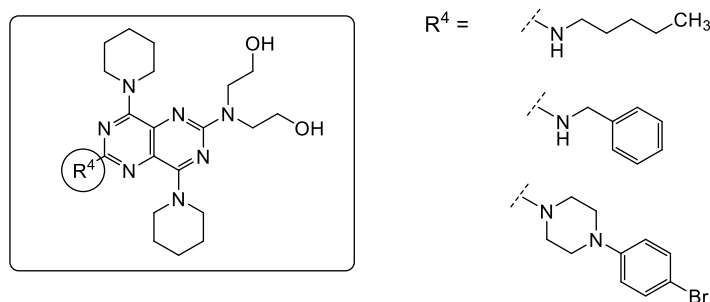
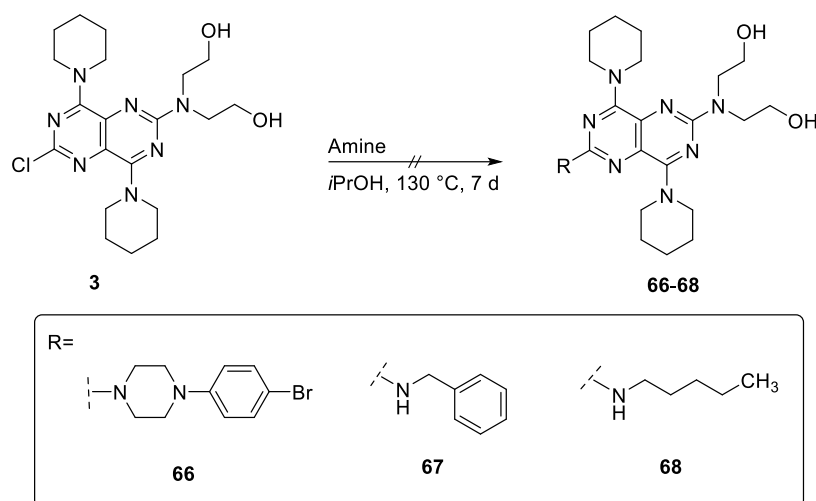


Figure 6. Planned structures of 2-[bis(2-hydroxyethyl)amino]-4,8-di(piperidin-1-yl)pyrimido[5,4-*d*]pyrimidin derivatives

The obvious strategy to synthesize the 2-[bis(2-hydroxyethyl)amino]-4,8-di(piperidin-1-yl)pyrimido[5,4-*d*]pyrimidin derivatives is to react **3** with the appropriate amines, 1-(4-bromophenyl)piperazine, benzylamine and pentylamine (cf. Scheme 29). However, none of the reactions was successful. The product could either not be isolatable due to too many side products (**67** and **68**) or only unreacted starting material was obtained (**66**).



Scheme 29. Attempted synthesis of **66-68**.

It might have been a better approach to start from **1** and introduce the varied residue at the beginning, as the “third substituent” since the reaction conditions for this step are not as harsh. The diethanolamine moiety would be introduced subsequently as the last reaction step.

4.4.3.8. Synthesis of 2,6-bis[bis(2-hydroxyethyl)amino]-4-piperidinopyrimido[5,4-*d*]pyrimidine derivatives (variation of R³)

The screening of an independent library of 2,4,6,8-tetrasubstituted pyrimido[5,4-*d*]pyrimidines revealed several hits with diverse substitution patterns and substituents.²² A pattern that delivered many good compounds was R² and R⁴ being diethanolamine (-derivatives), R¹ being a comparably small substituent and R³ being diverse. Figure 7 illustrates a new scaffold based on these findings. It was decided to leave R¹ as piperidine and R² = R⁴ = diethanolamine. R³ was planned to be modified with substituents of different sizes (cf. Figure 7).

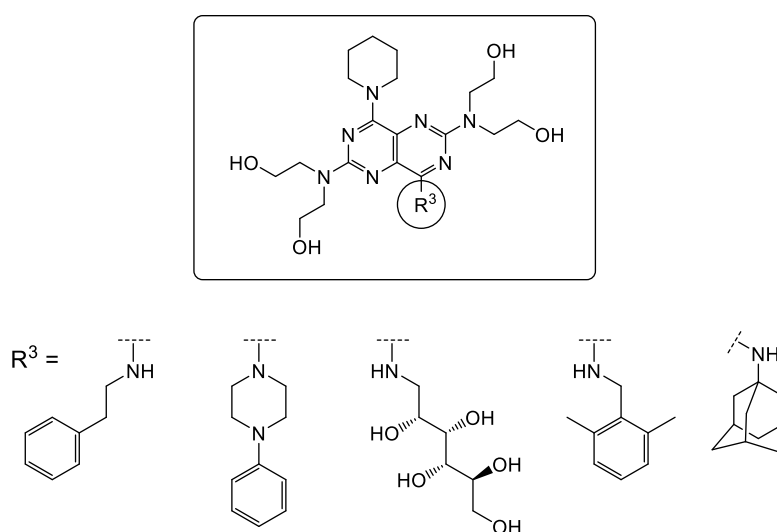
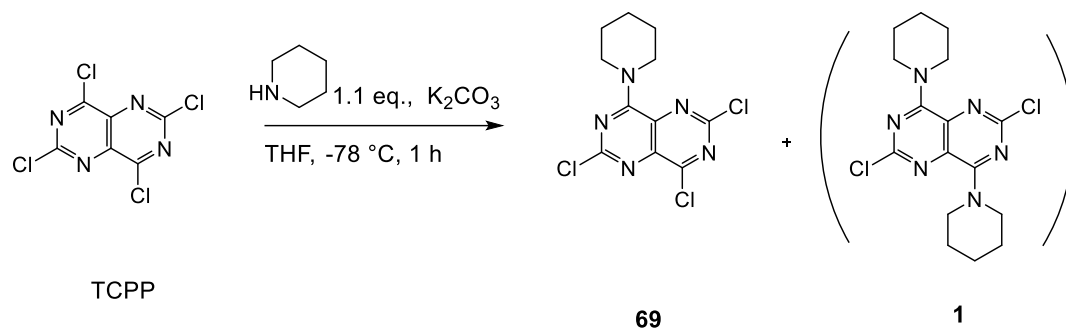


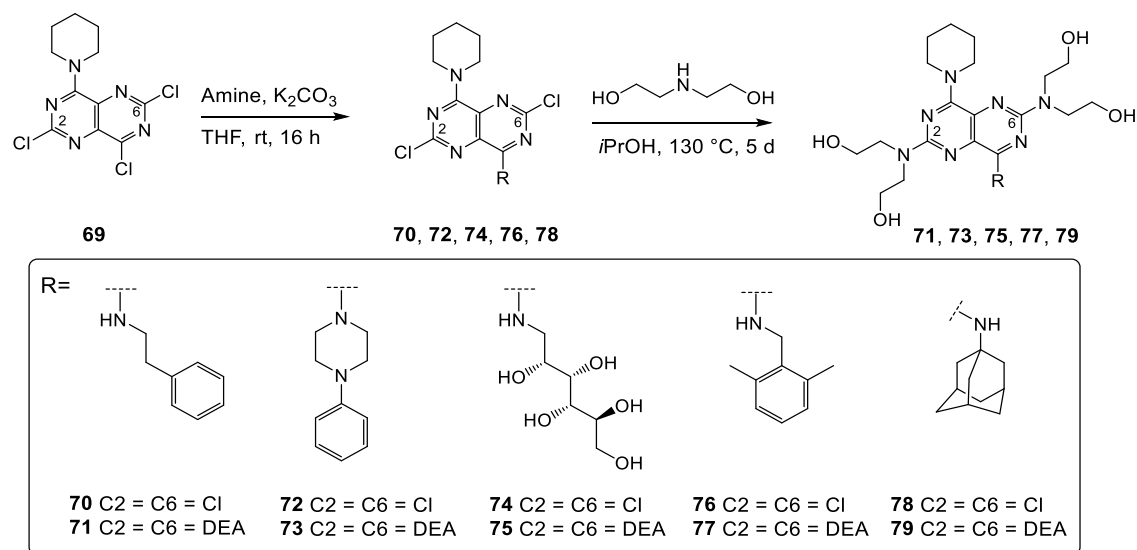
Figure 7. Planned structures of 2,6-bis[bis(2-hydroxyethyl)amino]-4-piperidinopyrimido[5,4-*d*]pyrimidine derivatives

In order to selectively modify R¹ and R³ of the 2,4,6,8-tetrasubstituted pyrimido[5,4-*d*]pyrimidine scaffold with different substituents, a different reaction sequence than used before needed to be exploited. Firstly, piperidine was introduced as first substituent at R¹. Therefore, a diluted solution of 1.1 eq. piperidine in THF was added to a -78 °C cold, highly diluted solution of TCPP and K₂CO₃ in THF. The resulting mixture of unreacted TCPP, the desired monosubstituted intermediate **69** and the disubstituted side product **1** were subsequently separated by column chromatography.



Scheme 30. Synthesis of **69**.

The second reaction step was the introduction of the variable substituents at the R³ position:



Scheme 31. Synthesis route of **71**, **73**, **75**, **77** and **79**.

The appropriate amines (2-phenylethylamine, *N*-phenylpiperazine, *D*-glucamine, 2,5-dimethylbenzylamine or 1-adamantidylamine, respectively) were added to **69** at rt and the mixture was stirred overnight in THF in presence of a base affording the intermediates **70**, **72**, **74**, **76** and **78**. Strong heating with a large excess of diethanolamine eventually afforded the desired final products **71**, **73**, **75**, **77** and **79**. All of them were isolated using RP flash HPLC (water / MeOH). This synthetic route was successful providing good yields.

4.4.3.9. Separation and purification products

Mixtures like TCPP, **69** and **1** were hard to separate, since all of the compounds are poorly water-soluble and lipophilic exhibiting very similar properties on TLC and column chromatography. Typical solvents would not lead to appropriate separation of compound mixtures as illustrated in Figure 8. RP chromatography was not possible due to limited solubility in water. This constituted a problem, since the synthesis of a particular compound of the depicted derivatives was often accompanied by the formation of side products.

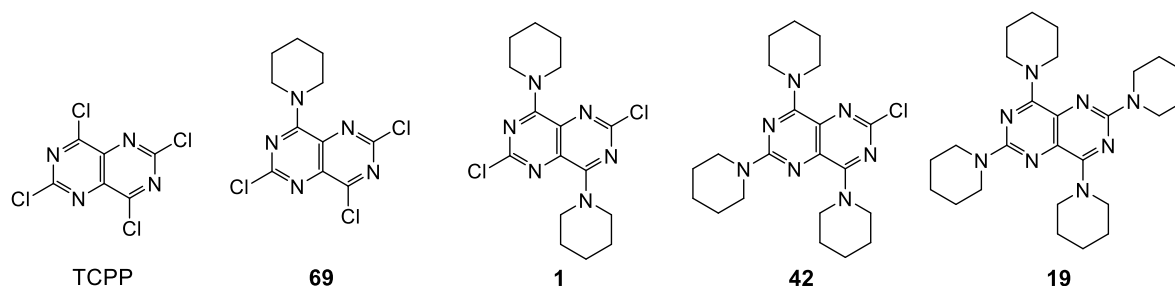


Figure 8. Structures of TCPP and its piperidine-derivatives **69**, **1**, **42** and **19**.

However, the following strategy led to successful separation: All compounds are similarly lipophilic, the only noteworthy difference between them are the numbers of nitrogen atoms. Although none of the structures is particularly basic, the addition of acid to the solvent used for chromatography will affect their polarity due to protonation. Using the solvent combination petrolether / ethyl acetate - 10 : 1 + 1% acetic acid made separation possible. Thereby, higher substituted derivatives were more polar and stayed longer on the silica gel phase. In literature, reactions were often performed with impure compounds due to separation issues. The developed new procedure is therefore very helpful.

4.4.3.10. Upscaling of the synthesis of **82**

One of the potent MRGPRX3 agonists, **82**, was selected for upscaling to be used as a standard agonist and the antagonist screening. Compound **82** was chosen due to its good chemical accessibility (see Figure 9).

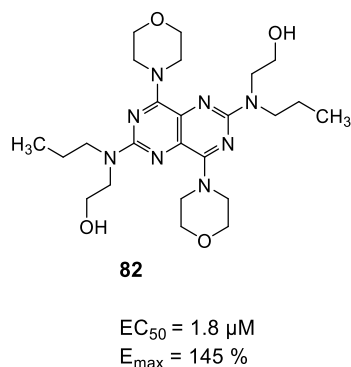
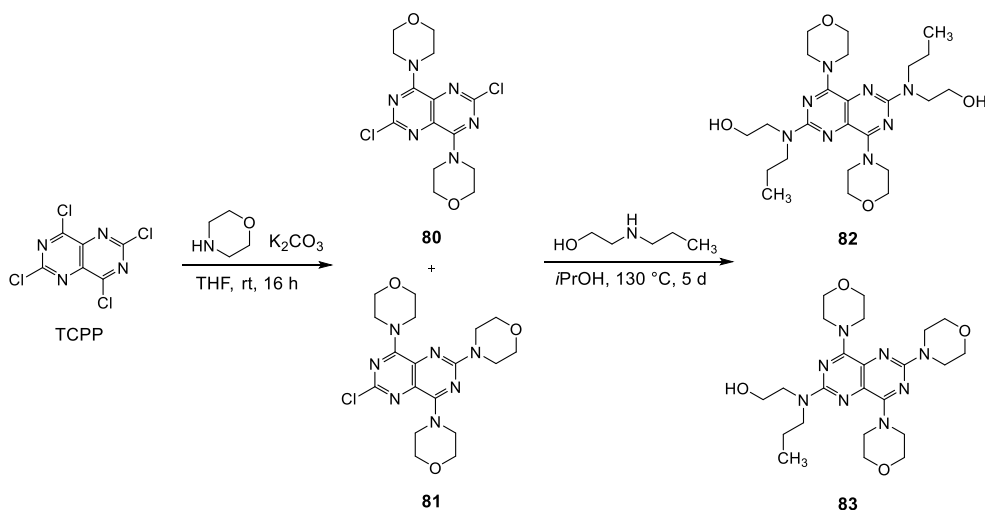


Figure 9. Biological activity compound **82**.

The synthesis of **82** followed the classic route of ABAB-substituted pyrimido[5,4-*d*]pyrimidines like dipyridamole.^{10;16;17} TCPP was treated with morpholine and K_2CO_3 as a base at rt in THF for 16 h to form **80**. Surprisingly, the trisubstituted side product **81** was formed as well (cf. Scheme 32). Both compounds were separated and isolated by column chromatography.



Scheme 32. Synthesis of **82** and **83**.

Both intermediates were subsequently heated with an excess of *N*-propylethanolamine for 5 days to form the final products **82** and **83**, which were purified using RP flash HPLC (water / MeOH). Both compounds could be obtained in good yields. The unplanned side product **83** is very interesting due to the resemblance to **4** which had been selected as a lead structure.

4.4.3.11. Synthesis of 2,6-bis[bis(2-hydroxyethyl)amino]-4-benzylthiopyrimido[5,4-d]pyrimidine derivatives (different amines at R³)

Substitution with a benzyl thiol residue at the R¹ position (with R² = R⁴ = diethanolamine) led to several potent compounds in the independent library.²² Hence, this substitution pattern was supposed to be used as a basis for new compounds. Thereby, R³ is substituted with different amines of varying size and degree of substitution. Figures 10 and 11 illustrates the planned molecules.

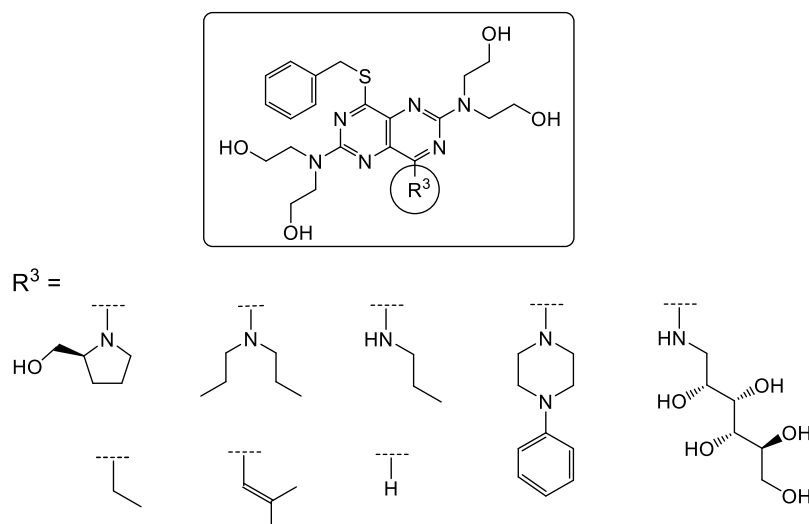


Figure 10. Planned structures with different residues at R³.

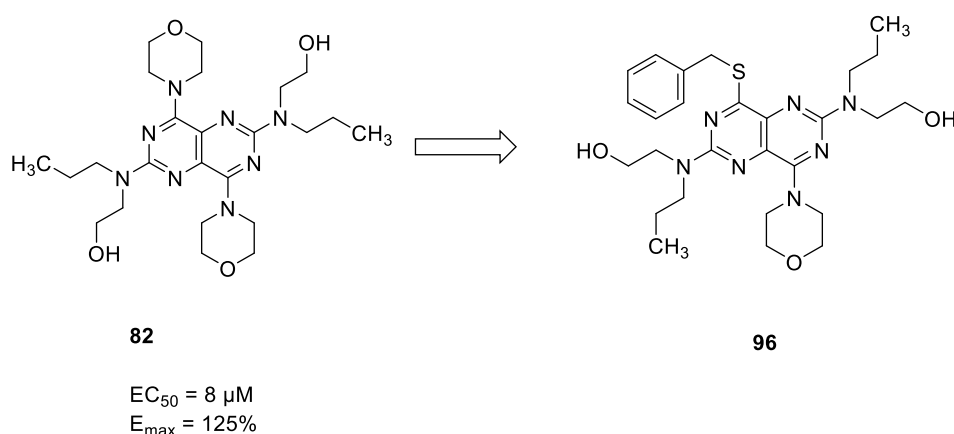
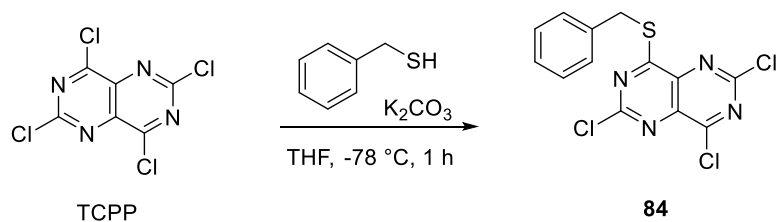


Figure 11. Planned compound **96** is based on the activity of **82**.

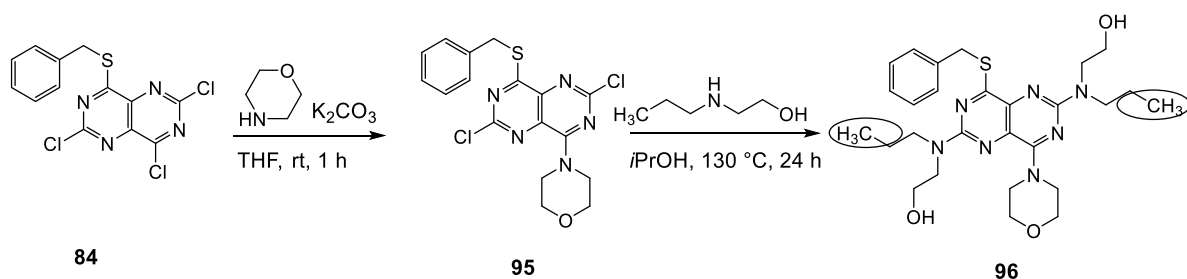
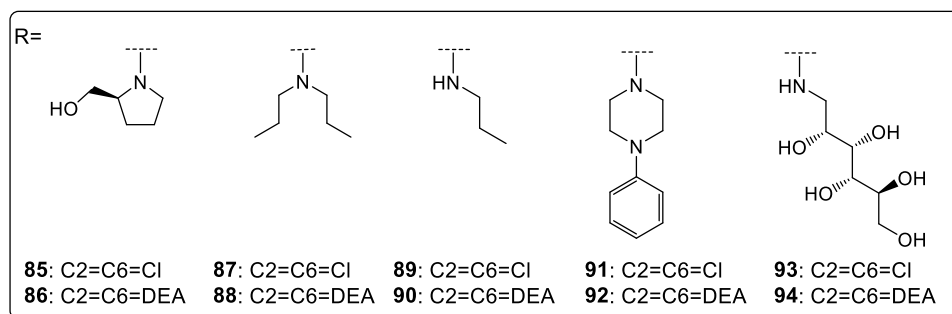
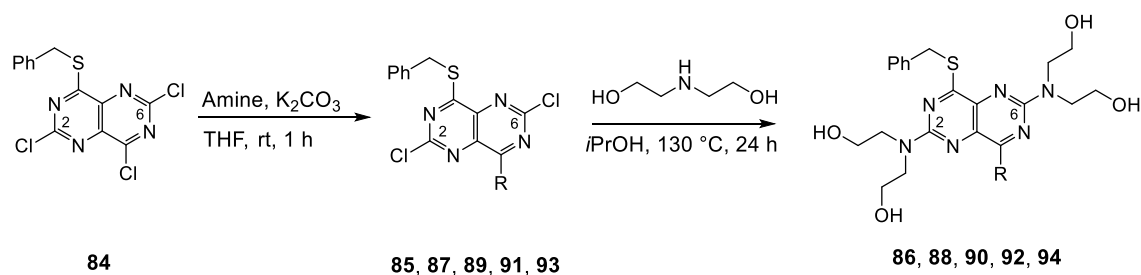
The planned compound in Figure 11 is based on the potent MRGPRX3 agonist **82**. It can be expected, that this compound will be one of the best since it combines the best substituents that are known so far. Also, the combination of a thiol at R¹ and an alkyl group at R³ or no substituent at all (R³ = H) would be interesting. In all cases except for **96**, diethanolamine was to be left at R² and R⁴ due to its beneficial effect on the solubility of the compounds.

For this particular substitution pattern, a reaction sequence was used that was established for the synthesis of the corresponding 2,6-bis[bis(2-hydroxyethyl)amino]-4-piperidino-pyrimido[5,4-*d*]pyrimidine derivatives (see 4.4.3.8.). Following this approach, benzyl thiol was introduced as a first substituent as R¹. A diluted solution of 1.1 eq. benzyl thiol in THF was added to a -78 °C cold, strongly diluted solution of TCPP and K₂CO₃ in THF. The resulting mixture of unreacted TCPP, the desired monosubstituted intermediate **84** and the disubstituted side product were subsequently separated by column chromatography.



Scheme 33. Synthesis of **84**.

The second reaction step was the introduction of the variable substituents at the R³ position:



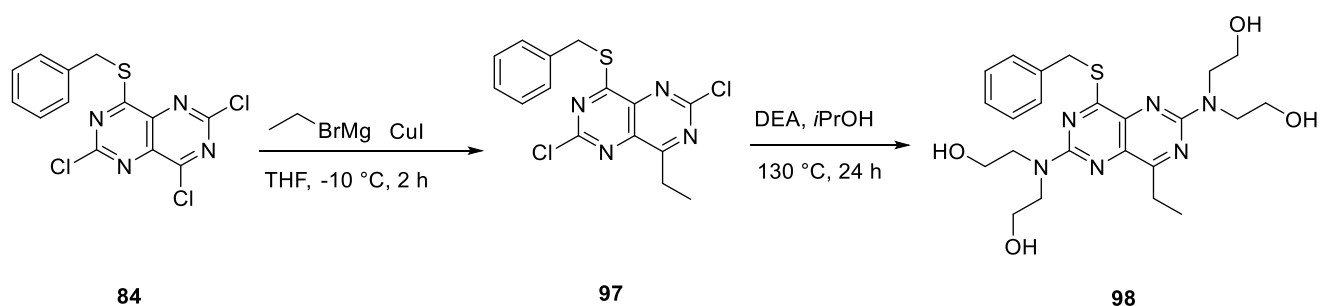
DEA = diethanolamine

Scheme 34. Synthesis of **86, 88, 90, 92, 94** and **96**.

The appropriate amines (*L*-prolinol, dipropylamine, propylamine, 1-phenylpiperazine and *D*-glucamine, respectively) were added to **84** at rt, and the mixture was stirred for one hour in THF in the presence of a base. Strong heating with a large excess of diethanolamine (*N*-propylethanolamine in case of **96**) led to the desired final products **86**, **88**, **90**, **92** and **94**. All of them were isolated using RP flash HPLC (water / MeOH). This synthetic route was straightforward resulting in moderate to good yields. In case of **94**, the desired compound was not formed, only the intermediate **93** could be detected. The disubstituted intermediates were obtained after only one hour, and the final products were formed after only 24 h. Typically, the last reaction step had taken at least 3 days for analogue. Apparently, the sulfur-containing substituent for R¹ enhances the reactivity of the remaining chlorine atoms which become more susceptible to nucleophilic substitution.

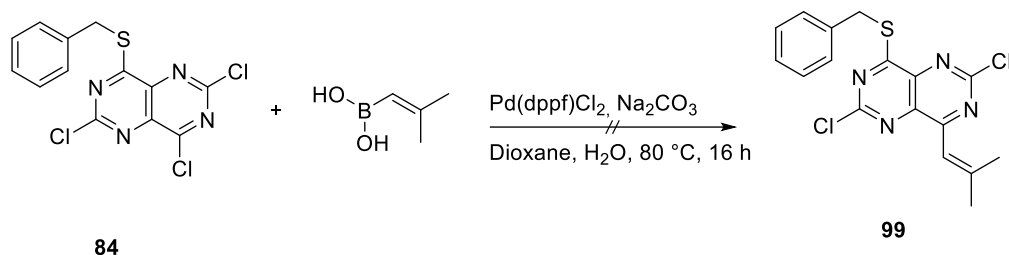
4.4.3.12. Synthesis of 2,6-bis[bis(2-hydroxyethyl)amino]-4-benzylthiopyrimido[5,4-*d*]pyrimidine derivatives (alkyl residues and H for R³)

A number of attempts were made to introduce various substituents to the pyrimido[5,4-*d*]pyrimidine core by methods other than simple nucleophilic substitution. Scheme 35 illustrates an attempted synthesis employing the Grignard reaction. Ethylmagnesium bromide and Cu(I) as a catalyst were used to introduce an ethyl residue at the R³ position.²³ However, a complex mixture of product (**97**) and side products were obtained. This crude mixture was reacted with diethanolamine expecting that the final product might be easier to isolate than the intermediate. As a result, only 8.5% of **98** was found by LC-MS analysis, and the product was not isolated due to the obtained complex mixture.



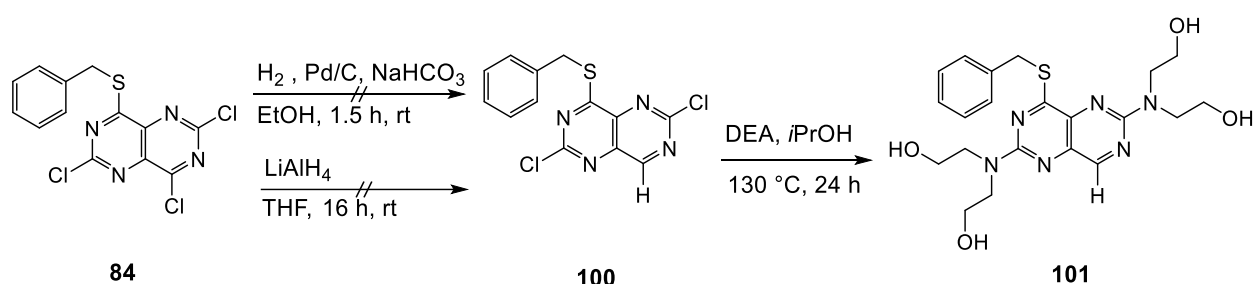
Scheme 35. Attempted synthesis of **98**.

A different approach was a Suzuki type reaction. 2,2-Dimethylethenylboronic acid and the catalyst Pd(dppf)Cl₂ were utilized (cf. Scheme 36). However, an LC-MS analysis of the crude mixture did not show the mass of the desired compound.²⁴



Scheme 36. Attempted synthesis of **99**.

Next, the replacement of the chlorine atom at position 3 with a hydrogen atom was investigated (cf. Scheme 37). Hydration with hydrogen gas under Pd-catalysis²⁵ and reaction with LiAlH₄ in THF were tried, however the desired product **100** could not be obtained.



Scheme 37. Attempted synthesis of **101**.²⁵

4.4.3.13. Attempts to replace hydroxyl groups by amino groups

Another idea was to exchange the OH groups of dipyrnidamole with NH₂ groups. These would be positively charged at physiological pH value and hence would offer a very different kind of interaction with target proteins. Moreover, water-solubility would be enhanced. Figure 12 illustrates potential examples.

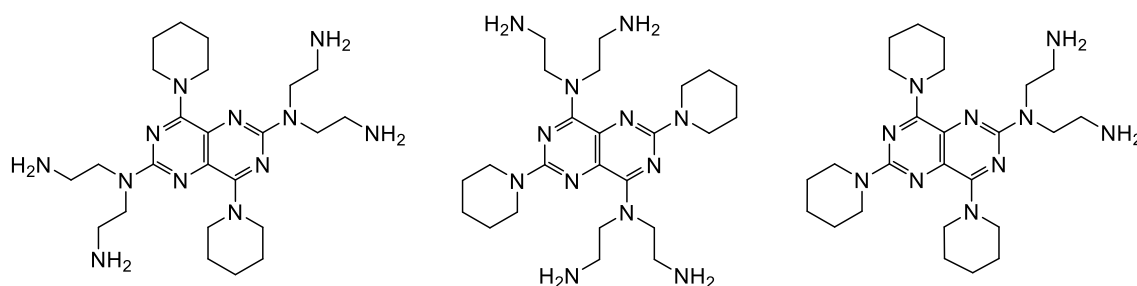
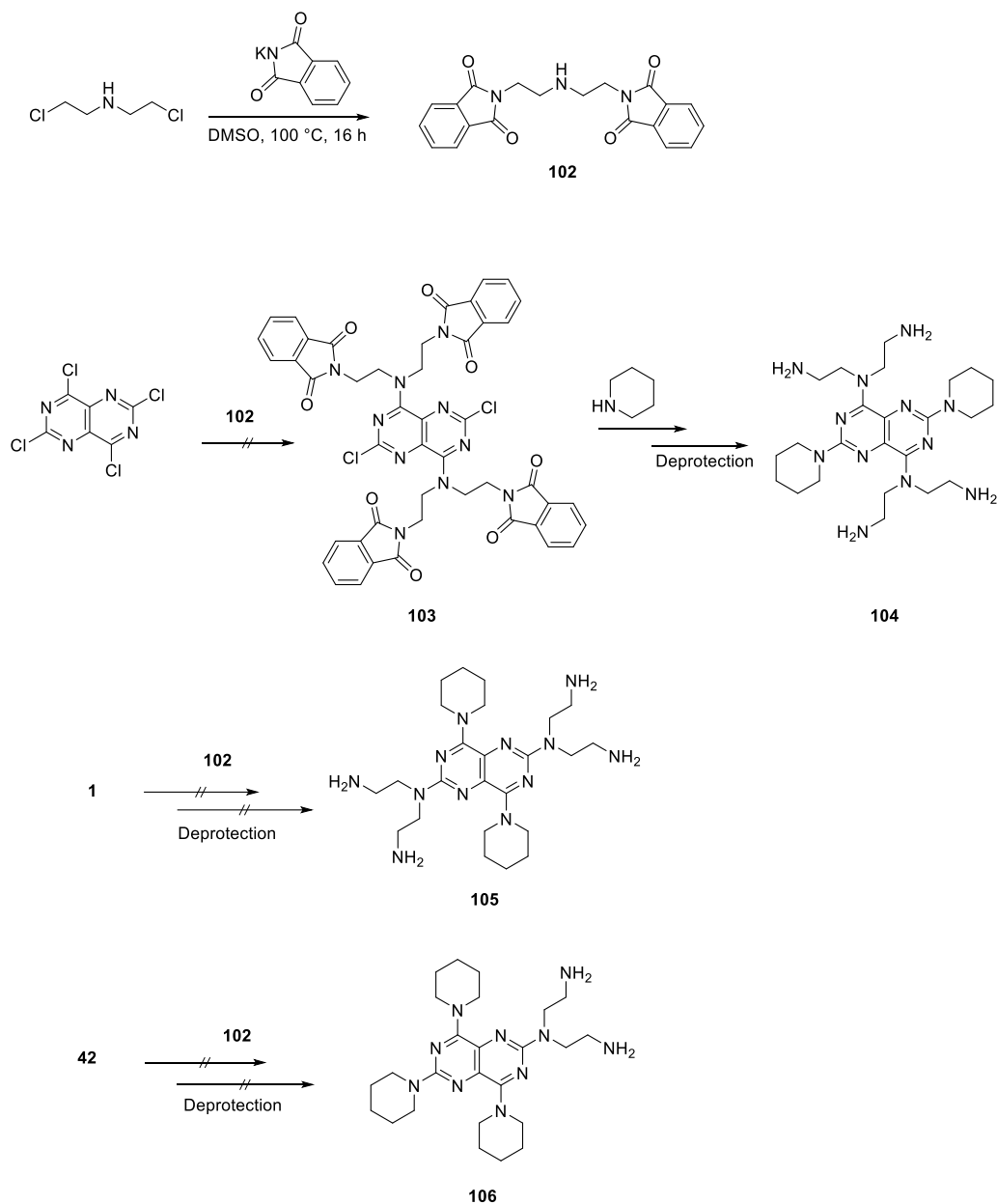


Figure 12. Amino-derivatives of dipyrnidamole, **31** and **4**.

In order to synthesize such compounds, a protection group strategy is necessary. Three free amino groups (like the reagent bis(2-aminoethyl)amine exhibits) would lead to mixed products and hence was not suitable. Therefore, the protected compound **102** was prepared as depicted in Scheme 38:



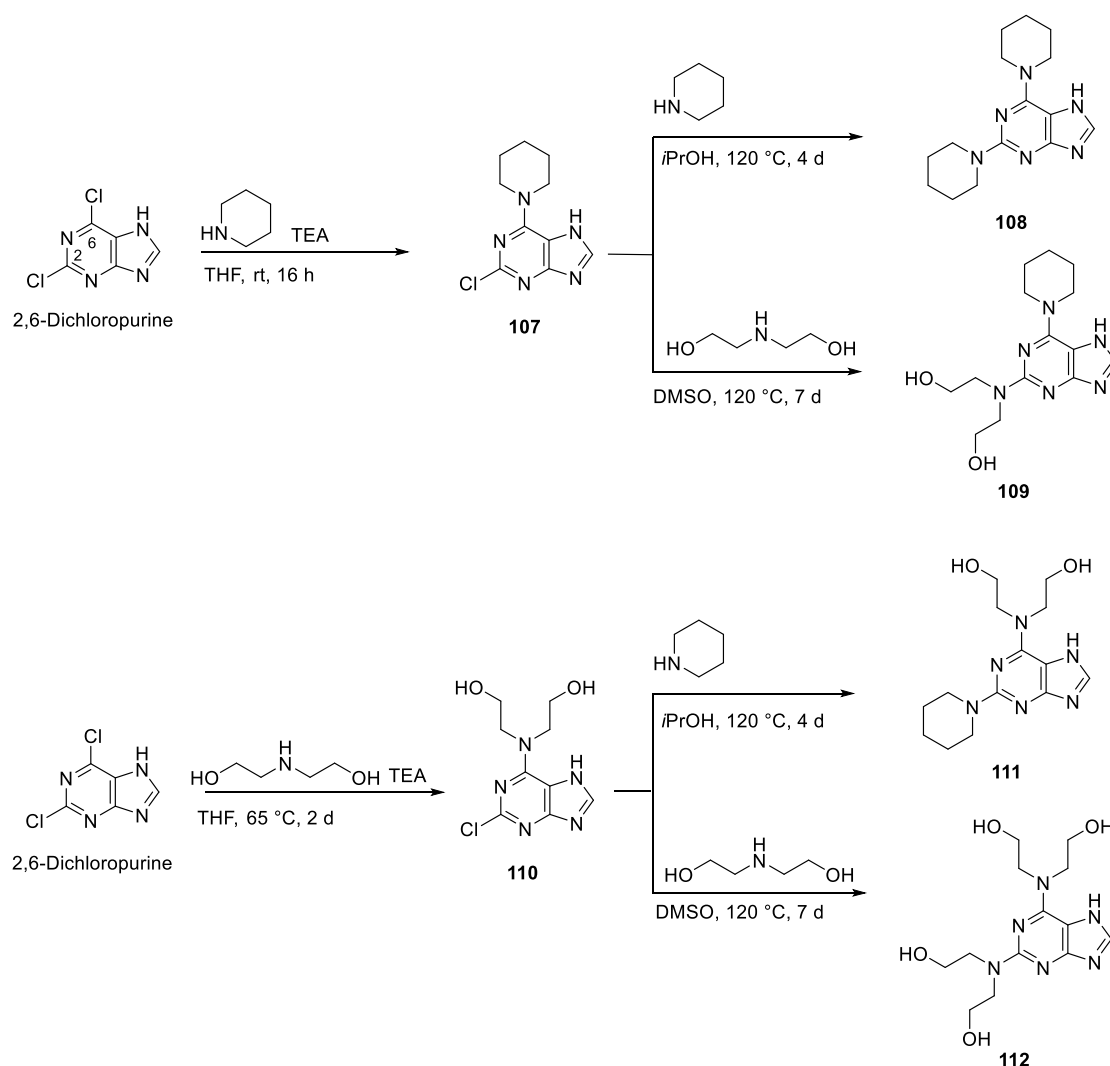
Scheme 38. Attempted syntheses of amino substituted analogs of dipyrnidamole.

Bis(2-chloroethyl)amine hydrochloride was reacted with potassium phthalimide under elevated temperatures in DMSO to afford **102**. This building block was tried to be reacted with small amounts of TCPP, **1** and **42** employing different solvents (*i*PrOH, DMSO, THF). The potential products were supposed to be subsequently deprotected. In every case, **102** was not soluble and the reactions resulted in unreacted starting material or unidentified side products.

All in all, 40 compounds based on the pyrimido[5,4-*d*]pyrimidine scaffold could be isolated and submitted to biological testing.

4.4.3.14. Synthesis of purine derivatives

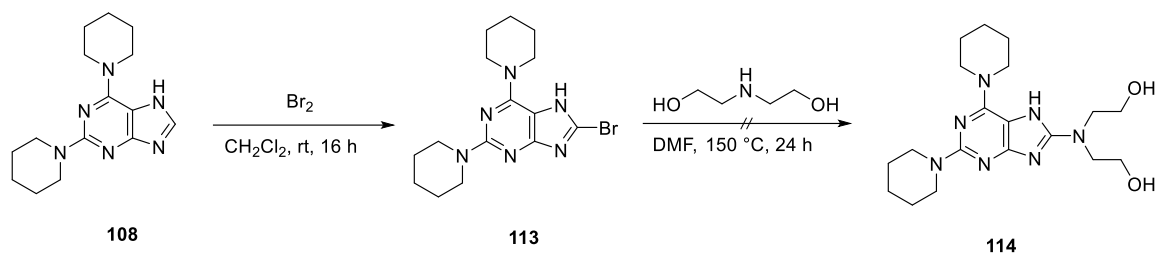
The reactivity of 2,6-dichlorpurine (DCP) is quite similar to that of TCPP: While C6 is very reactive towards nucleophiles (readily reacting at rt), the C2 position needs the same harsh conditions as TCPP to react in substitution reactions (several days at 120 °C with excess of amine). With these established conditions, the 4 illustrated compounds **108**, **109**, **111** and **112** were prepared (cf. Scheme 39).³²



Scheme 39. Synthesis of 2,6-disubstituted purine derivatives.³²

It needs to be noted, that again the reactions involving diethanolamine (particularly the preparation of **110**) took comparably longer and sometimes even needed heating. All reactions with piperidine as nucleophile went very well. For the substitution at C2, DMSO was chosen as solvent due to solubility problems with *i*PrOH.

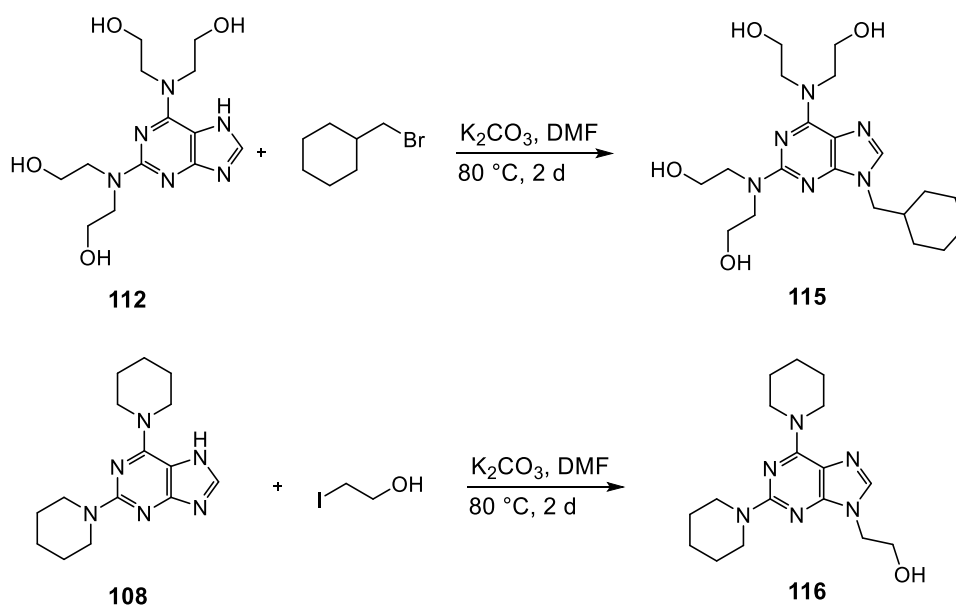
In order to be able to attach more substituents to the purine scaffold, it was tried to brominate the 8-position and to subsequently introduce amines via substitution reactions (cf. Scheme 40).



Scheme 40. Attempted synthesis of **113** and **114**.³²

Compound **108** was treated with bromine at rt and the mixture was stirred overnight. The correct mass of the desired product **113** could be found by MS, however, the compound could not be isolated since the bromination was accompanied by many side reactions. A trial to react impure **113** with diethanolamine resulted in unreacted starting material and unclear products. Hence, this attempt was stopped.

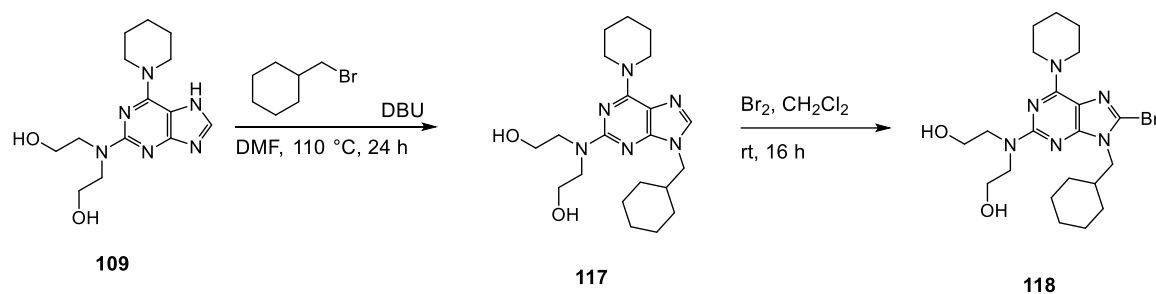
Another, more straightforward reaction step was alkylation at the N9-position.³² Methylcyclohexyl- and ethanoly- residues were selected as substituents to simulate the building blocks piperidine and diethanolamine.



Scheme 41. Synthesis of **115** and **116**.³²

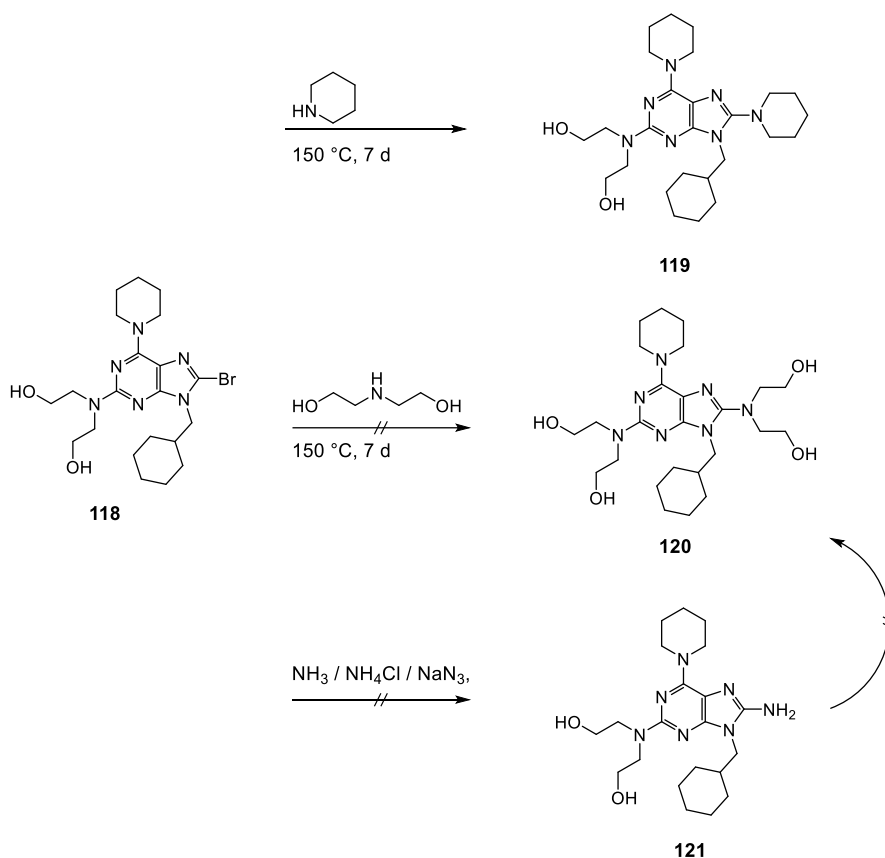
Standard conditions for nucleophilic substitution (K_2CO_3 as a base, DMF as solvent, moderate temperature) were applied for reacting **112** with (bromomethyl)cyclohexane affording **115**, and **108** with 2-iodoethanol affording **116**. The products were obtained in moderate yields, a lot of starting material remained unreacted even with an excess of alkyl halogenides and long reaction times.

For the preparation of **118**, **109** was reacted with (bromomethyl)cyclohexane. Reaction conditions were altered to improve the yield, however only a slight improvement could be observed (cf. Scheme 42). Subsequent bromination of the C8 position using Br₂ in CH₂Cl₂ yielded **117** in moderate yield (58%). This compound was supposed to be further functionalized at C8.



Scheme 42. Synthesis of **118**.³²

A substitution reaction of **118** using the appropriate amine as a solvent was planned to lead to the final 2,6,8,9-tetrasubstituted purine derivatives **119** and **120** (cf. Scheme 43).³²



Scheme 43. Synthesis of **119** and attempted synthesis of **120**.³²

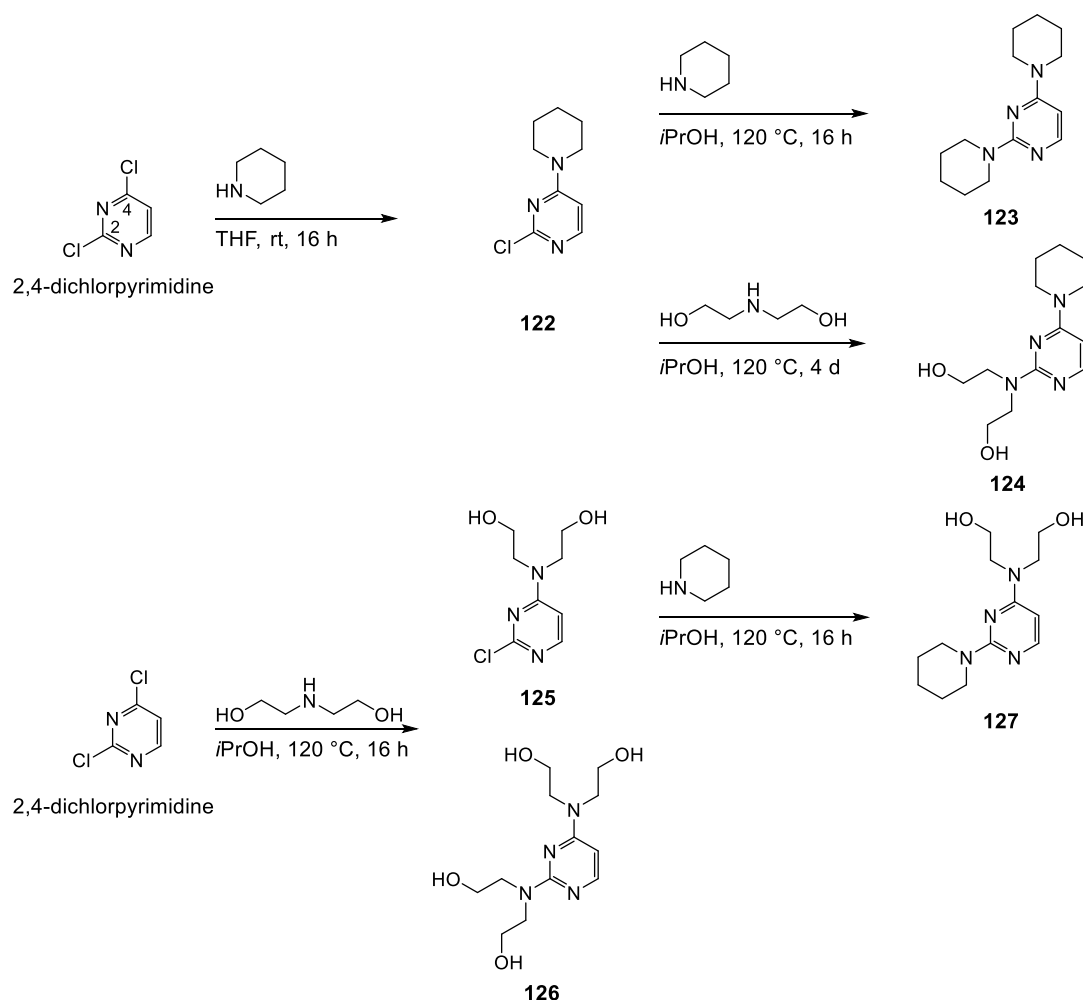
In case of **119**, the desired compound could be obtained after several purification steps using column chromatography. However, the compound **120** could not be obtained. Even after very

harsh reaction conditions, only unreacted starting material was found. Different attempts to firstly introduce an amino group (via ammonia solution, ammonium chloride and base or sodium azide and subsequent reduction) to obtain **121** and subsequent reactions were made, all of them being unsuccessful. The use of microwave irradiation might lead to the desired compound.

Altogether, 8 different purine derivatives could be isolated, characterized and submitted to biological testing.

4.4.3.15. 2,4-Disubstituted pyrimidine derivatives

Based on 2,4-dichloropyrimidine, 4 compounds were synthesized similar to the purine derivatives. Again, the reactivity of the two chlorine atoms is comparable to that of TCPP: C4 is very reactive while C2 needs harsh conditions. Thus, the established synthetic routes could be utilized (cf. Scheme 44). Piperidine and diethanolamine were introduced either at both positions (**123** and **126**) or as combinations (**124** and **127**).³³



Scheme 44. Synthesis of 2,4-disubstituted pyrimidine derivatives **123**, **124**, **126** and **127**.³³

In comparison to the purines and pyrimido[5,4-*d*]pyrimidines, the pyrimidine derivatives were more reactive, and many reactions were completed after 16 h instead of 4 days. In case of the formation of **126**, it was directly tried to form the final product. Conveniently, after 16 h of reaction, **125** was detected by TLC analysis, and the reaction was stopped to isolate both the mono- and the disubstituted products. All other compounds were obtained stepwise using the established procedures as illustrated in Scheme 20. Only a small series of 4 compounds was prepared and submitted to biological testing.

4.4.3.16. Comments on the reactivity of the starting compounds

In theory, the scaffold based on TCPP should be reactive towards all kinds of nucleophiles. In many cases however, the employed amines did not react with TCPP and its derivatives. Especially the chlorine atoms at position 2 and 6 were often hard to substitute, and a large excess of reagent was needed to get satisfying results. For amines like piperidine, this is readily possible since it is a strong nucleophile by nature, and most importantly, it is a liquid. It can be used as a solvent, and applied in large excess. A look into the literature with regard to the synthesis of 2,4,6,8-tetrasubstituted pyrimido[5,4-*d*]pyrimidines reveals that nearly all of the employed nucleophiles were liquid at rt or reaction temperature.^{10;16-18} In case of the tris(hydroxymethyl)aminomethane building block that was used to prepare **60**, a solvent is needed for the reaction since the amine is a solid under the employed conditions. However, not all common solvent will dissolve enough of the reagent. On the other side, if too much solvent is used, the reagent is diluted so that the needed excess might be too small. Reagents like 4-piperidinecarboxylic acid form zwitterions. Thus, they need the addition of bases like K₂CO₃ which might again result in dilution with solvent and solubility problems due to the charge of the reagent. These facts make the utilization of solid reagents challenging in this reaction.

Furthermore, some nucleophiles like tris(hydroxymethyl)aminomethane or diethanolamine will form intramolecular hydrogen bonds between the nitrogen atoms and the OH groups. This phenomenon was discussed in the literature (cf. Figure 13).²⁶ Consequently, these aminoalcohols are less reactive because the free electron pair that is needed for nucleophilic attack is “blocked” by a hydrogen bond.

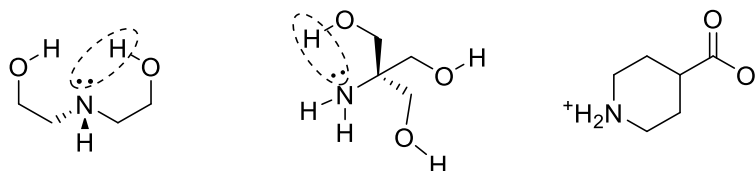


Figure 13. Assumed intramolecular hydrogen bonds of diethanolamine and tris(hydroxymethyl)aminomethane and betaine structure of 4-piperidinecarboxylic acid, both reducing or abolishing their nucleophilicity.²⁶

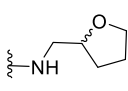
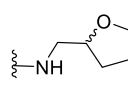
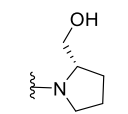
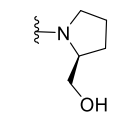
4.4.4. Pharmacological evaluation

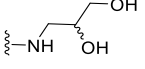
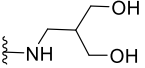
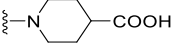
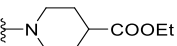
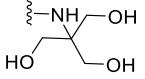
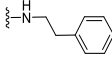
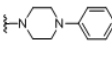
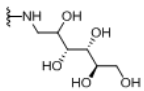
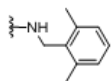
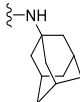
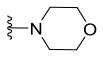
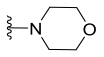
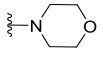
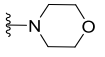
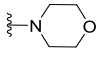
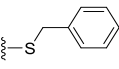
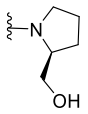
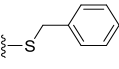
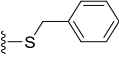
The pharmacological testing was performed with the PathHunter β -arrestin recruitment assay (DiscoverX). The assay employed β -arrestin CHO-K1 cells overexpressing MRGPRX3 being fused to the ProLink2 ARMS1 variant. (PathHunter®, Discoverx) The compounds were initially tested at a concentration of 20 μ M ($n = 3$, in duplicates). The effect was normalized to the maximal effect of dipyrindamole = 100% (300 μ M). At 20 μ M, dipyrindamole showed approximately 30 % of the maximal effect. Compounds that showed an effect that was greater than 50% at 20 μ M were fully characterized, a concentration-response curve was obtained and an EC_{50} value was determined.

4.4.4.1. Biological evaluation of 2,4,6,8-tetrasubstituted pyrimido[5,4-*d*]pyrimidines

Altogether, 40 compounds of the for 2,4,6,8-tetrasubstituted pyrimido[5,4-*d*]pyrimidine scaffold were evaluated regarding their potency at MRGPRX3. The results are collected in Table 2.

Table 2. Dipyridamole and its derivatives tested as MRGPRX3 agonists using the β -arrestin recruitment assays.^a

Compd.	R ₁	R ₂	R ₃	R ₄	EC ₅₀ ± SEM	E _{max}
					(μ M)	% ^c
					(% activation at 20 μ M) ^b	
Dipyridamole	1-Piperidinyl	-N(CH ₂ CH ₂ OH) ₂	1-Piperidinyl	-N(CH ₂ CH ₂ OH) ₂	71.5 ± 1.5	100
3	1-Piperidinyl	-N(CH ₂ CH ₂ OH) ₂	1-Piperidinyl	-Cl	(2)	-
4	1-Piperidinyl	1-Piperidinyl	1-Piperidinyl	-N(CH ₂ CH ₂ OH) ₂	27.9 ± 4.5	99
6	-N(CH ₂ CH ₂ OH) ₂	-N(CH ₂ CH ₂ OH) ₂	-N(CH ₂ CH ₂ OH) ₂	-N(CH ₂ CH ₂ OH) ₂	(3)	-
7	-N(CH ₂ CH ₂ OH) ₂	1-Piperidinyl	-N(CH ₂ CH ₂ OH) ₂	-N(CH ₂ CH ₂ OH) ₂	(37)	-
9	1-Piperidinyl	1-Piperidinyl	-N(CH ₂ CH ₂ OH) ₂	1-Piperidinyl	(37)	-
16	1-Piperidinyl	1-Piperidinyl	-OH	1-Piperidinyl	(3)	-
19	1-Piperidinyl	1-Piperidinyl	1-Piperidinyl	1-Piperidinyl	(36)	-
22	1-Piperidinyl	-N(CH ₂ CH ₂ OAc) ₂	1-Piperidinyl	-N(CH ₂ CH ₂ OAc) ₂	(-1)	-
24	1-Piperidinyl	-NHCH ₂ CH ₂ OH	1-Piperidinyl	-Cl	(3)	-
25	1-Piperidinyl	-NHCH ₂ CH ₂ OH	1-Piperidinyl	-N(CH ₂ CH ₂ OH) ₂	(3)	-
28	1-Piperidinyl		1-Piperidinyl		(-16)	-
29	1-Piperidinyl		1-Piperidinyl		(19)	-
31	-N(CH ₂ CH ₂ OH) ₂	1-Piperidinyl	-N(CH ₂ CH ₂ OH) ₂	1-Piperidinyl	14.2 ± 1.5	83
33	-N(CH ₂ CH ₂ OCH ₃) ₂	1-Piperidinyl	-N(CH ₂ CH ₂ OCH ₃) ₂	1-Piperidinyl	32.7 ± 4.3	61
39	-NH ₂	-N(CH ₂ CH ₂ OH) ₂	-NH ₂	-N(CH ₂ CH ₂ OH) ₂	(3)	-
40	-NH ₂	1-Piperidinyl	-NH ₂	1-Piperidinyl	(2)	-

41	1-Piperidinyl	1-Piperidinyl	-NH ₂	1-Piperidinyl	(16)	-
43	1-Piperidinyl	1-Piperidinyl	1-Piperidinyl	-N-propyl ethanolamine	(30)	-
44	1-Piperidinyl	1-Piperidinyl	1-Piperidinyl		(-4)	-
45	1-Piperidinyl	1-Piperidinyl	1-Piperidinyl		(-6)	-
46	1-Piperidinyl	1-Piperidinyl	1-Piperidinyl	-CN	(-2)	-
47	1-Piperidinyl	1-Piperidinyl	1-Piperidinyl	-C=NH-NH-OH	(1)	-
48	1-Piperidinyl	1-Piperidinyl	1-Piperidinyl	-CONH ₂	(-3)	-
50	1-Piperidinyl	1-Piperidinyl	1-Piperidinyl	-NHCH ₂ CH ₂ SO ₃ H	(29)	-
56	1-Piperidinyl	1-Piperidinyl	1-Piperidinyl		(25)	-
58	1-Piperidinyl	1-Piperidinyl	1-Piperidinyl		(20)	-
60	1-Piperidinyl	1-Piperidinyl	1-Piperidinyl		20.3 ± 3.3	98
61	1-Piperidinyl	1-Piperidinyl	1-Piperidinyl	-NHCH ₂ CH ₂ OH	(15)	-
71	1-Piperidinyl	-N(CH ₂ CH ₂ OH) ₂		-N(CH ₂ CH ₂ OH) ₂	(25)	-
73	1-Piperidinyl	-N(CH ₂ CH ₂ OH) ₂		-N(CH ₂ CH ₂ OH) ₂	(4)	-
75	1-Piperidinyl	-N(CH ₂ CH ₂ OH) ₂		-N(CH ₂ CH ₂ OH) ₂	(-3)	-
77	1-Piperidinyl	-N(CH ₂ CH ₂ OH) ₂		-N(CH ₂ CH ₂ OH) ₂	(-11)	-
79	1-Piperidinyl	-N(CH ₂ CH ₂ OH) ₂		-N(CH ₂ CH ₂ OH) ₂	(-6)	-
82		-N-propyl ethanolamine		-N-propyl ethanolamine	8.49 ± 1.23	125
83				-N-propyl ethanolamine	18.0 ± 2.7	53
86		-N(CH ₂ CH ₂ OH) ₂		N(CH ₂ CH ₂ OH) ₂	(37)	-
88		-N(CH ₂ CH ₂ OH) ₂	-N(CH ₂ CH ₂ CH ₃) ₂	-N(CH ₂ CH ₂ OH) ₂	(39)	-
90		-N(CH ₂ CH ₂ OH) ₂	-N(CH ₂ CH ₂ CH ₃)	-N(CH ₂ CH ₂ OH) ₂	(19)	-

92		-N(CH ₂ CH ₂ OH) ₂		-N(CH ₂ CH ₂ OH) ₂	(-7)	-
96		-N-propyl ethanolamine		-N-propyl ethanolamine	0.942 ± 0.325	607

^aThe pharmacological testing was performed with β arr CHO K1 cells expressing the MRGPRX3 with ProLink2 ARMS1 variant.

^bThe screening was performed at concentration of 20 μ M (n=3, in duplicates). The signal was normalized to the effect of 300 μ M dipyridamole (set to 100 %) and buffer (set to 0 %).

^cThe maximal effect of each active was normalized to the effect of 300 μ M dipyridamole (set to 100 %) and buffer (set to 0 %).

Similar compounds showed diverse activities indicating steep SARs. Compounds with different structures and properties showed in some cases comparable activities. The nature of the scaffold (bearing 4 variable residues) makes comparison of the compounds difficult, especially because alternative binding modes can be expected. In order to appropriately compare the structures and their potencies, the synthesized compounds were clustered with regard to residues or particular substitution patterns. Figure 14 illustrates the curves of selected compounds.

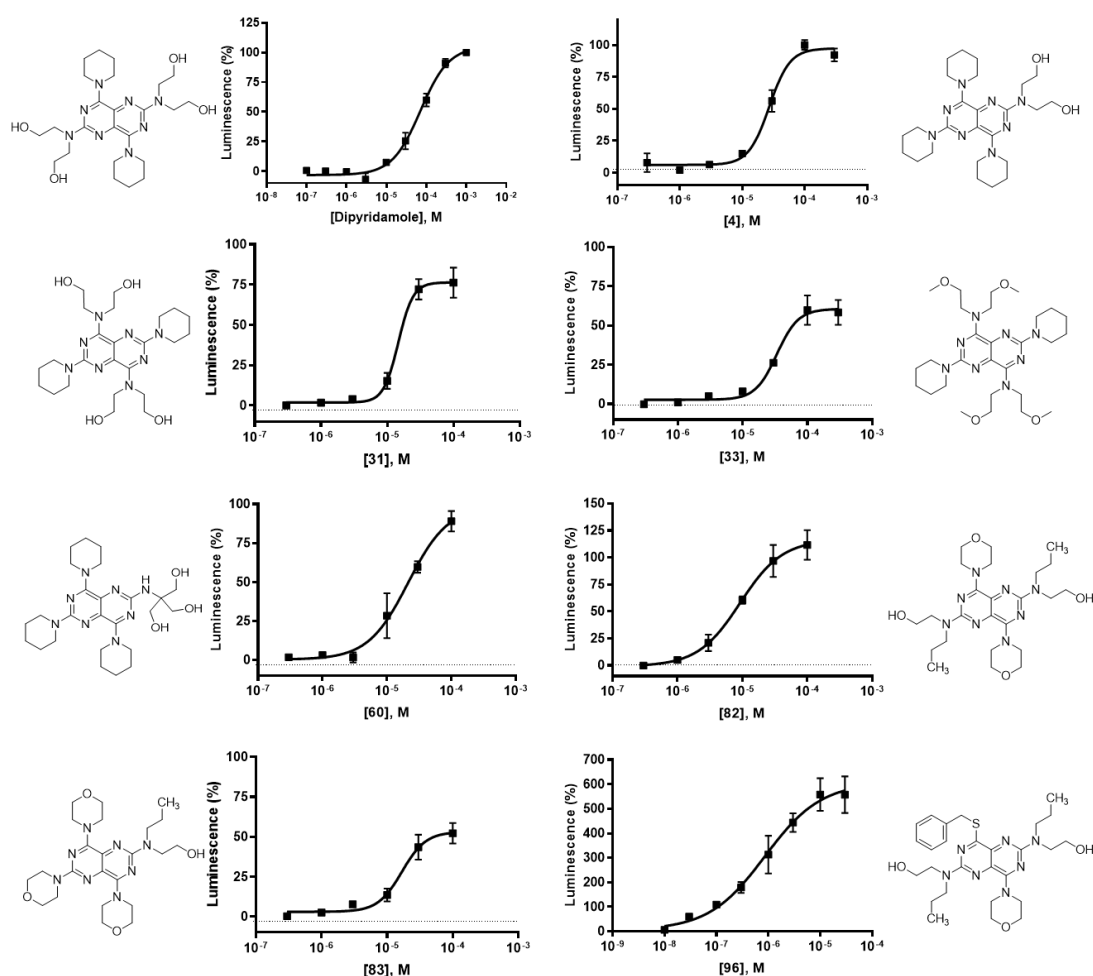


Figure 14. Concentration-response curves of compounds dipyridamole, **4**, **31**, **33**, **60**, **82**, **83** and **96**.

4.4.4.2. Pyrimido[5,4-d]pyrimidine derivatives bearing established residues

Figure 15 depicts the potency of 2,4,6,8-tetrasubstituted pyrimido[5,4-d]pyrimidines bearing an AAAB substitution pattern. Compound **4** was the first relatively potent MRGPRX3 agonist among the synthesized substances, exhibiting an EC₅₀ value of 27.9 μM and the same efficacy as the parent compound dipyridamole. It showed 49% inhibition at 20 μM. Switching the position of a piperidine (C4/C8) with the diethanolamine residue (C6) led to a decrease in potency, compound **9** showed 37% activation at 20 μM. Compound **7**, bearing the diethanolamine residue at three positions (C4/C6/C8) and only one piperidine at C2 exhibited the same potency as **9**. The physicochemical properties of these compounds are different, **7** is much more polar than **9** (cf. Figure 14).

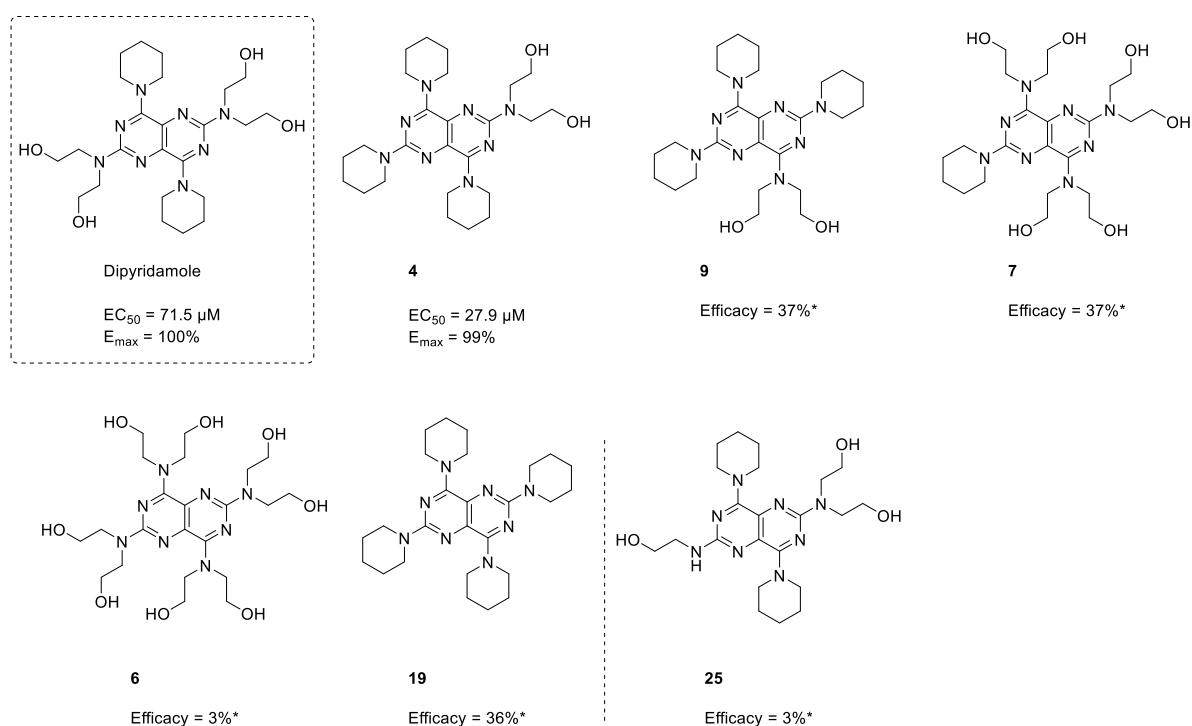


Figure 15. 2,4,6,8-Tetrasubstituted pyrimido[5,4-d]pyrimidines bearing an AAAB substitution pattern and **19** and **25** (*MRGPRX3 activation at 20 μM, normalized to the effect of 300 μM dipyridamole (set to 100 %)).

The very lipophilic compound **19** is in the same range of activity (36% activation at 20 μM) as **7** and **9**. At the first glance, it seems enough to have any residue at the pyrimido[5,4-d]pyrimidine core to observe potency at MRGPRX3 as long as the scaffold is tetra-substituted. However, many compounds did not show any activity at the receptor despite high resemblance to the aforementioned compounds. Compound **6**, for example, exhibiting four diethanolamine units was inactive (3% activation at 20 μM, see table 2 and Figure 15 and 17). Compound **25**, on the other hand, is similar to the structure of dipyridamole, but one diethanolamine residue is exchanged for ethanolamine. Despite the strong resemblance to the parent compound, **25**

is inactive at the tested concentration (3% activation at 20 μ M). These findings indicate steep SARs, which is typical for GPCR ligands since the membrane proteins display limited flexibility.

Figure 16 illustrates all compounds that exhibit at least one small residue at the pyrimido[5,4-*d*]pyrimidines (NH_2 , Cl or oxygen). All of those compounds, namely **3**, **16**, **24** and **39-41** were inactive (2-3% activation at 20 μ M). Only compound **41** showed somewhat higher potency at the tested concentration (16% activation at 20 μ M).

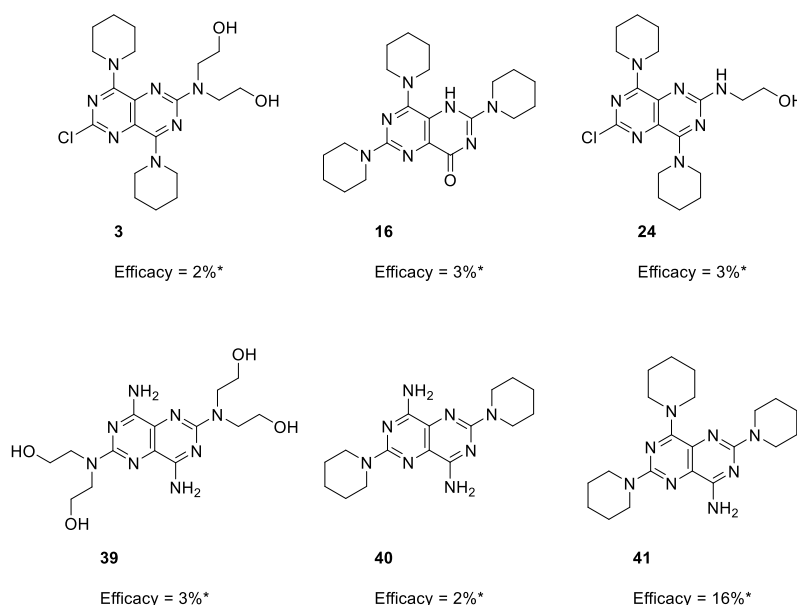


Figure 16. Biological data of pyrimido[5,4-*d*]pyrimidines bearing at least one small residue (*MRGPRX3 activation at 20 μ M, normalized to the effect of 300 μ M dipyridamole (set to 100 %)).

These findings indicate that tetra-substitution with residues of a particular size might be necessary for activity at MRGPRX3. Furthermore, the receptor might not tolerate small polar moieties (like NH_2) attached to the pyrimido[5,4-*d*]pyrimidine core structure.

4.4.4.3. Symmetrically substituted pyrimido[5,4-*d*]pyrimidine derivatives

The compounds depicted in Figure 17 all exhibit a symmetric structure of the substitution pattern ABAB which is similar to the substitution pattern of dipyrnidamole.

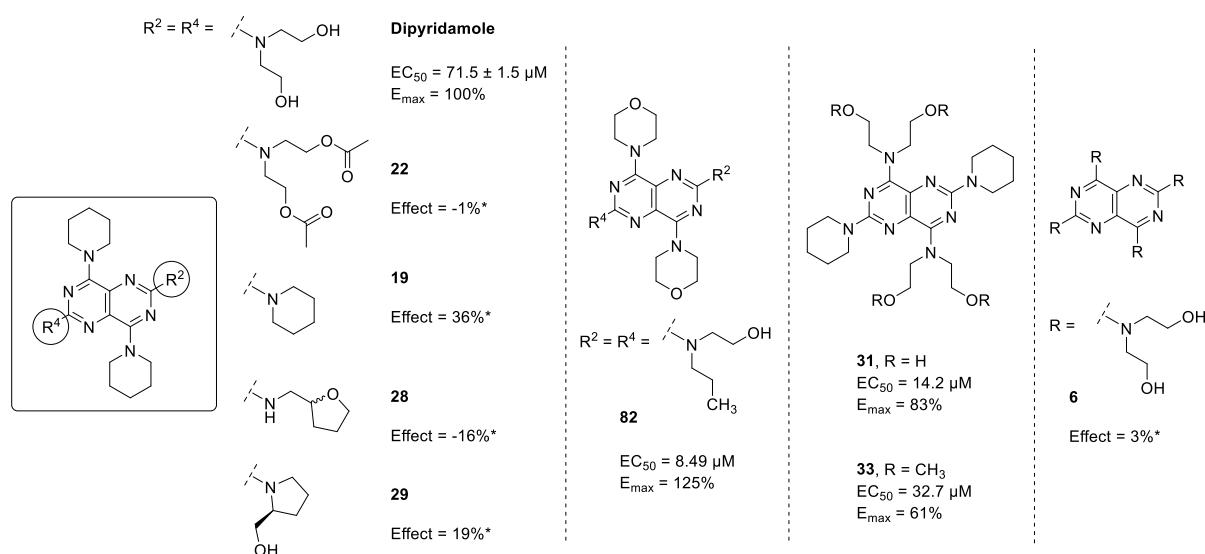


Figure 17. Biological data of symmetric 2,4,6,8-tetrasubstituted pyrimido[5,4-*d*]pyrimidines (*MRGPRX3 activation at 20 μM, normalized to the effect of 300 μM dipyrnidamole (set to 100 %)).

Among the symmetrical compounds, *N*-propylethanolamine was the best substituent for positions R² = R⁴ (when C4/C8 was morpholine). Compound **82** was the most potent compound from this cluster exhibiting an EC₅₀ value of 8.49 μM and an E_{max} of 125% compared to dipyrnidamole c = 100%. Replacing diethanolamine at C2/C6 (= dipyrnidamole) with diol-mimetics (e.g. in **28** and **29** and planned for compounds **26** and **27**) did not seem to be beneficial (see Table 2 and Figure 17 and 18.) Compound **28** was inactive (R² = R⁴ = 2-tetrahydrofurylamine) while compound **29** (R² = R⁴ = *L*-prolinol, 19% efficacy) showed at least a little activity, maybe because the prolinole residue resembles the successful *N*-propylethanolamine moiety. Since **44** and **45** were inactive (see Table 2), the planned but not realized compounds **26** (R² = R⁴ = 3-amino-1,2-propanediol) and **27** (R² = R⁴ = 2-amino-1,3-propanediol) might have been inactive as well. Masking the terminal OH groups of the diethanolamine moiety with acetyl residues led to an inactive compound; either at least one OH group is needed for activity or the compound does not fit into the protein anymore due to its increased size.

Interestingly, the dipyrnidamole-isomer **31** (bearing the flipped substitution pattern of dipyrnidamole) was more potent than the parent compound itself, sharing an EC₅₀ value of 14.2 μM and an E_{max} of 85% at 20 μM. Also, the methylated compound **33** showed some potency (EC₅₀ 32.7 μM, E_{max} = 61% at 20 μM). This finding might suggest different binding

modes for pyrimido[5,4-*d*]pyrimidines depending on the substitution pattern. However, a look at the different potencies of the isomers **4** and **9** (three residues being piperidine, one being diethanolamine, **4** exhibiting a 3-fold higher potency than **9**) indicates, that the position of the substituents *does* matter. Altogether, the approach to systematically rotate the established residues (and some new ones) around the scaffold was not successful, only compound **4** could be highlighted as a new lead structure.

4.4.4.4. 4,6,8-Tripiperidinopyrimido[5,4-*d*]pyrimidine derivatives

On the basis of the comparably great potency of **4**, several 4,6,8-tripiperidinopyrimido[5,4-*d*]pyrimidine derivatives and compound **83** were synthesized and evaluated (cf. Figure 18).

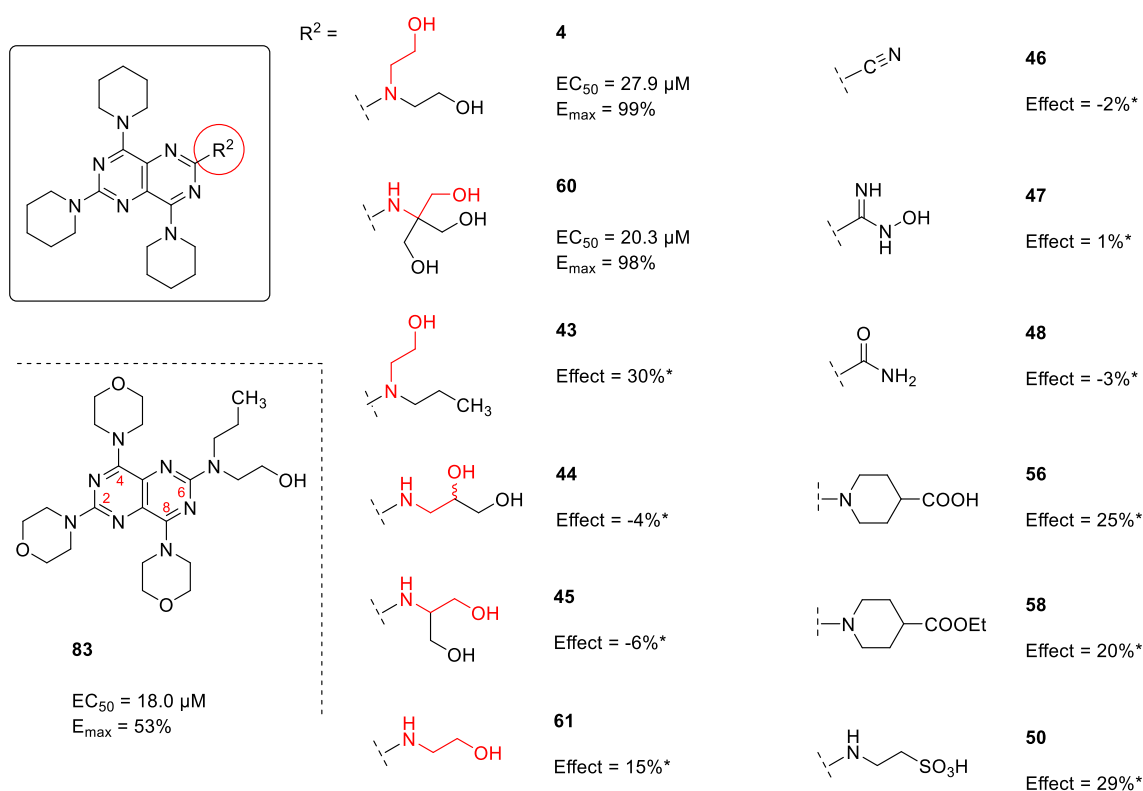


Figure 18. Biological data of 4,6,8-tripiperidinopyrimido[5,4-*d*]pyrimidine derivatives and **83** (*MRGPRX3 activation at 20 μM, normalized to the effect of 30 μM dipyrindamole (set to 100 %)).

As a result, only compound **60**, bearing a tris(hydroxymethyl)aminomethane moiety for R² (EC₅₀ 20.3 μM, E_{max} = 98% at 20 μM) and compound **83** (C2/C4/C8 = morpholine, C6 = *N*-propylethanolamine, EC₅₀ 18.0 μM, E_{max} = 53% at 20 μM) were found to be noteworthy active. A change from piperidine moieties to morpholine and a change from diethanolamine to *N*-propylethanolamine (**4** vs. **83**) led to a small increase in potency, but a decrease in efficacy. Compound **43** only differs in a single OH group in the diethanolamine moiety that is changed to a methyl group (**4** vs. **43**). This change, led to a decrease in potency, compound **43** exhibiting

only 30% activation at 20 μM . Morpholine is a slightly better residue compared to piperidine at C2/C4/C8 when C6 is bound to *N*-propylethanolamine (**43** vs. **83**).

Compounds **4** (R^2 = diethanolamine), **60** (R^2 = tris(hydroxymethyl)aminomethane), **43** (R^2 = *N*-propylethanolamine), **44** (R^2 = 3-aminopropane-1,2-diol), **45** (R^2 = 2-aminopropane-1,3-diol) and **61** (R^2 = ethanolamine) all bear a more or less modified version of ethanolamine for R^2 (Figure 18, ethanolamine moiety is indicated in red). The activity of these molecules at MRGPRX3 differs. This suggests that not only any alcohol function is required at this moiety but a very particular arrangement of OH groups is needed for interaction. For this compound family, it is beneficial to offer at least two OH groups that are separated by a particular spacer. Two OH groups (**44** and **45**) or only one OH groups subsequent to a NHCH_2CH_2 group (**61**) for R^2 led to low potency. Also replacing one ethanol residue with a propyl residue led to a decrease in potency. Figure 19 illustrates the assumed interactions that might take place within the modified ethanolamine moieties of compounds **4**, **44**, **45**, **60** and **61**. Intramolecular H-bonds between the OH group and the electron pair of the nitrogen might presumably lead to the formation of ring-structures that might place the attached OH groups in a particular spacial position. Intramolecular H-bonds have been reported in literature for diethanolamine and triethanolamine derivatives.²⁶

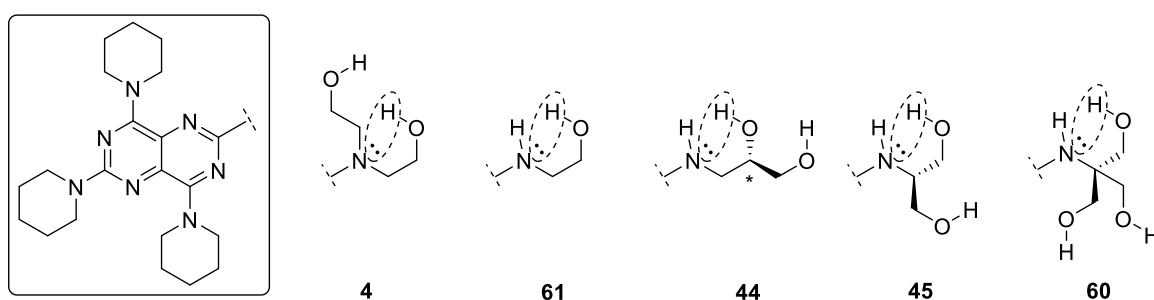


Figure 19. Proposed intramolecular interactions of **4**, **44**, **45**, **60** and **61**.²⁶

A compound that bears piperidine (or morpholine) residues at C4/C8 and tris(hydroxymethyl)aminomethane residues at C2/C6 would be very interesting, however it has not been synthetically accessible.

Compounds **46**, **47** and **48** did not show any activity at MRGPRX3. Seemingly, small polar residues for R^2 are not well tolerated by the receptor. Compounds **50** and **56** exhibit a 4-piperidinecarboxylic acid and a 2-aminoethanesulfonic acid function for R^2 . Both compounds are similarly potent as dipyridamole. Thus, a polar acidic function at C6 is tolerated but not superior to the parent compound. This finding might still be interesting with regard to the enhancement of the solubility of the very lipophilic pyrimido[5,4-*d*]pyrimidines.

4.4.4.5. 2,6-Bis[bis(2-hydroxyethyl)amino]-4-piperidinopyrimido[5,4-*d*]pyrimidine derivatives

Figure 20 illustrates the biological data of 2,6-bis[bis(2-hydroxyethyl)amino]-4-piperidinopyrimido[5,4-*d*]pyrimidine derivatives. Only compound **71** (R^3 = phenylethylamine) showed low potency (25% activation at 20 μ M). The other residues at R^3 may be too large or too polar to be tolerated by MRGPRX3.

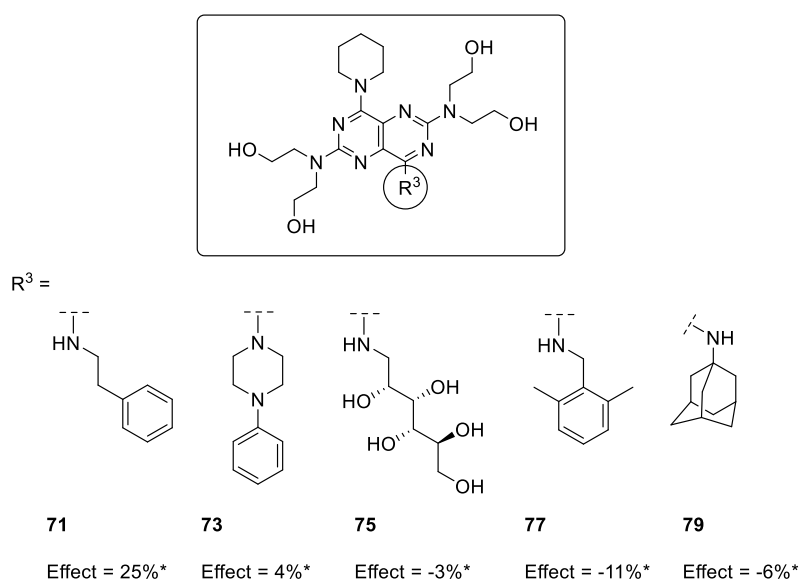


Figure 20. Biological data of 2,6-bis[bis(2-hydroxyethyl)amino]-4-piperidinopyrimido [5,4-*d*]pyrimidine derivatives (*MRGPRX3 activation at 20 μ M, normalized to the effect of 300 μ M dipyrindamole (set to 100 %)).

4.4.4.6. 2,6-bis[bis(2-hydroxyethyl)amino]-4-benzylthiopyrimido[5,4-d]pyrimidine derivatives

All synthesized 2,6-bis[bis(2-hydroxyethyl)amino]-4-benzylthiopyrimido[5,4-d]pyrimidine derivatives and **96** are depicted in Figure 21.

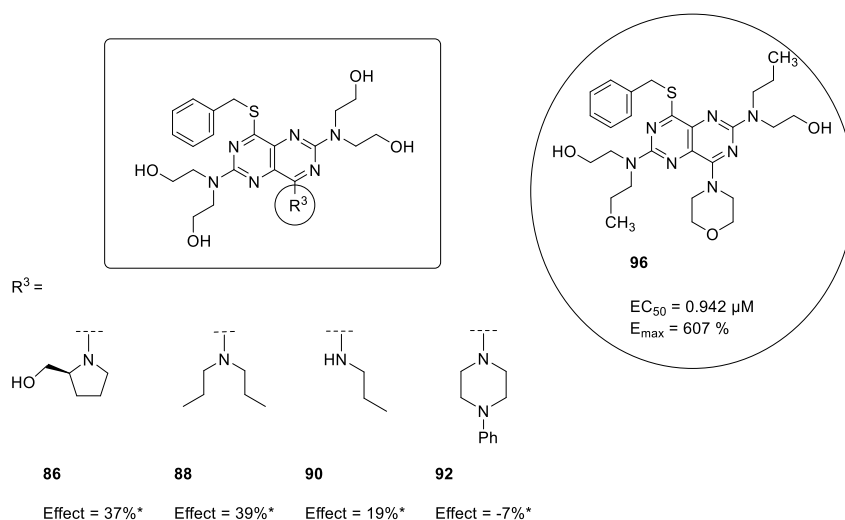


Figure 21. Biological data of 2,6-bis[bis(2-hydroxyethyl)amino]-4-benzylthiopyrimido[5,4-d]pyrimidine derivatives and **96** (*MRGPRX3 activation at 20 μM, normalized to the effect of 30 μM dipyrindamole (set to 100 %)).

The 2,6-bis[bis(2-hydroxyethyl)amino]-4-benzylthiopyrimido[5,4-d]pyrimidine derivatives were weakly potent or inactive. Compounds **86** and **88** showed 37-39% activation at 20 μM, similar to dipyrindamole. The phenylpiperazine residue of **92** (inactive) seems to be too large at this position. Compound **96** displayed the highest potency with an EC₅₀ value of 0.942 μM and 607% E_{max}. This result, however, needs to be carefully considered since it is an outlier and an artifact cannot be excluded. The compound combines features of the potent agonist **82** and the scaffold of 2,6-bis[bis(2-hydroxyethyl)amino]-4-benzylthiopyrimido[5,4-d]pyrimidine derivatives (see Figure 22).²²

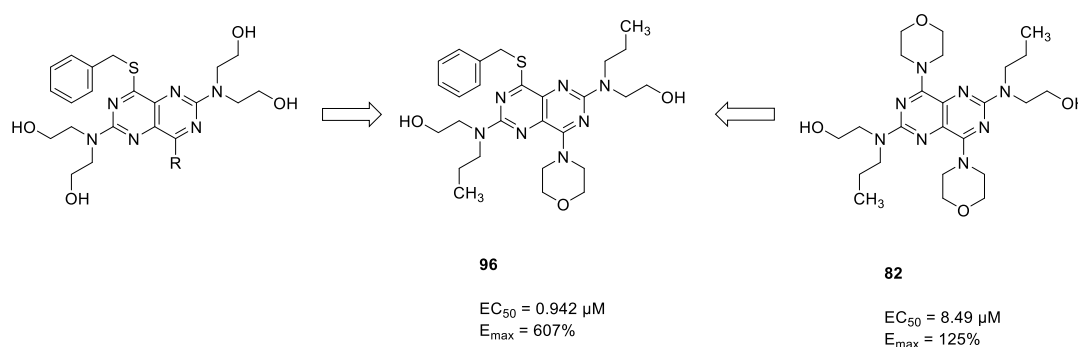


Figure 22. Biological data of derivatives **82** and **96** (*MRGPRX3 activation at 20 μM, normalized to the effect of 300 μM dipyrindamole (set to 100 %)).

4.4.4.7. Biological evaluation of substituted purine derivatives

In order to investigate a possible approach of scaffold hopping for MRGPRX3 agonists, eight purine derivatives, decorated with piperidine (-like) and diethanolamine (-like) residues were prepared to mimic the structure of 2,4,6,8-tetrasubstituted pyrimido[5,4-*d*]pyrimidines. The purines exhibited different degrees of substitution (2,6-disubstituted, 2,6,9-trisubstituted and 2,6,8,9-tetrasubstituted) and varying substitution patterns. Table 3 illustrates all test results: none of the purines showed activity at MRGPRX3. These findings indicate that the scaffold hopping approach has not worked out.

Table 3. Purine derivatives tested at the MRGPRX3 using the β -arrestin recruitment assay.^a

Compd	R ₁	R ₂	R ₃	R ₄	(% Effect) ^b	E _{max} % ^c
108	1-Piperidinyl	H	H	1-Piperidinyl	(-1)	-
109	1-Piperidinyl	H	H	-N(CH ₂ CH ₂ OH) ₂	(-3)	-
111	-N(CH ₂ CH ₂ OH) ₂	H	H	1-Piperidinyl	(-3)	-
112	-N(CH ₂ CH ₂ OH) ₂	H	H	-N(CH ₂ CH ₂ OH) ₂	(-2)	-
115	-N(CH ₂ CH ₂ OH) ₂	H	Methylcyclohexyl	-N(CH ₂ CH ₂ OH) ₂	(-3)	-
116	1-Piperidinyl	H	-CH ₂ CH ₂ OH	1-Piperidinyl	(-3)	-
117	1-Piperidinyl	H	Methylcyclohexyl	-N(CH ₂ CH ₂ OH) ₂	(0)	-
119	1-Piperidinyl	1-Piperidinyl	Methylcyclohexyl	-N(CH ₂ CH ₂ OH) ₂	(-3)	-

^aThe pharmacological testing was performed with β arr CHO K1 cells expressing the MRGPRX3 with ProLink2 ARMS1 variant.

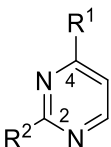
^bThe screening was performed at concentration of 20 μ M (n=3, in duplicates). The signal was normalized to the effect of 300 μ M Dipyridamole (set to 100 %) and buffer (set to 0 %).

^cThe maximal effect of each active was normalized to the effect of 300 μ M Dipyridamole (set to 100 %) and buffer (set to 0 %).

4.4.4.8 Biological evaluation of 2,4-disubstituted pyrimidine derivatives

Another approach to develop agonists for MRGPRX3 was the preparation 2,4-disubstituted pyrimidines decorated with piperidine and diethanolamine in order to mimic half of the structure of dipyridamole. As a result, all 4 prepared compounds were inactive (see Table 4). This finding indicates, that only 2,4,6,8-tetrasubstituted pyrimido[5,4-*d*]pyrimidines are appropriate agonists for MRGPRX3 at this point. No alternative scaffold could be identified yet so far.

Table 4. Pyrimidine derivatives tested at the MRGPRX3 using the β -arrestin recruitment assay.^a



Compd.	R ₁	R ₂	(% Effect) ^b	E _{max} % ^c
123	1-Piperidinyl	1-Piperidinyl	(-1)	-
124	1-Piperidinyl	-N(CH ₂ CH ₂ OH) ₂	(-3)	-
126	-N(CH ₂ CH ₂ OH) ₂	-N(CH ₂ CH ₂ OH) ₂	(-3)	-
127	-N(CH ₂ CH ₂ OH) ₂	1-Piperidinyl	(-2)	-

^aThe pharmacological testing was performed with β arr CHO K1 cells expressing the MRGPRX3 with ProLink2 ARMS1 variant.

^bThe screening was performed at concentration of 20 μ M (n=3, in duplicates). The signal was normalized to the effect of 300 μ M Dipyridamole (set to 100 %) and buffer (set to 0 %).

^cThe maximal effect of each active was normalized to the effect of 300 μ M Dipyridamole (set to 100 %) and buffer (set to 0 %).

In conclusion, the first structure-activity relationships for 2,4,6,8-tetrasubstituted pyrimido [5,4-*d*]pyrimidines as MRGPRX3 agonists have been established. However, alternative binding modes are likely. All residues are interdependent and, if a particular residue is tolerated by the receptor depends on the nature all other residues. The inactivity of purine and pyrimidine derivatives indicates that the entire molecule is required for binding and not just a part of it. The so far moderate potency of the compounds makes SAR analysis difficult.

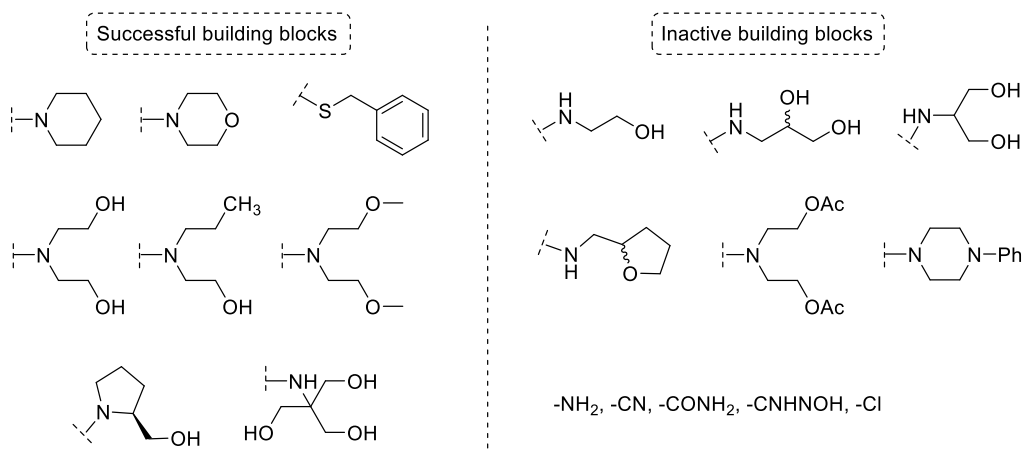


Figure 23. Evaluation of used building blocks.

The left side of Figure 23 illustrates all building blocks that led to potent compounds. Derivatives **4**, **31**, **33**, **60**, **82**, **83** and **96** showed particularly high potency as agonists for the MRGPRX3. Figure 23 furthermore depicts some selected residues that led to inactive compounds.

4.4.4.9. Selectivity studies

100 μM dipyrindamole was tested against MRGPRX1, X2, X3 and X4 in the β -arrestin assays and normalized to the E_{max} concentration of each receptor of standard agonist (cf. Figure 24). For MRGPRX3, the effect of 100 μM dipyrindamole was normalized to dipyrindamole E_{max} at 300 μM . As a result, dipyrindamole displayed no significant agonism for MRGPRX1, X2 and X4 and can therefore be regarded as selective for MRGPRX3.

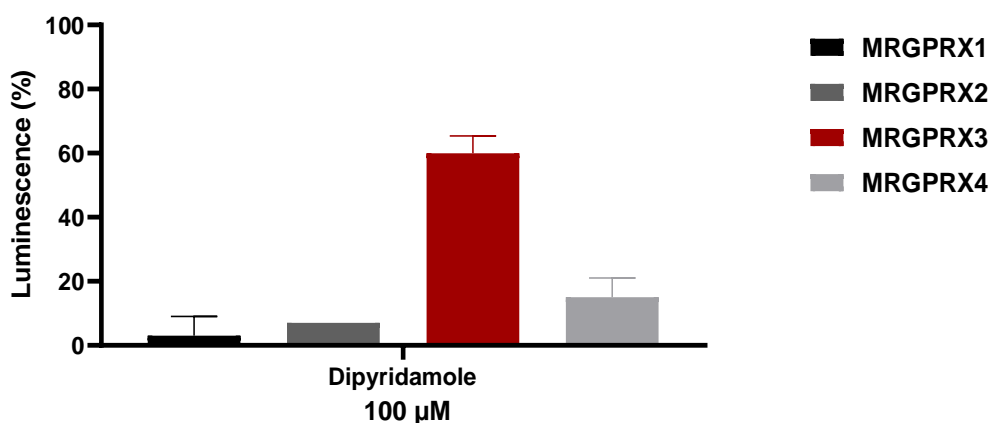


Figure 24. Selectivity studies employing β -arrestin assays of dipyrindamole at MRGPRX1, X2, X3 and X4; signal was normalized to the E_{max} concentration of each receptor of standard agonist.

4.4.4.10. Antagonist Screening

Since compounds that did not activate MRGPRX3 might actually block the receptor, they were tested at a concentration of 20 μM versus MRGPRX3 activation by 20 μM (EC_{80}) of **82**. As a result, none of the synthesized compounds among this project showed any antagonistic activity at MRGPRX3 at a concentration of 20 μM .

4.4.5. Conclusions and outlook

The MRGPRX3 is an interesting drug target since it still has the orphan status and it is proposed to be involved with pain and itch perceptions. To explore 2,4,6,8-tetrasubstituted pyrimido[5,4-*d*]pyrimidines as agonists for the MRGPRX3, compounds with defined substitution patterns were synthesized. Altogether, 40 pyrimido[5,4-*d*]pyrimidines, 8 purine derivatives and 4 2,4-disubstituted pyrimidines were obtained. Thereby, 8 to pyrimido[5,4-*d*]pyrimidines (**4**, **6**, **19**, **22**, **25**, **31**, **39** and **82**),^{10;17;27-29} one purine derivative (**108**)³⁰ and one pyrimidine derivative (**123**)³¹ have already been reported in literature in connection with other targets and issues. However, other synthetic pathways were used to obtain the products or the synthesis could be improved during the course of this project. For the rational synthesis of 2,4,6,8-tetrasubstituted pyrimido[5,4-*d*]pyrimidines, sequential nucleophilic substitutions of 2,4,6,8-tetrachloropyrimido[5,4-*d*]pyrimidine (TCPP) was utilized. Different reaction conditions were applied leading to pyrimido[5,4-*d*]pyrimidines mostly with patterns of substitution denoted as ABAB / BABA (reaction with nucleophile 1 at C4 and C8, followed by nucleophile 2 at C2 and C6), AAAB and ABAC (reaction with nucleophile 1 at C4, nucleophile 2 at C8 and nucleophile 3 at C2 and C6). However, several more products were designed and tried to be synthesized. Since the chemistry based on sequential substitution of TCPP does not allow all kinds of nucleophiles (in the literature,^{10;16-18} only nucleophiles that are liquid under reaction conditions have been used), the introduction of several designed building blocks was not possible or difficult. Nevertheless, the syntheses of compounds bearing special residues, e.g. **50**, **56** and **60** were successful.

To sum up, most of the noteworthy potent compounds that were synthesized (illustrated in Figure 25) exhibit a combination of piperidine (or derivatives) and diethanolamine (or derivatives) similar to the parent compound dipyridamole. Initial structure-activity relationships were established. The activity of compounds **31** and **33** in comparison to dipyridamole might suggest different binding modes of the scaffold in the protein. The investigation of compound **4** and its derivatives (see section 4.4.4.4.) revealed that only very particular ethanolamine derivatives (most notably tris(hydroxymethyl)aminomethane) were tolerated by the receptor within this cluster.

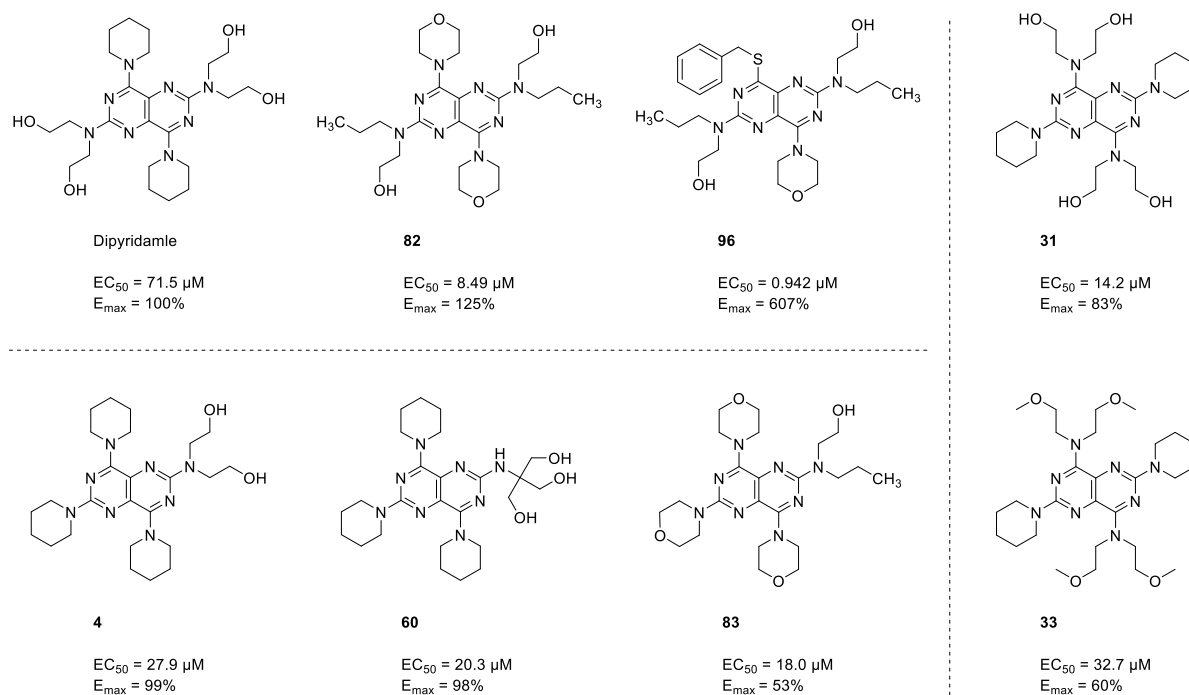


Figure 25. Biological data of the most potent compounds.

All compounds based on purines or pyrimidines were inactive, showing that actually the entire 2,4,6,8-tetrasubstituted pyrimido[5,4-*d*]pyrimidine scaffold is needed to activate MRGPRX3. The best compound by far was **96** with an EC₅₀ value of 0.942 μM and a 6-fold higher efficacy than dipyrindamole. This compound could be a new lead structure for further optimization of the scaffold. Also, some combinations of “active residues” have not yet been prepared thus for future investigations many more possibilities substitution patterns can still be realized.

Since many active compounds exhibit alcohol or ether structures (cf. Figure 25), the natural attempt is to introduce similar structures that copy these successful structures or to introduce more or differently arranged OH groups. Figure 26 shows some related building blocks that might be used for further synthesis.

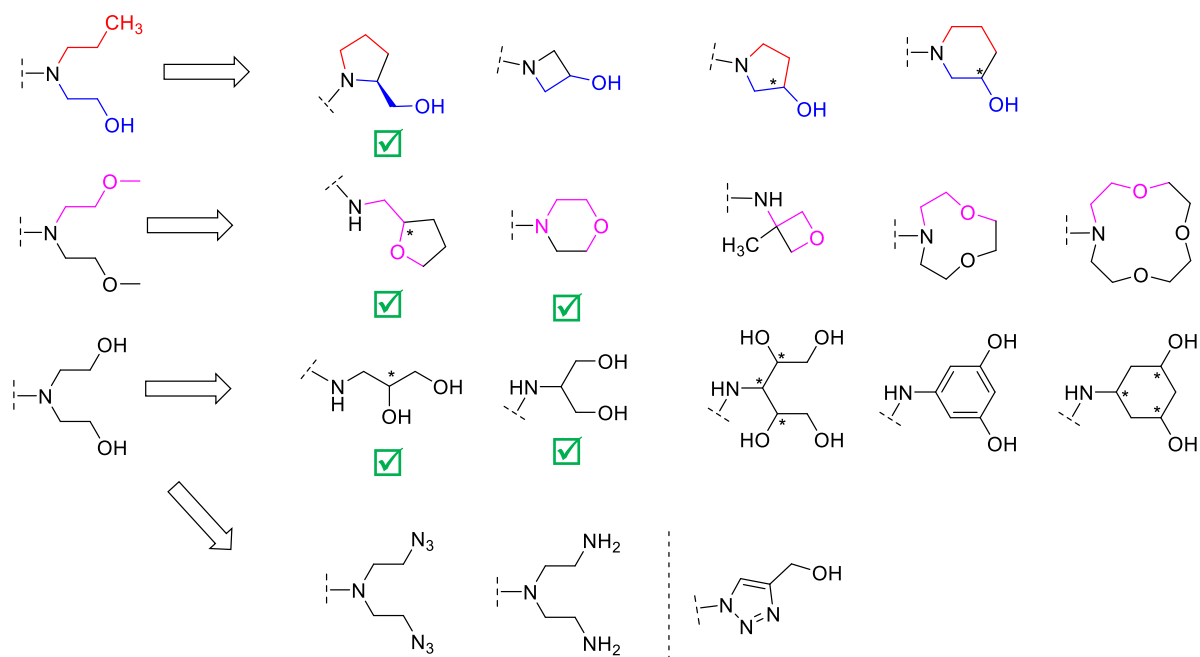
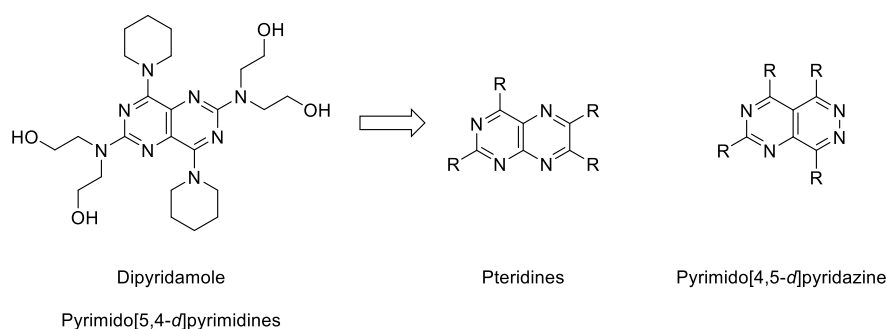


Figure 26. Suggested building blocks on the basis of active compounds

It is a common approach in medicinal chemistry to convert open chain structures like diethanolamine and its derivatives to rigid structures, e.g. rings. In case of *N*-propylethanolamine, structures like 3-azetidino-, 3-pyrrolidino- or 3-piperidino- could very well replace the chain structures (first column, Figure 26). An *L*-prolinole residue was already inserted in course of this exchange approach. The ether structure of bis(2-methoxyethyl)amine could, for example, be simulated by 3-methyl-3-oxetanamine or hexahydro-5*H*-1,4,7-dioxazine. Morpholine and 2-tetrahydrofurylamine have already been explored as residues on the scaffold (second column, Figure 26). Structures with at least two OH groups are particularly interesting since they are similar to the diethanolamine moiety of dipyrindamole and the derivatives of **4** (section 4.4.4.4.) showed that a very particular orientation of OH groups is needed for potent agonists. Two aminodiols and tris(hydroxymethyl)aminomethane have already been evaluated. Building blocks like 1,1'-iminobis-1,2-ethanediol, 3,5-dihydroxyaniline or 3,5-piperidinediol would offer even more different pharmacophores with regard to the orientation of OH groups (third column, Figure 26). Also, hydrogen bond donors and acceptors may enhance water solubility of the rather lipophilic dipyrindamole derivatives. The introduction of amino groups as a replacement for OH groups was tried, but their syntheses failed. Therefore, another protection group strategy would be necessary. Employment of azido groups masking the amino groups up to the final reaction step could be a new strategy for that approach. Furthermore, exotic building blocks like 1*H*-1,2,3-triazole-5-methanol could offer completely different interactions towards the protein (fourth column, Figure 26).

Another approach in the course of scaffold hopping could utilize pteridines or pyrimido[4,5-*d*]pyridazines as new scaffolds due to their resemblance to pyrimido[5,4-*d*]pyrimidines (ct. Figure 27).



Scheme 27. Suggested new scaffolds pteridines and pyrimido[4,5-*d*]pyridazines.

4.4.6. Experimental part

4.4.6.1. General methods

The general methods were the same as in script 4.1. and 4.2..

4.4.6.2. Synthesis of pyrimido[5,4-*d*]pyrimidine derivatives

All pyrimido[5,4-*d*]pyrimidine derivatives were synthesized employing procedures from literature.^{10,16-18}

4.4.6.2.1. Synthesis of AAAB-substituted pyrimido[5,4-*d*]pyrimidine derivatives bearing traditional substituents

Synthesis of 2,6-dichloro-4,8-di(piperidin-1-yl)pyrimido[5,4-*d*]pyrimidine (1)

A suspension of TCPP (200 mg, 0.74 mmol) and K₂CO₃ (100 mg, 0.74 mmol) in dry THF (6 ml) was treated with piperidine (157 mg, 1.85 mmol) in dry THF (6 ml) at 0 °C. This reaction mixture was allowed to warm up to rt and stirred at rt for 16 h. TLC analysis suggested the emergence of **2** as an undesired side product. Subsequently, the solvent was removed under reduced pressure, the residue was suspended in water and the resulting solid was filtered off under reduced pressure and washed with water (2 x 20 ml). The crude product was purified by column chromatography (pure CH₂Cl₂) yielding **1** as 178 mg (66%) of a yellow solid. ¹H NMR (600 MHz, DMSO-*d*₆) δ: 4.15 (m, 8H, NCH₂), 1.58 (m, 12H, CH₂CH₂CH₂) ppm. ¹³C NMR (151 MHz, DMSO-*d*₆) δ: 158.8 (C_{arom.}), 152.3 (C_{arom.}), 136.2 (C_{arom.}), 48.5 (NCH₂), 26.1 (CH₂CH₂CH₂), 24.3 (CH₂CH₂CH₂) ppm. HPLC-UV (254 nm) ESI-MS, purity: 95%. LC-MS (m/z): 367.1 [M + H]⁺.

Synthesis of 2,2'-((6-chloro-4,8-di(piperidin-1-yl)pyrimido[5,4-*d*]pyrimidin-2-yl)azanediyl)bis(ethan-1-ol) (3)

A stirred solution of **1** (200 mg, 0.55 mmol) and diethanolamine (3660 mg, 19.6 mmol) in THF (2 ml) was heated at 70 °C for 16 h in a sealed tube. Subsequently, the mixture was treated with water and extracted with CH₂Cl₂ (3 x 20 ml), the combined organic layers were dried over MgSO₄, filtered off and the solvent was evaporated under reduced pressure. The residue was purified by column chromatography (CH₂Cl₂ / MeOH - 9 : 1). The product **3** was obtained as 185 mg (77%) of a yellow solid. ¹H NMR (600 MHz, Chloroform-*d*) δ: 4.76 (s, 2H, OH), 4.14-4.04 (m, 4H, NCH₂CH₂OH), 4.05-3.95 (m, 4H, NCH₂CH₂OH), 3.93-3.87 (m, 4H, NCH₂), 3.79-3.73 (m, 4H, NCH₂), 1.74-1.62 (m, 12H, CH₂CH₂CH₂) ppm. ¹³C NMR (151 MHz, CDCl₃) δ: 164.9, 160.0, 159.1, 149.2, 132.5, 62.3, 48.9, 47.9, 25.8, 24.6 ppm. HPLC-UV (254 nm) ESI-MS, purity: 95%. LC-MS (m/z): 436.6 [M + H]⁺.

Synthesis of 2,2'-((4,6,8-tri(piperidin-1-yl)pyrimido[5,4-*d*]pyrimidin-2-yl)azanediyl)bis(ethan-1-ol) (4)²⁸

A stirred solution of **3** (10 mg, 0.02 mmol) and an excess of piperidine in *i*PrOH (2 ml) was heated at 120 °C for 4 days in a sealed tube. Subsequently, the solvent was removed under reduced pressure and the residue was purified by column chromatography (pure ethyl acetate). The product **4** was obtained as 10 mg (90%) of a yellow, fluorescent solid. ¹H NMR (600 MHz, DMSO-*d*₆) δ: 4.70-4.61 (m, 2H, OH), 4.07-3.98 (m, 8H, NCH₂ / NCH₂CH₂OH), 3.61-3.53 (m, 12H, NCH₂ / NCH₂CH₂OH), 1.60-1.45 (m, 18H, CH₂CH₂CH₂) ppm. ¹³C NMR (151 MHz, DMSO-*d*₆) δ: 159.5, 159.4, 153.7, 153.5, 132.3, 131.8, 59.7, 51.7, 48.1, 48.0, 45.1, 26.0, 24.7, 24.6 ppm. HPLC-UV (254 nm) ESI-MS, purity: 96%. LC-MS (m/z): 485.3 [M + H]⁺. Mp.: 172-173 °C.

Synthesis of 2,2',2'',2''',2''''',2''''''-((6-chloropyrimido[5,4-*d*]pyrimidine-2,4,8-triyl)tris(azanetriyl))hexakis(ethan-1-ol) (5) and 2,2',2'',2''',2''''',2''''''',2''''''''-(pyrimido[5,4-*d*]pyrimidine-2,4,6,8-tetrayltetrakis(azanetriyl))octakis(ethan-1-ol) (6)^{27;28}

A stirred solution of TCPP (50 mg, 0.17 mmol) and an excess of diethanolamine in *i*PrOH (2 ml) was heated at 120 °C for 7 days in a sealed tube. Subsequently, the solvent was removed under reduced pressure and the residue was purified by column chromatography (CH₂Cl₂ / MeOH - 8 : 2). The desired product **6** was obtained as 10 mg (11%) of a yellow, fluorescent solid. LC-MS analysis was not perfectly clear due to tailing of the compound in the chromatogram and a bid injection peak. NMR analysis was also not possible due to solubility problems.

The impure side product **5** was obtained as 40 mg (49%) of a yellow solid. LC-MS (m/z): 476.2 [M + H]⁺. The crude product was directly used to prepare **7**.

Synthesis of 2,2',2'',2''',2''''-(6-(piperidin-1-yl)pyrimido[5,4-*d*]pyrimidine-2,4,8-triyl)tris(azanetriyl)hexakis(ethan-1-ol) (7)

A stirred solution of impure **5** (40 mg, 0.08 mmol) and piperidine (70 mg, 0.83 mmol) in *i*PrOH (2 ml) was heated at 120 °C for 4 days in a sealed tube. Subsequently, the solvent was removed under reduced pressure and the residue was purified by column chromatography (CH₂Cl₂ / MeOH - 8 : 2). The product **7** was obtained as 24 mg (27% over two steps) of a yellow, fluorescent solid. ¹H NMR (600 MHz, DMSO-*d*₆) δ: 4.83-4.75 (m, 2H, OH), 4.73-4.63 (m, 4H, OH), 4.09-3.95 (m, 8H, NCH₂CH₂OH), 3.70-3.61 (m, 8H, NCH₂CH₂OH/ NCH₂CH₂OH), 3.58-3.49 (m, 12H, NCH₂ / NCH₂CH₂OH), 1.60-1.50 (m, 2H, CH₂CH₂CH₂), 1.49-1.39 (m, 4H, CH₂CH₂CH₂) ppm. ¹³C NMR (151 MHz, DMSO-*d*₆) δ: 158.1, 153.8, 153.6, 132.0, 131.6, 59.8, 54.2, 54.0, 53.9, 53.9, 51.3, 45.3, 25.3, 24.8 ppm. HPLC-UV (254 nm) ESI-MS, purity: 97%. LC-MS (m/z): 525.3 [M + H]⁺. Mp.: 193-195 °C.

Synthesis of 2,6,8-trichloropyrimido[5,4-*d*]pyrimidin-4(1*H*)-one (11)

600 mg of TCPP (2.24 mmol) was added to a mixture of water / acetone (25 ml each) and stirred for 24 h. The solvent was evaporated under reduced pressure and the product was suspended in isopropanol, filtered off under reduced pressure, and dried at 70 °C. Product **11** was obtained as 511 mg (91%) of a rose colored solid. ¹H NMR (600 MHz, DMSO-*d*₆) δ: 14.03 (s, 1H) ppm. HPLC-UV (254 nm) ESI-MS, purity: 97%. LC-MS (m/z): 250.9 [M + H]⁺.

Synthesis of 2,6-dichloro-8-(piperidin-1-yl)pyrimido[5,4-*d*]pyrimidin-4(1*H*)-one (2)

A suspension of **11** (200 mg, 0.8 mmol) and K₂CO₃ (200 mg, 1.4 mmol) in dry THF (6 ml) was treated with piperidine (85 mg, 1 mmol) in dry THF (6 ml) at rt. This reaction mixture was stirred for 16 h at rt. Subsequently, the solvent was removed under reduced pressure, the residue was suspended in water, filtered off under reduced pressure and dried at 70°C. The product **2** was obtained as 208 mg (87%) of a colorless solid. ¹H NMR (600 MHz, DMSO-*d*₆) δ: 8.90 (s, 1H, NH), 4.15 (m, 4H, NCH₂), 1.58 (m, 6H, CH₂CH₂CH₂) ppm. ¹³C NMR (151 MHz, DMSO-*d*₆) δ: 169.3 (C_{arom.}), 159.1 (C_{arom.}), 155.8 (C_{arom.}), 152.5 (C_{arom.}), 141.9 (C_{arom.}), 134.9 (C_{arom.}), 48.1 (NCH₂), 26.0 (CH₂CH₂CH₂), 24.3 (CH₂CH₂CH₂) ppm. HPLC-UV (254 nm) ESI-MS, purity: 96%. LC-MS (m/z): 299.9 [M + H]⁺.

Synthesis of 2,6,8-tri(piperidin-1-yl)pyrimido[5,4-*d*]pyrimidin-4(1*H*)-one (16)

A stirred solution of **2** (50 mg, 0.17 mmol) and piperidine (70 mg, 0.83 mmol) in *i*PrOH (2 ml) was heated at 120 °C for 4 days in a sealed tube. Subsequently, the mixture was treated with water and extracted with CH₂Cl₂ (3 x 20 ml), the combined organic layers were dried over MgSO₄, filtered off and the solvent was evaporated under reduced pressure. The crude product was purified by column chromatography (ethyl acetate / MeOH - 9 : 1). The product **16** was

obtained as 38 mg (58%) of a yellow, fluorescent solid. ¹H NMR (600 MHz, DMSO-*d*₆) δ: 11.48 (s, 1H, NH), 3.98 (m, 4H, NCH₂), 3.66-3.60 (m, 4H, NCH₂), 3.45-3.34 (m, 4H, NCH₂), 1.46-1.66 (m, 18H, CH₂CH₂CH₂) ppm. ¹³C NMR (151 MHz, DMSO-*d*₆) δ: 161.7 (C=O), 159.1 (C_{arom.}), 156.4 (C_{arom.}), 146.5 (C_{arom.}), 127.4 (C_{arom.}), 62.9, 48.1 (NCH₂), 46.7 (NCH₂), 44.7 (NCH₂), 25.9 (CH₂CH₂CH₂), 25.5 (CH₂CH₂CH₂), 25.0 (CH₂CH₂CH₂), 24.6 (CH₂CH₂CH₂), 24.5 (CH₂CH₂CH₂), 24.1 (CH₂CH₂CH₂) ppm. HPLC-UV (254 nm) ESI-MS, purity: 92%. LC-MS (m/z): 398.2 [M + H]⁺. Mp.: 177-178 °C.

4.4.6.2.2. Synthesis of pyrimido[5,4-*d*]pyrimidine derivatives closely related to dipyridamole

Synthesis of ((4,8-di(piperidin-1-yl)pyrimido[5,4-*d*]pyrimidine-2,6-diyl)bis(azanetriyl)) tetrakis(ethane-2,1-diyl) tetraacetate (**22**)¹⁷

A solution of dipyridamole (30 mg, 0.06 mmol), Ac₂O (31 mg, 0.3 mmol) and TEA (40 mg, 0.4 mmol) in CH₂Cl₂ was stirred at rt for 2 days. Subsequently, the mixture was treated with water and extracted with CH₂Cl₂ (3 x 20 ml), the combined organic layers were dried over MgSO₄, filtered off and the solvent was evaporated under reduced pressure. The crude product was purified by flash RP-HPLC (10 to 100% MeOH). The product **22** was obtained as 21.8 mg (54%) of a yellow, fluorescent solid. ¹H NMR (600 MHz, Chloroform-*d*) δ: 4.26 (t, *J* = 5.9 Hz, 8H, NCH₂CH₂OH), 4.02 (s, 8H, NCH₂), 3.82 (t, *J* = 7.3 Hz, 8H, NCH₂CH₂OH), 2.03 (s, 12H, CH₃), 1.70-1.64 (m, 12H, CH₂CH₂CH₂) ppm. ¹³C NMR (151 MHz, Chloroform-*d*) δ: 171.02, 62.85, 48.69, 48.05, 26.23, 24.91, 20.98 ppm. HPLC-UV (254 nm) ESI-MS, purity: 95%. LC-MS (m/z): 673.4 [M + H]⁺. Mp.: 124-125 °C (lit.121-122°C).

Synthesis of 2-((6-chloro-4,8-di(piperidin-1-yl)pyrimido[5,4-*d*]pyrimidin-2-yl)amino) ethan-1-ol (**24**)

A stirred solution of **1** (75 mg, 0.2 mmol) and ethanolamine (800 mg, 13.08 mmol) in THF (2 ml) was heated at 75 °C for 16 h in a sealed tube. Subsequently, the mixture was treated with water and extracted with CH₂Cl₂ (3 x 20 ml), the combined organic layers were dried over MgSO₄, filtered off and the solvent was evaporated under reduced pressure. The residue was purified by column chromatography (petrol ether / ethyl acetate - 25 : 75 to pure ethyl acetate). The product **24** was obtained as 72 mg (92%) of a yellow, fluorescent solid. ¹H NMR (600 MHz, DMSO-*d*₆) δ: 6.67 (t, *J* = 5.8 Hz, 1H, NH), 4.59 (t, *J* = 5.5 Hz, 1H, OH), 4.24-4.08 (m, 4H, NCH₂), 4.06-3.97 (m, 4H, NCH₂), 3.50 (t, *J* = 5.9 Hz, 2H, NCH₂CH₂OH), 3.28 (t, *J* = 5.9 Hz, 2H, NCH₂CH₂OH), 1.66-1.49 (m, 12H, CH₂CH₂CH₂) ppm. ¹³C NMR (151 MHz, DMSO-*d*₆) δ: 159.2, 156.8, 59.9, 48.3, 48.2, 43.9, 26.1, 25.9, 24.4, 24.3 ppm. HPLC-UV (254 nm) ESI-MS, purity: 97%. LC-MS (m/z): 392.1 [M + H]⁺.

Synthesis of 2,2'-((6-((2-hydroxyethyl)amino)-4,8-di(piperidin-1-yl)pyrimido[5,4-d]pyrimidin-2-yl)azanediyl)bis(ethan-1-ol) (25)²⁹

A stirred solution of **24** (30 mg, 0.08 mmol) and diethanolamine (80 mg, 0.8 mmol) in *i*PrOH (2 ml) was heated at 120 °C for 16 h in a sealed tube. Subsequently, the solvent was removed under reduced pressure and the residue was purified by column chromatography (CH₂Cl₂ / MeOH - 9 : 1). The product **25** was obtained as 12 mg (34%) of a yellow, fluorescent solid. ¹H NMR (600 MHz, Chloroform-*d*) δ: 3.96-3.90 (m, 8H, NCH₂), 3.85 (t, *J* = 4.8 Hz, 4H, NCH₂CH₂OH), 3.77 (t, *J* = 4.8 Hz, 2H, NCH₂CH₂OH), 3.72 (t, *J* = 4.8 Hz, 4H, NCH₂CH₂OH), 3.52-3.48 (m, 2H, NCH₂CH₂OH), 1.24-1.22 (m, 12H, CH₂CH₂CH₂) ppm. ¹³C NMR (151 MHz, CDCl₃) δ: 160.8, 160.2, 155.8, 155.1, 132.8, 64.1, 62.9, 52.0, 49.1, 48.7, 44.7, 26.0, 26.0, 24.7, 24.7 ppm. HPLC-UV (254 nm) ESI-MS, purity: 93%. LC-MS (*m/z*): 461.2 [M + H]⁺. Mp.: 166 °C.

Synthesis of 2,4,6,8-tetra(piperidin-1-yl)pyrimido[5,4-d]pyrimidine (19)^{27;28}

A stirred solution of TCPP (30 mg, 0.11 mmol) and piperidine (excess) in DMSO (2 ml) was heated at 120 °C for 3 days in a sealed tube. Subsequently, the mixture was treated with water, the precipitate was filtered off under reduced pressure and dried at 70 °C. The product **19** was obtained as 27 mg (52%) of a yellow, fluorescent solid. ¹H NMR (600 MHz, DMSO-*d*₆) δ: 4.09-3.94 (m, 8H, NCH₂), 3.69-3.49 (m, 8H, NCH₂), 1.68-1.36 (m, 24H, CH₂CH₂CH₂) ppm. ¹³C NMR (151 MHz, DMSO-*d*₆) δ: 159.5, 159.4, 153.7, 153.5, 132.3, 131.8, 48.0, 45.1, 26.0, 24.7, 24.6 ppm. HPLC-UV (254 nm) ESI-MS, purity: 95%. LC-MS (*m/z*): 465.3 [M + H]⁺. Mp.: 168 °C.

Synthesis of ((4,8-di(piperidin-1-yl)pyrimido[5,4-d]pyrimidine-2,6-diyl)bis(2-tetrahydrofurylamine))dimethanol (28)

A stirred solution of crude **1** (30 mg, 0.08 mmol) and 2-tetrahydrofurylamine (excess) in *i*PrOH (2 ml) was heated at 130 °C for 5 days in a sealed tube. Subsequently, the mixture was treated with water and extracted with CH₂Cl₂ (3 x 20 ml), the combined organic layers were dried over MgSO₄, filtered off and the solvent was evaporated under reduced pressure. The crude product was purified by flash RP-HPLC (water / MeOH - 10 to 100%). The product **28** was obtained as 3.5 mg (9%) of a yellow, fluorescent solid. ¹H NMR (600 MHz, Chloroform-*d*) δ: 9.24 (s, 1H, NH), 3.98-3.60 (m, 12H, NCH₂), 2.05 (q, *J* = 8.2, 7.7 Hz, 2H, CH), 1.95-1.82 (m, 6H, CH₂), 1.79-1.53 (m, 14H, CH₂) ppm. ¹³C NMR was not possible due to solubility problems of the sample. HPLC-UV (254 nm) ESI-MS, purity: 89%. LC-MS (*m/z*): 497.2 [M + H]⁺. Mp.: 165 °C.

Synthesis of ((4,8-di(piperidin-1-yl)pyrimido[5,4-d]pyrimidine-2,6-diyl)bis(pyrrolidine-1,2-diyl))dimethanol (**29**)

A stirred solution of **1** (30 mg, 0.08 mmol) and *L*-prolinole (excess) in *i*PrOH (2 ml) was heated at 130 °C for 5 days in a sealed tube. Subsequently, the mixture was treated with water and extracted with CH₂Cl₂ (3 x 20 ml), the combined organic layers were dried over MgSO₄, filtered off and evaporated under reduced pressure. The crude product was purified by flash RP-HPLC (water / MeOH - 10 to 100%). The product **29** was obtained 22 mg (55%) as a yellow, fluorescent solid. ¹H NMR (600 MHz, Chloroform-*d*) δ: 1.51 (m, 4H CH₂), 1.56-2.12 (m, 16H, CH₂), 3.22-3.37 (6H, 3.28 (ddd, *J* = 13.1, 6.9, 1.7 Hz), 3.30 (ddd, *J* = 12.8, 10.3, 2.7 Hz)), 3.52 (2H, ddd, *J* = 13.1, 7.7, 6.9 Hz, NCH₂), 3.74 (4H, ddd, *J* = 12.8, 2.9, 2.6 Hz, NCH₂), 3.96-3.99 (m, 4H, NCH₂), 3.98 (d, *J* = 4.5 Hz), 4H, CH₂OH), 4.15 (2H, ddt, *J* = 7.7, 6.9, 4.5 Hz, CH) ppm. ¹³C NMR (151 MHz, CDCl₃) δ: 49.8, 49.5, 48.9, 46.1, 45.8, 29.2, 26.8, 26.7, 26.0, 25.8, 24.4, 23.8, 23.7, 23.6 ppm. HPLC-UV (254 nm) ESI-MS, purity: 95%. LC-MS (*m/z*): 497.2 [M + H]⁺. Mp.: 179 °C.

4.4.6.2.3. Synthesis of 4,8-bis(2-dihydroxyethylamino)-2,6-dichloropyrimido[5,4-d]pyrimidine derivatives

Synthesis of 2,2',2'',2'''-((2,6-dichloropyrimido[5,4-d]pyrimidine-4,8-diyl)bis(azanetriyl))tetrakis(ethan-1-ol) (**30**)

A suspension of TCPP (100 mg, 0.37 mmol), K₂CO₃ (100 mg, 0,74 mmol) and molecular sieve Å4 (100 mg) in dry THF (6 ml) was treated with diethanolamine (85 mg, 0.81 mmol) in dry THF (6 ml) at 0 °C. This reaction mixture was stirred for 16 h at rt. Subsequently, the solvent was removed under reduced pressure and the residue was purified by column chromatography (CH₂Cl₂ / MeOH - 9 : 1). The product **30** was obtained was 72 mg (48%) of a colorless solid. LC-MS (*m/z*): 407.1 [M + H]⁺.

Synthesis of 2,2',2'',2'''-((2,6-di(piperidin-1-yl)pyrimido[5,4-d]pyrimidine-4,8-diyl)bis(azanetriyl))tetrakis(ethan-1-ol) (**31**)^{10;27;28}

A stirred solution of **30** (40 mg, 0.1 mmol) and piperazine (101 mg, 1 mmol) in *i*PrOH (2 ml) was heated at 120 °C for 4 days in a sealed tube. Subsequently, the mixture was treated with water and extracted with CH₂Cl₂ (3 x 20 ml), the combined organic layers were dried over MgSO₄, filtered off under reduced pressure and the solvent was evaporated under reduced pressure. The residue was purified by column chromatography (CH₂Cl₂ / MeOH - 9 : 1). The product **31** was obtained as 13 mg (26%) of a yellow, fluorescent solid. ¹H NMR (600 MHz, DMSO-*d*₆) δ: 4.70 (t, *J* = 5.2 Hz, 4H, OH), 4.12 - 3.92 (m, 8H, NCH₂), 3.67 (q, *J* = 5.8 Hz, 8H, NCH₂CH₂OH), 3.54 (t, *J* = 5.4 Hz, 8H, NCH₂CH₂OH), 1.57 (q, *J* = 6.2 Hz, 4H, CH₂CH₂CH₂), 1.51 - 1.42 (m, 8H, CH₂CH₂CH₂) ppm. ¹³C NMR (151 MHz, DMSO-*d*₆) δ: 158.1, 154.1, 131.8,

59.8, 54.2, 45.3, 25.4, 24.8 ppm. HPLC-UV (254 nm) ESI-MS, purity: 96%. LC-MS (m/z): 505.4 [M + H]⁺. Mp.: 178 °C (lit. 180-181°C).

Synthesis of 2,6-dichloro-*N4,N4,N8,N8*-tetrakis(2-methoxyethyl)pyrimido[5,4-*d*]pyrimidine-4,8-diamine (32)

A suspension of TCPP (200 mg, 0.74 mmol) and K₂CO₃ (204 mg, 1.48 mmol) in dry THF (6 ml) was treated with bis(2-methoxyethyl)amine (296 mg, 2.22 mmol) in dry THF (6 ml) at 0°C. The reaction mixture was allowed to warm up to rt and was stirred at rt for 16 h. Subsequently, the mixture was treated with water and extracted with CH₂Cl₂ (3 x 20 ml), the combined organic layers were dried over MgSO₄, filtered off and the solvent was evaporated under reduced pressure. The product **32** was obtained as 340 mg (99%) of a yellow solid. ¹H NMR (600 MHz, DMSO-*d*₆) δ: 4.37 (m, 2H, NCH₂CH₂OCH₃), 3.88 (m, 2H, NCH₂CH₂OCH₃), 3.62 (m, 4H, NCH₂CH₂OH), 3.26 (s, 6H, OCH₃) ppm. ¹³C NMR (151 MHz, DMSO) δ: 159.2 (C_{arom.}), 152.1 (C_{arom.}), 135.9 (C_{arom.}), 71.4 (NCH₂CH₂OCH₃), 68.9 (NCH₂CH₂OCH₃), 58.4 (OCH₃), 51.4 (NCH₂CH₂OCH₃) ppm. HPLC-UV (254 nm) ESI-MS, purity: 97%. LC-MS (m/z): 286.0 [M + H]⁺.

Synthesis of *N4,N4,N8,N8*-tetrakis(2-methoxyethyl)-2,6-di(piperidin-1-yl)pyrimido[5,4-*d*]pyrimidine-4,8-diamine (33)

A stirred solution of **32** (150 mg, 0.32 mmol) and piperidine (275 mg, 3.2 mmol) in *i*PrOH (2 ml) was heated at 120 °C for 4 days in a sealed tube. Subsequently, the solvent was removed under reduced pressure, the residue was suspended in water, filtered off under reduced pressure and dried at 70°C. The product was **33** was obtained as 179 mg (96%) of a yellow, fluorescent solid. ¹H NMR (600 MHz, DMSO-*d*₆) δ: 4.32-3.77 (m, 8H, NCH₂CH₂OCH₃), 3.59 (t, *J* = 6.2 Hz, 8H, NCH₂), 3.56-3.52 (m, 8H, NCH₂CH₂OH), 3.29 (s, 12H, OCH₃), 1.61-1.53 (m, 4H), 1.52-1.42 (m, 8H, CH₂CH₂CH₂) ppm. ¹³C NMR (151 MHz, DMSO-*d*₆) δ: 158.0 (C2/C6), 154.0 (C4/C8), 131.8 (C_{arom.}), 58.4 (OCH₃), 71.4 (NCH₂CH₂OCH₃), 51.1 (NCH₂CH₂OCH₃), 45.1 (NCH₂), 25.3 (CH₂CH₂CH₂), 24.7 (CH₂CH₂CH₂) ppm. HPLC-UV (254 nm) ESI-MS, purity: 98%. LC-MS (m/z): 561.3 [M + H]⁺. Mp.: 189 °C.

Synthesis of tetraethyl 2,2',2'',2'''-((2,6-dichloropyrimido[5,4-*d*]pyrimidine-4,8-diyl)bis(azanetriyl))tetraacetate (34)

A suspension of TCPP (100 mg, 0.37 mmol) and K₂CO₃ (100 mg, 0.74 mmol) in dry THF (6 ml) was treated with diethyl iminodiacetate (175 mg, 0.92 mmol) in dry THF (6 ml) at 0°C. This reaction mixture was allowed to warm up to rt and stirred at rt for 2 h. Subsequently, the mixture was treated with water and extracted with CH₂Cl₂ (3 x 20 ml), the combined organic layers were dried over MgSO₄, filtered off under reduced pressure and the solvent was evaporated under reduced pressure. The product **34** was obtained as 158 mg (74%) of a colorless solid. ¹H NMR (600 MHz, DMSO-*d*₆) δ: 4.90 (s, 4H, NCH₂COOEt), 4.45 (s, 4H, NCH₂COOEt), 4.13

(q, $J = 7.1$ Hz, 8H, COOCH₂CH₃), 1.19 (q, $J = 7.0$ Hz, 12H COOCH₂CH₃) ppm. ¹³C NMR (151 MHz, DMSO-*d*₆) δ: 169.4 (COO), 168.6 (COO), 159.7, 152.5, 135.8, 61.2 (COOCH₂CH₃), 55.5 (NCH₂COOEt), 54.6 (NCH₂COOEt), 14.6 (COOCH₂CH₃) ppm. HPLC-UV (254 nm) ESI-MS, purity: 95%. LC-MS (m/z): 575.1 [M + H]⁺. The side product **36** was formed during this reaction, it was isolated and subsequently used for the preparation of product **20**.

Synthesis of tetraethyl 2,2',2'',2'''-((2,6-di(piperidin-1-yl)pyrimido[5,4-*d*]pyrimidine-4,8-diyl)bis(azanetriyl))tetraacetate (35)

A stirred solution of **34** (75 mg, 0.13 mmol) and piperidine (111 mg, 1.3 mmol) in *i*PrOH (2 ml) was heated at 120 °C for 4 days in a sealed tube. Subsequently, the mixture was treated with water and extracted with CH₂Cl₂ (3 x 20 ml), the combined organic layers were dried over MgSO₄, filtered and the solvent was evaporated under reduced pressure. The residue was purified by column chromatography (petrol ether / ethyl acetate - 2 : 1). The product **35** was obtained as 78 mg (89%) of a yellow, fluorescent solid. During the reaction, a transesterification with *i*PrOH took place so that a mixture of ethyl- and isopropylesters arose. This didn't matter since the ester function was supposed to be cleaved or reduced. ¹H NMR (600 MHz, Chloroform-*d*) δ: 5.04 (s, 8H, NCH₂COOEt), 4.15 (q, $J = 7.1$ Hz, 8H, COOCH₂CH₃), 3.52 (s, 8H, NCH₂), 1.61-1.56 (m, 8H, CH₂CH₂CH₂), 1.55-1.43 (m, 4H, CH₂CH₂CH₂), 1.23 (t, $J = 7.1$ Hz, 12H, COOCH₂CH₃) ppm. ¹³C NMR (151 MHz, CDCl₃) δ: 170.6 (COO), 158.5, 154.0, 132.2, 60.8 (COOCH₂CH₃), 53.7 (NCH₂COOEt), 45.4 (NCH₂), 25.6 (CH₂CH₂CH₂), 24.9 (CH₂CH₂CH₂), 14.2 (COOCH₂CH₃) ppm. LC-MS (m/z): 673.5 [M + H]⁺.

Synthesis of 2,2',2'',2'''-((2,6-di(piperidin-1-yl)pyrimido[5,4-*d*]pyrimidine-4,8-diyl)bis(azanetriyl))tetrakis(ethan-1-ol) (31)

A stirred solution of **35** (20 mg, 0.03 mmol) in THF (5 ml) was treated with LiAlH₄ (6 mg, 0.15 mmol) and refluxed for 2 h. Subsequently, the mixture was treated with NaOH solution and extracted with CH₂Cl₂ (3 x 20 ml), the combined organic layers were dried over MgSO₄, filtered off under reduced pressure and the solvent was evaporated under reduced pressure. TLC control with previously prepared **31** and LC-MS analysis showed that reduction of **35** actually leads to the formation of **31**.

Synthesis of 2,2'-((2,6,8-tri(piperidin-1-yl)pyrimido[5,4-*d*]pyrimidin-4-yl)azanediyl)bis(ethan-1-ol) (20)

A stirred solution of impure **36** (31 mg, ~0.07 mmol) and piperidine (excess) in *i*PrOH (2 ml) was heated at 120 °C for 4 days in a sealed tube. Subsequently, the mixture was treated with water and extracted with CH₂Cl₂ (3 x 20 ml), the combined organic layers were dried over MgSO₄, filtered and the solvent was evaporated under reduced pressure. The crude intermediate was dissolved in THF (3 ml), treated with LiAlH₄ (6 mg, 0.16 mmol) and refluxed

for 2 h. Subsequently, the mixture was treated with 0.5 M NaOH solution (15 ml) at rt and extracted with CH₂Cl₂ (3 x 20 ml), the combined organic layers were dried over MgSO₄, filtered off under reduced pressure and the solvent was evaporated under reduced pressure. The residue was purified by column chromatography (CH₂Cl₂/ MeOH - 9 : 1). The product **20** was obtained as 6 mg (3.5%, 3 steps, based on TCPP) of a yellow, fluorescent solid. ¹H NMR (600 MHz, Chloroform-*d*) δ 4.05-3.89 (m, 8H, NCH₂CH₂OH / NCH₂), 3.78-3.54 (m, 12H, NCH₂), 1.69 (d, *J* = 9.4 Hz, 12H, CH₂CH₂CH₂), 1.55 (t, *J* = 6.1 Hz, 6H, CH₂CH₂CH₂) ppm. ¹³C NMR (151 MHz, Chloroform-*d*) δ: 159.6, 159.2, 153.5, 153.5, 132.1, 131.9, 59.5, 51.5, 48.9, 48.0, 45.1, 26.1, 24.7, 24.5 ppm. HPLC-UV (254 nm) ESI-MS, purity: 95%. LC-MS (*m/z*): 485.3 [M + H]⁺. Mp.: 174-175 °C.

4.4.6.2.4. Synthesis of 4,8-bis(amino)-2,6-dichloropyrimido[5,4-*d*]pyrimidine-derivatives

Synthesis of 2,6-dichloropyrimido[5,4-*d*]pyrimidine-4,8-diamine (**38**)

A suspension of TCPP (150 mg, 0.56 mmol) in dry THF (6 ml) was treated with NH₃ in MeOH (7 N, 2.5 ml, 2.8 mmol) at 0°C. This reaction mixture was allowed to warm up to rt and stirred at rt for 1 h. Subsequently, the solvent was removed under reduced pressure, the residue was suspended in water, filtered off under reduced pressure and dried at 70°C. The product **38** was obtained as 123 mg (95%) of a colorless solid ¹H NMR (600 MHz, DMSO-*d*₆) δ: 8.46 (s, 2H, NH₂), 8.11 (s, 2H, NH₂) ppm. LC-MS (*m/z*): 231.0 [M + H]⁺.

Synthesis of 2,2',2'',2'''-((4,8-diaminopyrimido[5,4-*d*]pyrimidine-2,6-diyl)bis(azanetriyl)) tetrakis(ethan-1-ol) (**39**)¹⁷

A stirred solution of **38** (25 mg, 0.11 mmol) and diethanolamine (116 mg, 1.1 mmol) in *i*PrOH (2 ml) was heated at 120 °C for 4 days in a sealed tube. Subsequently, the solvent was removed under reduced pressure and the residue was purified by column chromatography (CH₂Cl₂/ MeOH - 8 : 2). The product **39** was obtained as 25 mg (63%) of a yellow, fluorescent solid. ¹H NMR (600 MHz, DMSO-*d*₆) δ: 7.14 (s, 2H, NH₂), 6.63 (s, 2H, NH₂), 4.64 (s, 4H, OH), 3.60 (t, *J* = 6.2 Hz, 8H, NCH₂CH₂OH), 3.55 (t, *J* = 6.2 Hz, 8H, NCH₂CH₂OH) ppm. ¹³C NMR (151 MHz, DMSO-*d*₆) δ: 160.2, 155.3, 127.4, 59.7(NCH₂CH₂OH), 51.0 (NCH₂CH₂OH) ppm. HPLC-UV (254 nm) ESI-MS, purity: 96%. LC-MS (*m/z*): 369.1 [M + H]⁺. Mp.: 222-223 °C (lit. 225-226 °C).

Synthesis of 2,6-di(piperidin-1-yl)pyrimido[5,4-*d*]pyrimidine-4,8-diamine (**40**)

A stirred solution of **38** (25 mg, 0.11 mmol) and piperidine (94 mg, 1.1 mmol) in *i*PrOH (2 ml) was heated at 120 °C for 4 days in a sealed tube. Subsequently, the solvent was removed under reduced pressure and the residue was purified by column chromatography (petrol ether / ethyl acetate - 8 : 2 to pure ethyl acetate). The product **40** was obtained as 25 mg (63%) of a

yellow, fluorescent solid. ^1H NMR (600 MHz, $\text{DMSO-}d_6$) δ : 7.01 (s, 2H), 6.78 (s, 2H), 3.77-3.58 (m, 8H, NCH_2), 1.76-1.54 (m, 4H, $\text{CH}_2\text{CH}_2\text{CH}_2$), 1.55-1.37 (m, 8H, $\text{CH}_2\text{CH}_2\text{CH}_2$) ppm. ^{13}C NMR could not be interpreted due to solubility problems. HPLC-UV (254 nm) ESI-MS, purity: 93%. LC-MS (m/z): 329.2 $[\text{M} + \text{H}]^+$. Mp.: 199 °C.

4.4.6.2.5. Synthesis of 4,6,8-tripiperidinopyrimido[5,4-*d*]pyrimidin derivatives

Synthesis of 2-chloro-4,6,8-tri(piperidin-1-yl)pyrimido[5,4-*d*]pyrimidine (42)

A stirred solution of **1** (75 mg, 0.2 mmol) and piperazine (521 mg, 6.1 mmol) in THF (2 ml) was heated at 75 °C for 3 days in a sealed tube. Subsequently, the solvent was removed under reduced pressure and the residue was purified by column chromatography (pure ethyl acetate). The product **42** was obtained as 80 mg (96%) of a yellow solid. ^1H NMR (600 MHz, Chloroform-*d*) δ : 4.21-4.08 (m, 4H, NCH_2), 4.05 (s, 4H, NCH_2), 3.69 (t, $J = 5.2$ Hz, 4H, NCH_2), 1.67-1.60 (m, 12H, $\text{CH}_2\text{CH}_2\text{CH}_2$), 1.60-1.54 (m, 6H, $\text{CH}_2\text{CH}_2\text{CH}_2$) ppm. ^{13}C NMR could not be interpreted due to solubility problems. HPLC-UV (254 nm) ESI-MS, purity: 93%. LC-MS (m/z): 416.0 $[\text{M} + \text{H}]^+$. Mp.: 144 °C.

Synthesis 2-(propyl(4,6,8-tri(piperidin-1-yl)pyrimido[5,4-*d*]pyrimidin-2-yl)amino) ethan-1-ol (43)

A stirred solution of **42** and 2-(propylamino)ethan-1-ol (excess) in *i*PrOH (2 ml) was heated at 130 °C for 7 days in a sealed tube. The crude product was directly purified by column chromatography (CH_2Cl_2 / MeOH - 9 : 1). The product **43** was obtained as 14.4 mg (35%) of yellow, fluorescent solid. ^1H NMR (600 MHz, Chloroform-*d*) δ : 4.40-4.28 (m, 2H, NCH_2), 4.01-3.92 (m, 2H, NCH_2), 3.88-3.80 (m, 4H, NCH_2), 3.80-3.75 (m, 2H, NCH_2), 3.70-3.56 (m, 4H, NCH_2), 3.55-3.45 (m, 2H, CH_2), 1.81-1.58 (m, 18H, $\text{CH}_2\text{CH}_2\text{CH}_2$), 0.96-0.86 (m, 3H, CH_3) ppm. ^{13}C NMR could not be interpreted due to solubility problems. HPLC-UV (254 nm) ESI-MS, purity: 92%. LC-MS (m/z): 483.3 $[\text{M} + \text{H}]^+$. Mp.: 185 °C.

Synthesis of 3-((4,6,8-tri(piperidin-1-yl)pyrimido[5,4-*d*]pyrimidin-2-yl)amino)propane-1,2-diol. (44)

A stirred solution of **42** and 3-aminopropane-1,2-diol (excess) in *i*PrOH (2 ml) was heated at 130 °C for 7 days in a sealed tube. The crude product was directly purified by column chromatography (CH_2Cl_2 / MeOH - 9 : 1). The product **44** was obtained as 6.2 mg (15%) of yellow, fluorescent solid. ^1H NMR (600 MHz, Chloroform-*d*) δ : 8.99-8.77 (m, 1H, NH), 4.84-4.42 (m, 2H, NCH_2), 4.15-3.85 (m, 2H, CH_2OH), 3.71 (s, 1H, CHOH), 3.68-3.61 (m, 4H, NCH_2), 3.56 (s, 8H, NCH_2), 2.82-2.48, 1.75 (d, $J = 15.9$ Hz, 12H, $\text{CH}_2\text{CH}_2\text{CH}_2$), 1.67-1.60 (m, 6H, $\text{CH}_2\text{CH}_2\text{CH}_2$) ppm. ^{13}C NMR could not be interpreted due to solubility problems. HPLC-UV (254 nm) ESI-MS, purity: 89%. LC-MS (m/z): 471.3 $[\text{M} + \text{H}]^+$. Mp.: 179 °C.

Synthesis of 2-((4,6,8-tri(piperidin-1-yl)pyrimido[5,4-*d*]pyrimidin-2-yl)amino)propane-1,3-diol (**45**)

A stirred solution of **42** and 2-aminopropane-1,3-diol (excess) in *i*PrOH (2 ml) was heated at 130 °C for 7 days in a sealed tube. The crude product was directly purified by column chromatography (CH₂Cl₂ / MeOH - 9 : 1). The product **45** was obtained as 10 mg of a yellow, fluorescent solid. ¹H NMR (600 MHz, Chloroform-*d*) δ: 9.07 (d, *J* = 7.2 Hz, 1H, NH), 4.66 (s, 4H, NCH₂), 4.07 (s, 1H, NCH), 3.96 (s, 4H, NCH₂), 3.85 (tt, *J* = 11.5, 5.8 Hz, 4H, CH₂OH), 3.64 (t, *J* = 5.3 Hz, 4H, NCH₂), 3.53 (t, *J* = 5.2 Hz, 4H, NCH₂), 1.85-1.60 (m, 18H, CH₂CH₂CH₂) ppm. HPLC-UV (254 nm) ESI-MS, purity: 90%. LC-MS (m/z): 471.0 [M + H]⁺. Mp.: 187 °C.

Synthesis of 4,6,8-tri(piperidin-1-yl)pyrimido[5,4-*d*]pyrimidine-2-carbonitrile (**47**)

A stirred solution of **42** (100 mg, 0.24 mmol) and NaCN (118 mg, 2.4 mmol) in DMSO (2 ml) was heated at 90 °C for 2 days in a sealed tube. Subsequently, the mixture was treated with water and extracted with CH₂Cl₂ (3 x 20 ml), the combined organic layers were dried over MgSO₄, filtered and the solvent was evaporated under reduced pressure. The crude product was purified by column chromatography (petrol ether / ethyl acetate - 8 : 2). The product **47** was obtained as 56 mg (58%) of a colorless solid. ¹H NMR (600 MHz, Chloroform-*d*) δ: 4.10-4.07 (m, 8H, NCH₂), 3.76-3.67 (m, 4H, NCH₂), 1.76-1.59 (m, 18H, CH₂CH₂CH₂) ppm. ¹³C NMR (151 MHz, CDCl₃) δ: 159.7, 158.4, 157.0, 140.1, 131.8, 130.0, 117.6 (C≡N), 48.7 (NCH₂), 45.1 (NCH₂), 25.8 (CH₂CH₂CH₂), 24.9 (CH₂CH₂CH₂), 24.8 (CH₂CH₂CH₂), 24.8 (CH₂CH₂CH₂), 24.8 (CH₂CH₂CH₂) ppm. HPLC-UV (254 nm) ESI-MS, purity: 94%. LC-MS (m/z): 407.3 [M + H]⁺. Mp.: 163 °C.

Synthesis of *N*-hydroxy-4,6,8-tri(piperidin-1-yl)pyrimido[5,4-*d*]pyrimidine-2-carboximidamide (**48**)

A stirred solution of **46** (50 mg, 0.12 mmol) and H₂NOH • HCl (86 mg, 1.2 mmol) in MeOH (2 ml) was heated reflux for 2 days in a sealed tube. Subsequently, the mixture was treated with water and extracted with CH₂Cl₂ (3 x 20 ml), the combined organic layers were dried over MgSO₄, filtered off under reduced pressure and the solvent was evaporated under reduced pressure. The crude product was purified by column chromatography (CH₂Cl₂ / MeOH - 9 : 1 and afterwards ethyl acetate / MeOH - 9 : 1). The product **48** was obtained as 28 mg (53%) of a colorless solid. ¹H NMR (600 MHz, Chloroform-*d*) δ: 5.68 (s, 2H, NH), 4.14-4.04 (m, 8H, NCH₂), 3.75-3.69 (m, 4H, NCH₂), 1.73-1.56 (m, 18H, CH₂CH₂CH₂) ppm. ¹³C NMR (151 MHz, CDCl₃) δ: 160.7, 159.0, 156.6, 150.6, 144.7, 139.2, 129.8, 49.1 (NCH₂), 48.7 (NCH₂), 45.2 (NCH₂), 26.3 (CH₂CH₂CH₂), 26.2 (CH₂CH₂CH₂), 26.1 (CH₂CH₂CH₂), 25.8 (CH₂CH₂CH₂), 25.7 (CH₂CH₂CH₂), 24.9 (CH₂CH₂CH₂) ppm. HPLC-UV (254 nm) ESI-MS, purity: 95%. LC-MS (m/z): 440.4 [M + H]⁺. Mp.: 202 °C.

Synthesis of 4,6,8-tri(piperidin-1-yl)pyrimido[5,4-d]pyrimidine-2-carboxamide (49)

A stirred solution of **46** (15 mg, 0.04 mmol), 0.1 ml of 0.2 N NaOH, 2 ml water and 2 ml dioxane were heated at reflux for 16 h in a sealed tube. Subsequently, the solvent was removed under reduced pressure and the residue was purified by column chromatography (CH₂Cl₂ pure to CH₂Cl₂ / MeOH - 95 : 5). The product **49** was obtained as 7 mg (41%) of a yellow, fluorescent solid. ¹H NMR (600 MHz, Chloroform-*d*) δ: 7.34-7.15 (m, 5H, CH_{arom}), 4.06 (s, 4H, NCH₂CH₂OH), 4.04-3.69 (m, 8H, NCH₂CH₂OH / NCH₂), 3.65 (q, *J* = 6.9 Hz, 2H, NHCH₂CH₂Ph), 2.99-2.85 (t, *J* = 7.3 Hz, 2H, NHCH₂CH₂Ph), 1.66 (m, 6H, CH₂CH₂CH₂) ppm. ¹³C NMR (151 MHz, CDCl₃) δ: 138.7, 128.8, 128.7, 126.5, 67.0, 62.6, 52.1, 51.4, 48.6, 42.0, 35.2, 34.1, 29.6, 29.6, 29.3, 24.6, 22.6, 14.1 ppm. HPLC-UV (254 nm) ESI-MS, purity: 95%. LC-MS (m/z): 425.2 [M + H]⁺. Mp.: 178 °C.

Synthesis of 2-((4,6,8-tri(piperidin-1-yl)pyrimido[5,4-d]pyrimidin-2-yl)amino)ethane-1-sulfonic acid (50)

A stirred solution of **1** (50 mg, 0.14 mmol) and taurine (150 mg, 1.4 mmol) and TEA (0.5 ml) in DMSO (2 ml) was heated at 90 °C for 3 days in a sealed tube. Subsequently, the mixture was treated with water and extracted with CH₂Cl₂ (3 x 20 ml), the combined organic layers were dried over MgSO₄, filtered and the solvent was evaporated under reduced pressure. The residue was purified by column chromatography (CH₂Cl₂ / MeOH - 9:1 + 1% acetic acid). The intermediate **55** was obtained as 35 mg (58%) of a brownish solid. ¹H NMR (600 MHz, DMSO-*d*₆) δ: 11.93 (s, 1H, SO₃H), 6.69 (t, *J* = 5.5 Hz, 1H, NH), 4.16 (s, 4H, NCH₂), 4.01 (s, 4H, NCH₂), 3.47 (q, *J* = 6.5 Hz, 2H, NHCH₂CH₂SO₃H), 2.66 (t, *J* = 6.9 Hz, 2H, NHCH₂CH₂SO₃H), 1.69-1.53 (m, 12H, CH₂CH₂CH₂) ppm. ¹³C NMR (151 MHz, DMSO-*d*₆) δ: 179.2, 172.8, 159.3, 159.2, 156.5, 110.6, 50.5 (NHCH₂CH₂SO₃H), 48.3 (NCH₂), 38.3 (NHCH₂CH₂SO₃H), 25.9 (CH₂CH₂CH₂), 24.4 (CH₂CH₂CH₂) ppm. HPLC-UV (254 nm) ESI-MS, purity: 94%. LC-MS (m/z): 456.2 [M + H]⁺.

A stirred solution of **55** (34 mg, 0.075 mmol) and piperidine (excess) in *i*PrOH (2 ml) was heated at 120 °C for 4 days in a sealed tube. Subsequently, the mixture was treated with water and extracted with CH₂Cl₂ (3 x 20 ml), the combined organic layers were dried over MgSO₄, filtered off under reduced pressure and the solvent was evaporated under reduced pressure. The residue was purified by column chromatography (CH₂Cl₂ / MeOH - 9 : 1). The product **50** was obtained as 27 mg (71%) of a yellow, fluorescent solid. ¹H NMR (600 MHz, Chloroform-*d*) δ: 7.88 (s, 1 H, NH) 4.63 (s, 2H, NCH₂), 3.96 (s, 2H, NCH₂), 3.83-3.78 (m, 2H, NHCH₂CH₂SO₃H), 3.61 (t, *J* = 5.3 Hz, 4H, NCH₂), 3.44 (t, *J* = 4.5 Hz, 4H, NCH₂), 3.11 (dd, *J* = 6.9, 3.8 Hz, 2H, NHCH₂CH₂SO₃H), 1.75-1.57 (m, 18H, CH₂CH₂CH₂) ppm. ¹³C NMR (151 MHz, CDCl₃) δ: 158.0, 157.7, 156.0, 149.6, 133.2, 117.8, 48.8 (NCH₂), 48.3 (NCH₂), 47.8 (NCH₂) 45.2 (NHCH₂CH₂SO₃H), 37.7 (NHCH₂CH₂SO₃H), 25.5 (CH₂CH₂CH₂), 25.1 (CH₂CH₂CH₂), 24.7

(CH₂CH₂CH₂), 24.3 (CH₂CH₂CH₂), 24.2 (CH₂CH₂CH₂) ppm. HPLC-UV (254 nm) ESI-MS, purity: 97%. LC-MS (m/z): 505.5 [M + H]⁺. Mp.: 211 °C.

Synthesis of 1-(4,6,8-tri(piperidin-1-yl)pyrimido[5,4-d]pyrimidin-2-yl)piperidine-4-carboxylic acid (**52**)

A stirred solution of **1** (50 mg, 0.14 mmol) and 4-piperidinecarboxylic acid (182 mg, 1.4 mmol) and TEA (0.5 ml) in DMSO (2 ml) was heated at 90 °C for 3 days in a sealed tube. Subsequently, the mixture was treated with water and extracted with CH₂Cl₂ (3 x 20 ml), the combined organic layers were dried over MgSO₄, filtered off under reduced pressure and the solvent was evaporated under reduced pressure. The residue was purified by column chromatography (CH₂Cl₂ / MeOH - 9 : 1). The intermediate **56** was obtained as 53 mg (82%) of a brown solid. ¹H NMR (600 MHz, DMSO-*d*₆) δ: 12.19 (s, 1H, COOH), 4.37 (dt, *J* = 13.6, 3.9 Hz, 4H, NCH₂), 4.13 (s, 4H, NCH₂), 4.03 (s, 4H, NCH₂), 3.04-2.99 (m, 1H, CH), 1.88-1.81 (m, 2H, CH₂CH₂), 1.69-1.55 (m, 12H, CH₂CH₂CH₂), 1.53-1.43 (m, 2H, CH₂CH₂) ppm. ¹³C NMR (151 MHz, DMSO-*d*₆) δ: 176.0 (COOH), 159.3, 159.1, 155.8, 147.5, 137.3, 131.1, 48.4 (NCH₂), 43.4 (NCH₂), 43.4 (NCH₂), 27.6 (CH₂CH₂), 25.8 (CH₂CH₂CH₂), 24.3 (CH₂CH₂CH₂) ppm. HPLC-UV (254 nm) ESI-MS, purity: 95%. LC-MS (m/z): 460.2 [M + H]⁺.

A stirred solution of **56** (50 mg, 0.11 mmol) and piperidine (excess) in *i*PrOH (2 ml) was heated at 120 °C for 4 days in a sealed tube. Subsequently, the mixture was treated with water and extracted with CH₂Cl₂ (3 x 20 ml), the combined organic layers were dried over MgSO₄, filtered off under reduced pressure and the solvent was evaporated under reduced pressure. The residue was purified by column chromatography (CH₂Cl₂ / MeOH - 9 : 1). The product **52** was obtained as 45 mg (81%) of a yellow, fluorescent solid. ¹H NMR (600 MHz, DMSO-*d*₆) δ: 12.19 (s, 1H, COOH), 4.37 (dt, *J* = 13.6, 3.9 Hz, 4H, NCH₂), 4.13 (s, 4H, NCH₂), 4.03 (s, 8H, NCH₂), 3.04-2.99 (m, 1H, CH), 1.88-1.81 (m, 2H, CH₂CH₂), 1.69-1.55 (m, 18H, CH₂CH₂CH₂), 1.53-1.43 (m, 2H, CH₂CH₂) ppm. ¹³C NMR (151 MHz, DMSO-*d*₆) δ: 176.0 (COOH), 159.3, 159.1, 155.8, 147.5, 137.3, 131.1, 48.4 (NCH₂), 43.4 (NCH₂), 43.4 (NCH₂), 27.6 (CH₂CH₂), 25.8 (CH₂CH₂CH₂), 24.3 (CH₂CH₂CH₂) ppm. HPLC-UV (254 nm) ESI-MS, purity: 92%. LC-MS (m/z): 508.4 [M + H]⁺. Mp.: 192,5 °C.

Synthesis of ethyl 1-(4,6,8-tri(piperidin-1-yl)pyrimido[5,4-d]pyrimidin-2-yl)piperidine-4-carboxylate (**58**)

A stirred solution of **1** (50 mg, 0.14 mmol) and 4-piperidinecarboxylic acid ethyl ester (220 mg, 1.4 mmol) in THF (2 ml) was heated at 90 °C for 3 days in a sealed tube. Subsequently, the mixture was treated with water and extracted with CH₂Cl₂ (3 x 20 ml), the combined organic layers were dried over MgSO₄, filtered off under reduced pressure and the solvent was evaporated under reduced pressure. The residue was purified by column chromatography

(petrol ether / ethyl acetate - 10 : 1 + 1% acetic acid). The intermediate **57** was obtained as 55 mg (80%) of a brown solid. ¹H NMR (600 MHz, Chloroform-*d*) δ: 4.52 (dt, *J* = 13.6, 3.8 Hz, 2H, NCH₂), 4.13 (q, *J* = 7.1 Hz, 2H, CH₂CH₃), 4.05 (s, 4H, NCH₂), 3.02-2.95 (m, 2H, NCH₂), 2.52 (ddd, *J* = 11.1, 7.2, 3.9 Hz, 1H, CH), 1.96-1.89 (m, 2H, NCH₂), 1.73-1.62 (m, 10H, CH₂CH₂CH₂), 1.39 (s, 6H, CH₂CH₂CH₂), 1.24 (t, *J* = 7.1 Hz, 3H, CH₃) ppm. ¹³C NMR (151 MHz, CDCl₃) δ: 174.9 (ester), 160.2, 159.9, 156.1, 148.6, 137.5, 131.9, 60.4, 59.5, 48.9 (NCH₂), 43.7 (NCH₂), 41.6 (NCH₂), 38.1 (CH₂), 31.2 (CH₂), 27.9 (CH₂CH₂CH₂), 26.3 (CH₂CH₂CH₂), 26.0 (CH₂CH₂CH₂), 24.9 (CH₂CH₂CH₂), 24.8 (CH₂CH₂CH₂), 14.2 (CH₃) ppm. HPLC-UV (254 nm) ESI-MS, purity: 98%. LC-MS (m/z): 488.3 [M + H]⁺.

A stirred solution of **57** (50 mg, 0.11 mmol) and piperidine (excess) in *i*PrOH (2 ml) was heated at 120 °C for 4 days in a sealed tube. Subsequently, the mixture was treated with water and extracted with CH₂Cl₂ (3 x 20 ml), the combined organic layers were dried over MgSO₄, filtered off under reduced pressure and the solvent was evaporated under reduced pressure. The residue was purified by column chromatography (petrolether / ethyl acetate - 8 : 2). The product **58** was obtained as 11 mg (21%) of a yellow, fluorescent solid. ¹H NMR (600 MHz, Chloroform-*d*) δ: 4.50 (dd, *J* = 10.7, 6.5 Hz, 2H, NCH₂), 4.12 (q, *J* = 7.2 Hz, 2H, CH₂CH₃), 4.08-3.94 (m, 8H, NCH₂), 3.64 (d, *J* = 6.3 Hz, 4H, NCH₂), 2.91 (t, *J* = 12.4 Hz, 2H, NCH₂), 2.53-2.44 (m, 1H, CH), 1.97-1.85 (m, 2H, CH₂CH₂), 1.62-1.52 (m, 10H, CH₂CH₂CH₂), 1.33-1.13 (m, 12H, CH₂CH₂CH₂), 0.86 (d, *J* = 7.0 Hz, 3H, CH₂CH₃) ppm. ¹³C NMR (151 MHz, CDCl₃) δ: 175.2 (ester), 160.7 (CH), 154.4, 132.6, 124.4, 124.0, 119.1, 60.3 (NCH₂), 48.7 (NCH₂), 45.5 (NCH₂), 44.1 (NCH₂), 41.8 (NCH₂), 31.9 (CH₂), 31.4 (CH₂), 30.2 (CH₂), 29.78 (CH₂CH₂CH₂), 29.71 (CH₂CH₂CH₂), 29.6 (CH₂CH₂CH₂), 29.3 (CH₂CH₂CH₂), 27.9 (CH₂CH₂CH₂), 26.1 (CH₂CH₂CH₂), 25.7 (CH₂CH₂CH₂), 25.0 (CH₂CH₂CH₂), 22.7 (CH₂CH₂CH₂), 14.1 (CH₃) ppm. HPLC-UV (254 nm) ESI-MS, purity: 92%. LC-MS (m/z): 536.6 [M + H]⁺. Mp.: 178 °C.

Synthesis of 2-(hydroxymethyl)-2-((4,6,8-tri(piperidin-1-yl)pyrimido[5,4-*d*]pyrimidin-2-yl)amino)propane-1,3-diol (**60**)

A stirred solution of **1** (100 mg, 0.28 mmol) and tris(hydroxymethyl)aminomethane (440 mg, 2.8 mmol) in DMSO (2 ml) was heated at 90 °C for 3 days in a sealed tube. Subsequently, the mixture was treated with water and extracted with CH₂Cl₂ (3 x 20 ml), the combined organic layers were dried over MgSO₄, filtered off under reduced pressure and the solvent was evaporated under reduced pressure. The intermediate **59** was obtained as 52 mg (41%) of a yellow solid. LC-MS (m/z): 452.3 [M + H]⁺.

A stirred solution of **59** (50 mg, 0.11 mmol) and piperidine (excess) in *i*PrOH (2 ml) was heated at 120 °C for 4 days in a sealed tube. Subsequently, the mixture was treated with water and extracted with CH₂Cl₂ (3 x 20 ml), the combined organic layers were dried over MgSO₄, filtered off and the solvent was evaporated under reduced pressure. The residue was purified by

column chromatography (CH₂Cl₂/ MeOH - 9 : 1). The product **60** was obtained as 14 mg (21%) of a yellow, fluorescent solid. ¹H NMR (600 MHz, Chloroform-*d*) δ: 5.27 (s, 1H, NH), 4.70-4.67 (m, 12H, NCH₂), 3.80-3.75 (m, 6H, CH₂OH), 1.69-1.66 (m, 18H, CH₂CH₂CH₂) ppm. ¹³C NMR was not interpretable due to solubility problems. HPLC-UV (254 nm) ESI-MS, purity: 92%. LC-MS (m/z): 500.6 [M + H]⁺. Mp.: 236 °C.

Synthesis of 2-(4,6,8-tri(piperidin-1-yl)pyrimido[5,4-*d*]pyrimidin-2-yl)ethan-1-ol (51)

A stirred solution of **61** (30 mg, 0.08 mmol) and piperidine (excess) in *i*PrOH (2 ml) was heated at 120 °C for 4 days in a sealed tube. Subsequently, the mixture was treated with water and extracted with CH₂Cl₂ (3 x 20 ml), the combined organic layers were dried over MgSO₄, filtered off and the solvent was evaporated under reduced pressure. The residue was purified by column chromatography (CH₂Cl₂/ MeOH - 9 : 1). The product **51** was obtained as 12 mg (34%) of a yellow, fluorescent solid. ¹H NMR (600 MHz, Chloroform-*d*) δ: 4.09-4.06 (m, 4H, NCH₂), 3.83-3.79 (m, 4H, NCH₂), 3.75 (m, 2H, NCH₂CH₂OH), 3.64-3.59 (m, 4H, NCH₂), 3.51-3.46 (m, 2H, NCH₂CH₂OH), 1.70-1.56 (m, 18H, CH₂CH₂CH₂) ppm. ¹³C NMR (151 MHz, CDCl₃) δ: 160.4, 160.1, 155.1, 133.8, 64.0, 49.1, 48.8, 45.4, 44.8, 44.5, 26.3, 25.8, 25.7, 25.7, 25.7, 25.0, 24.8 ppm. HPLC-UV (254 nm) ESI-MS, purity: 94%. LC-MS (m/z): 441.3 [M + H]⁺. Mp.: 178°C.

4.4.6.2.6. Synthesis of 2,6-bis[bis(2-hydroxyethyl)amino]-4-piperidinopyrimido[5,4-*d*]pyrimidine derivatives

Synthesis of 4-piperazine-2, 6, 8-trichloropyrimido[5, 4-*d*]pyrimidine (69)

To a solution of TCPP (200 mg, 0.75 mmol) and K₂CO₃ (124 mg, 0.9 mmol) in dry THF (6 ml), stirred under argon at -78°C, was added piperazine (68 mg, 0.8 mmol) in THF (6 ml) drop wise from a syringe at a rate of 1 ml per minute. A cloudy yellow solution was obtained which was allowed to warm up for 10 min. Subsequently, the mixture was treated with water and was extracted with CH₂Cl₂ (3 x 20 ml), the combined organic layers were dried over MgSO₄, filtered off and the solvent was evaporated under reduced pressure. The crude product was purified by column chromatography (petrol ether / ethyl acetate - 10 : 1 + 1% acetic acid). The product **69** was obtained as 167 mg (70%) of a colorless solid. HPLC-UV (254 nm) ESI-MS, purity: 95%. LC-MS (m/z): 318.1 [M + H]⁺.

Synthesis of 2,6-dichloro-*N*-phenylethyl-8-(piperidin-1-yl)pyrimido[5,4-*d*]pyrimidin-4-amine (70)

A stirred solution of **69** (40 mg, 0.13 mmol), phenylethylamine (17 mg, 0.14 mmol) K₂CO₃ (26 mg, 1.9 mmol) in THF (10 ml) was stirred at rt for 16 h. Subsequently, the mixture was treated with water and extracted with CH₂Cl₂ (3 x 20 ml), the combined organic layers were dried over MgSO₄, filtered off and the solvent was evaporated under reduced pressure. The intermediate

70 was obtained as 43 mg (84%) of a yellow solid. ¹H NMR (600 MHz, Chloroform-*d*) δ: 7.32-7.28 (m, 2H, CH_{arom.}), 7.24-7.21 (m, 2H, CH_{arom.}), 7.06-7.02 (m, 1H, CH_{arom.}), 4.75-4.54 (m, 2H, NCH₂), 4.05-3.85 (m, 2H, NCH₂), 3.80 (q, *J* = 6.9 Hz, 2H, NHCH₂CH₂Ph), 2.96 (t, *J* = 7.3 Hz, 2H, NHCH₂CH₂Ph), 1.77-1.63 (m, 6H, CH₂CH₂CH₂) ppm. ¹³C NMR (151 MHz, CDCl₃) δ: 159.8, 157.8, 155.4, 153.7, 138.3, 135.0, 132.9, 126.7, 42.3, 35.2, 26.1, 24.5 ppm. HPLC-UV (254 nm) ESI-MS, purity: 95%. LC-MS (*m/z*): 403.2 [M + H]⁺.

Synthesis of 2,2',2'',2'''-((4-(phenylethylamino)-8-(piperidin-1-yl)pyrimido[5,4-*d*]pyrimidine-2,6-diyl)bis(azanetriyl))tetrakis(ethan-1-ol) (71)

A stirred solution of **70** (40 mg, 0.1 mmol) and diethanolamine (excess) in *i*PrOH (2 ml) was heated at 120 °C for 5 days in a sealed tube. Subsequently, the mixture was treated with water and extracted with CH₂Cl₂ (3 x 20 ml), the combined organic layers were dried over MgSO₄, filtered off and the solvent was evaporated under reduced pressure. The crude product was purified via flash RP-HPLC (10 to 100% MeOH). The product **71** was obtained as 31 mg (57%) of a yellow, fluorescent solid. ¹H NMR (600 MHz, Chloroform-*d*) δ: 7.34-7.15 (m, 5H, CH_{arom.}), 4.06 (s, 4H, NCH₂CH₂OH), 4.04-3.69 (m, 8H, NCH₂CH₂OH / NCH₂), 3.65 (q, *J* = 6.9 Hz, 2H, NHCH₂CH₂Ph), 2.99-2.85 (t, *J* = 7.3 Hz, 2H, NHCH₂CH₂Ph), 1.66 (m, 6H, CH₂CH₂CH₂) ppm. ¹³C NMR (151 MHz, CDCl₃) δ: 138.7, 128.8, 128.7, 126.5, 67.0, 62.6, 52.1, 51.4, 48.6, 42.0, 35.2, 34.1, 29.6, 29.6, 29.3, 24.6, 22.6, 14.1 ppm. HPLC-UV (254 nm) ESI-MS, purity: 95%. LC-MS (*m/z*): 541.4 [M + H]⁺. Mp.: 133 °C.

Synthesis of 2,6-dichloro-4-(4-phenylpiperazin-1-yl)-8-(piperidin-1-yl)pyrimido[5,4-*d*]pyrimidine (72)

A stirred solution of **69** (40 mg, 0.13 mmol), 1-phenylpiperazine (23 mg, 0.14 mmol) and K₂CO₃ (26 mg, 1.9 mmol) in THF (10 ml) was stirred at rt for 16 h. Subsequently, the mixture was treated with water and extracted with CH₂Cl₂ (3 x 20 ml), the combined organic layers were dried over MgSO₄, filtered off and the solvent was evaporated under reduced pressure. The intermediate **72** was obtained as 53 mg (94%) of a yellow solid. ¹H NMR (600 MHz, Chloroform-*d*) δ 7.31-7.25 (m, 2H, CH_{arom.}), 6.99-6.88 (m, 3H, CH_{arom.}), 4.36 (s, 8H, NCH₂), 3.41-3.26 (m, 4H, NCH₂), 1.77-1.66 (m, 6H, CH₂CH₂CH₂) ppm. HPLC-UV (254 nm) ESI-MS, purity: 93%. LC-MS (*m/z*): 403.2 [M + H]⁺.

Synthesis of 2,2',2'',2'''-((4-(4-phenylpiperazin-1-yl)-8-(piperidin-1-yl)pyrimido[5,4-*d*]pyrimidine-2,6-diyl)bis(azanetriyl))tetrakis(ethan-1-ol) (73)

A stirred solution of **72** (53 mg, 0.12 mmol) and diethanolamine (excess) in *i*PrOH (2 ml) was heated at 120 °C for 5 days in a sealed tube. Subsequently, the mixture was treated with water and extracted with CH₂Cl₂ (3 x 20 ml), the combined organic layers were dried over MgSO₄, filtered off and the solvent was evaporated under reduced pressure. The crude product was

purified via flash RP-HPLC (10 to 100% MeOH). The product **73** was obtained as 31 mg (44%) of a yellow, fluorescent solid. ¹H NMR (600 MHz, Chloroform-*d*) δ: 7.26 (t, *J* = 7.7 Hz, 2H, CH_{arom}), 6.95 (d, *J* = 8.1 Hz, 2H, CH_{arom}), 6.87 (t, *J* = 7.3 Hz, 1H, CH_{arom}), 4.05 (s, 4H, NCH₂ piperazine), 4.00-3.95 (m, 4H, NCH₂ piperazine), 3.90-3.84 (m, 8H, NCH₂CH₂OH), 3.76-3.69 (m, 8H, NCH₂CH₂OH), 3.36-3.28 (m, 4H, NCH₂), 1.72-1.66 (m, 6H, CH₂CH₂CH₂) ppm. ¹³C NMR (151 MHz, CDCl₃) δ: 159.1, 158.8, 150.7, 129.2, 129.2, 120.4, 116.4, 61.7, 53.7, 53.4, 49.2, 49.2, 47.8, 30.9, 26.1, 24.4 ppm. HPLC-UV (254 nm) ESI-MS, purity: 96%. LC-MS (m/z): 582.4 [M + H]⁺. Mp.: 142 °C.

Synthesis of (2*S*,3*S*,4*S*,5*R*)-6-((2,6-dichloro-8-(piperidin-1-yl)pyrimido[5,4-*d*]pyrimidin-4-yl)amino)hexane-1,2,3,4,5-pentaol (74)

A stirred solution of **69** (30 mg, 0.09 mmol), *N*-glucamine (20 mg, 0.11 mmol) and K₂CO₃ (19 mg, 1.4 mmol) in THF (10 ml) was stirred at rt for 16 h. Subsequently, the mixture was treated with water and extracted with CH₂Cl₂ (3 x 20 ml), the combined organic layers were dried over MgSO₄, filtered and the solvent was evaporated under reduced pressure. The crude intermediate was directly used to prepare product **75**. LC-MS (m/z): 463.0 [M + H]⁺.

Synthesis of (2*S*,3*S*,4*S*,5*R*)-6-((2,6-bis(bis(2-hydroxyethyl)amino)-8-(piperidin-1-yl)pyrimido[5,4-*d*]pyrimidin-4-yl)amino)hexane-1,2,3,4,5-pentaol (75)

A stirred solution of crude **74** and diethanolamine (excess) in *i*PrOH (2 ml) was heated at 120 °C for 5 days in a sealed tube. Subsequently, the mixture was treated with water and extracted with CH₂Cl₂ (3 x 20 ml), the combined organic layers were dried over MgSO₄, filtered off and the solvent was evaporated under reduced pressure. The crude product was purified via flash RP-HPLC (10 to 100% MeOH). The product **75** was obtained as 26 mg (48% over 2 steps) of a yellow, fluorescent solid. ¹H NMR (600 MHz, Chloroform-*d*) δ: 4.00 (s, 1H, NH), 3.87-3.74 (m, 8H, NCH₂ / NCH₂CH₂OH), 3.74-3.54 (m, 18H, NCH₂CH₂OH / CHOH), 3.30 (d, *J* = 8.4 Hz, 2H, NHCH₂), 1.63 (d, *J* = 9.2 Hz, 6H, CH₂CH₂CH₂) ppm. ¹³C NMR (151 MHz, CDCl₃) δ: 158.9, 158.0, 155.0, 153.1, 135.1, 132.7, 72.5, 71.2, 69.6, 63.3, 60.7, 52.7, 52.2, 43.6, 25.8, 24.3 ppm. HPLC-UV (254 nm) ESI-MS, purity: 95%. LC-MS (m/z): 601.5 [M + H]⁺. Mp.: 188 °C.

Synthesis of 2,6-dichloro-*N*-(2,6-dimethylbenzyl)-8-(piperidin-1-yl)pyrimido[5,4-*d*]pyrimidin-4-amine (76)

A stirred solution of **69** (30 mg, 0.09 mmol), 2,6-dimethylbenzylamine (14 mg, 0.11 mmol) and K₂CO₃ (19 mg, 1.4 mmol) in THF (10 ml) was stirred at rt for 16 h. Subsequently, the mixture was treated with water and extracted with CH₂Cl₂ (3 x 20 ml), the combined organic layers were dried over MgSO₄, filtered and the solvent was evaporated under reduced pressure. The crude intermediate **76** was directly used to prepare product **77**. ¹H NMR (600 MHz, Chloroform-*d*) δ: 7.14 (dd, *J* = 8.2, 6.9 Hz, 1H, CH_{arom}), 7.06 (d, *J* = 7.5 Hz, 2H, CH_{arom}), 6.87

(s, 1H, NH), 4.70 (d, $J = 4.8$ Hz, 2H, NHCH_2Ar), 3.94 (s, 4H, NCH_2), 2.37 (s, 6H, $\text{CH}_2\text{CH}_2\text{CH}_2$), 1.71 (d, $J = 7.1$ Hz, 6H, CH_3) ppm. ^{13}C NMR (151 MHz, CDCl_3) δ : 159.4, 157.7, 155.3, 153.7, 137.8, 134.7, 132.9, 128.6, 128.3, 40.1, 26.3, 24.5, 19.9 ppm. HPLC-UV (254 nm) ESI-MS, purity: 85%. LC-MS (m/z): 417.0 $[\text{M} + \text{H}]^+$.

Synthesis of 2,2',2'',2'''-((4-((2,6-dimethylbenzyl)amino)-8-(piperidin-1-yl)pyrimido[5,4-*d*]pyrimidine-2,6-diyl)bis(azanetriyl))tetrakis(ethan-1-ol) (77)

A stirred solution of crude **76** and diethanolamine (excess) in *n*PrOH (2 ml) was heated at 120 °C for 5 days in a sealed tube. Subsequently, the mixture was treated with water and extracted with CH_2Cl_2 (3 x 20 ml), the combined organic layers were dried over MgSO_4 , filtered off and the solvent was evaporated under reduced pressure. The crude product was purified via flash RP-HPLC (10 to 100% MeOH). The product **77** was obtained as 38 mg (76% over 2 steps) of a yellow, fluorescent solid. ^1H NMR (600 MHz, Chloroform-*d*) δ : 10.00 (s, 1H, NH), 7.11 (t, $J = 7.5$ Hz, 1H, $\text{CH}_{\text{arom.}}$), 7.03 (d, $J = 7.6$ Hz, 2H, $\text{CH}_{\text{arom.}}$), 4.78 (s, 2H, NHCH_2Ar), 4.02-3.76 (m, 12H, $\text{NCH}_2/\text{NCH}_2\text{CH}_2\text{OH}$), 2.39 (d, $J = 8.5$ Hz, 6H, $\text{CH}_2\text{CH}_2\text{CH}_2$), 1.76 (s, 6H, CH_3) ppm. ^{13}C NMR (151 MHz, CDCl_3) δ : 155.7, 154.2, 154.0, 152.2, 137.8, 131.5, 128.5, 128.3, 63.7, 59.4, 55.1, 52.9, 50.2, 41.4, 26.4, 23.9, 20.6, 20.4 ppm. HPLC-UV (254 nm) ESI-MS, purity: 93%. LC-MS (m/z): 555.6 $[\text{M} + \text{H}]^+$. Mp.: 158 °C.

Synthesis of *N*-((3*R*,5*S*)-adamantan-1-yl)-2,6-dichloro-8-(piperidin-1-yl)pyrimido[5,4-*d*]pyrimidin-4-amine (78)

A stirred solution of **69** (30 mg, 0.09 mmol), 1-adamantidylamine (17 mg, 0.11 mmol) and K_2CO_3 (19 mg, 1.4 mmol) in THF (10 ml) was stirred at rt for 16 h. Subsequently, the mixture was treated with water and extracted with CH_2Cl_2 (3 x 20 ml), the combined organic layers were dried over MgSO_4 , filtered and the solvent was evaporated under reduced pressure. The crude intermediate **78** was directly used to prepare **79**. ^1H NMR (600 MHz, Chloroform-*d*) δ : 6.85 (s, 1H, NH), 4.64 (s, 2H, NCH_2), 3.95 (s, 2H, NCH_2), 2.22-2.17 (m, 6H, $\text{CH}_2\text{CH}_2\text{CH}_2$), 2.17-2.12 (m, 3H, CH), 1.77-1.67 (m, 12H, CH_2) ppm. ^{13}C NMR (151 MHz, CDCl_3) δ : 158.9, 158.0, 155.0, 153.1, 135.1, 132.7, 53.5, 40.7, 36.3, 29.4, 26.5, 24.6 ppm. HPLC-UV (254 nm) ESI-MS, purity: 89%. LC-MS (m/z): 433.0 $[\text{M} + \text{H}]^+$.

Synthesis of 2,2',2'',2'''-((4-(((3*R*,5*S*)-adamantan-1-yl)amino)-8-(piperidin-1-yl)pyrimido[5,4-*d*]pyrimidine-2,6-diyl)bis(azanetriyl))tetrakis(ethan-1-ol) (79)

A stirred solution of crude **78** and diethanolamine (excess) in *n*PrOH (2 ml) was heated at 120 °C for 5 days in a sealed tube. Subsequently, the mixture was treated with water and extracted with CH_2Cl_2 (3 x 20 ml), the combined organic layers were dried over MgSO_4 , filtered off and the solvent was evaporated under reduced pressure. The crude product was purified via flash RP-HPLC (10 to 100% MeOH). The product **79** was obtained as 33 mg (64% over 2

steps) of a yellow, fluorescent solid. ^1H NMR (600 MHz, Chloroform-*d*) δ : 7.67 (s, 1H, NH), 3.85 (d, $J = 5.0$ Hz, 4H, $\text{NCH}_2\text{CH}_2\text{OH}$), 3.80-3.74 (m, 8H, $\text{NCH}_2 / \text{NCH}_2\text{CH}_2\text{OH}$), 2.18 (d, $J = 2.8$ Hz, 6H, $\text{CH}_2\text{CH}_2\text{CH}_2$), 2.13 (s, 3H, CH), 1.74-1.64 (m, 12H, CH_2) ppm. ^{13}C NMR (151 MHz, CDCl_3) δ : 158.9, 158.0, 155.0, 153.1, 135.1, 132.7, 60.6, 55.6, 53.1, 49.4, 40.8, 36.2, 29.3, 25.7, 24.2 ppm. HPLC-UV (254 nm) ESI-MS, purity: 95%. LC-MS (m/z): 571.7 $[\text{M} + \text{H}]^+$. Mp.: 174 °C.

4.4.6.2.7. Synthesis of 2,2'-((4,8-dimorpholinopyrimido[5,4-*d*]pyrimidine-2,6-diyl)bis(propylazanediy))bis(ethan-1-ol) and derivatives

Synthesis of 4,4'-(2,6-dichloropyrimido[5,4-*d*]pyrimidine-4,8-diyl)dimorpholine (80)

A stirred solution of TCPP (200 mg, 0.75 mmol) and morpholine (162 mg, 1.87 mmol) in THF (10 ml) was stirred at rt for 16 h. Subsequently, the mixture was treated with water and extracted with CH_2Cl_2 (3 x 20 ml), the combined organic layers were dried over MgSO_4 , filtered off and the solvent was evaporated under reduced pressure. The residue was purified by column chromatography (petrolether / ethyl acetate - 10:1 +1% acetic acid). The product **80** was obtained as 116 mg (42%) of a yellow solid. ^1H NMR (600 MHz, Chloroform-*d*) δ : 4.82-3.95 (m, 8H, $\text{NCH}_2\text{CH}_2\text{O}$), 3.85-3.77 (m, 8H, $\text{NCH}_2\text{CH}_2\text{O}$) ppm. ^{13}C NMR (151 MHz, CDCl_3) δ : 159.0, 153.1, 136.4, 67.0 ppm. HPLC-UV (254 nm) ESI-MS, purity: 99%. LC-MS (m/z): 371.2 $[\text{M} + \text{H}]^+$.

Also, the side product **81** was isolated as 47 mg (15 %) of a yellow, fluorescent solid. ^1H NMR (600 MHz, Chloroform-*d*) δ : 4.28 (s, 4H, $\text{NCH}_2\text{CH}_2\text{O}$), 3.90-3.78 (m, 12H, $\text{NCH}_2\text{CH}_2\text{O}$), 3.77-3.72 (m, 4H, $\text{NCH}_2\text{CH}_2\text{O}$), 3.69-3.60 (m, 4H, $\text{NCH}_2\text{CH}_2\text{O}$) ppm. ^{13}C NMR (151 MHz, CDCl_3) δ : 159.0, 153.1, 136.4, 67.0, 66.8 ppm. LC-MS (m/z): 422.7 $[\text{M} + \text{H}]^+$.

Synthesis of 2,2'-((4,8-dimorpholinopyrimido[5,4-*d*]pyrimidine-2,6-diyl)bis(propylazanediy))bis(ethan-1-ol) (**82**)^{27;28}

A stirred solution of **80** (110 mg, 0.3 mmol) and *N*-propylethanolamine (excess) in *i*PrOH (2 ml) was heated at 140 °C for 5 days in a sealed tube. Subsequently, the mixture was treated with water and extracted with CH_2Cl_2 (3 x 20 ml), the combined organic layers were dried over MgSO_4 , filtered off and the solvent was evaporated under reduced pressure. The residue was purified via flash RP-HPLC (10 to 100% MeOH). The product **82** was obtained as 103 mg (68%) of a yellow, fluorescent solid. ^1H NMR (600 MHz, Chloroform-*d*) δ : 3.84 (d, $J = 4.9$ Hz, 18H, $\text{NCH}_2\text{CH}_2\text{O} / \text{NCH}_2\text{CH}_2\text{OH}$), 3.62 (s, 4H, $\text{NCH}_2\text{CH}_2\text{OH}$), 3.46 (d, $J = 7.9$ Hz, 4H, $\text{NCH}_2\text{CH}_2\text{CH}_3$), 1.60 (q, $J = 7.4$ Hz, 4H, $\text{NCH}_2\text{CH}_2\text{CH}_3$), 0.88 (t, $J = 7.2$ Hz, 6H, CH_3) ppm. ^{13}C NMR (151 MHz, CDCl_3) δ : 158.2, 66.8, 66.8, 66.6, 66.3, 61.6, 51.8, 51.4, 48.8, 48.3, 48.3, 20.8, 11.4 ppm. no aromatic C atoms displayed. HPLC-UV (254 nm) ESI-MS, purity: 93%. LC-MS (m/z): 505.4 $[\text{M} + \text{H}]^+$. Mp.: 195-196 °C.

Synthesis of 2-(propyl(4,6,8-trimorpholinopyrimido[5,4-*d*]pyrimidin-2-yl)amino)ethan-1-ol (**83**)

A stirred solution of **81** (47 mg, 0.11 mmol) and *N*-propylethanolamine (excess) in *i*PrOH (2 ml) was heated at 140 °C for 5 days in a sealed tube. Subsequently, the mixture was treated with water and extracted with CH₂Cl₂ (3 x 20 ml), the combined organic layers were dried over MgSO₄, filtered off and the solvent was evaporated under reduced pressure. The residue was purified via flash RP-HPLC (10 to 100% MeOH). The product **83** was obtained as 6 mg (11%) of a yellow, fluorescent solid. ¹H NMR (600 MHz, Chloroform-*d*) δ: 4.29-4.05 (m, 2H, NCH₂CH₂OH) 3.86 (d, *J* = 4.5 Hz, 4H, NCH₂CH₂O), 3.82 (t, *J* = 4.8 Hz, 4H, NCH₂CH₂O), 3.76-3.72 (m, 4H, NCH₂CH₂O), 3.65 (t, *J* = 4.6 Hz, 2H, NCH₂CH₂OH), 3.61 (t, *J* = 4.8 Hz, 4H), 3.48 (t, *J* = 7.6 Hz, 2H, NCH₂CH₂CH₃), 1.63 (q, *J* = 7.5 Hz, 2H, NCH₂CH₂CH₃), 0.90 (t, *J* = 7.4 Hz, 3H, CH₃) ppm. ¹³C NMR (151 MHz, CDCl₃) δ: 67.0, 66.8, 66.6, 51.7, 48.3, 44.8, 21.1, 11.4 ppm. no aromatic C atoms displayed. HPLC-UV (254 nm) ESI-MS, purity: 95%. LC-MS (m/z): 489.3 [M + H]⁺. Mp.: 172-173 °C.

4.4.6.2.8. Synthesis of 2,6-bis[bis(2-hydroxyethyl)amino]-4-benzylthiopyrimido[5,4-*d*]pyrimidin derivatives

Synthesis of 4-(benzylthio)-2,6,8-trichloropyrimido[5,4-*d*]pyrimidine (**84**)

A suspension of TCPP (300 mg, 1.12 mmol) and K₂CO₃ (309 mg, 2.24 mmol) in THF (6 ml) was treated with benzylthiol (152 mg, 1.23 mmol) in THF (6 ml) at -78 °C under argon atmosphere. After an hour of stirring at -78 °C, the mixture was allowed to warm up to rt. Subsequently, the mixture was treated with water and extracted with ethyl acetate (3 x 20 ml), the combined organic layers were dried over MgSO₄, filtered off and the solvent was evaporated under reduced pressure. The product **84** was obtained as 415 mg of a beige solid. ¹H NMR (500 MHz, DMSO-*d*₆) δ: 7.50-7.44 (m, 2H, CH_{arom.}), 7.36-7.30 (m, 2H, CH_{arom.}), 7.30-7.23 (m, 1H, CH_{arom.}), 4.47 (s, 2H, CH₂Ph) ppm. ¹³C NMR (126 MHz, DMSO-*d*₆) δ: 173.3, 159.2, 155.0, 145.7, 141.6, 139.0, 136.6, 129.4, 129.4, 128.7, 128.6, 127.7, 127.6, 33.5. LC-MS (m/z): 358.6 [M + H]⁺.

Synthesis of (S)-(1-(8-(benzylthio)-2,6-dichloropyrimido[5,4-*d*]pyrimidin-4-yl)pyrrolidin-2-yl)methanol (**85**)

A mixture of **84** (50 mg, 0.14 mmol), K₂CO₃ (38.6 mg, 0.28 mmol) and *L*-prolinole (22 mg, 0.21 mmol) in THF (5 ml) was stirred for 1 h at rt. Subsequently, the mixture was treated with water and extracted with ethyl acetate (3 x 20 ml), the combined organic layers were dried over MgSO₄, filtered off and the solvent was evaporated under reduced pressure. The crude product was purified via flash RP-HPLC (10 to 100% MeOH). The intermediate **85** was obtained as 39 mg (66%) of a colorless solid. ¹H NMR (600 MHz, Chloroform-*d*) δ: 7.43 (dd, *J*

= 7.1, 1.7 Hz, 2H, CH_{arom.}), 7.29 (t, *J* = 7.5 Hz, 2H, CH_{arom.}), 7.24 (d, *J* = 6.9 Hz, 1H, CH_{arom.}), 4.64 (s, 1H, OH), 4.44 (s, 2H, CH₂Ph), 4.37-4.29 (m, 1H, HOCH₂), 3.89-3.52 (m, 4H, CH / CH₂), 2.15-1.82 (m, 4H, CH₂) ppm. HPLC-UV (254 nm) ESI-MS, purity: 92%. LC-MS (*m/z*): 422.1 [M + H]⁺.

Synthesis of (S)-2,2',2'',2'''-((4-(benzylthio)-8-(2-(hydroxymethyl)pyrrolidin-1-yl)pyrimido[5,4-*d*]pyrimidine-2,6-diyl)bis(azanetriyl))tetrakis(ethan-1-ol) (86)

A stirred solution of **85** (35 mg, 0.08 mmol) and diethanolamine (excess) in *i*PrOH (1 ml) was heated at 130 °C for 24 h in a sealed tube. Subsequently, the mixture was treated with saturated NH₄Cl solution and extracted with CH₂Cl₂ (3 x 20 ml), the combined organic layers were dried over MgSO₄, filtered off and the solvent was evaporated under reduced pressure. The crude product was purified via flash RP-HPLC (10 to 100% MeOH). The product **86** was obtained as 13 mg (29%) of a yellow, fluorescent solid. ¹H NMR (600 MHz, Methanol-*d*₄) δ: 7.49-7.46 (m, 2H, CH_{arom.}), 7.37 (t, *J* = 7.5 Hz, 2H, CH_{arom.}), 7.32 (t, *J* = 7.3 Hz, 1H, CH_{arom.}), 5.78 (s, 1H, OH), 4.67 (s, 2H, CH₂Ph), 4.55 (t, *J* = 7.0 Hz, 1H, CH), 4.04-3.83 (m, 10H, NCH₂ / NCH₂CH₂OH), 3.82 (t, *J* = 5.8 Hz, 6H, NCH₂CH₂OH), 2.31-1.98 (m, 4H, CH₂) ppm. ¹³C NMR (151 MHz, MeOD) δ: 158.3, 158.1, 157.7, 153.3, 137.6, 137.6, 135.0, 134.2, 129.1, 65.5, 63.8, 62.9, 61.7, 61.1, 55.8, 54.2, 53.2, 52.7, 35.6, 29.4, 27.3, 26.0, 21.3 ppm. HPLC-UV (254 nm) ESI-MS, purity: 95%. LC-MS (*m/z*): 560.5 [M + H]⁺. Mp.: 188 °C.

Synthesis of 8-(benzylthio)-2,6-dichloro-*N,N*-dipropylpyrimido[5,4-*d*]pyrimidin-4-amine (87)

A mixture of **84** (50 mg, 0.14 mmol), K₂CO₃ (38.6 mg, 0.28 mmol) and *N*-dipropylamine (18 mg, 0.18 mmol) in THF (5 ml) was stirred for 1 h at rt. Subsequently, the mixture was treated with water and extracted with ethyl acetate (3 x 20 ml), the combined organic layers were dried over MgSO₄, filtered off and the solvent was evaporated under reduced pressure. The crude product was purified via flash RP-HPLC (10 to 100% MeOH). The intermediate **87** was obtained as 28 mg (47%) of a colorless solid. ¹H NMR (600 MHz, Chloroform-*d*) δ: 7.44-7.40 (m, 2H, CH_{arom.}), 7.31-7.26 (m, 2H, CH_{arom.}), 7.24 (d, *J* = 11.2 Hz, 1H, CH_{arom.}), 4.42 (s, 2H, CH₂Ph), 4.15-3.99 (m, 2H, NCH₂), 3.72-3.55 (m, 2H, NCH₂), 1.71 (dq, *J* = 15.2, 7.7 Hz, 4H, CH₂CH₂CH₃), 0.97 (dt, *J* = 23.6, 7.4 Hz, 6H, CH₃) ppm. HPLC-UV (254 nm) ESI-MS, purity: 95%. LC-MS (*m/z*): 422.2 [M + H]⁺.

Synthesis of 2,2',2'',2'''-((4-(benzylthio)-8-(dipropylamino)pyrimido[5,4-*d*]pyrimidine-2,6-diyl)bis(azanetriyl))tetrakis(ethan-1-ol) (88)

A stirred solution of **87** (26 mg, 0.06 mmol) and diethanolamine (excess) in *i*PrOH (1 ml) was heated at 130 °C for 24 h in a sealed tube. Subsequently, the mixture was treated with saturated NH₄Cl solution and extracted with CH₂Cl₂ (3 x 20 ml), the combined organic layers were dried over MgSO₄, filtered off and the solvent was evaporated under reduced pressure. The crude product was purified via flash RP-HPLC (10 to 100% MeOH). The product **88** was obtained as 4.5 mg (13%) of a yellow, fluorescent solid. ¹H NMR (500 MHz, Chloroform-*d*) δ: 7.36 (d, *J* = 7.0 Hz, 2H, CH_{arom.}), 7.29 (t, *J* = 7.6 Hz, 2H, CH_{arom.}), 7.27-7.18 (m, 1H, CH_{arom.}), 4.46 (s, 2H, CH₂Ph), 4.29 (s, 2H, NCH₂CH₂OH), 4.14 (s, 2H, NCH₂CH₂OH), 3.83-3.76 (m, 4H, NCH₂CH₂OH), 3.74 (t, *J* = 4.7 Hz, 4H, NCH₂CH₂OH), 3.60 (s, 4H, NCH₂), 1.74 (s, 4H, CH₂), 0.93 (t, *J* = 7.5 Hz, 6H, CH₃)ppm. HPLC-UV (254 nm) ESI-MS, purity: 95%. LC-MS (m/z): 560.5 [M + H]⁺. Mp.: 168 °C.

Synthesis of 8-(benzylthio)-2,6-dichloro-*N*-propylpyrimido[5,4-*d*]pyrimidin-4-amine (89)

A mixture of **84** (50 mg, 0.14 mmol), K₂CO₃ (38.6 mg, 0.28 mmol) and propylamine (11 mg, 0.18 mmol) in THF (5 ml) was stirred for 1 h at rt. Subsequently, the mixture was treated with water and extracted with ethyl acetate (3 x 20 ml), the combined organic layers were dried over MgSO₄, filtered and the solvent was evaporated under reduced pressure. The crude product was purified via flash RP-HPLC (10 to 100% MeOH). The intermediate **89** was obtained as 21 mg (40%) of a colorless solid. ¹H NMR (600 MHz, Chloroform-*d*) δ: 7.47-7.41 (m, 2H, CH_{arom.}), 7.32-7.27 (m, 2H, CH_{arom.}), 7.27-7.21 (m, 1H, CH_{arom.}), 7.04 (t, *J* = 5.9 Hz, 1H, NH), 4.46 (s, 2H, CH₂Ph), 3.63-3.50 (m, 2H, NHCH₂), 1.72 (q, *J* = 7.3 Hz, 2H, CH₂CH₂CH₃), 1.00 (t, *J* = 7.4 Hz, 3H, CH₃). HPLC-UV (254 nm) ESI-MS, purity: 94%. LC-MS (m/z): 380.1 [M + H]⁺.

Synthesis of 2,2',2'',2'''-((4-(benzylthio)-8-(propylamino)pyrimido[5,4-*d*]pyrimidine-2,6-diyl)bis(azanetriyl))tetrakis(ethan-1-ol) (90)

A stirred solution of **89** (20 mg, 0.05 mmol) and diethanolamine (excess) in *i*PrOH (1 ml) was heated at 130 °C for 24 h in a sealed tube. Subsequently, the mixture was treated with saturated NH₄Cl solution and extracted with CH₂Cl₂ (3 x 20 ml), the combined organic layers were dried over MgSO₄, filtered and the solvent was evaporated under reduced pressure. The crude product was purified via flash RP-HPLC (10 to 100% MeOH). The product **90** was obtained as 21 mg (40%) of a yellow, fluorescent solid. ¹H NMR (500 MHz, Chloroform-*d*) δ: 7.36 (d, *J* = 7.0 Hz, 2H, CH_{arom.}), 7.29 (t, *J* = 7.6 Hz, 2H, CH_{arom.}), 7.27-7.18 (m, 1H, CH_{arom.}), 4.46 (s, 2H, CH₂Ph), 4.29 (s, 2H, NCH₂CH₂OH), 4.14 (s, 2H, NCH₂CH₂OH), 3.83-3.76 (m, 4H, NCH₂CH₂OH), 3.74 (t, *J* = 4.7 Hz, 4H, NCH₂CH₂OH), 3.60 (s, 4H, NCH₂), 1.74 (s, 4H, CH₂),

0.93 (t, $J = 7.5$ Hz, 6H, CH₃) ppm. HPLC-UV (254 nm) ESI-MS, purity: 94%. LC-MS (m/z): 380.1 [M + H]⁺. Mp.: 181 °C.

Synthesis of 4-(benzylthio)-2,6-dichloro-8-(4-phenylpiperazin-1-yl)pyrimido[5,4-*d*]pyrimidine (91)

A mixture of **84** (50 mg, 0.14 mmol), K₂CO₃ (38.6 mg, 0.28 mmol) and 1-phenylpiperazine (18 mg, 0.16 mmol) in THF (5 ml) was stirred for 1 h at rt. Subsequently, the mixture was treated with water and extracted with ethyl acetate (3 x 20 ml), the combined organic layers were dried over MgSO₄, filtered off and the solvent was evaporated under reduced pressure. The crude product was purified via flash RP-HPLC (10 to 100% MeOH). The intermediate **91** was obtained as a complex mixture of compounds and was directly used for the next reaction step. LC-MS (m/z): 484.1 [M + H]⁺.

Synthesis of 2,2',2'',2'''-((4-(benzylthio)-8-(4-phenylpiperazin-1-yl)pyrimido[5,4-*d*]pyrimidine-2,6-diyl)bis(azanetriyl))tetrakis(ethan-1-ol) (92)

A stirred solution of crude **91** (26.5 mg, 0.07 mmol) and diethanolamine (excess) in *i*PrOH (1 ml) was heated at 130 °C for 24 h in a sealed tube. Subsequently, the mixture was treated with saturated NH₄Cl solution and extracted with CH₂Cl₂ (3 x 20 ml), the combined organic layers were dried over MgSO₄, filtered off and the solvent was evaporated under reduced pressure. The crude product was purified via flash RP-HPLC twice (10 to 100% MeOH). The product **92** was obtained as 4.3 mg (34% based on **84**) of a yellow, fluorescent solid. ¹H NMR (600 MHz, Methanol-*d*₄) δ: 7.75-7.70 (m, 2H, CH_{arom.}), 7.62 (qd, $J = 7.3, 2.0$ Hz, 3H, CH_{arom.}), 7.55-7.45 (m, 2H, CH_{arom.}), 7.42-7.29 (m, 3H, CH_{arom.}), 5.43 (d, $J = 56.3$ Hz, 4H, NCH₂CH₂OH), 4.70 (s, 2H, NCH₂Ph), 3.96-3.91 (m, 4H, NCH₂CH₂OH), 3.89 (d, $J = 4.5$ Hz, 4H, NCH₂), 3.85 (t, $J = 5.2$ Hz, 4H, NCH₂), 3.83-3.79 (m, 4H, NCH₂), 3.74 (t, $J = 5.3$ Hz, 4H, NCH₂) ppm. ¹³C NMR (151 MHz, MeOD) δ: 164.2, 159.4, 157.8, 153.2, 152.8, 137.5, 131.9, 131.9, 130.3, 130.1, 129.2, 125.6, 121.9, 121.8, 61.3, 57.9, 53.9, 50.6, 37.7, 35.8 ppm. HPLC-UV (254 nm) ESI-MS, purity: 91%. LC-MS (m/z): 621.6 [M + H]⁺. Mp.: 198 °C.

Synthesis of 4-(8-(benzylthio)-2,6-dichloropyrimido[5,4-*d*]pyrimidin-4-yl)morpholine (95)

A mixture of **84** (50 mg, 0.14 mmol), K₂CO₃ (38.6 mg, 0.28 mmol) and morpholine (18 mg, 0.16 mmol) in THF (5 ml) was stirred for 1 h at rt. Subsequently, the mixture was treated with water and extracted with ethyl acetate (3 x 20 ml), the combined organic layers were dried over MgSO₄, filtered off and the solvent was evaporated under reduced pressure. The crude product was purified via flash RP-HPLC (10 to 100% MeOH). The intermediate **95** was obtained as 30 mg (47%) of a colorless solid. ¹H NMR (600 MHz, Chloroform-*d*) δ: 7.45-7.41 (m, 2H, CH_{arom.}), 7.31-7.26 (m, 2H, CH_{arom.}), 7.27-7.21 (m, 1H, CH_{arom.}), 4.83 (s, 2H, CH₂

morpholine), 4.43 (s, 2H, CH₂Ph), 4.06 (s, 2H, CH₂_{morpholine}), 3.88-3.76 (m, 4H, CH₂_{morpholine}) ppm. HPLC-UV (254 nm) ESI-MS, purity: 97%. LC-MS (m/z): 408.3 [M + H]⁺.

Synthesis of 2,2'-((4-(benzylthio)-8-morpholinopyrimido[5,4-*d*]pyrimidine-2,6-diyl)bis(propylazanediy))bis(ethan-1-ol) (96)

A stirred solution of **95** (26.5 mg, 0.07 mmol) and *N*-propylethanolamine (excess) in *i*PrOH (1 ml) was heated at 130 °C for 24 h in a sealed tube. Subsequently, the mixture was treated with saturated NH₄Cl solution and extracted with CH₂Cl₂ (3 x 20 ml), the combined organic layers were dried over MgSO₄, filtered off and the solvent was evaporated under reduced pressure. The crude product was purified via flash RP-HPLC (10 to 100% MeOH). The product **96** was obtained as 16 mg (45%) of a yellow, fluorescent solid. ¹H NMR (500 MHz, Chloroform-*d*) δ: 7.44-7.39 (m, 2H, CH_{arom.}), 7.32-7.25 (m, 2H, CH_{arom.}), 7.26-7.19 (m, 1H, CH_{arom.}), 4.46 (s, 2H, CH₂Ph), 4.08-3.99 (m, 2H, NCH₂), 3.83 (t, *J* = 4.8 Hz, 4H, CH₂_{morpholine}), 3.76-3.70 (m, 2H, NCH₂), 3.67 (q, *J* = 4.9, 3.9 Hz, 4H, CH₂_{morpholine}), 3.59-3.50 (m, 2H, NCH₂), 3.51-3.40 (m, 2H, NCH₂), 1.67-1.62 (m, 2H, CH₂), 1.60-1.54 (m, 2H, CH₂), 0.92 (t, *J* = 7.4 Hz, 3H, CH₃), 0.85 (t, *J* = 7.4 Hz, 3H, CH₃) ppm. ¹³C NMR (151 MHz, CDCl₃) δ: 155.7, 154.2, 154.0, 152.2, 137.8, 131.5, 128.5, 128.3, 63.7, 59.4, 55.1, 52.9, 50.2, 41.4, 26.4, 23.9, 20.6, 20.4 ppm. HPLC-UV (254 nm) ESI-MS, purity: 98%. LC-MS (m/z): 542.4 [M + H]⁺. Mp.: 173 °C.

4.4.6.3. Synthesis of purine derivatives

Synthesis of 2-chloro-6-(piperidin-1-yl)-7*H*-purine (107)

A solution of 2,6-dichloropurine (1000 mg, 5.29 mmol) in THF (10 ml) was treated with TEA (1070 mg, 6.35 mmol) and piperidine (540 mg, 6.35 mmol) in THF (10 ml) at rt and stirred for 16 h. Subsequently, the solvent was evaporated under reduced pressure and the residue was suspended in water, filtered off under reduced pressure and dried at 70 °C. The product **107** was obtained as 1.21 g (96%) of a white solid. ¹H NMR (600 MHz, DMSO-*d*₆) δ: 13.10 (s, 1H, NH), 8.09 (s, 1H, Imidazol), 3.80-4.50 (m, 4H, NCH₂), 1.79-1.44 (m, 6H, CH₂CH₂CH₂) ppm. ¹³C NMR (151 MHz, DMSO-*d*₆) δ: 153.3, 152.7, 152.6, 138.5, 117.7, 25.8, 24.2 ppm. HPLC-UV (254 nm) ESI-MS, purity: 97%. LC-MS (m/z): 237.8 [M + H]⁺.

Synthesis of 2,6-di(piperidin-1-yl)-7*H*-purine (108)^{30,32}

A stirred solution of **107** (200 mg, 0.34 mmol) and piperidine (70 mg, 0.83 mmol) in *i*PrOH (2 ml) was heated at 120 °C for 4 days in a sealed tube. Subsequently, the mixture was treated with water, the precipitate was filtered off under reduced pressure and dried at 70 °C. The product **108** was obtained as 228 mg (95%) of a colorless solid. ¹H NMR (600 MHz, DMSO-*d*₆) δ: 12.21 (s, 1H, NH), 7.67 (s, 1H, Imidazol), 4.09 (m, 4H, NCH₂), 3.69-3.52 (m, 4H, NCH₂), 1.44-1.65 (m, 12H, CH₂CH₂CH₂) ppm. ¹³C NMR (151 MHz, DMSO-*d*₆) δ: 158.3, 153.9, 153.3,

134.9, 113.0, 45.5, 45.1, 25.8, 25.4, 24.7, 24.6 ppm. HPLC-UV (254 nm) ESI-MS, purity: 97%. LC-MS (m/z): 286.8 [M + H]⁺. Mp.: 211-212 °C (lit: 214°C).

Synthesis of 2,2'-((6-(piperidin-1-yl)-7H-purin-2-yl)azanediyl)bis(ethan-1-ol) (109)³²

A stirred solution of **107** (200 mg, 0.84 mmol) and diethanolamine (443 mg, 4.22 mmol) DMSO (2 ml) was heated at 120 °C for 7 days in a sealed tube. The mixture was directly purified by column chromatography (CH₂Cl₂ / MeOH - 95 : 5 to 9 : 1). The product **109** was obtained as 151 mg (59%) of a colorless solid. ¹H NMR (600 MHz, DMSO-*d*₆) δ: 12.27 (s, 1H, NH), 7.64 (s, 1H, Imidazole), 4.72 (m, 2H, NCH₂CH₂OH), 4.08 (m, 2H, NCH₂CH₂OH), 3.67-3.77 (m, 2H, 3.60 (m, 8H, NCH₂CH₂OH, NCH₂), 1.63 (q, *J* = 5.8 Hz, 2H), 1.52 (p, *J* = 5.6 Hz, 4H) ppm. ¹³C NMR (151 MHz, DMSO) δ: 158.0, 153.9, 153.2, 134.7, 112.9, 59.7, 51.7, 45.6, 25.8, 24.6 ppm. HPLC-UV (254 nm) ESI-MS, purity: 95%. LC-MS (m/z): 307.1 [M + H]⁺. Mp.: 231-232 °C.

Synthesis of 2,2'-((2-chloro-7H-purin-6-yl)azanediyl)bis(ethan-1-ol) (110)³²

A solution of 2,6-dichloropurine (1000 mg, 5.29 mmol) in THF (10 ml) was treated with TEA (1070 mg, 6.35 mmol) and diethanolamine (667 mg, 6.35 mmol) in THF (10 ml) at rt and stirred for 16 h. TLC analysis indicated that a lot of starting material was left, hence, the reaction mixture was heated to 65 °C for 2 additional days. Subsequently, the solvent was evaporated under reduced pressure and the residue was suspended in water, filtered off under reduced pressure and dried at 70 °C. The crude product was purified by column chromatography (CH₂Cl₂ / MeOH - 7 : 3). The product **110** was obtained as 680 mg (50%) of a white solid. LC-MS (m/z): 258.7 [M + H]⁺.

Synthesis of 2,2',2'',2'''-((7H-purine-2,6-diyl)bis(azanetriyl))tetrakis(ethan-1-ol) (112)³²

A stirred solution of 2,6-dichloropurine (200 mg, 1.06 mmol) and diethanolamine (667 mg, 6.35 mmol) in DMSO (2 ml) was heated at 120 °C for 7 days in a sealed tube. The mixture was directly purified by column chromatography (CH₂Cl₂ / MeOH - 8 : 2). The product **112** was obtained as 285 mg (83%) of a colorless solid. ¹H NMR (600 MHz, DMSO-*d*₆) δ: 12.26 (s, 1H, NH), 7.65 (s, 1H, Imidazole), 4.66-4.75 (m, 4H, NCH₂CH₂OH), 4.10-4.26 (m, 2H, NCH₂CH₂OH), 3.68-3.77 (m, 2H, NCH₂CH₂OH) 3.62-3.66 (m, 4H, NCH₂CH₂OH), 3.54-3.62 (m, 8H, NCH₂CH₂OH) ppm. ¹³C NMR (151 MHz, DMSO-*d*₆) δ: 157.9, 153.60, 153.55 135.0, 112.7, 59.8, 51.7 ppm. HPLC-UV (254 nm) ESI-MS, purity: 98%. LC-MS (m/z): 327.1 [M + H]⁺. Mp.: 259 °C.

Synthesis of 2,2'-((2-(piperidin-1-yl)-7H-purin-6-yl)azanediyl)bis(ethan-1-ol) (111)³²

A stirred solution of **110** (150 mg, 0.58 mmol) and piperidine (248 mg, 2.92 mmol) in *i*PrOH (2 ml) was heated at 120 °C for 4 days in a sealed tube. Subsequently, the solvent was removed under reduced pressure, the residue was suspended in water, filtered off under

reduced pressure and dried at 70 °C. The product **111** was obtained as 25 mg (14%) of a colorless solid. ¹H NMR (600 MHz, DMSO-*d*₆) δ: 12.20 (s, 1H, NH), 7.67 (s, 1H, Imidazol), 4.75-4.70 (m, 2H, NCH₂CH₂OH), 4.18 (s, 2H, NCH₂CH₂OH), 3.68-3.61 (m, 8H, NCH₂CH₂OH, NCH₂), 1.57 (q, *J* = 6.1, 5.4 Hz, 2H, CH₂CH₂CH₂), 1.47 (q, *J* = 6.0, 5.4 Hz, 4H, CH₂CH₂CH₂) ppm. ¹³C NMR (151 MHz, DMSO-*d*₆) δ: 158.2, 153.7, 135.3, 112.8, 60.7, 58.9, 52.3, 45.2, 25.4, 24.8 ppm. HPLC-UV (254 nm) ESI-MS, purity: 95%. LC-MS (*m/z*): 307.1 [M + H]⁺. Mp.: 225-226 °C.

Synthesis of 2,2',2'',2'''-((9-(cyclohexylmethyl)-9*H*-purine-2,6-diyl)bis(azanetriyl)) tetrakis(ethan-1-ol) (**115**)³²

A stirred solution of **112** (75 mg, 0.23 mmol), (bromomethyl)cyclohexane (82 mg, 0.46 mmol) and K₂CO₃ (63 mg, 0.46 mmol) in DMF (3 ml) was heated at 80 °C for 2 days in a sealed tube. Subsequently, the mixture was treated with water and extracted with CH₂Cl₂ (3 x 20 ml), the combined organic layers were dried over MgSO₄, filtered off and the solvent was evaporated under reduced pressure. The residue was dried at 70 °C to remove the surplus (bromomethyl)cyclohexane. The product **115** was obtained as 46 mg (47%) of a beige solid. ¹H NMR (600 MHz, Chloroform-*d*) δ: 7.40 (s, 1H, NH), 4.06-3.95 (m, 4H, NCH₂CH₂OH), 3.89 (t, *J* = 5.2 Hz, 4H, NCH₂CH₂OH), 3.85 (t, *J* = 4.9 Hz, 4H, NCH₂CH₂OH), 3.79 (d, *J* = 7.1 Hz, 2H, NCH₂ cyclohexyl), 3.74 (t, *J* = 5.0 Hz, 4H, NCH₂CH₂OH), 1.80-1.72 (m, 1H, cyclohexyl), 1.72-1.66 (m, 2H, cyclohexyl), 1.65-1.61 (m, 2H, cyclohexyl), 1.26-1.07 (m, 4H, cyclohexyl), 1.02-0.84 (m, 2H, cyclohexyl) ppm. ¹³C NMR (151 MHz, CDCl₃) δ: 159.0, 155.3, 152.2, 137.3, 113.7, 62.4, 61.0, 52.4, 51.9, 49.7, 38.3, 30.6, 26.0, 25.6. HPLC-UV (254 nm) ESI-MS, purity: 92%. LC-MS (*m/z*): 423.3 [M + H]⁺. Mp.: 239 °C.

Synthesis 2-(2,6-di(piperidin-1-yl)-9*H*-purin-9-yl)ethan-1-ol (**116**)³²

A stirred solution of **108** (50 mg, 0.17 mmol), 2-iodoethanol (39 mg, 0.22 mmol) and K₂CO₃ (46 mg, 0.34 mmol) in DMF (3 ml) was heated at 80 °C for 2 days in a sealed tube. Subsequently, the mixture was treated with water and extracted with CH₂Cl₂ (3 x 20 ml), the combined organic layers were dried over MgSO₄, filtered off and the solvent was evaporated under reduced pressure. The residue was purified by column chromatography (CH₂Cl₂/ MeOH - 9 : 1). The product **116** was obtained as 19 mg (34%) of a beige solid. ¹H NMR (600 MHz, Chloroform-*d*) δ: 7.34 (s, 1H, NH), 4.19-4.14 (m, 2H, NCH₂CH₂OH), 4.14 (s, 4H, NCH₂), 3.95-3.90 (m, 2H, NCH₂CH₂OH), 3.68-3.62 (m, 4H, NCH₂), 1.71-1.52 (m, 12H, CH₂CH₂CH₂) ppm. ¹³C NMR (151 MHz, CDCl₃) δ: 153.8, 135.9, 114.0, 62.8 (NCH₂CH₂OH), 48.8 (NCH₂CH₂OH), 46.1 (NCH₂), 45.7 (NCH₂), 26.0 (CH₂CH₂CH₂), 25.6 (CH₂CH₂CH₂), 24.83 (CH₂CH₂CH₂), 24.80 (CH₂CH₂CH₂) ppm. HPLC-UV (254 nm) ESI-MS, purity: 94%. LC-MS (*m/z*): 331.0 [M + H]⁺. Mp.: 219-221 °C.

Synthesis of 2,2'-((9-(cyclohexylmethyl)-6-(piperidin-1-yl)-9H-purin-2-yl)azanediyl)bis(ethan-1-ol) (117)³²

A stirred solution of **109** (580 mg, 1.89 mmol), (bromomethyl)cyclohexane (1006 mg, 5.69 mmol) and DBU (575 mg, 3.78 mmol) in DMF (3 ml) was heated at 110 °C for 24 h in a sealed tube. Subsequently, the mixture was treated with water and extracted with CH₂Cl₂ (3 x 20 ml), the combined organic layers were dried over MgSO₄, filtered off and the solvent was evaporated under reduced pressure. The residue was purified by column chromatography (CH₂Cl₂ / MeOH - 99 : 1 to 95 : 5). The product **117** was obtained as 380 mg (50%) of a brownish solid. ¹H NMR (600 MHz, Chloroform-*d*) δ: 7.38 (s, 1H), 4.24-3.96 (m, 4H, NCH₂), 3.87 (t, *J* = 4.3 Hz, 4H, NCH₂CH₂OH), 3.80 (d, *J* = 7.1 Hz, 2H, NCH₂), 3.76 (t, *J* = 5.0 Hz, 4H, NCH₂CH₂OH), 1.78-1.72 (m, 1H, cyclohexyl), 1.72-1.59 (m, 10H cyclohexyl / piperidine), 1.20-1.11 (m, 2H, cyclohexyl), 1.00-0.90 (m, 2H, cyclohexyl), 0.88-0.77 (m, 2H, cyclohexyl) ppm. ¹³C NMR (151 MHz, CDCl₃) δ: 159.8, 153.3, 151.9, 136.5, 114.1, 63.1, 52.1, 49.6, 46.6, 38.4, 38.4, 30.6, 30.6, 26.1, 26.1, 26.1, 26.0, 25.6, 24.7, 22.6 ppm. HPLC-UV (254 nm) ESI-MS, purity: 98%. LC-MS (*m/z*): 403.4 [M + H]⁺. Mp.: 224 °C.

Synthesis of 2,2'-((8-bromo-9-(cyclohexylmethyl)-6-(piperidin-1-yl)-9H-purin-2-yl)azanediyl)bis(ethan-1-ol) (118)³²

A solution of **117** (360 mg, 0.9 mmol) and bromine (287 mg, 1.8 mmol) in CH₂Cl₂ (3 ml) was stirred for 16 h at rt. Subsequently, the mixture was treated with saturated Na₂S₂O₃ solution and extracted with CH₂Cl₂ (3 x 20 ml), the combined organic layers were dried over MgSO₄, filtered off and the solvent was evaporated under reduced pressure. The residue was purified by column chromatography (CH₂Cl₂ / MeOH - 9 : 1). The product **118** was obtained as 250 mg (58%) of a brownish solid. LC-MS (*m/z*): 481.1 [M + H]⁺.

Synthesis of 2,2'-((9-(cyclohexylmethyl)-6,8-di(piperidin-1-yl)-9H-purin-2-yl)azanediyl)bis(ethan-1-ol) (119)³²

A mixture of **118** (70 mg, 0.15 mmol) and piperidine (2 ml) was stirred at 150 °C for 2 days. Subsequently, the mixture was treated with water and extracted with CH₂Cl₂ (3 x 20 ml), the combined organic layers were dried over MgSO₄, filtered off and the solvent was evaporated under reduced pressure. The residue was purified using column chromatography (CH₂Cl₂ / MeOH - 95 : 5) and flash RP-HPLC (10 to 100% MeOH). The product **119** was obtained as 30 mg (41%) of a brownish solid. ¹H NMR (600 MHz, Chloroform-*d*) δ: 4.21-3.98 (m, 4H, NCH₂), 3.97-3.85 (m, 4H, NCH₂CH₂OH), 3.85-3.66 (m, 6H, NCH₂ methylene, NCH₂CH₂OH), 3.13-3.00 (m, 4H, NCH₂), 2.07-1.83 (m, 1H, cyclohexyl), 1.78-1.63 (m, 13H, CH₂), 1.64-1.54 (m, 2H, CH₂), 1.54-1.45 (m, 2H, CH₂), 1.19-1.09 (m, 3H, CH₂), 0.99-0.89 (m, 2H, CH₂) ppm. HPLC-UV (254 nm) ESI-MS, purity: 88%. LC-MS (*m/z*): 486.3 [M + H]⁺. Mp.: 254-256 °C.

4.4.6.4. Synthesis of pyrimidine derivatives

Synthesis of 2,4-di(piperidin-1-yl)pyrimidine (**123**)^{31,33}

A stirred solution of 2,4-dichloropyrimidin (100 mg, 0.67 mmol) and piperidine (570 mg, 6.7 mmol) in *i*PrOH (2 ml) was heated at 120 °C for 16 h in a sealed tube. Subsequently, the mixture was treated with water and extracted with CH₂Cl₂ (3 x 20 ml), the combined organic layers were dried over MgSO₄, filtered and the solvent was evaporated under reduced pressure. Subsequently, the solvent was removed under reduced pressure and the residue was purified by column chromatography (pure ethyl acetate). The product **123** was obtained as 145 mg (88%) of a brownish solid. ¹H NMR (600 MHz, DMSO-*d*₆) δ: 7.80 (d, *J* = 6.0 Hz, 1H, C₆H_{arom.}), 5.98 (d, *J* = 6.0 Hz, 1H, C₅H_{arom.}), 3.68-3.60 (m, 4H, NCH₂), 3.55-3.47 (m, 4H, NCH₂), 1.63-1.53 (m, 4H, CH₂CH₂CH₂), 1.51-1.42 (m, 8H, CH₂CH₂CH₂) ppm. ¹³C NMR (151 MHz, DMSO-*d*₆) δ: 161.9 (C₂), 161.2 (C₄), 156.5 (C₆), 92.6 (C₅), 44.4 (NCH₂), 44.3 (NCH₂), 25.4 (CH₂CH₂CH₂), 25.2 (CH₂CH₂CH₂), 24.7 (CH₂CH₂CH₂), 24.4 (CH₂CH₂CH₂) ppm. HPLC-UV (254 nm) ESI-MS, purity: 99%. LC-MS (m/z): 246.9 [M + H]⁺. Mp.: 55 °C (lit. 52-54 °C).

Synthesis of 2,2'-((4-(piperidin-1-yl)pyrimidin-2-yl)azanediyl)bis(ethan-1-ol) (**124**)³³

A suspension of 2,4-dichloropyrimidin (100 mg, 0.67 mmol) and K₂CO₃ (185 mg, 1.34 mmol) in dry THF (6 ml) was treated with piperidine (157 mg, 1.85 mmol) and was stirred at rt for 16 h. Subsequently, the mixture was treated with water and extracted with CH₂Cl₂ (3 x 20 ml), the combined organic layers were dried over MgSO₄, filtered off and the solvent was evaporated under reduced pressure. The crude intermediate **122** (being identified via TLC-MS) was directly used to prepare **124**.

Therefore, a stirred solution of crude **122** (123 mg, 0.62 mmol) and an excess of diethanolamine in *i*PrOH (2 ml) was heated at 120 °C for 4 days in a sealed tube. Subsequently, the solvent was removed under reduced pressure and the residue was purified by column chromatography (CH₂Cl₂/ MeOH - 9 : 1). The product **124** was obtained as 67 mg (38% over two steps) of a brownish solid. ¹H NMR (600 MHz, DMSO-*d*₆) δ: 7.78 (d, *J* = 6.0 Hz, 1H, C₆H_{arom.}), 6.02 (d, *J* = 6.1 Hz, 1H, C₅H_{arom.}), 4.72 (s, 2H, OH), 3.59-3.53 (m, 8H, NCH₂/NCH₂CH₂OH), 3.51 (t, *J* = 5.5 Hz, 4H, NCH₂CH₂OH), 1.64-1.56 (m, 2H, CH₂CH₂CH₂), 1.51-1.42 (m, 4H, CH₂CH₂CH₂) ppm. ¹³C NMR (151 MHz, DMSO-*d*₆) δ: 161.7 (C₂), 160.7 (C₄), 155.8 (C₆), 92.6 (C₅), 59.4 (NCH₂CH₂OH), 51.2 (NCH₂CH₂OH), 44.6 (NCH₂), 25.3 (CH₂CH₂CH₂), 24.4 (CH₂CH₂CH₂) ppm. HPLC-UV (254 nm) ESI-MS, purity: 99%. LC-MS (m/z): 267.0 [M + H]⁺. Mp.: 64-66 °C.

Synthesis of 2,2',2'',2'''-(pyrimidine-2,4-diylbis(azanetriyl))tetrakis(ethan-1-ol) (**126**) and 2,2'-((2-chloropyrimidin-4-yl)azanediyl)bis(ethan-1-ol) (**125**)³³

A stirred solution of 2,4-dichloropyrimidin (100 mg, 0.67 mmol) and diethanolamine (704 mg, 6.7 mmol) in *i*PrOH (2 ml) was heated at 120 °C for 16 h in a sealed tube. TLC-MS analysis indicated that a monosubstituted and the disubstituted product were formed. The solvent of the mixture was removed under reduced pressure and the residue was purified by column chromatography (CH₂Cl₂/ MeOH - 9 : 1 to 8 : 2). The disubstituted product **126** was obtained as 91 mg (47%) of a colorless solid. ¹H NMR (600 MHz, Methanol-*d*₄) δ: 7.80 (d, *J* = 6.3 Hz, 1H, C₆H_{arom.}), 6.09 (d, *J* = 6.3 Hz, 1H, C₅H_{arom.}), 3.80 (q, *J* = 5.5 Hz, 8H, NCH₂CH₂OH), 3.76 (t, *J* = 5.7 Hz, 4H, NCH₂CH₂OH), 3.74-3.67 (m, 4H, NCH₂CH₂OH) ppm. ¹³C NMR (151 MHz, MeOD) δ: 163.7 (C₂), 161.8 (C₄), 155.0 (C₆), 94.9 (C₅), 62.0 (NCH₂CH₂OH), 61.0 (NCH₂CH₂OH), 53.2 (NCH₂CH₂OH), 52.8 (NCH₂CH₂OH) ppm. HPLC-UV (254 nm) ESI-MS, purity: 95%. LC-MS (*m/z*): 286.8 [M + H]⁺. Mp.: 82-85 °C.

The monosubstituted product **125** was isolated as 36 mg (25%) of a colorless solid. ¹H NMR (600 MHz, DMSO-*d*₆) δ: 7.98 (d, *J* = 6.2 Hz, 1H, C₆H_{arom.}), 6.69 (d, *J* = 6.2 Hz, 1H, C₅H_{arom.}), 4.85-4.72 (m, 2H, OH), 3.68-3.58 (m, 2H, NCH₂CH₂OH), 3.56 (q, *J* = 5.0 Hz, 4H, NCH₂CH₂OH), 3.53-3.47 (m, 2H, NCH₂CH₂OH) ppm. ¹³C NMR (151 MHz, DMSO) δ: 162.8 (C₂), 159.5 (C₄), 156.6 (C₆), 102.8 (C₅), 58.2 (NCH₂CH₂OH), 51.5 (NCH₂CH₂OH), 50.5 (NCH₂CH₂OH) ppm. HPLC-UV (254 nm) ESI-MS, purity: 99%. LC-MS (*m/z*): 218.1 [M + H]⁺.

Synthesis of 2,2'-((2-(piperidin-1-yl)pyrimidin-4-yl)azanediyl)bis(ethan-1-ol) (**127**)³³

A stirred solution of **125** (36 mg, 0.17 mmol) and piperidine (140 mg, 1.7 mmol) in *i*PrOH (2 ml) was heated at 120 °C for 4 days in a sealed tube. Subsequently, the mixture was treated with water and extracted with CH₂Cl₂ (3 x 20 ml), the combined organic layers were dried over MgSO₄, filtered off and the solvent was evaporated under reduced pressure. The crude product was purified by column chromatography (CH₂Cl₂/ MeOH - 9 : 1). The product **127** was obtained as 39 mg (89%) of a brownish solid. ¹H NMR (600 MHz, DMSO-*d*₆) δ: 7.77 (d, *J* = 6.0 Hz, 1H, C₆H_{arom.}), 5.88 (d, *J* = 6.0 Hz, 1H, C₅H_{arom.}), 4.71 (s, 2H, OH), 3.62 (t, *J* = 5.5 Hz, 4H, NCH₂CH₂OH), 3.58-3.42 (m, 8H, NCH₂ / NCH₂CH₂OH), 1.57 (m, 2H, CH₂CH₂CH₂), 1.48-1.40 (m, 4H, CH₂CH₂CH₂) ppm. ¹³C NMR (151 MHz, DMSO) δ: 161.6 (C₂), 160.8 (C₄), 155.6 (C₆), 92.7 (C₅), 58.7 (NCH₂CH₂OH), 51.1 (NCH₂CH₂OH), 44.4 (NCH₂), 25.4 (CH₂CH₂CH₂), 24.7 (CH₂CH₂CH₂) ppm. HPLC-UV (254 nm) ESI-MS, purity: 97%. LC-MS (*m/z*): 266.9 [M + H]⁺. Mp.: 69 °C.

4.4.7. References

- (1) Melani, A.; Cipriani, S.; Corti, F.; Pedata, F. Effect of intravenous administration of dipyridamole in a rat model of chronic cerebral ischemia. *Ann. N. Y. Acad. Sci.* **2010**, *1207*, 89-96.
- (2) Brown, D. G.; Wilkerson, E. C.; Love, W. E. A review of traditional and novel oral anticoagulant and antiplatelet therapy for dermatologists and dermatologic surgeons. *J. Am. Acad. Dermatol.* **2015**, *72*, 524-534.
- (3) Rogosnitzky, M.; Isakov, I.; Wlassoff, W.; Ingram, A.; Barishak, Y. R. Ocular applications of dipyridamole: A review of indications and routes of administration. *J. Ocul. Pharmacol. Ther.* **2016**, *32*, 83-89.
- (4) Schröder, J.; Esteban, M.; Müller, M. R.; Kasimir-Bauer, S.; Bamberger, U.; Heckel, A.; Seeber, S.; Scheulen, M. E. Modulation of multidrug resistance by BIBW22BS in blasts of de novo or relapsed or persistent acute myeloid leukemia ex vivo. *J. Cancer Res. Clin. Oncol.* **1996**, *122*, 307-312.
- (5) Jansen, W.; Pinedo, H. M.; van der Wilt, C. L.; Feller, N.; Bamberger, U.; Boven, E. The influence of BIBW22BS, a dipyridamole derivative, on the antiproliferative effects of 5-fluorouracil, methotrexate and gemcitabine in vitro and in human tumor xenografts. *Eur. J. Cancer.* **1995**, *31*, 2313-2319.
- (6) Tonew, M.; Tonew, E.; Mentel, R. The antiviral activity of dipyridamole. *Acta Virol.* **1977**, *21*, 146-150.
- (7) Tonew, E.; Indulen, M. K.; Dzeguze, D. R. Antiviral action of dipyridamole and its derivatives against influenza virus A. *Acta virologica.* **1982**, *26*, 125-129.
- (8) Liu, X.; Li, Z.; Liu, S.; Sun, J.; Chen, Z.; Jiang, M.; Zhang, Q.; Wei, Y.; Wang, X.; Huang, Y.; Shi, Y.; Xu, Y.; Xian, H.; Bai, F.; Ou, C.; Xiong, B.; Lew, A. M.; Cui, J.; Fang, R.; Huang, H.; Zhao, J.; Hong, X.; Zhang, Y.; Zhou, F.; Luo, H.-B. Potential therapeutic effects of dipyridamole in the severely ill patients with COVID-19. *Acta Pharm. Sin. B.* **2020**, *10*, 1205-1215.
- (9) Wang, C.; Lin, W.; Playa, H.; Sun, S.; Cameron, K.; Buolamwini, J. K. Dipyridamole analogs as pharmacological inhibitors of equilibrative nucleoside transporters. Identification of novel potent and selective inhibitors of the adenosine transporter function of human equilibrative nucleoside transporter 4 (hENT4). *Biochem Pharmacol.* **2013**, *86*, 1531-1540.
- (10) Curtin, N. J.; Barlow, H. C.; Bowman, K. J.; Calvert, A. H.; Davison, R.; Golding, B. T.; Huang, B.; Loughlin, P. J.; Newell, D. R.; Smith, P. G.; Griffin, R. J. Resistance-modifying agents. 11. Pyrimido[5,4-*d*]pyrimidine modulators of antitumor drug activity. Synthesis and structure-activity relationships for nucleoside transport inhibition and binding to alpha1-acid glycoprotein. *J. Med. Chem.* **2004**, *47*, 4905-4922.

- (11) Yamagishi, H.; Kawaguchi, M. Characterization of central- and peripheral-type benzodiazepine receptors in rat salivary glands. *Biochem. Pharmacol.* **1998**, *55*, 209-214.
- (12) Weishaar, R. E.; Cain, M. H.; Bristol, J. A. A new generation of phosphodiesterase inhibitors: multiple molecular forms of phosphodiesterase and the potential for drug selectivity. *J. Med. Chem.* **1985**, *28*, 537-545.
- (13) Regan, J.; Bruno, J.; McGarry, D.; Poli, G.; Hanney, B.; Bower, S.; Travis, J.; Sweeney, D.; Miller, B.; Souness, J.; Djuric, S. 2-Substituted-4-methoxybenzimidazole-based PDE4 inhibitors. *Bioorg. Med. Chem. Lett.* **1998**, *8*, 2737-2742.
- (14) Watanabe, N.; Adachi, H.; Takase, Y.; Ozaki, H.; Matsukura, M.; Miyazaki, K.; Ishibashi, K.; Ishihara, H.; Kodama, K.; Nishino, M.; Kakiki, M.; Kabasawa, Y. 4-(3-Chloro-4-methoxybenzyl)aminophthalazines: synthesis and inhibitory activity toward phosphodiesterase 5. *J. Med. Chem.* **2000**, *43*, 2523-2529.
- (15) Manallack, D. T.; Hughes, R. A.; Thompson, P. E. The next generation of phosphodiesterase inhibitors: structural clues to ligand and substrate selectivity of phosphodiesterases. *J. Med. Chem.* **2005**, *48*, 3449-3462.
- (16) Northen, J. S.; Boyle, F. T.; Clegg, W.; Curtin, N. J.; Edwards, A. J.; Griffin, R. J.; Golding, B. T. Controlled stepwise conversion of 2,4,6,8-tetrachloropyrimido[5,4-d]pyrimidine into 2,4,6,8-tetrasubstituted pyrimido[5,4-d]pyrimidines. *J. Chem. Soc. Perkin Trans. 1.* **2002**, 108-115.
- (17) Lin, W.; Buolamwini, J. K. Synthesis, flow cytometric evaluation, and identification of highly potent dipyridamole analogues as equilibrative nucleoside transporter 1 inhibitors. *J. Med. Chem.* **2007**, *50*, 3906-3920.
- (18) Scott L. DAX. Preparation of pyrimido[5,4-d]pyrimidine derivatives as novel breathing control modulating compounds for preventing and/or treating respiratory diseases, United states, WO 002017003822 A1, **2017**.
- (19) Wan, Z.-K.; Wacharasindhu, S.; Binnun, E.; Mansour, T. An efficient direct amination of cyclic amides and cyclic ureas. *Org. Lett.* **2006**, *8*, 2425-2428.
- (20) Fischer, F. G.; Roch, J.; Neumann, W. P. Über pyrimido-pyrimidine, III chlor-, hydroxy- und amino-derivate des dyrimido[5.4-d]pyrimidins. *Liebigs Ann. Chem.* **1960**, *631*, 147-162.
- (21) Teno, N.; Gohda, K.; Wanaka, K.; Tsuda, Y.; Sueda, T.; Yamashita, Y.; Otsubo, T. Pyrrolopyrimidine-inhibitors with hydantoin moiety as spacer can explore P4/S4 interaction on plasmin. *Bioorg. Med. Chem.* **2014**, *22*, 2339-2352.
- (22) Unpublished data from Müller group.

- (23) Scheiper, B.; Bonnekessel, M.; Krause, H.; Fürstner, A. Selective iron-catalyzed cross-coupling reactions of Grignard reagents with enol triflates, acid chlorides, and dichloroarenes. *J. Org. Chem.* **2004**, *69*, 3943-3949.
- (24) Kuduk, S. D.; Liverton, N.; Luo, Y. Preparation of heteroaryl compounds as orexin receptor antagonists, United States WO2016095205 A1, **2016**.
- (25) Zhang, Y.-M.; GU, M.; MA, H.; TANG, J.; LU, W.; NAN, F.-J. An efficient synthesis of 2-chloropyrimidines via Pd-catalyzed regioselective dechlorination of 2,4-dichloropyrimidines in the presence of NaHCO₃. *Chin. J. Chem.* **2008**, *26*, 962-964.
- (26) Mulla, S. T.; Jose, C. I. Intramolecular hydrogen bonding and conformational behavior of *N*-methyldiethanolamine and triethanolamine. *J. Chem. Soc., Faraday Trans. 1.* **1986**, *82*, 681.
- (27) Dr. Karl Thomae, G.m.b.H., Derivatives of pyrimido[5,4-*d*]pyrimidine, GB807826, **1959**.
- (28) Fischer, F. G.; Roch, J.; Kottler, August, Substituted pyrimido[5,4-*d*]pyrimidines, US3031450, **1962**.
- (29) Y. D. Bommegowda, D. B. Shenoy, M. T., Chethan B. P., Nagaraja G., F. Baig, Sandeep K. N., V. Babu. Synthesis of novel pyrimido-[5,4-*d*]pyrimidines by sequential nucleophilic substitution reaction. *J. Chem. Pharm. Res.* **2012**, *4(11)*, 4888-4893.
- (30) Breshears, S. R.; Wang, S. S.; Bechtolt, S. G.; Christensen, B. E. Purines. VIII. The aminolysis of certain chlorosubstituted purines 1. *J. Am. Chem. Soc.* **1959**, *81*, 3789-3792.
- (31) Bhujabal, Y. B.; Vadagaonkar, K. S.; Gholap, A.; Sanghvi, Y. S.; Dandela, R.; Kapdi, A. R. HFIP promoted low-temperature SNAr of chloroheteroarenes using thiols and amines. *J. Org. Chem.* **2019**, *84*, 15343-15354.
- (32) Lenselink, E. B.; Louvel, J.; Forti, A. F.; van Veldhoven, J. P. D.; Vries, H; Mulder-Krieger, T.; McRobb, F. M.; Negri, A.; Goose, J.; Abel, R. van Vlijmen, Herman W. T.; Wang, L.; Harder, E.; Sherman, W.; IJzerman, A. P.; Beuming, T. Predicting binding affinities for GPCR ligands using free-energy perturbation. *ACS Omega.* **2016**, *2*, 293-304.
- (33) Maier, J. A.; Brugel, T. A.; Clark, M. P.; Sabat, M.; Golebiowski, A.; Bookland, R. G.; Laufersweiler, M. J.; Laughlin, S. K.; VanRens, J. C.; De, B.; Hsieh, L. C.; Brown, K. K.; Juergens, K.; Walter, R. L.; Janusz, M. J. Development of *N*-2,4-pyrimidine-*N*-phenyl-*N*-alkyl ureas as orally active inhibitors of tumor necrosis factor alpha (TNF-alpha) synthesis. Part 2. *Bioorg. Med. Chem. Lett.* **2006**, *13*, 3514-3518.

5. Summary and outlook

5.1. Adenosine receptors

The A_{2A} and A_{2B} adenosine receptors (ARs) are promising drug targets in Alzheimer's and Parkinson's disease, inflammatory diseases, autoimmune diseases, diabetes and, most importantly, in cancer (immuno)therapy. The A_{2A} AR is expressed on a variety of immune cells including natural killer cells and T-lymphocytes, and its stimulation decreases cytokine production causing immunosuppression. Stimulation of A_{2B} ARs supports cancer cells by inducing tumor proliferation, metastasis, angiogenesis, and it mediates immunosuppressive effects by activation of A_{2B} ARs on immune cells. Consequently, blocking of A_{2A} - and A_{2B} ARs is a promising strategy in cancer (immuno)therapy. In this thesis, a series of xanthine-based receptor antagonists was synthesized, their SARs were analyzed, and fluorescence-labeled probes for biological studies were developed. In another sub-project, a series of A_{2A} AR antagonists was developed and explored with regard to its SARs.

5.1.1. Exploration of *N*-acyl-8-(4-piperazine-1-sulfonyl)phenylxanthines as potent and selective adenosine A_{2B} receptor antagonists

Potent and selective A_{2B}AR antagonists based on the xanthine scaffold have been reported in literature.¹⁻³ On the basis of parent compound **7**, the new scaffold 8-(4-acylpiperazine-1-sulfonyl)phenyl-1-propylxanthine was explored by straightforward acylation of the piperazine moiety of precursor **12** with a variety of carboxylic acids, yielding 19 novel A_{2B}AR antagonists (see Figure 1). *N*-Acyloxanthines can be formed by employing the coupling reagent HBTU at rt. An SAR analysis of the new compounds revealed that benzoyl moieties bearing lipophilic substituents (such as halogens or CF₃) and substituted 2-phenylfuran moieties attached to the piperazine residue lead to A_{2B}AR antagonists with subnanomolar affinities and high selectivities versus the other AR subtypes. Derivative **29** turned out to be the most potent (K_i A_{2B} 0.246 nM) and selective (>4,000-fold) compound in this series (see Figure 1), and can be considered as a new lead structure for further optimization, e.g. regarding pharmacokinetic properties.

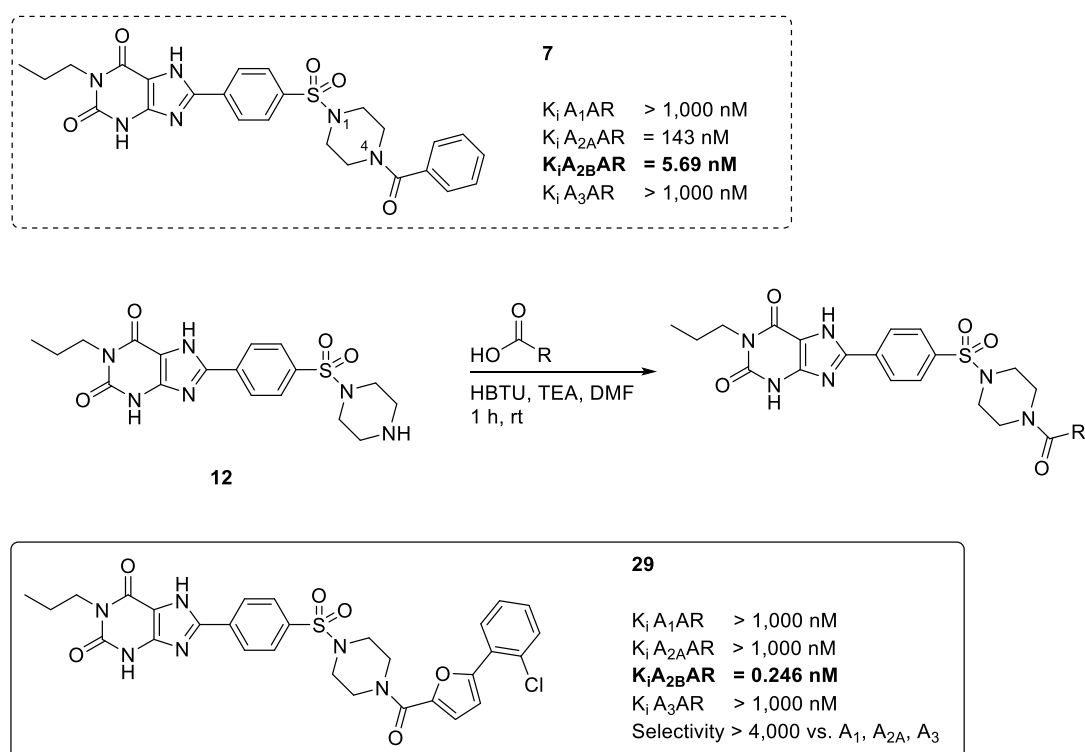


Figure 1. Biological data at AR subtypes of parent compound **7** and derivative **29**; the general acylation reaction of precursor **12** is shown which allows an easy access to a broad range of target compounds.

5.1.2. Functionalized potent and selective 8-(4-acylpiperazinyl-1-sulfonyl)phenylxanthines providing a platform for fluorescence-labeling of adenosine A_{2B} receptor antagonists

Fluorescence-labeled AR antagonists are versatile biological probes for a variety of applications including microscopy, flow cytometry, and ligand binding assays. In this project, a functionalized cyanine fluorophore was combined with 8-substituted xanthine derivatives forming novel potent and selective A_{2B}AR antagonists as biological probes. Xanthine precursor **12** was conjugated with a variety of benzoic acid derivatives that exhibited reactive groups. Cyanine dyes bearing functionalized linkers were coupled to these xanthines forming fluorescent A_{2B}AR ligands. Compounds **39** (PSB-20077) and **40** (PSB-20104) showed high potency (K_i A_{2B}AR 149 nM and 159 nM) and subtype-selectivity, and they were investigated in confocal microscopy studies, revealing specific binding to the A_{2B}AR (see Figure 2). Currently, **39** and **40** will be evaluated as pharmacological probes, e.g. for BRET-based binding assays.

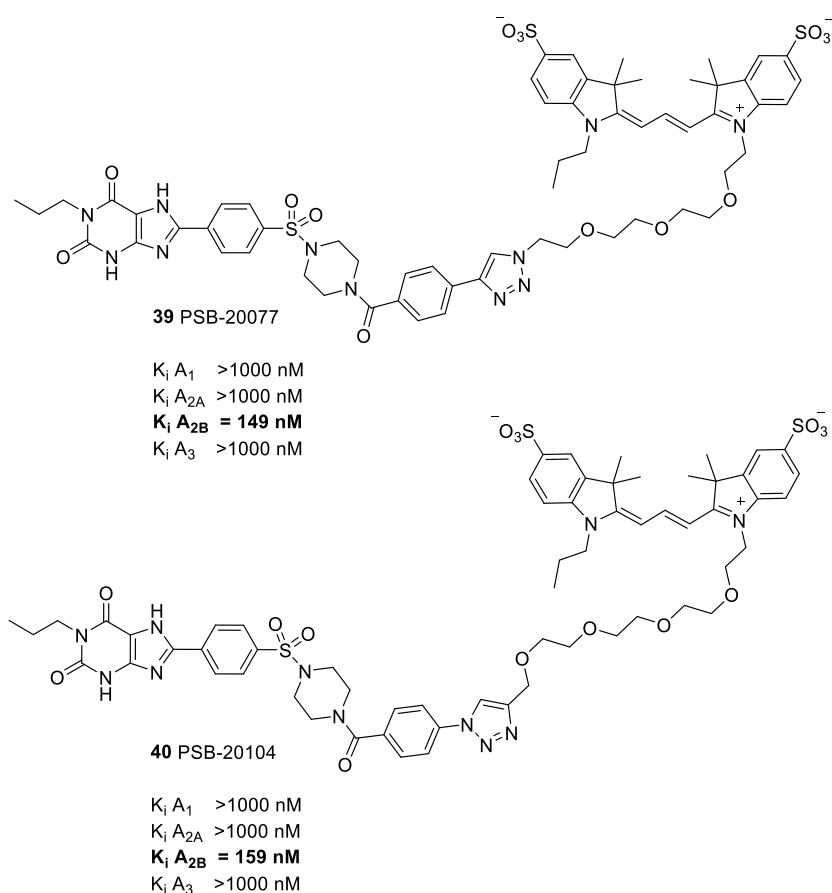


Figure 2. Fluorescence-labeled A_{2B}AR antagonists **39** and **40** and their biological data at AR subtypes.

5.1.3. Synthesis of 3-amino-*N*-benzyl-1-phenyl-1*H*-pyrazole-4-carboxamides as A_{2A} AR antagonists

5-Amino-2-phenyl-1,2,3-triazole derivatives have been reported as A_{2A} AR antagonists in literature.⁴⁻⁵ In this study, closely related 3-amino-*N*-benzyl-1-phenyl-1*H*-pyrazole-4-carboxamide derivatives were explored as A_{2A} AR antagonists. Therefore, a regioselective synthesis, starting from the appropriate phenylhydrazines, was employed and improved. A protecting group strategy could exclude the formation of undesired regioisomers. Moreover, copper-catalyzed coupling reactions were explored with regard to the formation of N1-substituted aminopyrazoles. A compound library of 53 new A_{2A} -antagonists was prepared and analyzed with regard to SARs at the four AR subtypes. Figure 3 illustrates the most potent compound **36a** as well as the general insights in the SARs observed for this scaffold.

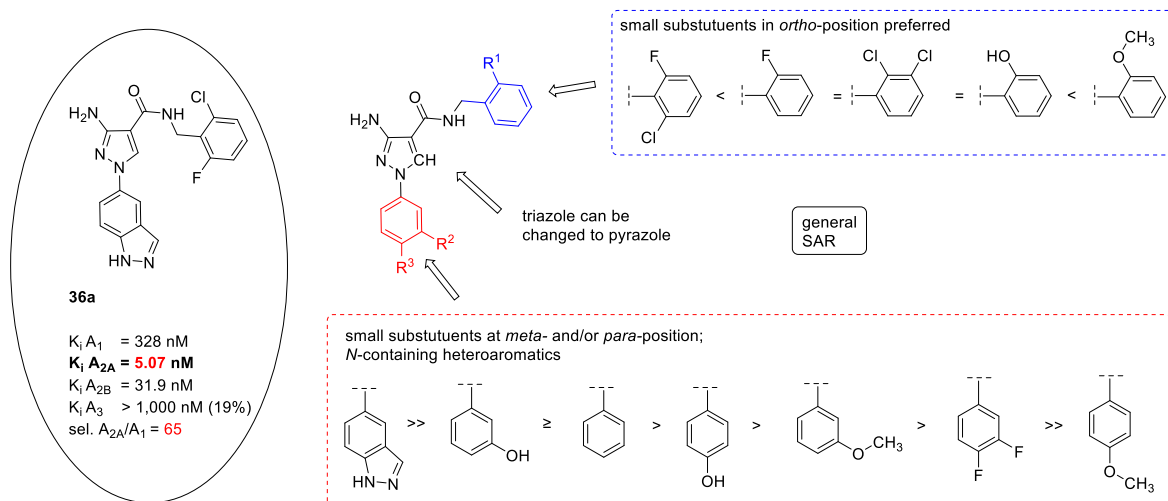


Figure 3. SAR analysis of 3-amino-*N*-benzyl-1-phenyl-1*H*-pyrazole-4-carboxamides as A_{2A} AR antagonists and biological data of derivative **36a**.

As a result, the 1*H*-indazol-5-yl residue turned out to be the most favorable moiety at the N1-position leading to compounds with affinities in the low nanomolar range between 5.07 and 68.2 nM (**36a-36f**). Small residues (such as a hydroxy group) at the *meta*- and/or *para*-position were very well tolerated by the A_{2A} AR. 2-Chloro-6-fluorobenzylamine stood out as the best substituent for the benzylamine moiety. However, small substituents in the *ortho*-position (such as halogens or hydroxy groups) showed good results as well. Compounds **9a**, **21a** and **21c** were submitted to metabolic stability studies, and water-solubility of **9a** was measured. Our studies suggested drug-like properties for this scaffold. Compounds **21e** and **36a** are planned to be tested as therapeutics in cancer models.

5.2. Synthesis of 2,4,6,8-tetrasubstituted pyrimido[5,4-*d*]pyrimidines as MRGPRX3 agonists

The MRGPRX3 is an orphan GPCR that is predicted to be involved in pain and itch perception. In the present study, the first agonist screening hit, dipyridamole, was the prototype for the synthesis of various MRGPRX3 agonists on the basis of 2,4,6,8-tetrasubstituted pyrimido[5,4-*d*]pyrimidines. For a rational synthesis, 2,4,6,8-tetrachloropyrimido[5,4-*d*]pyrimidine (TCPP) was stepwise substituted with nucleophiles under controlled conditions. This yielded 40 compounds with defined substitution patterns. An analysis of their biological activity revealed steep SARs; only very specific substitution patterns led to potent compounds. SARs indicated that alternative binding modes are likely. Derivative **96** was the most potent compound with an EC₅₀ value of 0.942 nM.

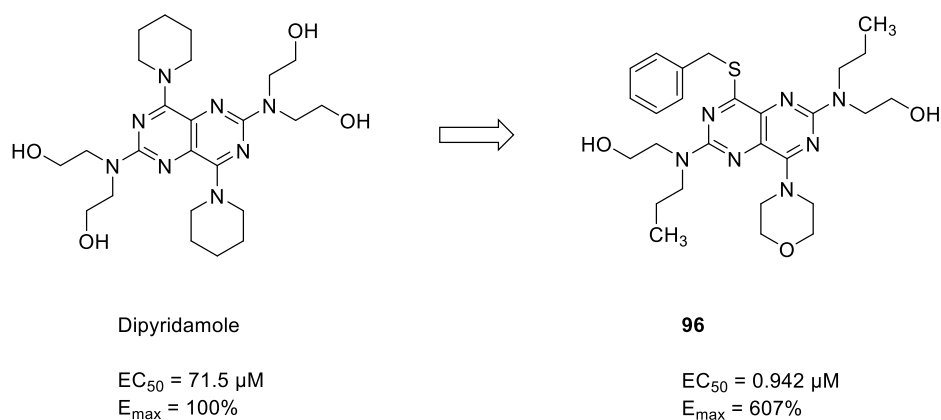


Figure 4. Biological data of dipyridamole and derivative **96** at MRGPRX3.

In addition, 8 compounds based on a purine scaffold and 4 compounds based on a 2,4-disubstituted pyrimidine scaffold were prepared, however, none of those compounds showed any significant activity for MRGPRX3. All derivatives of this project were additionally tested as antagonists but no compound showed antagonistic activity. For the future, **96** can be considered as the new lead structure. Furthermore, new scaffolds should be tested as ligands for MRGPRX3, especially antagonists would be of great interest due to their expected biological activities, e.g. in pain therapy.

5.3. References

- (1) Yan, L.; Müller, C. E. Preparation, properties, reactions, and adenosine receptor affinities of sulfophenylxanthine nitrophenyl esters: toward the development of sulfonic acid prodrugs with peroral bioavailability. *J Med Chem.* **2004**, *47*, 1031-1043.
- (2) Borrmann, T.; Hinz, S.; Bertarelli, D. C. G.; Li, W.; Florin, N. C.; Scheiff, A. B.; Müller, C. E. 1-alkyl-8-(piperazine-1-sulfonyl)phenylxanthines: development and characterization of adenosine A_{2B} receptor antagonists and a new radioligand with subnanomolar affinity and subtype specificity. *J. Med. Chem.* **2009**, *52*, 3994-4006.
- (3) Jiang, J.; Seel, C. J.; Temirak, A.; Namasivayam, V.; Arridu, A.; Schabikowski, J.; Baqi, Y.; Hinz, S.; Hockemeyer, J.; Müller, C. E. A_{2B} adenosine receptor antagonists with picomolar potency. *J. Med. Chem.* **2019**, *62*, 4032-4055.
- (4) Sun, B.; Bachhawat, P.; Chu, M. L.-H.; Wood, M.; Ceska, T.; Sands, Z. A.; Mercier, J.; Lebon, F.; Kobilka, T. S.; Kobilka, B. K. Crystal structure of the adenosine A_{2A} receptor bound to an antagonist reveals a potential allosteric pocket. *P. Natl. Acad. Sci. U.S.A.* **2017**, *114*, 2066-2071.
- (5) Jaiteh, M.; Zeifman, A.; Saarinen, M.; Svenningsson, P.; Brea, J.; Loza, M. I.; Carlsson, J. Docking screens for dual inhibitors of disparate drug targets for Parkinson's Disease. *J. Med. Chem.* **2018**, *61*, 5269-5278.

6. Danksagung

Zunächst möchte ich meiner Doktormutter **Prof. Dr. Christa E. Müller** meine aufrichtige und tiefe Dankbarkeit dafür aussprechen, dass sie mir die Möglichkeit gegeben hat, in ihrer Forschungsgruppe mitzuarbeiten. Außerdem möchte ich mich bei ihr für die interessanten Projekte und ihre Inspiration, Geduld, Mentorenschaft und Unterstützung während meines gesamten Promotionsstudiums bedanken. Ich hatte das gute Gefühl bei jedem Meeting etwas Wichtiges dazu gelernt zu haben. Danke für dein Vertrauen und danke für die viele Arbeit die du dir machst, um so vielen Menschen eine Promotion zu ermöglichen.

Ich möchte **Prof. Dr. Finn Hansen** herzlich für seine Zeit und seine Bereitschaft danken, als zweiter Betreuer zu fungieren.

Außerdem möchte ich **Prof. Dr. Günther Weindl** und **Prof. Dr. Rainer Manthey** sehr dafür danken, dass sie sich bereit erklärt haben, als Korreferenten in meinem Promotionsausschuss mitzuarbeiten.

Ich möchte mich ganz herzlich bei Dr. Jörg Hockemeyer bedanken der nicht nur mein Betreuer, Ratgeber und Büro-Kollege war, sondern vor allem ein sehr guter Freund.

Ich möchte Ghazl Al Hamwi danken für die tolle Zusammenarbeit in unserem gemeinsamen Projekt. Es war mir eine Ehre und eine Freude mit dir zu arbeiten. Bleib weiterhin so fleißig und liebenswert.

Außerdem möchte ich Christin Vielmuth für die Durchführung der Radioligandenbindungs-Studien danken. Ich danke Marion Schneider, Sabine Terhart-Krabbe und Annette Reiner für die LC-MS- und NMR-Analysen.

Ich möchte dem gesamten Arbeitskreis Müller dafür danken, eine sehr nette und produktive Umgebung geschaffen zu haben. Es hat Spaß gemacht mit euch allen zusammenzuarbeiten.

Zuletzt möchte ich meiner Familie danken. Ihr habt mich bedingungslos und in jeder Hinsicht privat wie beruflich unterstützt und ich wäre nicht der Mensch der ich heute bin ohne euch.

Tim Harms

Bonn, September 2021